ARCHAEOMAGNETIC WORK IN BRITAIN AND IRAQ

by

NIMAT BADEEL HAMMO YASSI

A thesis submitted for the Degree of Doctor of Philosophy
at the University of Newcastle upon Tyne

DECLARATION

I declare that the contents of this thesis have not previously been presented for a degree at this or any other University.

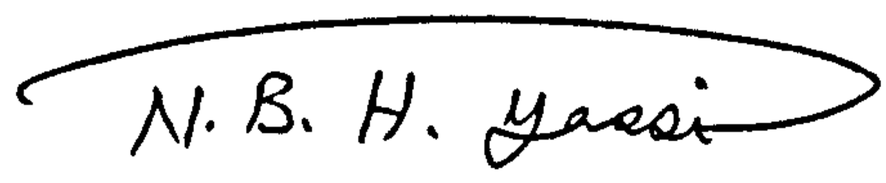

Nimat Badeel Hammo Yassi

School of Physics
The University of Newcastle
upon Tyne

DEDICATION

To my husband Nabeel, whose care, patience and encouragement made this work possible.

ACKNOWLEDGEMENTS

I would like to thank Professor S.K. Runcorn for giving me the opportunity to work in the School of Physics.

I sincerely thank my supervisor, Dr. D.H. Tarling, for his continued cheerful supervision and invaluable constant encouragement and guidance.

Dr. A.J. Clark, Department of the Environment kindly provided his unpublished archaeomagnetic data, for which I thank him most gratefully and my thanks also go to him for his continued help and interest.

Much assistance was provided by the archaeologists during field work, who most kindly provided archaeological information.

The State Organization of Antiquities in Baghdad,Iraq, kindly provided me with the permission to collect samples. Thanks are especially due to Dr. M. Saa'd, head of the State Organization of Antiquities.

I should also like to record my debt to all my friends in the School of Physics, who have, at one time or another, helped me whilst I have been in Newcastle, particularly Mrs. D. Cooper for her help in the design of the thesis, Miss Anne Codling for typing the thesis, Mrs. M. Summersby for her help in processing the data and to my husband Nabeel, for his computing assistance. I also offer my apologies to all those who I have failed to mention, but who have not been forgotten.

Finally, I would like to thank my son, Nawaf, who, despite making this thesis very late, gave me the chance to enjoy motherhood.

ABSTRACT

Archaeomagnetic studies were carried out on fired and sediment samples collected from predominantly 'rescue' British archaeological sites. Four of the fired sites were suitable for refraction and wall movement studies. The results showed no clear evidence for systematic wall movements or refraction. The scattered directions were explained in terms of local movements, inhomogeneous refraction, small scale anisotropy, fabric anisotropy and the presence of iron objects.

The grain size and colour of some of the sediments were studied and it was found that the presence of shards affects the magnetization of the sediments but this will depend on the percentage of shards and their magnetization. No direct relation was found between the intensity and the stability of the sediments . The brown and red samples appear to have the highest intensities and relatively higher stabilities.

The accumulated British and French archaeomagnetic data were assessed and presented as an archaeomagnetic data bank which was re-evaluated. Revised archaeomagnetic curves were plotted for both Britain and Paris.

A total of 96 samples were collected from 19 Iraqi archaeological sites. These were used to build an initial archaeomagnetic curve for Iraq.

A comparison of different palaeointensity methods on specimens taken from a single Roman brick, 3 other Roman bricks, and on nine Iraqi samples showed that the Thellier and Kono and Ueno methods give the most reliable results.

Magnetic characterization of 28 Iraqi obsidian artefacts (using their magnetizations and refractive indices) indicated that all samples except one came from a single source.

TABLE OF CONTENTS

TABLE OF CONTENTS (continued)

CHAPTER I INTRODUCTION

1.1 Archaeomagnetism and the Geomagnetic Field:-

Archaeomagnetism is concerned with the magnetic properties of materials in an archaeological context. It is most commonly used as a dating technique based on the fact that the directions and strength of the geomagnetic field may be preserved in, for example, baked archaeological materials such as pottery, kilns and fireplaces (section 1.3). The directional properties can then be determined if the material has remained in position after cooling although the past intensity of the field can be measured even if the materials are no longer in situ. These parameters for the ancient geomagnetic field can then be compared with records of the long term variations of the geomagnetic field (secular variation) in order to determine the time at which the magnetization was acquired (Thellier, 1938).

The geomagnetic field at any point on the earth's surface is defined by three elements: a) Declination (D) is the angle, measured clockwise, between the horizontal component of the magnetic field and the geographic north. b) Inclination (I) is the dip of the total intensity vector, positive downwards, from the horizontal plane, and c) the total intensity (F) measured in units of Tesla (Table 1.1).

The present geomagnetic field has a total dipole moment of 8×10^{25} mAm^{-1}, and can be represented by an inclined geocentric dipole field plus an additional non-dipole field. Spherical harmonic analysis shows that some 80% of the earth's field can be attributed to a single geocentric dipole inclined at 11½% to the earth's axis of rotation. When the inclined dipole field is subtracted from the total field, the remaining non-dipole field shows some eight to ten regions of continental dimensions displaying either positive or negative value with an amplitude of some 1.5 mT.

Magnetic Parameter		e.m.u.	MKs (Sommerfeld)	MKS (Kennelly)
Field	B	Gauss	10^{-4} T ($^{Wb}/_{m}$)	
	H	Oe	$10^{3}/4\pi$ $^{A}/_{m}$	
Magnetization or Moment per unit vol.		G (emu/cc)	10^{3} $^{A}/_{m}$	$4\pi 10^{-4}$ $^{Wb}/_{m^2}$
Dipole moment or total moment		Gcm^3	10^{-3} Am	$4\pi 10^{-10}$ Wb m
Specific (mass) moment		Gcm^3/gm (emu/gm)	1 Am^2/kg	$4\pi 10^{-7}$ Wb m/kg
Total susceptibility		Gcm /Oe	$4\pi 10^{-6}$ m^3	
Vol susceptibility		G/Oe (emu/cc)	4π (dimensionless)	
Specific (mass) susceptibility		$Gcm^3gm^{-1}Oe^{-1}$(emu/gm)	$4\pi 10^{-3}$ m^3/kg	

Table 1.1 Units of Magnetic Elements

These regions are asymmetrically distributed, and are strongest in the southern hemisphere and weakest in the Pacific region.

Observatory records show that the field gradually changes in both intensity and direction, showing regional growth or decay of the field pattern, superimposed on an apparent westerly drift of the non-dipole field at 0.2 - 0.3 degrees of longitude per year (Bullard and Gellman, 1950). These secular variations correspond, in London and Paris, to changes of some 0.25^{o} $year^{-1}$ in direction and 0.05% $year^{-1}$ intensity during the last 150 years. If such changes are regarded as typical of the rate of secular change, then this would imply that archaeomagnetic dating, using directional changes, should be possible to within about 5-20 years, while intensity changes would give a potential dating accuracy of some ±20-50 years. However, studies of observatory records elsewhere indicate that the rates of secular change can be either faster or slower, with corresponding increases or decreases. in the accuracy of the dating.

Archaeomagnetic dating can thus be very accurate for periods where the past variations of the geomagnetic field are well established, and can also be used for relative dating between different samples when such records are not available. The fundamental problem in archaeomagnetic dating is therefore to obtain an accurate record of the past geomagnetic field changes. Observatory records are only available since 1600, from London and Paris, and most other observatories only date from the mid-19th Century. For earlier times, therefore, these records can only be established by archaeomagnetic studies of materials dated by other means (Carbon 14, Thermoluminescence, etc.) and can therefore only be as reliable as the original dating method.

The main advantages of this method over the conventional

dating methods is that it is fairly simple, cheap and often non-destructive, and can be applied to a variety of materials which may not be datable by other methods. It also has the advantage that as more data becomes available the record of the geomagnetic field changes becomes more accurate and hence the precision of the technique will improve with time.

1.2 Other Dating Methods of Archaeological Materials

Archaeologists depend on different methods for dating archaeological materials. These can be stratigraphical, physical, chemical, climatic or astronomical. The reliability of the dating methods depends on a variety of factors. Generally, time-scales and records have been obtained by the evaluation of several dating methods in order to get calibration scales.

One of the most common archaeological dating physical methods is Carbon 14. This depends on the decay of ^{14}C isotopes which have been generated in the ionosphere by cosmic ray neutron interactions. The ^{14}C is oxidized to radioactive carbon dioxides and then mixed diffusively with the non-radioactive CO_2. During photosynthesis plants obtain all their carbon from the atmospheric CO_2 and they cease to absorb CO_2 when they die. Hence their ratio of ^{14}C compared with non-radioactive ^{13}C will gradually decrease with age according to the half life of 5568 years. However comparison of ^{14}C ages with dendrochronological dates showed major and minor differences (Damon et al., 1966; Ralph, 1972). The major fluctuations are thought to relate to changes in ^{14}C produced in ionosphere, possibly resulting from changes in height of ionosphere due to changes in the strength of the earth's magnetic field (Bucha, 1970). The origin of the minor fluctuations, 'Suess Wriggles' is uncertain (Suess, 1970; Stuiver, 1982). The long-term changes in the ^{14}C concentration can give rise to discrepancies

of several hundred years, while the Suess wriggles also give potential errors of a decade or so. There are also other errors in this method, for example, inter-laboratory correlation indicates differences of up to ±3% (Klein et al., 1982). Additionally it is known that different results can be obtained from different materials of the same age, although the reason for this remains unclear. Some caution is therefore necessary in using any age for archaeomagnetic values based on this method. It is also of interest to check for possible correlations between ^{14}C production and the past intensity of the earth's magnetic field.

Similar caution must also be used in assessing other methods of archaeological dating. Thermoluminescence, for example, requires adequate calibration of the environmental radioactivity, while clearly other archaeological dating can be highly subjective.

1.3 The British Archaeomagnetic Curve:-

Observations of the declinations and inclinations of the geomagnetic field in London have been recorded since 1600 (Bauer, 1899) and form the basis of the appropriate part of the curve in fig. 4.1. Following early work at Cambridge (Cook and Belshé, 1958), the Oxford Research Laboratory for Archaeology carried out measurements on some seventy archaeological structures, involving well over 1000 samples (Aitken and Weaver, 1962; Aitken, Hawley and Weaver, 1963; Aitken and Hawley, 1966, 1967; Aitken, 1970). They also sampled two dozen prehistoric hearths but these were not sufficiently well dated to allow a curve to be drawn. In producing the initial British archaeomagnetic curve, these authors used a subjective estimate of the general reliability of the results:-

A. Complete confidence

B. Reasonable Confidence

C. Doubtful but worth considering

D. Very doubtful.

The dates were presented in terms of local declinations of remanence, but with the inclinations modified to London on the assumption of an axial geocentric dipole field. This approach does not take into account the changes in declination resulting from changes in locations. In order to represent the magnetic directions of a number of sites from various localities and of different ages, the published "London" inclinations, Noel (1976) corrected them back to their original site values and the entire data were re-analysed in terms of a virtual polar wander path. Noel later (personal communication) corrected the polar data to the expected values at a central English location, Meriden (section 1.6.2). Subsequently, a new curve was determined by Clark (1980) incorporating new archaeomagnetic results and integrating them with the previous data. This curve has been used for determining the magnetic ages of sampled materials described in the following two chapters.

The work presented here on fired (Chapter 2) and deposited (Chapter 3) archaeological materials has been used to construct a new curve for Britain (Chapter 4) and to provide an initial curve for Iraq (Chapter 5). Comparisons are made between the results from fired and sedimented materials in order to assess their relative potentials and a brief comparison is also made between different palaeointensity methods (Chapter 6). Some Iraqi obsidians were also sourced on the basis of their magnetic properties (Chapter 7).

1.4 Type of Remanent Magnetizations and Magnetic Minerals

Primary magnetization in rocks and archaeological materials is acquired at, or not significantly later than the time of formation of

the material. Most fired archaeological material contains primary thermal magnetization (TRM) which develops as the temperature falls below the Curie points of the magnetic minerals. Other magnetizations can also take place as a result of the growth of new magnetic minerals (chemical remanent magnetization (CRM)) or lightning (isothermal remanent magnetization (IRM)). Deposited sediments usually contain primary depositional or post depositional magnetization (DRM or PDRM) acquired as a result of alignment of magnetic grains during or after deposition. Secondary magnetizations may be acquired at any time after the formation of the magnetic material. Since most archaeological materials have been lying in the earth's magnetic field for a very long time, viscous magnetization (VRM) which is time-dependent, can be acquired. Chemical magnetization may also be acquired after the formation of the magnetic materials. In addition, anhysteretic remanent magnetization (ARM) can be introduced in the laboratory during measurements as a result of impure alternating fields.

1.4.1 Magnetic Minerals

The most common magnetic minerals responsible for the magnetic properties in rocks and archaeological materials are listed below (Stacey, 1977; McElhinny, 1979):-

Magnetite (Fe_3O_4, Cubic) is ferromagnetic, with a Curie point of 578^{o}C and a saturation magnetization of 480 mAm^2/g. This mineral is common in many fired materials as well as in sediments.

Maghemite (Fe_2O_3, Cubic) is usually formed by low-temperature oxidation of magnetite. It has an inverse spinel structure similar to magnetite, but has a defective lattice. It is chemically metastable and inverts to haematite (Fe_2O_3, rhombohedral) irreversibly, on being heated to temperatures in the range 300^{o} to 700^{o} C. The saturation magnetization is about 450 mAm^2/g.

Haematite (Fe_2O_3, rhombohedral) is antiferromagnetic but carries a weak, parasitic ferromagnetism with a Curie temperature of 680°C, while at temperatures below about -20°C, this intrinsic weak ferromagnetism disappears. Its saturation magnetization is low, 2.2 mAm^2/g. Although the magnetization is weak, haematite shows an extremely high stability of remanence compared with other minerals which make it an important magnetic carrier, particularly in well-oxidized fired materials and sediments (Collinson, 1965a,1966).

Goethite (FeOOH, Orthorhombic) is an important hydroxide of iron, occurring naturally in sediments. Its magnetic structure is antiferromagnetic, with a Neél temperature ranging from 60°C to 170°C (O'Reilly, 1976). At room temperatures the saturation magnetization lies in the range 10^{-3} to 1 mAm^2/g. Goethite dehydrates to haematite at 100 - 300°C and is therefore not found in unweathered fired materials.

Pyrrohtite ($Fe\ S_{1+x}$) is a ferrimagnetic iron sulphide for $0.09 < x < 0.14$ with a Curie temperature around 300°C and a saturation magnetization of 19.5 mAm^2/g. This mineral is not common in archaeological contexts.

1.4.2 Thermoremanent Magnetization (TRM):-

Thermoremanent magnetization is the remanence acquired when a rock containing magnetic mineral grains is cooled down through their Curie temperatures in the presence of a magnetic field. Upon cooling from a high temperature, spontaneous magnetization appears at the Curie point, Tc, and this assumes an equilibrium magnetization in the presence of an applied field. The time for this alignment to take place between the equilibrium magnetization and the applied field is termed the relaxation time. For any magnetic grains the relaxation time increases spontaneously as the temperature falls, so that each grain will have a characteristic temperature, the blocking temperature, T_b, at which its relaxation time becomes of the order

of a few minutes. As the temperature cools down below T_c and passes through each T_b the equilibrium magnetization becomes 'frozen in' and subsequent changes in the applied field direction, occurring at temperatures below T_b, are ineffectual in changing the directions of magnetization. The total TRM may be considered to have been acquired in steps over successive temperature intervals. The partial TRM (PTRM) acquired in any temperature interval depends only on the field applied during that interval and is not affected by the field applied at subsequent intervals on cooling. Thus the total TRM is equal to the sum of the PTRMs - the additivity law of TRM (Thellier, 1937). Conversely, on reheating to any temperature $T<Tc$, the original magnetization of all grains with blocking temperatures less than T will be destroyed.

In grains less than 1μm diameter (single domain) the grain will become magnetized in a specific direction determined by the crystal lattice structure. This is the direction of the easy magnetization axis. Antiparallel. alignment is possible when the thermal agitation energy of the grains becomes comparable with the potential energy of the constraints tending to keep the magnetization along their preferred axes.

In multidomain grains, the remanence is acquired by irreversible domain-wall movements, i.e. the domain walls are forced past energy barriers to new potential minima. Since this process can be thermally activated, it follows that domain walls, and therefore multidomain grains, have blocking temperatures, just as do single-domain grains. At high temperatures the domain walls are free to move to the positions of minimum total energy but they are immobilized by cooling and thus "freeze-in" any high temperature (thermoremanent magnetization). The process of blocking is not as simple as with single domains because domain walls tend to lock into a pattern and the whole pattern must be changed and not a single wall.

However the concept is the same, though with quantitative difference (Stacey and Banerjee, 1974).

The TRM of a sample of baked clay is proportional to the field intensity in which it cooled down and archaeomagnetic measurements can be used to determine both the ancient geomagnetic field strength and the direction (Thellier, 1937). The determination of the ancient intensity requires a knowledge, or reliable estimate, of the probable rate of cooling (section 1.7.1).

1.4.3 Chemical Remanent Magnetization (CRM)

Chemical processes can create magnetic minerals at temperatures below their Curie point. The growth of any magnetic mineral will result in the acquisition of a CRM as they increase their size from a very small superparamagnetic state into a single domain state, and possibly to multidomain, during which its relaxation time increases to millions of years, blocking in any magnetization it carried at its critical blocking volume (which is the volume at which the magnetization becomes frozen in) and as the grain grows further, has no effect upon direction of magnetization.

Several possible chemical and mineralogical changes may be significant in archaeological environments:-

a) Dehydration of iron hydroxides, for example goethite to maghemite.

b) Oxidation of (titano) magnetite to (titano) haematite.

c) Conversion of maghemite to haematite (Porath, 1968).

d) Reduction of haematite to magnetite (Haigh, 1958; Kobayashi, 1959).

e) Alteration of iron silicates into clay minerals and haematite or magnetite.

1.4.4 Isothermal Remanent Magnetization (IRM):-

When a weak field is applied to a specimen the domain walls move in the direction of the applied field but are able to return to their original position when the field is removed. In a stronger field the domain walls may move past energy barriers such as lattice imperfections, impurities etc., which prevent them returning. This leaves them with a magnetization (IRM) when the field is removed. This magnetization increases until a saturation ($M_{sat.}$) value is reached. At this point all possible domain wall movements have been made (Cox, 1961). The application of increasing magnetic field, first in one direction and then in the reverse direction therefore causes the magnetization to behave in a systematic manner, forming a hysteresis loop. Such a loop defines some important rock magnetic parameter such as the saturation moment M_{sat} and the field required to obtain it, H_{sat} as well as the back field required to reduce the isothermal remanence to zero Hcr., the back field coercivity. IRMs occurring naturally are usually associated with lightning strikes.

1.4.5 Depositional Remanent Magnetization (DRM):-

This is a magnetization acquired by a sediment through mechanical means during and after deposition. It can be produced by the alignment of magnetized particles when falling through water (Ising, 1943) and by the rotation of particles in water-filled, interstitial holes within the sediment (post-depositional remanent magnetization, PDRM). The main magnetic mineral to carry a DRM is magnetite, often in very fine particle sizes of a few microns, although a DRM in fine-grained haematite can also occur. Laboratory tests on current effects have been carried out using redeposited sediments (King, 1955; Collinson, 1965b). These show that the direction taken up is approximately that of the ambient field although the

inclinations tend to be shallower. Such inclination shallowing occurs as each particle makes contact with the bed when it assumes a position of minimum energy by rolling into the hollows between particles previously deposited. Elongated grains will also come to rest with their longest axes horizontal, and as these grains tend to be magnetized along their long axes, a sediment which contains a proportion of platey particles will have a remanent magnetization, I_o, which will be less than the inclination of the ambient field, I_f. This leads to an inclination error, δ, given by $\delta = I_f - I_o$ (Noel, 1976). In experiments with redeposited varve clays, Johnson et al (1948) and King (1955) found that inclination error could amount to 20^o. Such depositional effects are also influenced by water currents, the relative size of magnetic and matrix particles. Post-depositional realignment can also occur as a result of surface tension, compaction, drying out of the sediments and to other post-depositional factors. The nature of the sediments can thus determine whether it is likely to have acquired a DRM or PDRM reflecting the geomagnetic field at its time of formation. Very coarse-grained sediments deposited in turbulent conditions, would only acquire a weak, essentially random, DRM magnetization (Strangway, 1970), while fine grained sediments such as clay, silt and sand will have a magnetization which should be higher as they are deposited in a quiet environment.

Sediments are common in archaeological sites, but only a few studies were carried out on such materials. Nonetheless, various sediments, such as basal sediments in ditches or post-holes, pond infills, old soils and cave deposits in an archaeological context, have provided successful results (Creer and Kopper, 1976; Latham et al., 1979; Tite and Mullins, 1971; Mullins, 1977).

1.4.6 Viscous Remanent Magnetization (VRM)

This is a time-dependent isothermal remanence. For a constant time the rate at which viscous remanence is acquired depends on the temperature, the strength of the magnetic properties of the material and the strength of the ambient field. The relaxation time can also be used to describe the processes in an individual domain and is defined as:-

$$\frac{1}{\tau} = \frac{1}{c} \exp \left(\frac{vH_c J_s}{2KT}\right)$$

where ċ is a frequency factor, v is the volume of the grain, H_c is the coercive force, J_s is the saturation magnetization, K is Boltzman's constant and T the absolute temperature. Over prolonged periods in zero field, the original magnetization gradually "relaxes" towards an equilibrium state which has the effect of moving back the domain walls in multidomain grains and randomizing the directions of single domain grains. In the presence of a field, a VRM will develop along the direciton of the ambient field. Hence at constant temperature the acquisition of VRM depends logarithmically on time and therefore some rocks may be completely or partially remagnetized in geologically short periods of time (Dunlop,, 1973). Since all archaeological materials have been lying in an ambient magnetic field (geomagnetic field), they will thus have varying degrees of viscous magnetizations, depending on the time they have been lying in the field, the strength and constancy of the field, and the relaxation times of the magnetic particles in them. The magnetization of these viscous remanences can be removed by partial demagnetization (section 1.5), but in specimens with low magnetic stability, the natural remanence will be dominated by viscous components.

1.4.7 Anhysteretic Remanent Magnetization (ARM):-

Anhysteretic remanent magnetization is produced accidentally or deliberately during decreasing alternating magnetic field demagnetization if this is done in the presence of a steady magnetic field. A large alternating field initially saturates the sample during each cycle. As the field decays, the remanence is frozen in the direction of the direct field as the peak value of the applied alternating field falls below the coercivity of the individual magnetic grains in the sample. This effect is very similar to that occurring during the cooling of a sample through the blocking temperature and so ARM is considered to be an analog of TRM. Accordingly, several methods have been presented using ARM properties instead of TRM for the determination of the ancient intensity as no chemical changes are possible when imparting an ARM (Chapter 6).

Other types of remanent magnetizations can also be produced when the rock is rotated during AF demagnetization. This has been termed Rotational Remanent Magnetization (RRM) (Wilson and Lomax, 1972) and can be partially explained in terms of gyroremanent magnetization (GRM) which is likely produced whenever there is an asymmetry in the number of moments which flip in a particular sense (Stephenson, 1980 a,b,c).

1.5 Methods and Techniques:-

1.5.1 Sampling

In sampling fired materials for archaeomagnetic dating using directional properties, it is vital that the samples are oriented while in situ, i.e. they have not moved since baking. Thus in kilns and furnaces, the most undisturbed samples would be expected to come from the floors, unless the structure has tilted as a whole. The area to be sampled is usually brushed gently and sometimes washed with acetone to make sure that it is

clean from any material which may affect the measurements or prevent a good adhesion. A plastic disc method was used for sampling hearths and kilns. Solid plastic discs were cut with a smooth upper surface on which the fiducial marks could be drawn. The discs were usually attached to the archaeological material using an epoxy resin glue. A small piece of plasticine was also used which helped to retain the disc in position until the glue set. The disc was sometimes levelled using a spirit level, but when its surface was inclined, its dip was measured using a clinometer. (The shape of the discs was designed to allow them, with the attached sample, to fit inside a plastic cylinder which could then be placed in the archaeomagnetic magnetometer).

A fiducial mark was placed on the surface of the disc which was arbitrary in direction if the disc was level, and corresponded with a strike line if the disc was tilted. Its orientation was then measured before the disc, with attached sample, was removed. Wherever possible, this orientation was measured with a sun compass, but a magnetic compass was sometimes used despite the possibility of local field distortions (see later). The sun compass consists of a horizontal 360^{o} scale which can be read counter-clockwise from the direction defined by its marking edge. A centrally situated hole accommodates a vertical silver steel rod and the direction of the shadow of the rod is then read from the scale to within 1^{o} of the arc. In order to check the accuracy of the magnetic compass, both methods were usually used. Generally no differences were found, and where they did differ, the difference was within $\pm 1^{o}$, except for one site from North Wales in which the difference between the two readings was 30^{o}. This site had extremely high intensity (>10,000 mAm^{-1}) compared with the intensity obtained for all other sites. Accordingly it is thought that the magnetic compass can often be used with reasonable confidence, unless

the structure is particularly highly magnetized when the sun compass is impossible to use. The sample, with attached disc, was then separated from the structure and the sample was then reduced in volume so that it would fit into the archaeomagnetic magnetometer (i.e. within a 5.5 x 4.8 cm. cylinder). The magnetization of the materials used (disc, plasticine and glue) were all below the noise level of the magnetometer.

Sediment samples were collected using plastic cylinders of 5.3 cm. diameter and 4.8 cm. length. Samples were obtained by simply pushing a plastic cylinder into the sediment, where possible, or carving a pillar over which a plastic cylinder could be placed. As it is very important to keep the sediment sample unmoved inside the cylinder, the unfilled spaces within the cylinder were packed with polystyrene, paper and sometimes plaster of Paris. To reduce the rate of drying out of the sediments, plastic discs were used to cover the tops of the cylinders and fixed using lassotape. Fiducial marks were then put on the upper disc using the same orthogonal system as for solid materials. The main difficulty with this technique is when dealing with hard sediments and those containing pebbles and shards. Forcing the cylinders into their positions can then cause displacements within the sediments and also distortion of the shape of the cylinder, leading to unreliable results. Some deformed samples were collected but had to be rejected because of their uncertain reliability. In sampling hard sediments a brass cylinder was used which had an inner diameter slightly bigger than the outer diameter of the plastic cylinder. This brass cylinder made it possible to hammer the cylinder into the sediment without displacing the sediment or deforming the plastic cylinder. However, it is also important not to have pieces of pebbles or shards within the sample as they may have different magnetizations and could dominate the weak magnetization of the

sediments themselves, but this situation was difficult to establish until later.

1.5.2 Magnetic Measurements and Instrumentation:-

Natural Remanent Magnetization (NRM):-

The initial NRM was measured using a Digico spinner magnetometer, usually including a primary component, and secondary components (e.g. viscous magnetization). These components are commonly isolated by means of partial demagnetization using thermal or alternating field methods.

Digico Spinner Magnetometer:-

The Digico spinner magnetometer (Molyneux, 1971) was used for measuring the natural remanent magnetization of all of the samples studied in this thesis. This magnetometer is basically a balanced ring-fluxgate spinner in which the rock sample is placed in a holder on a shaft and rotated at about 7HZ within the centre of the fluxgate. The specimen is surrounded by a cylindrical triple mu-metal shield which screens the sample and the fluxgate from most of the ambient magnetic field. As the sample rotates, the amplitude of the analogue signal from the fluxgate rises and falls as a sine wave. This signal is amplified and passed through a digital converter (ADC). Attached to the sample shaft is a disc with 128 slots . As each slot passes a photocell, the ADC converts the fluxgate signal into a digital number which is stored in the computer's memory in such a way that each reading is referred to a particular memory location where they are added for successive rotations. After a fixed number of rotations (determined by the operator on the basis of the signal to noise ratio), the accumulated results are subjected to Fourier analysis. The results are given in terms of two othogonal components of the first harmonic within the plane of the fluxgate, X and Y, together with the magnitude of the resultant. Where X

is the direction of the fiducial line, Y is perpendicular to it within the plane of the fluxgate. The total vector could be determined by spinning the sample about a second orthogonal axis, but in practice the sample is successively rotated in six orientations to obtain average values of the NRM components and to reduce the effect of inhomogeneity. Random noise is reduced by increasing the total spin time measured in terms of 2^n spins. After four and six spins declination , inclination and mean volume magnetization and its components $\overline{X}$, $\overline{Y}$ and $\overline{Z}$ relative to the fiducial mark on the surface are printed out in units of mAm^{-1}.

The noise level (measurement carried out without a sample) should, ideally, be the lowest possible, but if the noise is random, then simple computational considerations show that it is sufficient if the signal to noise ratio does not fall below 10 : 1. The maximum absolute directional displacement from the true direction will then be less than 6^{o}. The signal-noise ratio increases linearly as the square root of the number of revolutions. Hence more spins can be used on weak samples to obtain more accurate results. The lowest noise level achieved during this work had an effective intensity of 0.014 mAm^{-1} (2^5 spins). The noise level reading was taken at the begining and end of each set of measurememements. Many attempts were undertaken to achieve the lowest noise level, when measuring weakly magnetized samples (mainly sediments) and most of the samples were measured twice or even three times (using longer spinning time) to check on their repeatability. A source of non-random noise, still subject to investigation (Xu, 1984), is that weakly magnetized samples with high susceptibility could acquire short-term viscous magnetization during measurements despite the mu-metal shielding. This short-term viscous magnetization effect can be checked from the first four readings of the magnetometer, which

represents the component of magnetization in each direction. These readings should be repeatable and if there are consistent differences between them, they may be attributable to viscous magnetization, particularly if all such samples show vectors which move to the same direction within the magnetometer. However even in weak samples if the first four readings are consistent with each other and above the noise level the results can still be considered reliable.

In an attempt tocheck the short-term viscous effect on weakly magnetized samples, the noise level readings were compared with readings obtained from a weakly magnetized (within the noise level) but highly susceptible sample. The individual results were scattered and the components did not show any vectors moving in a consistent direction (Fig. 1.1). Another weakly magnetized sample was then measured in both normal and reversed directions. The two sets of readings were also scattered (Fig. 1.1). Accordingly it was found that the effect of the magnetometer noise level was to give random directions even when the specimens involved had a very high susceptibility.

Low Field Susceptibility:-

A bridge system (Collinson and Molyneux ,1967) was used to determine the low field susceptibility of samples used for palaeointensity work. The bridge consists of two ferrite rings, with an air gap in each. Primary windings on each ring carry a current that produces an alternating magnetic field across the air gap of up to 10^{-3}T. A ferrite plug in one gap is used to initially balance the circuit so that the introduction of a specimen into the other air gap unbalances the circuit in proportion to the magnetic susceptibility of the specimen. Susceptibility measurements are used to record any chemical changes during thermal heating for the determin-

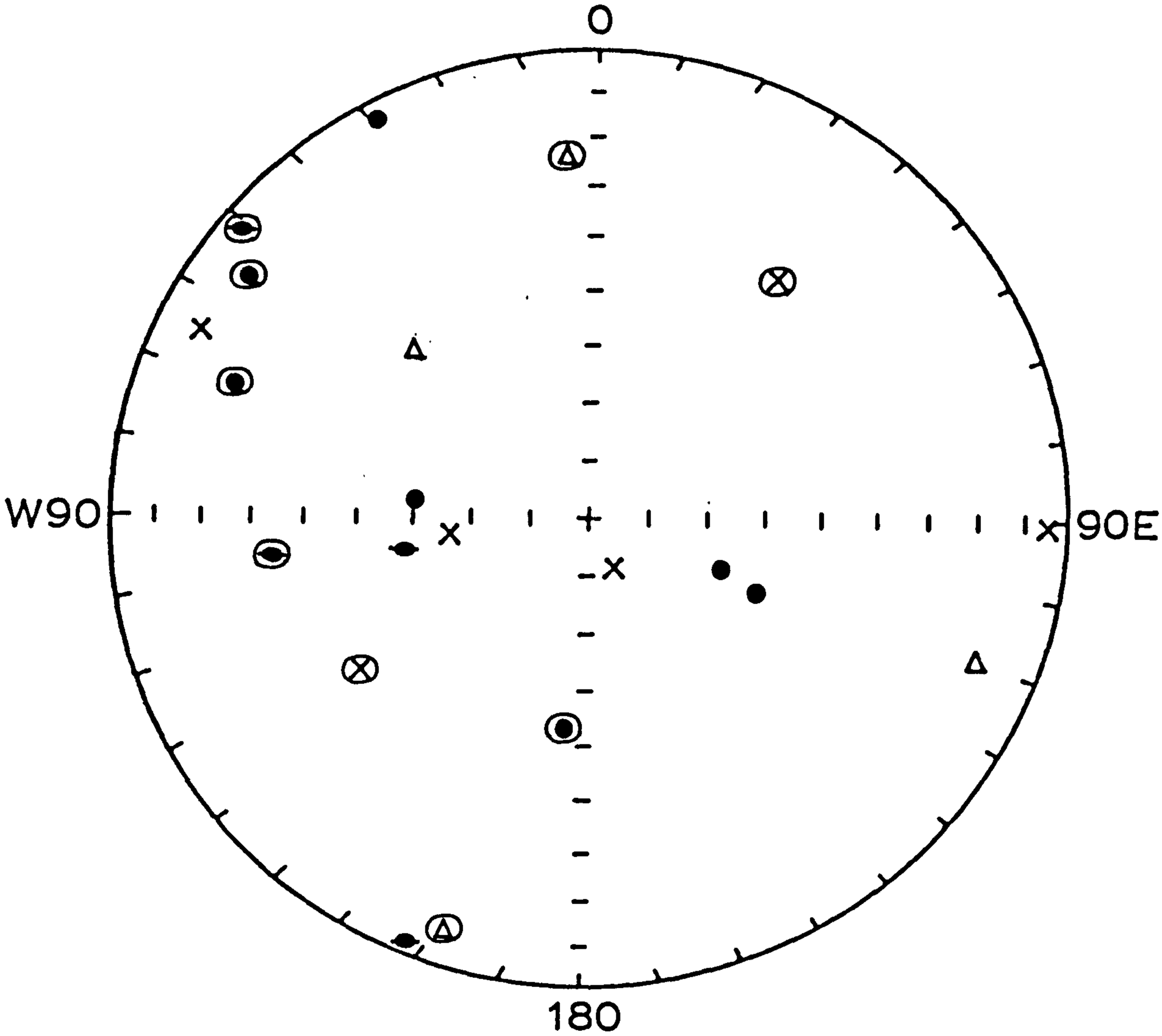

Δ Noise Level

X Weak but highly susceptible

Sample with very low remanent

● Normal

◆ Reversed

Upper hemisphere inside a circle

Fig. 1.1 Measurements of the noise level effects

ation of ancient intensity (Chapter 6). However, it was not practicable to measure the susceptibility of the other samples, because their sizes were too large to fit within the susceptibility bridge and, in any case, the demagnetization was by alternating field and did not involve any chemical changes.

Alternating Field Demagnetization:-

An alternating magnetic field demagnetizer was used in order to partially demagnetize the natural remanence of the samples. The demagnetizer consists of a coil through which is passed a very pure alternating current to create an alternating magnetic field along the axis of the coil. Specimens are usually rotated within the centre of the coil so that all directions within the specimen are eventually rotated into alignment with the peak field along the coil axis. The current is then gradually reduced while the specimen continues to rotate. In rotating the sample in increasing alternating field the magnetization of grains of low coercivity will follow the applied field. As this is reduced, the magnetization of these particles is left in random position (As and Zijderveld, 1958). Successive increments in the applied field, with the remanence of the specimen measured after each increment, allows the coercivity spectra to be determined and will leave only the remanence of the particles with coercivities greater than that of the applied field. To avoid the acquisition of ARM the geomagnetic field is cancelled over the specimen by mu-metal shields, and the wave form of the alternating field has been made very pure. To some extent, the process of tumbling the specimen in two or three axis also tends to reduce the effects of any ARM acquired accidentally. However, rotation procedures can give rise to rotational and gyromagnetic magnetizations and so the alternating magnetic field demagnetizer tends to become increasingly 'noisy'

at fields over 50 mT (Tarling, 1983).

The intensity of magnetization of the sample was corrected to its volume. Pilot samples from each site were chosen according to the NRM measurements and the size of the samples. The samples selected were chosen as representative of the site's average values, and their sizes were not too small or too large compared with the standard size (12.86 cm^3), to prevent inaccuracies that may arise from off-centred measurements. The number of pilot samples varied at different sites. This was based on the total number of samples collected and the consistency in the NRM directions and intensity within individual sites. Sites with less than 10 samples had all of their samples demagnetized, while sites with more samples normally had between 6 - 8 pilot samples analysed. Sites with inconsistent NRM directions and intensities irrespective of the total number of samples, had all their samples demagnetized. Accordingly all the Iraqi samples and most of the sediments were demagnetized in incremental A.F. Fired samples were found to be much more stable than sediments and hence they were demagnetized at fewer steps but using relatively higher field (5, 10, 15, 20, 30, 40 and 50 mT) while more steps were used for demagnetizing the sediments and some of the unstable samples (3, 4, 5, 7.5, 10, 12.5, 15, 20 and 30 mT). The remaining samples were bulk demagnetized using the steps with the most stable directions.

1.6 Stability Estimates:-

1.6.1 Stability Indices:-

Objective estimates of the stability during AC demagnetization were based on the following indices:-

a) The Stability Index

This parameter is an estimate of the stability of the

NRM in materials which have been subjected to step demagnetization by incrementally increased alternating magnetic fields or temperatures (Tarling and Symons, 1967). This index is a function of the change in direction of remanence, over two or more sucesslve increases in field or temperature and the range of field or temperature over which the directional change is least. The formula is:-

$$SI = \max ((R)^{\frac{1}{2}}/\theta^{o}_{63})$$

for 3 or more successive observations of the remanence direction. It is thus defined by the circular standard deviation, θ^{o}_{63}, and over successive increases in field or temperature as defined by the range R. The use of this index facilitates an objective comparison of different specimens from the same or different suites of rocks and also indicates the optimum range of treatment over which the most stable component of remanence has been isolated. Comparison of the stability indices with the subjective classification allows a specimen's remanence stability in response to AC or thermal demagnetization to be defined as:-

S.I.	Subjective Classification
over 15	Extremely stable
5 - 15	Very stable
2.5 - 5	Stable
1 - 2.5	Poorly stable
0.5 - 1	Metastable
under 0.5	Unstable

Since this index depends on directional changes only, any changes in intensity will not be reflected on the S.I. value if

the directional changes are small.

b) The Briden Index

This index combines the effect of direction and intensity changes at successive steps in the demagnetization procedure (Briden, 1972). It varies between +1 and -1; large values indicating small combined changes have occured. The maximum value of Briden Index during a demagnetizing run may then be used as the choice of optimum cleaning field. However, the Briden index will give low stability for a vector that remained of constant direction but of rapidly decreasing intensity.

1.6.2 Fisherian Statistics

The mean direction for each site and the related statistical parameter reflecting the reliability of the results were computed following Fisher (1953). The Fisherian model simulates the Gaussian (normal) distribution in three dimensions whereby points on a sphere (directions or poles) can be described in terms of a probability density (P) given by:-

$$P = \frac{K}{4\pi \sinh K} \exp (k \cos \theta)$$

where θ is the angle between the observed individual directions and the true mean direction and K is the precision parameter, varying from 0 for a perfectly random distribution, to infinity for identical directions. On this model, it is possible to estimate the precison parameter:-

$$k = \frac{N - 1}{N - R}$$

where N is the number of samples and R is the resultant vector ($\bar{D}$ and $\bar{I}$).

The reliability of the observed mean direction can then be defined by measuring the radius (α) of a circle on the sphere's surface, centred on the observed mean direction, within which there is a particular

probability (P) of the true mean direction lying, the cone of confidence:

$$\alpha = \cos^{-1} 1 - \frac{N - R}{R} (P - 1 / (N - 1) - 1)$$

conventionally, P is taken as 0.05, i.e. 95% probability.

The two precision parameters k and α_{95} can therefore be used as a measure of the reliability of the observed mean direction of a group of directions or poles which have a Fisherian distribution, the highest reliability being for the largest k and the smallest α_{95} . These precision estimates are less reliable for low numbers and there is increasing uncertainty about the reliability of k, particularly for N less than 7 and α_{95} when k becomes less than 10 (Watson, 1956).

The estimate of the precision of the mean direction is not measurement of the actual scatter of the vectors and it is often the magnitude of the scatter that is of interest. The Fisher distribution involves the angular distance of any individualpoint from the true mean. The angular radius (θ) of a circle about the mean containing either 63% of the observation can be given by:-

$$\theta_{63} = 81 K^{-1}$$

The 63% level is analogous to the standard deviation and is thus a good measure of the magnitude of scatter.

1.7 Archaeomgnetic Dating:-

The most stable direction of magnetization was selected according to the directional and intensity behaviour during AC-demagnetization mainly based on the values of different stability indices. In this work the stability index (Tarling and Symons, 1967) was mainly used for the

selection of the most stable range of magnetization, but the Briden index was also considered in most cases as a double check for establishing the most stable range of magnetization, particularly where there were both directions and intensity changes.

The mean values of the most stable directions were calculated for each site and dating was evaluated by comparing the mean values with the available archaeomagnetic curve. The statistical accuracy of these observed data is measured by the value of α_{95}, which can be converted directly to the inclination error ($\delta I = \alpha_{95}$), while the declination error (δD) is also dependent on the mean inclination value $\delta D = \frac{\alpha_{95}}{\cos I}$. Hence the circle of confidence (α_{95}) was corrected to an ellipse of confidence around the mean direction. Theoretically the mean value of the sites should fall on or very near to the archaeomagnetic curve but such agreement, even within the circle of confidence was often not achieved. Where the mean direction was close to the curve, the possible age range could be determined from those parts of the curve sectors that were cut by the ellipse of confidence, but when the mean direction was located away from the curve, the age estimates were obtained using the mid-point of intersection of the tangents of the edges of the ellipse, which are perpendicular to the curve.

The reliability for such dating is obviously lower than such an estimate and the differences between the mean direction and the curve were themselves interpreted as indications of the statistical error.

1.7.1 Corrections of Archaeomagentic Data:-

Archaeomagnetism has been found to be a generally reliable dating method which, under ideal conditions, should normally give data within ±5 years. However, recent application of this dating method shows much larger errors in direction and intensity. Studies have been undertaken

on different structures in order to find solutions of some uncertainties, and hence some corrections have been recommended in particular cases. Some of these corrections are related to the theoretical background of the method which concerns the uncertainties about the real nature of the earth's magnetic field, while the others are concerned with the practical application of the method on different structures.

1) Meriden Correction:-

The actual geomagnetic field at the present time is a combination of some 80% geocentric dipole with some 20% non-dipolar field. The strength of the non-dipole field at the surface amounts to about 5% of the dipole field (section 1.1), and so the local geomagnetic field cannot be adequately represented by a simple first harmonic inclined geocentric field. The geomagnetic field is better represented by higher harmonic which includes the non-dipole or irregular component of the field, but neither the behaviour of the non-dipole field nor the inclined dipole field are adequately known for proper regional corrections. Aitken et al (1962, 1963) used a correction based on the assumption of axial dipole, i.e. correction was only concerned with inclinations in relation to latitude.

In order to compare archaeomagnetic data from different localities in Britain, archaeomagnetic directions determined at sites have been corrected to their corresponding directions at a central locality, Meriden (Lat. = 52.43N, Long. = 358.38). This is based on a model in which the observed regional field is considered to largely correspond to that of an inclined geocentric dipole.

The pole position $P(\lambda', \phi')$ for an inclined geocentric dipole can be calculated from site (Lat., Long.) $(S(\lambda, \phi))$ and magnetic declination (D) and inclination (I) (Irving, 1964) (fig. 1.2).

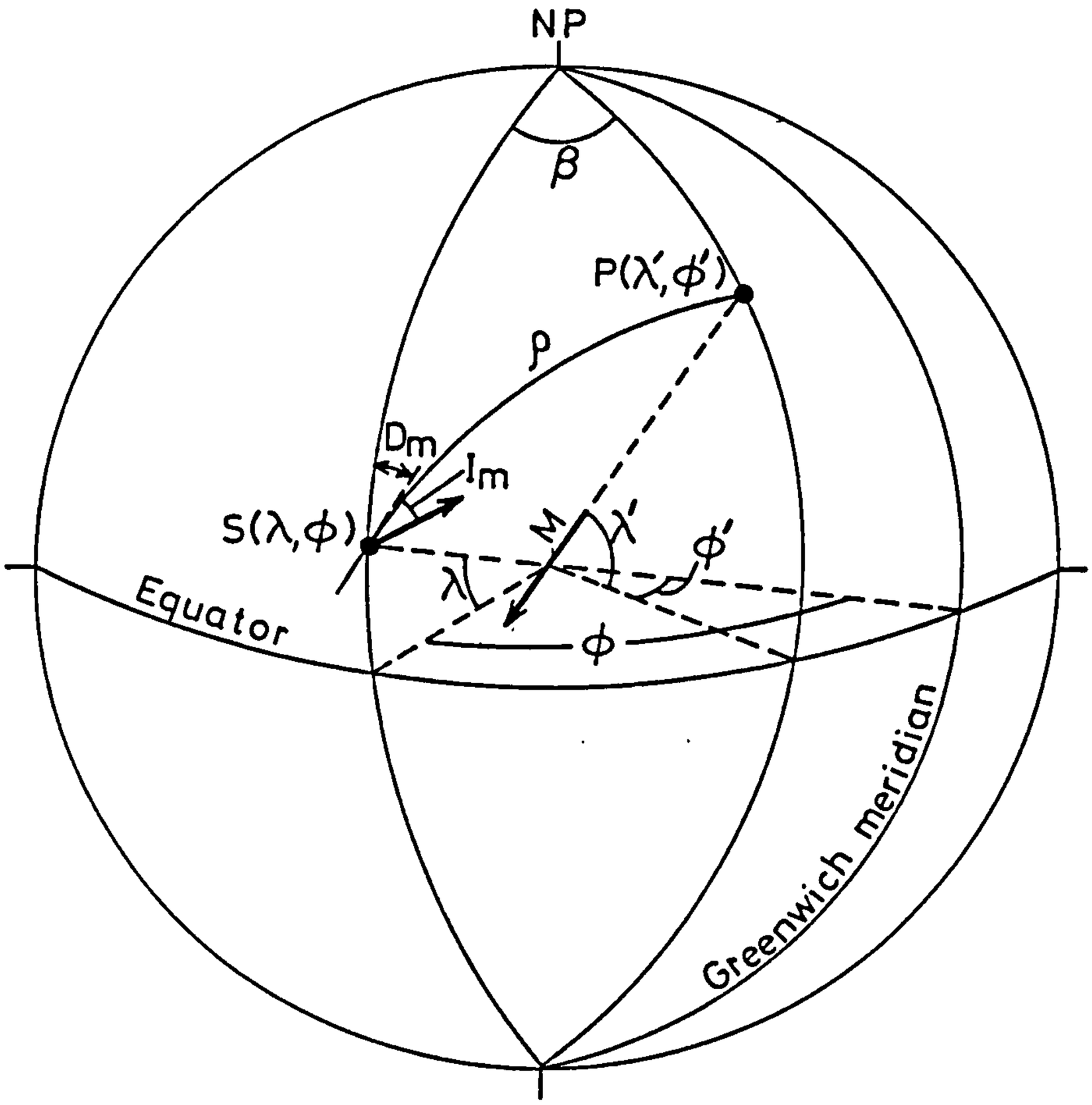

Fig. 1.2 Calculation of palaeomagnetic poles

M = elementary dipole placed at the centre

N_p = North geographic pole

P = Palaeomagnetic pole

S = Sampling locality

Dm, Im = Coordinates of the observed palaeomagnetic directions

ρ = Virtual geomagnetic pole

colatitude

× 41

$$\rho = \tan^{-1}\left(\frac{2}{\tan I}\right)$$

$$\lambda' = \sin^{-1}\left(\sin\lambda\cos\rho + \cos\lambda\sin\rho\cos D\right)$$

$$\cdots\cdots\cdots \quad (-90^{o} < \lambda' < 90^{o})$$

$$\beta = \sin^{-1}\left(\frac{\sin\rho\sin D}{\cos\lambda'}\right) \quad \cdots\cdots\cdots \quad (-90^{o} < \beta < 90^{o})$$

$$\phi' = \phi + \beta \qquad \text{when } \cos\rho > \sin\lambda_m\sin\lambda'$$

$$\phi' = \phi + 180 - \beta \qquad \text{when } \cos\rho < \sin\lambda\sin\lambda'$$

The D_m and I_m corrected to a reference locality $S(\lambda_m, \phi_m)$ can be calculated from the locality latitude and longitude and the pole position $P(\lambda', \phi')$.

$$\rho = \cos^{-1}\left(\sin\lambda'\sin\lambda_m + \cos\lambda'\cos\lambda_m\cos(\overline{\phi} - \phi_m)\right)$$

$$\beta = \phi' - \phi_m \qquad \text{when } \cos\rho > \sin\lambda_m\sin\lambda'$$

$$\beta = \phi_m + 180 - \phi' \qquad \text{when } \cos\rho < \sin\lambda_m\sin\lambda$$

$$D_m = \sin^{-1}\left(\frac{\sin\beta\cos\lambda'}{\sin\rho}\right)$$

$$I_m = \tan^{-1}\left(\frac{2}{\tan\rho}\right)$$

where D is measured clockwise from true north and I is positive downward. (Positive latitudes lie between 0^{o} and 90^{o}N and negative latitudes between 0^{o} and 90^{o}S. Longitudes 0^{o} to 180^{o}E are positive and 0^{o} to 180^{o}W negative).

The reliability of this correction was tested using the recorded magnetic observations at London and Paris, corrected to Meriden,

and then compared with each other (fig. 1.3). The two sets of data coincide with each other except for the period between 1700 - 1780 AD,where the French data are about 1-2^{o} steeper than the British data. This difference can also be observed in the shapes of the two original curves. Therefore any geographical correction will result in poor agreement for this period. However, the similarity obtained between the two data in the other periods indicates the general validity of the Meriden correction between Paris and England. Further corrections have been carried out for other European localities to estimate the probable distance over which the correction is applicable (table 1.2).

Table (1.2) Some European Magnetic Directions Corrected to Meriden

	Lat.	Long.	Dec.	Inc.	δD	δI	Approx. distance from Meriden km
Meriden	52.43	358.4	353.5	67.6	0	0	
Paris	48.90	2.3	355.2	67.5	1.7E	-0.1	484
Bonn	50.7	7.1	356.8	67.7	3.3E	0.1	623
Madrid	40.4	356.3	353.7	66.1	0.2E	-1.5	1344
Naples	40.8	14.2	358.8	66.8	5.3E	-0.8	1768
Athens	38.0	23.7	0.2	66.5	6.7E	-1.1	2554
Iceland	64.1	339.0	345.2	66.3	8.3W	-1.3	1741
Sofia	42.7	23.3	0.9	67.1	7.4E	0.5	2154

According to the above results, it was found that this correction can be applied within about 2000 km. with an inclination error of about ±1^{o} but with a declination error of up to 8^{o}.

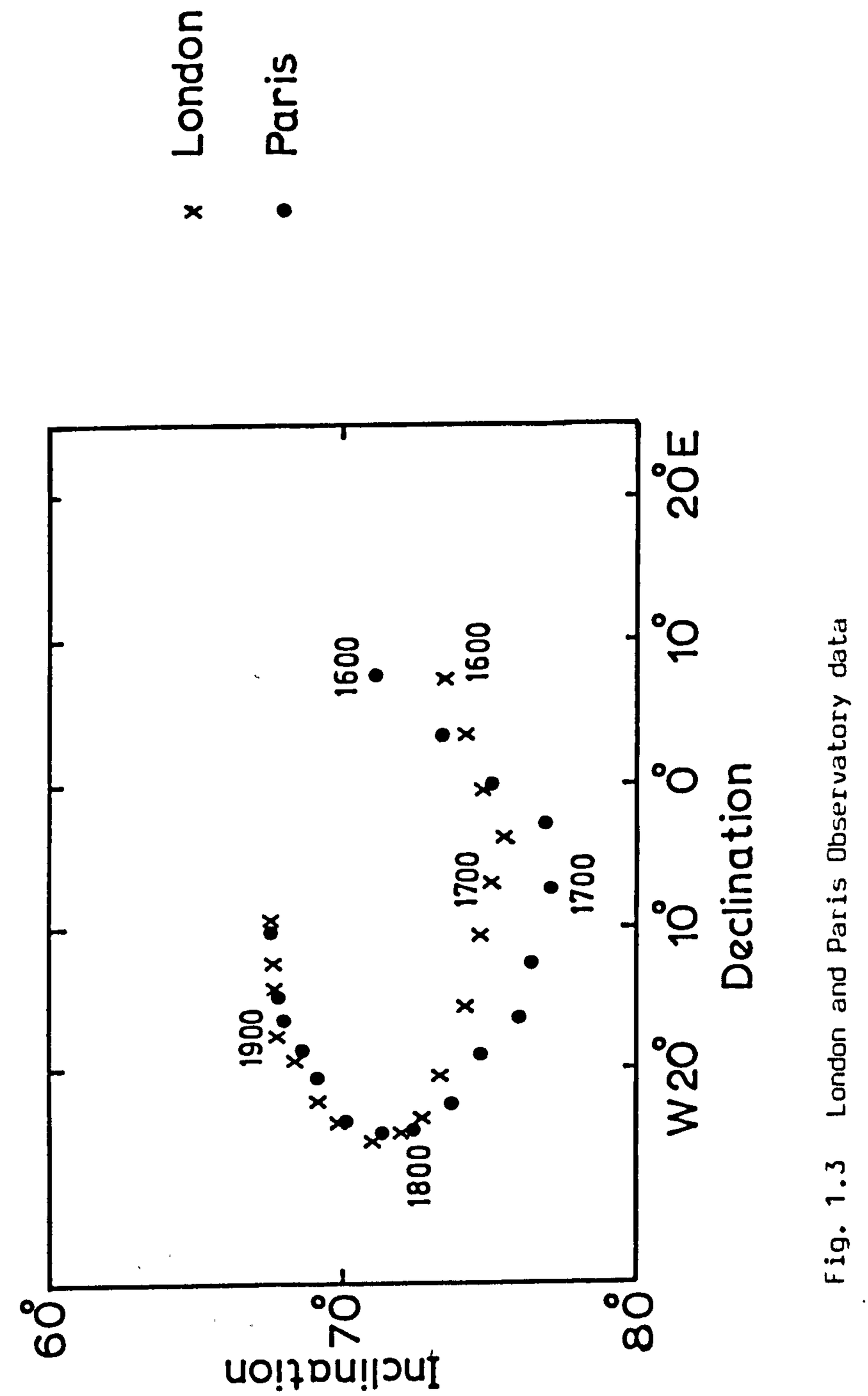

Fig. 1.3 London and Paris Observatory data

2) Kiln Wall Fall-Out and Magnetic Refraction:-

Archaeomagnetic measurements on samples collected round a circular Roman kiln wall at Hartshill by Harold (1960) showed a systematic deviation from their average value. This deviation, in declination and inclination, approximated to a sine wave for declination and another for inclination, depending on azimuth of the sample with respect to magnetic north (fig. 1.4). The angle of dip was too steep in the region of 0^{o} and too shallow in the region of 180^{o}; the declination was too westerly in the region of 90^{o} and too easterly in the region of 270^{o}. The amplitude of the variation for declination wasapproximately twice that for the angle of dip. It was pointed out that the dependence on azimuth was consistent with a uniform fall out of the kiln walls by about 3^{o} subsequent to the last firing of the kiln. Harold pointed out that if such an interpretation is valid then an average of the directions would give misleading results (this is only true if the samples were taken from one part of the kiln and not uniformly round the kiln). He also suggested that the true value of declination and inclination can be deduced by taking the mean of the maximum and minimum of the best fitting smooth curves of the declination and inclination sine curves (Harold, 1960). If this systematic dispersion is due to physical tilting of the wall then the average remanent direction in the floor sample would represent the true ancient direction. An experiment was carried out by sampling at 0^{o}, 90^{o}, 180^{o} and 270^{o} around the wall of two experimental replica kilns of circular plan. These data also showed results consistent with kiln wall fall-out of 4^{o}, although there was no evidence for any such uniform outward tilting and irregular movements were less than 1.5^{o} (Weaver, 1961, 1962). It was therefore concluded that the cause of the dispersion (both systematic and random) was likely to be distortion

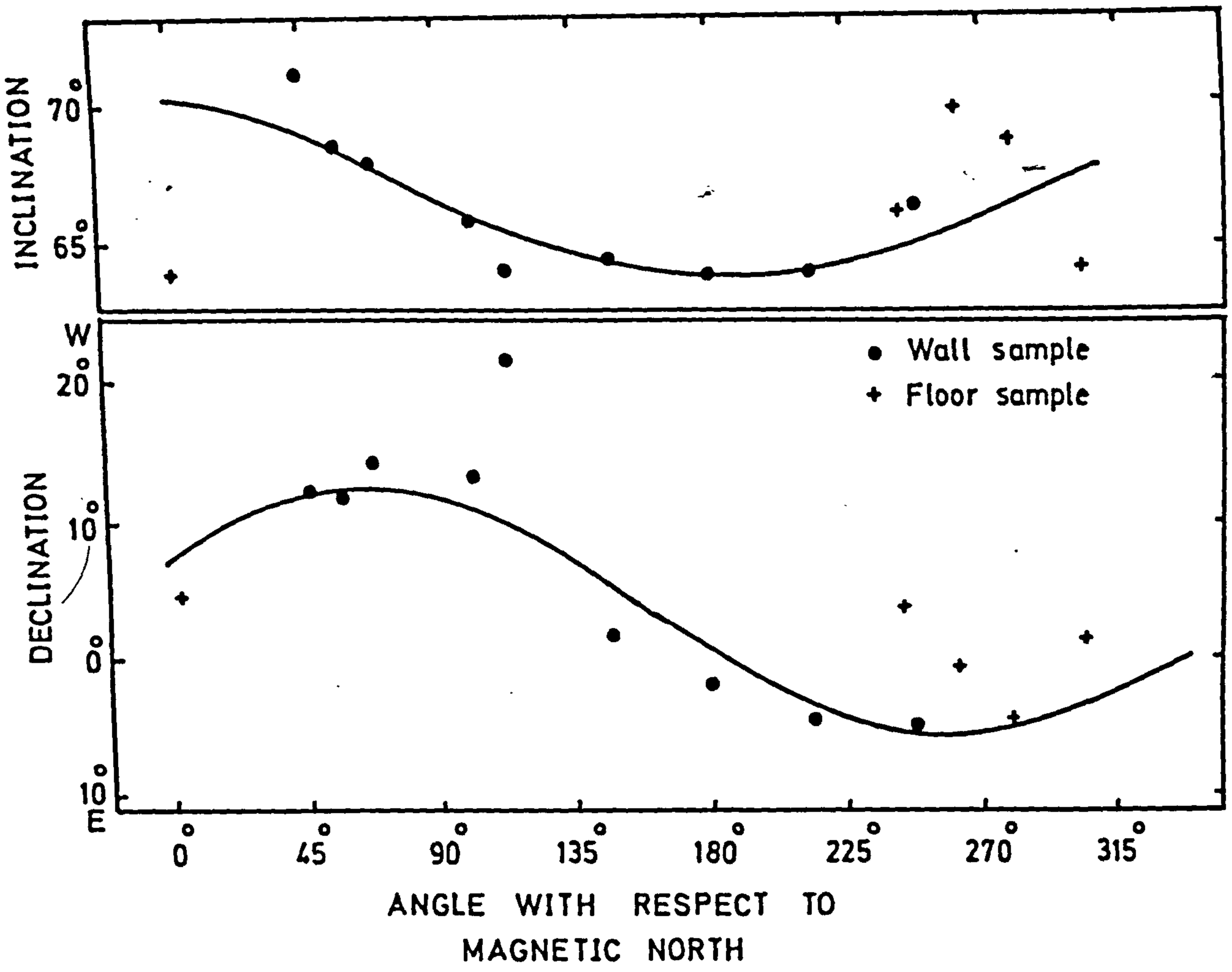

Fig. 1.4 The expected sine curve for kiln wall fall out (Harold, 1960)

of the ambient field direction by the magnetism of the structure itself.

Magnetic refraction may occur as the kiln cools from its firing temperature. The magnetism it acquires may be strong enough to distort the local earth's field, so that some parts of the kiln will cool in a magnetic field whose direction does not correspond with that of the earth's field (Aitken and Hawley, 1971). Accordingly, the angle of dip recorded in the floor will be too shallow and the average for the walls will be too steep, with the true value lying in between (Weaver, 1964). Results obtained from structures in which comprehensive sampling of both floors and walls was possible (Aitken and Hawley, 1971), showed that the scatter of directions in floor samples is usually very much less than in wall samples and that the floor values were shallower than the true value by about 2.4^{o}. This value could correspond to an apparent age difference of about ±25 years. The intensity of magnetization that would give rise to an angle of deviation of 2.4^{o} for a flat horizontal sheet having a volume intensity of magnetization, M, in a field, F, the angle of deviation is approximately : $2\pi(M/F) \sin (2I)$ radians, where I is the angle of dip, so that for 2.4^{o} the value M is about 4×10^{-3} A/m taking F = 0.048 mT and I = 60^{o}. This is the effective value of M at the time when the remanent magnetization was being acquired. M decreases with increase of temperature and so grains with a high blocking temperature should exhibit less deviation than grains whose direction is locked in at a lower temperature. Since there is a possibility for a strong temperature gradient through the thickness of the floor and possibly a gradient in magnetic properties as well, the effective value of M will not be simply related to the value M measured for the sample at room temperature and consequently there will not necessarily be a strong correlation between deviation and the strength of magnetization (Aitken and Hawley, 1971).

Archaeomagnetic directional studies of an Italian kiln, terminally fired in 1960, suggests that neither magnetic refraction nor fall out could explain the observed shallower inclination relative to the known field from bricks taken from a vertical wall (no floor samples) (Hoye, 1982).

3) Cooling Rate Dependence:-

Palaeointensity results can be affected by the rate at which the sample is cooling while the TRM is being acquired (Dodson and McClelland-Brown, 1980; Walton, 1982). An experiment was carried out by Fox and Aitken (1980) to show the cooling rate effect. The Thellier method was carried out on samples of known geomagnetic intensity, all effects due to sample shape or fabric anisotropy were avoided and a consistent cooling time of the order of 30 minutes was used. The field magnitude, evaluated by the Thellier analysis, was found to be higher than the known field in which the samples had cooled during acquisition of the TRM by an average, 6% - 12%. Fox and Aitken (1980) found that the TRM acquired for slow cooling is greater than that for fast cooling. This is because, for a given group of grains, the effective blocking temperature is lower in the case of slow cooling and therefore the fractional alignment that is blocked in is higher, because of the reduced thermal agitation at the lower temperature and because of the intrinsic increase of activation energy (McClelland-Brown, 1980). Accordingly, to avoid errors in palaeointensity determinations, laboratory cooling time should ideally be the same as the archaeological cooling time. This is rarely practicable. Walton (1980) and Dodson et al. (1980) found that a correction of 10% is required for the normal laboratory methods which they employ in which very fast cooling rates are involved.

4) Anisotropy of Samples:-

The magnetic anisotropy is the difference of magnetic susceptibility in different directions. This anisotropy can cause the observed directions of remanence to depart from that of the applied field. Anisotropy arises primarily from crystalline alignments in samples containing haematite and from shape alignments in samples with magnetite. Additional anisotropy can also occur if magnetic grains, even if individually isotropic, occur in rows or plans (Bathal, 1971). Shape and crystal alignments can occur in a variety of ways and the resultant magnetic anisotropy can be used to determine the nature and direction of the forces causing them.

In sediments, the effect of stresses during deposition result in elongated and platey minerals being oriented within the bedding plane, and elongated minerals being further constrained into directions either parallel or perpendicular to the flow direction and so most sediments exhibit an oblate magnetic fabric slightly imbricated in the direction of flow (Tarling, 1983).

In archaeological fired materials, alignment of different minerals may take place during the moulding processes, such as striae formed during the turning of clays on a wheel, potter's marks of the physical manipulation and rolling of clays as pots are shaped.

The effect of magnetic anisotropy is generally small and is less than 10 to 20 per cent with expected deflections of less than 5 or 10°, which should also be averaged out if observations are taken from different parts of the structure. The effect of anisotropy of TRM has mainly been considered on pottery in which the anisotropy is present prior to the acquisition of remanence. This was observed during measuring the ancient field intensity of a pottery disc samples. It was found that the

ease with which the TRM is acquired depends on the angle at which the remagnetizing field is applied. The hardest direction was found to be perpendicular to the plane of pottery samples while the easy plane lies within the plane. Accordingly the palaeointensity value obtained when the applied laboratory field is perpendicular to the plane of the pottery will have an error by a factor equal to the anisotropy ratio.

This effect of anisotropy was found to be higher in wheel pottery, however some British Iron Age non-wheel pottery also showed some effect. This anisotropy effect of brick, tiles and kilns was assumed to be relatively unimportant (Roger, Fox and Aitken, 1979; Aitken et al., 1981).

TRM experiments were carried out by Hoye (1982) on sub-samples cut from six specimens to test the possibility of distortions caused by anisotropy. The easy plane of some of these samples did not lie in the plane of the brick and thus the results did not support the idea of systematic easy-plane fabric anisotropy.

Another source of error due to anisotropy was found to be produced as a result of sample shape (Kent and Lowrie, 1975; Turner and Tarling, 1975).

Errors in anisotropy meter readings were found to be dependent on the shape of the specimen. These errors depend on the ratio l/d (length to the diameter). However, these errors are negligible on the magnetometer.

CHAPTER 2 ARCHAEOMAGNETIC STUDIES ON BRITISH FIRED MATERIALS

Fired archaeological materials were collected, or obtained, from the following sites and the refraction effect is discussed at the end of this Chapter:-

1. Alice Holt - Surrey
2. Coppergate - Yorkshire
3. Eshott - Northumberland
4. Harlech - N. Wales
5. Holyhead - N. Wales
6. Piercebridge - Durham
7. Prudhoe Castle - Northumberland
8. Loftus, N. Yorkshire
9. Bryn y Castell - N. Wales

2.1 Alice Holt Forest - Surrey (Roman)

This site is about 7 km. south-west of Farnham, Surrey (Lat. 51.2N, Long. 1.4W). A total of 9 samples were collected by Dr. A.J. Clark (Ancient Monuments Laboratory) from the site. These samples were taken from the floor of the lowest kiln which was composed of fired grey layers, one above the other, distinctly separated by thick layers of partly-fired red clay. While cutting the samples into measurable sizes, some of the discs fell apart, and only five samples were measurable.

The intensity of NRM of these samples ranged between 289-985 mAm^{-1} and their directions were consistent with each other (Table 2.1). The intensity decrease and the direction changes were smooth, with increasing AC demagnetization steps (fig. 2.1) and the directions showed high stability

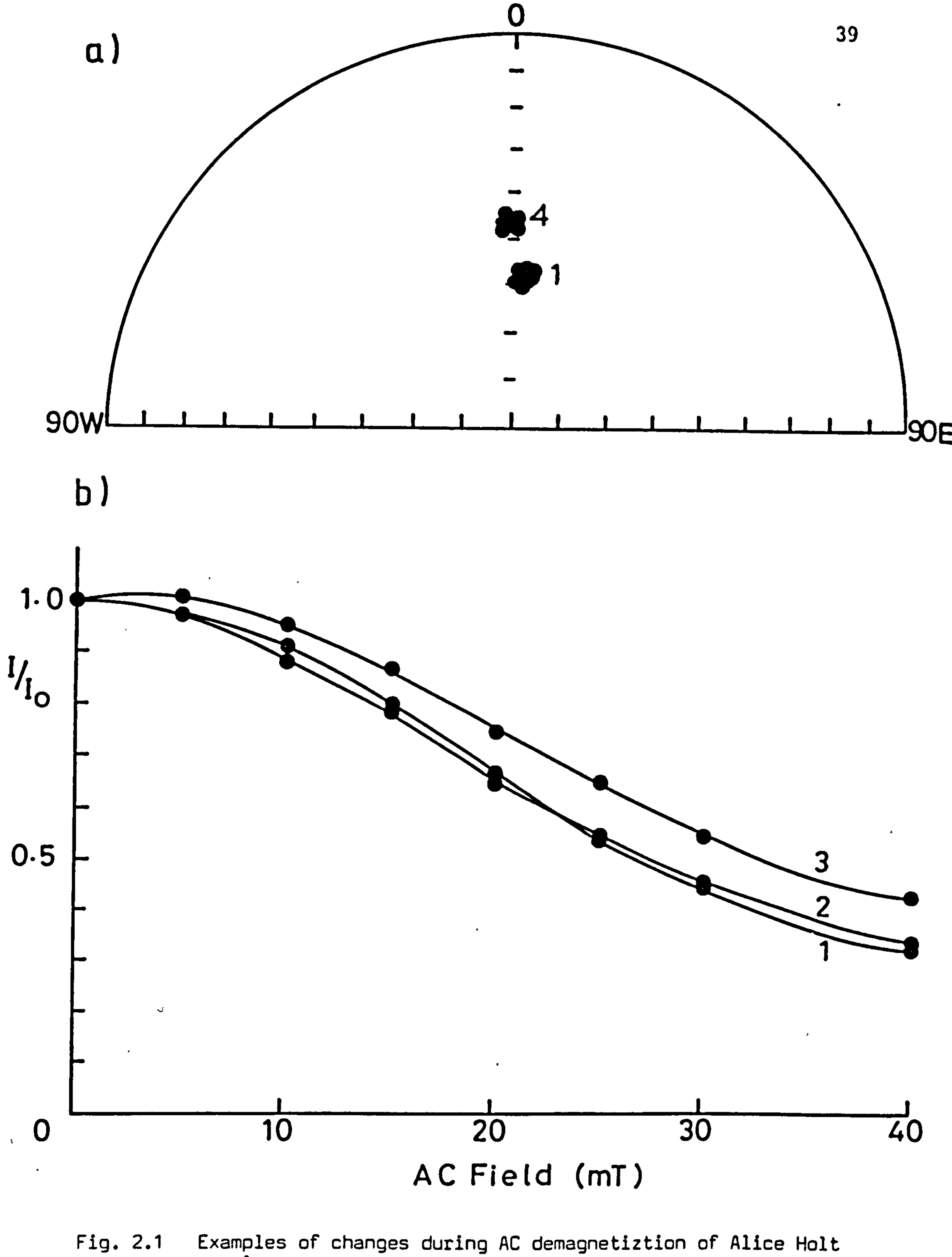

Fig. 2.1 Examples of changes during AC demagnetiztion of Alice Holt samples

a) Directions
b) Intensity

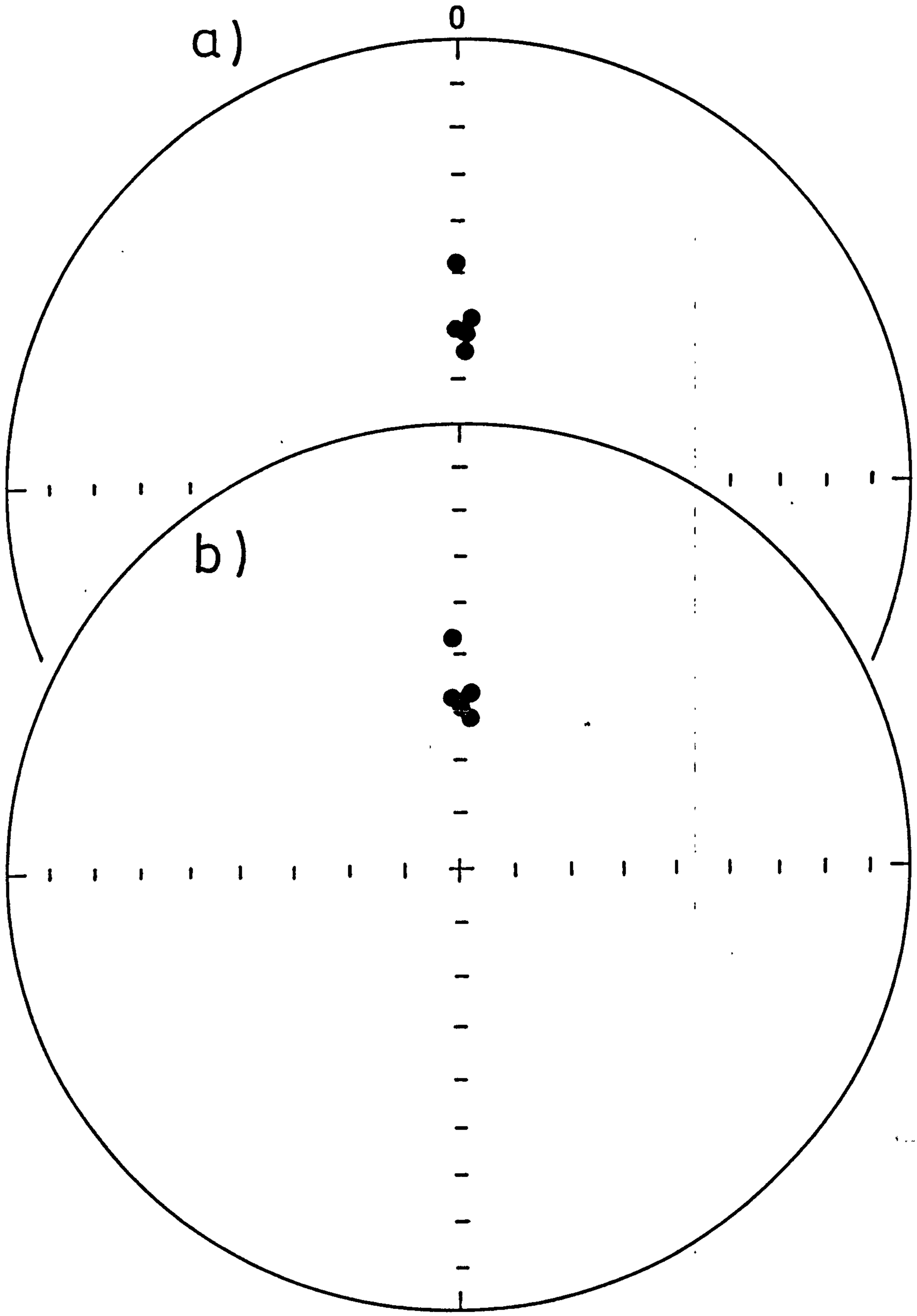

Fig. 2.2. Magnetic directions of Alice Holt samples
a) NRM
b) Stable

indicated by the high stability indices. The components remaining during AC-demagnetization were well-grouped, having a northerly direction, and the components removed showed a similar grouping in the same direction (fig. 2.2). The mean value of the most stable directions was calculated and plotted on the archaeomagnetic curve. The age of these samples was found to be around 220 AD ±15 years, which is consistent with its estimated archaeological age (200 - 250 AD).

	Initial			Most stable		
Sample No.	Dec.	Inc.	Int, mAm^{-1}	Dec.	Inc.	S.I.
1	1.0	60.6	985.58	359.9	59.9	15.74
2	3.8	64.9	522.43	4.8	62.5	33.63
3	0.3	48.0	189.71	359.0	47.8	13.41
4	5.3	58.8	543.64	4.9	57.8	18.35
5	3.9	60.9	409.04	2.2	60.8	16.15

Mean Dec. = 1.1, Inc. = 58.8, α_{95}= 5.6, k = 182.4

Table 2.1 Initial, most stable, stability indices and the mean value of Alice Holt samples

2.2 Coppergate - York

2.2.1 Introduction

Between 860 AD and 870 AD, the Viking raids turned into negotiated settlements, with a Viking colony being established at York. It was ruled by a succession of Danish and Norwegian kings until 954 AD (Addyman, 1980).

Excavation at Coppergate, in the centre of York (Lat. 53.8N, Long. 1.05W), commenced in 1976 and exposed hearths and ovens, presumably belonging to shopkeepers. Four hearths were sampled at different times and at different levels. These hearths were all composed of soft, fired clay

their colour ranging between red and black, for the well-fired areas, to light red for the less fired areas. Since most of the hearth materials were soft, caution was taken during sampling in order to get the well-fired materials and also hard in situ pieces within the hearth. The sizes of these hearths ranged between 60 - 90 cm. and their estimated archaeological ages were:-

	Hearth	Archaeological age
1.	25134	910 - 925 AD
2.	22441+ bricks	900 - 920 AD
3.	30757	850 AD
4.	22720	900 AD

2.2.2 Hearth 25134

This hearth had a rounded shape and was composed of fired soft red clay. A total of nine samples were collected. The intensity of NRM ranged betwen 1 - 85 mAm^{-1} while the directions were consistent having a mean value of Dec. = 21.7, Inc. = 70.8, α_{95}= 6.1 (table 2.2).

AC demagnetization studies showed that the decreases in intensity were smooth and there were only small directional changes, indicating high stability (fig. 2.3). The remanences remaining in all samples were well-grouped, having a north-northeasterly direction and the removed components showed the same grouping indicating that only one component of remanence was present (fig. 2.4). The mean value of the most stable directions was calculated (Table 2.2) and plotted on the archaeomagnetic curve. The age of the hearth was found to be around 900 A.D. ±20 years, which is near to the estimated archeological age based on a coin (dated between 910 - 925 AD) found in the lower layer of the hearth.

a)

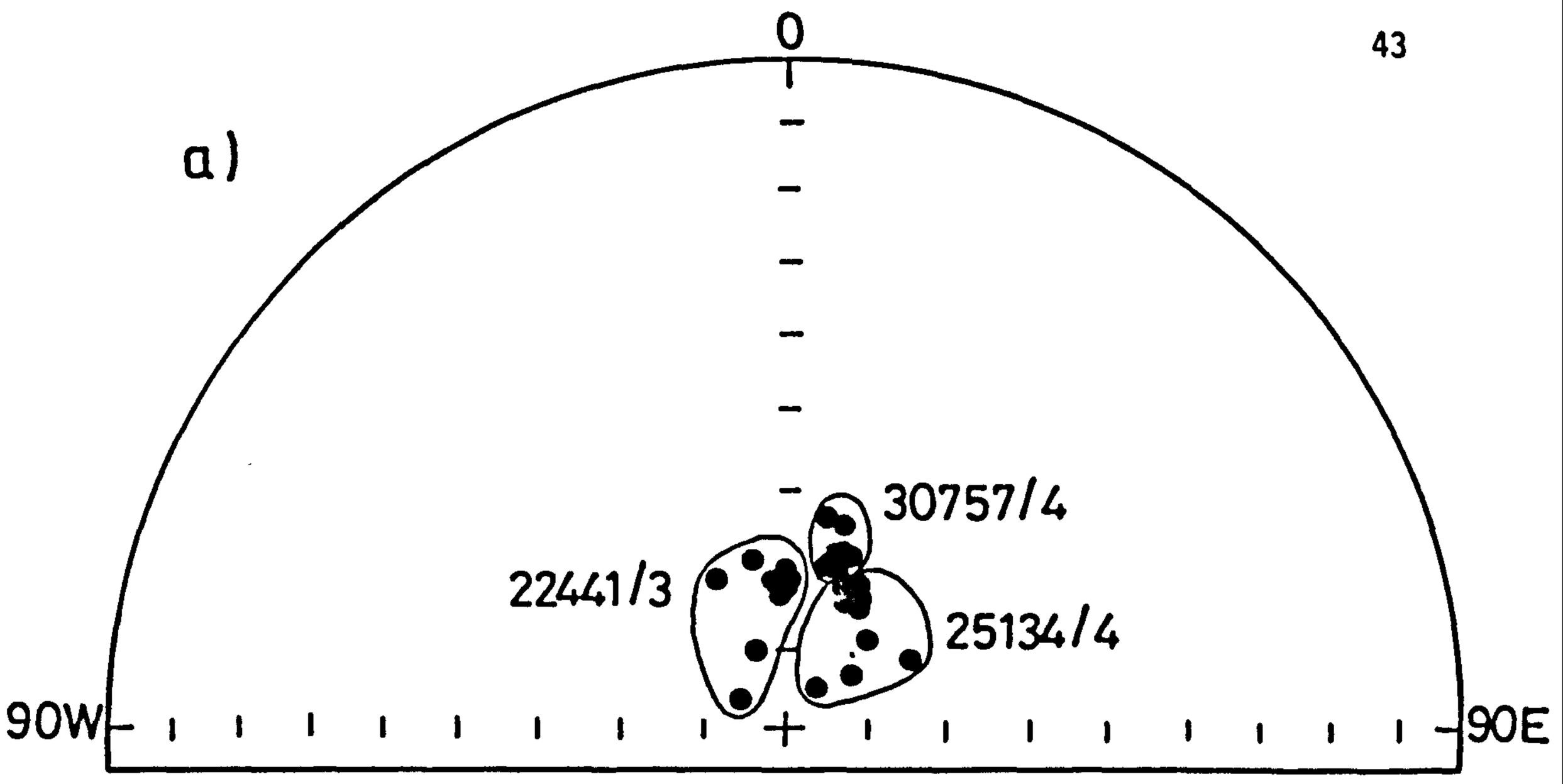

b)

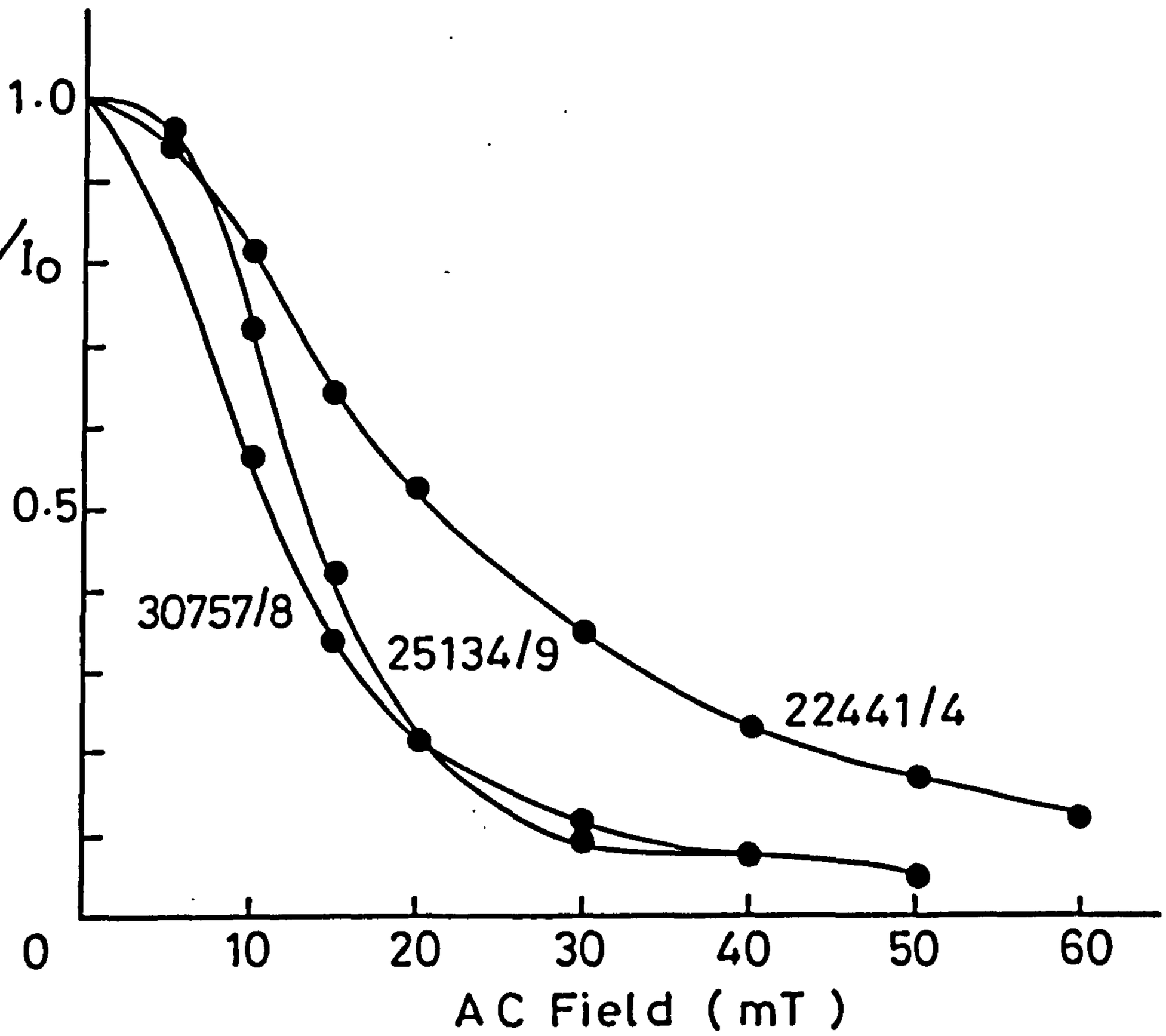

Fig. 2.3 Examples of changes during AC demagnetiation of Coppergate site samples

a) Directions
b) Intensity

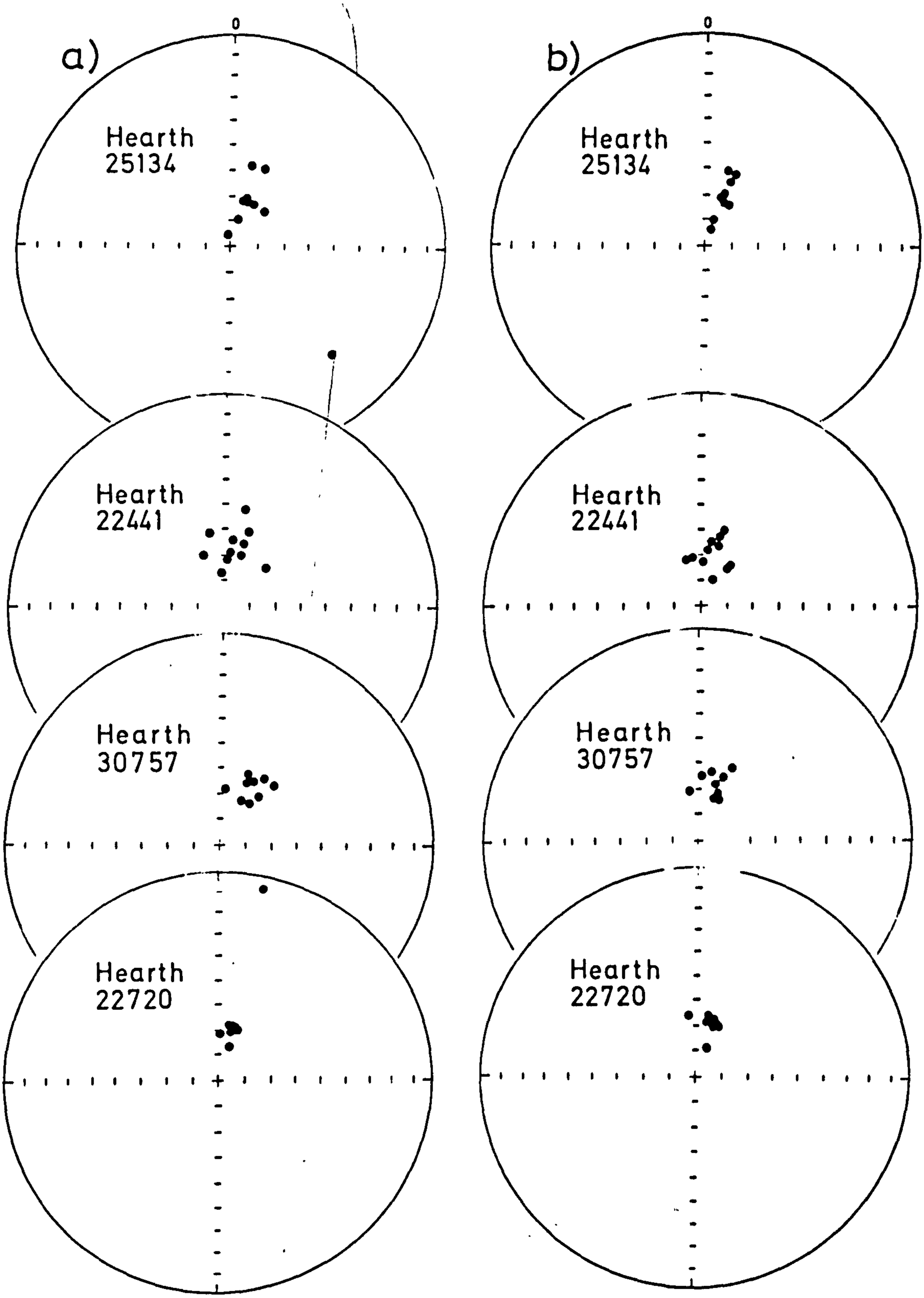

Fig. 2.4 Magnetic directions of Coppergate site samples
a) NRM b) Most stable

Sample No.	Initial Dec.	Inc.	Int. mAm^{-1}	Most stable directions Dec.	Inc.	S.I.
1	351.4	85.1	1.68	16.1	82.8	2.96
2	42.3	71.4	34.89	20.8	63.6	7.27
3	17.1	71.8	66.21	20.0	68.3	2.93
4	27.8	71.7	56.75	29.0	71.5	20.50
5	14.3	57.4	8.03	16.8	59.8	7.81
6	22.5	56.9	8.46	23.1	60.1	4.05
7	27.0	71.6	65.66	24.0	71.9	5.96
8	16.1	79.2	9.50	17.2	79.3	10.44
9	17.2	70.5	37.72	17.2	70.5	6.87

Mean Dec = 19.9 Inc. = 68.2 α_{95} = 5.1 k = 101.9

Table 2.2 Initial, most stable, stability indices and the mean values of Hearth 25134

2.2.3 Hearth 22441 and nearby bricks

This hearth was at the same level as hearth 22720 and was surrounded by some firedbricks which were Roman and had been put around the hearth during Viking times. Eight samples were collected from the hearth, and three samples from the bricks.

The intensity of NRM of the hearth samples ranged betwen 0.6 - 125 mAm^{-1}, except sample 3 which had a very high intensity (0.7 Am^{-1}). The initial directions were mutually consistent (table 2.3) having a mean value of Dec. = 11.6, Inc. = 67.6, α_{95} = 7.3. Pilot samples showed high magnetic stability with smooth changes in intensity and small directional changes (fig. 2.3). The remaining components were well-grouped in a north-northeasterly direction (fig. 2.4). The mean value of the most stable directions was calculated and plotted on the archaeo-magnetic curve. The age of the hearth was found to be 840 AD ±25 years.

This date is somewhat earlier than the expected archaeological stratigraphical age which was thought to be around 900 AD ±20 years.

	Initial			Most stable directions		
Sample No	Dec.	Inc.	Int. mAm^{-1}	Dec.	Inc.	S.I.
Hearths						
1	357.2	78.6	1.61	23.2	77.9	2.58
2	7.4	68.5	2.97	6.8	67.0	5.56
3	3.7	71.8	693.89	3.2	72.1	15.79
4	339.4	68.7	6.77	345.1	70.3	15.16
5	47.5	68.1	0.65	34.3	70.4	1.98
6	18.2	68.8	1.53	33.4	71.8	3.64
7	18.1	59.6	11.35	14.7	61.3	12.09
8	12.0	50.9	18.72	17.2	58.0	4.58
Mean Dec. = 13.8, Inc. = 68.1, α_{95}=5.9 , k= 91						
Bricks						
1	348.2	60.8	164.30	351.2	70.2	14.02
2	7.6	63.9	195.80	9.1	63.9	34.28
3	17.2	64.3	125.40	16.2	64.7	25.42
Mean Dec. = 6.1, Inc. = 65.3, α_{95} = 9.1, k = 177.5						

Table 2.3 Initial, most stable, stability indices and the mean value of hearth 22441, and bricks

The intensity of NRM of the three brick samples ranged between 125 - 195 mAm^{-1} while the directions were moderately consistent with each other. They were very stable during demagnetization, and the remaining and removed components for each of the three samples were well-grouped indicating that only one component of remanence is present, i.e. the bricks have either not been refired, or were refired to above their Curie temperatures. The mean value of the most stable directions of the bricks was calculated and

plotted on the archaeomagnetic curve. This value was about 8^{o} west of the 800-900 AD curve and about 3^{o} shallower. On the other hand, it is about 5^{o} east of the Late Roman curve with relatively similar inclination. Accordingly the age of these bricks is thought to be between 300 - 400 AD, and are thought not to have been heated later. Since the archaeological evidence suggests that the bricks were put in a straight line around the hearth during the Viking age, it would seem unlikely that they were put around the hearth in the same directions as when they were fired. However, it seems more likely that these bricks were completely refired in the Viking period and then tilted from their original position. In this case, the direction of remanence cannot be used to date them.

2.2.4 Hearth 30757

This hearth had a slightly elongated shape. Within the hearth, there were some brick fragments, but the firing was not very clear in most of the hearth. A total of nine samples were collected from the well-fired areas within the hearth. The intensity of NRM ranged between 45 - 632 mAm^{-1} and the initial directions were consistent having a mean value of Dec. = 29.7, Inc. = 65.0, α_{95} = 4.1 (table 2.4).

During AC demagnetization the intensity decrease was smooth and the changes in directions were small indicating a high stability (fig. 2.3). The components remaining after AC demagnetization were well grouped having a north-northeasterly steep direction (fig. 2.4). The mean value of the most stable directions was calculated and plotted on the archaeomagnetic curve. The age of the hearth was found to be around 850 AD ±20 years, which is similar to the archaeological age (850 AD) and consistentwith the Thermo-luminescence date (830 ±30 years).

Sample No.	Initial Dec.	Inc.	Int. mAm^{-1}	Most stable Dec.	Inc.	S.I.
1	39.9	66.5	111.1	21.4	73.7	13.22
2	26.4	71.1	135.7	23.1	71.0	6.20
3	34.3	59.7	297.7	25.6	60.1	6.96
4	24.7	63.8	345.3	18.1	67.9	18.44
5	22.4	60.8	632.3	3.7	66.2	18.18
6	28.9	62.7	368.7	11.8	64.2	41.02
7	36.1	70.4	252.0	25.3	73.0	5.81
8	7.2	68.6	45.3	351.2	71.7	8.38
9	43.2	58.9	95.9	22.0	64.7	4.44

Mean: Dec, = 15.3, Inc. = 67.2, α_{95}= 3.9, k = 170.9

Table 2.4 Initial, most stable, directions, stability indices and the mean value of hearth 30757

2.2.5 Hearth 22720

This hearth is composed of fired clay with a colour ranging between red and black. Eight samples were collected and had NRM intensities ranging betwen 8 - 154 mAm^{-1} and consistent directions with an initial mean value of Dec. = 15.8, Inc. = 68.7, α_{95} = 2.8 (table 2.5).

AC-demagnetization of pilot samples showed smooth decreases in intensity and small changes in directions indicating a high stability (fig. 2.3). The components remaining after demagnetization were well grouped, having a north-northeasterly direction (fig. 2.4). Two mean values were calculated (table 2.5); the overall mean, corrected to Meriden, gave an age around 840 AD ±15 years. The second mean

Sample No.	Initial Dec.	Inc.	Int, mAm^{-1}	Most stable directions Dec.	Inc.	S.I.
1	13.2	6.5	20.20	12.1	65.6	15.79
2	19.2	75.5	133.70	20.4	77.8	7.92
3	13.2	67.5	154.30	11.6	67.3	13.02
4	19.4	67.3	22.98	17.2	66.2	8.30
5	23.5	67.4	14.81	25.1	68.3	8.25
6	16.8	66.8	27,25	20.0	67.4	5.10
7	16.6	68.7	29.98	17.8	69.0	9.01
8	4.3	71.3	8.93	354.1	66.0	1.14

Overall Mean: Dec -= 13.5, Inc. = 67.3, α_{95} = 3.6, k = 23.3
Mean (excl. 2,8) " = 16.3 " = 66.1 " = 1.9, " = 1221

Table 2.5 Initial, most stable directions, stability indices and the mean value of Hearth 22720

excluded sample 2, which had a steep inclination, and sample 8, which was poorly stable, and gave a date around 860 AD ±10 years and this is considered to be the more reliable date. However, it is earlier than the expected archaeological age of around 900 AD although not inconsistent with it.

2.2.6 Conclusions

These four hearths (Table 2.6) were mostly found to be very stable. Their directions of most stable remanence matched the existing archaeomagnetic curve between 840 - 900 AD with a maximum displacement in inclination of about 1.5^{o}. This displacement is within the accuracy of the method but it could also indicate that the actual inclination values between 800 - 900 AD were slightly shallower than on the established curve. The expected archaeological ages for these hearths are close to each other

(within ±20 years), with hearth 25134 being the oldest and 30757 the youngest. The archaeomagnetic dates also showed hearth 25134 to be the oldest and 22441 and 30757 the youngest. However, these dates are all within ±20 years and this is within the accuracy of the method.

Hearth Code	Dec.	Inc.	N	α_{95}	Archaeomagnetic age
25134	19.9	68.2	9	5.1	900 ±20
22441	13.8	68.1	8	5.8	840 ±25
bricks	6.1	65.3	3	9.1	300 - 400
30757	15.3	67.2	9	3.9	850 ±20
22720	16.4	66.1	6	1.9	860 ±10

Table 2.6 Summary of Blackgate Site

2.3 Eshott - Alnwick (Medieval)

During construction of a gas pipeline through Northumberland, a dense concentration of 12th - 14th century pottery and fragments of fired clay were recovered from a field and a low east-west ridge on the south side of the Longdyke Burn (Lat. 55.1N, Long. 1.6W) about 18km. south of Alnwick, and 600 metres from a 14th Century moated manor of Eshott. It was suspected that a pottery kiln and village settlement had been discovered. The study of pottery collections from the site suggested an age around 1200 AD (Dickson, 1981).

The kiln was elliptical in shape, 0.85 x 1.2 m, and about 10 cm. deep. The surface of the hearth had been reddened by heat, and

filled with grey sand which had been cleaned out after firing. Since most parts of the kiln-hearth seemed to have been disturbed, a total of 18 samples were collected in order to have a better chance of detecting the disturbed samples.

The intensity of the natural remanent magnetization ranged betwen 3 - 299 mAm^{-1} and the initial directions were somewhat scattered. All samples were found to be very stable during AC demagnetization, as indicated by their high values of stability indices (table 2.7, fig. 2.5). The components remaining after AC-demagnetization were all well-grouped in the same direction of the remaining components indicating the existence of only one component of remanence. The components remaining after demagnetization in pilot samples 5 and 7 were grouped in a north-north-westerly direction, while samples 8, 9, 13 and 15 had the components remaining grouped in a north-northeasterly direction.

Although nearly all the samples were very stable, some of them had directions away from the main grouping (fig. 2.6), probably due to the suspected disturbance of the hearth material. On this basis, only the directions of eleven better-grouped samples were chosen for calculating the mean direction. Five of the rejected samples (1, 2, 3, 4 and 6) were collected from the same area within the hearth and were all near each other. This could indicate disturbances of that part of the hearth. Samples 14 and 16, which were also rejected, were from an area surrounding the hearth which were well fired but also appeared to have been disturbed prior to collection. It is therefore thought that the closely grouped samples retained the genuine field direction which was found to be around 1200 AD ±15 years which is exactly the same as indicated by the pottery styles.

No.	Initial Dec.	Inc.	Int mAm^{-1}	Most stable Dec.	Inc.	S.I.
Samples Used						
ET/5	354.6	69.2	125.07	355.3	66.2	5.51
ET/7	348.2	69.2	62.22	351.0	66.2	8.78
ET/8	34.6	64.1	36.44	27.3	65.4	7.05
ET/9	19.4	64.5	43.86	20.2	64.3	21.37
E T/10	15.7	64.5	3.79	15.9	57.1	1.53
ET/11	18.7	65.8	299.52	29.8	62.3	6.65
ET/12	3.8	65.5	181.70	2.7	66.1	16.01
ET/13	18.7	63.5	15.39	23.2	63.7	5.01
ET/15	30.0	61.5	207.74	27.3	62.0	8.80
ET/17	8.8	59.7	178.71	7.7	60.8	10.17
ET/18	23.6	60.5	127.42	14.1	59.7	9.27
Mean Dec = 13.0, Inc. = 61.0, α_{95} = 3.6, k = 154.3						
Samples Excluded						
ET/1	344.9	74.1	268.05	345.5	75.6	7.75
ET/2	326.4	73.8	111.89	325.3	74.0	20.51
ET/3	347.8	71.9	212.71	347.4	71.0	14.72
ET/4	277.9	80.3	18.17	265.3	87.7	3.93
ET/6	41.2	69.3	51.37	38.6	69.1	12.16
ET/14	53.9	74.9	3.43	69.1	75.0	3.75
ET/16	300.5	56.1	82.12	303.4	56.6	11.19
Overall Mean Dec = 7.5, Inc. = 67.1, α_{95} = 5.7, k = 37.4						

Table 2.7 Initial, most stable direction, stability indices and the mean values of Eshott site samples

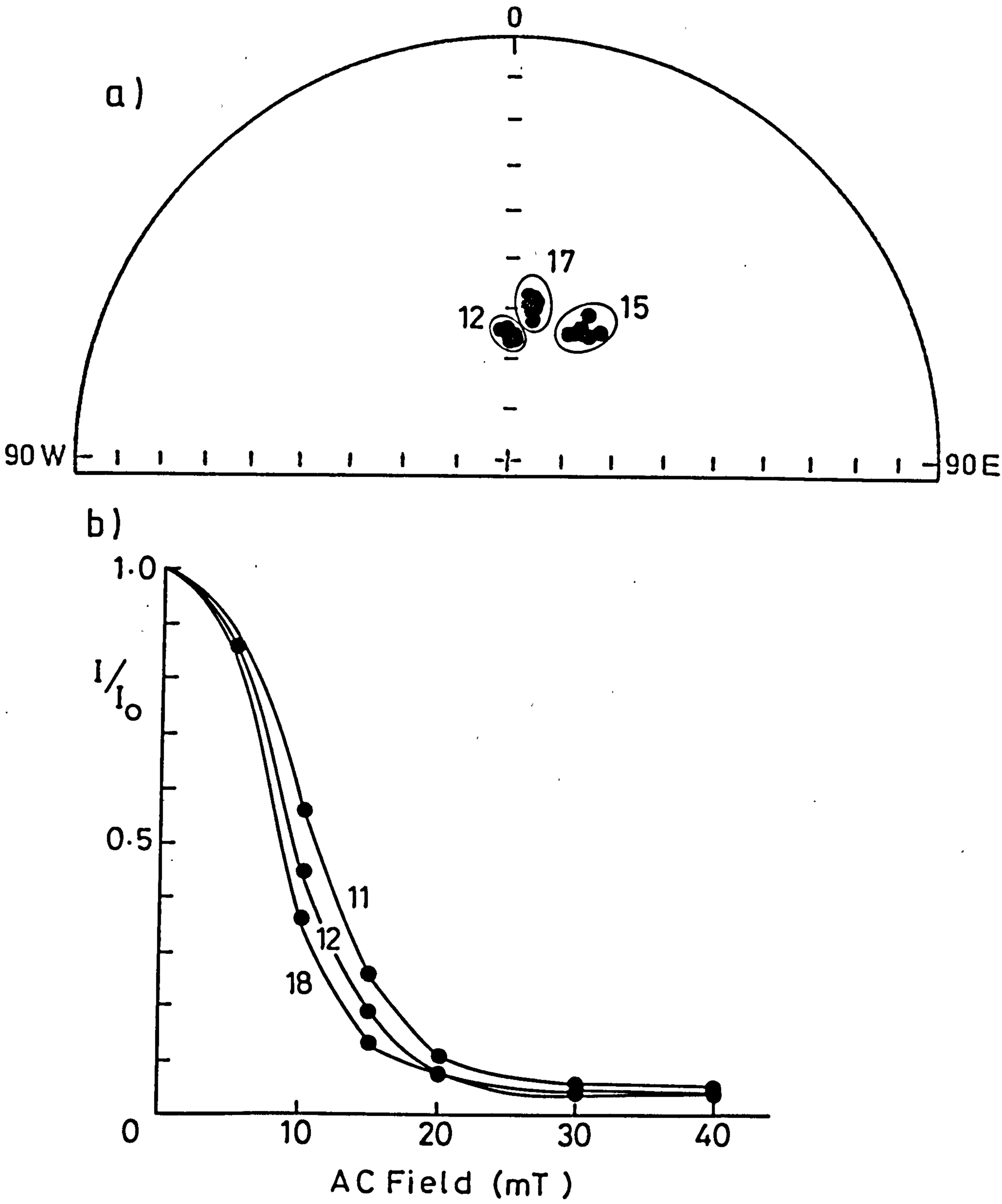

Fig. 2.5 Examples of changes during AC demagnetization of Eshott site samples

a) Directions
b) Intensity

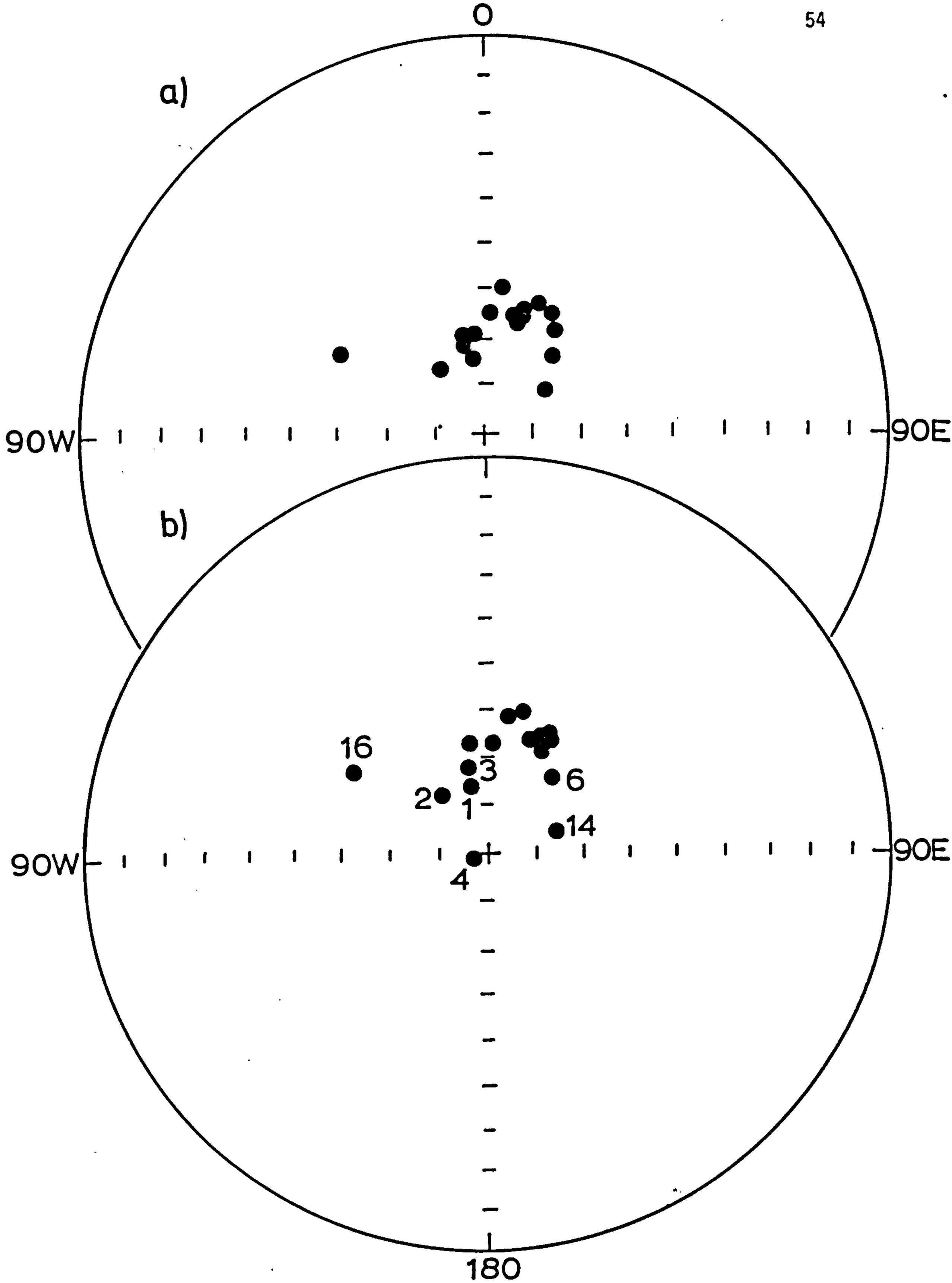

Fig. 2.6 Magnetic direction of Eshott site samples
a) NRM
b) Most stable

2.4 Harlech, N. Wales (Pre-Roman, Iron Age Settlement)

The site is situated on the summit of a small ridge about 330m above sea level, some 4km. east of Harlech (Lat. 52.8, Long 4.1 W). The knoll itself and the surrounding slopes to the south of the Moel Goldog are regularly ploughed. Two hearths were sampled, the first (S004) is located almost in the centre of two concentric stone circles and the hearth stone is composed of large pieces of dolerite (40 x 30 cm.) with red, burnt upper surfaces. The stone was already broken into separate blocks, possibly by ploughing but these blocks still appear to be in situ. The second hearth (S036) is on the bottom of a shallow pit or scoop, dug into the hut floor. It is composed of local shale (30 x 30 cm.). This hearth is thought to have a date similar to S004 or slightly earlier by not more than 100 years.

Hearth S004

Five hand samples were collected from this hearth. Cores, 2.5 cm. diameter, were drilled from the burnt tops of the cores to make cylindrical samples of 2.1 cm. height. Two cores were drilled in the first hand sample, three in the third, two in the fourth and four in the fifth (sample 2 was broken). A total of eleven samples were measured and demagnetized. The intensity of the natural remanent magnetization ranged between 0.3 - 7.1 mAm^{-1}. The NRM directions were consistent with steep inlincation (table 2.8). The behaviour during AC-demagnetization ranged between stable to very stable. The components remaining were well-grouped in a north-northwesterly direction and the removed components showed a similar grouping. The most stable directions of magnetization were all well-grouped having a steep, essentially northerly direction.

The mean values of the most stable directions of these samples, Meriden, was Dec. = 355.5, Inc. = 79.5, α_{95} = 2.7 and lies around the 1700 AD value but with a slightly steeper inclination of about 4^{o}. Since most of the samples were stable it could be that the hearth was either last heated at about 1700 AD, or that the age of this hearth is pre-100 BC, and thus its magnetic direction lies on an earlier, unknown part of the archaeomagnetic curve which happens to be close to the 1700 AD position. Alternatively, if the hearth was in fact last heated in Roman times and was subsequently tilted to the south by at least 10^{o}, then this would rotate Roman magnetic vectors to the observed direction. It is more likely that the age of this hearth corresponds to an unknown older part of the curve. This is based on the lack of any burning evidence of significant intensity that could affect the hearthstone as it was buried by 10 cm. of peat.

2.4.2 Hearth SO36

Three hand samples were taken from this hearth. Six cores were drilled and two samples were obtained from each core except core 2 from which only one sample was obtained. The initial NRM directions were consistent with each other and the intensity ranged between 7 - 541 mAm^{-1} (table 2.8). These samples were all very stable during demagnetization except sample (80.1.2) which was metastable (fig. 2.7). The components remaining after demagnetization were all grouped in a north-northwesterly direction and the removed components showed a similar grouping indicating the presence of only one component (fig. 2.8).

The mean value of the most stable directions (Dec. = 345.5, Inc. = 73.2, α_{95}= 2.5) was plotted on the archaeomagnetic curve and compared with the mean value of hearth SO04. These two values had close but statistically different directions with hearth SO36 being magnetized 10^{o}W of

a)

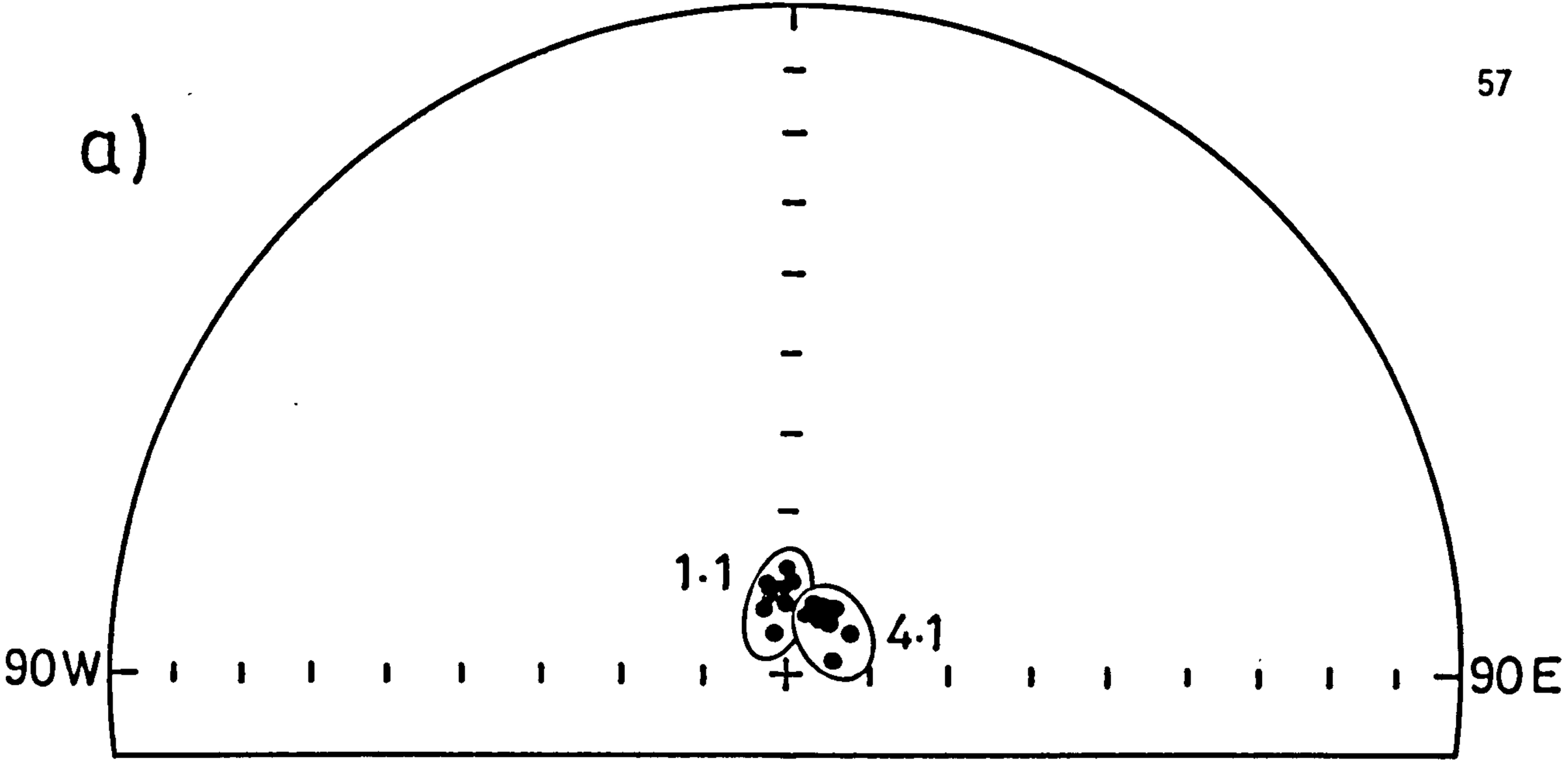

b)

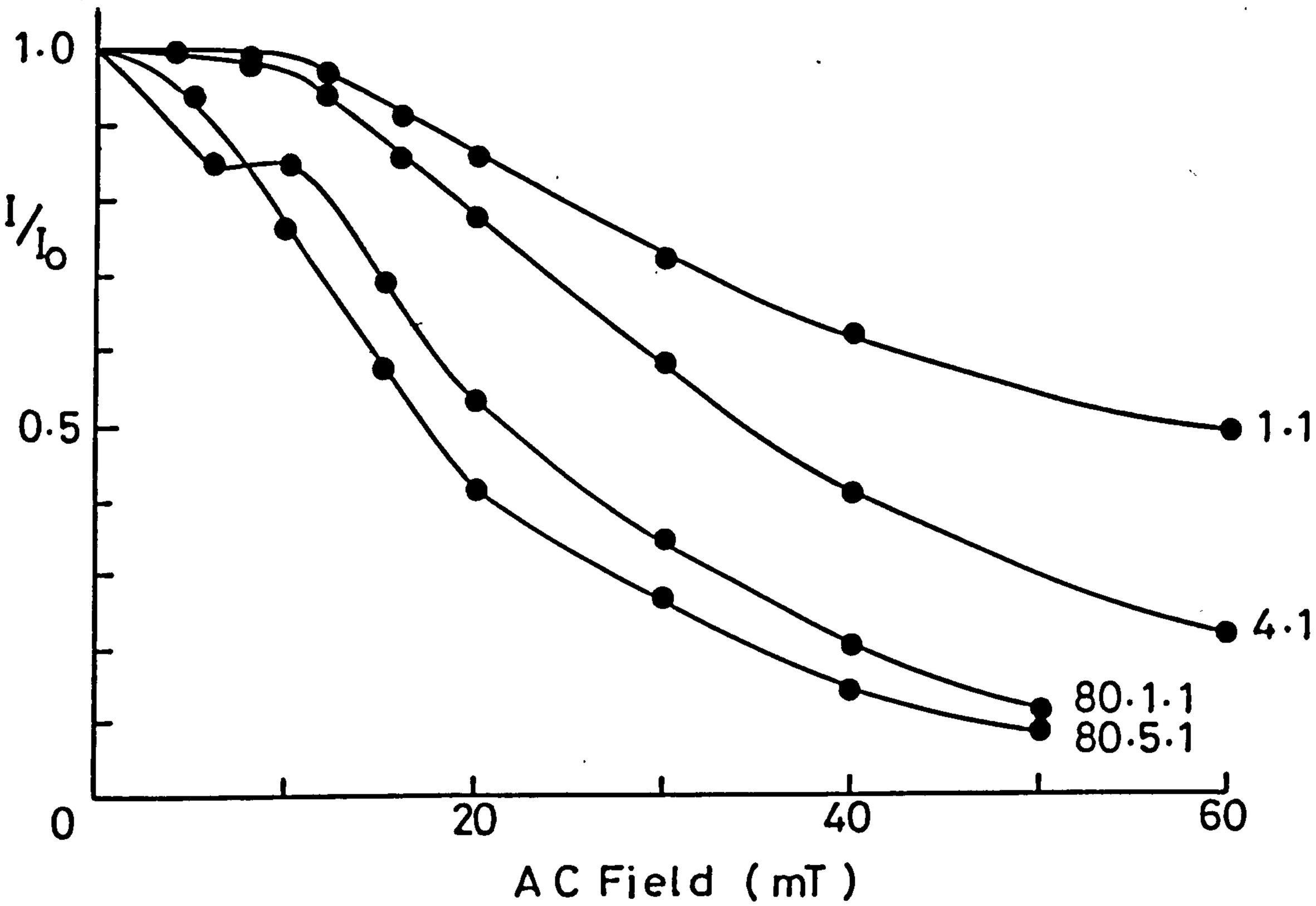

Fig. 2.7 Examples of changes during AC demagnetization of Harlech samples

a) Directions

b) Intensity

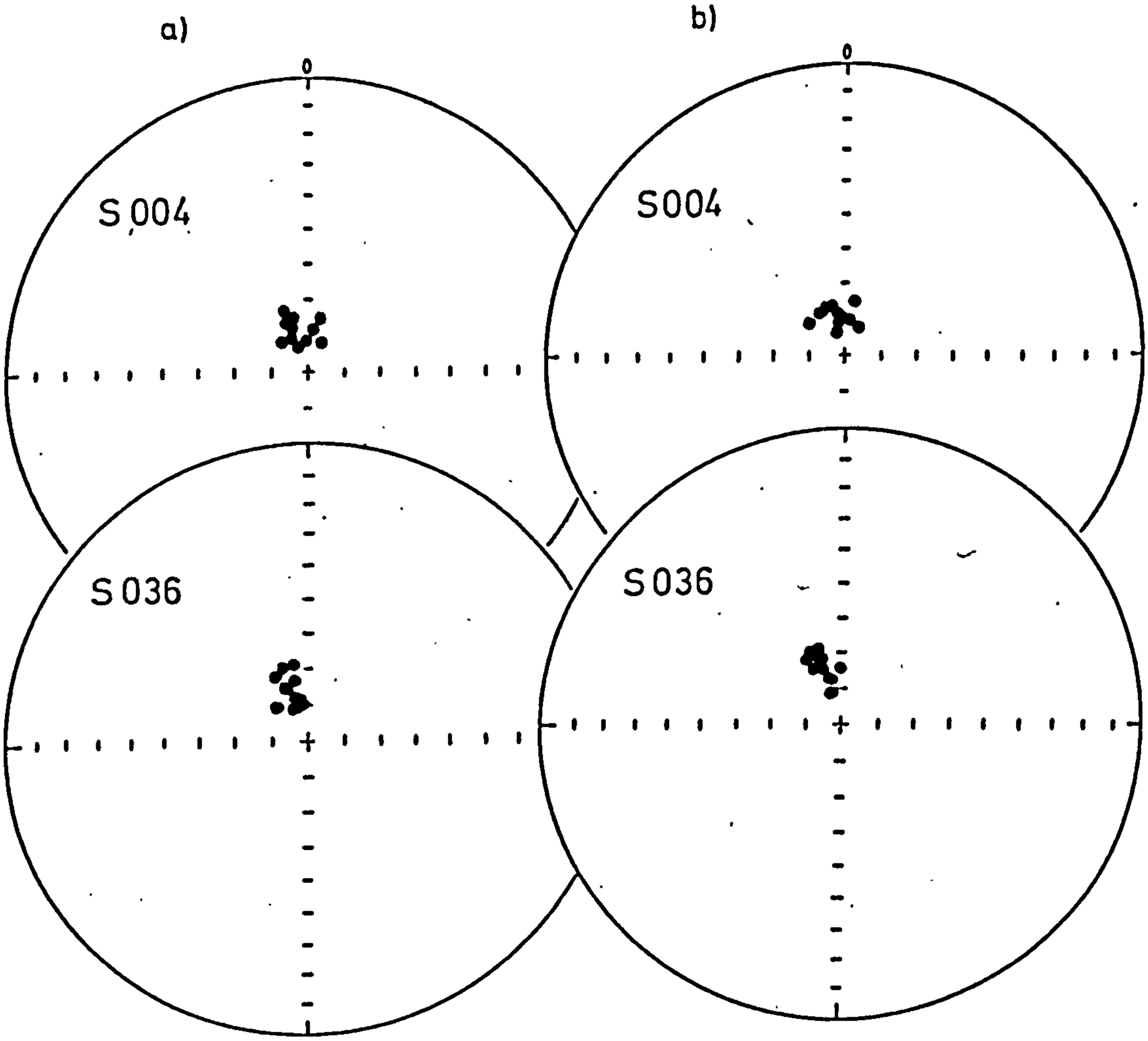

Fig. 2.8 Magnetic direction of Harlech samples
a) NRM
b) Most stable

Sample No.	Initial Dec.	Inc.	Int mAm^{-1}	Most stable Dec.	Inc.	S.I.
Hearth (S004)						
HL/1.1	347.7	79.3	1.2	354.8	79.7	6.1
HL/1.2	10.3	74.4	2.8	13.4	74.9	12.0
HL/3.1	347.0	75.8	7.1	347.2	76.3	5.6
HL/3.2	346.7	79.1	2.4	350.8	79.3	5.4
HL/3.3	341.1	76.0	4.6	341.5	76.6	6.8
HL/4.1	21.9	82.	3.3	26.9	81.7	10.3
HL/4.2	11.3	82.0	1.2	15.6	81.3	7.4
HL/5.1	320.7	73.9	0.3	311.7	77.8	4.6
HL/5.2	342.6	81.5	0.6	345.2	83.4	3.0
HL/5.3	328.5	76.8	1.7	332.3	75.6	4.5
HL/5.4	352.7	81.3	1.2	353.2	81.4	3.6
Mean Dec. = 355.5, Inc. = 79.5, α_{95} = 2.7, k = 278.0						
Hearth (S036)						
80.1.1	339.7	74.8	314.9	337.3	73.2	29.0
80.1.2	347.2	77.9	233.4	352.4	77.0	2.9
80.2	342.9	69.1	457.8	340.9	68.2	17.6
80.3.1	321.2	77.8	334.5	341.4	68.0	11.9
80.3.2	346.6	81.0	20.7	351.0	80.1	8.7
80.4.1	349.9	68.9	124.4	346.6	70.5	6.3
80.4.2	359.9	79.9	7.7	349.8	76.6	5.1
80.5.1	340.2	74.6	521.1	340.3	69.9	19.4
80.5.2	353.2	78.6	18.8	0.3	74.0	10.2
80.6.1	335.0	70.7	541.0	334.5	69.5	8.8
80.6.2	348.9	73.4	16.7	344.6	73.5	14.8
Mean Dec = 345.5, Inc. = 73.2, α_{95} = 2.5, k = 322.2						

Table 2.8 Initial most stable and S.I. of hearths S004 and S036 (Harlech)

S004 and its inclination was about 6^{o} shallower. Assuming that these differences in directions are not a result of tilting the hearthstone, which is most unlikely, the changes in directions can be attributed to time changes in the direction of the geomagnetic field between the last firing of each hearthstone. Such an age difference between the two mean values would be of the order of 100 years on the basis of the average rate of variation of the geomagnetic field during the last 400 years but as the earth's magnetic field behaviour is not adequately known for earlier periods, the actual time difference could be different.

2.5 HOLYHEAD - N. WALES (Late Roman)

The twenty huts at Holyhead Mountain, Wales (Lat. 53.3N, Long. 4.6W), are remains of a formerly much larger settlement. Since the early excavations by W.O. Stanley, the site has been regarded as a classic example of an unenclosed village. Stanley argued for a pre-Roman age for some of the buildings, but the only datable finds recovered during his excavation suggested occupation during the 2nd to the 4th centuries A.D., and this is now generally regarded as the age of this site (Smith, 1979).

A total of 17 samples were collected from three hearths. Five samples were collected from the first (context 113), nine samples from the second (context 149), and three samples from a third hearth (context 30).

2.5.1 Hearth 1 (context 113)

The intensity of NRM of samples from the first hearth ranged between 0.3 - 6.7 mAm^{-1}, and their directions showed only poor consistency (table 2.9). The behaviour during AC demagnetization ranged from unstable to very stable (fig. 2.9).

The components remaining after AC-demagnetization in

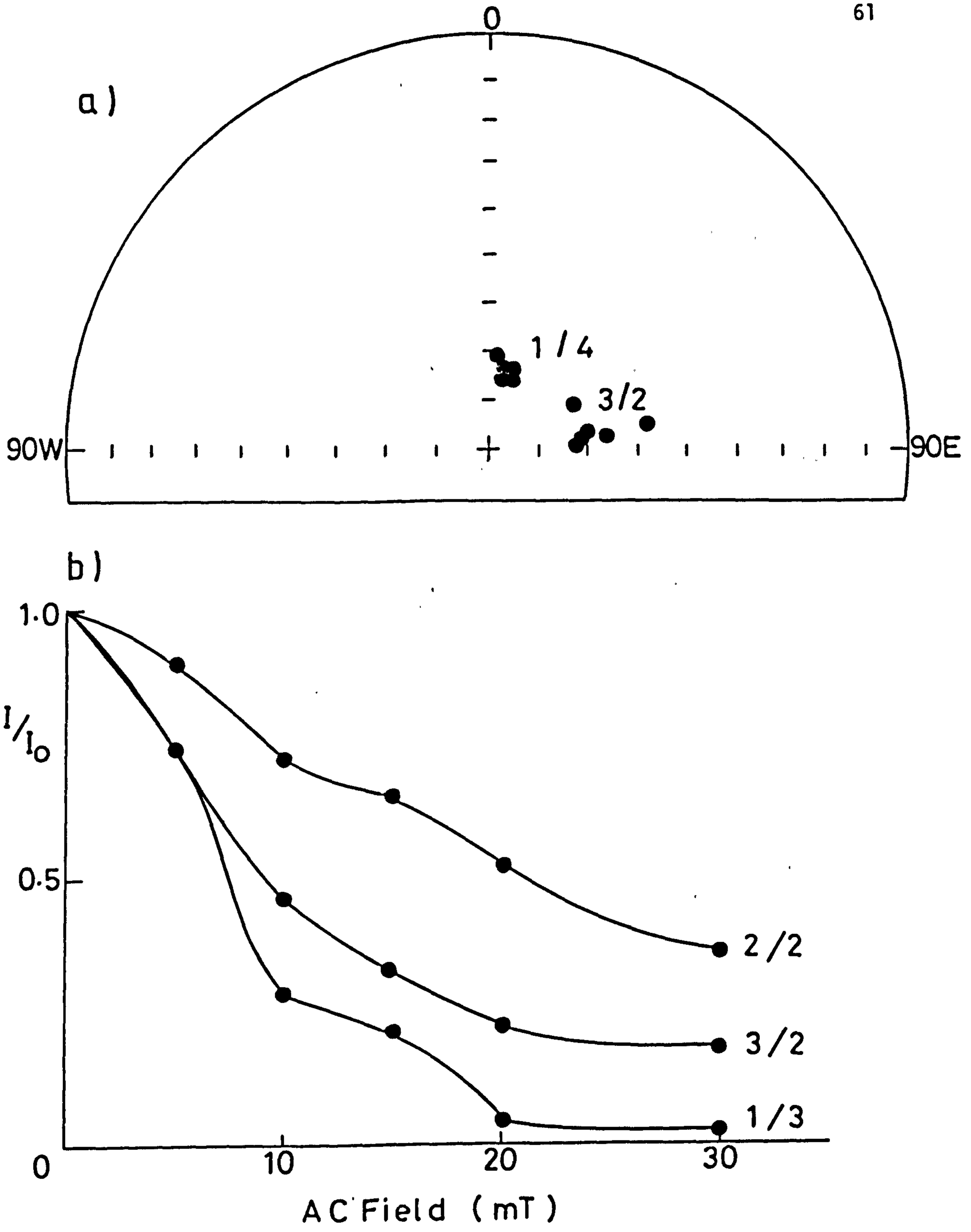

Fig. 2.9 Examples of changes during AC demagnetiation of Holyhead samples

a) Directions
b) Intensity

sample 2 were well grouped having a northerly direction, while the removed components had their low coercivity components grouped in the northerly direction and the higher coercivity components were scattered. Sample 3 had the remaining components grouped in the north-northwesterly direction and the removed components showed a similar grouping. Sample 4 had the remaining components grouped in the northerly direction while the removed components were scattered. (Samples 1 and 5 were demagnetized using only three steps of alternating field). The mean value of samples 1, 2 and 3 were calculated; the other two samples were rejected because of the aberrant declination of sample 4 and the low stability of sample 5. The mean value was plotted on the archaeomagnetic curve and the age of these samples was found to be around 100 AD. This date is archaeologically acceptable but is poorly defined because of the high α_{95} value.

2.5.2 Hearth 2 (context 149)

Nine samples were collected from this hearth. The intensity of NRM of these samples ranged between 4 - 54 mAm^{-1}, while their directions were very scattered including negative inclinations (table 2.9). The behaviour of these samples during AC demagnetization ranged from poorly stable to very stable as indicated by their stability indices (fig. 2.9).

The components remaining after AC demagnetization in sample 1 were very well grouped having a northwesterly direction but with very shallow inclination. The removed components showed a similar behaviour. The components remaining in sample 2 were well grouped having a south-westerly direction and the removed components showed some grouping in the same direction. Sample 3 had both the remaining and the removed components scattered in the southeasterly direction. Sample 4 had the remaining components grouped in the southwesterly direction with negative inclin-

ations while the removed components were scattered. Sample 5 had the remaining components well grouped having a nearly easterly direction and the removed components showed a similar grouping in the same direction. Sample 6 had the remaining components well grouped in the northerly direction in the upper hemisphere, while the removed components had some of the high coercivity components grouped in the same northerly direction, and the other lower coercivity components were scattered. Samples 7 and 8 both had the remaining and the removed components grouped in the north-easterly direction but with negative inclinations for sample 7. Sample 9 also had both the remaining and the removed components grouped in a northerly direction with steep inclinations.

The most stable directions of even the more steady magnetized samples were so scattered (fig. 2.10) that it was not considered possible to calculate the mean value for this hearth.

2.5.3 Hearth 3 (context 30)

Only three samples were measured from this hearth. The intensity of NRM of these samples ranged between 0.65 - 4.7 mAm^{-1} and the directions were very scattered (Table 2.9, Fig.2.10). AC demagnetization showed that sample 1 was very stable and samples 2 and 3 were poorly stable.

The components remaining after AC demagnetization in sample 1 were well grouped having a northeasterly direction, and the removed components were scattered in the same direction. The components remaining in sample 2 were well grouped near the origin, while the removed components were scattered. The components remaining in sample 3 were loosely grouped, having a north-northwesterly direction and the removed components were scattered.

Hearth 3 had two of its samples showing moderately

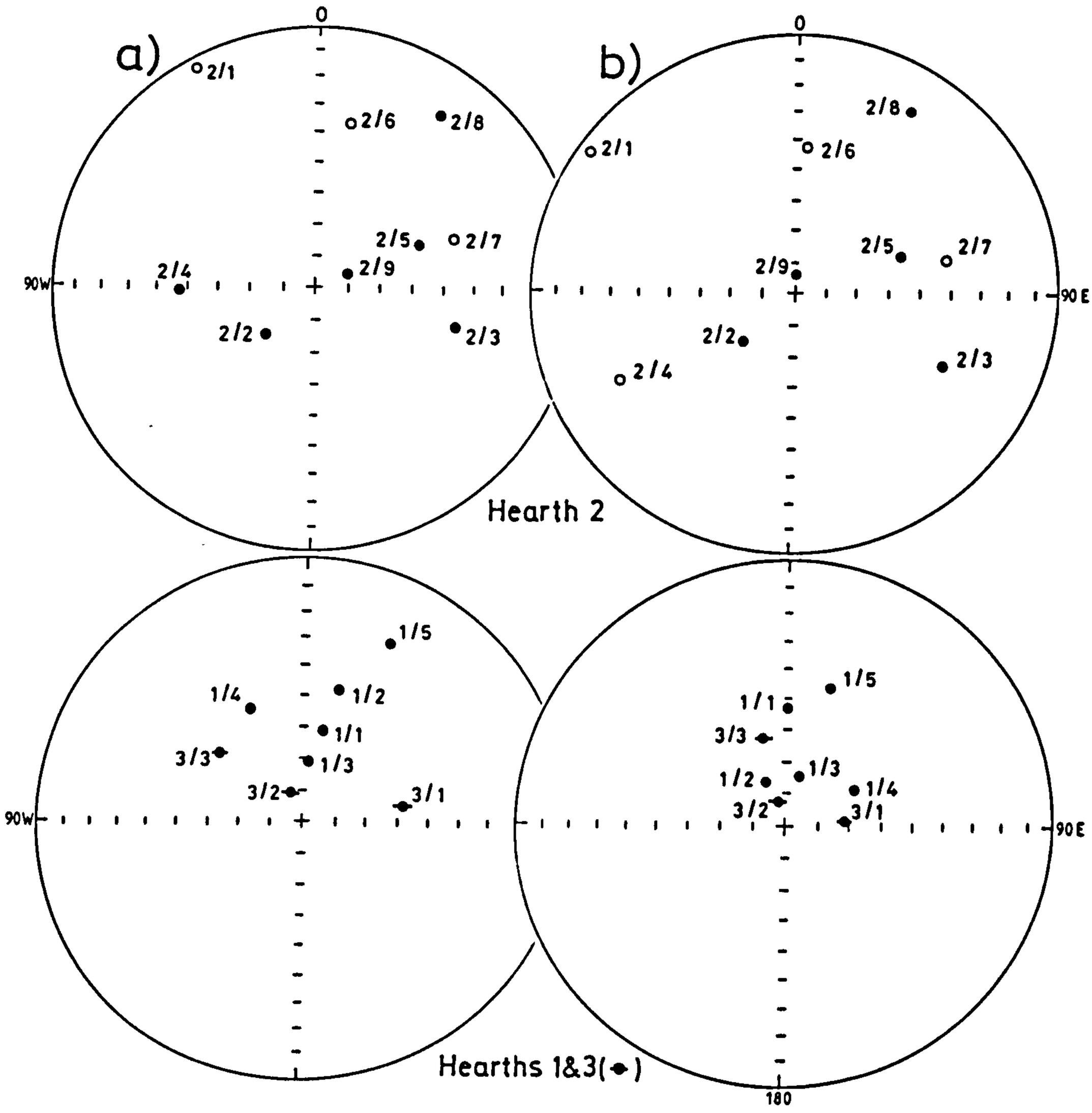

Fig. 2.10 Magnetic directions of Holyhead samples (hearths 1,2 and 3)
a) NRM b) Most stable

Sample	Initial			Most stable		
No.	Dec.	Inc.	Int mAm^{-1}	Dec.	Inc.	S.I.
Hearth 1						
1	12.2	61.8	0.35	I.2	52.4	2.21
2	15.5	47.4	1.87	344.8	74.8	1.68
3	6.0	71.4	5.67	15.5	73.6	16.74
4	334.2	51.4	6.77	61.8	65.5	1.93
5	25.9	26.2	3.75	17.7	44.0	0.54
Mean 1 (all samples)	Dec. = 13.8, Inc. = 62.9, α_{95} = 17.8, k = 193					
Mean 2 (reject 4,5)	Dec. = 1.1, Inc. = 66.7 α_{95} = 20.8, k = 35.0					
Hearth 2						
1	301.0	-4.7	4.03	304.8	-5.4	7.91
2	226.1	68.5	44.88	226.0	68.1	20.78
3	105.4	44.5	25.04	115.9	37.9	1.11
4	267.3	46.9	18.43	242.1	-26.1	1.74
5	67.4	55.5	54.05	70.6	54.9	10.36
6	10.7	-37.1	8.31	4.1	-42.8	6.22
7	71.3	-45.0	48.16	78.0	-41.2	4.85
8	35.2	20.5	8.43	31.9	19.1	4.95
9	70.4	80.0	38.23	5.8	84.3	5.98
Mean	Dec = 24.99, Inc. = 47.2 α_{95} = 90, k = 1.2					
Hearth 3						
1	81.5	58.0	4.73	84.2	71.2	9.72
2	340.2	80.8	0.65	343.7	81.8	2.03
3	309.4	56.2	1.26	345.4	61.1	1.06
Mean 2 and 3	Dec. = 345.2, Inc. = 70.5, α_{95} = 46.7, k = 30.7					

Table 2.9 Initial, Most Stable, S.I. and mean values of Holyhead samples

consistent directions (2 and 3) while the other ones showed scattered directions. Interpretation of the results was therefore based on the directions of 2 samples. The mean value of these two samples lay about 10^{o} west of the Roman period curve and about 1^{o} steeper. This could either indicate that the age of these samples is on an unknown earlier part of the curve, or it could indicate complete rotation and tilting of this part of the hearth by about 10^{o} to the west and probably with 10^{o} steeper if the age of the site is between 200 - 400 AD.

Conclusions

Samples collected from this location showed variable magnetic stability and with scattered directions within each site. In some samples the scatter may be due to measurement errors, in others it may be due to instability. However, even stable strong directions still show a large, more systematic scatter which cannot be due to refraction and is more likely to be due to disturbance in the hearth materials. Subsequent information indicated that there was some archaeological evidence that all hearths had been disturbed.

2.6 PIERCEBRIDGE - DURHAM (Roman)

Piercebridge is primarily a Roman-British site with some evidence of Medieval occupation. It is about 8 km. west of Darlington, at Lat. 54.4N, Long. 1.66W. It is probable that the Roman army came to Piercebridge in 70 AD. By about 125 AD, well-built stone structures were being erected in the vicinity of Dere street site, in the Tofts field, and a bakery and copper working industry had been established. But some time after 130 AD, and before 170 AD, the bridge ceased to exist, probably due to a massive flooding of the river Tees. The pottery from the field

indicates a slow build-up of occupation until about 140 AD, and it is to this age the sampled kiln is attributed.

A total of eight samples were collected from a rounded kiln which is about 1.5m. deep and 0.8m diameter. The samples collected were all of red fired clay. The intensity of NRM ranged between 1091 - 3413 mAm^{-1}, while the directions of NRM were consistent with each other, having a mean value of Dec. = 355.8, Inc. = 68.9 (table 2.10). The four pilot samples (1,2,6 and 7) were very stable during AC demagnetization (S.I. > 5) and the decrease in intensity and changes in direction were very smooth (Fig. 2.11). The components remaining after AC-demagnetization were well-grouped, having a northerly direction in all samples (fig.2.12).The removed component behaved similarly in the four pilot samples showing grouping in a northerly direction, i.e. indicating the presence of only one component of remanence. The remaining samples were demagnetized at fewer steps and they were also very stable. The mean value of the most stable directions (table 2.10) was calculated and plotted on the archaeomagnetic curve. The mean

	Initial			Most stable		
Sample No	Dec.	Inc.	Int, mAm^{-1}	Dec.	Inc.	S.I.
1	7.1	67.4	1823.6	9.2	68.5	26.5
2	13.8	71.2	1176.0	10.0	68.0	30.0
3	355.8	89.2	1141.1	356.3	70.6	11.6
4	354.8	54.8	1521.1	354.9	54.3	5.7
5	350.3	62.4	1824.6	352.5	62.5	17.7
6	344.0	66.9	1840.9	344.8	66.7	25.1
7	358.8	66.8	3413.8	358.8	67.2	8.0
8	345.9	71.2	1091.6	346.3	70.9	45.2

Mean Dec. = 356.0, Inc. = 64.9, α_{95} = 4.4, k = 155.0

Table 2.10 Initial, most stable, S.I. and the mean value of samples from Roman Piercebridge.

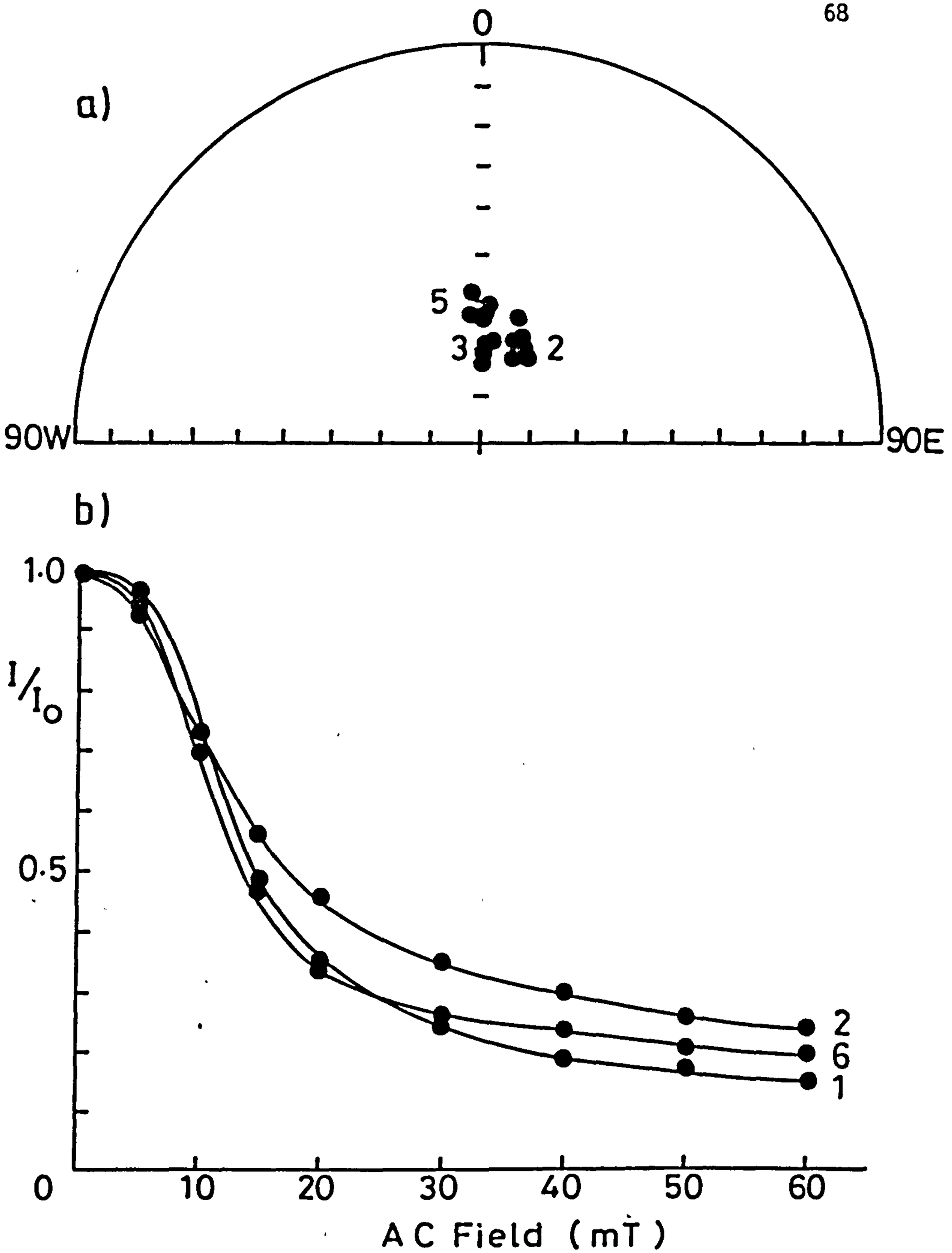

Fig. 2.11 Examples of changes during AC demagnetization of Roman Piercebridge samples

a) Directions
b) Intensity

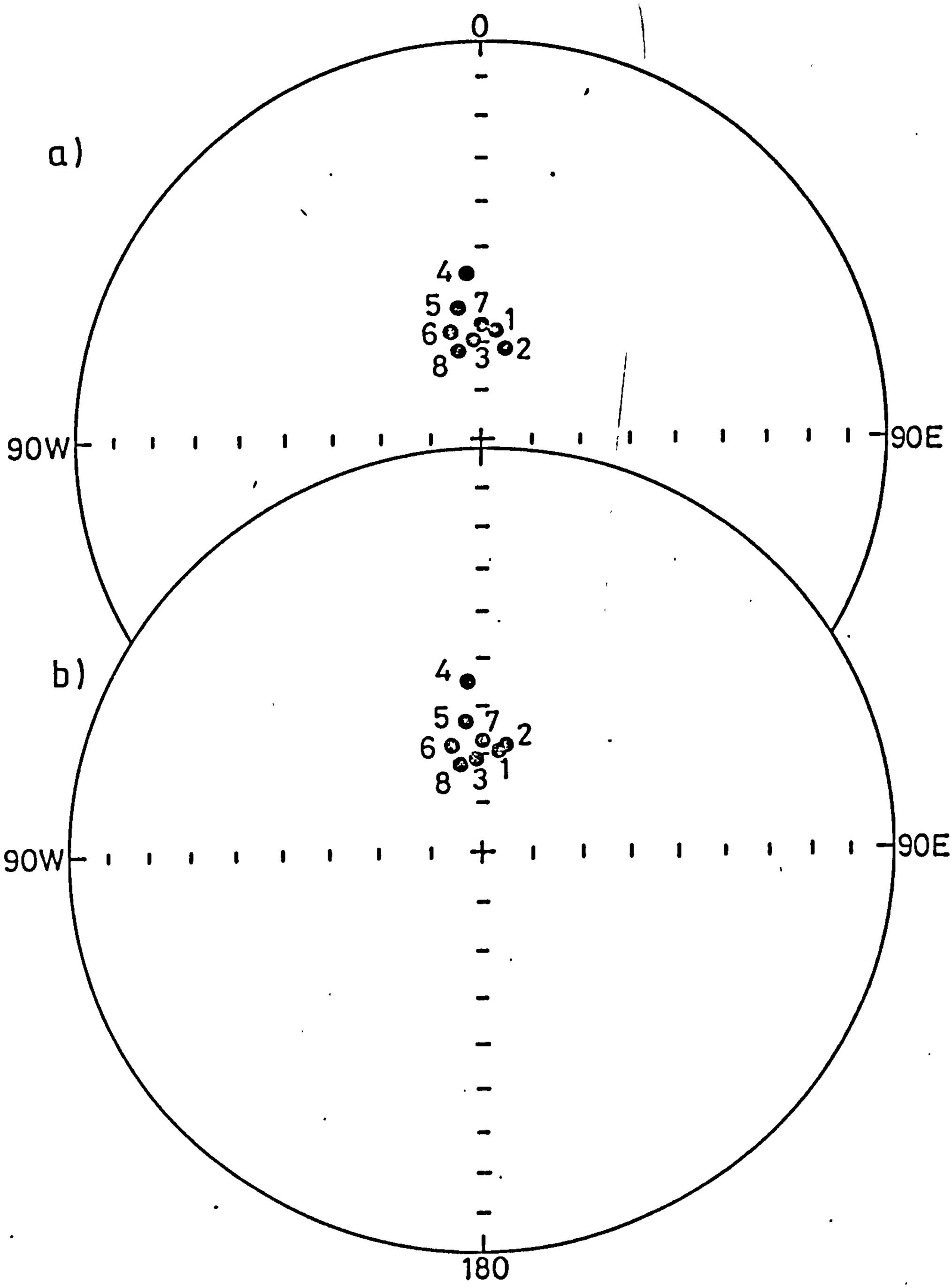

Fig. 2.12 Magnetic Direction of Piercebridge Samples

a) NRM
b) Most stable

direction had the α_{95} bars intersecting the curve at 140 AD and 330 AD, with about 2^{o} difference in declination (which is considered to be within the accuracy of the technique). The age of the kiln was therefore thought to be around 140 AD, which is consistent with the archaeological date. The other age (330 AD), is thought to be unlikely archaeologically. However, when the mean value was plotted on the revised curve (Ch. 4), it was found to correspond to about 140 AD.

2.7 PRUDHOE CASTLE, NORTHUMBERLAND (Medieval)

The castle is situated to the south of the River Tyne about 13 km. west of Newcastle at Lat. 54.9N, Long. 1.8W. The castle was of importance during the wars with Scotland and resisted two sieges in 1173 and 1174 AD.

Samples were collected on two trips. Two hearths were sampled during the first trip (A1502, B1524), and were later resampled together with another four fired areas (A1500, C1622/1646, D1327, E1402) and a fired wall (F1663).

2.7.1 Hearth A(1502)

This hearth had a rounded shape with a red burnt edge and a grey depression. On top of the burnt sides there was white mortar. The burnt areas were mainly concentrated in two sides of the hearth and were composed of soft, reddened clay. 13 samples were initially collected from this hearth (A1-13). The intensity of NRM ranged betweeen 3 - 236 mAm^{-1} (except sample A1 which had lower intensity) (table 2.11). Most of the samples were very stable during AC-demagnetization (fig. 2.13) except sample A1 which was unstable and sample A5 and A7 were poorly stable. The components remaining after demagnetization were grouped in a north-northeasterly

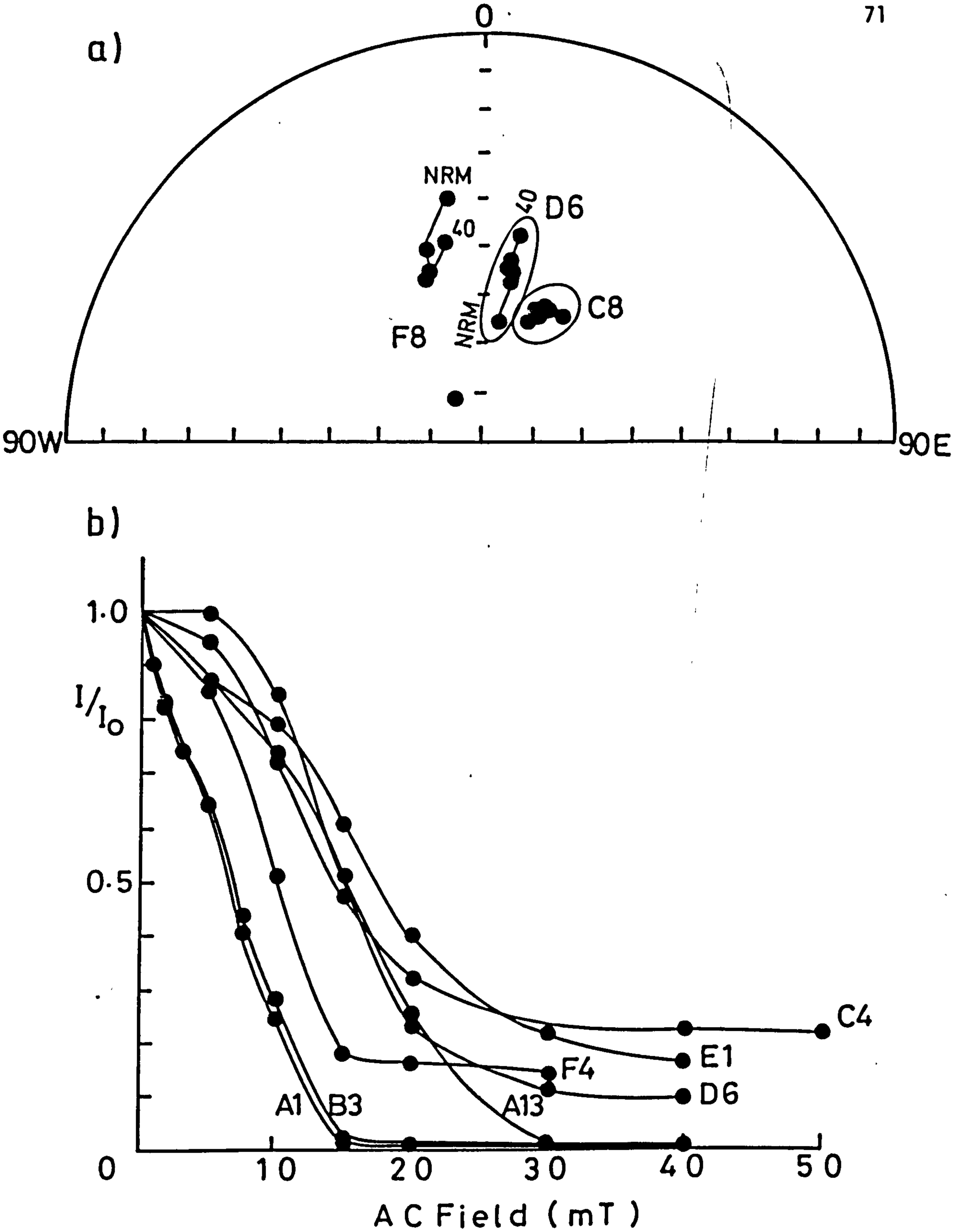

Fig. 2.13 Examples of changes during AC demagnetiation of Prudhoe Castle samples

a) Directions
b) Intensity

	Initial			Most stable		
Sample No.	Dec.	Inc.	Int. mAm^{-1}	Dec.	Inc.	S.I.
A1	16.7	-0.8	0.9	18.4	5.4	0.9
A2	7.2	54.7	21.4	348.3	57.9	3.9
A3	16.7	60.8	208.1	17.6	57.1	5.5
A5	6.0	35.2	3.6	5.9	37.9	2.1
A5	25.4	33.1	37.6	25.4	34.8	4.1
A6	12.2	40.7	70.0	9.4	40.5	5.4
A7	41.4	54.6	10.1	23.6	48.3	1.7
A8	18.1	61.2	131.2	20.7	59.4	3.6
A9	35.8	57.9	19.3	26.1	60.8	4.5
A10	4.2	66.6	236.6	0.2	59.8	8.6
A11	65.3	77.9	61.5	31.8	76.8	9.9
A12	70.7	72.6	60.8	29.4	71.2	4.7
A13	33.9	65.1	123.7	31.7	66.2	8.0
Mean Dec = 15.4, Inc. = 62.5, α_{95} = 6.9, k = 65.3 rej. 1,4,5,6 and 7						
			Dec. = 19.5, Inc. = 60.2, α_{95} = 6.8, k = 66.0 (rej.1,2,4,5,6)			
A14	24.9	66.5	15.8	35.1	58.6	1.7
A15	10.0	60.9	67.2	14.7	62.8	12.7
A16	7.1	59.6	30.2	6.7	60.7	7.0
A17	359.5	75.7	34.1	359.5	74.7	8.5
Mean Dec. = 14.7, Inc. = 62.4, α_{95} = 11.1, k = 68.9						
Overall Mean Dec. = 15.5, Inc. = 62.6, α_{95} = 5.1, k = 73.0						

Table 2.11 Initial, most stable, stability indices, and corrected mean values of samples from Hearth A (1502)

direction and the removed components showed a similar grouping (fig. 2.14). The mean value of the most stable directions was calculated, but excluding five samples (A1, A4, A5, A6 and A7). Sample A1 was rejected because it was unstable and had very weak intensity. All the rejected samples had been collected from the same area within the hearth and all showed shallow inclinations when compared with the main grouping of the other samples. This could indicate some disturbance in the hearth which was also suspected during sampling.

The mean value of the most stable directions was plotted on the archaeomagnetic curve. This value was exactly on the curve and gave a date around 1170 ±65 years.

In an attempt to increase the dating reliability, another four samples were collected during a second trip to the site. Three of these samples were very stable during demagnetization, as indicated by their high values of stability indices, but sample A14 was poorly stable (table 2.11, A14-A17). The mean value of the most stable directions of these four samples gave an age around 1170 AD. The overall mean, which is considered to be most reliable, suggests an age of 1170 AD ±50 years, which is consistent with the expected archaeological age of the hearth, which was 1100-1200 AD.

2.7.2 Hearth A" (1500)

This hearth lies over hearth A and is therefore younger. It is somewhat elliptical in shape and about 20 cm. in diameter. Five samples (A1-A5) were collected from this hearth. The natural remanent magnetization had consistent directions with the intensity ranging between 9 - 178 mAm^{-1} (table 2.12). AC-demagnetization showed that these samples were all very stable during demagnetization. The components remaining were well grouped having a northerly direction and the removed components were

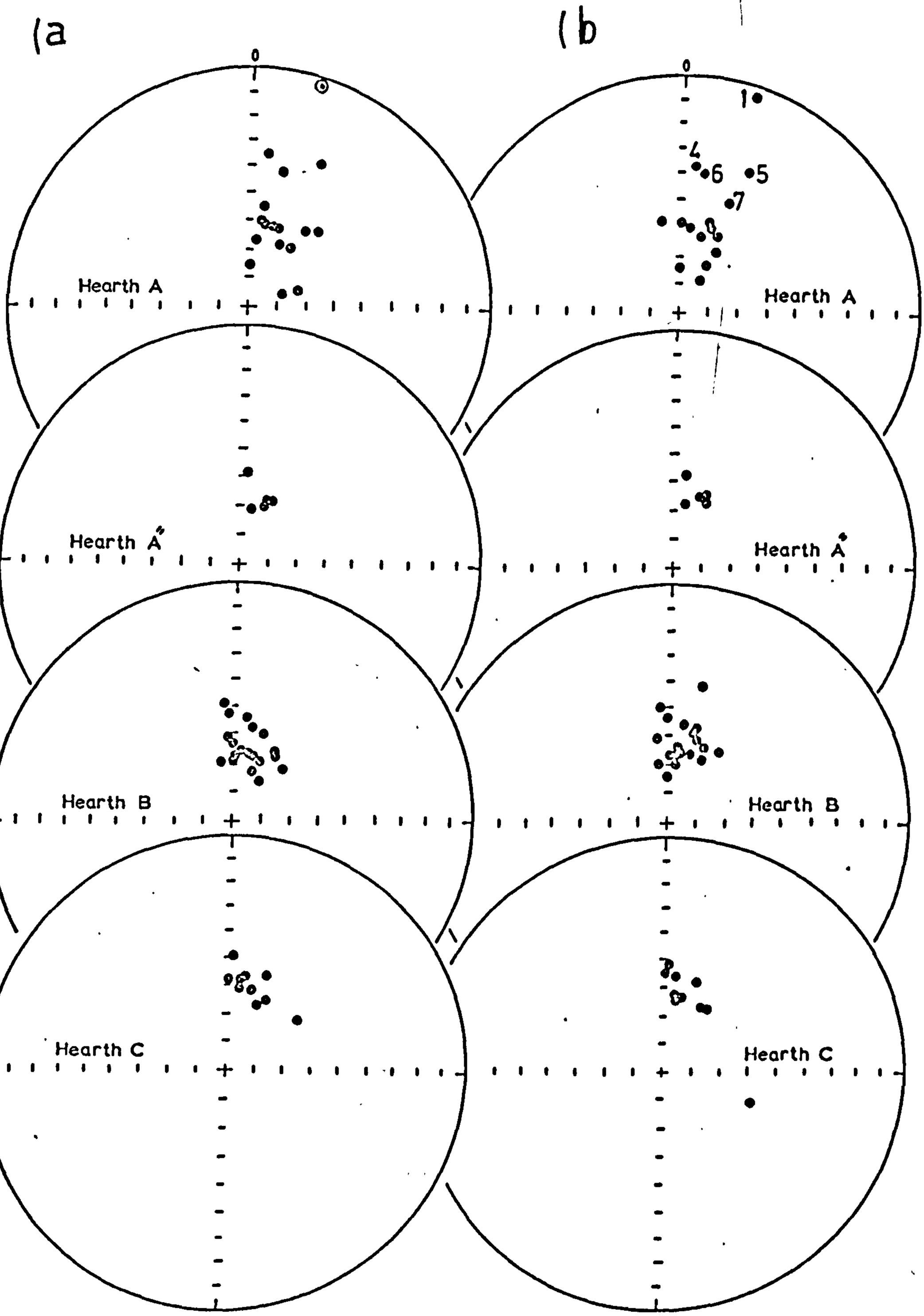

Fig. 2.14 Magnetic directions of Prudhoe site samples
a) NRM
b) Most stable

also grouped in the same directions (fig. 2.13). The mean value of the most stable directions was calculated and plotted on the archaeomagnetic curve. The age of this hearth was found to be around 1215 AD ±35 years, which is also consistent with the archaeological age for this hearth (1200-1250 AD).

	Initial			Most stable		
Sample	Dec.	Inc.	Int, mAm^{-1}	Dec.	Inc.	S.I.
B1	10.0	70.4	44.8	7.7	67.1	23.8
2	22.6	66.1	23.7	18.3	63.8	6.3
3	24.3	65.5	183.6	20.9	61.1	13.6
4	20.5	68.0	177.7	24.3	64.9	6.1
5	3.0	57.4	91	6.5	56.8	5.3

Mean Dec. = 13.8, Inc. = 60.4, α_{95} = 5.1, k = 225.0

Table 2.12 Initial, most stable directions, stability indices and the mean value of samples from hearth A" (1500)

2.7.3 Hearth B (1524)

This hearth consists of a flattish area of reddish soft clay, with an irregular shape, about 6m. from hearth A and at approximately the same level. 13 samples were collected from this hearth. The intensity of the natural remanent magnetization ranged between 3-500 mAm^{-1} (table 2.13). Pilot samples (B3, B4, B7 and B13) were very stable during demagnetization. Samples B3 and B4 had the components remaining well grouped in a north-northeasterly direction while the removed components were scattered. Sample B13 had the remaining components grouped in the north-northwesterly direction and the removed components showed a similar grouping. Sample B7 had the components remaining well grouped in a northerly direction and the removed components showed a similar grouping (fig. 2.14). The

	Initial			Most stable		
Sample No.	Dec.	Inc.	Int. mAm^{-1}	Dec.	Inc.	S.I.
B1	33.7	63.7	35.6	35.5	60.2	2.5
B2	12.2	66.0	397.8	11.3	64.7	8.0
B3	19.4	58.7	102.2	16.1	57.5	18.8
B4	22.9	66.7	285.0	26.7	65.1	8.0
B5	7.7	54.3	502.1	9.2	55.7	5.4
B6	20.4	71.5	16.5	18.9	69.7	5.2
B7	332.8	73.5	76.1	350.9	69.5	13.9
B8	1.0	67.9	446.3	5.2	66.4	6.0
B9	5.9	65.4	3.3	7.5	63.8	6.6
B10	16.2	66.6	11.5	13.4	53.5	1.9
B11	31.9	63.2	155.7	24.9	60.8	7.5
B12	355.6	61.2	17.0	351.5	60.2	4.4
B13	356.9	52.7	13.7	358.8	52.9	6.7
Mean Dec. = 11.1, Inc. = 60.0, α_{95} = 4.2, k = 94.8, N = 13						
B14	11.6	57.2	134.8	15.6	56.1	2.8
B15	354.7	48.9	129.5	355.5	48.8	3.0
B16	359.5	68.9	7.7	5.8	69.5	4.4
B17	0.1	63.1	8.1	4.1	66.3	2.7
B18	348.3	68.9	11.1	358.9	60.8	1.3
B19	43.5	65.8	36.4	15.9	64.3	1.8
Mean Dec. = 5.2, Inc. = 59.0, α_{95} = 7.2, k = 87.3, N = 6						
Overall Mean Dec = 9.3, Inc. = 59.7, α_{95} = 3.4, k = 95.0, N = 19						

Table 2.13 Initial, most stable, stability indices, and corrected mean value of Hearth B (1524)

remaining samples were all demagnetized at 7.5, 15, 30 and 40 mT. The mean value of the most stable directions was calculated and then plotted on the archaeomagnetic curve, giving an age of around 1220 AD. ±25 years.

A further six samples were collected from this hearth during the second trip (Table 2.13, B14-B19). Most of the samples were stable during demagnetization. The mean value of these most stable directions was calculated and plotted on the archaeomagnetic curve, the value gave an age around 1450 AD. ±65 years. This date is later than the expected archaeological age of 1250 AD ±25 years. The overall mean value was then calculated and plotted on the archaeomagnetic curve. This now lay inbetweeen the 1200 - 1250 AD and 1450 - 1500 AD part of the curve, but slightly nearer to the 1200 - 1250 AD curve. Since the archaeological evidence suggested an age of about 1250 AD., hence the site was archaeomagnetically dated as 1225 AD ±25 years. This value was subsequently plotted on the revised archaeomagnetic curve (Chapter 4) and was found to correspond to an age of 1250 AD ±15 years.

2.7.4 Hearth C (1622/1646)

This hearth was composed of fired clay surrounded by some bricks. A total of 10 samples (C1-C10) were collected from the clay and from brick fragments within the hearth. The natural remanent magnetization had intensities ranging between 0.3 - 129 mAm^{-1} with reasonably consistent directions, except sample 7 which had a scattered direction (table 2.14). AC-demagnetization results showed that most of the samples were very stable during demagnetization except samples C3 and C9 which were metastable and sample C7, which was unstable with a weak intensity. As the directions for C3 and C9 were consistent with the other samples, only sample C7 was eliminated from further analysis. The components remaining

after demagnetization were well-grouped having a north-northeasterly direction (fig. 2.14) and the removed components were grouped in the same direction. The mean value of the most stable direction was calculated for the 9 samples and gave an age of 1260 AD.±20 years, which is consistent with its archaeological age (1250 - 1300 AD).

Sample No	Initial Dec.	Initial Inc.	Initial Int. mAm^{-1}	Most stable Dec.	Most stable Inc.	Most stable S.I.
C1	7.1	60.4	14.8	5.0	64.0	9.9
C2	9.7	56.1	129.0	359.7	54.6	3.5
C3	8.1	57.3	1.0	6.2	65.1	2.3
C4	22.9	64.4	93.0	26.9	65.1	6.9
C5	20.6	54.0	3.7	16.7	57.6	5.1
C6	2.0	49.6	10.9	20.1	52.9	4.4
C7	52.0	59.9	0.3	109.0	59.4	0.3
C8	26.0	61.7	19.2	29.4	65.3	7.03
C9	14.9	60.7	1.9	4.6	57.0	2.05
C10	10.2	62.8	24.6	10.0	59.4	4.5

Mean = Dec. = 8.4, Inc. = 57.9, α_{95} = 4.4, k = 127

Table 2.14 Initial, most stable, stability indices and the mean value of Hearth C (1622/1646)

2.7.5 Hearth D (19327)

This hearth lies within a kitchen corner and is surrounded by fired bricks. A total of six samples were collected from the bricks and the baked clay. The natural remanent magnetization intensity ranged between 6 - 559 mAm^{-1} and the directions were reasonably

consistent (table 2.15). AC-demagnetization results showed that samples D1, D4 and D5 (brick) were very stable, while samples D2 (brick), D3 and D5 (clay) were poorly stable. The components remaining after demagnetization were moderately well-grouped in a northerly direction (fig. 2.15) and the removed components showed some grouping in the same northerly direction. The mean value of the most stable directions was calculated and plotted on the archaeomagnetic curve and the age was found to be around 1240 AD ±25 years, which is very close to their supposed archaeological age of 1250 - 1300 AD.

Sample No		Initial Dec.	Initial Inc.	Initial Int mAm^{-1}	Most stable Dec.	Most stable Inc.	S.I.
D1	B	26.9	63.7	9.3	24.6	62.4	8.1B
D2	B	6.6	63.4	6.8	11.1	60.2	1.3B
3		6.4	72.9	6.9	4.8	66.1	1.3
4	B	9.4	52.3	61.2	9.8	51.8	10.5B
5		10.0	62.2	61.3	9.2	61.7	1.4
6	B	10.5	66.5	559.1	10.6	54.8	8.7B

Mean ' Dec. = 10.5, Inc. = 58.1, α_{95} = 5.0, k = 173

Table 2.15 Initial, most stable, stability indices and the mean value of Hearth D (1327)

2.7.6 Hearth E (1402)

This hearth had a nearly circular shape and was composed of fired red clay. Eight samples (E1-E8) were collected from the hearth. The intensity ranged between 6 - 725 mAm^{-1} and the directions were reasonably consistent (table 2.16). AC-demagnetization showed that most of the samples were stable, but samples E2, E3 and E6 were poorly stable. The

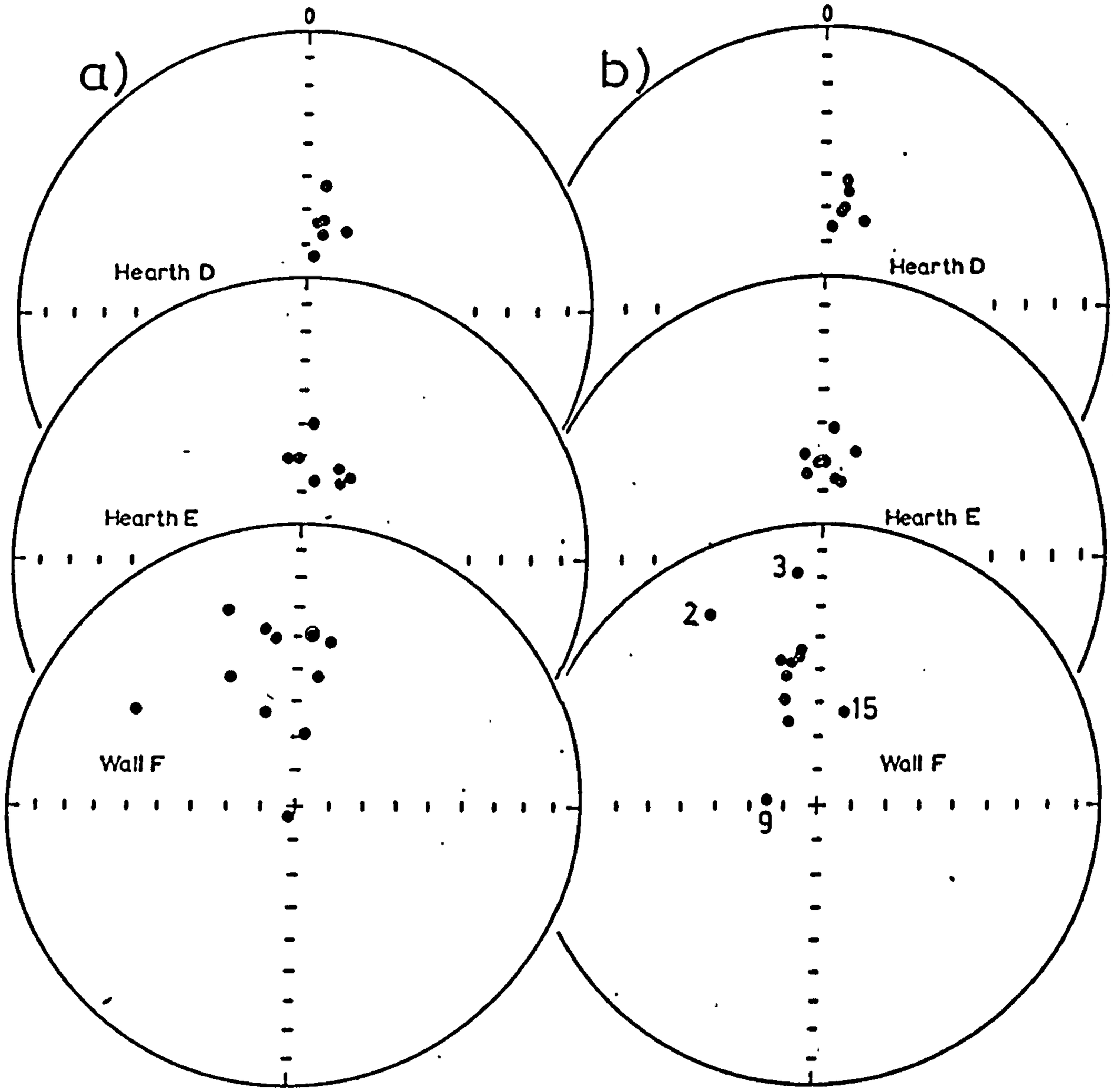

Fig. 2.15 Magnetic directions of Prudhoe sites. D, E and F
a) Initial
b) Most stable

components remaining were well-grouped in a northerly direction and the removed components showed a similar grouping (fig. 2.15). The mean value of the most stable directions was calculated and plotted on the archaeomagnetic curve and it was found to be near the Roman curve which is not archaeologically acceptable. The value was subsequently plotted on the revised curve (Chapter 4), and gave an age around 1305 AD ±15 years, which is very consistent with the archaeological age (1300 AD).

Sample No.	Initial Dec.	Inc.	Int. mAm^{-1}	Most stable Dec.	Int.	S.I.
E1	10.4	66.1	125.0	10.3	68.5	6.6
E2	29.5	61.1	236.8	6.7	67.6	1.1
E3	24.7	64.5	150.3	346.3	66.5	1.7
E4	5.5	50.0	201.0	3.0	52.9	3.8
E5	2.8	59.2	725.3	355.0	63.1	3.7
E6	353.4	59.4	541.2	347.9	60.0	1.8
E7	0.0	59.0	25.4	358.2	62.9	7.6
E8	20.8	60.5	6.4	14.7	57.7	3.3

Mean Dec. = 0.4, Inc. = 60.7, α_{95} = 4.6, k = 130

Table 2.16 Initial, most stable, stability indices and the mean value of Hearth E (1402)

2.7.7 Wall F (1663)

Twelve samples were collected from fired areas on a stone wall, recognized by a reddish colouration. The initial intensity of these samples ranged between 0.067 - 1.205 mAm^{-1} and the initial directions were scattered (table 2.17). AC-demagnetization results showed that these samples were poorly stable except samples 1 and 11, which were metastable

and sample 8 which was stable. The components remaining after AC-demagnetization showed some grouping in the north-northwesterly direction, while the removed components were scattered (fig. 2.15). The most stable direction of all the samples were somewhat consistent with each other except samples 2,3,4 and 9 which departed from the main grouping of the sample.

Sample No	Initial Dec.	Initial Inc.	Initial Int_{-1} mAm	Most stable Dec.	Most stable Inc.	Most stable S.I.
F1	340.5	26.5	0.067	345.1	46.5	0.7
F2	332.8	47.6	1.205	330.5	23.1	1.2
F3	4.5	-38.6	0.083	345.2	18.5	1.2
F4	7.0	89.1	0.934	15.4	62.4	1.2
F5	9.3	51.4	0.354	352.3	46.4	1.3
F6	10.7	40.4	0.306	352.9	44.0	1.1
F7	341.1	60.9	0.250	340.5	64.3	2.2
F8	352.3	40.0	0.328	345.7	50.9	2.7
F9	208.8	87.7	0.356	276.1	75.5	1.3
F11	301.3	34.9	0.295	340.9	57.8	0.6
F12	349.9	36.3	0.174	348.7	47.2	1.3

Mean,rej. 2,3,4,9 Dec. = 347.0, Inc. = 51.0, α_{95} = 5.9, k = 103

overall mean Dec. = 346.3, Inc. = 44.3, α_{95} = 10.2, k = 23.2

Table 2.17 Initial, most stable and stability indices of sample from the Wall (F) (1663)

Since the samples had relatively weak intensities, their directions were checked after each step of demagnetization. These directions did not show any consistent change towards a particular direction and hence

they were considered genuine and not affected by errors as a result of magnetometer effects. Accordingly the scatter in directions could be due to:

1) Insufficient firing of the wall: the samples were taken from the reddish parts which were assumed to be well fired. This firing could have been insufficient because the wall was only partly fired in two small locations.

2) According to the size and position of the wall (located near a cliff), displacement in the wall is possible. Such displacement after firing could affect the directions. However, there was no clear evidence of such movements.

3) 'Washing out' of the wall due to weathering throughout its archaeological history. The area had been open to the air subsequent to firing.

The mean value of the most stable directions was calculated after samples 2,3,4 and 9 were rejected because of their scattered positions. This mean value was away from the 1200 AD directions (which is the estimated archaeological age of the heating of the wall) by about 25^{o} in declination and about 10^{o} in inclination (shallow). Clearly such dating must be considered doubtful, and further work is necessary to establish the reasons for the low , stability and scatter.

2.7.8 Summary

Most of the samples collected from Prudhoe castle were found to be stable during demagnetization, except those collected from the wall (F) which were generally poorly stable. Since these sites were all archaeologically well-dated, and also magnetically stable (apart from the wall samples), hence any shift in mean directions from the archaeomagnetic curve was thought to correspond to an error in the position of the present

curve. (This does not include hearth A which appeared to be somewhat disturbed). On this basis most of the samples were plotted on a revised archaeomagnetic curve which showed a different route for the period between 1200 - 1400 AD. The results obtained from Prudhoe site sample are all summarized in table 8 and their relevance to the British archaeomagnetic curve is assessed in Chapter 4.

Hearth	Dec.	Inc.	α_{95}	Archaeological Age	A.M. age
A/1502	18.0	60.9	5.1	1100-1200 AD	1170±50
A/1500	13.8	60.4	5.1	1200-1250 AD	1215±50
B/1524	9.3	59.7	3.4	1250 AD ± 25	1225±25
C/1622/1646	8.4	57.9	4.4	1250-1300 AD	1260±20
D/1327	10.5	58.1	5.0	1250-1300 AD	1240±25
E/1402	0.4	60.7	4.6	1300 AD	1305±15
F/1663	348.4	47.1	6.5	1200 AD	

Table 2.18 Summary of Prudhoe Castle site

2.8 LOFTUS, N. YORKSHIRE (Neolithic)

This site is about 3 km. north-east of Loftus, in the county of Cleveland (Lat. 54.6N, Long. 0.86W). It was originally thought to be a round barrow, but, after excavation, was found to be a Neolithic long barrow. The excavated area was about 4m. long and 1.5m. wide and consisted of loose and friable burnt sandstone blocks overlain by some unburnt human bones.

A total of 14 samples were collected from separate, apparently unmoved, hard blocks (samples 1 and 11 were broken). The intensity of

remanence was generally high, ranging between 272-16001 mAm^{-1}, except samples 2 and 9 which had lower intensity, and the directions were very scattered (table 2.19).

	Initial			Most stable		
Sample	Dec.	Inc.	Int. mAm^{-1}	Dec.	Inc.	S.I.
2	124.2	53.0	132.2	129.2	47.8	4.4
3	323.7	38.1	16001.6	322.8	37.7	10.5
4	334.9	81.6	1144.8	330.3	82.2	30.2
5	326.0	86.0	433.8	338.9	88.1	13.8
7	275.8	63.7	369.3	269.8	63.9	53.9
8	324.1	0.4	272.3	304.8	-22.4	3.3
9	47.0	27.5	4.2	48.4	29.4	3.5
10	23.8	55.5	352.5	23.3	55.0	16.9
12	45.4	24.5	955.6	46.5	23.6	9.6
13	351.7	29.6	626.1	352.1	28.7	28.3
14	357.8	61.4	365.5	358.1	62.7	48.7

Table 2.19 Initial, most stable directions and stability indices (S.I.) of Stree House Farm, Loftus, samples

Pilot samples (2,4,5,7,8, 13 and 14) were stable to very stable during AC demagnetization (fig. 2.16). Sample 2 showed that the components remaining were grouped in a southeasterly direction, while the removed components were scattered but they tend to show the same grouping as the components remaining, indicating that, above 10 mT, only one component of remanence was present. Sample 4 had the components remaining in a northwesterly direction, near to the present earth field. Only the high coercivity components of the components removed were scattered and the low coercivity components were grouped in a northwesterly direction,

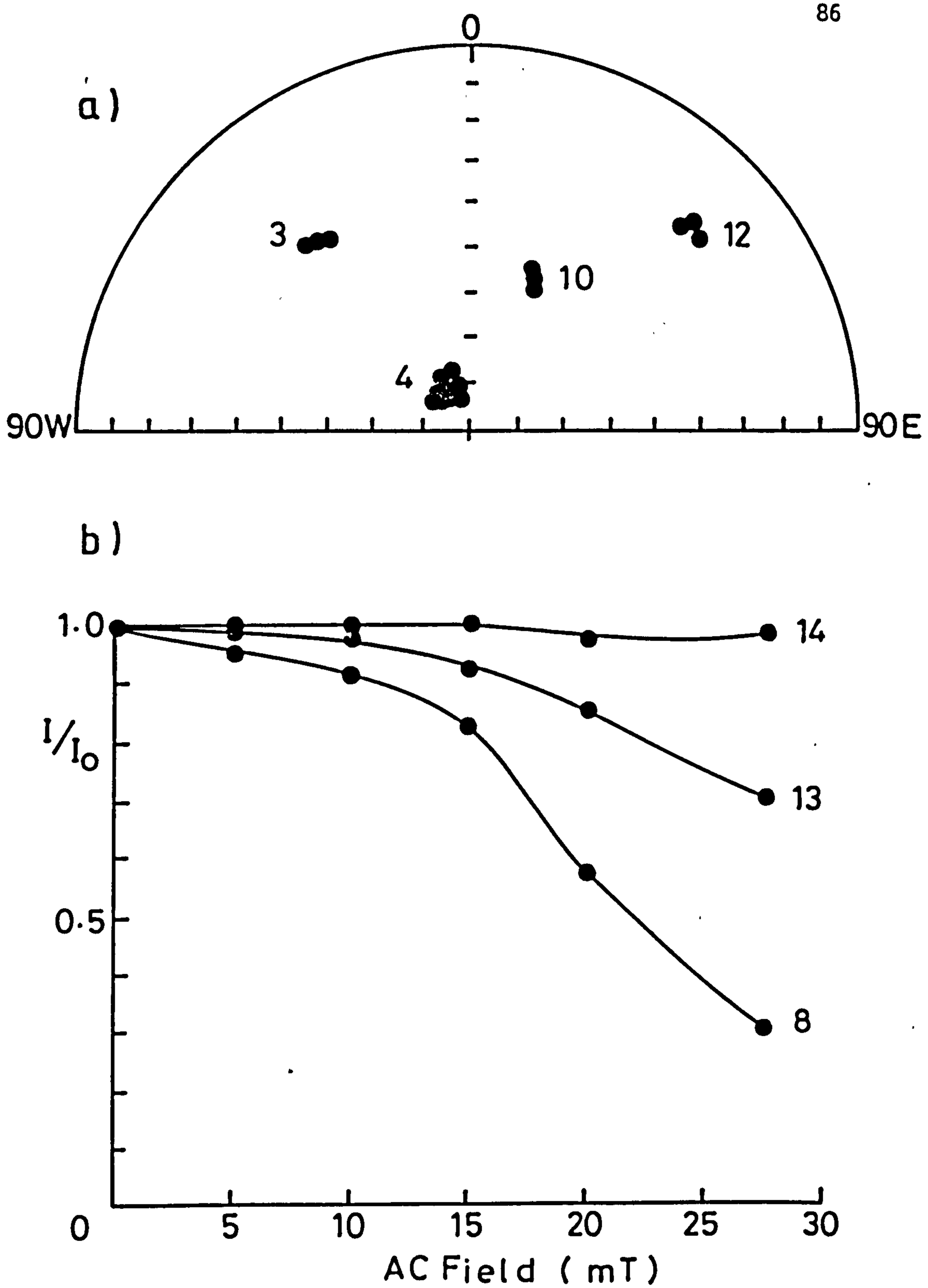

Fig. 2.16 Examples of changes during AC demagnetization of Street House Farm samples

a) Directions

b) Intensity

again indicating the removal of the same single component. Sample 7 behaved similarly, having the remaining components in the westerly direction and the removed components having the same grouping. The components remaining in sample 5 were well grouped near to the present earth field and the removed components were similarly grouped near the present earth field. The remanence of sample 8 was somewhat less stable although the components remaining were all in the upper hemisphere and had a northwesterly direction, while the components removed were all scattered. Samples 13 and 14 had the remaining components grouped in a north-northwesterly direction, but with a shallow inclination for sample 13, while the removed components in the two samples were scattered. The remaining samples (3,6,9 and 10) were all demagnetized at 5, 15 and 27.5 mT. Despite the magnetic stability of these samples (S.I. all greater than 3.0) and the evidence for single component remanence after removal of various components, their remanent directions were not consistent except for samples which were very close to each other (fig. 2.17). This scatter cannot be due to different components, nor to instability, and, since there were no systematic patterns to the scattered directions, it cannot be due to magnetic refraction. The most likely cause for this scatter of directions is some disturbance of the material after the firing had taken place. Since the bones which accompanied the sampled area were unfired, the most likely interpretation is that the funeral area was fired first and was left until it cooled down, after which ashes and burnt rocks were moved, and the human bones placed on them. The disturbance could have been accidental or deliberate. This conclusion is somewhat surprising as it had been thought that the sampled blocks were still in situ. Sampling of larger blocks, which are less likely to have been moved, may still provide useful archaeomagnetic information, if available.

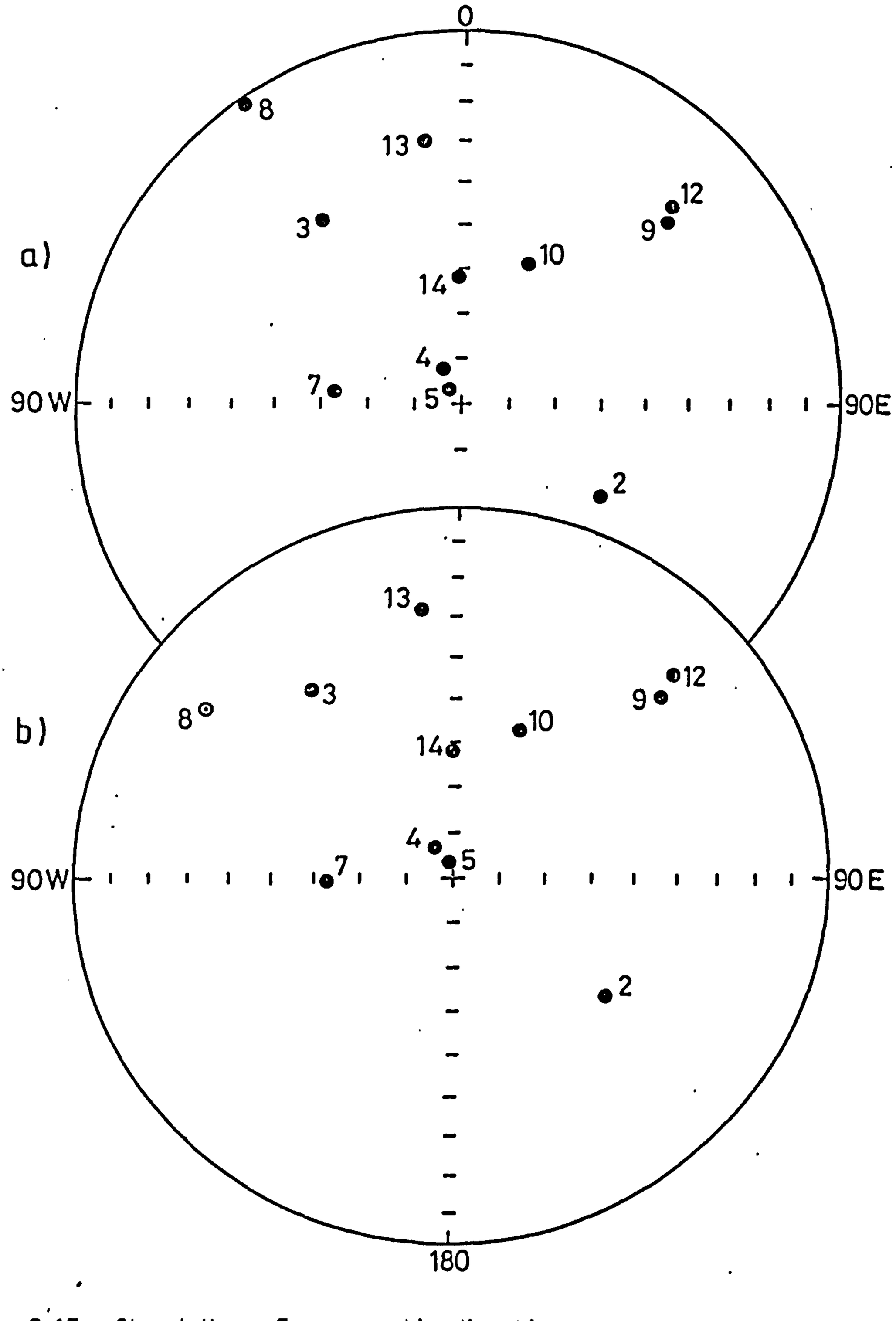

Fig. 2.17 Street House Farm magnetic directions

a) NRM directions
b) Most stable directions

⊙ upper hemisphere

2.9 BRYN Y CASTELL - N. Wales

The site is a small hill fort on the summit of a steep-sided rock knoll about 14 km. from Maentwrog (Lat. 52.5N, Long. 3.59W). Outside the hill fort to the north-east is a sub-rectangular structure predominantly extensive evidence for iron smelting (Crew, 1981). A total of 21 samples were collected from four smelting furnaces in the extramural site. Most of the samples showed high content of iron, as indicated by their weights, colour and high intensity of magnetizations. Two samples were chosen from each site for pilot studies and the other samples were bulk demagnetized at 15, 30 and 50 mT. Most of the samples were stable during demagnetization except samples A3 and A1 which were poorly stable (Table 2.20) (fig. 2.18).

2.9.1 Hearth A (F37)

Six samples were collected from this hearth which is located at the northwestern corner of the site. The intensity of NRM of these samples ranged between 1597 - 21183 mAm^{-1} and the directions were consistent with each other.

The components remaining after AC-demagnetization in pilot samples A_1 and A_6 were well grouped in a north-northwesterly direction, while the removed components were scattered in the same direction. The mean value of the most stable directions of all samples was calculated (Dec. = 0.99, Inc. = 60.6, α_{95}= 3.6) and corrected to Meriden. This value was found to lie on the 210 AD ±15 years part of the curve.

2.9.2 Hearth B (F49)

Six samples were collected from this hearth which is near the central part of the site. The intensity of NRM of these samples ranged between 290 - 11638 mAm^{-1} and the directions were consistent with

each other. Pilot samples B_2 had the components remaining after AC-demagnetization well grouped in the north-northwesterly direction while the removed components were scattered. The components remaining in sample B_5 were also well grouped in a northerly direction while the removed components were scattered.

The mean value of the most stable directions of all samples was calculated (Dec. = 357.8, Inc. = 61.5, α_{95} = 5.2) and corrected toMeriden and the age of the hearth was found to be around 200 A.D. ±30 years.

2.9.3 Hearth C (F28)

Four samples were collected from this hearth which is about 2m. away from hearth B. The intensity of NRM of these samples ranged betwen 2724 - 23501 mAm^{-1} and the directions were consistent with each other. The components remaining after AC demagnetization in pilot samples C_2 were well grouped in the northerly direction while the remaining components in sample C_4 were well grouped in the north-northeasterly direction, and the removed components were scattered in both samples. The mean value of the most stable directions was calculated (Dec. = 3.1, Inc. = 57.6, α_{95} = 6.7) and corrected to Meriden and the age was found to be either 240 A.D. or near 1400 A.D. According to the archaeological evidence the age is more likely to be around 240 A.D. ±25 years).

2.9.4 Hearth D (F41)

Four samples were collected from hearth D which is located at the southeastern corner of the site. The intensity of NRM of these samples ranged between 1073 - 16272 mAm^{-1} and the directions were scattered. The components remaining after AC demagnetization in pilot samples D_2 and D_3 were well grouped in the northerly direction while the removed components were

scattered.

The NRM and most stable directions of all samples are presented in fig. 2.19.

Sample No.	Initial Dec.	Inc.	Int mAm^{-1}	Most Stable Dec.	Inc.	S.I.
Hearth A (F37)						
A1	357.5	53.3	21183.0	6.4	64.9	6.5
A2	353.7	63.3	3907.0	4.6	60.8	1.8
A3	10.7	55.8	5410.0	8.7	59.6	3.0
A4	356.9	52.0	5686.0	357.0	57.5	4.3
A5	353.5	53.3	1597.0	351.2	58.7	3.4
A6	16.4	63.5	13441.0	8.4	62.9	4.1
Mean	Dec. = 0.99	Inc. = 60.6		α_{95} = 3.6	k = 330.0	
Hearth B(F49)						
B1	5.6	60.3	11638.0	3.9	56.9	2.5
B2	.3.3	60.5	9863.0	352.0	66.5	5.3
B3	1.4	68.6	290.8	4.9	61.5	2.7
B4	6.8	59.2	7881.0	1.2	53.6	3.1
B5	5.0	59.6	568.6	2.6	67.3	2.8
B6	353.6	67.6	8589.0	347.5	63.0	3.7
Mean	Dec. = 357.8	Inc. = 61.56		α_{95} = 5.2	k = 164.1	
Hearth C(F28)						
C1	353.5	55.1	2724.0	356.4	59.6	3.1
C2	358.5	61.1	23501.0	356.5	60.8	12.3
C3	15.0	53.0	6431.0	9.3	58.0	5.1
C4	20.6	57.8	14849.0	14.3	53.0	7.6
Mean	Dec = 3.17	Inc. = 57.67		α_{95} = 6.7	k = 185.1	
Hearth D (F41)						
D1	351.9	51.5	1819.0	359.2	64.4	1.8
D2	6.4	60.7	3382.0	0.7	63.3	4.2
D3	2.0	66.9	1073.0	3.1	66.3	4.5
D4	2.8	65.6	16272.0	358.3	64.3	4.0
Mean	Dec. = 359.38	Inc. = 64.4		α_{95} = 1.7	k = 2789.2	

Table 2.20 Initial, most stable, stability indices and mean values of Bryn y Castell samples

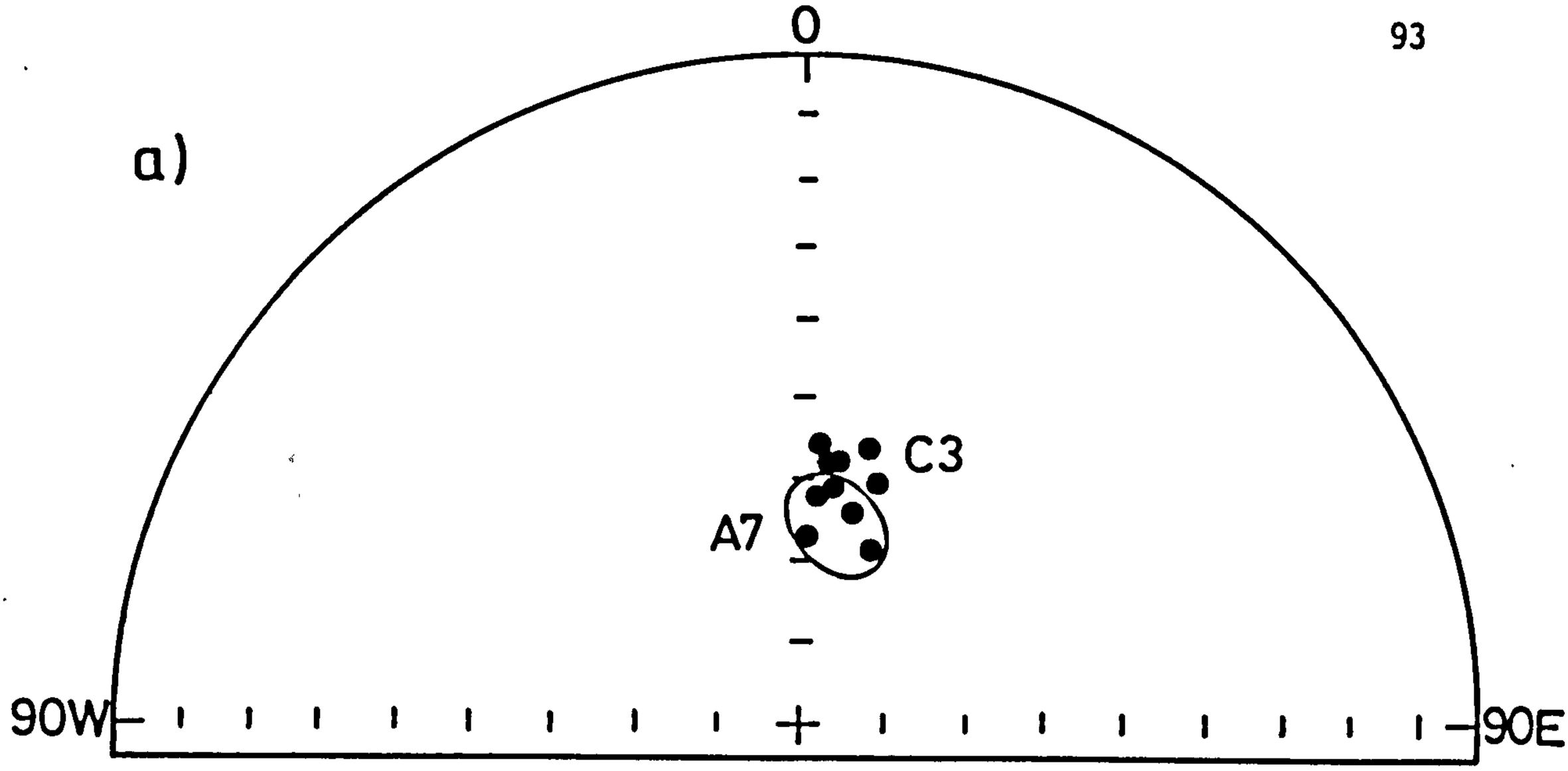

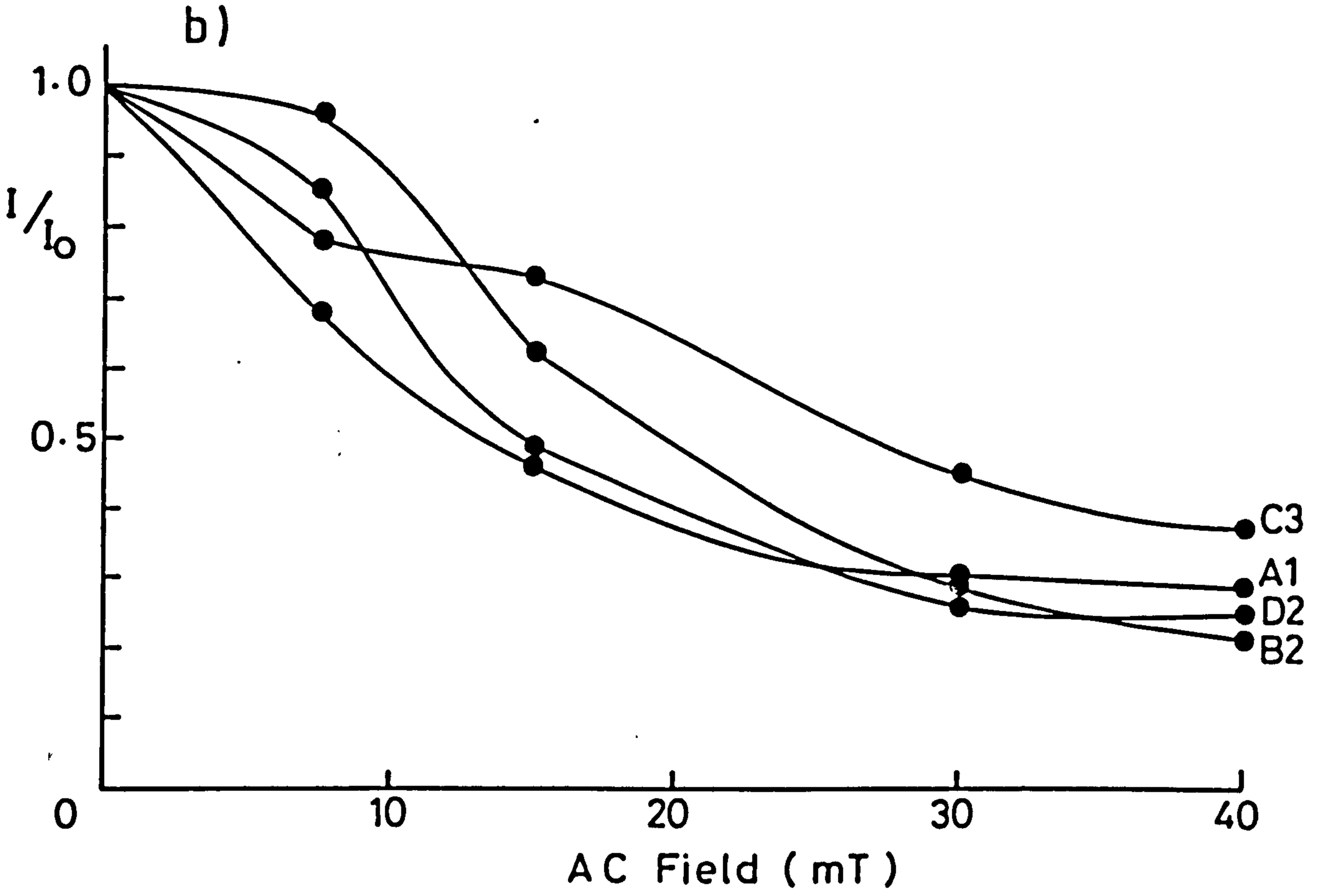

Fig. 2.18 Examples of changes during AC demganetization of Bryn y-Castel λ 63 samples

a) Directions

b) Intensity

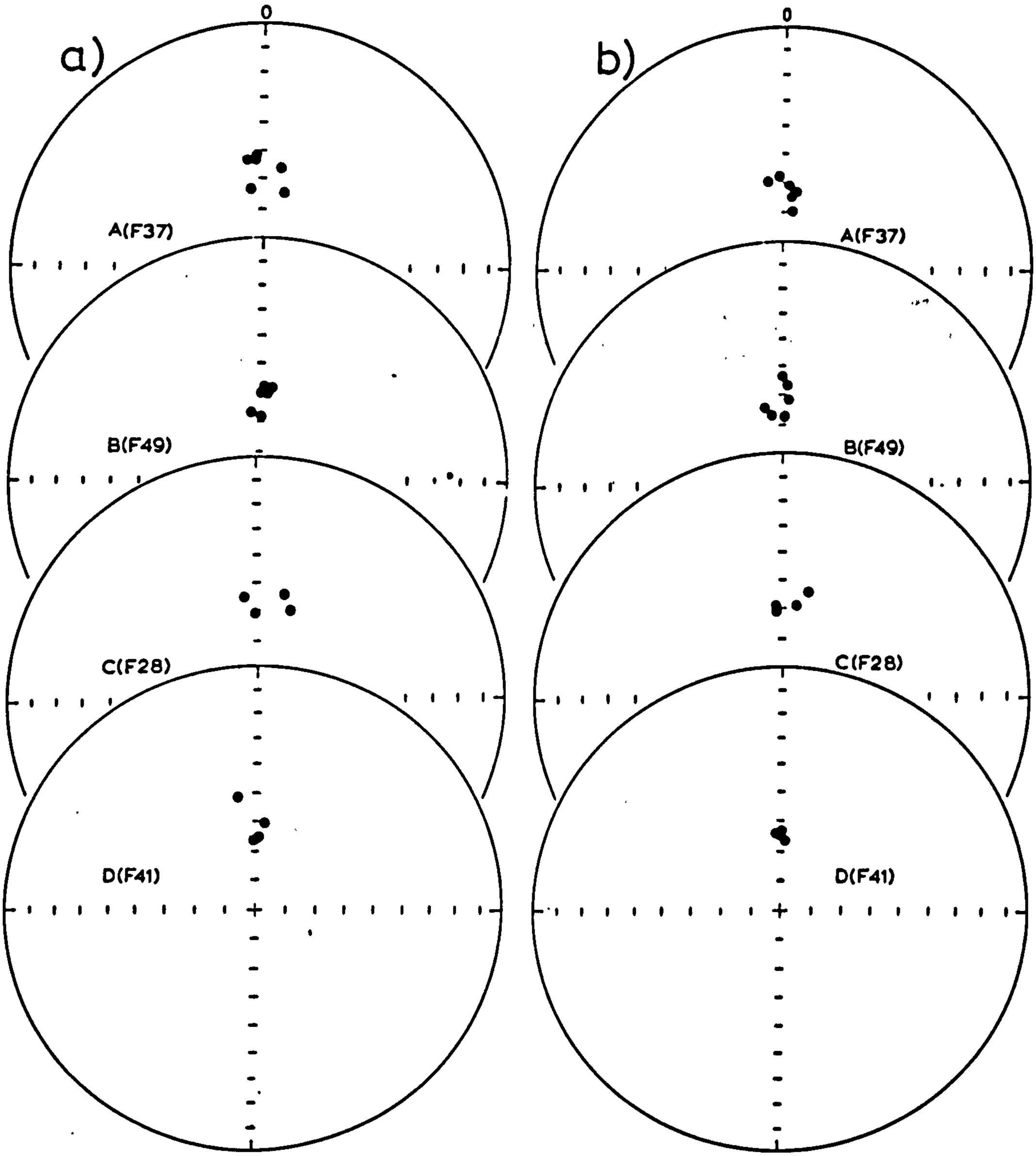

Fig. 2.19 Magnetic directions of Bryn Y-Castel samples
a) NRM b) Most stable

× 64

2.10 Kiln Wall Movements and Magnetic Refraction

Introduction

A total of 105 samples were collected from 3 kilns and a kiln pillar which were considered suitable for refraction and wall fall studies. These kilns were round and samples were collected systematically from the walls and from the floors wherever possible. The pillar had been taken by Dr. A.J. Clark of the Ancient Monuments Laboratory from the centre of a kiln. All orientations were taken using a sun compass, so that any scatter in directions should not be due to orientation errors. The initial magnetizations of all samples were measured and pilot samples were demagnetized at 7.5, 15, 30, 40 and 50 mT. The stability of pilot samples ranged between stable to very stable. The remaining samples were bulk demagnetized.

The causes of the magnetic directions scatter around ancient kilns have been explained in terms of wall fall-out, magnetic refraction and later, Hoye (1980), suggested wall fall-in rather than fall-out.

Theoretically if a kiln is perfectly rigid and cools uniformly in a homogeneous magnetic field, the directions should be uniform. But some kilns lack rigidity and have moved after firing. However, it was clear that kilns do not cool identically so it is possible that the magnetization acquired by those parts of the kiln which cooled first, or nearby magnetic objects, may cause a local distortion of the field in the kiln within which the later cooling parts become magnetized. The effect of refraction is dependent on factors like cooling pattern and magnetic properties. The refraction effect was thought to be of second harmonic, localised and not strong enough to account for most of the scattered directions (Weaver, 1961;

Aitken and Hawley, 1971).

To study the kiln wall movements the most stable directions of magnetization at each site were plotted with respect to the magnetic north and a theoretical sine curve was plotted showing a kiln wall movement. An arbitrary value of 2.4^{o} fall-out and fall-in was adopted as this corresponds to the errors suspected by Aitken and Hawley (1971) due to either refraction effects or kiln wall movements.

Deviations have also been observed between floor and wall samples. Previous work by Aitken and Hawley (1971) showed that floor samples are less scattered than wall samples. It was also thought that if physical tilting occurred on the walls then the average remanence directions in floor samples represent the true ancient direction. On the other hand, if the floor direction is due to magnetic distortion then the angle of dip recorded in the floor may be too shallow and the average for the walls will be too steep, the true value lying in between (Weaver, 1964).

1) Green Lea Kiln - Lincoln (Late Roman $\tilde{\sim}$ 300 AD)

A total of 54 samples were collected from a round kiln (1.5m. diameter, 1m. depth); 28 samples were from the wall (5 - 32) (sample 33 was broken), at about 50 cm. depth. 14 samples were from the floors (43 - 57) (sample 47 was broken), 9 samples were from the mouth of the kiln (1 - 4, 34 - 38) and 4 samples from slag near the outlet of the kiln (fig. 2.20).

The mean value of most stable directions for different parts of the kiln are:-

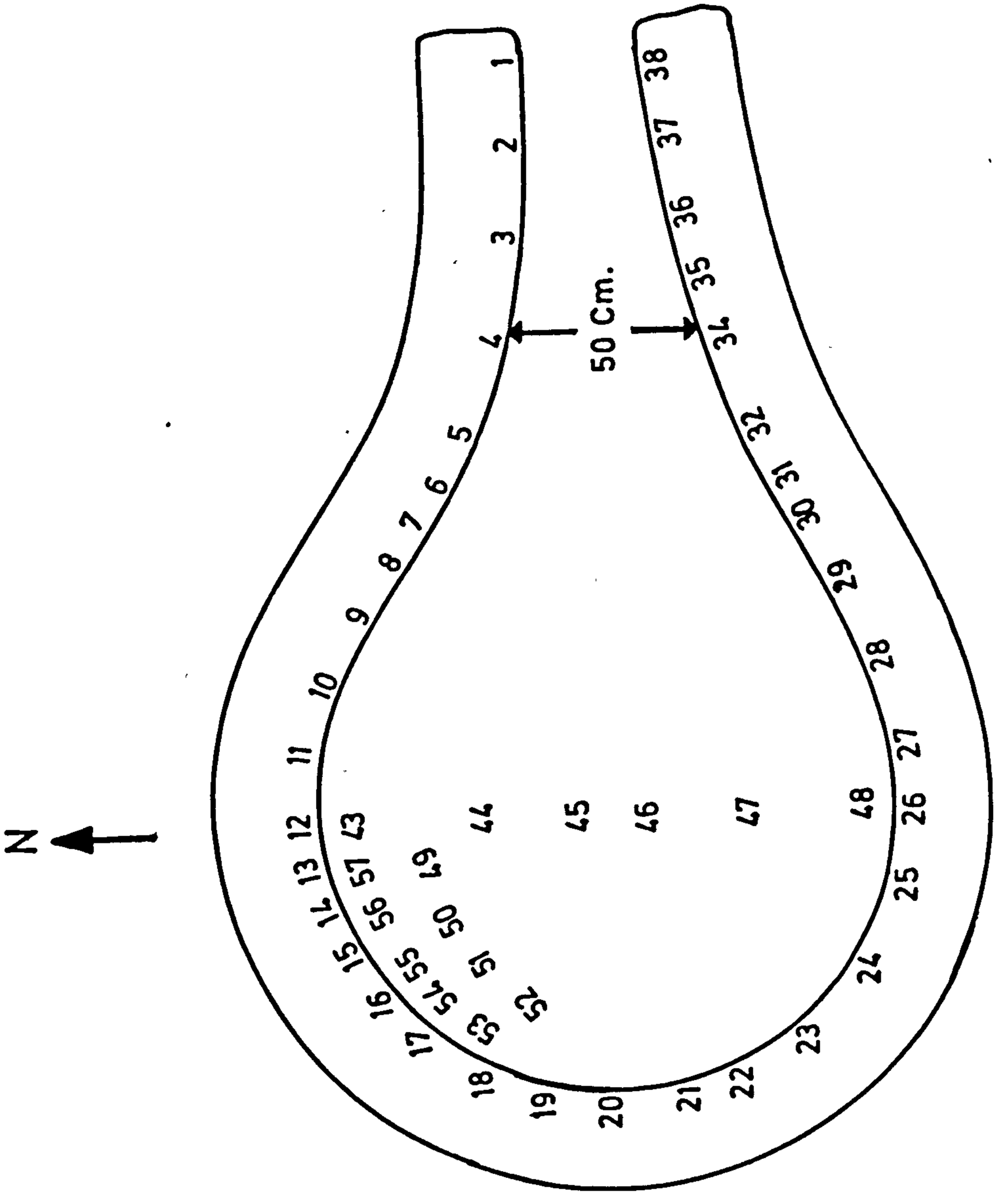

Fig. 2.20 Samples distribution of Green Lea kiln

	Dec.	Inc.	α_{95}	N	δD	δI	Dec.	Inc.	α_{95}	N	δD	δI
Wall	7.9	71.6	3.0	28	-	-	4.3	60.6	2.2	23	-	-
Floor	346.5	66.0	8.2	14	21.5W	-5.6	352.8	63.2	5.4	11	11.5W	-6.4
Mouth	8.4	72.9	4.5	8	0.5E	1.4	4.2	73.9	4.0	7	0.1W	4.3
Overall	0.9	70.5	2.9	50			1.9	68.8	2.1	41		

where N is the number of samples and δD, δI are the errors in declination and inclination with reference to the wall directions

Wall samples

The most stable directions of magnetization of the wall samples were plotted with respect to their positions around the wall relative to magnetic north and then compared with the theoretical sine curves for wall fall in and out by 2.4^{o} relative to the mean value of the most stable directions of the wall samples only. The declination plot (fig. 2.21) shows that the values are distributed randomly along the two curves, showing no evidence for systematic wall movement. The inclination values are also distributed along both curves but show some weak evidence for a possible fall in. Hence no systematic wall movement was observed as was also indicated by the field appearance of the kiln. The most deviant stable directions (table 2.21) are 5 and 30 (eastern side, near the mouth of the kiln), 20 (90^{o} west) and 26 (south). The distribution of these samples does not suggest any apparent cause although the fact that two of these are from the corner of the entrance may be significant.

The site as a whole shows somewhat large scatter when compared with other kilns studied here, possibly reflecting very local movements due to clay shrinkage during, and possibly subsequent to, firing

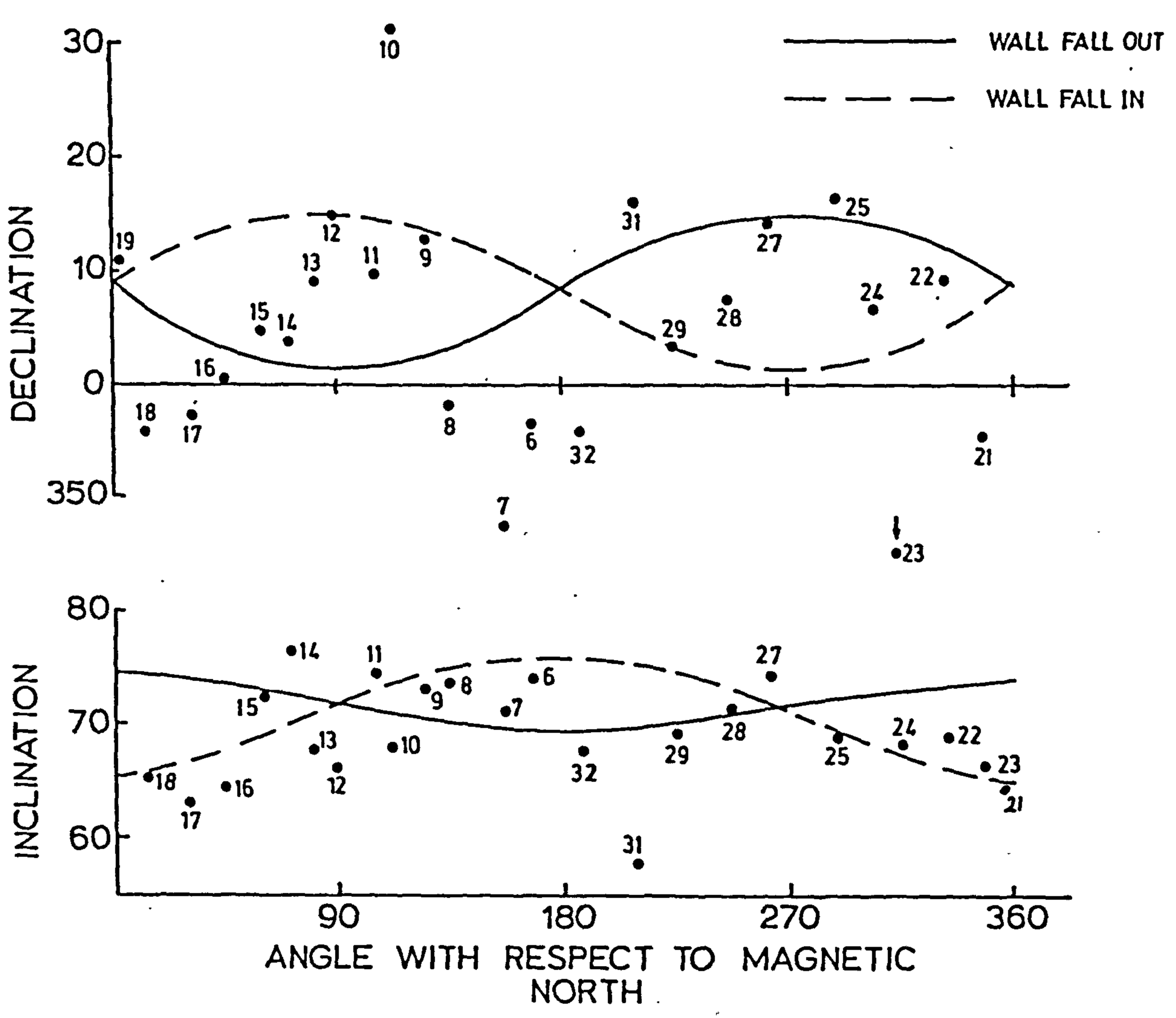

Fig. 2.21 The most stable directions of Green Lea kiln walls samples and their expected wall fall in and out sine curve

Table 2.21 Initial, most stable and pilot samples stability indices of Green Lea kiln

No.	Dec.	Inc.	Int. (mAm^{-1})	Dec.	Inc.	S.I.
M1	23.5	61.0	1743.6	27.1	64.3	
M2	6.7	73.1	1761.5	8.5	74.8	
M3	350.9	85.6	754.6	356.5	81.7	5.2
M4	359.0	67.9	1753.8	0.8	71.1	
W5	201.3	79.8	1096.1	247.9	82.8	
W6	3.0	69.7	1209.0	356.1	74.2	
W7	344.5	73.2	3423.4	347.4	71.2	
W8	353.9	76.8	6148.9	358.7	73.8	
W9	16.1	71.4	6813.9	13.0	73.4	4.7
W10	25.6	66.9	3412.9	31.4	68.0	
W11	12.1	73.2	1359.9	9.8	74.9	
W12	13.8	62.5	3289.2	15.3	66.3	
W13	19.7	60.8	7886.7	9.1	68.0	
W14	354.8	79.3	32928.0	3.5	76.5	
W15	342.6	80.1	17598.0	4.9	72.8	3.2
W16	357.9	59.8	4089.0	0.7	64.9	
W17	7.1	68.6	3089.0	357.3	63.6	
W18	340.3	70.1	1292.6	355.6	65.2	
W19	16.7	70.3	4545.1	10.9	68.9	
W20	30.7	79.9	48597.0	11.7	84.0	6.7
W21	359.2	65.3	7142.3	355.1	66.5	
W22	14.1	70.9	1580.9	9.1	68.9	
W23	344.7	65.8	1056.5	334.5	68.4	
W24	10.8	66.3	1243.7	6.9	68.1	
W25	7.5	66.5	7008.9	21.1	68.5	
W26	53.1	71.5	8380.9	45.7	71.6	
W27	15.8	76.3	3584.9	19.5	74.1	
W28	359.7	65.6	2951.7	7.9	71.6	
W29	355.8	66.3	6848.9	3.5	69.1	
W30	50.0	71.3	9240.2	39.2	70.6	

Table 2.21 (continued)

No.	Dec.	Inc.	Int. (mAm^{-1})	Dec.	Inc.	S.I.
W31	12.9	65.2	1193.2	20.9	57.6	4.0
W32	349.0	63.5	1615.4	356.3	67.5	
M34	25.6	70.4	2099.5	9.3	77.4	
M35	344.8	69.9	11705.2	359.3	64.9	
M36	356.7	74.1	1660.2	5.6	72.1	
M37	15.3	69.6	4799.6	9.8	74.6	
M38	8.2	58.3	5814.3	1.7	71.7	3.9
S39	203.7	-23.0	8475.0	246.5	-56.3	
S40	253.6	-8.7	9327.7	265.8	-7.2	2.6
S41	277.9	-40.6	11055.8	255.8	-14.2	
S42	346.0	41.2	16634.0	351.7	29.7	3.1
F43	326.7	59.6	1779.9	310.9	61.7	
F44	348.1	54.7	520.9	355.1	53.1	
F45	330.9	55.9	126.3	337.0	56.8	
F46	339.6	57.8	451.5	343.3	53.7	
F48	210.9	55.6	7115.8	265.1	52.5	
F49	340.5	69.3	3206.0	332.4	72.0	
F50	333.6	60.7	6704.6	340.5	57.1	
F51	10.5	60.9	7477.2	9.3	68.8	
F52	54.0	71.3	8844.3	54.6	68.5	4.7
F53	7.7	59.6	4616.9	14.9	63.6	
F54	5.3	55.5	2026.7	11.7	58.8	
F55	14.6	65.5	3033.5	4.1	70.0	
F56	342.3	67.8	1442.3	352.2	69.2	
F57	349.8	60.7	932.3	345.8	65.6	

W : wall

F : floor

M : mouth

S : slag

although such movements do not show any systematic pattern.

Assuming that the magnetic directions of the wall samples were refracted by the field of an already cooled floor, then such a scatter would be expected to be systematic, but no such pattern is observed.

Floor samples

The directions of floor samples collected along a NS profile in the kiln, together with the wall samples at each end, 26, 12 (of which 26 is anomalous) were plotted (fig. 2.22). The plot shows sudden directional changes between the floor and the wall. The floor samples have more westerly directions and relatively shallow inclinations, with a possible decrease from north to south.

Two other sets of samples were collected parallel to the NW wall, one close to it and the other some 20 cm. away. The declination plot shows that both sets of samples change easterly towards the west, while the wall samples show the opposite directional change. The plot of inclination curves show that samples nearest to the wall are less scattered than those further away from it. In fact the shape of the inclination curve of the set of samples near the wall is similar to that of the wall samples. However, the directions of the floor samples show a higher degree of scatter than the wall samples.

Mouth samples

Samples were collected from both parallel sides, the NE (1 - 4) and SE (34 - 38) of the kiln entrance. The most stable directions, together with samples 5 and 32 which are in the corner, are plotted in fig. 2.23. The directions on both sides show similar degrees of scatter, about 7^{o} in declinations and inclinations (apart from sample 1). This

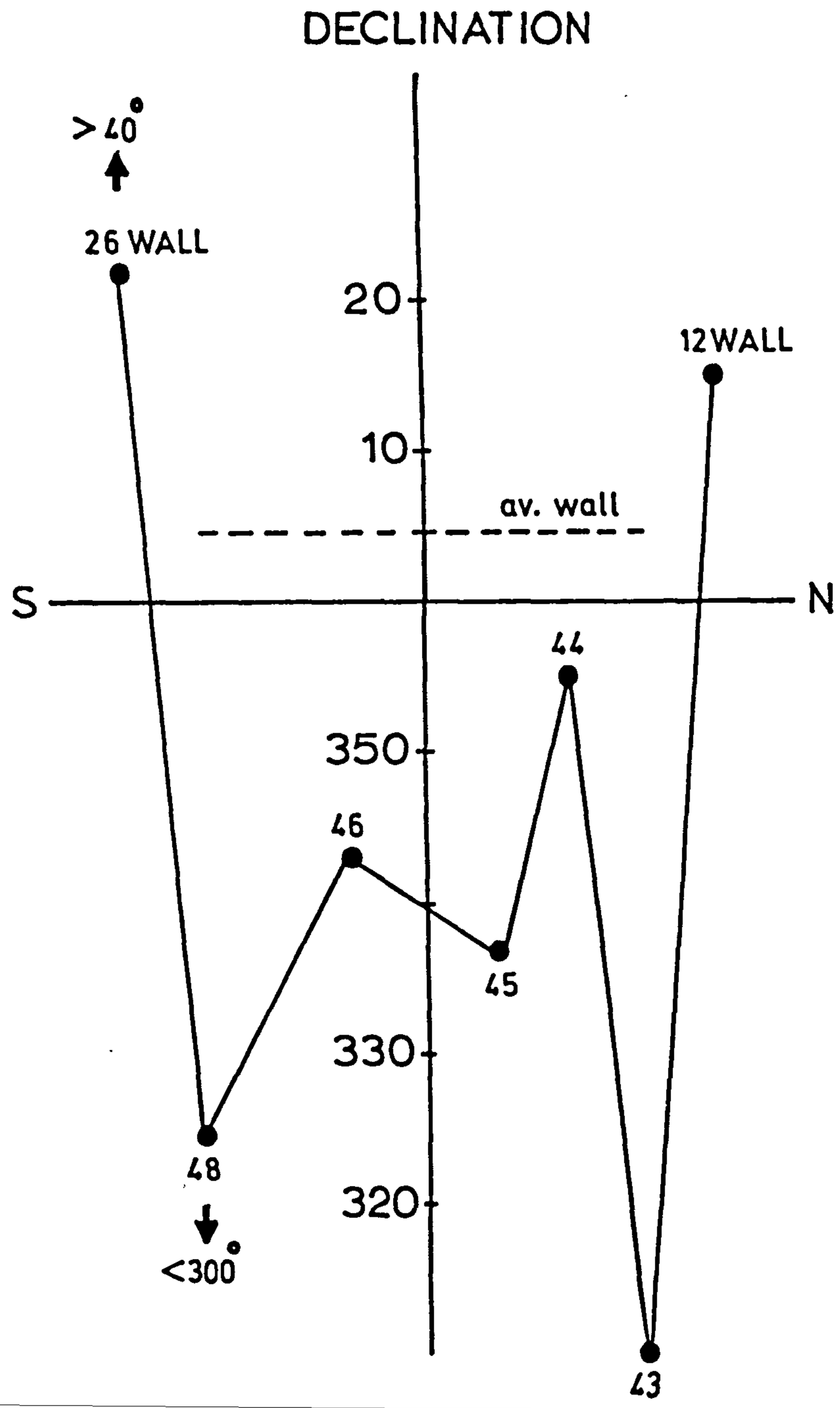

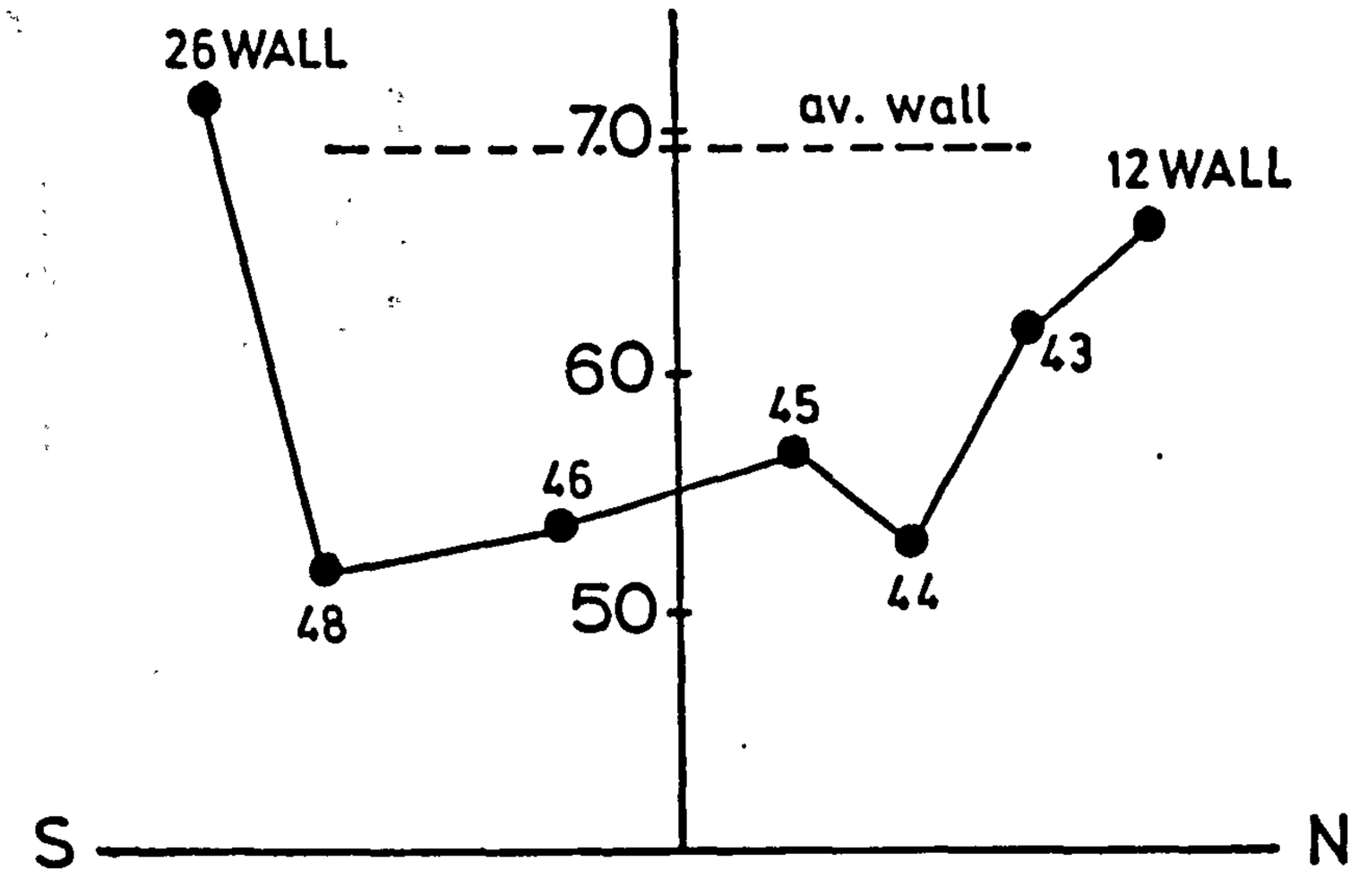

Fig. 2.22a Magnetic directions of Green Lea kiln NS profile floor samples, with wall samples 26 and 12

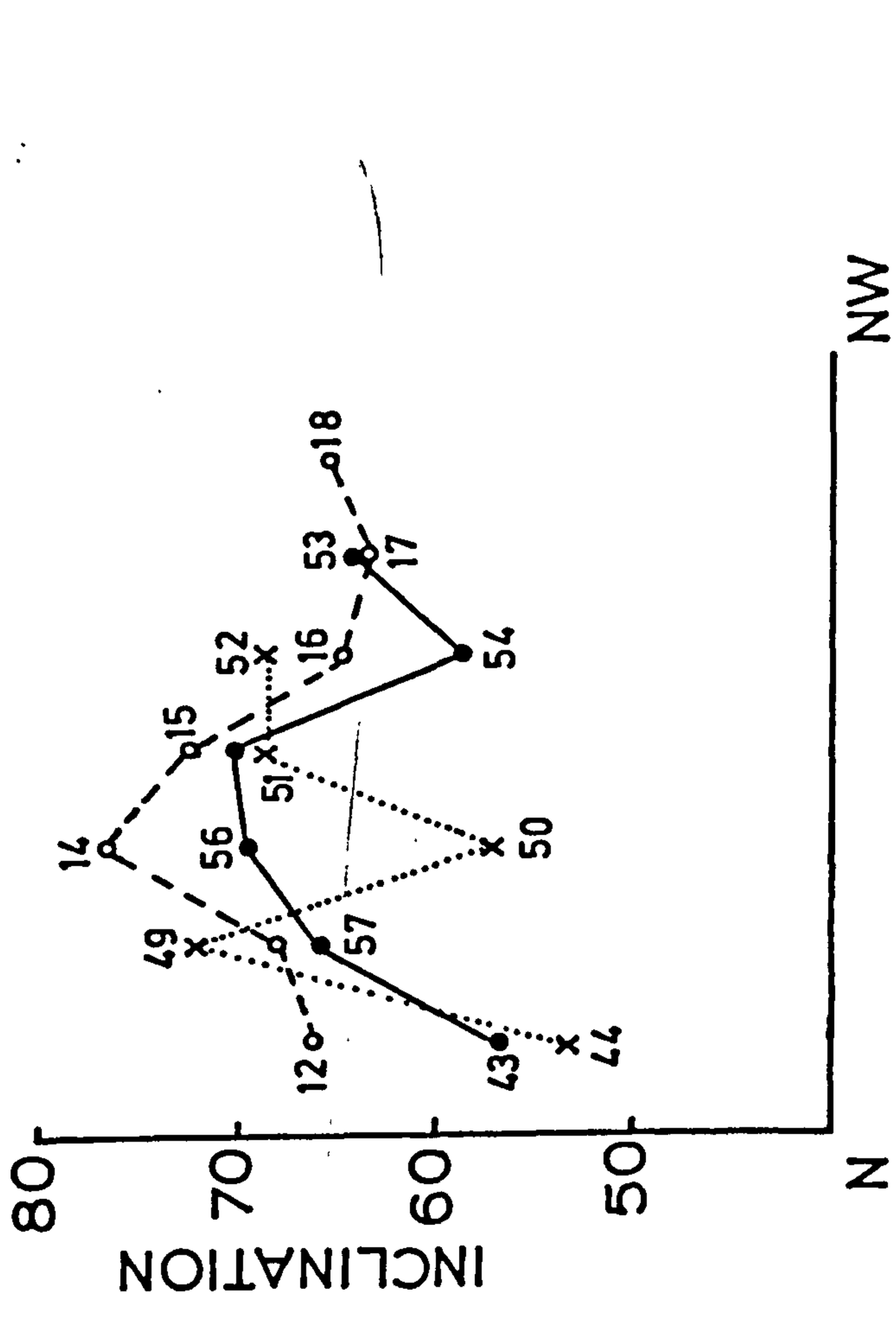

Fig. 2.22b Magnetic directions of floor and wall samples along the north-west

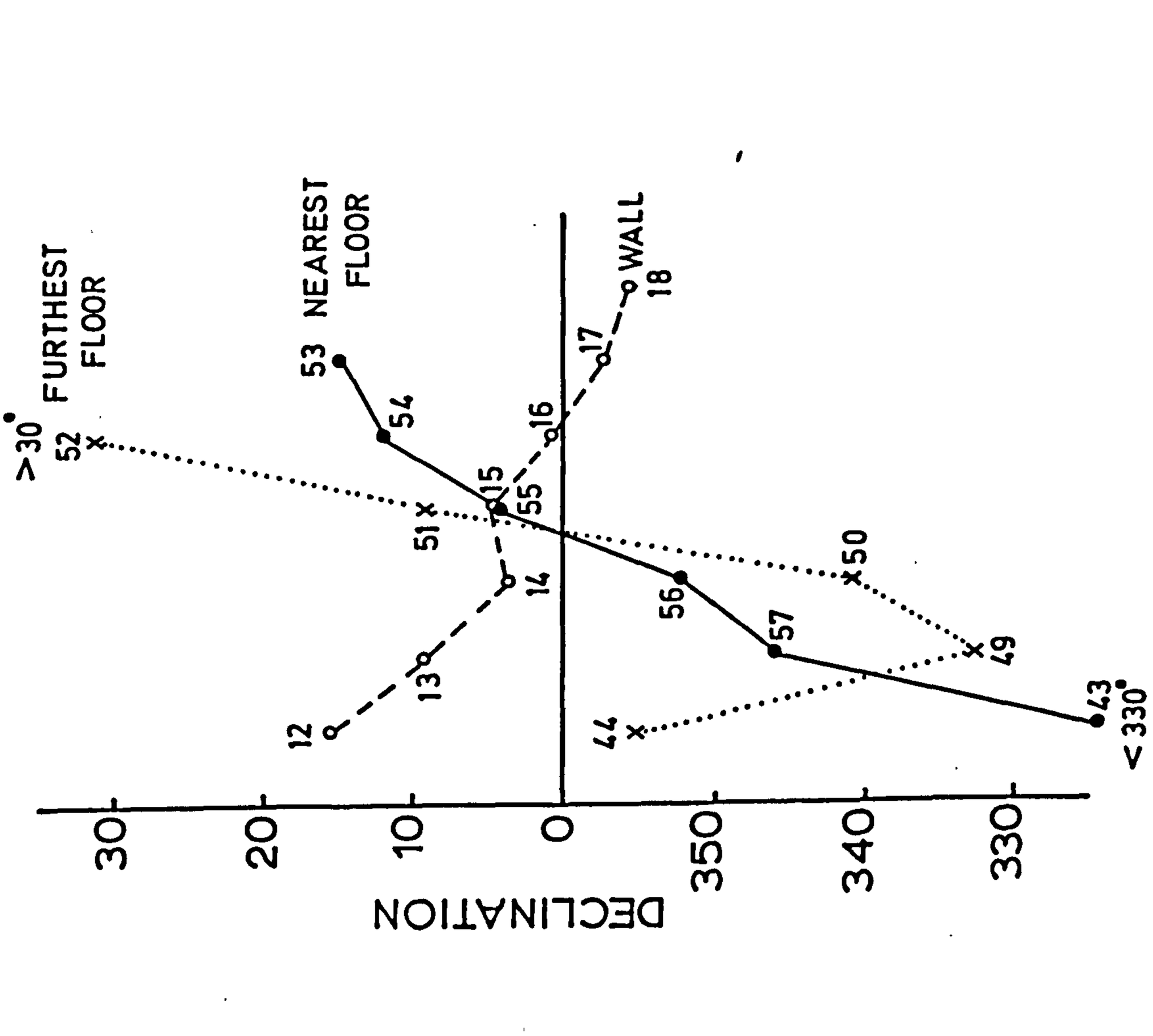

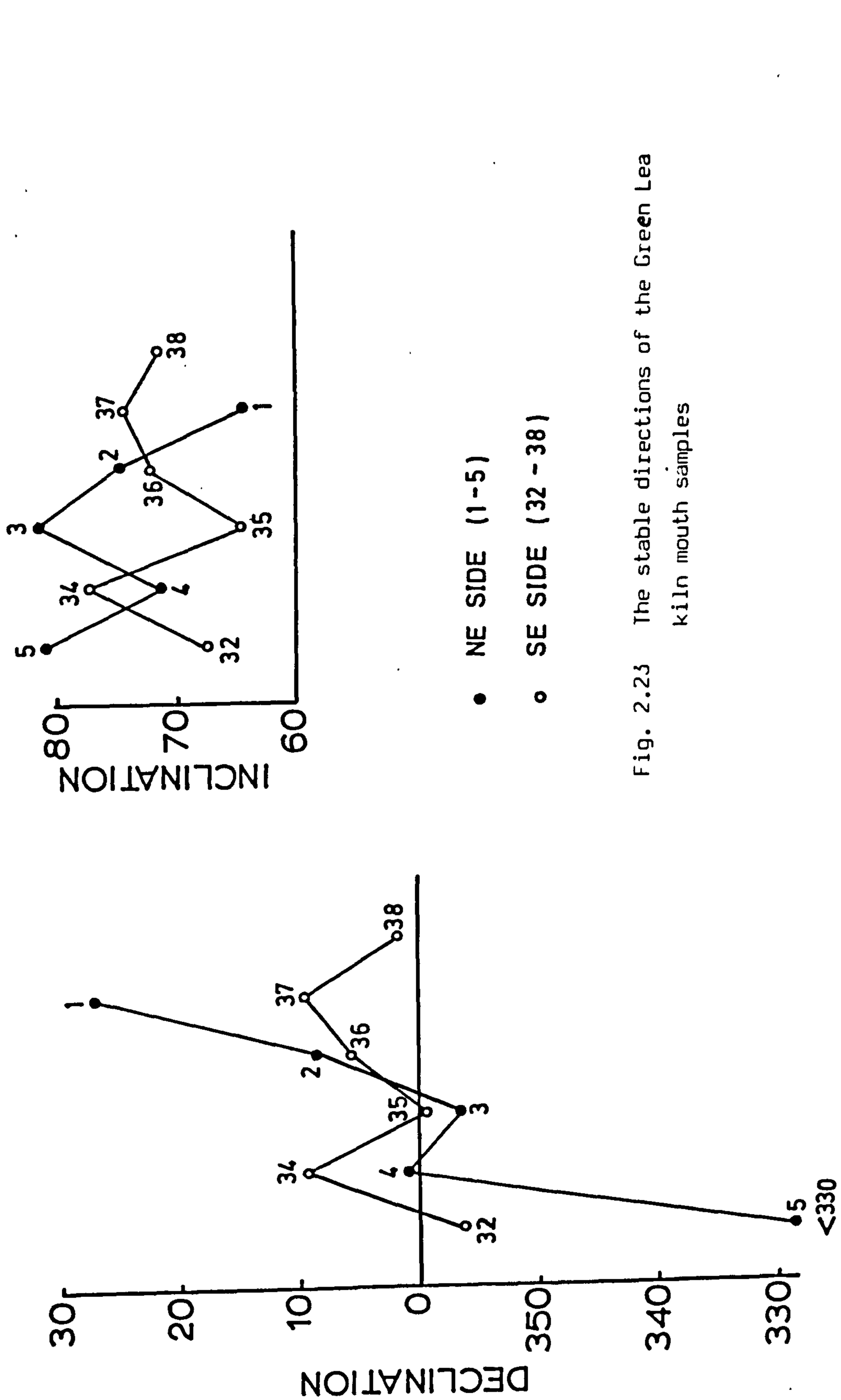

- NE SIDE (1-5)
- SE SIDE (32-38)

Fig. 2.23 The stable directions of the Green Lea kiln mouth samples

scatter is similar to that observed for the walls but less than that for the floors. Their mean declination values were similar to the wall samples but their average inclination was 4.3^{o} steeper.

Slag samples

Four samples were collected and appeared to be not in situ. These samples had very high intensities and their directions deviated from those observed in the other parts of the kiln, as the slag had very shallow inclination. These slag samples could either be of different age or, more probably, they had been moved since cooling.

Discussion

Samples collected from Green Lea kiln site showed a greater scatter in directions than is expected for such a well-preserved structure. Floor samples were more scattered than wall and mouth samples and they tend to show shallower inclinations. The mean directions of the wall and mouth samples were consistent with each other and they agree with the expected late Roman archaeological age of the kiln, while the floor samples are 12^{o} westerly and 6.4^{o} shallower than the expected directions.

The scatter in the directions of the wall samples could be due to random movement. This is more likely to occur in large kilns, like GreanLea kiln, as the structure of the kiln cannot perfectly support the weight of the walls and the resultant movement will probably be inward, i.e. the kiln wall will tend to collapse inwards. However, only weak evidence of fall-in were observed in the inclination curve. Movements in the walls could also be due to inhomogeneous loading. The scatter in directions could also have been due to distortion of the magnetic field by magnetization of the floor, if this cooled first. Such an effect

would be expected to be systematic and also tend to make the intensities lower in the wall than the floors. However, there is no systematic pattern and the intensities are comparable with each other so any refraction effects appear to be low. On the other hand, refraction could be in the wall itself as the outer face is expected to cool quicker and hence distort the magnetization acquired by the inner face. Such effect cannot be determined in this kiln as all samples were collected from the inner face. (This effect is studied in the later kilns in this section).

Distortion of the magnetic field could be due to the presence of iron objects within the kiln, which could have been introduced with the fuel and then removed after cooling. Disturbance could also be as a result of the slag located near the kiln.

The scatter of the directions of the floor samples could be due to distortion of the magnetic field by the magnetization of the wall, if this had cooled first. The inclination of the floor samples, collected along the NS profile, were steep in the region of north and shallow towards the south, similar to that predicted by Aitken and Hawley (1971). If this directional change is due to refraction then floor samples near the wall will be more affected and scattered than those which are away from the wall. In this kiln, samples away from the wall were more scattered than those close to it. This probably suggests that floors and walls were disturbed separately, and this disturbance is not uniform.

Floors are less likely to undergo consistent movement than walls, unless the whole structure was moved, but it is possible that the kiln was disturbed randomly either by different degrees of loading or shrinkage of the clay due to the heat. Similarly, floors could easily

be disturbed during pot removal or subsequent excavation. Walking over the floors, for example, could result in compaction, causing the magnetic particles to become shallower.

The mouth of the kiln can be expected to be less rigid than other parts of the kiln, as the construction of a kiln is based mainly on keeping the walls surrounding the kiln very rigid, while the mouth of the kiln is not necessarily well built.

The scattered directions could also be due to refraction in the mouth walls as the outer parts are expected to cool quicker and hence distort the magnetic field in which the inner faces are cooling. This could also occur between the two walls of the mouth, although it is not very likely in this kiln as the distance between the two sides of the kiln is about 50 cm. and the two parts are expected to cool at the same time.

The distortion in directions of the whole kiln could be due to refraction of the magnetic field by the magnetization of each part of the kiln. This effect is expected to be systematic if the magnetization of the whole kiln was homogeneous as the field will be refracted by the same degree on the whole kiln. However, since the intensities of the overall samples are not similar, this refraction will tend to be random. The intensities of some of the scattered samples (20, 26, 30, 42, 48, 52) and also slag samples are within the higher range of the overall intensities. However, there are still other samples with similar intensities but showing grouped directions. Although this refraction effect is very difficult to predict, it was noticed that samples with the highest intensities (table 2.21) tend to have relatively steeper inclinations (the same applies to floor samples). This steep inclination could be due to refraction of the magnetic field by the magnetization of the stucture.

2) Bryn-Castell, N. Wales (Roman)

A total of 14 samples were collected from a round (30 cm. diameter) kiln. All samples were taken from the walls because the floor appeared to be disturbed. Some parts of the kiln were thick enough to allow some sampling of both the inner and outer faces of the kiln walls (fig. 2.24). Both were well fired.

The declinations of the most stable directions (fig. 2.25) shows that samples 1,2,5,6,8 and 10-13 are consistent with fall out by about 1^{o} while samples 3,4,7,8 and 14 are more consistent with fall-in of some 2^{o}. Since samples 3 and 4 were collected from the outer face and samples 5 and 6 were from the inner face of the same part of the kiln, it is clearly not possible for both fall-in and fall-out to occur for this part of the wall. The inclination curve (fig. 2.25) shows that samples 2, 3, 9, 10 and probably 1 and 11, are consistent with a wall fall-out of about 2^{o}, while samples 4 - 8 and 12 - 14, and probably 1 and 11, are consistent with fall-in by more than 2.4^{o}.

This means that samples 12, 13, 5, 6 and 8 show evidence of fall-out for their declinations and fall-in for inclinations, also samples 3 and 9 show evidence for fall-in for their declination and fall-out for their inclination. Such interpretations are clearly incompatible.

Some distortion is observed in samples collected from the same position, but on inner and outer faces of the northwestern wall (3, 4, 5,6) (table 2.22), although the range is low; declination $\pm 3^{o}$ and $\pm 1^{o}$ in inclination. Samples 3 and 4 declinations are westerly and those of 5 and 6 are easterly. As the outer face cools quicker, therefore the inner face will cool in a field which is distorted by the magnetization of the

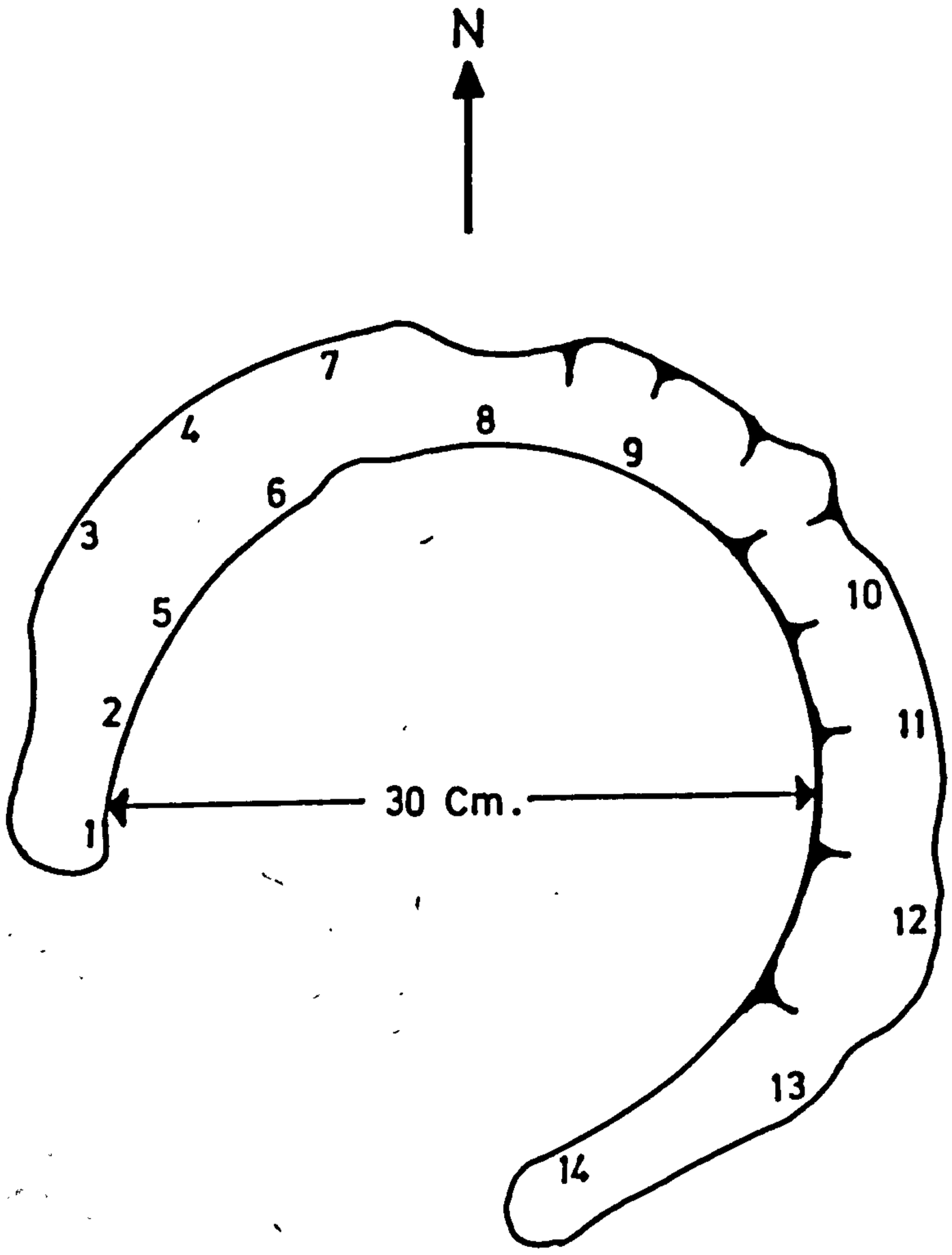

Fig. 2.24 Samples distribution of Bryn-y-Castell kiln

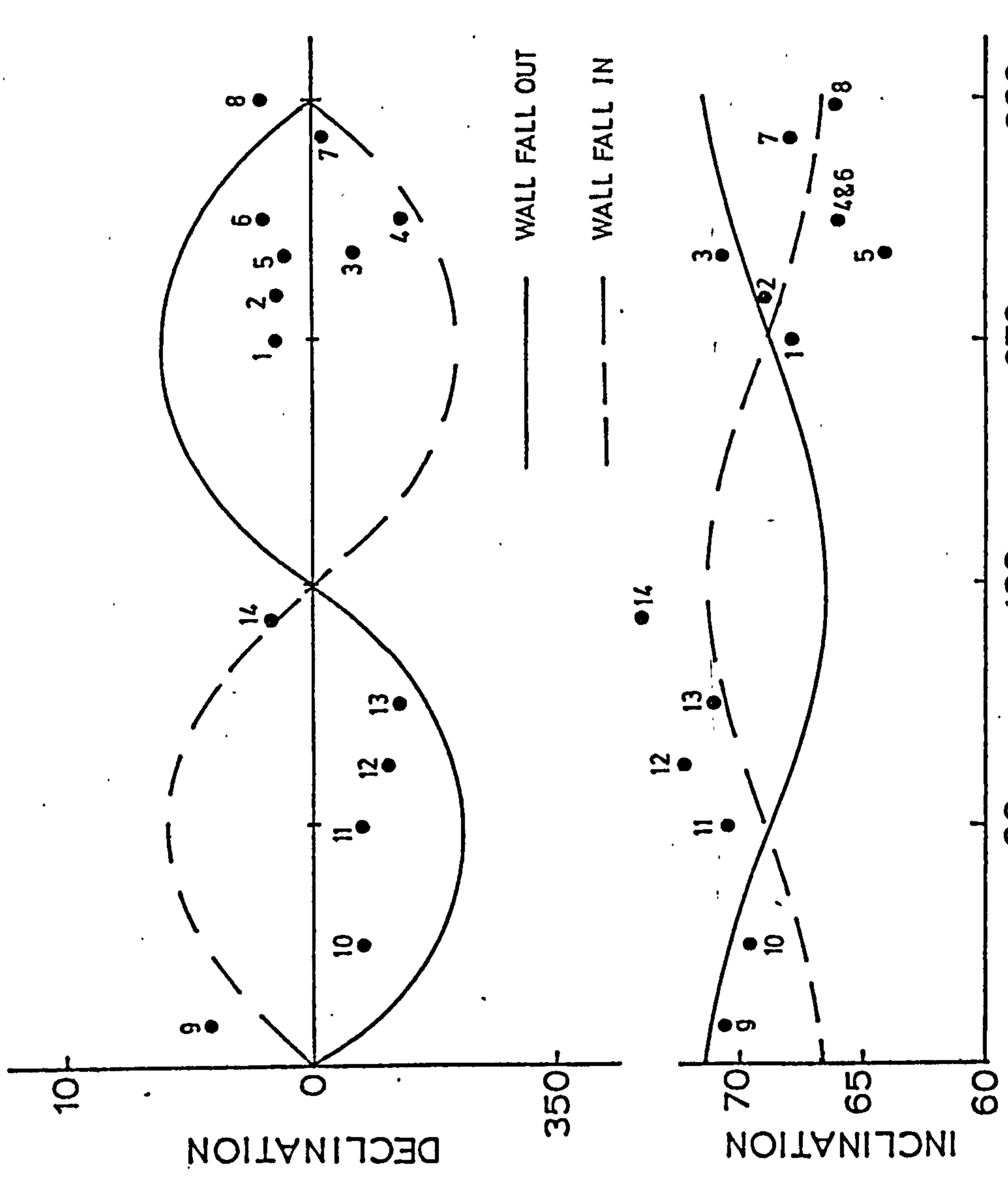

Fig. 2.25 The stable directions of Bryn-y-Castell samples, with their expected sine curve for kiln wall fall out and in

Table 2.22 Initial, most stable directions and pilot samples stability indices of Bryn Y Castell kiln

	Initial			Most Stable		
Sample	Dec.	Inc.	Int mAm^{-1}	Dec.	Inc.	S.I.
1	3.7	71.1	1678.7	1.7	67.9	
2	10.5	64.0	635.2	1.6	69.0	
3	3.7	73.1	28110.0	358.6	70.8	6.3
4	5.4	69.3	1311.1	356.4	66.8	
5	359.9	66.1	1453.7	1.2	64.0	
6	356.7	64.2	27431.0	2.0	66.6	
7	5.3	70.8	14578.0	359.9	68.1	4.5
8	357.5	71.1	9843.7	2.1	66.3	
9	1.2	65.2	1203.1	4.4	70.6	
10	356.8	68.1	1756.8	358.0	69.8	
11	359.8	69.0	15688.0	358.2	70.5	5.3
12	351.8	70.3	1041.0	357.0	72.2	
13	7.2	67.8	5234.5	356.5	71.0	
14	4.7	67.3	731.8	1.9	74.0	

outer side. The same applies for the other samples from the outer side (7, 10, 11, 12 and 13) which are westerly, while the inner face samples are more to the east (1, 2, 5, 6, 8, 9 and 14). This effect will probably vary depending on the magnetization of the overall kiln, its consistency and the precise distance apart of the samples, and therefore it is expected to be higher at certain parts of the kiln. As the intensity of magnetization of these samples was very high (table 2.22), it would be expected that most directions would have been distorted by the high magnetization of the kiln. Nevertheless, the mean direction of Bryn Castell kiln provided a reliable date and the mean value was nearly on the curve. It would appear, therefore, that the walls of this strongly magnetized kiln do not show significant effects of either wall movement or refraction.

3) Burrow Hill, Suffolk (750 - 840 AD)

A total of 12 samples were collected from this kiln (60 cm. diameter). Only one sample was taken from the floor (fig. 2.26).

The most stable directions of magnetizations show that the declinations of samples collected from the western side of the kiln are more easterly (including sample 12 from the floor and 11 from the mouth), than samples from the eastern side.

The most stable directions of magnetizations show that the declinations of samples collected from the western side of the kiln are more easterly (including sample 12 from the floor and 11 from the mouth), than samples from the eastern side.

The declination plot (fig. 2.27) shows that the samples are consistent with kiln wall fall-out (except samples 6 and 8) with a value which is near to 2.4^{o}. The inclination values also show a general trend

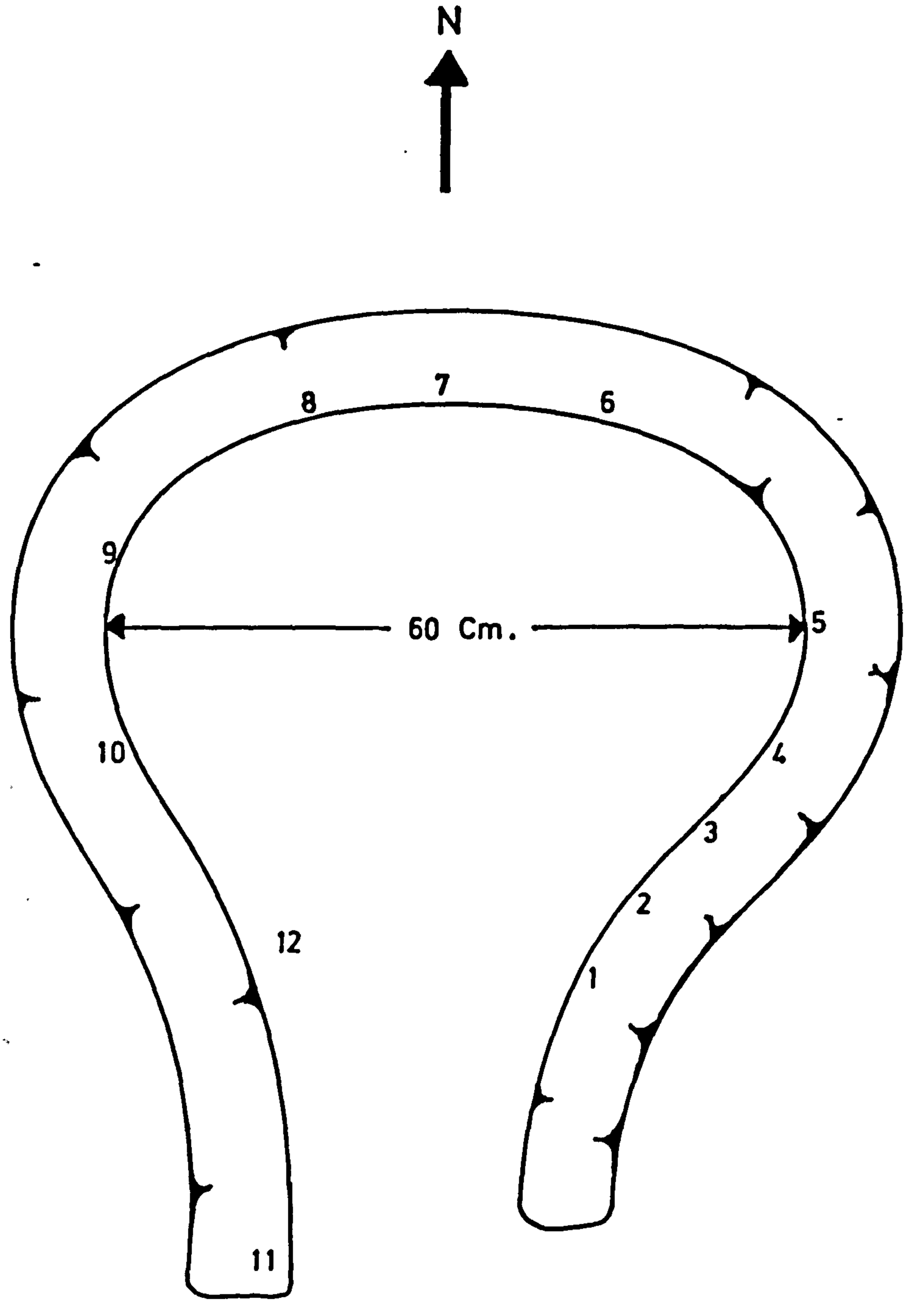

Fig. 2.26 Samples distribution of Burrow Hill kiln

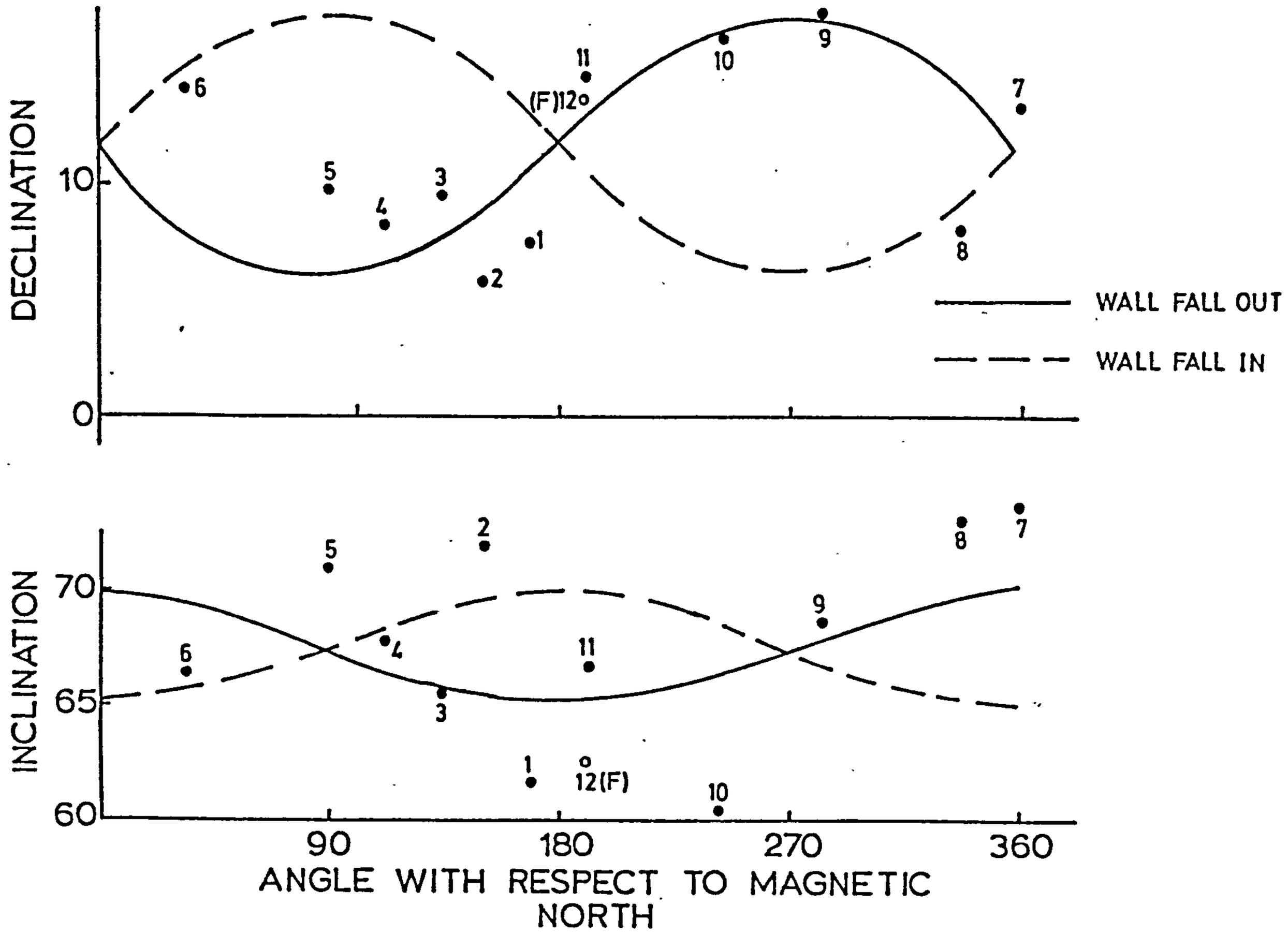

Fig. 2.27 The stable directions of Burrow Hill samples, with their expected kiln wall fall in and out sine curve

Table 2.23 Initial, most stable direction and pilot samples stability indices of Burrow Hill kiln

	Initial			Most stable		
Sample	Dec.	Inc.	Int. mAm^{-1}	Dec.	Inc.	S.I.
1	3.9	68.9	1256.1	7.5	61.8	
2	5.3	80.9	795.6	5.9	72.0	4.7
3	6.4	59.2	56.0	9.5	65.5	
4	358.5	75.2	166.0	8.3	67.8	5.7
5	359.7	74.0	103.0	9.9	71.0	3.2
6	6.7	75.2	465.2	14.1	66.6	
7	4.2	77.9	1012.7	13.3	73.9	
8	2.4	76.1	5.3	8.6	73.1	5.8
9	20.9	75.3	101.0	17.3	68.9	
10	7.1	73.2	230.0	16.4	60.3	4.0
11	21.0	67.2	831.1	14.8	66.9	
12	11.0	59.9	330.5	13.9	62.6	3.1

which is consistent with wall fall-out, but this is not clearly observed.

The floor sample (12) shows a declination consistent with the wall samples but with shallower inclination.

The intensity of magnetizations of these samples is not very strong (table 2.23) compared with the magnetization of the previous site (Bryn-Castell). Therefore the effect of refraction due to the magnetism of the structure is expected to be lower. The somewhat systematic directional changes are therefore more likely to be explained in terms of wall movement, although the scatter in direction is not very high (about 5^{o} for both declinations and inclinations). However, the walls were well packed and it is difficult to see how such fall-out movement could have occurred.

Spong: Hill Kiln

A total of 25 samples were taken from a pillar, 30 cm. high, 15 cm. wide, from inside this kiln (fig. 2.28). These were provided by Dr. A.J. Clark, Ancient Monuments Laboratory. The field orientations were done by attaching 2 plastic discs on the top of the kiln (samples 21 and 22). Additional discs were fitted later, and oriented in the laboratory (sun compass) relative to the two above samples. A large number of plastic discs were glued, but only 22 samples were obtained as there were some difficulties in breaking them, and large pieces were broken due to inhomogeneities within the kiln. As shown in plate 1, some of the discs on the right side of the plate were broken as a whole block fell away before orientation.

To prevent orientation errors during sampling the inner face, one of the outer samples was not removed from the kiln to allow

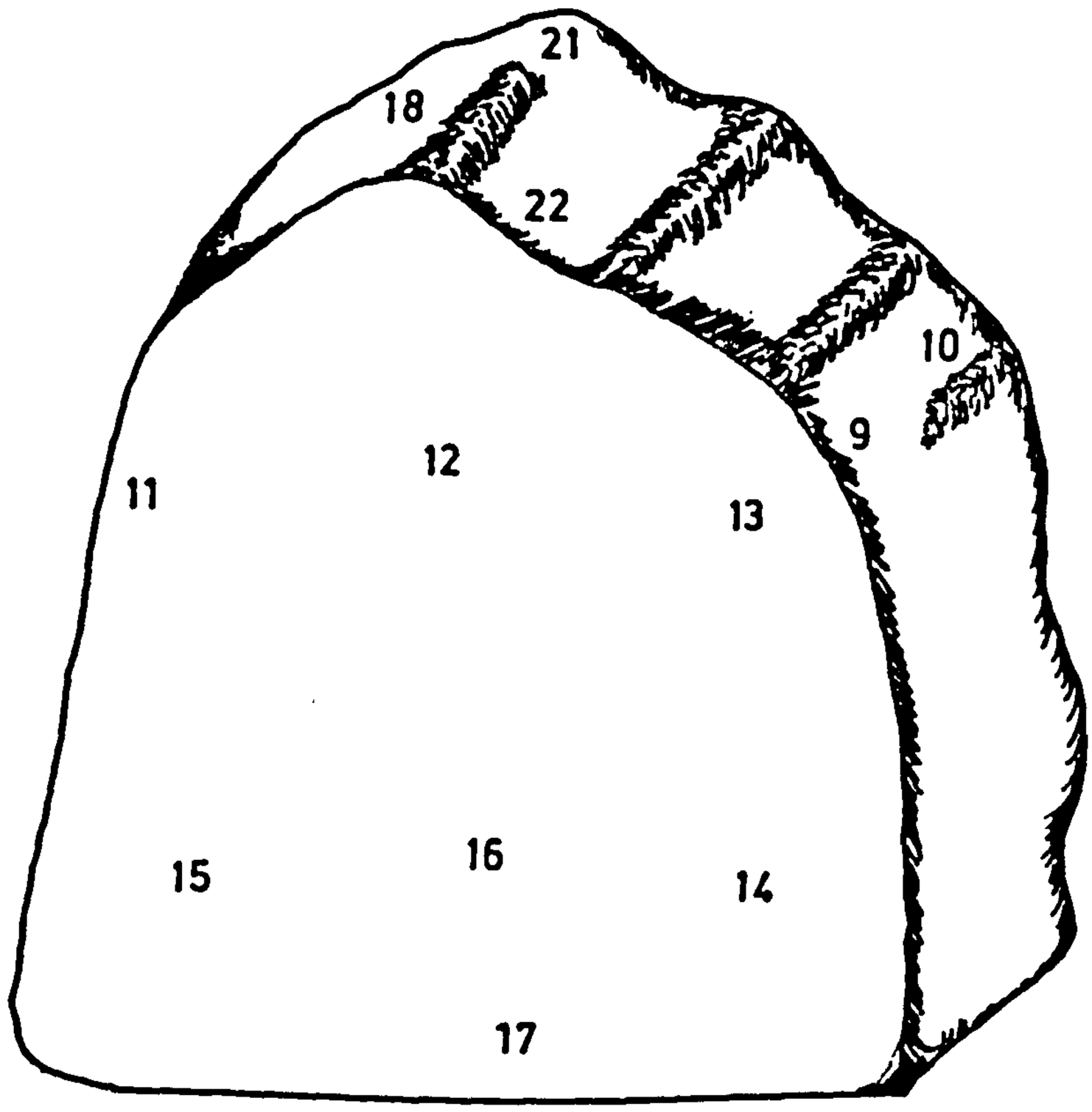

EASTERN FACE

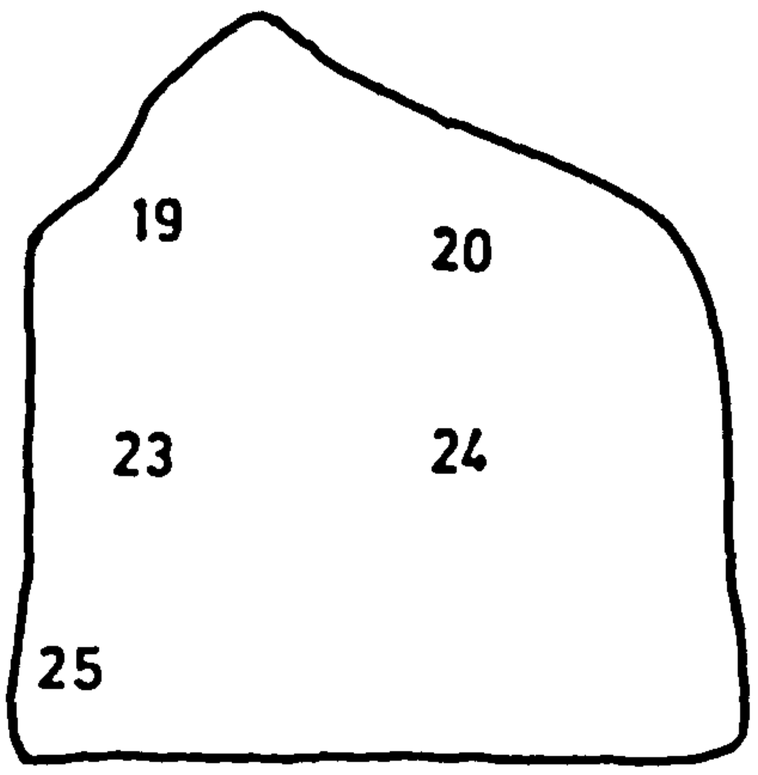

INNER EASTERN FACE

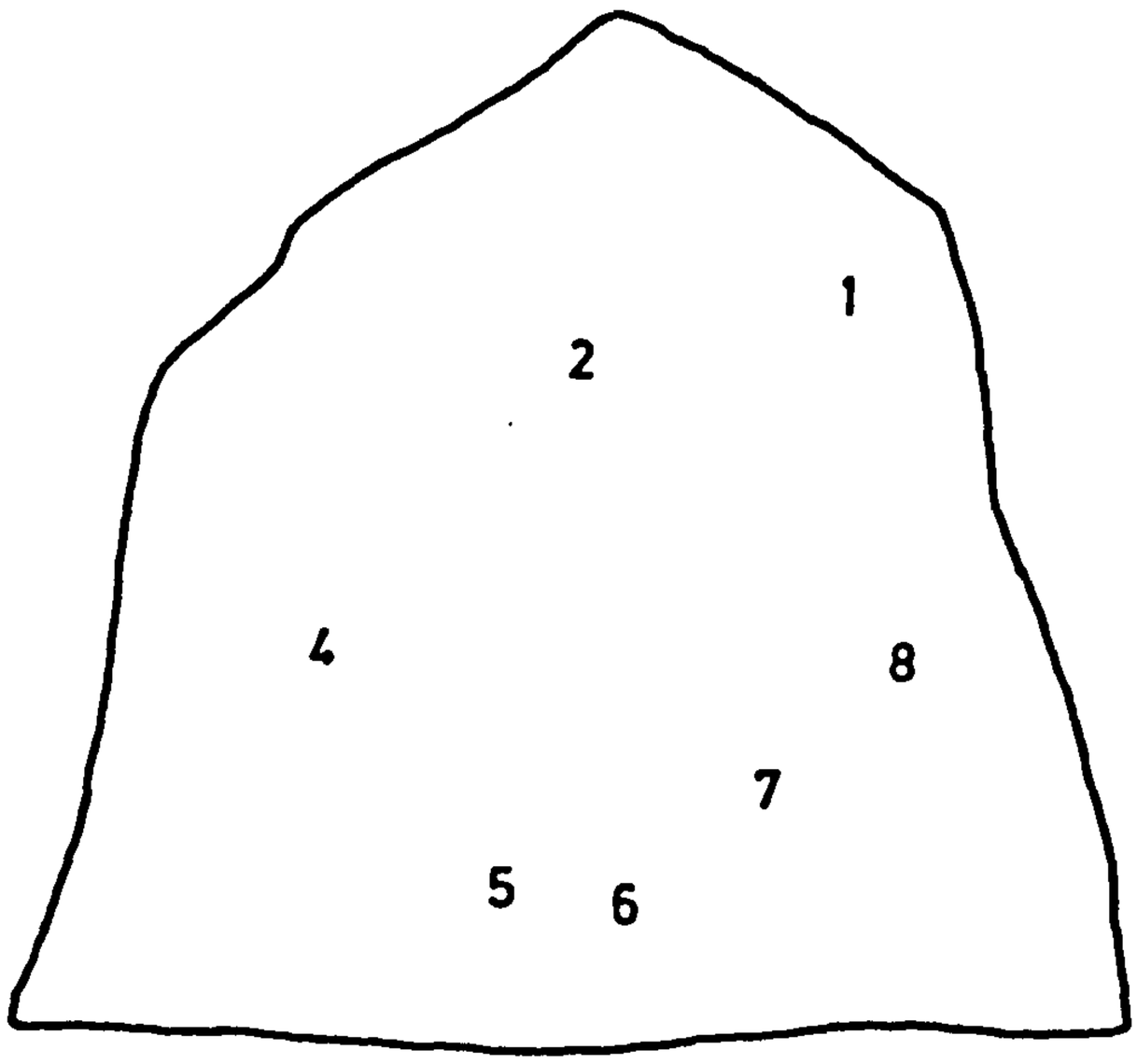

WESTERN FACE

Fig. 2.28 Samples distribution of Spong Hill kiln

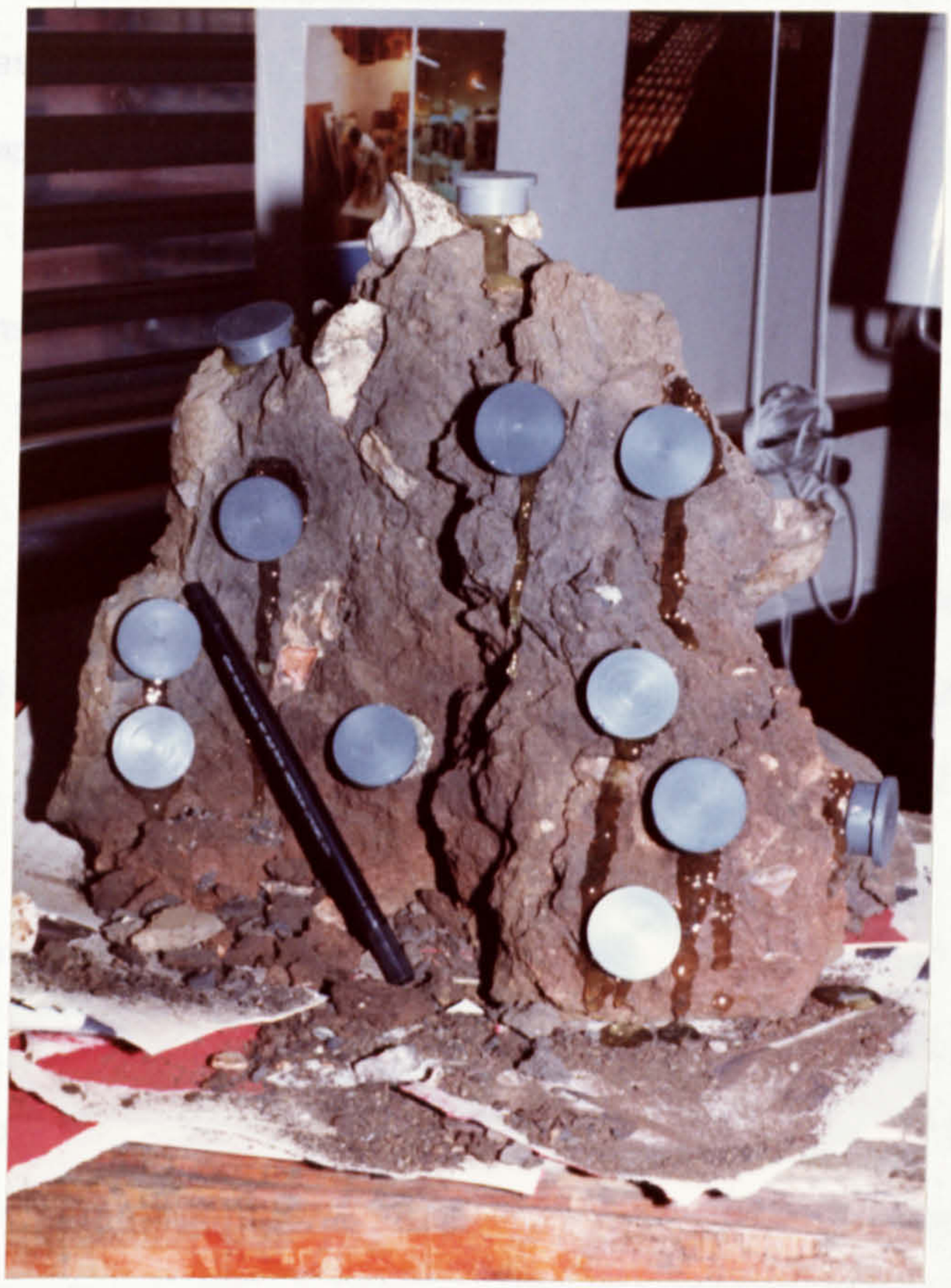

Plate 1 Spong Hill kiln

further comparison with the orientations of the inner samples. Although orienting the samples was difficult, they were considered reliable to within a few degrees.

The samples were from the eastern face (12 - 17), the western face (1, 2, 4 - 8) and the inside of the pillar (19, 20, 23 - 25). Samples 9 and 10 were taken from the top with sample 9 being in the middle, and sample 11 was taken from the edge, although its red colour was similar to the inner samples. The other samples were dark red.

The outer samples (eastern, western and top samples) showed directions which were consistent with each other (fig. 2.29) (table 2.24) while the inner samples gave very scattered directions.

The scattered directions in the inner samples could be explained in terms of refraction. The inner samples being expected to cool in a field which was probably distorted by the magnetization of the outer samples. However, such an effect would be expected to be systematic and not random. Additionally, the intensity of the inner samples is comparable with that of the outer samples, but would be expected to be lower if acquired in the geomagnetic field and an antiparallel field generated by the outer parts of the pillar. On the other hand the pillar contained lumps and these inhomogeneities could affect both directions and intensity.

Discussion and Conclusions

The observed scatter of magnetic directions in ancient kilns can be explained in terms of the following categories:-

1) Wall movements:- Although systematic wall movements were not observed in this work, they are considered possible, although only rarely for the whole structure. If these movements were consistent (wall fall-out or in)

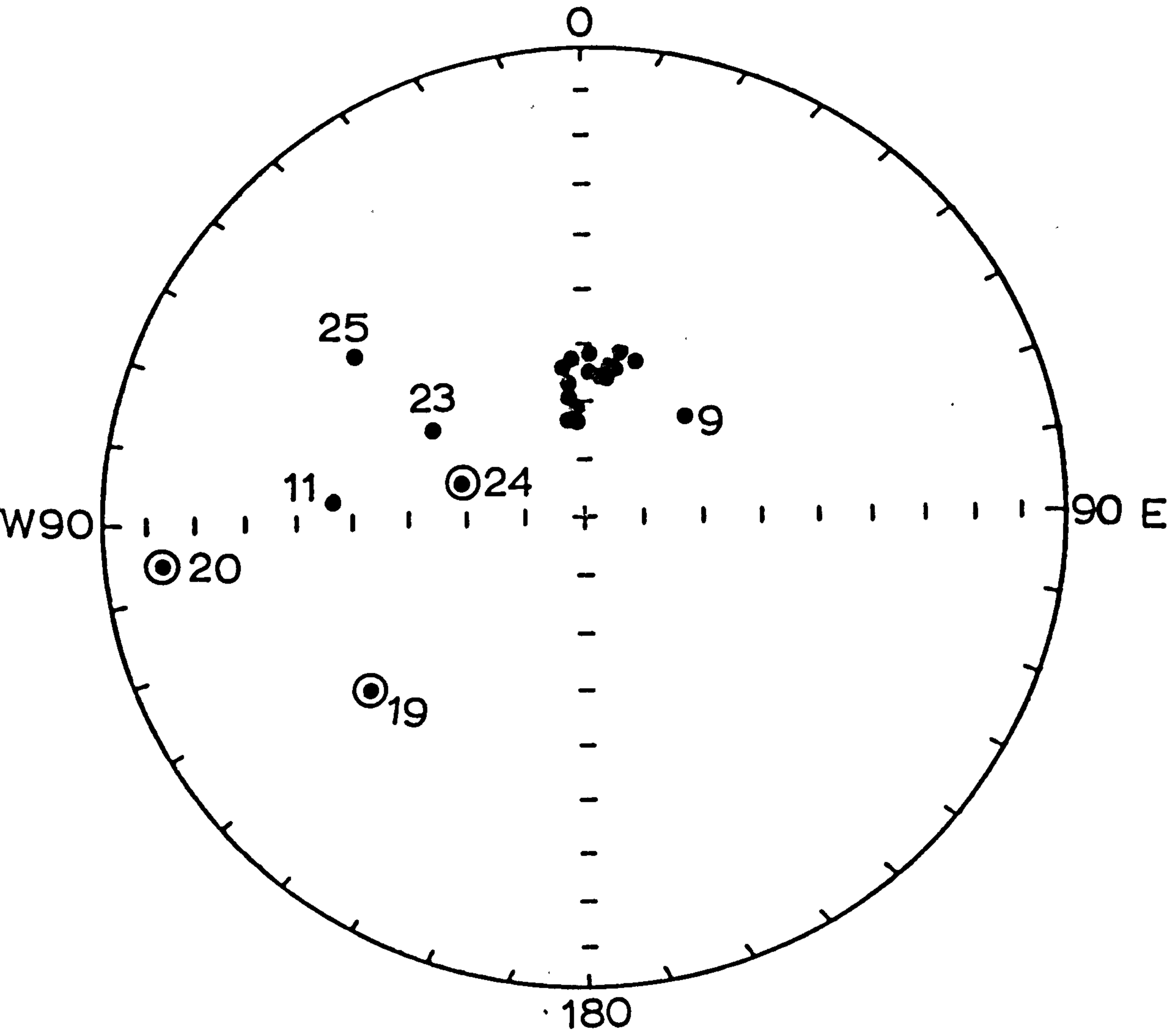

Fig. 2.29 Most stable direction of the Spong Hill samples

Table 2.24 Initial, most stable and stability indices of Spong Hill kiln samples

No.	Initial Dec.	Inc.	Int. (mAm^{-1})	Most stable Dec.	Inc.	S.I.
1	341.5	72.8	228.9	354.0	69.5	17.8
2	350.7	70.1	687.1	352.3	73.0	10.1
4	355.3	69.4	170.9	2.3	65.4	12.0
5	357.0	66.6	69.3	3.3	62.7	7.7
6	355.8	69.1	303.7	354.9	67.0	9.7
7	16.1	64.4	1128.0	19.2	62.2	10.1
8	358.5	78.0	174.9	455.6	73.0	8.3
9	39.7	62.5	245.3	45.1	65.0	44.7
10	354.1	62.5	708.5	354.5	62.4	17.0
11	277.3	44.4	2054.2	275.0	46.5	20.4
12	11.2	70.0	371.3	358.2	71.1	15.4
13	17.4	61.2	653.5	12.9	61.7	17.8
14	15.6	59.5	104.9	11.4	62.5	9.4
15	354.0	65.1	1915.3	353.7	64.4	16.9
16	3.5	62.0	504.1	351.9	64.3	11.2
17	11.8	62.1	3.5	8.3	65.6	3.9
18	5.4	63.7	1092.1	3.3	65.6	7.7
19	213.4	75.6	1671.3	232.4	-43.3	10.5
20	264.9	-14.8	101.7	264.9	-14.0	11.0
21	354.0	67.9	375.9	352.1	68.3	7.3
22	352.4	69.0	2023.8	357.8	71.8	32.9
23	290.3	59.0	503.9	301.3	60.0	5.9
24	287.9	67.5	1195.1	288.0	-68.1	14.5
25	306.3	40.3	401.1	306.0	41.0	13.7

then the directional changes would also be constant. However, it is possible to have local movements as a result of inhomogeneous loading, lack of rigidity or shrinkage in the clay. All these will cause scatter in the directions which could be partially systematic or random. The deviation in the magnetic directions will depend on the amount of the wall movement and are more likely to occur on large kilns, such as the Green Lea kiln, as the kiln will tend to collapse inwards due to the weight of the walls. The probability of movement will also depend on the height of the samples from the floor as parts of the wall nearer the floors probably undergo less movements than the higher ones.

2) Refraction:- This is a result of distortion of the earth's magnetic field by the already-cooled parts of the kiln. It could either affect the floors or walls, depending on which cools first, and depends on their distance apart as well as the relative strengths of the magnetization of the materials and the ambient earth's magnetic field. This refraction effect could be systematic if the already cooled parts had consistent intensities. On the other hand if the magnetization of the structure was inhomogeneous then this refraction effect could be more random.

The refraction effect could also occur within the wall itself, particularly if it was relatively thick. The outer face would then cool quicker, and hence its magnetization would distort the field in which the inner face was cooling. This effect was possibly detected at two of the kiln sites (Bryn-y-Castell and Spong Hill) but was found to be independent on intensity. The Bryn-y-Castell site had a high intensity yet only showed a consistent deviation (of about 6^{o}) between the directions of the outer and inner samples. On the other hand, the Spong Hill kiln

pillar, in which the intensity was relatively low and inhomogeneous (3.5 - 2054 mAm^{-1}) compared with the Bryn-y-Castell site (731 - 28110 mAm^{-1}), yet the directions showed a high degree of scatter. Therefore no evidence for refraction effects in these two kilns were clearly observed.

3) Small scale anisotropy:- Distortion in the directions could occur as a result of refraction of the geomagnetic field by the magnetic particles actually within each part of the structure. This could give systematic changes if the magnetization of the structure was homogeneous as the field would then be refracted to the same degree, otherwise the distortion would tend to be random. This effect was found to be independent of intensity, as the strongly magnetic kiln (Bryn-y-Castell) gave the most consistent directions. While the Spong Hill kiln pillar with relatively weak intensities, showed a higher degree of scatter in directions.

4) Iron objects and other magnetic disturbances:- Distortion of the magnetic field could also be due to the presence of iron or other magnetic objects within or around the kiln (Hoye, 1980) which were removed after firing the pottery. Such effects are probably localised and random, and would be very difficult to assess.

5) Fabric anisotropy:- Magnetic fabric anisotropy can significantly affect directions and intensities, and can be random or systematic. The construction of the kiln could result in a parallel alignment of the magnetic particles, particularly within the mud linings of the kiln walls, i.e. the easy planes of grains could become oriented parallel to the walls.

Under these circumstances the field acquired will not be that of the earth's magnetic field but partially turned into the directions of the easy planes. Such distortion in directions around the kiln would generally have a second

harmonic pattern, but no such effect was observed in any of the kilns, although inhomogeneous anisotropy could account for some of the observed directional distortions.

6) Local physical disturbances:- Floor samples in this work had shallower inclinations than the walls, as previously noticed by Aitken and Hawley (1971) who suggested that this could be explained in terms of refraction. Another explanation could be that shallower inclinations arise due to compaction during loading of the kiln as this will flatten the magnetic particles causing some anisotropy. Neither explanations are thought to account for the observations in this investigation. However, floors could easily be disturbed during pot removal, subsequent excavation or walking over the floors, thereby causing the directions to become scattered and probably causing some shallowing of the inclination due to vertical compaction.

In conclusion, it was found that most of the scattered directions observed in this work were random. Only weak systematic deviations were observed in two sites (Burrow Hill and some inclinations of floor samples from Green Lea kiln). These deviations were inversely dependent on intensity as the more strongly magnetic kiln gave the least scatter, yet most refractions and field distortions would be expected to be associated with the highest intensities. The largest kiln (Green Lea kiln) was the most scattered, and the smallest (Bryn-y-Castell) was the least scattered, therefore suggesting that the actual size of a kiln may be important. However, this was only the case for these four kilns and it is difficult to assess the effect of the size using the previously studied kilns, as most of them were collected from rescue archaeological sites in which sampling was only localised in the specific areas which appeared to be least disturbed. If the Green Lea kiln was sampled in only one area,

it too would show a low scatter.

Factors controlling the consistency of directions in kilns are considered to be variable and therefore no general correction for archaeomagnetic dating can be recommended at this stage. Each site needs to be treated or corrected separately according to an assessment of the previous factors. It is relevant that dating the structure with samples covering most of the kiln structure provides better data which allows a determination of the causes for the scatter in direction. However, if the deviation in directions is systematic then an average direction of samples taken systematically around the kiln will probably still give the true value as such a mean direction could reduce both first or second harmonic deviations as well as the random scatter.

The absence of systematic errors in the wall data and their consistency, both with each other and with the archaeomagnetic curve, suggests that walls may, in fact, be more reliable indicators of the ancient geomagnetic field than floors.

CHAPTER 3 ARCHAEOMAGNETIC WORK ON BRITISH SEDIMENTS

The following sites were investigated in an attempt to assess the potential of using sedimentary deposits in archaeological environments for archaeomagnetic dating purposes:

1. Lurk Lane, Beverley, Yorkshire
2. Carlisle Archaeological site, Carlisle
3. Grove Priory, Leighton Buzzard
4. Lincoln Archaeological site, Lincolnshire
5. Wharram Percy, Yorkshire
6. Westbury Sub-Mendip, Somerset

3.1 Lurk Lane, Beverley, Yorkshire (Medieval)

This excavation is located behind Beverley Minster, Lat. 53.8N, Long. 0.4W, and comprises various levels of habitation of the priory. Several hearths from this excavation have already been sampled by the Ancient Monuments Laboratory, Department of the Environment, each with a corresponding floor level formed mostly of puddled clays. Samples of these clays were taken corresponding approximately to the 13th and 14th centuries levels in order to test if such materials were suitable for archaeomagnetic dating. The section from which samples were collected (fig. 3.1) showed different layers of clay separated by silty layers, each clay layer representing floors of separate periods of time.

A total of 26 samples were collected from the archaeological section. Eight samples (3,4,6,7,8,9,16 and 24) were rejected because they were deformed during sampling. The intensity of NRM of the other samples ranged between 1-54 mAm^{-1}, except samples collected from the eastern face, some of which had much higher intensities (samples 23 and 25).

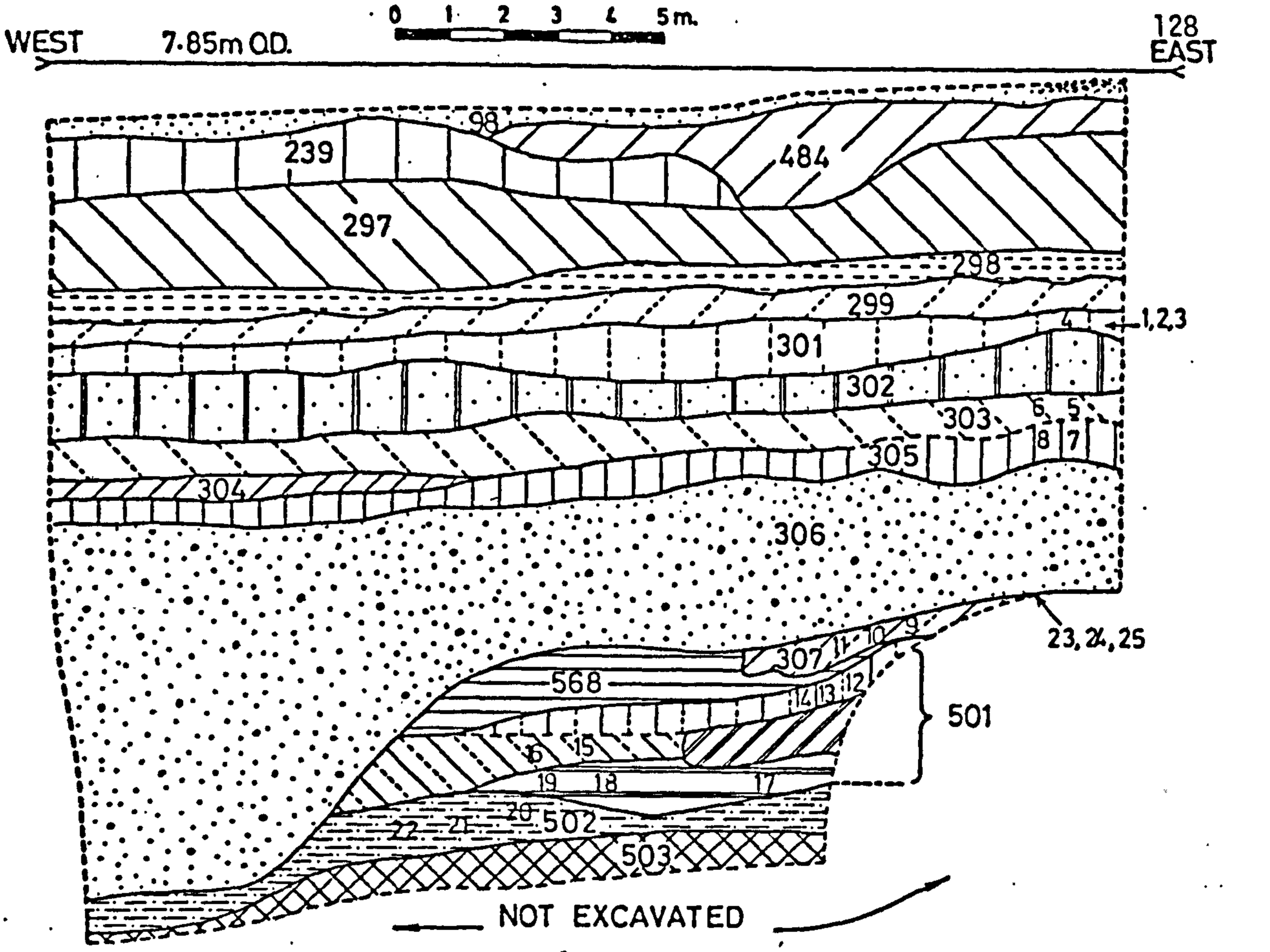

98 Mortar

299 Firm yellowish brown clay

305 Firm yellowish brown clay with organic stones

501 Light brown/yellow/ green sandy textured clay with chalk chips

239 Silty grey floor deposit with charcoal

301 Firm yellowish brown clay with blue/grey particles

306 Dark grey silt with much charcoal

501 Light brown/yellow/ green sandy clay with chalk chips

484 Grey mortary clay

302 Grey mortary silt in light grey clay

307 Firm yellow/ brown sandy clay

501 Greenish yellow clay

297 Hard yellowish brown clay

303 Firm reddish brown clay

568 Dark grey ash with charcoal

502 Grey green clay

298 Light grey mortary silt floor deposit

304 Black organic

501 Greenish yellow sandy clay

503 Black/brown peaty soil with much wood

Fig. 3.1 Beverley Lurk Lane section and samples distribution

The initial directions did not show any consistency with each other (table 3.1, fig. 3.3a).

Samples 1 and 2 (Munsell colour light yellowish brown) were from the eastern face of the section about 15cm. below the excavated surface. These samples were stable during demagnetization, the components remaining after AC demagnetization showed that the low coercivity components were grouped (sample 1 N-NW; sample 2 N-NE) while the somewhat higher coercivity components were scattered (fig. 3.2).

Sample 5 was from a firm, reddish brown clay (303) at a depth of 30 cm. This sample was stable during demagnetization. The components remaining had a northeasterly direction and the high coercivity components were scattered.

Samples 10 and 11 (Munsell colour light olive brown) were at about 75 and 77 cm. depth and were of a firm yellow/brown sandy clay (307). Sample 10, which was stable, had the components remaining grouped in a north-easterly direction, and in sample 11, which was very stable, the grouping was in a northerly direction.

Samples 12, 13 and 14 were collected from the greenish yellow sandy clay (501) at depths of 79, 83 and 85 cm. Samples 12 and 13 were stable during demagnetization while sample 14 was poorly stable. The components remaining in sample 12 were grouped in the northerly direction, while in sample 13 they were nearly in the northeasterly direction. Sample 14 had the remaining components scattered but showing an approximately northerly direction.

Sample 15 was of light brown yellow, green sandy textured clay with chalk chips (501). The sample was stable during demagnetization and the remaining components were grouped in the upper

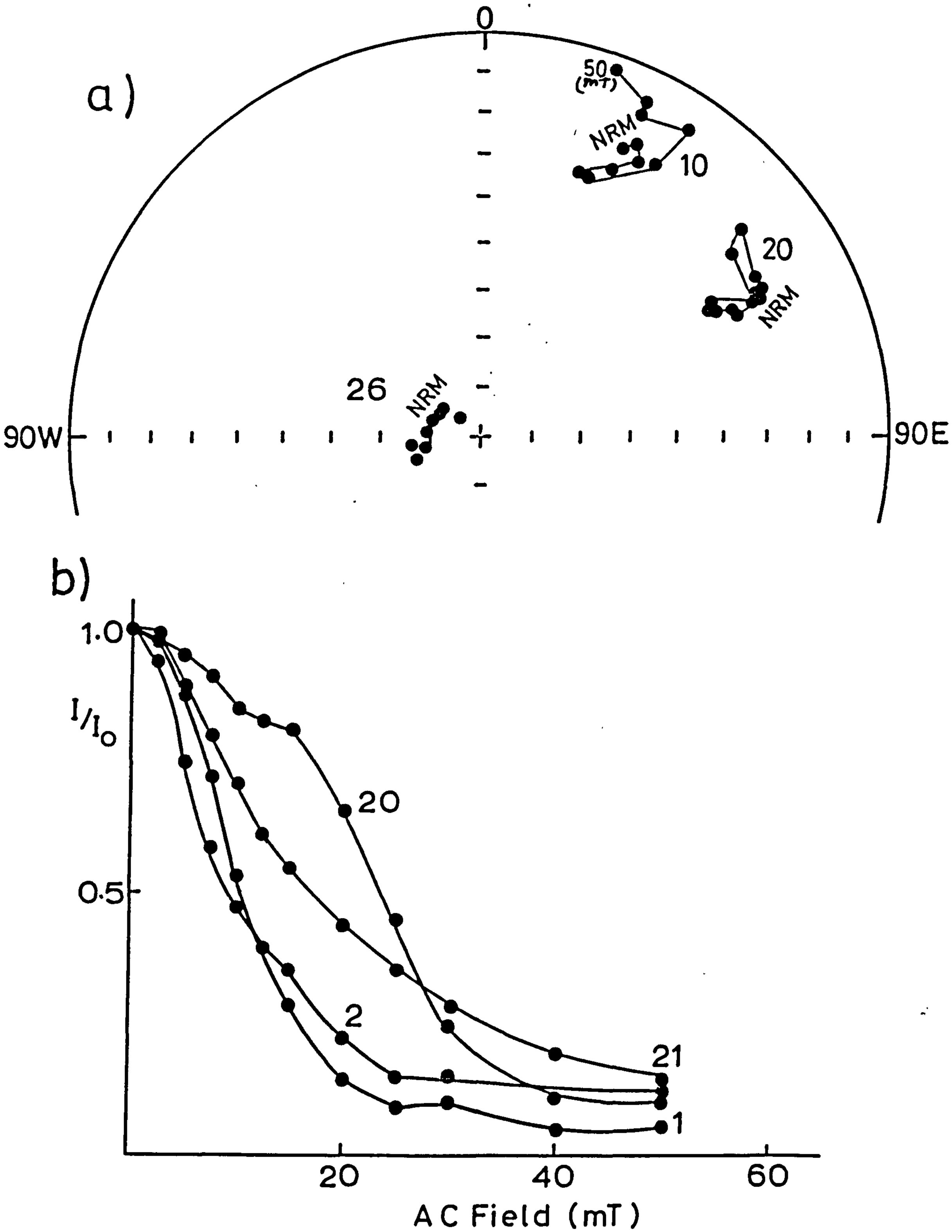

Fig. 3.2 Examples of changes during AC demagnetization of Beverley Lurk Lane samples
a) Direction b) Intensity

Sample No.	NRM Components Dec.	Inc.	Int. mAm^{-1}	Most stable Directions Dec.	Inc.	S.I.
1	333.8	53.0	31.32	331.6	52.2	3.33
2	37.6	63.4	14.48	34.4	64.5	5.13
5	48.6	59.7	10.63	46.8	61.7	2.80
10	21.1	30.7	3.97	28.7	21.5	2.46
11	10.9	65.3	5.06	12.1	66.4	5.79
12	358.8	49.9	3.28	358.7	48.7	4.92
13	19.6	40.6	8.0	17.7	41.9	4.37
14	12.0	2.7	1.88	35.1	30.1	1.63
15	54.1	-66.0	2.71	178.8	-26.2	3.24
17	299.3	-75.6	9.68	308.8	-70.3	5.61
18	6.0	64.2	3.88	6.7	64.8	9.82
19	224.1	-62.9	10.38	225.6	-62.8	5.40
20	60.0	35.2	54.13	62.3	24.2	10.17
21	16.1	29.7	21.42	23.7	-6.0	6.92
22	1.2	74.4	9.59	1.7	75.6	11.30
23	47.2	60.1	1339.5	110.4	28.6	3.82
25	27.4	62.2	1859.0	29.7	64.6	5.04
26	305.2	80.7	3.43	296.6	80.5	3.79

Table 3.1 Initial, most stable directions and stability indices (S.I.) of Beverley Lurk Lane samples.

hemisphere.

Samples 17, 18 and 19 were also at coordinate (501) at depths of 97, 94 and 93 cm. and were of greenish yellow clay. The samples were very stable during demagnetization. The components remaining in sample 17 were grouped in the upper hemisphere, while the removed components were scattered. Sample 18 had the remaining components grouped in the northern direction, and the removed components were scattered, but they did show some grouping in the north-northeasterly direction. The components remaining in sample 19 were in the upper hemisphere and the removed components were somewhat scattered, but showing some degree of grouping.

Samples 20 (Munsell colour light yellowish brown), 21 (Munsell colour; light olive grey) and 22 (Munsell colour dark olive grey) were collected from the grey-green clay (502) at 103, 106 and 105 cm. depth. The intensity of sample 20 was the highest and sample 22 was the lowest, i.e. the intensity increases towards the corner (fired) and thus these samples could have been affected by actual heating in the corner, or the difference in intensity could indicate systematic changes in the content of brown clay away from the hearth. These samples were very stable during demagnetization; the components remaining were well-grouped in a north-northeasterly direction with shallow inclination for samples 20 and 21.

Samples 23, 25 and 26 (Munsell colour, strong brown) were from the eastern face composing a red, burnt clay. Two samples were strongly magnetized (but sample 26 was weaker). Samples 23 and 26 were stable during demagnetization while sample 25 was very stable. The components remaining in sample 23 had the high coercivity components grouped better than the low coercivity components and in a southeasterly direction.

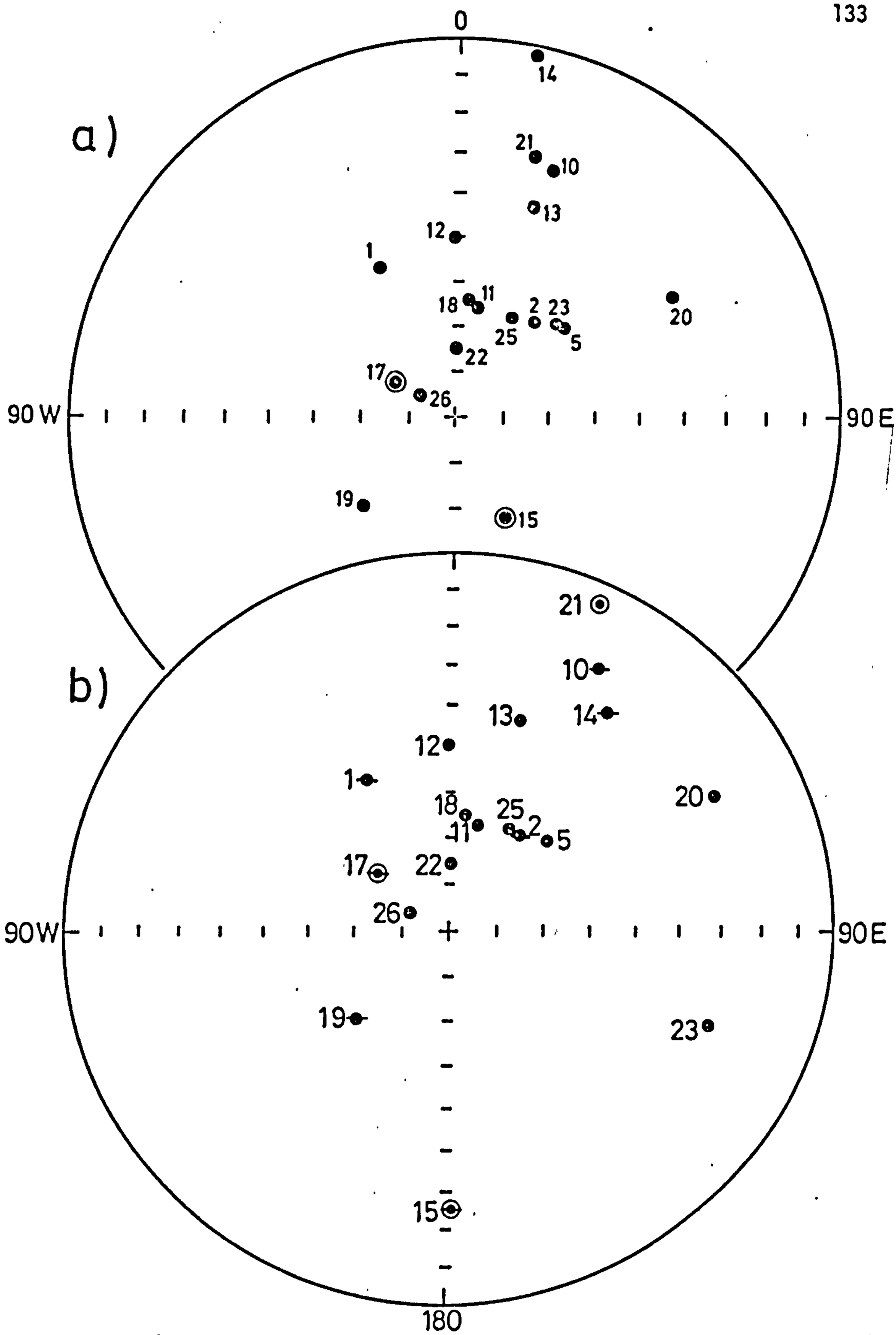

Fig. 3.3 Magnetic directions of Beverley Lurk Lane samples
a) Initial
b) Most stable
⊙ Upper hemisphere
●— Samples with >5% shard

The components remaining in sample 25 were 'loosely' grouped, having a northeasterly direction, and the removed components were scattered with some grouping in the same direction of the low coercivity components. Sample 26 had the remaining components grouped near the present earth field with a north-northwesterly direction.

The study of the colour of the above samples, using Munsell soil colour charts (1972), showed that the highest intensities were in the strong brown samples, except sample 26 which showed low intensity while the lowest intensities were for the light olive brown.

The most stable directions were plotted on a stereographic projection (fig. 3.3b). These directions were scattered and even the pure samples (5,11,18,21,22,23 and 25) showed a high degree of scatter; the only grouped directions were for samples 2,5,11,18,22 and 25. The mean value of these samples was calculated (excluding sample 2, which contained 5% shards), and corrected to meriden (Dec. = 20.8, Inc. = 66.4, α_{95} = 8.5). This mean value corresponds to an age of about 1050 AD ± 100 years. This age is considered to be significantly earlier than the archaeological age, 13th - 14th century (1200-1400 AD).

The observed mean value is about 10^{o} steeper and about 15^{o} east of what it is expected to be.

Since most of the samples were stable during demagnetization, as indicated by their values of stability indices, hence this scatter (and offset) in direction is not due to instability. The study of the grain size of the samples showed that samples 1,2,10,14,15,17,19 and 20 contained about 5% shards of sizes more than 1mm., while the other samples appeared to be pure and fine grained (<1mm.). The samples

containing shards showed the highest degree of dispersion (fig. 3.3b) (except sample 2) indicating that the presence of shard increases the scatter in directions, while not necessarily increasing the intensity. However, some of the pure samples (21 and 23) also showed a high degree of dispersion. On this basis it appears that there are other factors which are disturbing the directions. One of these factors could be fast deposition, which prevents the sediments from acquiring the directions of magnetization at the time of deposition. Another possibility is that post depositional disturbance occurred, such as weathering or disturbance during excavation.

3.2 Carlisle Archaeological Site (early Roman)

This site is a ditch of early Roman age, located near the centre of Carlisle city (Lat. 54.9N, Long. 357.5W). The ditch, of triangular cross section was composed of pebbly clay at the bottom and black clay at the top. A total of 15 samples were collected from the cleaned basal clay face.

The intensity of the Natural Remanent Mangetization ranged betweeen 4-191 mAm^{-1} and the initial directions of remanence were moderately consistent (table 3.2). The study of the grain size and colour showed that all these samples were pure and very fine..-grained (<1mm.) and the colour was mainly light brown except for samples 2,9 and 10, (which were brown to dark-brown) and sample 3 which was light yellow brown . Since the samples were all dominated by the brown colour, no systematic relation could be observed between the colour, intensity and stability.

Pilot samples (1,2,6,7,11 and 12) were found to be stable during demagnetization. The intensity decreased smoothly and changes in directions were smooth (fig. 3.4).

The components removed during demagnetization were

a)

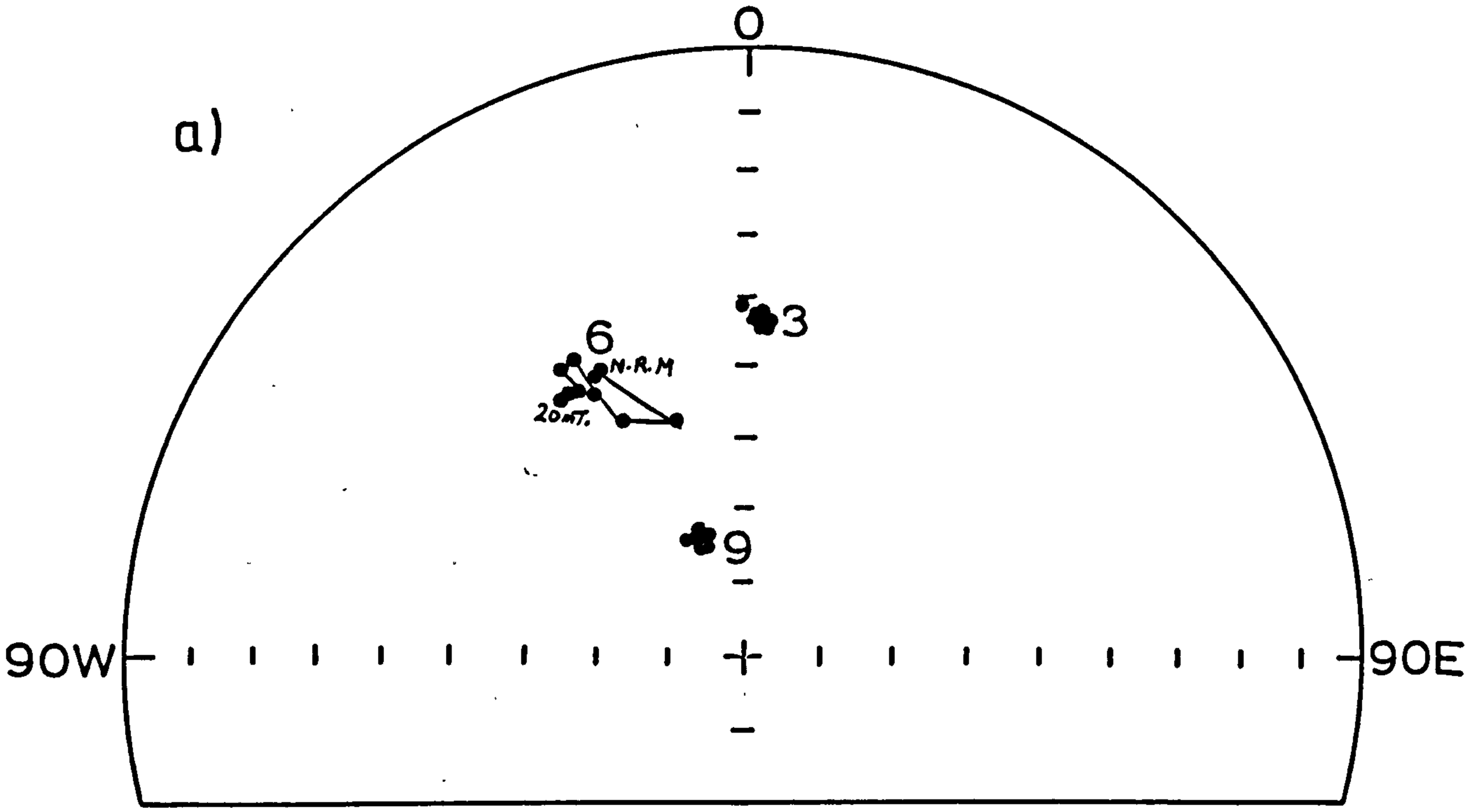

b)

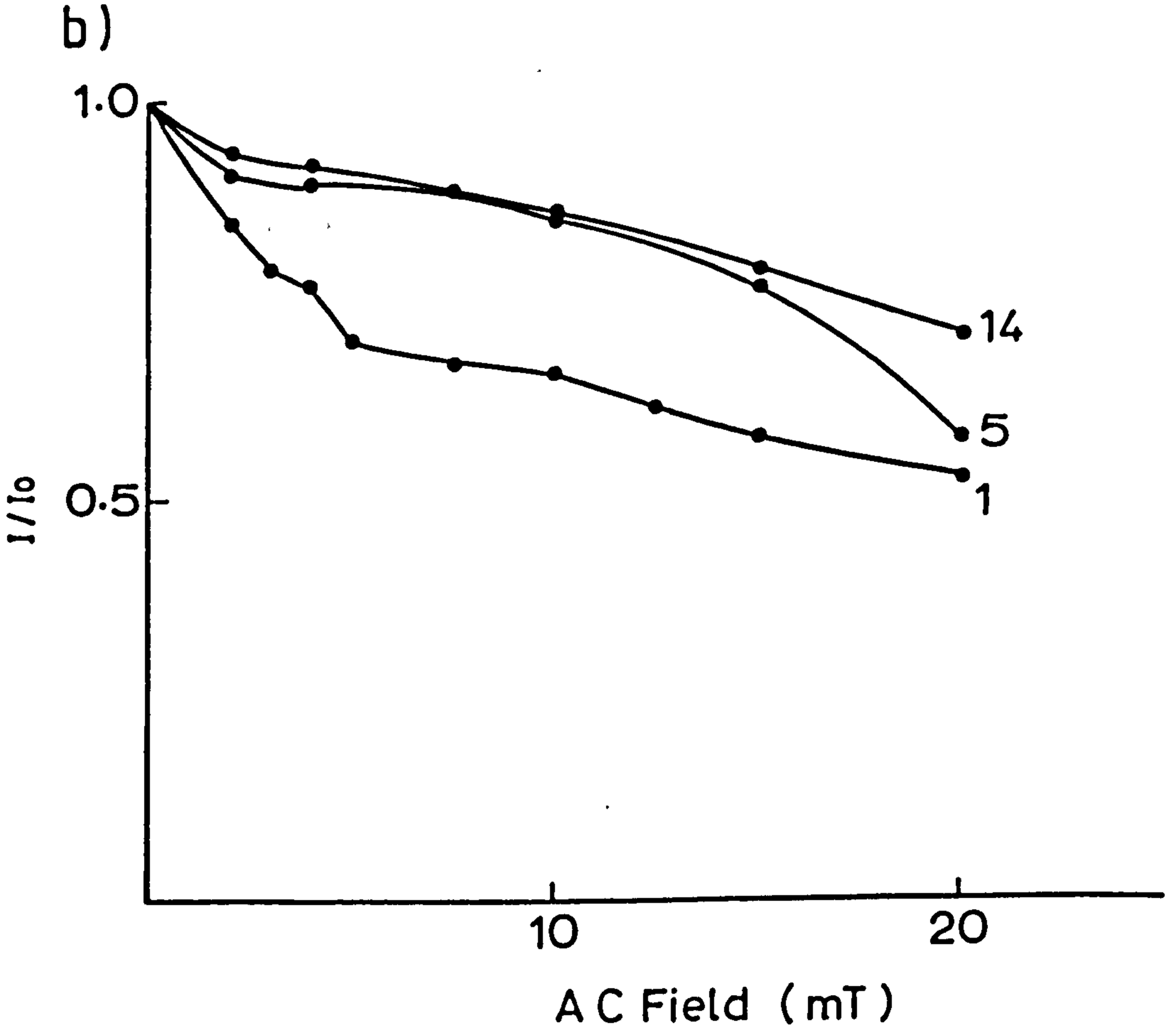

Fig. 3.4 Examples of changes during AC demagnetization of Carlisle archaeological site samples
a) Directions b) Intensity

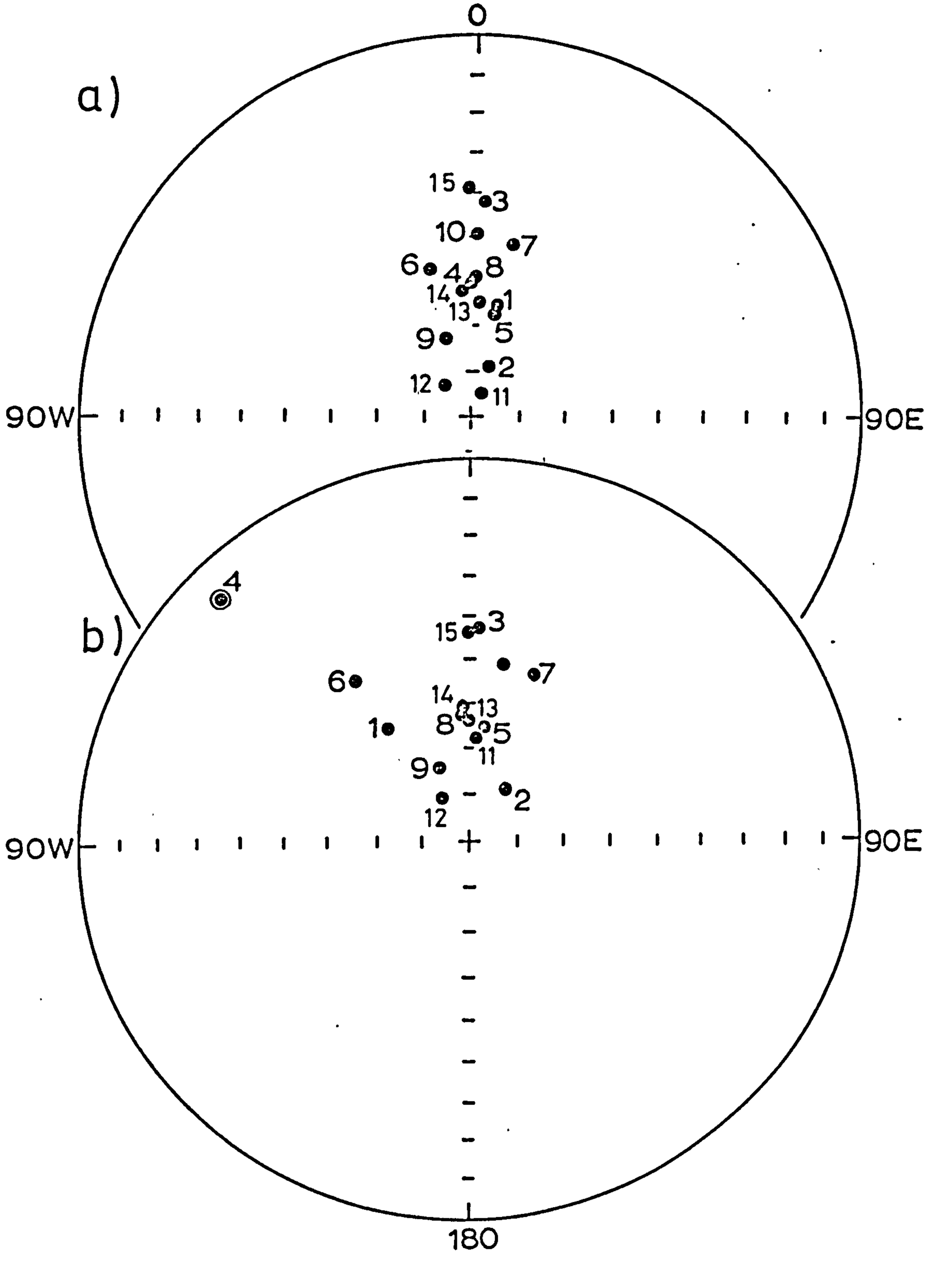

Fig. 3.5 Magnetic directions of Carlisle archaeological site samples
a) NRM
b) Most stable

Sample No.	Initial Dec.	Inc.	Int. mAm^{-1}	Most stable Dec.	Inc.	S.I.
1	12.7	65.6	81.31	326.0	60.4	5.39
2	20.7	79.1	47.31	39.2	76.0	7.80
3	2.8	42.5	68.48	3.2	43.3	13.79
4	0.4	60.7	56.9	315.5	-10.4	2.66
5	11.6	66.9	48.50	9.6	65.1	6.24
6	344.2	56.9	84.56	326.1	47.5	5.57
7	13.3	51.5	65.60	21.6	51.1	8.96
8	1.1	60.0	138.00	0.2	62.4	2.45
9	343.1	72.5	38.17	341.0	73.3	10.65
10	1.6	49.8	4.02	11.6	50.7	1.95
11	27.8	84.3	9.06	6.7	67.9	4.26
12	321.9	81.8	41.89	332.5	79.0	4.81
13	5.2	65.6	173.00	2.6	63.9	8.32
14	359.1	39.8	84.40	1.3	43.8	10.07
15	356.4	62.3	191.10	359.3	61.8	6.06
Mean	358.9	59.6	α_{95} = 7.4		k = 29.5	

Table 3.2 Initial, most stable, S.I. and the mean value of Carlisle samples.

scattered for all samples while the remaining components were all grouped in a northerly direction with the inclination ranging from 43-79^{o} (except sample 4 which had negative inclination). According to the behaviour of pilot samples the other samples were demagnetized in fewer steps and they were also found to be stable to very stable during demagnetization, except samples 8 and 10 which were only poorly stable.

The most stable directions were plotted on a stereographic projection (fig. 3.5) and the mean value was calculated after sample 4 had been rejected due to its scattered direction (negative inclination). Sample 4 had been slightly deformed during collection and it is thought that this affected the observed remanence. The mean value of the most stable directions, corrected to Meriden, was plotted on the archaeomagnetic curve. This value was only 2^{o} (in declination) away from the curve. This shift is considered to be within the accuracy of the technique, and an age of 225 ±40 AD was assigned. This archaeomagnetic date was archaeologically acceptable although it was somewhat younger than the archaeological date based on coin and pottery sequences which suggested an age earlier than 150 AD, probably 100 AD. However, such an early age would correspond to the same obtained declination but with a 7^{o} steeper inclination. Since these sediments are finely grained and pure, such shallow inclinations could be attributed to an inclination error in sediment samples.

3.3 Grove Priory - Leighton Buzzard (Saxon)

This site is about 27 km. south-west of Bedford, at Lat. 52,3^{o}N, Long. 1.5^{o}W. Saxon pottery of about the 7th C. has been found in various parts of the field under examination. Other probable Late Saxon ware has been found. Although the upper fills of the ditch have contained 12th and 13th C. pottery, the lower silts have contained exclusively

Saxon pottery. The ditch frequently changes character. It starts at the east end as a shallow feature about 1m. deep and becomes progressively deeper eastwards. Its profile is either V-shaped or rectangular, with a flat bottom. The east end probably remained visible until the end of the 13th C. or thereabout, since medieval buildings had their foundations constructed at a deeper level, crossing the ditch, and so held back the water to the east and kept the area wet after later back-filling. The material sampled from this site was brown clay containing some pebbles and shards of different sizes and shapes which made the material somewhat hard.

A total of 18 samples were collected from two sections. Four samples were deformed during sampling (3,12,13 and 16) and therefore rejected. The intensity of the Natural Remanent Magnetization varied between 1-73 mAm^{-1} (table 3.3). The study of the colour showed that samples 1,2,4,6,7 and 17 are dark yellowish brown; samples 5,8 and 10 are yellowish brown; 9 and 18 are dark brown; 11 is light olive-brown; 14 is light yellowish brown and 15 is brownish yellow. The highest intensity was for the dark brown colour and the dark yellowish brown showed lower intensity.

Pilot samples (1,2,4,5,6,10,11,14,15,17 and 18) were stable during AC demagnetization. The intensity decrease and the direction changes were smooth during increasing AC demagnetizing field. This behaviour indicates good magnetic stability which was also shown by their high stability indices. The results of partial demagnetization showed that the samples could be divided into two groups according to the similarity of their behaviour during demagnetization - the "Great Circle" group and the "Stable" group (fig. 3.6).

Sample	Initial		Intensity	Most stable directions		
No.	D	I	mAm^{-1}	D	I	S.I.
1	274.9	66.8	2.53	258.4	68.5	5.71
2	241.3	37.5	3.68	340.8	36.8	5.75
4	338.8	65.0	6.68	339.5	66.2	6.91
5	119.7	26.3	7.95	173.9	-34.3	8.89
6	73.3	87.6	2.80	114.3	85.5	4.29
7	251.0	60.1	9.03	258.5	54.4	6.02
8	177.8	-69.6	4.17	199.6	-55.2	4.31
9	299.7	63.7	73.21	299.9	63.8	48.96
10	328.9	65.8	8.77	330.1	65.5	9.75
11	331.9	30.9	18.82	331.9	30.2	4.91
14	207.0	50.3	4.65	200.2	47.5	12.30
15	84.4	29.0	3.15	71.3	26.3	8.62
17	12.7	37.2	4.08	13.2	37.2	5.97
18	344.9	-26.1	36.60	344.7	-26.1	17.88

Table 3.3 Initial, most stable directions and stability indices of Grove Priory standard samples

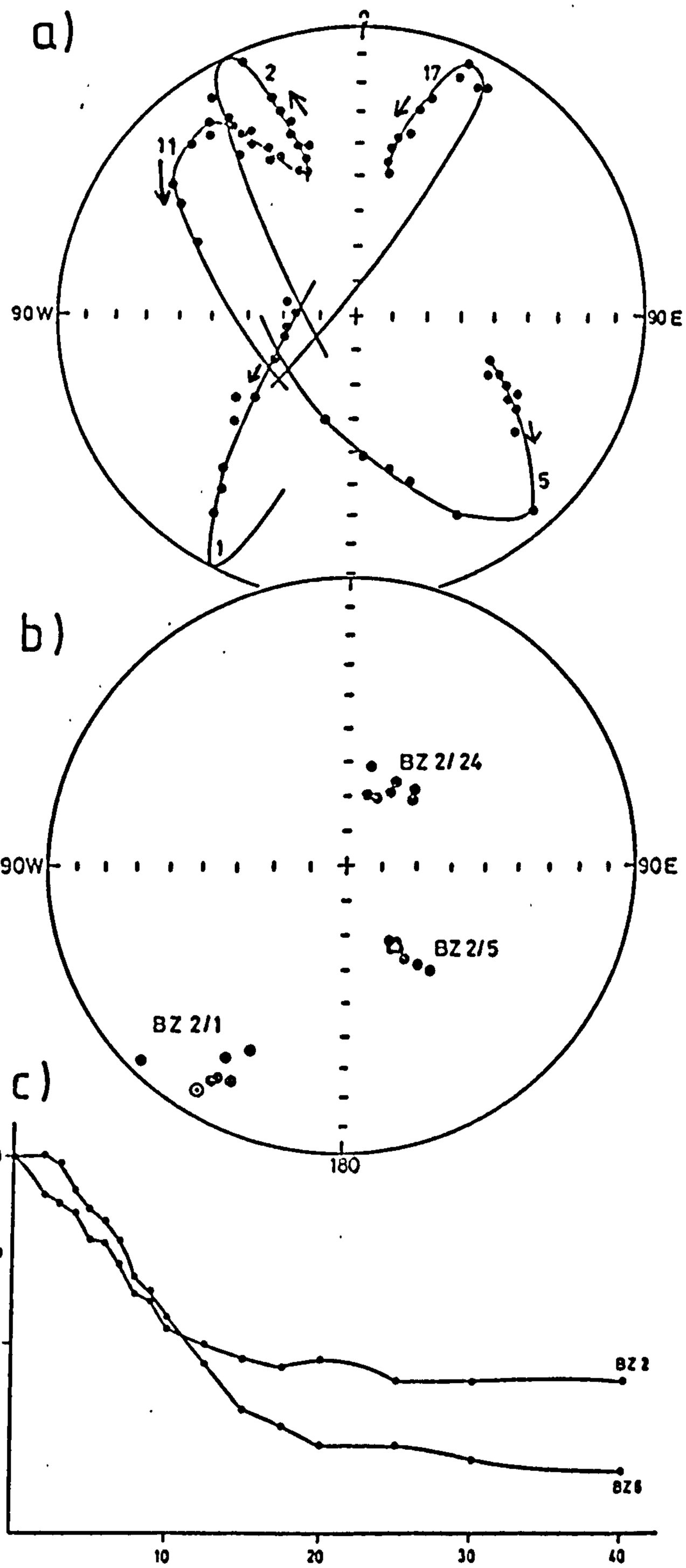

Fig. 3.6 Examples of changes during AC demagnetization of Grove Priory samples
a) Great circle
b) Stable
c) Intensity

(a) "Great Circle" group consists of five samples (1,2,5,11 and 17). Sample (1) showed southwesterly changes away from the present earth field with increasing field and no stable end was reached by a peak field of 40 mT. Sample (2) behaved similarly but moved in a northwesterly directionaway from the present earth field, but with increasing peak field, the high coercivity components moved into the same northwesterly direction but towards the present earth field. Sample (5) had low coercivity components in a southeasterly direction and they became shallower with increasing field. The high coercivity components had a southeasterly direction but they became steeper. Sample (11) had a northwesterly direction and the high coercivity components were near the present earth's field. Sample (17) which was collected from the second section had a northeasterly direction and the higher coercivity components were steeper and towards the present earth's field.

The remaining components from this group were drawn on a stereo projection (fig. 3:6a) and the great circles were completed to find their inter-sections; these were southwesterly. It is obvious that these samples have two distinct remanent components. However, neither of these values gave a sensible age for this site on the archaeomagnetic curve.

(b) "Stable Group". This group (4,6,10,14,15 and 18) each showed only one stable component of remanence but differed from the other. Three samples (4,9,10) had a northwesterly direction, sample (6) had a southeasterly direction and the other two (7 and 8) had a southwesterly direction, having sample (8) in the upper hemisphere. Samples from other sections (14,15 and 18)also had stable but scattered directions

with sample (14) having a southwesterly direction, sample (15) a north-easterly direction and sample (18) a northwesterly direction but in the upper hemisphere. (The remaining samples were demagnetized using fewer steps of demganetization).

Scattered directions were observed in these samples despite the remanence being very stable (fig. 3.7). Since these scattered directions are not due to instability they must be due to other factors such as inhomogeneity of magnetization, probably due to the presence of shards which are highly magnetized. These would have high magnetic stability but scattered directions. Hence dating this type of material is very difficult unless it is possible to collect samples of sediments which do not contain shards or other materials likely to cause inhomogeneity.

In order to test this, 27 small samples were collected using small cylinders of 2.1 cm. dimension. The intensity of Natural Remanent Magnetization ranged between 0.18 - 17.0 mAm^{-1}, but the directions were again scattered (table 3.4). Seven samples only were demagnetized for pilot treatment. Sample 1 was poorly stable, the components remaining were grouped in an elongated shape similar to those obtained from the bigger samples. This grouping had a southwesterly direction, the components removed were all scattered. Sample 2 was very stable during demagnetization, the components remaining were grouped in an easterly direction with the high coercivity components somewhat to the south, while the removed components were scattered. The components remaining in sample 3 which were unstable were grouped near to the present earth's field while the removed components were all scattered. Sample 5 (stable) had the components remaining grouped in a southeasterly direction while the removed components had a northwesterly direction and showed a movement towards this direction

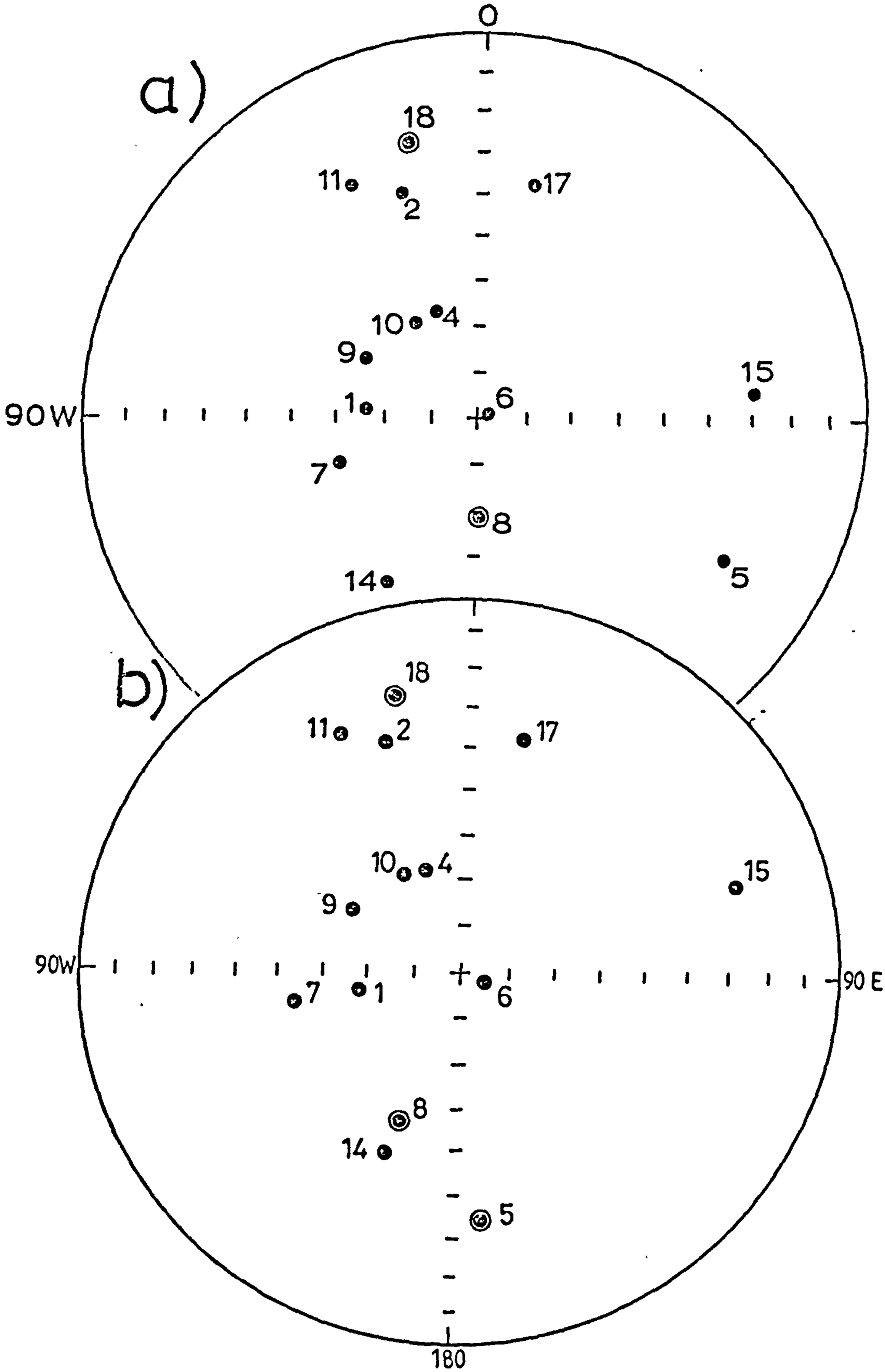

Fig. 3.7 Magnetic directions of Grove Priory standard samples
a) Initialb) Most stable
◉ Upper hemisphere

with increasing demagnetizing field. The components remaining in sample 20, which is also stable, showed two separate groupings for the low and high coercivity components. The low coercivity components were near to the present earth's field but they all had a southwesterly direction, while the removed components were all scattered. The components remaining in sample 21 (poorly stable) also showed two grouping for the low and high coercivity components, but this time the high coercivity components were nearer to the present earth's field and the removed components were all scattered. The components remaining in sample 27 (stable) had the low coercivity components well-grouped with a north-northwesterly direction, while the high coercivity components were scattered. The removed components were also scattered, but they were all near to the present earth's field. On the basis of the behaviour of pilot samples, the other samples were bulk demagnetized. Although some of the pilot samples were stable, the final directions were scattered, showing inconsistent directions (fig. 3.8). Hence, it was found that despite the smaller size of the samples, the same problems were faced concerning the stability of magnetization and the scattered directions.

All the small samples were opened to examine them for shard content. Eleven samples (table 3.5) were nearly pure, the directions of these samples showed consistent inclinations, except samples 12 and 16. The directions of samples 3,6,9 and 12 are on the western side of the archaeomagnetic curve. The mean value of samples 3,6 and 9 falls near the 1850 portion of the curve. Only two of the other samples had consistent directions (23 and 27) in which their mean value is near the 1200 part of the curve.

Sample No.	Initial			Most Stable directions		
	Dec.	Inc.	Int. mAm^{-1}	Dec.	Inc.	S.I.
1	161.2	70.1	0.98	209.6	15.2	1.84
2	242.9	-38.3	1.59	92.2	-57.9	7.09
3	93.2	9.2	0.33	331.3	68.7	0.67
4	45.7	12.0	0.88	299.2	21.3	
5	118.2	18.4	5.38	150.8	63.7	4.07
6	61.9	-8.1	0.54	320.9	68.8	
7	63.0	21.9	0.42	289.6	39.7	
8	46.6	-35.1	1.98	3.2	27.9	
9	71.9	-14.0	0.84	340.7	70.0	
10	85.8	17.9	1.70	263.7	67.5	
11	53.1	71.5	1.98	254.1	31.6	
12	57.7	4.5	0.60	324.9	35.2	
13	86.9	0.9	11.40	64.6	74.6	
14	80.3	-0.7	0.60	282.4	65.7	
15	87.2	-9.0	0.60	72.0	75.3	
16	78.9	-43.4	8.40	41.8	-38.8	
17	87.1	4.9	0.78	229.9	67.0	
18	91.9	40.4	0.66	194.3	35.0	
19	306.7	57.4	3.30	268.7	-21.9	
20	102.5	39.6	2.22	218.4	62.8	3.96
21	318.8	-2.8	0.30	299.2	-44.5	1.00
22	80.4	-5.0	0.72	303.0	60.7	
23	77.2	-30.6	3.60	7.9	50.3	
24	77.1	-9.3	1.20	23.5	69.3	
25	81.9	-6.9	1.20	249.4	67.1	
26	67.3	11.1	0.54	319.4	45.0	
27	85.6	-1.1	0.18	20.6	65.9	2.71

Table 3.4 Initial, most stable directions and stability Indices (S.I.) (Pilot Sample only) of Leighton Buzzard small samples

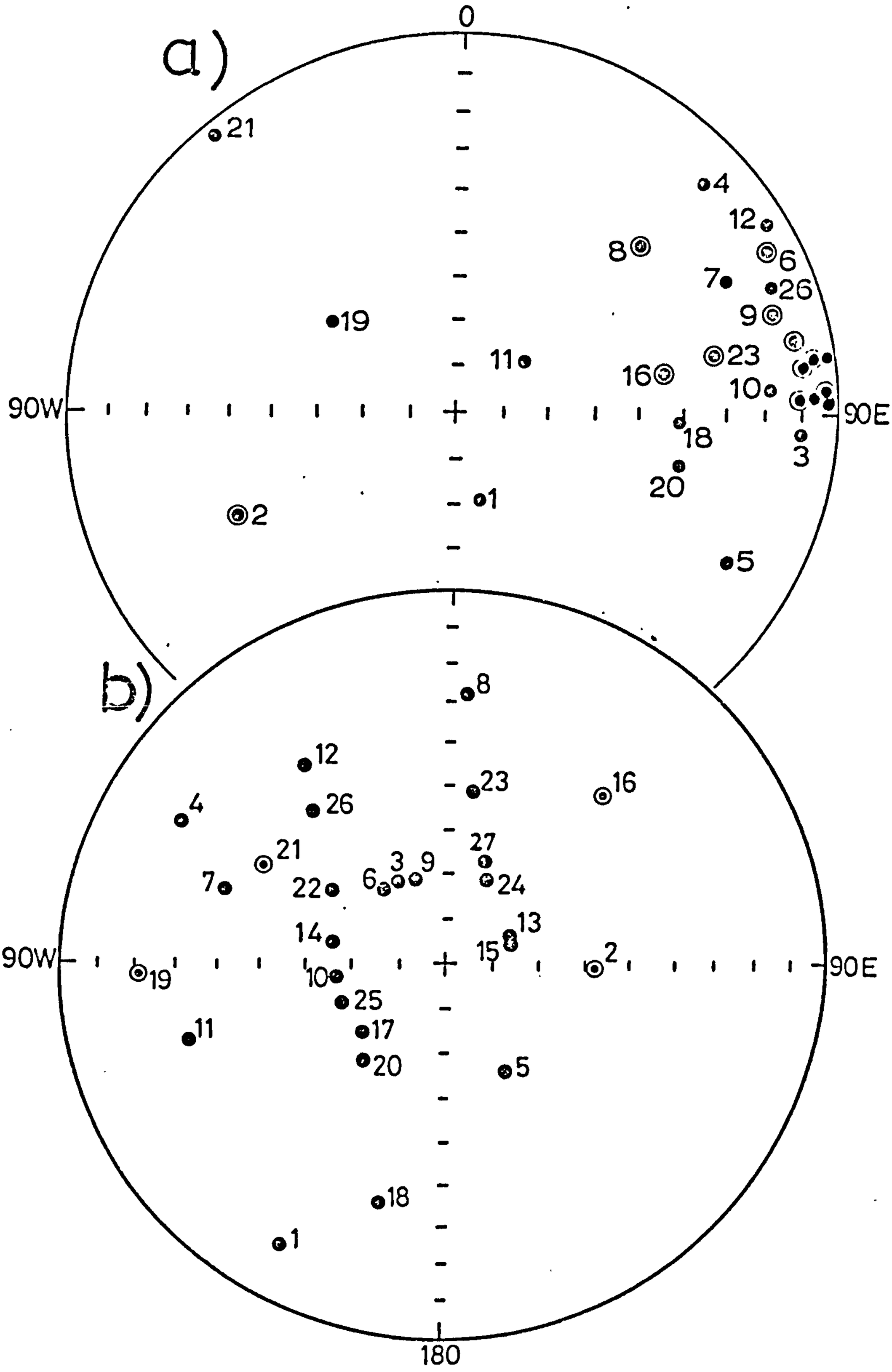

Fig. 3.8 Magnetic directions of Grove Priory small samples
a) NRM b(Most stable

Sample No.	Dec.	Inc.
3	331.3	68.7
6	320.9	68.8
9	340.7	70.0
12	324.9	35.2
13	64.6	74.6
14	282.4	65.7
16	41.8	-38.8
17	229.9	67.0
20	218.4	62.8
23	7.9	50.3
27	20.6	65.9

Table 3.5 Grove Priory Clean Samples

The intensity of magnetization of the small sample (normalized to standard size) was found to be generally lower than the standard samples, and although some of the small samples (pilot samples) were stable, the overall stability of the standard samples looked higher than the stability of the smaller samples. Accordingly, it is more likely that shards in this site are increasing both the intensity and stability of the sample and at the same time causing scattered directions. By collecting small samples, i.e. avoiding some of the shards, the intensity and stability were decreased but the directions were still scattered either because the shards were distributed homogeneously within the section, or that the sediments were disturbed by reworking or later back-filling of highly magnetized material. The study of the grain size and colour of the standard samples showed that most of the samples contained between 5-30% of shards and the only pure samples

were 2,11 and 15. However no systematic relation was observed between the magnetization and the percentage of shards, but the colour showed that the highest intensity was for the dark brown samples, and the dark yellow colour showed lower intensity.

3.4 Lincoln Archaeological Site - Lincolnshire

This site is about 8 km. east of Lincoln at Lat. 53.2°N and Long. 0.1°W. A total of 17 samples were collected. Samples 1 - 9 (context 3) were from a coarse river sediment lying near to a parish boundary These samples were taken from two silt layers. Samples 1 - 5 were taken from the upper layer, while samples 6 - 9 were from the lower layer, and it is not known whether they represent the same silt layer or not. The other samples were collected from a column of silt which contains Roman pottery. Samples 10 and 11 were from the lowest part (context 195), samples 12 and 13 were from context 192 and samples 14 - 17 were from context 26.

The intensity of NRM ranged between 0.2 - 3.6 mAm^{-1}, and the directions had scattered declination and somewhat consistent inclination. but all negative. These samples were found to be stable to very stable during demagnetization (except samples 2 and 15, which were poorly stable), as indicated by their values of stability indices (fig. 3.9, table 3.6).

The study of the colour showed that samples 1 - 9 were yellowish brown except samples 3, 4 and 5 which were dark yellowish brown, while samples 10 - 17 were black. The overall colour of these samples were darker than the other sediments and they showed relatively low intensities of magnetization. On the other hand, the study of the grain size showed that these samples were all fine-grained (<1mm.)

a)

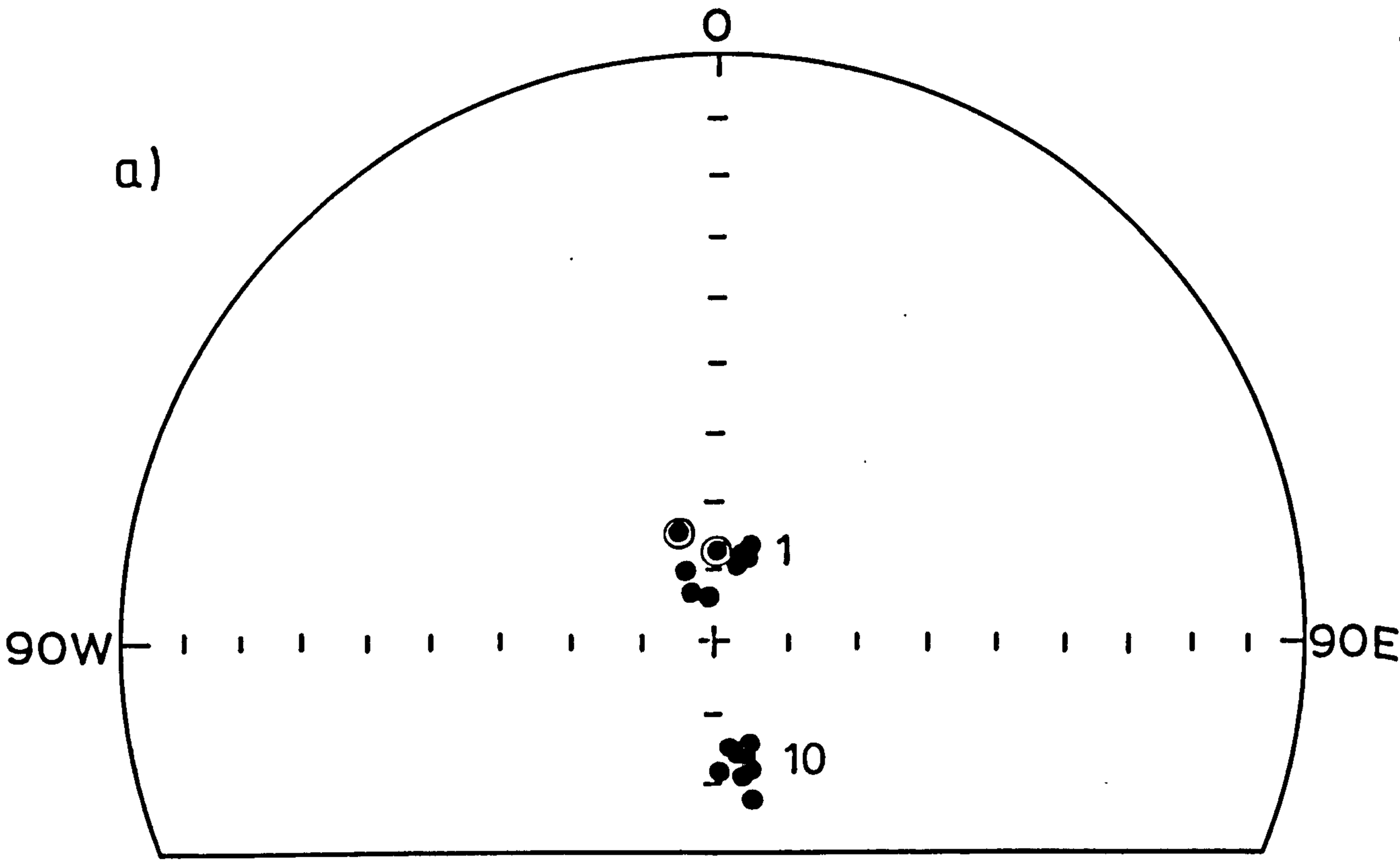

b)

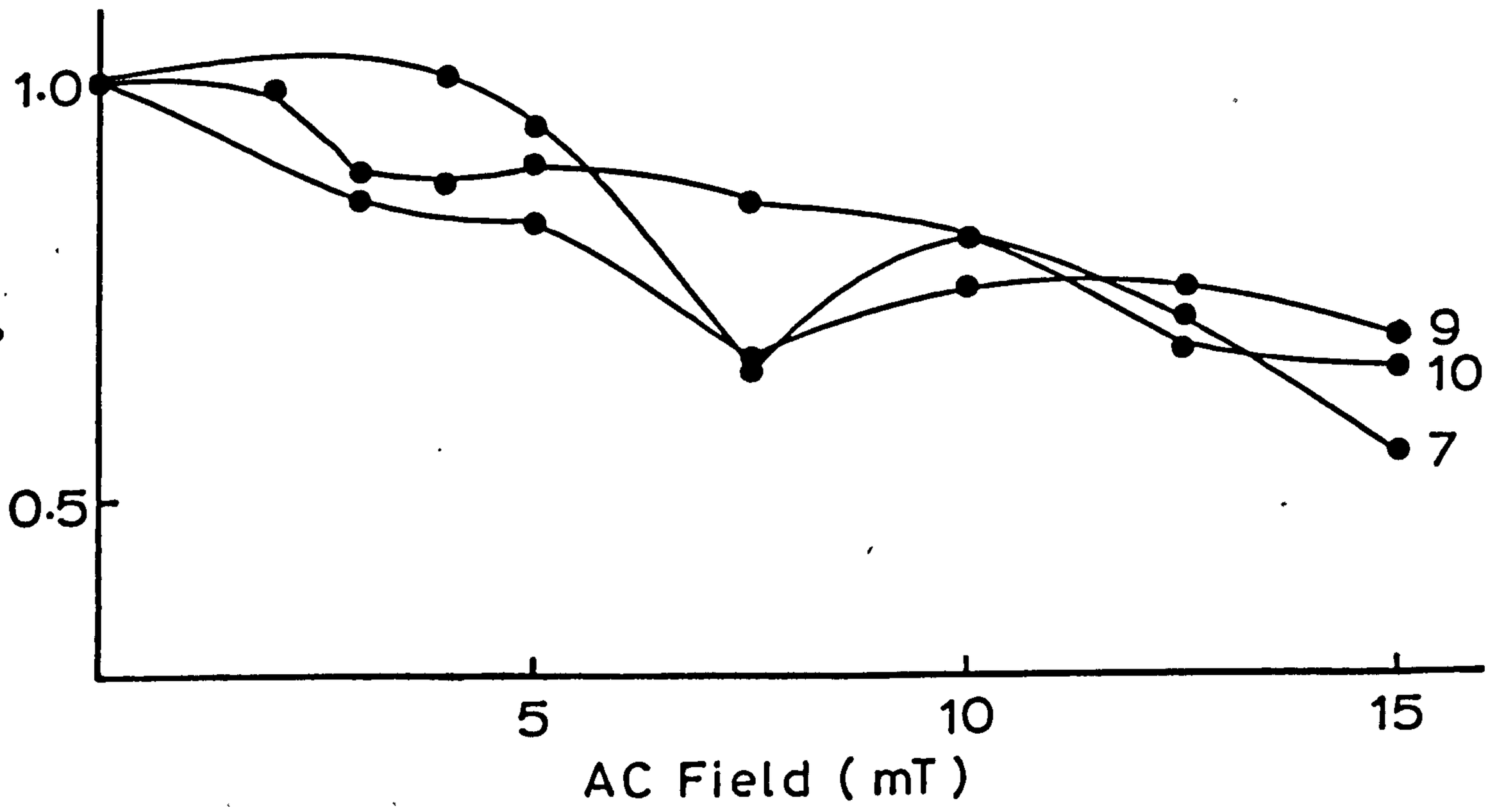

Fig. 3.9 Examples of changes during AC demagnetization of Lincoln site samples

a) Directions b) Intensity

Sample No	Initial Dec.	Inc.	Int, mAm^{-1}	Most stable Dec.	Inc.	S.I.
1	2.6	-76.8	1.88	20.0	77.1	6.1
2	28.6	-86.2	1.45	350.4	65.9	1.9
3	35.0	-82.0	1.87	345.4	77.2	2.2
4	99.1	178.6	1.32	333.2	66.2	2.6
5	78.8	-86.1	1.36	347.8	75.6	3.7
6	80.1	-67.4	0.86	336.2	77.2	1.2
7	185.8	-60.5	1.32	13.1	64.3	4.3
8	200.1	-71.4	1.34	8.5	70.3	5.2
9	191.8	-70.1	1.83	13.9	66.7	7.0
Mean	357.5,	71.4,	α_{95} = 5.0	k = 106.6		
10	344.5	-73.6	3.31	164.1	73.0	6.0
11	0.3	-80.3	3.63	180.9	77.9	11.9
12	249.5	-64.1	1.57	23.8	70.3	5.2
13	219.0	-77.9	1.16	60.1	78.0	3.8
15	8.2	-53.5	0.28	88.5	88.9	1.4
16	191.2	-57.9	0.51	28.4	62.1	3.8
17	195.3	-82.4	0.90	355.5	80.4	3.3

Table 3.6 Initial, most stable and stability indices of Lincoln samples

and samples 10 - 17 contained fine white fractures, distributed uniformly within the sediments.

The components remaining after AC demagnetization were well-grouped in all the samples having a north-northwesterly direction in samples 1 - 6, a northerly direction in samples 7 - 9, southern

direction in sample 10, southeasterly direction in samples 11 and 15, and a north-northeasterly direction in samples 12, 13, 16 and 17. The removed components in most of the samples showed a similar grouping as the remaining components, indicating a single component of remanence was present in each of the samples, and they were scattered only in a few samples.

Although the directions of samples 1 - 5 were northwesterly (except sample 1 , which was northeasterly) and samples 6 - 9 were northeasterly (except sample 6, which was northwesterly), the plot of the stable directions (fig.. 3.10) showed that they were all well-grouped. Accordingly, they were assumed to be from the same layer; this was also indicated by the study of the colour of the samples which showed that samples 1 - 9 were of the same colour. The mean value of the most stable directions corrected to Meriden, was plotted on the archaeomagnetic curve. This value was about 2^{o} shallower than the directions at 0 - 50 AD. However, the α_{95} bars were cutting the curve at 40 AD. This date is earlier than the expected archaeological age, which suggests a post-Roman age. According to the available records for the likely post-Roman period, the obtained mean value has been deflected to the west by at least 10^{o}. The shift in declination could be due to the effect of the course of the river which is more likely to be westerly.

The most stable directions of samples 10 - 17 had scattered declinations and somewhat consistent inclinations, hence it was not possible to date the samples. The study of the grain size showed that these samples contained fine fractures (probably shards); the scatter in directions was therefore attributed to the presence of shards within the sediments.

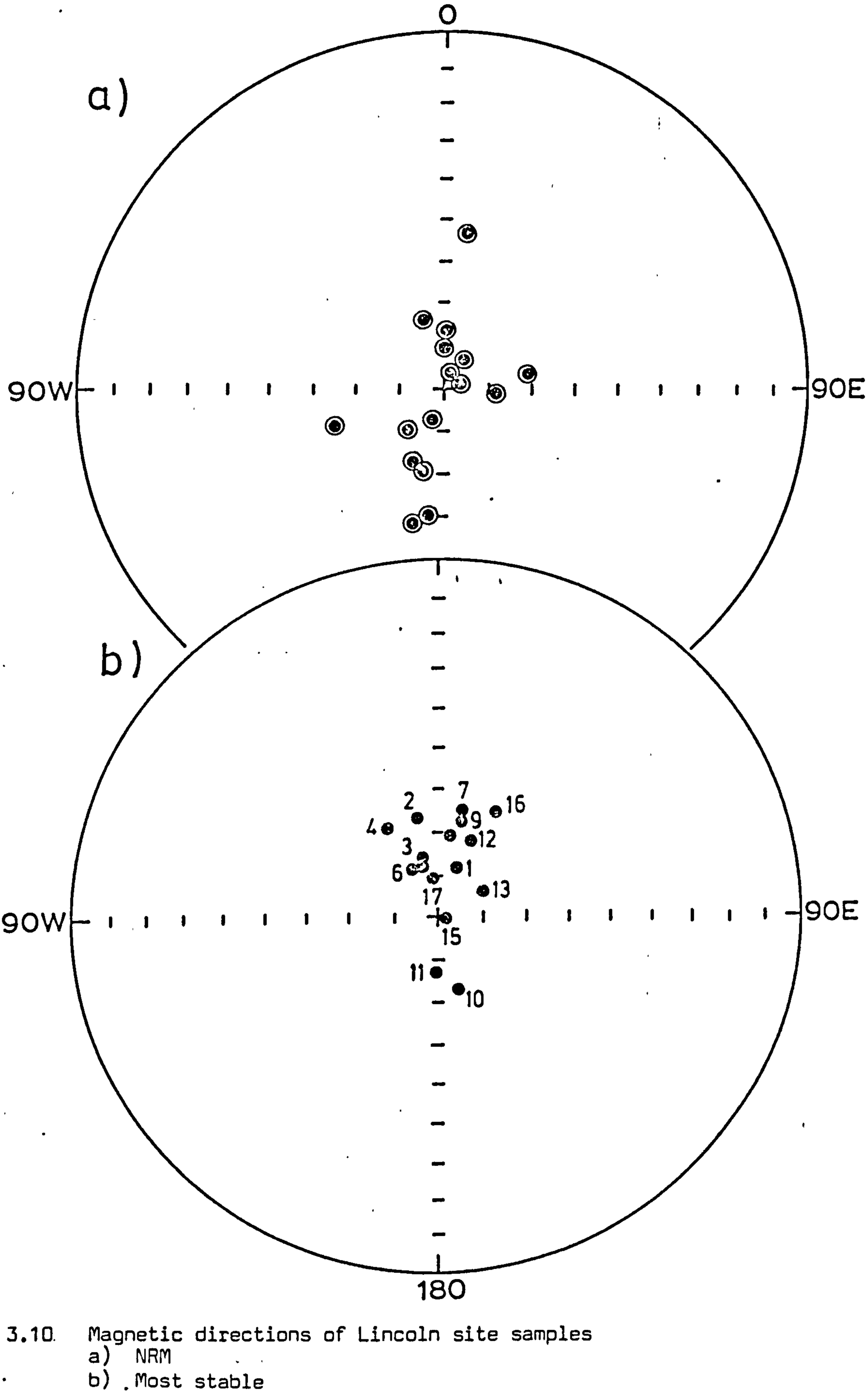

Fig. 3.10 Magnetic directions of Lincoln site samples
a) NRM
b) Most stable

3.5 Wharram Percy

New sites were sampled at Wharram Percy (Lat. 54.01 N, Long. 0.55 W) as a continuation of previous studies (Fig. 3.11).

The village of Wharram Percy was largely abandoned some time in the 18th Century, largely in response to the demand for land for sheep farming, although it is thought that the church continued to be used until later times. The mill pond may, or may not, have been cleaned during the final stages of abandonment. The site of the mill has not yet been ascertained but the dam and pond have been excavated in various places, over a period of several years.

Previous archaeomagnetic studies had been undertaken by Noel and Tarling (Tarling, 1983). In particular they studied samples from a trench excavated in 1974 through the pond sediments, extending approximately north-south from near the dam site at an 18th Century brick wall. Twelve samples were taken 3.35m. south of the wall and on the east face of the trench within a thick clay horizon. The clay was overlain by a well-defined rubble layer some 0.85m. thick and the samples (1 - 12) were taken at 11, 18, 36, 34, 53, 60, 68, 79, 83, 91 and 100 cm. below the rubble clay. It was found that the magnetization tended to show variations with depth that were, in most cases, irregular but with indications of an overall trend. A three-point average curve through the directions ranged between $4^{o}E$ - $20^{o}W$ while the inclinations ranged between 60^{o} - 70^{o}. Although this curve is similar in shape to the available archaeomagnetic records between 1600-1900, the inclinations were consistently about 10^{o} shallower than the historical records for this period (fig. 3.15).

Subsequently, samples were collected from the following locations:-

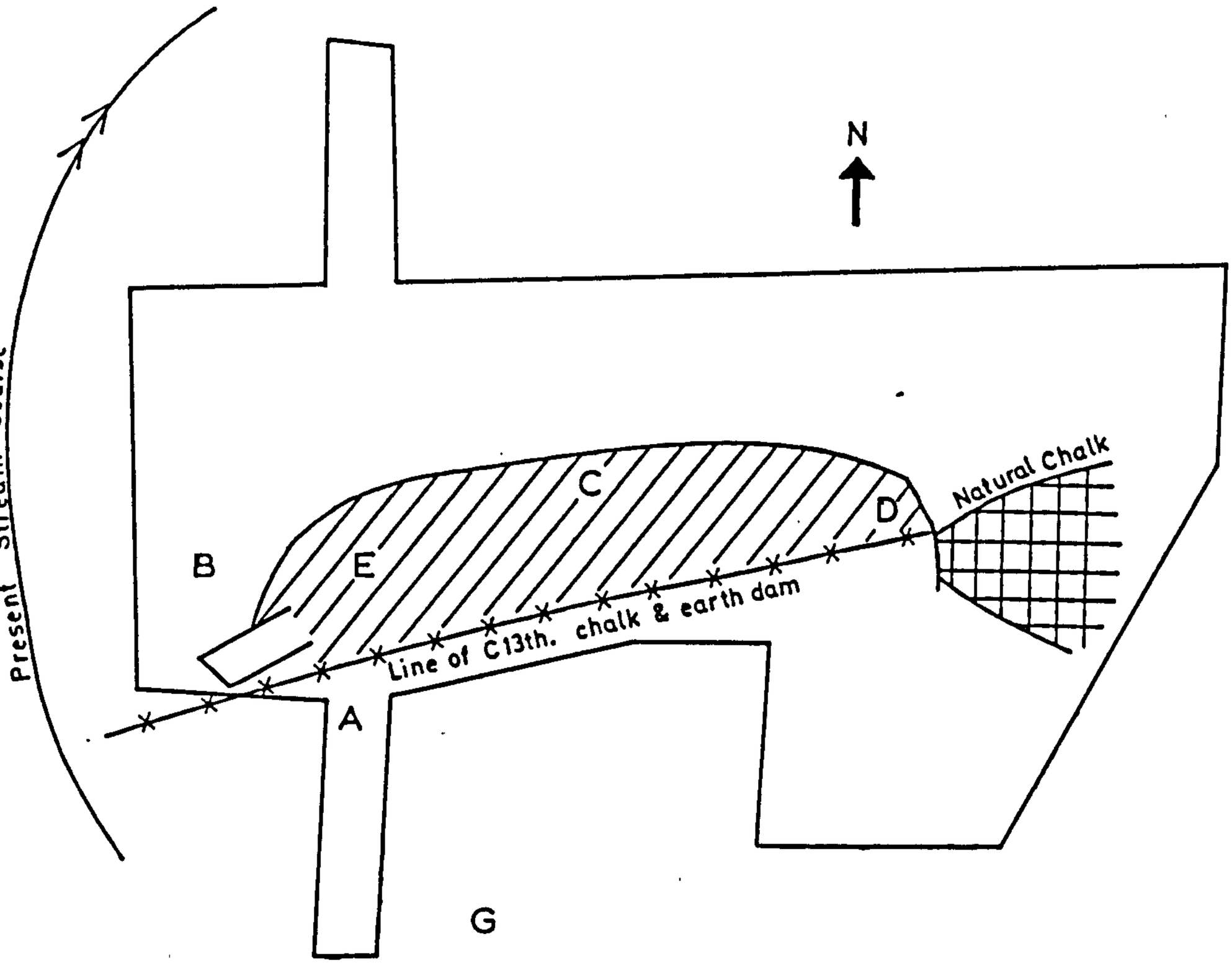

Area of pre C13th. dam pond silt preserved below chalk & earth dam.

A Original Noel & Tarling sampling site.

B Dam site (WW/VV 170/171).

C Wharram silts (W176).

D Pond silts (KK176).

E Pond silt E face & W face (QQ/RR 171).

F Water conduct.

G Sump (00/55).

Fig. 3.11 Wharram Percy site plan

3.5.1 Dam site, WW/VV, 170/171 (600 - 1300 AD)

A total of 18 samples were collected from a cross-section trench through the dam. The section is 1.8m. thick and includes 4 separate layers distinguished by their colour (Figure 3.12a). It was possible to collect 11 samples from the grey layer, and 5 samples from the black layer, but only one sample was taken from the grey and black layer (sample 18) because there were too many stones and pebbles. The chalk yellow pebbly layer was very thin and it was very difficult to sample and the only sample collected (Ds17) was so deformed that no measurements could be made on it.

The intensity of NRM of these samples ranged between 0.5 - 56 mAm^{-1}. Their initial directions were not very consistent, having a mean value of Dec. = 356.7^{o}, Inc. = 73.7^{o} (α_{95} = 7.1), (Table 3.7). Twelve of the samples were stable to very stable during AC-demagnetization. Samples 1, 2, 4 and 11 were poorly stable and sample 18 was metastable (fig. 3.13).

The most stable directions of these samples were scattered but showed systematic directional changes with depth. Samples 1 - 11 had northwesterly directions while the upper samples (12 - 18) showed northeasterly directions. These directional changes could reflect changes in the geomagnetic field direction over a period of time. The mean value of the most stable directions of samples collected at the same level were calculated (i.e. mean value of samples 1,2,3 ; 4,5,6 ; 7,8, and 9,10) and combined with all other samples at different levels to produce a three-point average curve, corrected to Meriden (fig. 3.15a). This curve was compared with the archaeomagnetic curve for the period 1500 - 1900 AD and the previous Wharram pond curve. The inclination value of the dam site

a)

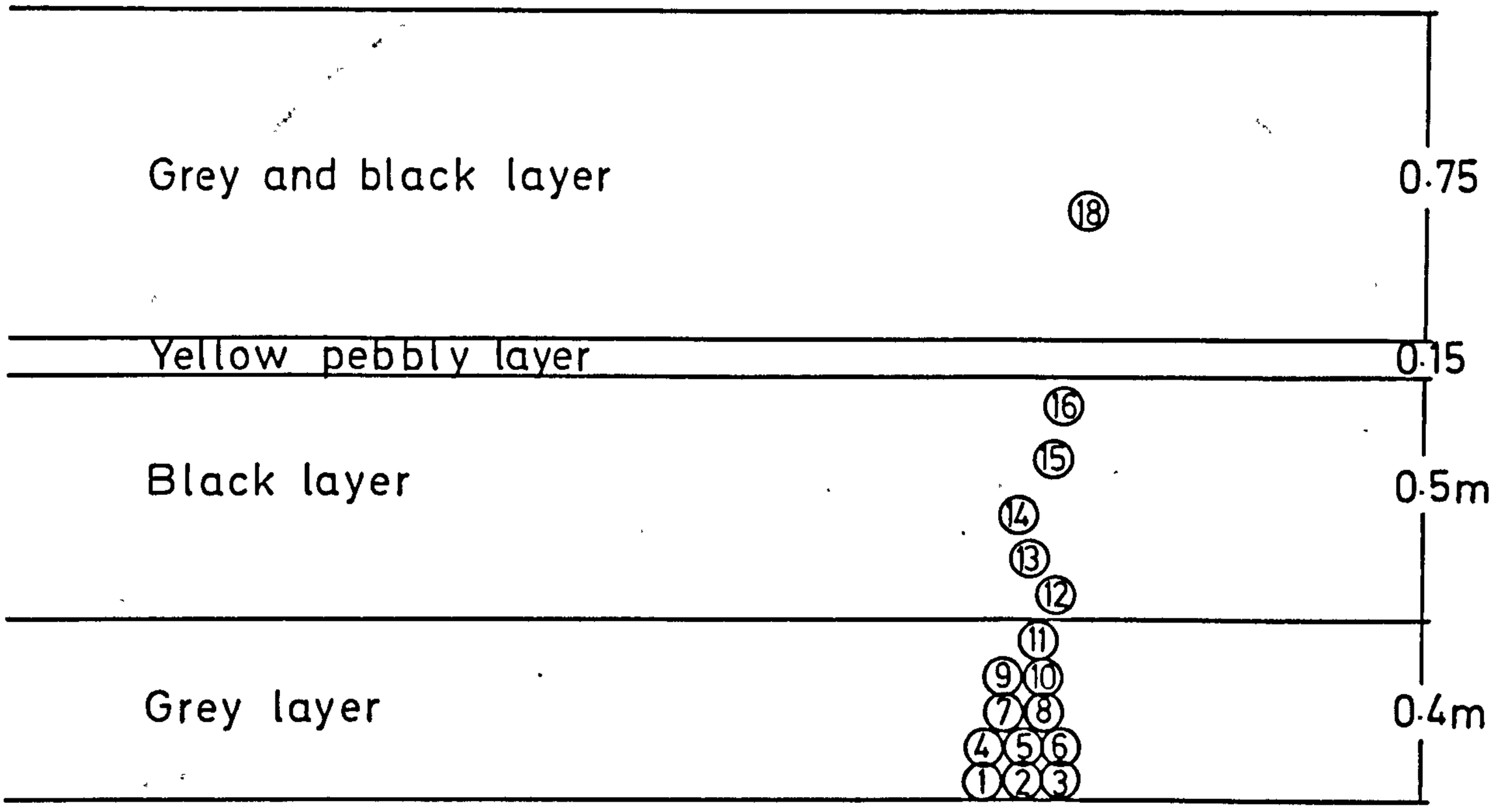

b)

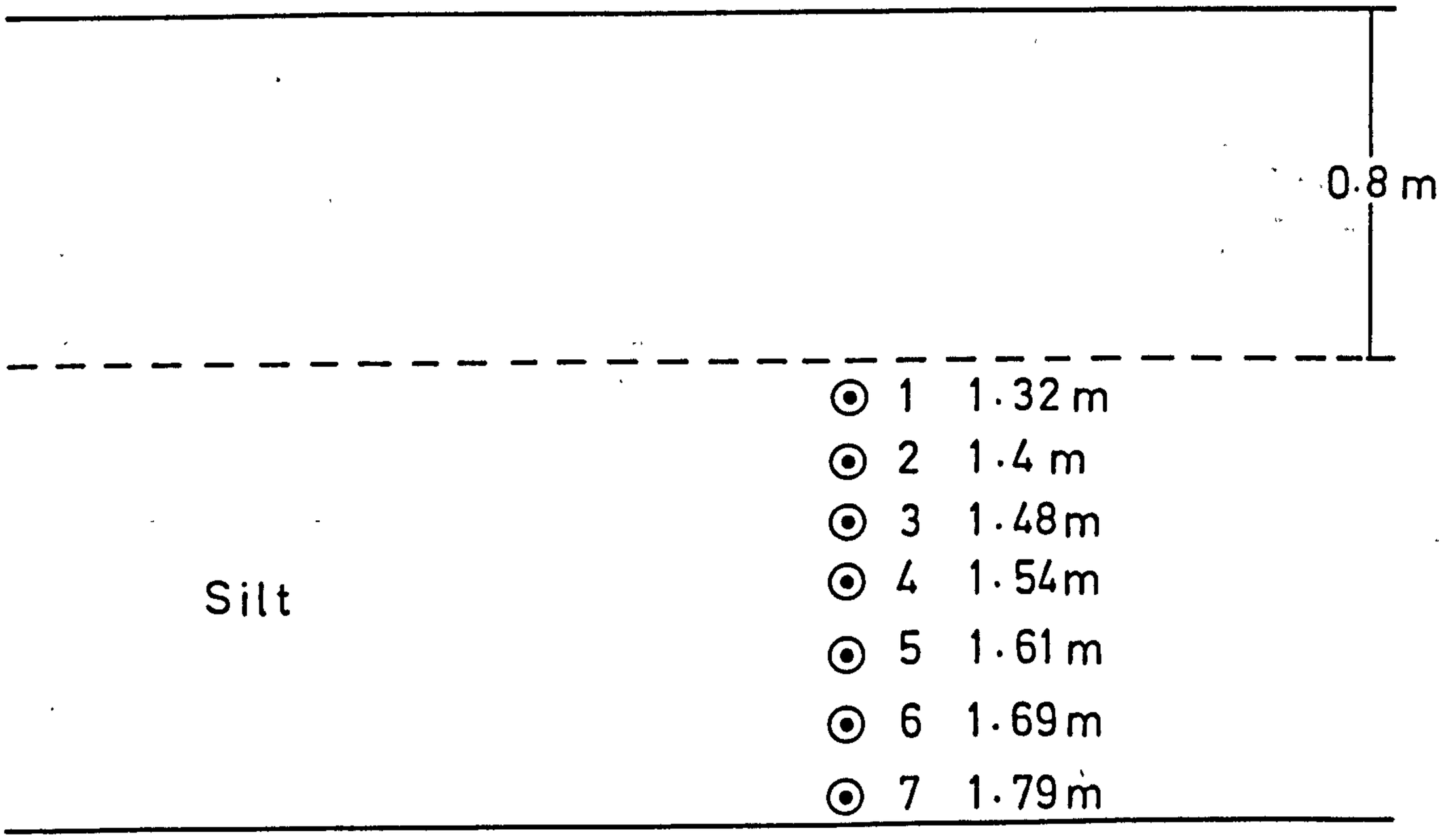

Fig. 3.12 Samples distribution of
a) Dam site
b) Silt (W_{176})

a)

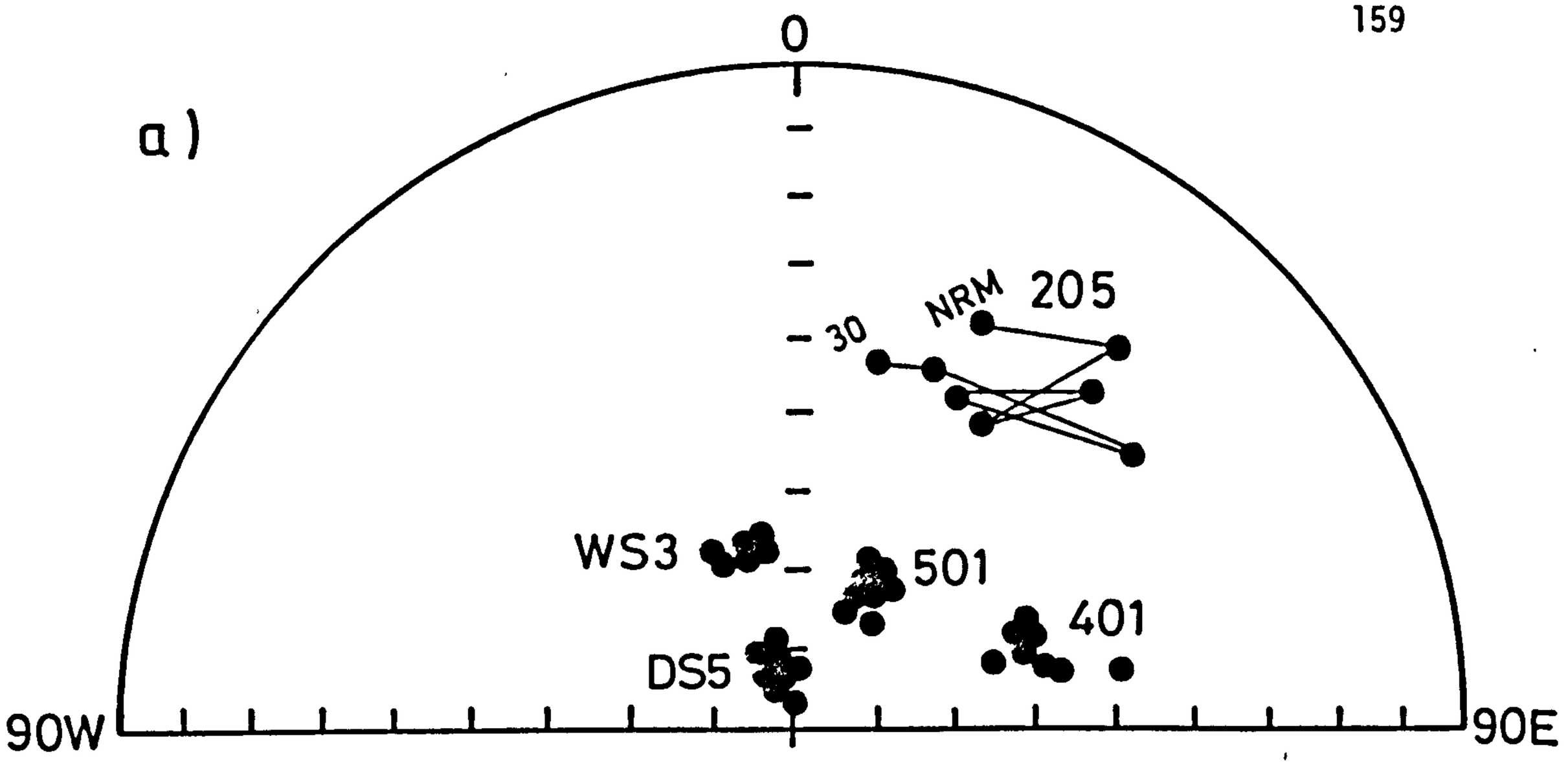

b)

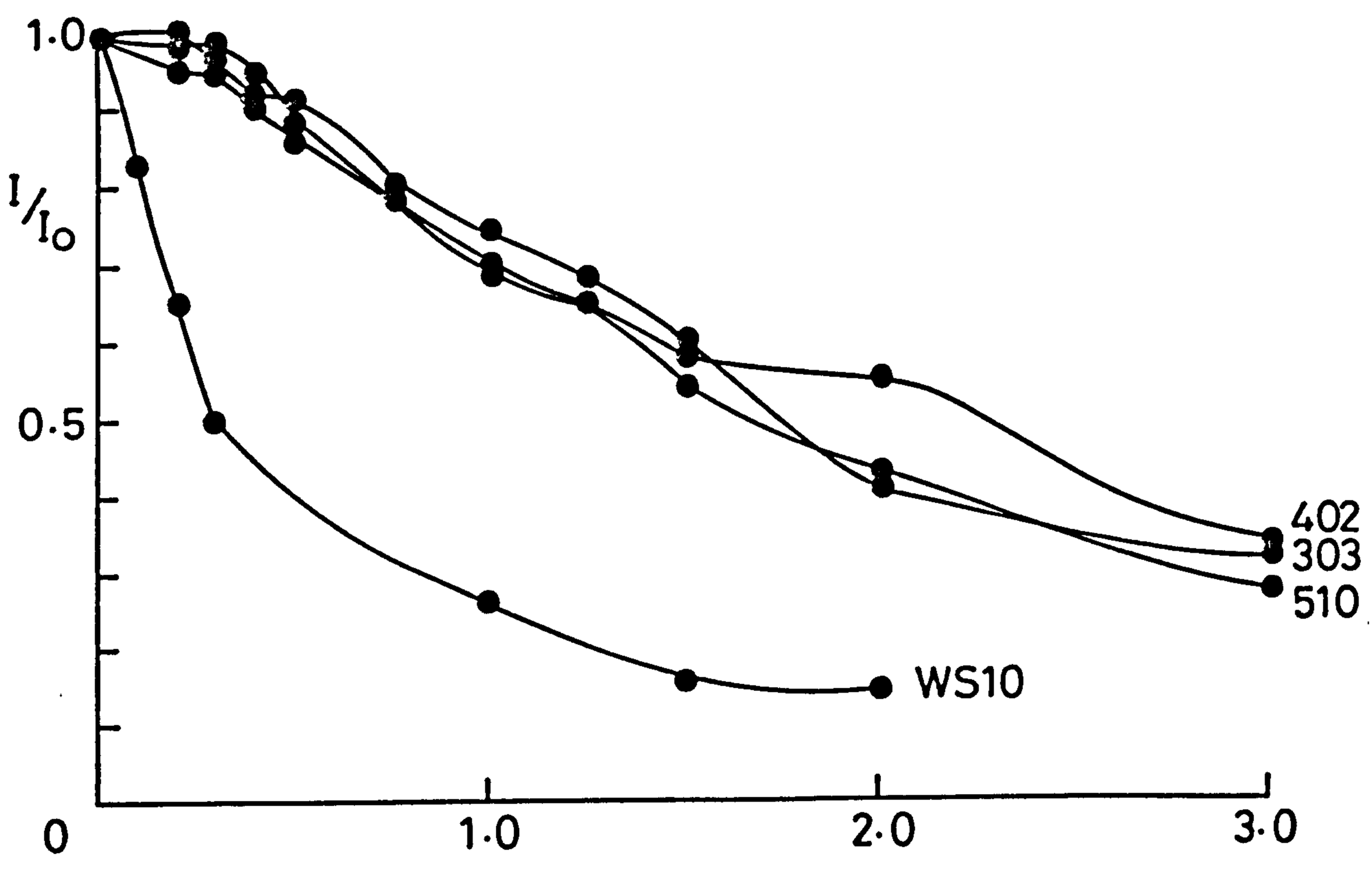

Fig. 3.13 Examples of changes during AC demagnetization of Wharram Percy samples

a) Directions
b) Intensity

	Sample No	Depth	Initial components Dec.	Inc.	Int. (mAm^{-1})	Most stable components Dec.	Inc.	S.I.
black layer	18	0.35	225.8	74.5	45.47	218.5	83.3	0.60
	16	0.70	51.5	60.1	49.56	48.0	60.3	8.45
	15	0.80	57.7	74.2	56.82	59.7	78.3	8.07
	14	0.90	49.2	70.2	30.69	31.3	69.1	4.05
	13	1.00	47.6	78.1	17.95	12.5	86.0	6.76
	12	1.05	26.1	71.4	27.63	358.9	73.2	5.69
grey layer	11	1.15	333.5	73.0	0.52	297.3	66.8	1.79
	10	1.20	348.3	79.2	2.18	330.6	77.1	5.04
	9	1.20	349.8	66.3	1.34	349.6	63.0	5.05
	8	1.25	18.9	61.3	2.20	7.0	69.9	6.49
	7	1.25	337.3	68.9	0.82	315.5	58.6	2.80
	6	1.35	7.4	69.6	4.25	1.0	69.1	11.14
	5	1.35	1.8	82.3	0.98	344.1	82.5	5.48
	4	1.35	331.2	55.8	0.58	321.8	47.5	1.89
	3	1.45	300.1	55.6	0.93	295.0	50.2	2.64
	2	1.45	332.9	65.9	0.57	319.3	57.3	1.55
	1	1.45	344.7	64.4	1.37	334.0	62.9	2.38

TABLE 3.7 Initial, most stable, stability indices and the mean values of the stable direction of the Dam Site samples

Black layer mean	33.4	74.2	α_{95} = 11.0	k = 48.6
Grey layer mean	326.4	65.4	α_{95} = 8.2	k = 31.2
overall mean	340.3	70.4	α_{95} = 7.9	k = 22.2

data were steeper than the inclination values of the archaeomagnetic curve and previous Wharram pond curve. The first point(point A) was shallower than the archaeomagnetic curve by about 3^{o} and about 12^{o} to the west. The other values from the grey layer, after point A, then show steeper inclinations with the declinations remaining westerly until point E, which is the transition between the grey and black layer, in which the declination started to become easterly with the inclinations remaining nearly constant but 4^{o} steeper than the archaeomagnetic curve, until between points F and G where the inclination starts to shallow.

The obtained curve from the dam site shows an easterly change in direction. The only part in the available archaeomagnetic records that shows such an easterly change is the period between 400 - 1000 AD, although the directions between 400 - 800 AD are based on sediment samples and are considered to be not very well defined. However, the two curves do not coincide, and only show broad regional similarities. Since the archaeological age of the site is expected to be between 600 - 1300 AD, the obtained directions could correspond to the part of the archaeomagnetic curve which shows anti-clockwise directional changes (i.e. 500 - 1000 AD), but there still appears to be a large scatter in the directions. This scatter is probably due to the presence of pebbles within the sampled section and also due to the effect of water flow.

The previous Wharram Pond results show a westerly directional change which was correlated with the period between 1600 - 1900 AD. It is possible that the present samples were collected from stratigraphically older layers, as the excavation in the site was still in progress.

The mean value of the black layer samples and

the grey layer samples were each calculated separately, and assuming that the declination has changed as a result of pebbles or water flow, the mean inclination was used for dating these samples. On this basis the grey layer samples could have an age around 1130 AD, 1520 AD, 330 AD or 150 (Roman), while the possibilities for the black layer samples are approximately 1750 AD, 1650 AD or between the 7th-8th century. However, for the overall mean value, the age could be around 1850 AD, or around 1570 AD. Although there are many possibilities, the archaeological evidence restricts the age range. According to the available information, the site cannot be Roman or even near-Roman; furthermore, the grey layer is stratigraphically older than the black layer (i.e. below the black layer) hence some of the proposed ages for the black layer (ages older than 11th century) are not applicable, and so the black layer age should be related to the end of the 15th or beginning of the 16th century. The overall age range for the site would then be 1130 - 1600 AD.

3.5.2 Wharram Silt (W_{176})

A total of 7 samples (Ws_{1-7}) were collected from a deposit of silt filling a high level depression to the downstream (north) side of the dam. These samples were collected successively from the top of the bottom covering a uniform column of silt of about 1.79 m. thickness (fig. 3.12b). Another three samples (Ws_8, Ws_9, Ws_{10}) were collected from a corner to the west of the first group of Wharram silt samples at coordinate 9R/S 171.

The NRM directions of samples Ws_1 - Ws_7 were well grouped with a mean value of Dec. = 329.5^o, Inc. = 62.8^o, ($\alpha_{95} = 4.4^o$), and the intensity ranged between 10 - 18 mAm^{-1} (fig.3.14). The other silt samples (8 - 10) had slightly weaker intensity ranging betwen 6 - 8 mAm^{-1} (table

Sample No.	Initial Components Dec.	Inc.	Int mAm^{-1}	Most stable components Dec.	Inc.	S.I.
1	337.7	63.3	18.14	336.0	73.5	3.64
2	332.6	60.0	16.19	337.9	53.7	1.64
3	337.4	67.6	13.74	347.7	67.2	5.65
4	333.6	70.5	18.09	342.3	74.7	2.43
5	320.4	56.5	14.41	322.5	59.1	6.12
6	329.0	59.4	14.03	335.6	60.2	6.77
7	320.7	61.4	10.11	327.9	63.2	3.98
Mean	334.8,	64.4	α_{95} = 6.3	k = 90.2		
8	286.3	76.6	7.99	307.0	69.9	1.91
9	310.3	68.6	8.90	311.6	68.1	4.90
10	297.8	65.1	6.65	317.6	73.2	1.23
Mean	312.0	70.1	α_{95} = 4.7	k = 680.7		
11	21.6	48.7	0.44	15.9	45.8	2.48
12	11.5	37.6	0.53	20.9	37.0	1.77
13	358.2	36.3	0.65	1.6	36.9	3.05
Mean	12.2	39.6	α_{95} = 14.2	k = 75.5		

Table 3.8 Initial, most stable, stability Indices and mean values of Wharram silt W_{176}, Ws_8-Ws_{10}, and ditch samples Ws_{11}-Ws_{13}.

3.8). The behaviour during AC-demagnetization ranged between stable to very stable, except samples 2 and 4 which were poorly stable. The components remaining after AC demagnetization in all samples (Ws_1 - Ws_{10}) had north-westerly directions while the components removed showed a similar grouping, indicating the removal of the same component. The most stable directions of magnetization of samples Ws_1 - Ws_7 show a clockwise rotation with decreasing age (Fig. 3.15b) and probably reflect deposition over a period of time. The curve shows small changes in declination values (about $\pm 10^{o}$) with inclinations ranging between 50^{o} to 80^{o}. These are stable and consistent but the directions are very different from those expected for any possible ages for them. However, they are still thought to reflect a waterlain deposit rather than shovelled deposits (which was suspected by the local archaeologist) as they are so uniform with only small, consistent vertical changes. The mean directions of the grey layer (same level as silt) from the dam site samples was plotted on the Wharram Silt curve and it was found to be near the end of the curve, with a shift of about 7^{o} in declination from the Wharram Silt mean value. This suggests that the end of the Wharram silt depositional cycle just preceeded the postulated refilling of the sediments of the dam site.

The mean value of the most stable directions was plotted on the archaeomagnetic curve. This value was found to be near the 1800 - 1900 AD part of the curve but about 8^{o} shallower. The mean inclination was also used for dating the site on the assumption that the declination was shifted to the west due to disturbance as a result of water flow. The mean inclination suggests the following possible ages; 1140 AD and 1530 AD. The 1530 AD is consistent with the archaeological age (1500 - 1600 AD) but it is poorly defined. Therefore the most reliable date will be the inter-

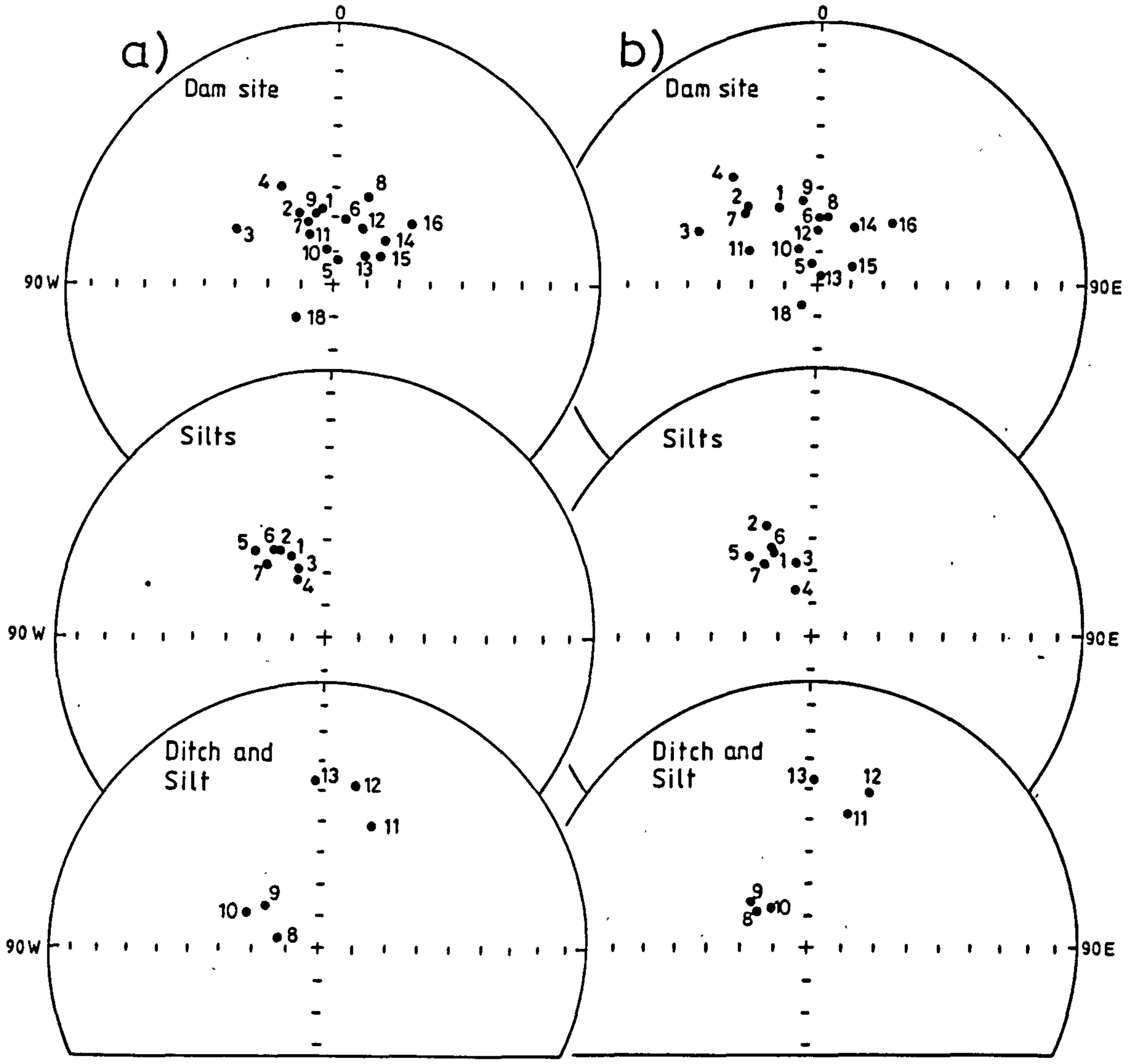

Fig. 3.14 Magnetic directions of Wharram Percy dam site, silts and ditch samples

a) NRM b) stable directions

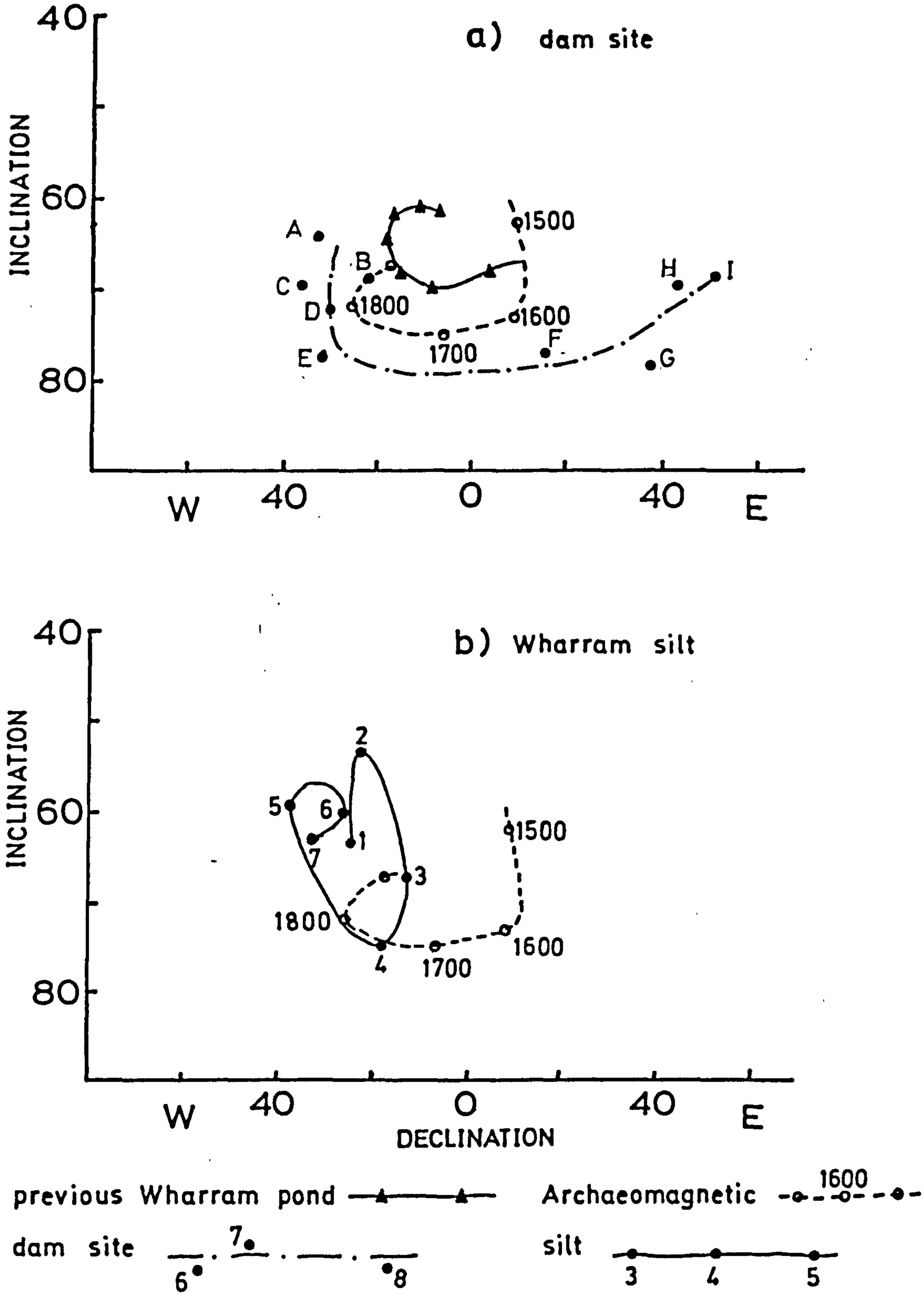

Fig. 3.15 Comparison of the most stable directions of the dam site and silt samples with previous Wharram Pond curve and the archaeomagnetic curve (1500-1900 AD)

section of the Wharram silt curve with the archaeomagnetic curve, 1750 - 1900 AD.

The other three samples (Ws_8, Ws_9 and Ws_{10}) had their most stable directions well grouped but their mean value was shifted to the west of the archaeomagnetic curve.

If these directions of remanence (particularly declination) of these silts is due to depositional factors then this could indicate a westerly change in the stream direction.

3.5.3 Pond Silts KK 172 (1000 - 1300 AD)

A total of 10 samples were collected from an east-west section through the chalk and earth dam. The sampled column is about 66 cm. thick and at the top of it there is a coarse pebble layer. Samples 201, 202 and 203 (top samples) were collected from silt layer 1921. Samples 204, 205 and 206 were collected from silt layer 1461. Samples 207 and 208 were collected from silt layer 1464, and samples 209 and 210 (lower samples) were collected from silt layer 1466. These silty layers were all separated by layers of pebbles.

The intensity of NRM was weak, ranging between 0.28 - 0.87 mAm^{-1}, and the directions were somewhat scattered (table 3.9). (Samples 201, 207, 208 and 210 were rejected because of the deformation in their shapes). All samples were metastable to poor during AC demagnetization. Sample 202 was poorly stable; the components remaining were all scattered in the northeasterly direction and the removed components were all scattered. Sample 203 was metastable with significant, but moderately smooth changes in intensity and direction. The components remaining were scattered but all in a southwesterly direction while the removed components were widely scattered. Sample 204 was metastable, changes in intensity were smooth

Sample No.	Initial Dec.	Inc.	Int, mAm^{-1}	Most stable Dec.	Inc.	S.I.
202	26.8	21.6	0.54	23.7	18.3	1.01
203	278.1	34.0	0.28	235.4	47.7	0.99
204	7.6	27.9	0.70	6.6	30.1	0.56
205	24.4	32.6	0.87	20.2	42.6	1.55
206	357.5	32.6	0.69	23.3	33.3	0.85
Mean (excluding sample 203)	14.6	31.8	α_{95} = 12.4, k = 39.0			

Table 3.9 Initial, most stable, stability indices, and the mean value of the pond silt sample KK 172

while the directional changes were inconsistent. The remaining components were grouped having a northeasterly direction while the removed components were scattered. Samples 205, 206 and 209 ranged from poorly stable to meta-stable during AC demagnetization. The components remaining were not well-grouped but all appear to have a north-northeasterly direction, while the removed components were scattered.

The most stable directions showed very shallow inclinations, much shallower than any historic directions of geomagnetic field (fig. 3.16). This could be due to reworking of the sediments. The declination values were not very consistent, but all had easterly directions except sample 203. The mean value of samples 202, 204, 205, 206 and 209 was calculated bu this mean value did not fall on the archaeomagnetic curve because of the shallow inclination. However, taking just the mean declination, the age of these samples could be around 1200 AD. This date is poorly defined but it was comparable with the archaeological data.

Since the archaeological data for this site is also poorly

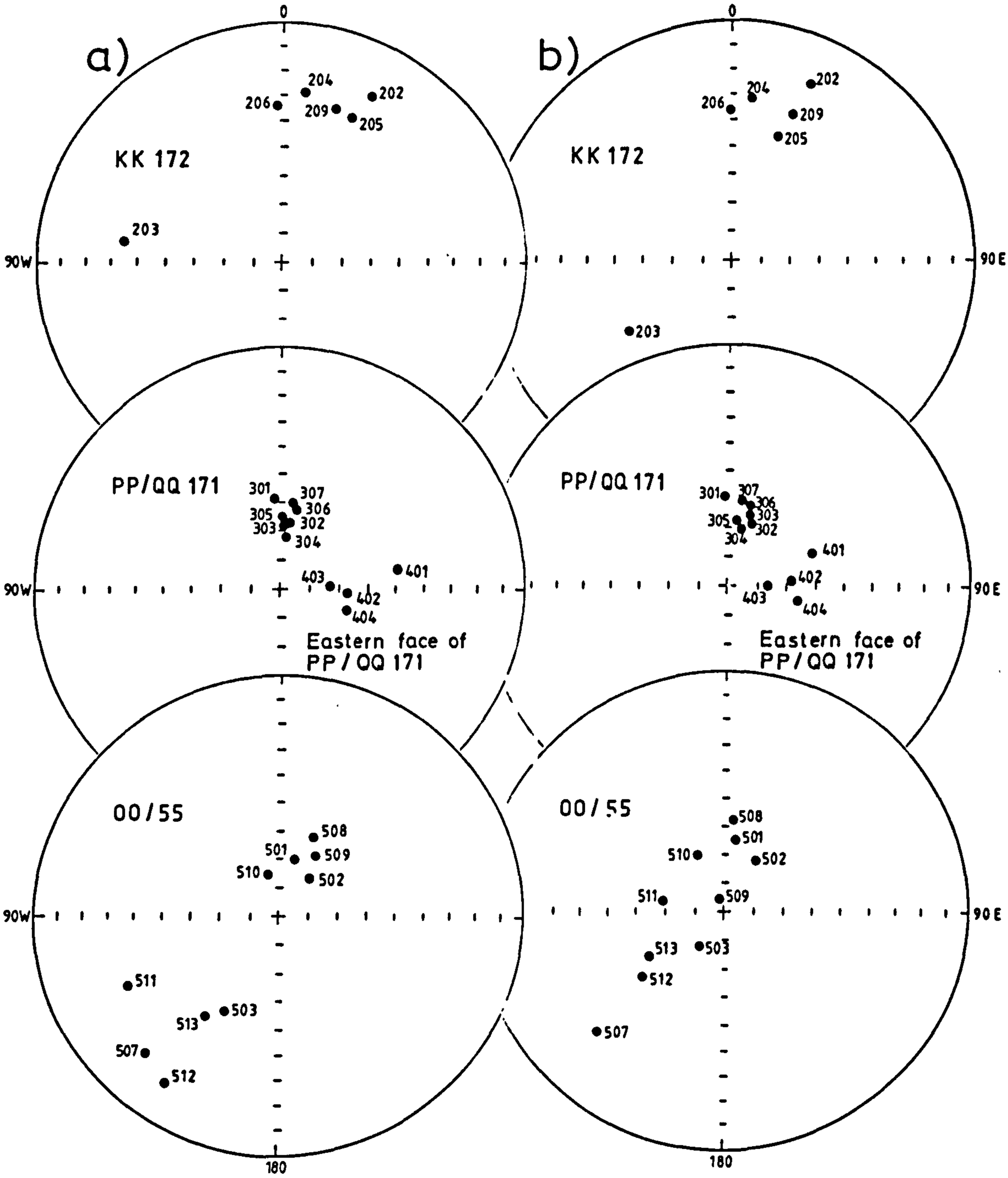

Fig. 3.16 Magnetic directions of Wharram Percy sites KK/72, PP/QQ171, Western face of PP/QQ171 and the sump

a) NRM b) Most stable

defined (1000 - 1300 AD), the difference between the obtained inclination and the expected inclination for the site can only be approximated as 30^{o}. This shallow inclination could be due to reworking of the sediments or to other sources of inclination errors in sediments.

3.5.4 Pond Silt PP/QQ 171 (Eastern face of section QQ/RR 171) (1200-1300 AD)

Seven samples were collected from the eastern face of a ditch distributed along 45 cm. column of coarse brown silt. Above the brown silt column there was a 10 cm. layer of blue clay, while at the bottom there was a layer of coarse gravel.

The intensity of NRM ranged betwen 4.9 - 7.3 mAm^{-1} and the directions were consistent with a mean value of Dec. = 13.4, Inc. = 64.4 (α_{95} = 3.8). Most of the samples were very stable, except sample 305 which was only just stable, the intensity decrease and the changes in directions were smooth during increasing AC demagnetizing field (table 3.10).

	Initial			Most stable		
Sample No.	Dec.	Inc.	Int. mAm^{-1}	Dec.	Inc.	S.I.
301	1.7	58.0	4.92	2.3	58.8	6.81
302	12.3	66.7	7.39	23.1	66.6	10.15
303	10.3	67.9	6.70	21.6	65.6	14.53
304	12.0	71.4	6.69	16.0	69.8	14.10
305	8.6	64.6	5.56	11.3	67.7	2.94
306	16.7	62.1	6.68	19.6	61.7	5.00
307	13.1	59.9	5.32	14.3	59.8	6.17
Mean	15.1	64.2	α_{95} = 3.9	k = 231.5		

Table 3.10 Initial, most stable, stability indices and the mean value of pond silt samples PP/QQ/171 (eastern face of the ditch)

The components remaining after AC demagnetization in sample 301 were well-grouped having a north-northeasterly direction, while the removed components showed a similar grouping indicating the existence of only one component and also the high stability of the samples. The other six samples behaved similarly during AC demagnetization. The components remaining were all well grouped having a northerly direction, with the components removed showing a similar grouping.

The mean value of the most stable directions were calculated and plotted on the archaeomagnetic curve. The α_{95} bars curve around 1180 AD and the mean value was only about 4^{o} away from the 1130 AD part of the curve. Accordingly the site was dated as 1060 - 1180 AD. This date was accepted archaeologically despite being somewhat earlier than expected (1200 - 1300 AD). The expected (for 1200 - 1300 AD) inclination was steeper by about 5^{o} and the declinations were shifted to the west. Such shift in declination is considered possible in sediments as it could be due to the local disturbance in the water flow; on the other hand, the error in inclination could also be as a result of the wet conditions or inclination error in sediments.

3.5.5 Western face of QQ section (PP/QQ/171) (1200-1300 AD)

A total of 4 samples were collected from a 30 cm. column of silt which was below a 15 cm. layer of chalk and earth dam.

The intensity of NRM ranged between 4.8 - 5.8 mAm^{-1} and the directions were not very consistent (table 3.11). Samples were all very stable during demagnetization (except sample 404 which was only stable) as indicated by their stability indices. The components remaining after AC demagnetization in sample 401 were well grouped having a northeasterly direction, while the removed components were scattered. The components

remaining in sample 402 were well grouped having approximately easterly direction and the removed components were all scattered but also in an eastern direction. Sample 403 had the component remaining well grouped having nearly an easterly direction while the removed components were scattered (fig. 3.16). The mean value of the most stable directions (samples 401, 402, 403) did not fall on the archaeomagnetic curve because of the shifted declination value and hence it was difficult to find the age of these samples.

The mean value of the most stable direction of these

Sample No.	Initial Dec.	Initial Inc.	Initial Int, mAm^{-1}	Most stable Dec.	Most stable Inc.	Most stable S.I.
401	80.5	48.2	4.83	68.7	59.2	5.04
402	93.7	66.8	5.88	84.1	68.3	8.30
403	85.8	72.3	5.04	89.4	76.5	7.00
404	105.2	65.9	4.98	102.0	66.5	4.17

Mean Dec. = 83.9, Inc. = 68.0, α_{95} = 10.3, k = 79.8

Table 3.11 Initial, most stable, stability indices and the mean value of samples collected from the western face of section PP/QQ/171

samples had their declination values well shifted towards the east while the inclination value was somewhat near the inclination value of the Eastern face group samples (PP/QQ/171). Since the sampled column of the Eastern face was 45 cm. thick and the Western face was 30 cm. thick, then this could mean that the main depositional site was near the Eastern face, i.e. the flow was eastward. As a result the sediments near the western face were under the effect of an eastward horizontal shifting which could affect the declination.

3.5.6 Water Conduit (ditch samples)

Samples Ws_{11}, Ws_{12} and Ws_{13} were of clay packed sandstone which were collected from a line and capped channel running from the pond area, west of the church towards either the vicarage or a post-desertion farm.

The intensity of NRM of these samples was weak, ranging between 0.44 - 0.65 mAm^{-1}, but the directions were fairly consistent (table 3.8). They were moderately stable to stable during AC demagnetization and the components remaining had a shallow northeasterly direction.

The most stable directions had very shallow inclination value, hence no possible age was found for this group (fig. 3.14) although the declination value is consistent with the 1500 - 1600 AD period. These shallow inclinations could be due to compaction as a result of the overloading sediments, or due to reworking of the sediments.

3.5.7 Sump 00/55

Thirteen samples were collected from silts exposed in a sump dug to keep the rest of the pond site dry. The silts probably therefore represent sedimentation since the last time that the pond was cleaned.

The intensity of NRM of these samples ranged between 2.7 - 8.4 mAm^{-1}, while the directions were scattered (table 3.12). Samples 504, 505 and 506 were rejected, because they were deformed during sampling.

Pilot samples 501, 502, 508 and 510 were stable during AC demagnetization. The components remaining in sample 501 were well grouped having nearly a northerly direction while the removed components were scattered. The components remaining in sample 502 had the low coercivity components well grouped in the northeasterly direction while the high

Sample No.	Initial Dec.	Initial Inc.	Initial Int, mAm^{-1}	Most stable Dec.	Most stable Inc.	Most stable S.I.
501	16.4	69.5	6.2	9.8	63.3	4.7
502	39.0	72.7	7.6	30.4	68.1	11.8
503	208.6	51.5	2.7	220.9	76.7	0.9
507	223.6	20.7	3.3	227.2	28.6	0.6
508	23.5	59.7	6.5	6.0	56.1	5.1
509	210.7	64.9	4.8	341.1	84.1	1.2
510	345.7	75.1	8.4	337.4	67.2	7.1
511	244.2	31.8	5.7	280.6	68.0	0.9
512	213.4	15.1	5.8	233.3	54.4	0.6
513	214.9	46.3	5.6	241.3	81.3	1.3

Mean Dec. = 292.7, Inc. = 78.6, α_{95} = 17.7, k = 8.3

Table 3.12 Initial, most stable, stability indices, and the mean value of the sump samples (PP155)

coercivity components were in the southwesterly direction, and the removed components were scattered. Sample 508 had the components remaining well grouped having a northerly direction while the removed components were scattered. Sample 510 also had the remaining components well grouped having a northwesterly direction while the removed components were scattered. The other samples were also demagnetized, and they were less stable than the pilot samples. The most stable directions of all samples were scattered and did not show any consistency (fig. 3.16). These scattered directions could be a result of the wet conditions of the sump during sampling which could make sedimentation movement very likely. Alternatively, or additionally, the scattered directions could be due to some disturbances in the

pond as a result of water currents during flooding.

Summary

The results from the dam site (table 3.13) showed directional changes with depth. Although the curve obtained for directional changes was similar to the archaeomagnetic curve (1500 - 1800) and the previous Wharram pond curve, the directional changes were in the opposite direction, hence suggesting a date between 400 - 1000 AD (which is the only part of the curve where the directional changes are easterly), which is archaeologically unrealistic. The site also showed high degree of scatter in directions and this was thought to be due to the presence of pebbles within the sampled section and also the effect of water flow during deposition.

The silt samples (W_{176}) also showed directional changes with depth and were therefore thought to reflect waterlain deposits rather than shovelled deposits. The age of these silts was obtained using the mean value and the intersection of the obtained directional curve with the archaeomagnetic curve (table 3.13). The directions of the other silt samples (Ws_8 - Ws_{10}) departed from the archaeomagnetic curve, and this could also be due to changes in the stream direction of flow.

The pond silts (KK172) had their mean inclinations much shallower than expected, by about 30^{o}, but with the declination consistent with 1200 AD. While the other pond silts PP/QQ171 (eastern and western face) gave better grouped directions. The mean value of the eastern face sample was only 4^{o} away from the curve (westerly) and 5 steeper. On the other hand, the western side of the section gave stable directions with the declination towards the east, indicating an easterly flow. The water conduit samples (clay) gave very shallow inclinations which could be due to the effect of compaction, reworking of the sediments or inclination

SITE	CODE	D	I	α_{95}	AGE	REM
Dam site, grey layer	ww/vv, 170/171	326.4	65.4	8.2	1130 - 1520 AD	
Dam site, black layer	ww/vv, 170/171	33.4	74.2	11.0	around 1600 AD	
Dam site, overall	ww/vv, 170/171	340.3	70.4	7.9	1130 - 1600 AD	or 400 - 1000 AD
Wharram Silt	w176	334.8	64.4	6.3	1140 - 1530 AD	or 1750 - 1900 AD
Wharram Silt	-	312.0	70.1	4.7	-	samples Ws_8, Ws_9 and Ws_{10}
Pond Silt	KK 172	14.6	31.8	12.4	1200 AD(,?)	
Pond silt	PP/QQ 171	15.1	64.2	3.9	1130 - 1200 AD	
Pond silt	PP/QQ 171	83.9	68.0	10.3	-	west of PP/QQ 171
Water Conduit - ditch	54	12.2	39.6	14.2	1500 - 1600 (?)	
Sump silt	00/55	292.7	78.6	17.7	-	

Table 3.13 Age summary of Wharram Percy sites

errors.

The sump samples 00/55 were collected from a very wet section and the directions were scattered.

3.6 Westbury-Sub-Mendip, Somerset

The Mendip hills are famous for the caves formed in their limestone. In 1969 a new cave was discovered during quarrying operations, 250 m. up on the south western edge of the Mendip, above the village of Westbury-Sub-Mendip (Lat. 51.2N, Long. 2.5W). As quarrying continued, an oblique cross-section of a vast cave filled with fossiliferous deposits, 100 m. long and 30 m. deep, was revealed in the precipitous north wall of the quarry. The rich fauna of fossil mammals indicated that the cave fill was not much older than that of the majority of other Mendip Caves, but was probably more ancient than that of any other known Pleistocene cave in Britain. Pieces of flint showed apparent human workmanship at an age far older than previous records of human occupation in Britain. The associated flora and fauna indicate that their age is between 300,000 and 700,000 BP (Stinger et al., 1979).

The cave deposits are exposed on a face of the limestone quarry (fig. 3.17). Samples were collected during three visits in 1979, 1980 and 1982. These samples were from sites W_2, W_9, W_1, W_3, W_4 and W_6. Five samples were collected from the Upper Red Breccia (sites W_2 and W_9), nine samples from the Calcareous/Siliceous transition (site W_1), and two samples were collected from the transition between the siliceous and the calcareous groups (site W_3). Ten samples were collected from the Yellow Sand of the siliceous group (W_4) during two separate trips (four samples in 1979 and six samples in 1980). A total of 17 samples were collected from the siliceous group of sand and gravel (W_6); eight of them were collected

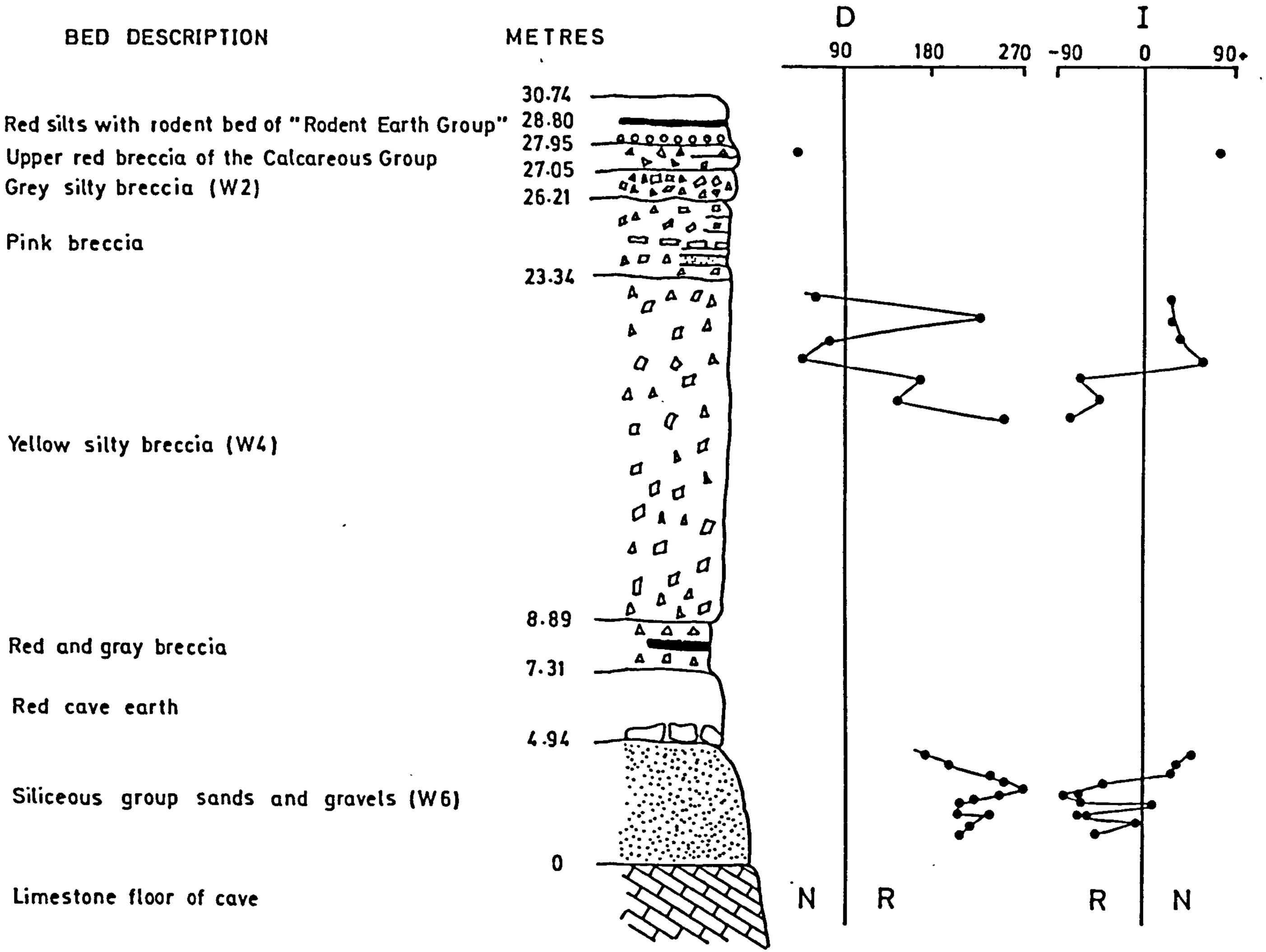

Fig. 3.17a Westbury sub-Mendip cave deposits, with their obtained magnetic directions

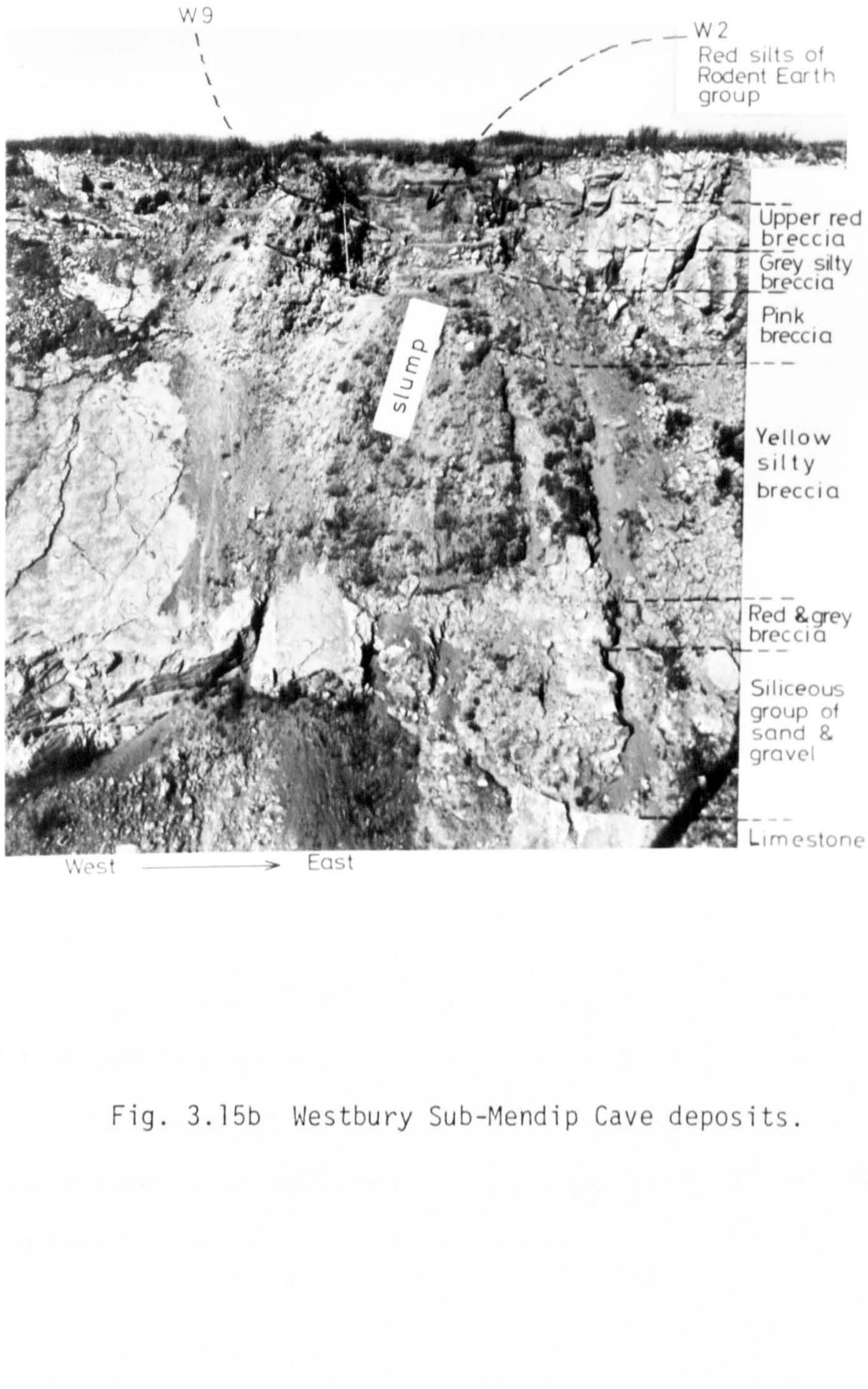

Fig. 3.15b Westbury Sub-Mendip Cave deposits.

from the site during two trips and 9 were subsequently taken from a core stored in the Natural History Museum.

The NRM of all samples were measured and most of them were demagnetized at 2, 4, 6, 10 and 14 mT, while the others were bulk demagnetized at 6 and 14 mT (fig. 3.18).

The intial intensities of all samples ranged between 0.02 - 96 mAm^{-1}. The highest intensity was obtained from layer W_2 (Munsell colour. yellowish red), W_9 (Munsell colour reddish brown) and from W_6 core samples (Munsell colour brown). The weakest intensity was obtained from layer W_4 (Munsell colour yellow and brownish yellow). As all the samples were fine grained(<1mm) no correlation could be observed between the grain size and the intensity.

3.6.1 Upper Red Breccia (W_2 and W_9)

The NRM intensity of samples collected from W_2 and W_9 ranged between 3 - 92 mAm^{-1}. These values were considered to be very high compared with the intensities obtained from the other sites. AC-demagnetization showed that samples $W_{2/4}$ were unstable while sample $W_{2/5}$ was metastable. The components remaining after AC-demagnetization in sample $W_{2/5}$ were grouped in a northeasterly direction and the components removed were in the same direction indicating the removal of some of the same vectors at high fields.

AC-demagnetization of samples collected from W_9 deposits showed that sample $W_{9/1}$ was stable, and samples $W_{9/2}$ and $W_{9/3}$ were unstable. The components remaining after demagnetization in sample $W_{9/1}$ were well grouped in a northeasterly direction while the removed components were scattered.

a

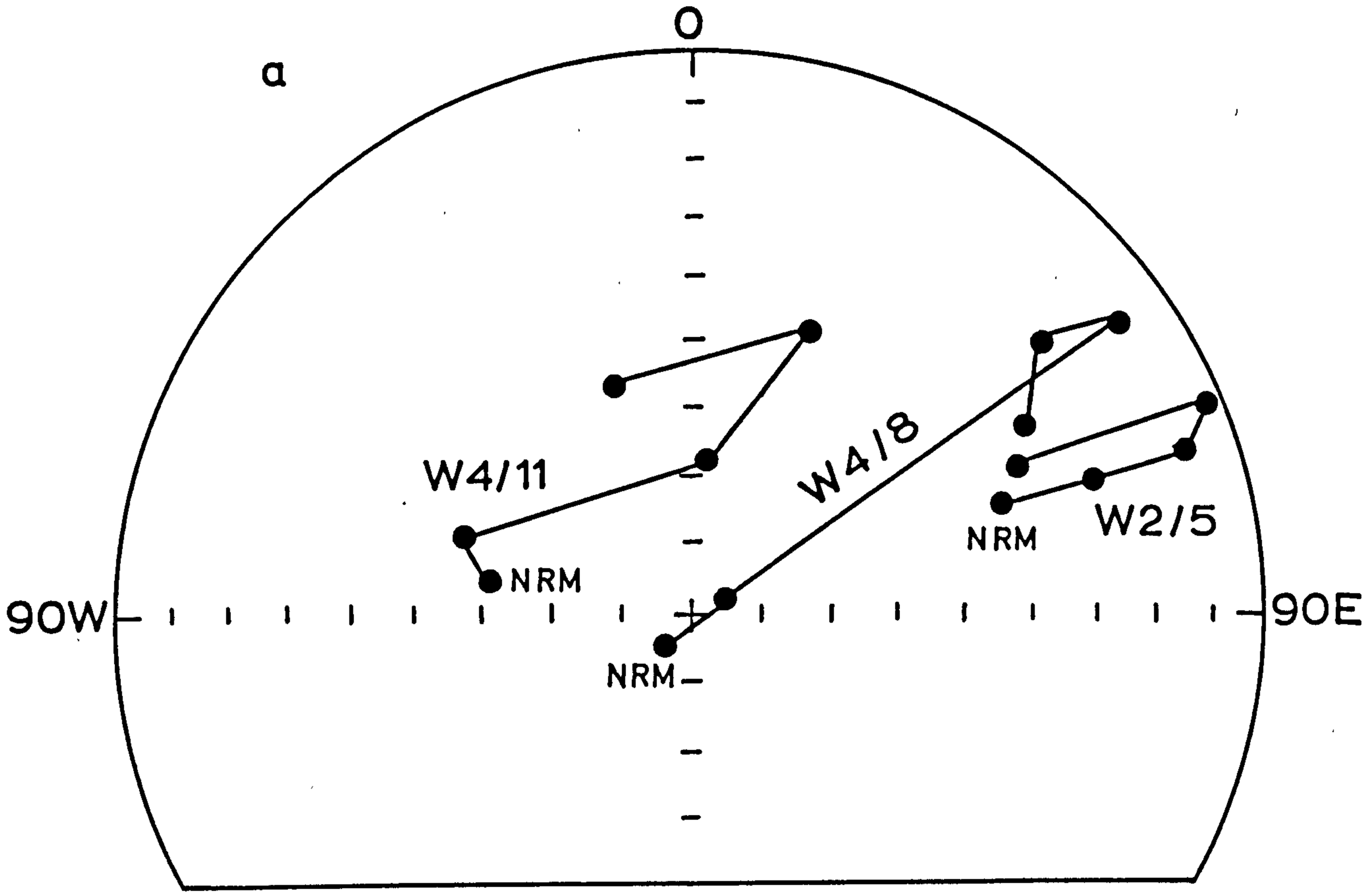

b

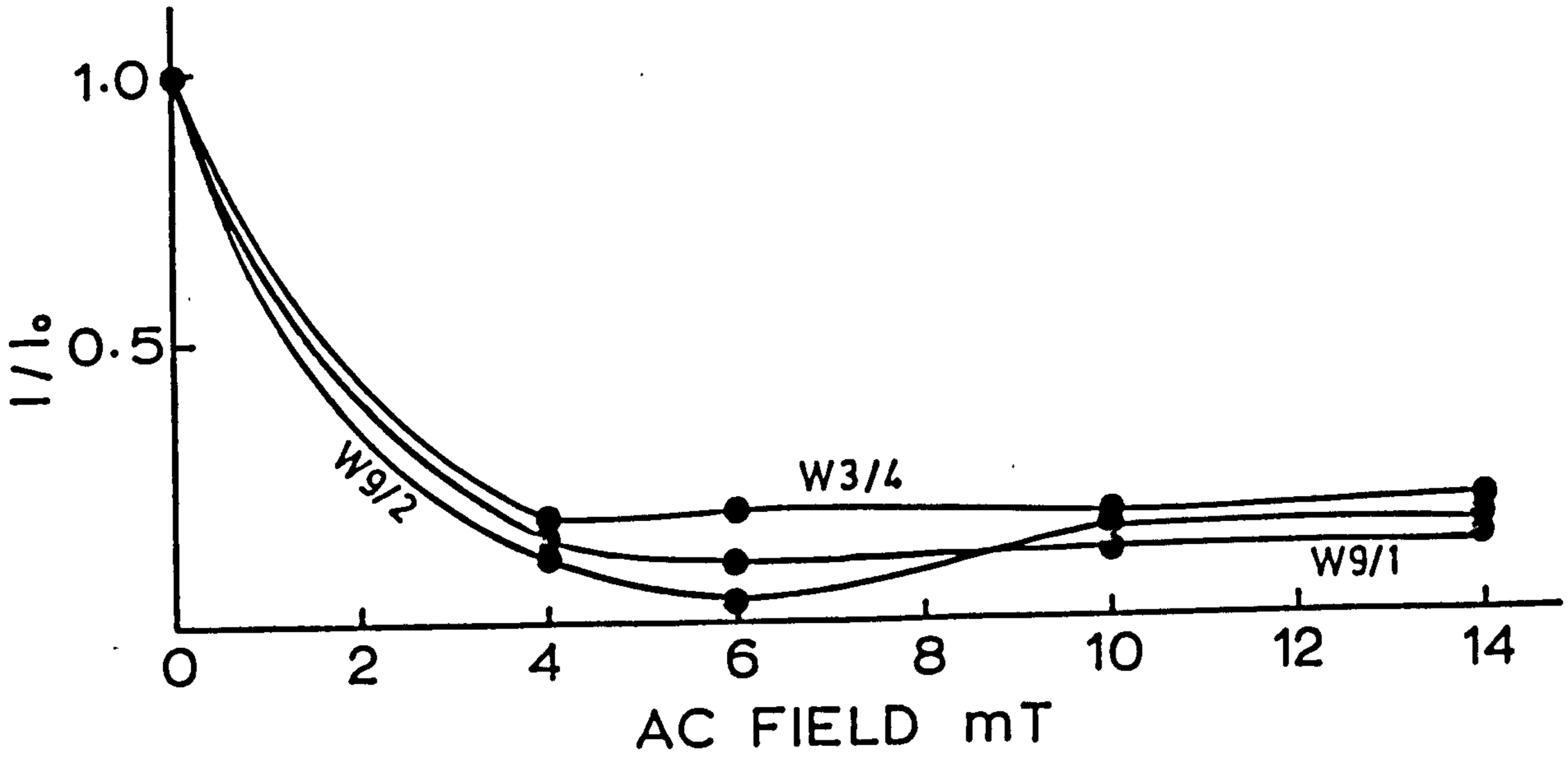

Fig.3.18a Examples of changes during AC demagnetization of Westbury sub-Mendip samples

a) Direction
b) Intensity

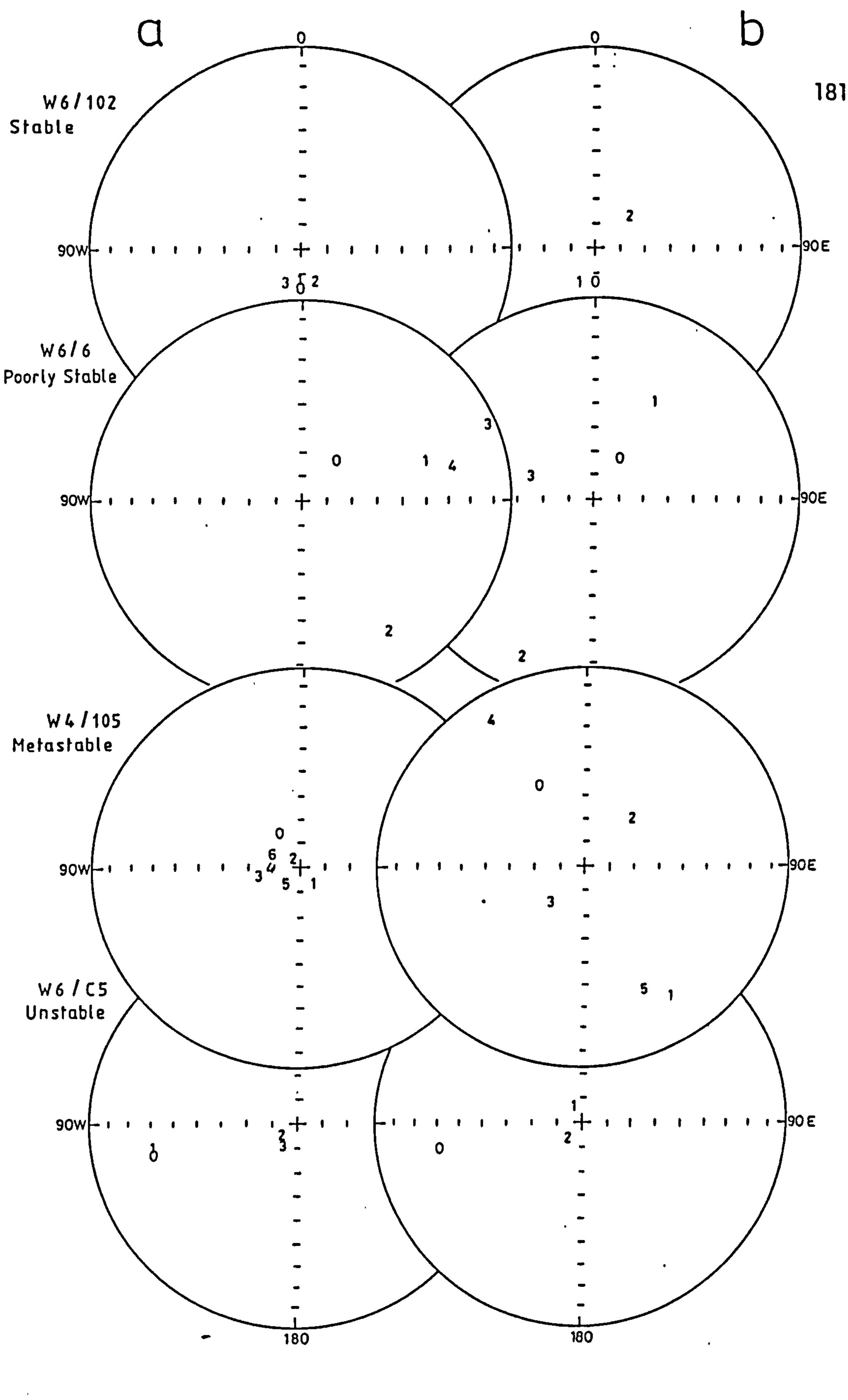

Fig. 3.18b Examples of changes during demagnetization of four reversed pilot samples
a) Components remaining
b) Components removed

3.6.2 Calcareous/Siliceous Transition (W_1)

The NRM intensity of samples collected from this site ranged between 0.3 - 0.23 mAm^{-1}, and the direction showed somewhat shallow inclination with a northeasterly declination. AC-demagnetization showed that sample $W_{1/5}$ was stable, $W_{1/1}$ and $W_{1/4}$ poorly stable, $W_{1/2}$ and $W_{1/3}$ metastable and $W_{1/6}$, $W_{1/7}$, $W_{1/8}$ and $W_{1/9}$ were unstable. The components remaining after demagnetization showed grouping in the north-northeasterly direction, with relatively shallow inclination.

3.6.3 Transition Beds between Siliceous and Calcareous Group (W_3)

Two samples of mixed clay and sands were collected from this site. The intensity of magnetization of these samples was 0.07 and 2.92 mAm^{-1}. AC-demagnetization showed that sample $W_{3/3}$ was metastable and $W_{3/4}$ unstable. The components remaining after AC demagnetization were scattered in the northeasterly direction. This scatter could be caused by the inhomogeneity due to the clay injections in the silt.

3.6.3 Yellow Sands of the Siliceous Group (W_4)

Ten samples were collected from this site during two trips. The intensity of NRM of the first four samples ranged between 0.18 - 3 mAm^{-1} while the directions were scattered. The remaining components in sample 8 (which was metastable) were moderately grouped having a shallow north-easterly direction, while the removed components had a south-westerly direction. Sample 9 (poorly stable showed a similar removed south-westerly low coercivity component, while the remaining components were well grouped in a southwesterly direction, indicating possibly reversed magnetization. For samples 10 and 11 (metastable) the components remaining were scattered in the north-northeasterly direction, while the removed components were scattered but showing some northeasterly vectors.

In order to check the apparent reversed magnetization observed in sample 9 another six samples were collected from these sands. The intensity of NRM of these samples ranged between 0.2 - 0.6 mAm^{-1}, while all the directions had negative inclinations with some of the samples also having reversed declinations. Sample 101 (metastable) had the components remaining grouped in the southern direction while the removed components were scattered. The components remaining in sample 103 (metastable) were not well grouped but they lay in a southeasterly direction. The remaining components in sample 105 were all grouped in the southwesterly direction while the removed components were all scattered. Sample 108 (metastable) had a similar behaviour, the remaining components were grouped in the south-westerly direction, while the removed components were all scattered.

The remaining components of these samples had a southern direction and were in the upper hemisphere (-ve inclination) indicating a reversed magnetization. These results confirm the previous maqnetic reversed direction observed in sample 9.

3.6.5 Siliceous Group (W_6)

Eight samples were collected from the site and another 9 samples were taken from a core stored in the Natural History Museum. The intensity of NRM of the two samples collected during the first trip were 2.13 and 0.55 mAm^{-1}. Sample 6 was unstable and sample 7 was poorly stable during demagnetization. The components remaining in sample W_6, showed a negative inclination with a possibly reversed declination.

The core samples had the NRM intensity ranging between 10 - 72 mAm^{-1} and the directions were scatterd showing reversed polarity in some samples. Samples (1, 2, 3, 5, 6 and 8) were demagnetized at 5, 10 and 15 mT. Sample 2 was poorly stable, samples 1, 3, 6 and 8 were

metastable and sample 5 was unstable during demagnetization. The most stable directions of pilot samples showed shallow inclinations, with a possible reversed direction in all samples. The remaining samples were bulk demagnetized and their directions also showed reversed polarity.

The NRM intensity of the other six samples (collected during a 1982 visit) ranged between 0.02 - 0.1 mAm^{-1} while the directions were scattered. These samples were demagnetized at 7.5, 15 and 20 mT. The stability of these samples ranged between poorly stable to unstable except sample $W_{6/02}$ which was stable. The components remaining after AC demagnetization were all in the upper hemisphere indicating reversed magnetization.

3.6.6 Conclusions

Doubts were raised in the analyses of this particular site due to the generally weak intensity of some of the samples and their generally poor stability. Accordingly the data were re-examined for the presence of spurious effects:-

1. Magnetometer effect: AC-demagnetization results did not show a systematic change towards any particular direction. Accordingly the results are not considered to be affected by systematic error rising from magnetometer effects or from the demagnetization procedure.

2. Stability and intensity relationship: The stability of the samples was found to be independent of intensity of magnetization (section 3.7).

3. Viscous magnetization: All samples were measured within less than 48 hours after sampling, except the core samples, hence the samples are not affected by short term viscous magnetizations or drying-out effects after collection. The core samples had been stored in the

British Museum for about 4 weeks, but those had been wrapped thoroughly and were still wet when the samples were extracted.

These considerations therefore suggest that the results can be considered to be reliable. Their interpretation was carried out using only samples with stability indices above 0.5 (metastable). The unstable samples were only tabulated (table 3.13) for comparison with the overall trend. The Upper Red Breccia (W_2 and W_9), the Calcareous/Siliceous Transition (W_1) and the Siliceous/Calcareous transitional rocks (W_3) show normal magnetization. On the other hand, reversed directions were observed in all samples from the Siliceous group, except for samples from the upper part of the Yellow Sand. Three of these samples had normal declination with somewhat shallow inclination, while the other sample had a probable reversed magnetization (figs.3.17b,3.19). The normal polarity in the three samples could be a result of mixing between normal and reversed magnetization i.e. the upper part of the Yellow Sand and/or the transition between the Siliceous and Calcareous group could be the transition between normal and reversed magnetization. The clear reversed magnetization observed in the Siliceous group samples suggests that these deposits acquired their magnetization during a period of earth's magnetic field reversal. Geologically many polarity reversals were recorded (Tarling, 1983) with the last being dated as 730,000 years B.P. Although the archaeomagnetic dating of this site is uncertain, a date of 730,000 years B.P. is probable on the available evidence and corresponds with the date of the last geomagnetic reversal.

3.7 Discussions and Conclusions

One of the main advantages of using sediments in archaeological dating is that sedimentary sections can reflect a continuous record of the magnetic directions during deposition, i.e. archaeomagnetic

Code	Initial			Most stable			
	D	I	Int mAm^{-1}	D	I	S.I.	Deposits
W2/4	68.3	12.8	28.76	70.2	2.2	0.4	
W2/5	70.7	40.6	92.46	69.5	22.3	0.6	Upper
W9/1	53.7	70.6	24.69	45.0	70.5	3.8	Red
W9/2	114.6	77.9	29.71	102.1	43.1	0.4	Breccia
W9/3	105.0	-79.5	3.07	91.7	29.5	0.4.	
W1/1	16.5	31.7	0.23	19.5	31.9	1.9	
W1/2	44.6	54.6	0.12	14.4	55.3	0.5	
W1/3	18.7	50.1	0.15	355.2	46.1	0.6	Calcareous/
W1/4	45.2	46.1	0.18	43.6	52.0	1.5	Siliceous
W1/5	5.0	23.8	0.14	42.2	21.1	2.5	Transition
W1/6	39.0	-51.0	0.03	35.8	15.0	0.2	
W1/7	102.3	53.7	0.03	82.6	11.2	0.2	
W1/8	68.3	28.4	0.10	52.1	13.7	0.4	
W1/9	115.8	39.9	0.04	135.3	10.3	0.2	
W3/4	38.2	74.0	0.11	351.3	58.4	0.4	Siliceous/Calcareous
W3/13	318.0	42.2	2.92	305.0	42.2	0.8	Transition
W4/8	216.8	85.9	1.26	60.3	25.0	0.7	
W4/9	23.9	70.6	1.43	224.6	20.8	1.1	
W4/10	72.0	14.4	2.98	74.4	38.5	0.9	Yellow Sands
W4/11	279.4	61.0	0.18	4.9	57.0	0.5	
W4/101	109.5	-23.4	0.32	166.4	-61.3	0.5	of the
W4/102	118.9	-40.0	0.21	141.7	-47.1	0.4	
W4/103	96.0	10.4	0.42	140.8	-45.3	0.9	Siliceous
W4/105	331.0	-73.4	0.46	248.1	-74.5	0.9	
W4/106	126.0	-64.1	0.62	174.4	-28.2	0.4	Group
W4/108	35.8	-21.5	0.23	231.2	-76.8	0.7	
W6/6	44.9	60.4	2.13	84.3	20.0	0.2	
W6/7	223.2	-34.7	0.55	152.7	- 83.9	2.0	
W6/C1	10.3	13.5	27.60	171.9	49.0	0.8	
W6/C2	48.0	77.1	10.80	191.3	33.0	1.4	
W6/C3	319.9	30.2	39.90	237.8	26.0	0.5	
W6/C4	294.1	-11.5	46.20	250.1	-40.8		Siliceous
W6/C5	257.6	-20.1	22.20	243.4	-61.4	0.3	
W6/C6	175.3	-18.4	72.60	204.0	6.4	0.5	
W6/C7	29.3	0.3	25.80	237.8	-55.7		
W6/C8	331.5	-72.4	39.00	216.0	-2.8	0.6	Group
W6/C9	224.6	-70.2	45.00	202.5	-50.1		
W6/101	143.7	42.6	0.02	112.6	-3.6	0.2	
W6/102	176.7	-68.6	0.04	176.0	-68.8	2.5	
W6/103	327.2	-82.0	0.09	270.3	-79.8	1.1	
W6/104	183.7	-82.0	0.10	214.0	-76.2	1.4	
W6/105	55.0	-53.0	0.09	64.6	-60.6	1.1	
W6/106	50.9	-31.2	0.03	79.4	-70.1	0.3	

Table 3.13 Initial, Most Stable and Stability Indices of Westbury-Sub-Mendip Cave Deposits

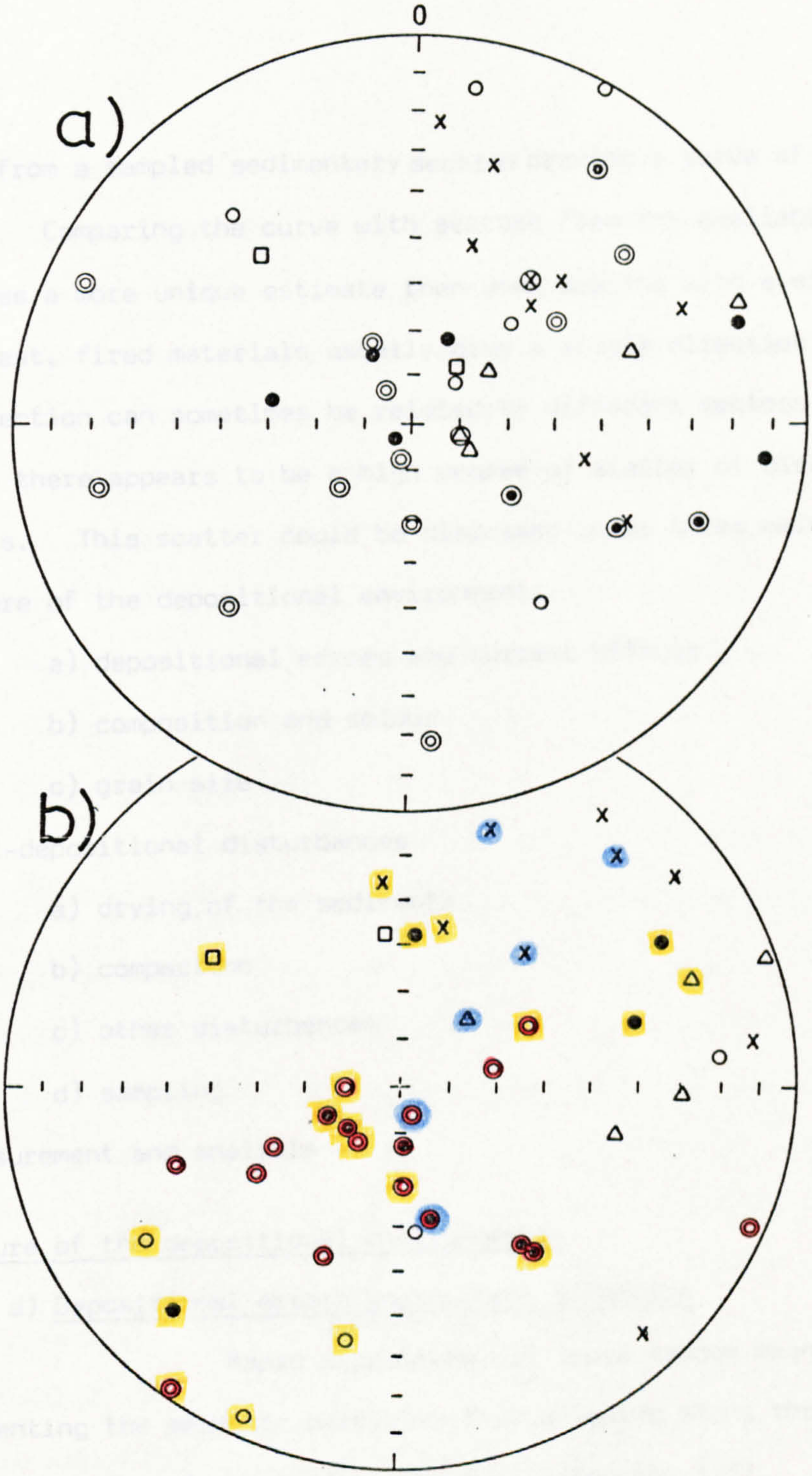

△ Upper Red Breccia — Blue S.I. ⩾ 1·5

x Calcareous / Siliceous Transition — Yellow S.I. ⩾ 0·5

□ Siliceous / Calcareous Transition — Others are unstable

● Yellow sands of the Siliceous Group

o Siliceous Group

Upper hemisphere, red circle

Fig. 3.19 Magnetic direction of Westbury Sub-mendip samples
a) NRM
b) Most stable

results from a sampled sedimentary section provide a curve of directional changes. Comparing the curve with sectors from the available records thus gives a more unique estimate than when dealing with a single point. In contrast, fired materials usually give a single direction for a site and this direction can sometimes be related to different sectors of the curve. However, there appears to be a high degree of scatter of directions in sediments. This scatter could be discussed under three main categories:-

1) Nature of the depositional environment:-
    a) depositional errors and current effects
    b) composition and colour
    c) grain size
2) Post-depositional disturbances
    a) drying of the sediments
    b) compaction
    c) other disturbances
    d) sampling
3) Measurement and analysis

1) <u>Nature of the depositional environment:-</u>

a) <u>Depositional errors and current effects:-</u>

Rapid deposition may cause random magnetic directions by preventing the magnetic particles from aligning along the earth's magnetic field at the time of deposition (Chapter 1, Section 1.3). Changes in the direction of water flow at different times could cause scatter in directions at different levels by causing alignment or partial alignment of magnetic minerals in the direction of the water flow. As clay and other very fine-grained sediments can only be deposited in quiet conditions,

these should become aligned along the earth's magnetic field. Most sediments depart from this ideal behaviour by an amount proportional to the rate of deposition and the particle shape and size. For example in a mixed clay-sand silt a high content of quartz grains may prevent the smaller magnetic minerals from aligning perfectly along the earth's magnetic field. In fact most of the collected clay deposits gave scattered directions (Beverley, Lurk Lane; Leighton Buzzard, and water conduit samples from Wharram Percy), on the other hand silt and sand deposits were better grouped (Wharram Percy and Lincoln), suggesting that the processes of deposition are not very significant in archaeomagnetic studies.

b) Composition effect:-

The colour studies of the available sediments using Munsel colour codes showed that the highest intensities were obtained from the strong brown and red coloured sediments (fig. 3.20). The stabilities of the yellow and black sediments were also relatively lower than the brown samples (fig. 3.21). The colour variation could reflect mineral composition of the sediments, for example a high percentage of limonite and goethite could result in a yellowish colour (both limonite and goethite are common in sediments and formed as a result of oxidation and weathering of iron minerals). On the other hand, the colour of the sediments in archaeological sites may be changed by many factors such as human, animal and plant activities. For example cave deposits probably have the most natural colour while pond and ditch sediments will have darker colour, because the original colour will be masked by the dark colour (organic materials) caused by biological activities. The composition of the sediments can also be strongly affected by a fixed component if they were near fireplaces, as in the case of the Lurk Lane (Beverley) samples. Such

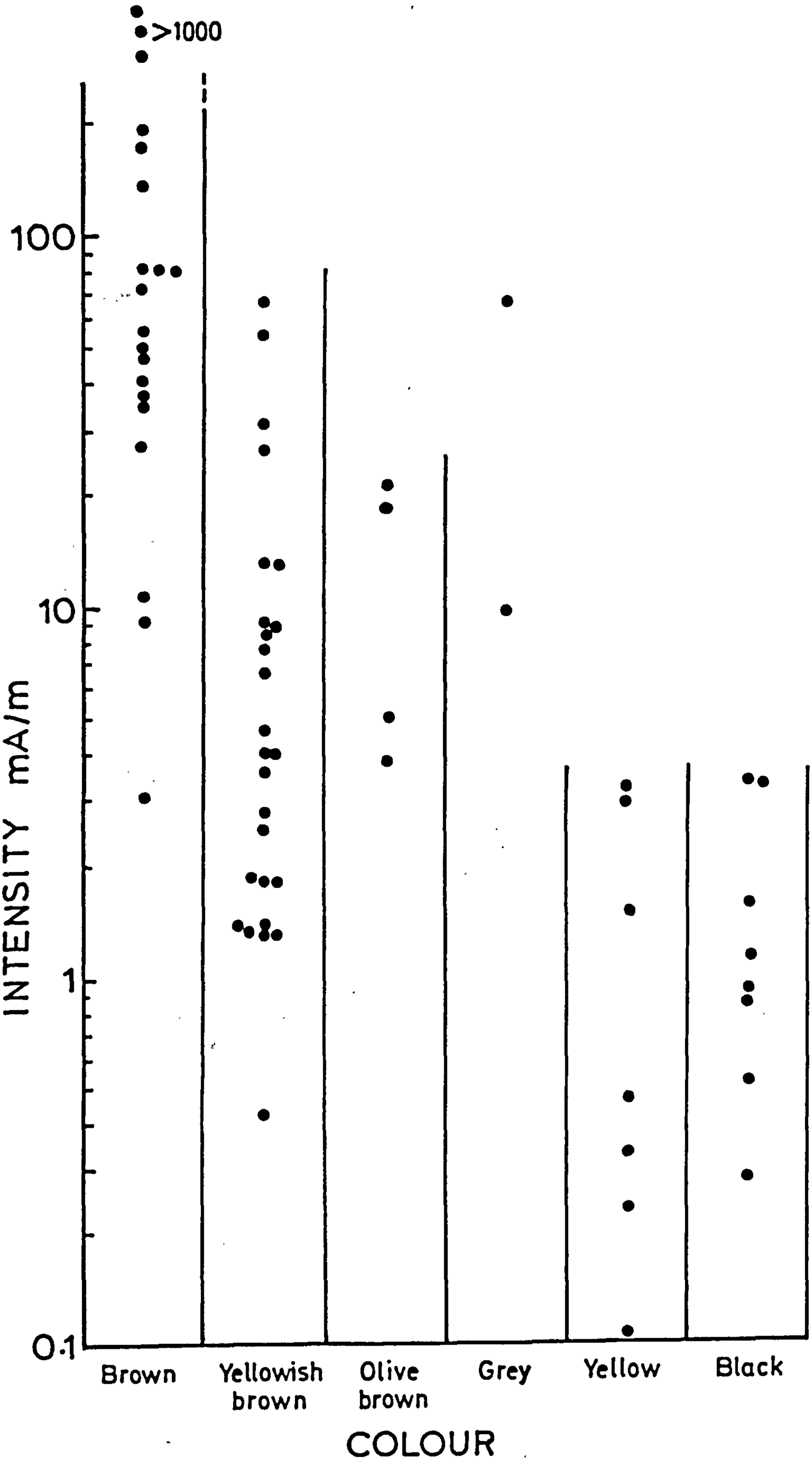

Fig. 3.20 Comparison between the colour of the sediments and the intensity of magnetization

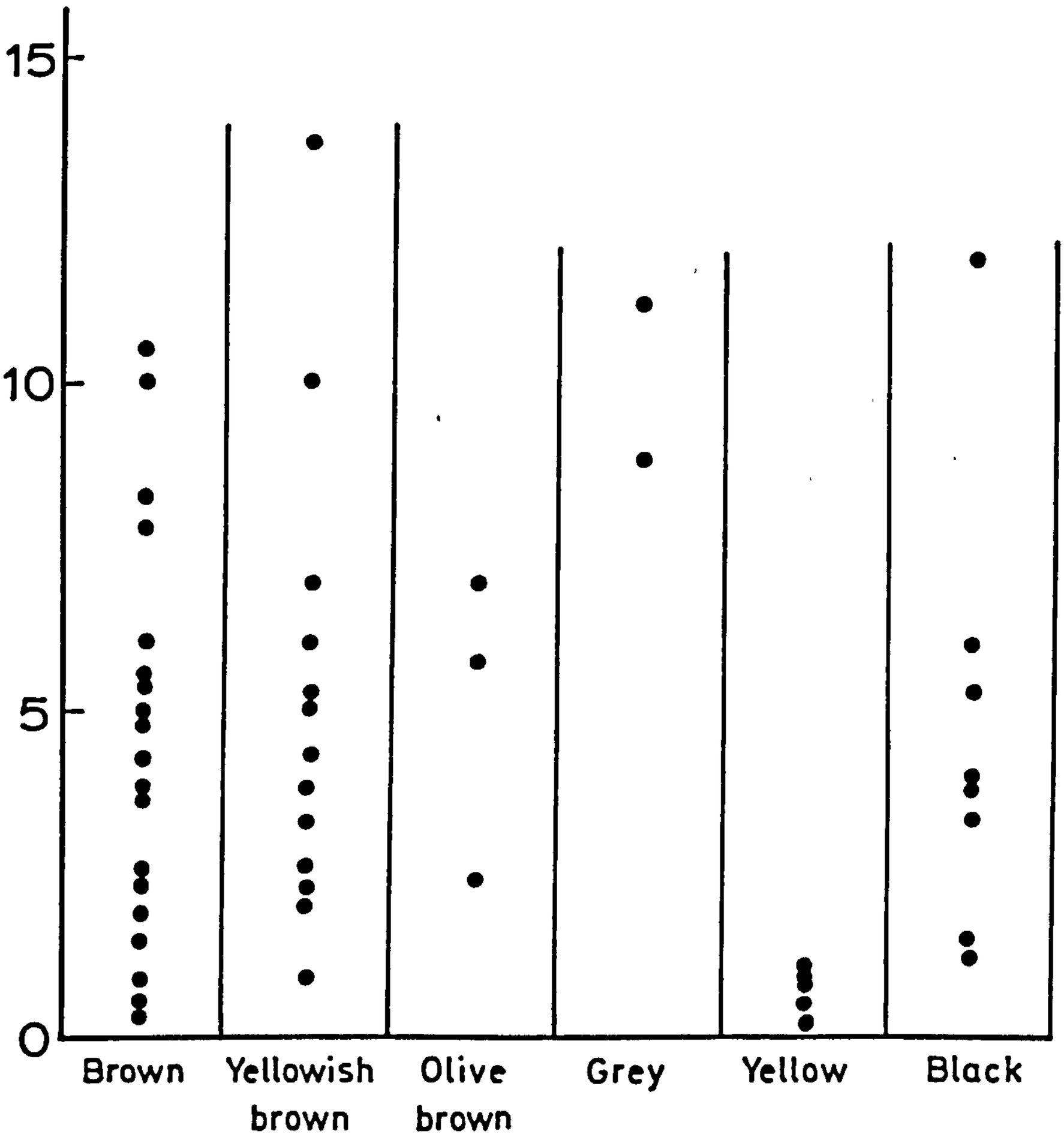

Fig. 3.21 Comparison between the colour of the sediments nad their stability indices

samples appear to be dominated by a red colouration and can have stabilities and intensities comparable with those of fired materials.

The above relation between colour and intensity was not found applicable for comparing intensities of different sites which are of the same colour, as this will depend on factors affecting the deposited sediments and maybe the mineral composition within the site.

c) Grain size:-

The grain size of the available sediment samples, obtained by sieving, were mostly fine-grained (sizes equal or less than 1mm.) with some of them containing additional large grains of shards and pebbles. The presence of highly magnetic shards and pebbles was found to have a great effect as their magnetization dominates the weak magnetization of their sedimentary matrix. The effect was found to vary depending on the magnetization of shards and pebbles themselves and also on their percentage within the sediments. Such effects were mainly observed on samples from Beverley and Leighton Buzzard. In the first site (fig. 3.3), samples with >5% shards showed a higher degree of scatter than the other samples which were nearly pure and showed better grouping. However, some of the pure samples were departed from the grouping, and this must be due to other factors than the presence of shards. On the other hand the degree of scatter will probably depend on the magnetization of the individual shards, as one of the samples which also contained shards was consistent with the grouping of the pure samples. This could, of course, be simply a random factor or the net magnetization of the shards within this sample could be weak and hence not dominating the magnetization of the sample.

The shards in Leighton Buzzard site were distributed uniformly within the sampled section, and the direction of the samples

were very scattered. It was therefore thought that this problem could be overcome by taking smaller samples which might be free of shards. Since the shards were widely distributed over the section and were of variable sizes, the small samples did not help in reducing their effect, as they still contained fine shards (≈1mm.). However, this technique using smaller samples could be useful in other sites where shards and pebbles can be recognised sufficiently easily (particularly by their big sizes) and so can be avoided during sampling.

2) Post-depositional disturbance:-

a) Changes in the water table can cause changes in the distribution of the surface tension between the grains within the sediments, and therefore affect the orientation of interstitial magnetic grains. This occurs when there is a loss of the interstitial water, the volume previously occupied by pore water must be filled by air and water vapour. Consequently, a liquid meniscus traverses each pore space during desiccation and any grains which are free to move within them may respond to surface tension force (Noel, 1980). Apart from the position of sediments relative to the past and present water tables, this effect will depend on the porosity of the sediments and so it can be expected to be more common in sand and silts than in clay.

Any drying out of the samples after collection can also have the same effect, but this was minimized in this study by airtight sealing of the samples and by undertaking the measurements as soon as possible after collection, usually within one or two days.

b) Compaction: As the wet sediments are deposited and loaded by later sediments, the magnetic particles start to re-align in a direction perpendicular to the compaction, hence shallowing the inclination

value. This post-depositional compaction is expected to be more effective in clays than in silt and sand as the high percentage of quartz grains in silt and sand help in strengthening the structural fabric, while clay could undergo severe deformation as a result of even weak compactional stresses.

c) Other post-depositional factors may also affect the magnetic record of the sediments. These can be sliding and slumping along the depositional slope, or disturbances by vegetation, animal and man.

d) Sampling errors: Sampling sediments involves pushing cylinders in the sediments. Such a procedure could sometimes cause displacement or movement in the particles and therefore result in change in the original directions of the sediments. This is particularly likely to happen when large pieces such as shards and pebbles are present within the sampled sediments. Post-sampling drying of the sediments can also change the magnetization.

3) Measurements and Analysis

Intensity of Magnetization

Sediments generally have a much weaker intensity than fired materials. In order to check whether weak samples are suitable for archaeomagnetic studies the intensities of magnetization after 1.5 mT alternating field demagnetization (generally the most stable field of demagnetization) of all samples were plotted against their stability indices. The plots (fig. 3.22) showed no clear relations between the two parameters as strong samples yield similar stabilities as weaker ones. Conversely some very weak samples, like the Westbury samples, had stabilities comparable with the same site and were also comparable with the stability of some of the highly magnetic samples from other sites. Therefore it was

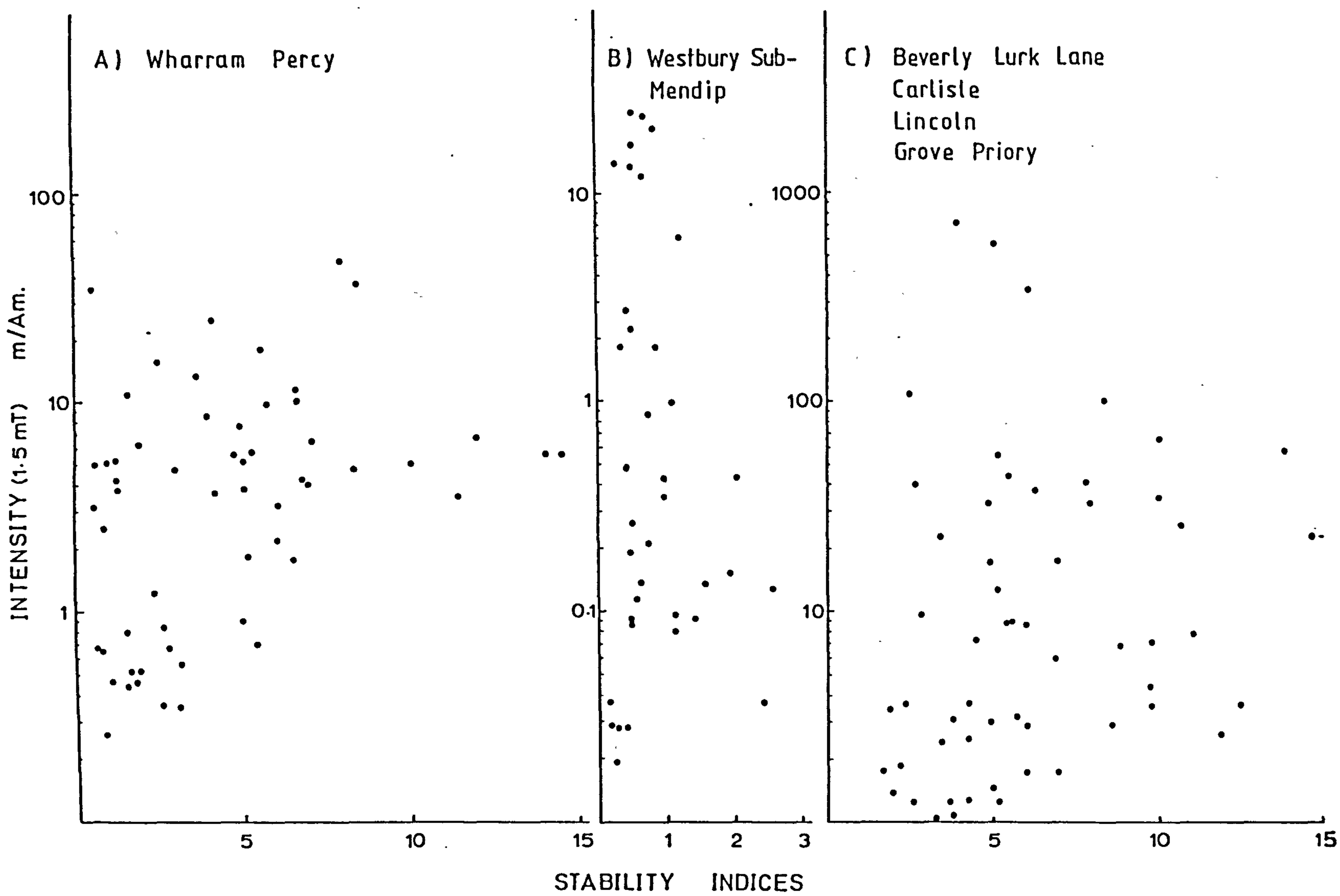

Fig. 3.22 Stability indices of all sediment samples verses the intensity of magnetization at 1.5 mT

concluded that even weak samples can have just as good stability for archaeomagnetic dating as fired materials.

Conclusions

Sediment samples which were used for dating showed poor reliability because of their directions departed from the curve. This was apparent even in the stable samples. The presence of shards and pebbles was found to cause scatter in directions, but this scatter was random as it would probably depend on the magnetization of the shards and pebbles. Most of the mean directions showed deviated inclinations, with most being shallower than expected, by between 4^{o} and 30^{o}. The shallow inclination is probably as a result of compaction of the sediments (in addition to the other previously mentioned factors) while steep inclinations could occur due to more complicated factors such as tilting and other deformations in the sediments like bioturbation or drying out. Accordingly it was concluded that depostional inclination errors are not always involved in most sediment samples.

Most of the previously mentioned parameters that can cause significant scatter of the directions in sediment samples and cannot be effectively compensated by different forms of measurements or analysis. It is thus necessary at this stage, to avoid collecting inhomogeneous samples, and also those that were deposited chaotically. The sediments examined also indicate sand and silts yield better archaeomagnetic results than do clays, although all these conclusions need further verification.

Despite these limitations, some sedimentary samples were useful in dating either by comparing their magnetic directions with the available archaeomagentic curve or by their polarity. However, the reliability of sediments for archaeomagnetic dating is not very high when compared

with fired archaeological materials, but are worth considering when no fired materials or other suitable archaeological materials are available.

CHAPTER 4 BRITISH ARCHAEOMAGNETIC CURVE

4.1 Introduction

For archaeomagnetic dating, new data are usually compared with available records of archaeomagnetic directions which form a master curve. These curves have been obtained by intensive archaeomagnetic work mainly during the last 25 years throughout which alterations and modifications have been made as more data have accumulated in order to obtain the optimum archaeomagnetic curve.

During this work, the original British archaeomagnetic curve (Aitken 1970) and Paris curve (Thellier 1981) have been re-examined. These two curves were originally plotted after careful sampling and measurements and are based on the most stable results for the sites. A reasonable number of sites has been sampled and a statistically good number of samples were obtained for most of the sites.

To study the data thoroughly and systematically, they have been divided into 200-year intervals, and each site was given a weight (Table 4.1) ranging from 1 to 5 (with 5 being very reliable), depending on the number of samples, magnetic stability (α_{95} and k) and the known age ranges (i.e. independent of the magnetic data). Since the accuracy of the curve depends highly on the age of each site the age range was given somewhat more weight than the magnetic factors. On this basis some of the sites with a reasonable number of samples and good magnetic stability were given low weight because of their uncertain archaeological age. In a few cases subjective assessment was used to place boundary line cases in one or the other category.

N	α_{95}	age range ± years	weight	symbols
≥ 7	≤ 3	≤ 25	5	*
≥ 5	≤ 5	≤ 50	4	□
≥ 2	≤ 9	≤ 75	3	Δ
> 9	≤ 100		2	X
>15	>100		1	+

Table 4.1

4.2 The British Archaeomagnetic Data

The previous British Archaeomagnetic Curve (Figure 4.1) (Aitken 1970) covers a period 50-350 A.D. and 1000-1600 A.D., after which the Bauer data begins. The curve showed sharp inclination changes within the Roman period with slight changes in declination. A steady movement of both inclination and declination occurs between 1000 and 1300 A.D., while near the turning points the declination starts to change within virtually no change in inclination, and after 1400 A.D. (where the directions are similar to 1200 A.D.), the inclination starts to steepen very rapidly until 1600 A.D. where the observatory records begin.

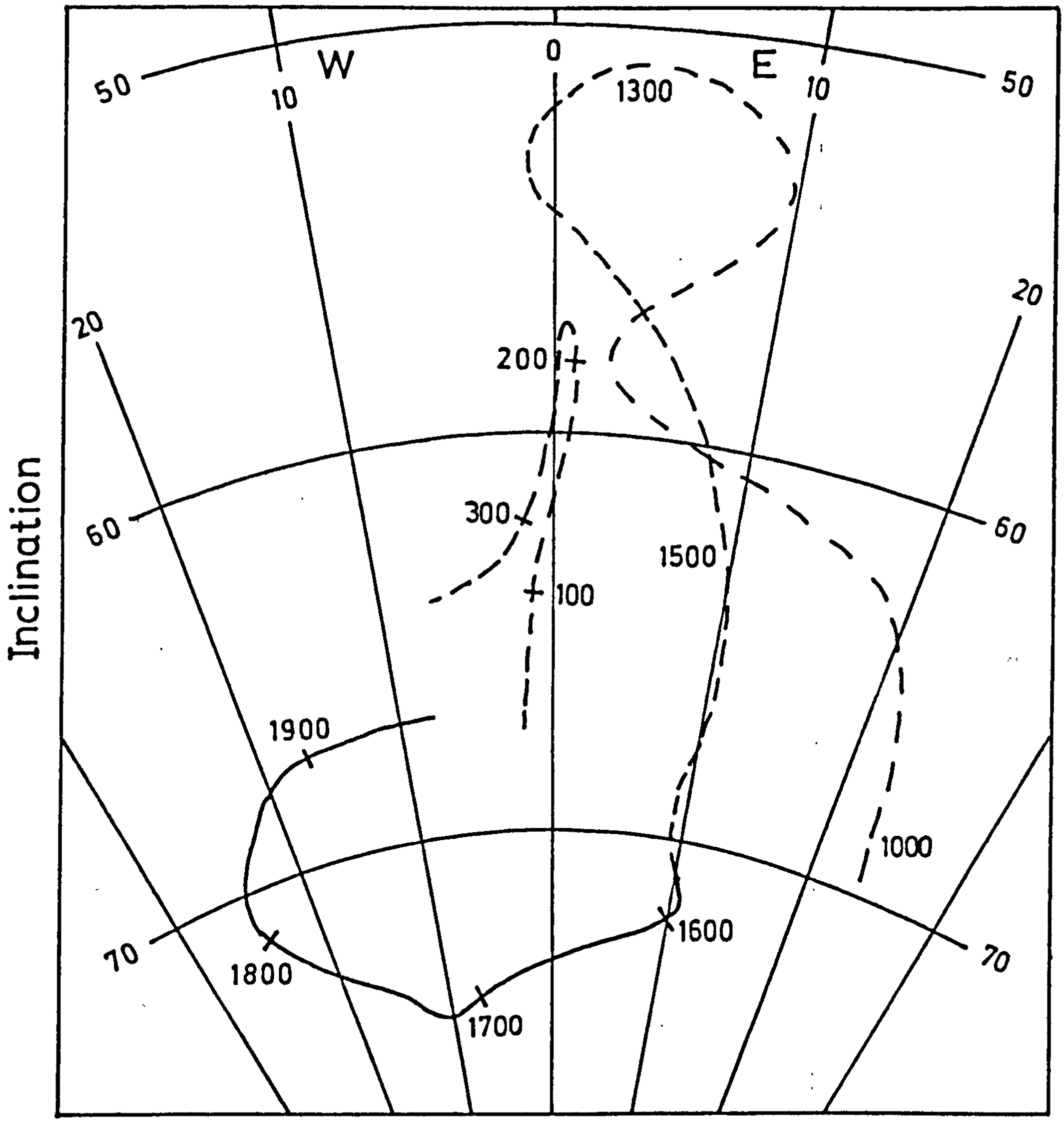

Fig. 4.1 British archaeomagnetic curve (Aitken, 1970)

Some archaeomagnetic data has been accumulated from recent research in Scotland (Turner and Thompson 1978) on cores taken from the sediments on the bed of Loch Lomond. Using the archaeomagnetic curve for comparison, the rate of sedimentation of Loch Lomond has been calibrated and reveals acceleration from about half a metre to one metre per thousand years. These results indicated that the period between Roman and medieval have a double loop between 600 and 800 A.D.; this clearly will depend heavily on precision of measurements and supplementary data (Clark 1980).

During this work the British archaeomagnetic data (Aitken and Weaver 1962; Aitken, Hawley and Weaver 1963; Aitken and Hawley 1966,1967), which had all their inclination values reduced to latitude 51.5° (London), were recorrected and referred back to their original site latitudes and α_{95} of each site was calculated using their θ_{80} and θ_{68} values. These data were then combined with other archaeomagnetic data provided by A.J. Clark (Ancient Monument Laboratory), and also data obtained during this work, and after giving each site its weight they were corrected to Meriden (Chapter One) and re-evaluated as follows (Appendix 1):

-2000 BC - 0 AD

A total of 38 sites are available within the range (Figure 4.2). Some of the sites have high weights, but because of the wide age range and the scattered directions, it was only possible to locate directions at 100 B.C. (between Site BIG/1, BIG/2 and MUC/2), 400 B.C. (between RA and FN) and 50 B.C. (between Sites GAR436, GAR315 and GAR433). These points were not joined due to the low number of sites.

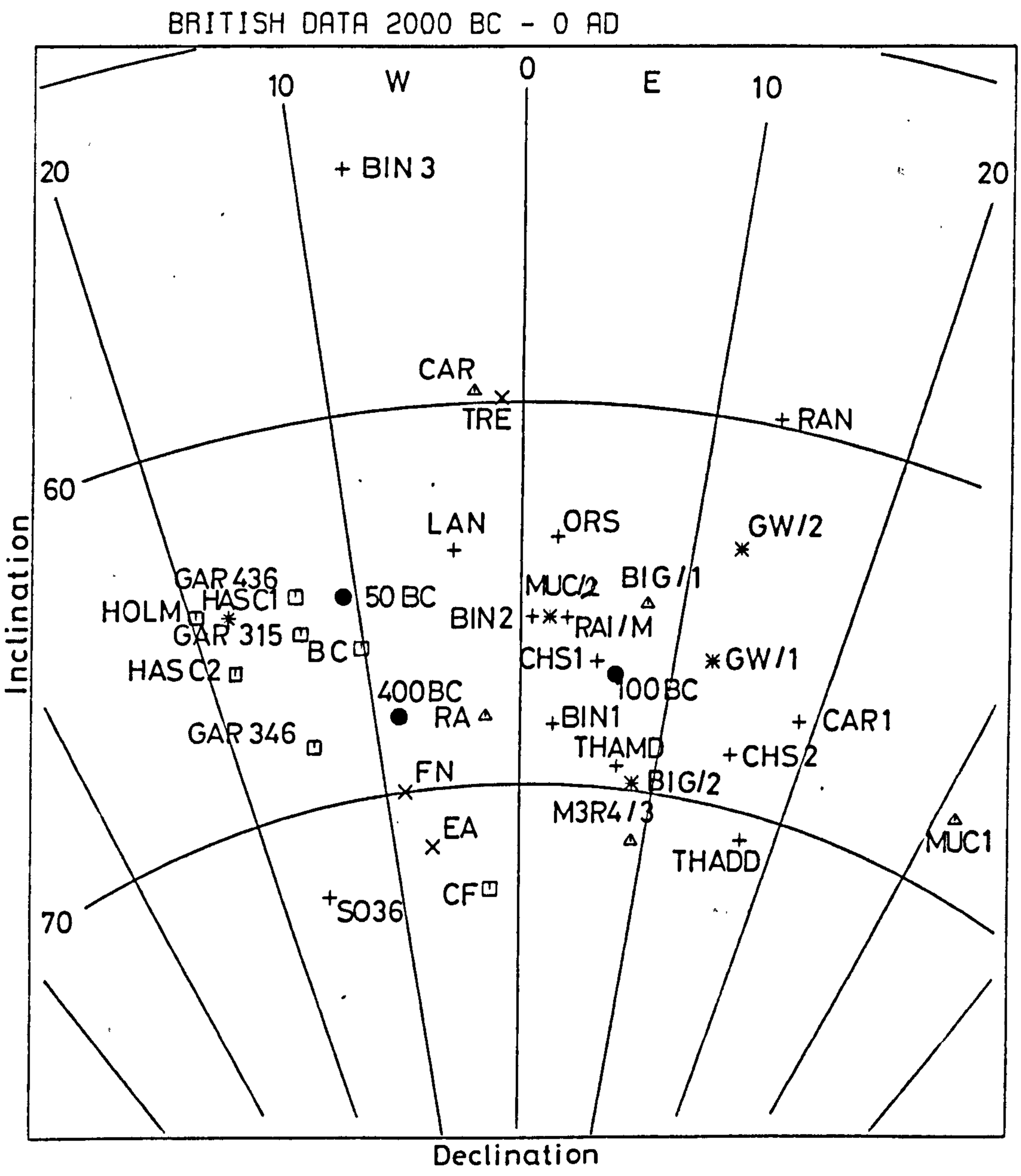
BRITISH DATA 2000 BC - 0 AD
10 W
0
E
10
20
20
+ BIN 3
CAR
TRE
+ RAN
60
LAN
+ ORS
GW/2
GAR 436
HASC1
50 BC
MUC/2
BIG/1
HOLM
BIN2
+*+ RAI/M
GAR 315
BC
CHS1 +
*GW/1
HASC2
400BC
100BC
RA
+BIN1
+ CAR1
GAR 346
THAMD
+CHS2
FN
*BIG/2
M3R4/3
EA
MUC1
THADD
CF
+SO36
70
Inclination
Declination

Fig. 4.2

0-200 AD

A total of 59 sites are available within this range (Figure 4.3). Most of these sites have high weights but they cover a wide range of directions (i.e. they are scattered). The direction at 50 AD can be located between site directions SAP1, SAP2, PEL and LH. This will make Site HW (40-70 AD) OB (50-70 AD), GL (60-80 AD) and DG (50-100 AD) away from this direction. The curve is then expected to have shallow inclinations towards 100 AD which is located using Sites HL/14A (100-130 AD), HL/11 (100-150 AD), HL/24 (100-140 AD), PIP/2 (43-100 AD) and HL/32 (100-150 AD). The 100 AD should be near Site HL/14A, PIP/2 and HL/11, taking into consideration the direction of the other sites which are about 10^{o} west of this direction. This will still leave many of the reliable sites of the same age away from this direction, such as Site SV (70-110 AD), RED (100-150 AD), DG (50-100 AD), GL (60-80 AD), HL/12 (100-200 AD) and DG2 (50-100 AD). The directions at 150 AD can be located in between sites HL/19 (135-160 AD), PIEG (150), MC/1 (155-180 AD), and PW (100-200 AD) and taking into consideration Site HL/11 (100-150 AD). This will make Site RB/1 (150-180 AD), RB/2 (150-180 AD), HL/12 (100-200 AD), MC/3A (150-180 AD) away from this direction. The direction at 200 AD was located using sites MC/2 (200-260 AD), RBA (150-250 AD) and SG (200-230 AD) and taking into consideration Site ALC (200-250 AD), HL/12 (100-200 AD) and CA/35 (200-300 AD). This direction will also leave site HL/31 (180-230 AD) and FB (100-300 AD) away from the curve. According to the plotted curve between 0-200 AD, many sites with high weights were found away from the curve with about $\pm$ 10^{o} difference in declination (mainly Easterly declinations).

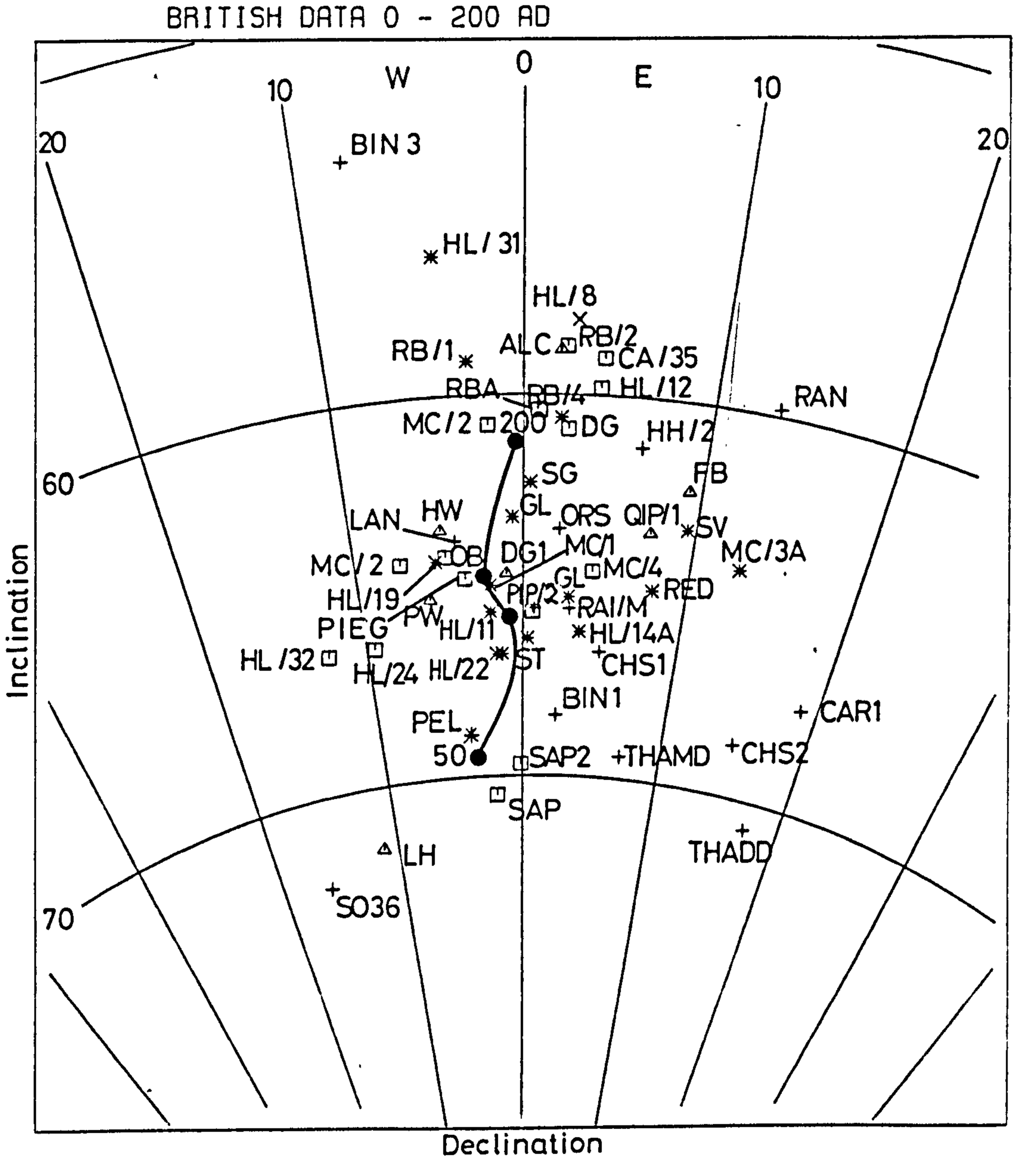
BRITISH DATA 0 - 200 AD
W
E
0
10
10
20
20
60
70
Inclination
Declination
BIN 3
HL / 31
HL/8
RB/1
ALC
RB/2
CA/35
RBA
RB/4
HL/12
RAN
MC/2
200
DG
HH/2
SG
FB
LAN
HW
GL
ORS
QIP/1
SV
MC/3A
OB
DG1
MC/1
MC/4
HL/19
PIP/2
RAI/M
RED
PW
PIEG
HL/11
HL/14A
HL/32
HL/24
HL/22
ST
CHS1
BIN1
CAR1
PEL
50
SAP2
THAMD
CHS2
SAP
LH
THADD
SO36

Fig. 4 · 3 a

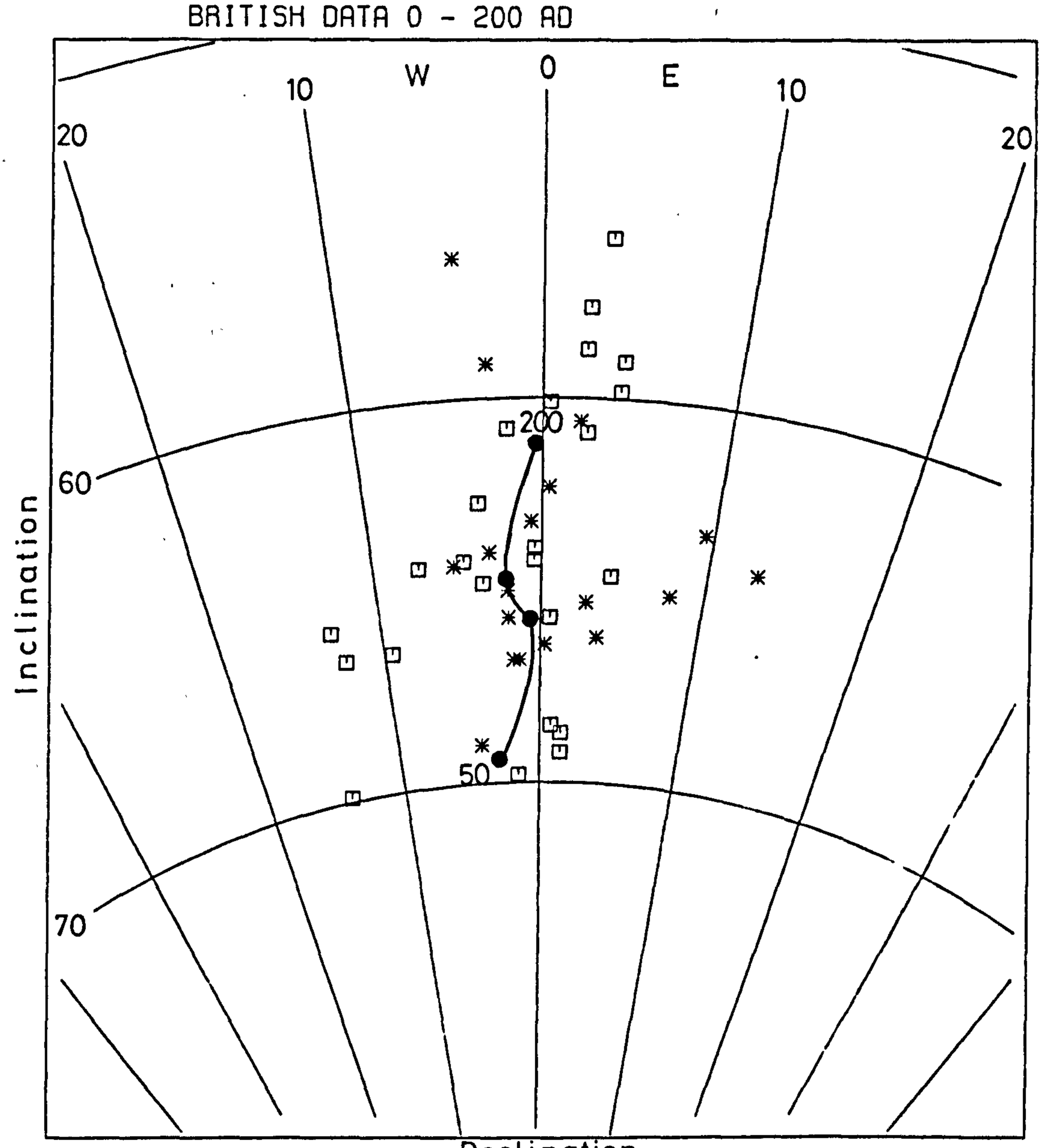

Fig. 4.3b

The most reliable sites (wt. 4 and 5) for the period 0 - 200 AD

200-400 AD

A total of 52 sites are available within this range (Figure 4.4). The direction at 250 AD was located using Sites ALC (200-250 AD), CA/35 (200-300 AD), HL/18 (240-290 AD), RBA (150-250 AD), HL/15 (260-300 AD) and HL/8 (180-350 AD). This will leave Sites SB/B (230-270 AD), HL/31 (180-320 AD), MC 2 (200-260 AD), and HL/9 (240-300 AD), which are of reasonable weights away from this direction.

The directions after 250 AD are expected to steepen towards 300 AD, which was located in between Sites MC/9 (260-310 AD), HL/9 (240-300 AD), CT (270-350 AD), SD (300-330 AD), HL/28 (270-320 AD), HM/2 (300-400 AD). The direction at 350 AD was located using Sites RI (330-370 AD), NEA (325-375 AD), WP/1 (300-350 AD), SB/C (300-400 AD), PW (300-385 AD), and HL/6 (300-400 AD), and taking into consideration the directions of Site HL/1 (300-350 AD), CG3 (300-385 AD).

400-600 AD

A total of 32 sites are available within this range (Figure 4.5). The 400 direction is expected to be between those of Sites HM/2 (300-400 AD), HM/1 (300-400 AD), CG/8 (315-400 AD), SB/E (300-400 AD), SB/C (300-400 AD), HM/3 (300-400 AD) and CA/39 (280-400 AD). After 400 AD, only three sites are available of which only two have a high weight. These three sites can only indicate that the curve moves easterly after 400 AD and becomes steeper. However, the 400 AD directions are not considered very well defined and, therefore, this point was not joined with the rest of the curve.

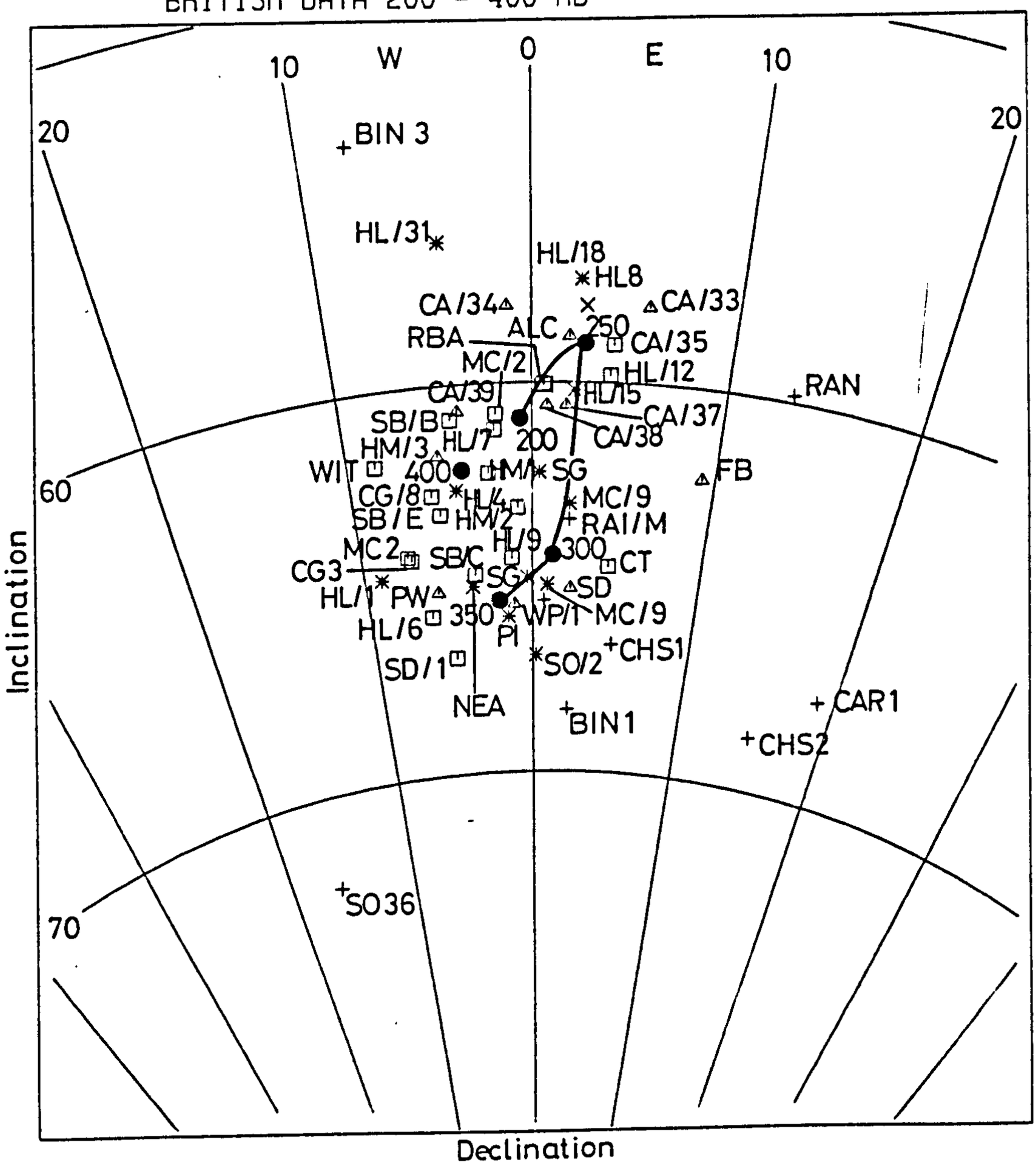
BRITISH DATA 200 - 400 AD
W
E
0
10
10
20
20
60
70
Inclination
Declination
BIN 3
HL/31
HL/18
HL8
CA/34
CA/33
RBA
ALC
250
CA/35
MC/2
HL/12
CA/39
HL/15
RAN
SB/B
CA/37
HL/7
200
CA/38
HM/3
WIT
400
HM/
SG
FB
CG/8
HL/4
MC/9
SB/E
HM/2
RAI/M
MC2
HL/9
300
CT
CG3
SB/C
SG
SD
HL/1
PW
350
WP/1
MC/9
HL/6
PI
SO/2
CHS1
SD/1
NEA
BIN1
CAR1
CHS2
SO36

Fig. 4.4a

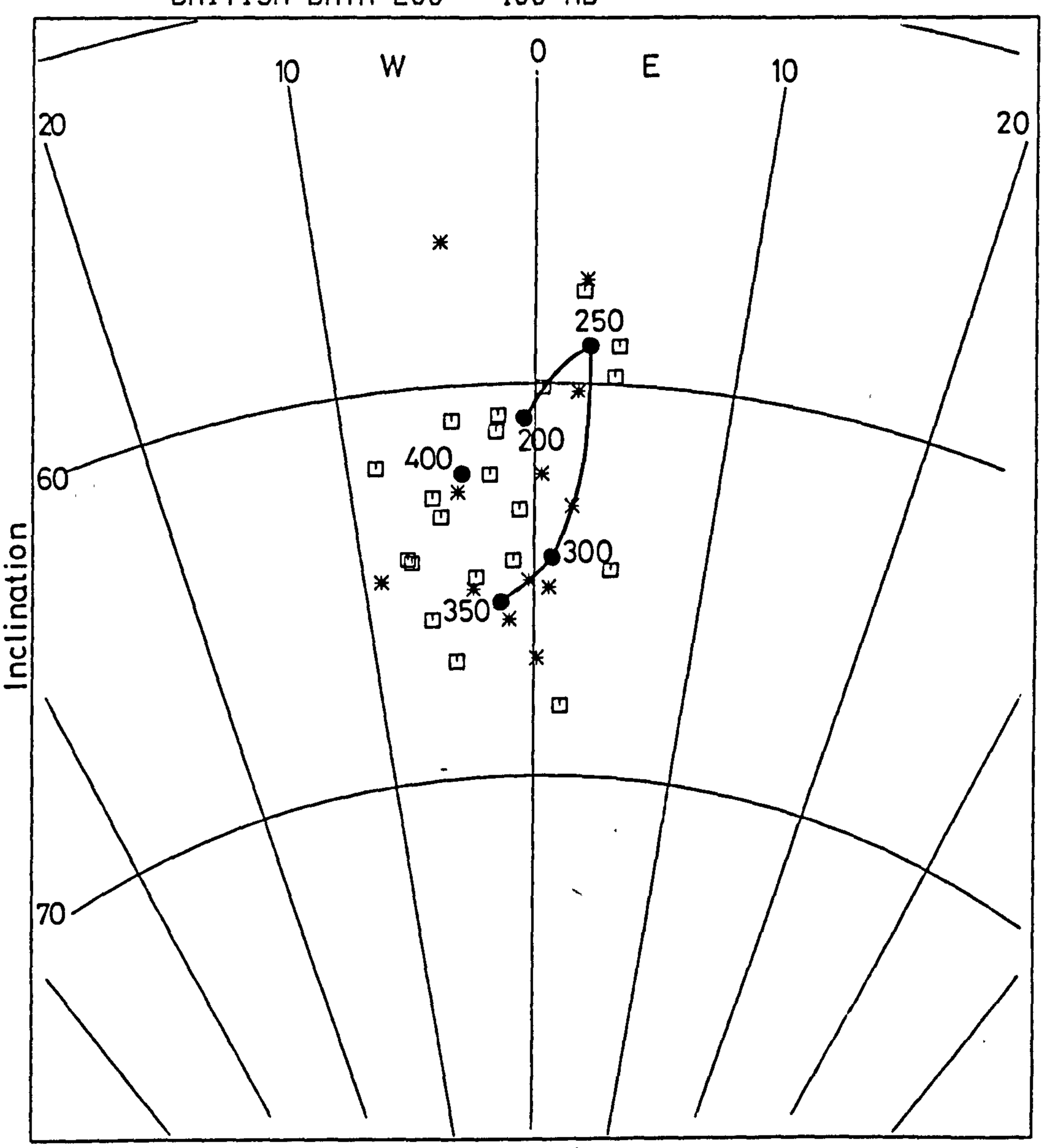

Fig. 4.4b

Fig. 4.4b The most reliable sites (wt. 4 and 5) for the period 200 - 400 AD

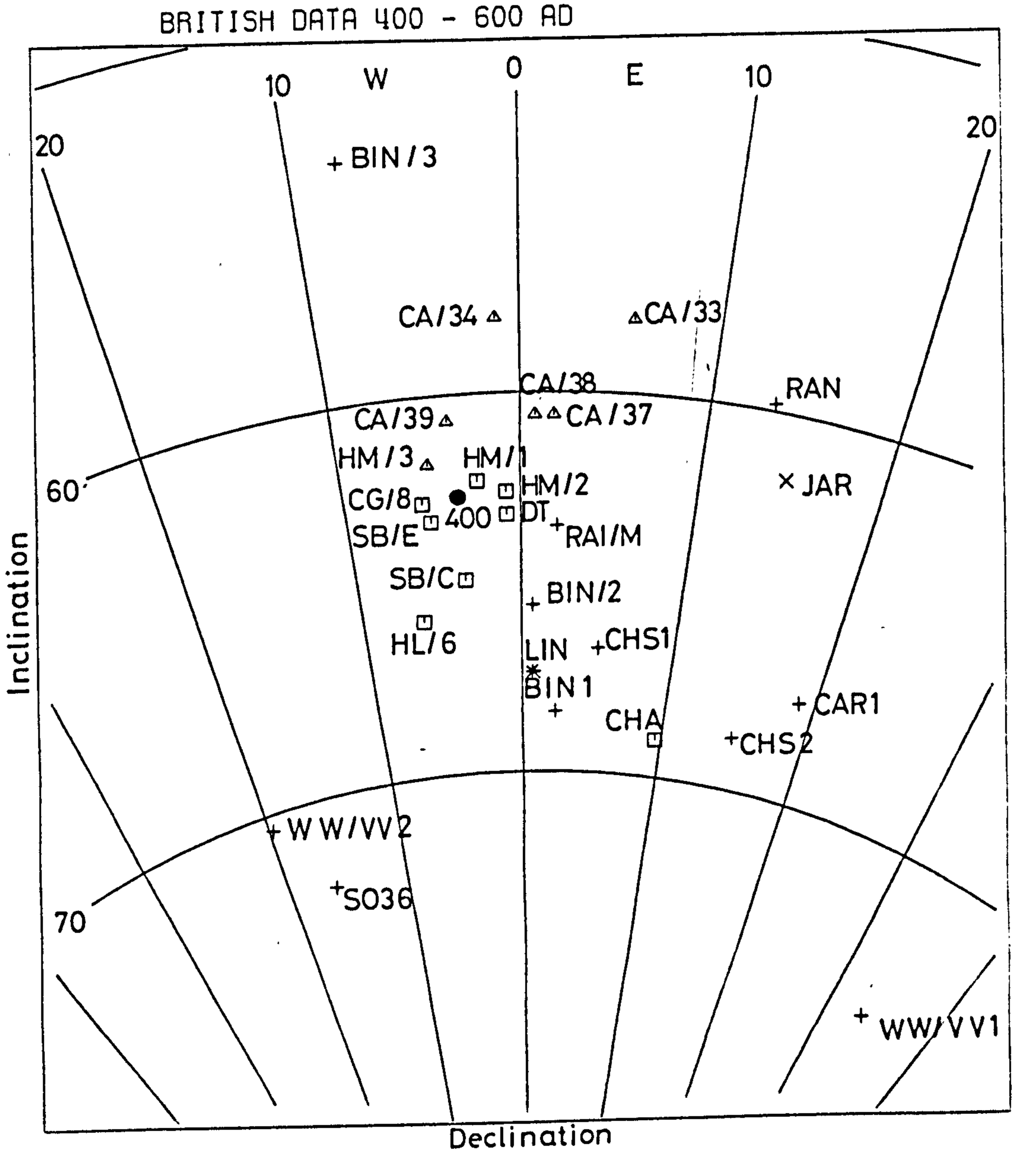
BRITISH DATA 400 - 600 AD
10 W
0
E
10
20
20
+ BIN/3
CA/34
CA/33
CA/38
RAN
CA/39
CA/37
HM/3
HM/1
HM/2
60
JAR
CG/8
400
DT
SB/E
RAI/M
SB/C
BIN/2
HL/6
LIN
CHS1
BIN1
CHA
CAR1
CHS2
WW/VV2
S036
70
WW/VV1
Inclination
Declination

Fig. 4·5

600-800 AD

Twelve sites are available within this range (Figure 4.6). Using these sites it is only possible to locate the direction around 800 AD which could be between site directions MON (800-900 AD), STAM1 (800-900 AD), CHA (600-700 AD), ASH (800-835 AD) and BH (750-850 AD). This direction is not very well defined due to the low number of sites.

800-1000 AD

A total of 59 sites are available within this range (Figure 4.7). The location at 800 AD and 850 AD is still not very well defined. However, according to Sites ASH (800-835 AD), 30757 (850 AD), MON (800-900 AD) and STAM1 (800-900 AD),the 850 AD direction should be somewhat in between these sites. The direction at 900 AD was located using Sites 22441 (900-920 AD), STAM1 (800-900 AD), 25134 (910-925 AD) WI/A (900-1000 AD). The direction at 950 AD was located using Sites WI/A (900-1000 AD), CC (950-1050 AD), TK/2 (900-1000 AD), TAV82 (900-950 AD), and also taking into consideration the directions of Sites IP (850-1150 AD) and TK/4 (900-1100 AD). The 1000 AD direction is not very well defined due to the limited number of sites with high weights. According to the available sites, the 1000 AD could be between CHI 123 (1000-1066 AD), CHI 1 (1000-1066 AD), CHI2 (1000-1066 AD) and SA (900-1100 AD) and also taking into consideration a group of sites which are of low weights.

1000-1200 AD

A total of 89 sites are available within this range (Figure 4.8). The direction at 1050 AD was located using Sites TK/1 (1050-1150 AD), CHI 123(1000-1066 AD). This location is not very well defined but,

according to these two sites, the curve is expected to pass between these two sites shortly after 1000 AD. The direction at 1100 AD was located using site directions TK/1 (1050-1150 AD), A1500 (1100-1200 AD), BAR (1000-1100 AD), and SWA2 (1150 AD). The curve after 1100 AD is expected to change westerly towards 1200 AD. However, the 1150 AD direction was located using site directions EAS (1160-1190), CC/2 (1100-1130 AD), SWA (1100-1200 AD), ES (1050-1150 AD) and A1500 (1100-1200 AD). The 1200 AD direction is well defined by site directions COP1 (1200 AD), QV195 (1190-1200 AD) A2 (1200-1300 AD) and ESH (1200-1300 AD) and WOO (1180-1250 AD).

The plotted directions for the range 1000-1200 AD showed scattered reliable (high weights) sites which were well away from the curve. These sites are: STAM2 (1150-1170 AD), NC/2 (1050-1100 AD), QV1 (1160 AD), SWA5 (1150 AD), EAST (1200-1300 AD), CAR (1200-1300 AD), QKE (1200-1300 AD), WI/P3 (1100-1130 AD) and EL (1170-1230 AD).

1200-1400 AD

A total of 94 sites are available within this range (Figure 4.9). The direction at 1250 AD is expected to be between site directions QV/115 (1250-1260 AD), DP (1250-1325 AD) OKE (1150-1250 AD), B (1250 AD), WF/4 (1250-1325 AD), WOO (1180-1250 AD) and D (1250-1300 AD). The direction at 1300 was located using Sites BR/E (1300-1350 AD), E (1300 AD), WF/2 (1250-1350 AD), LIM (1230-1366 AD), NEW/2 (1230-1360 AD) and T2 (1300-1560 AD). This location will make other sites with high weights and of similar ages away from this direction, such as Sites STAM3

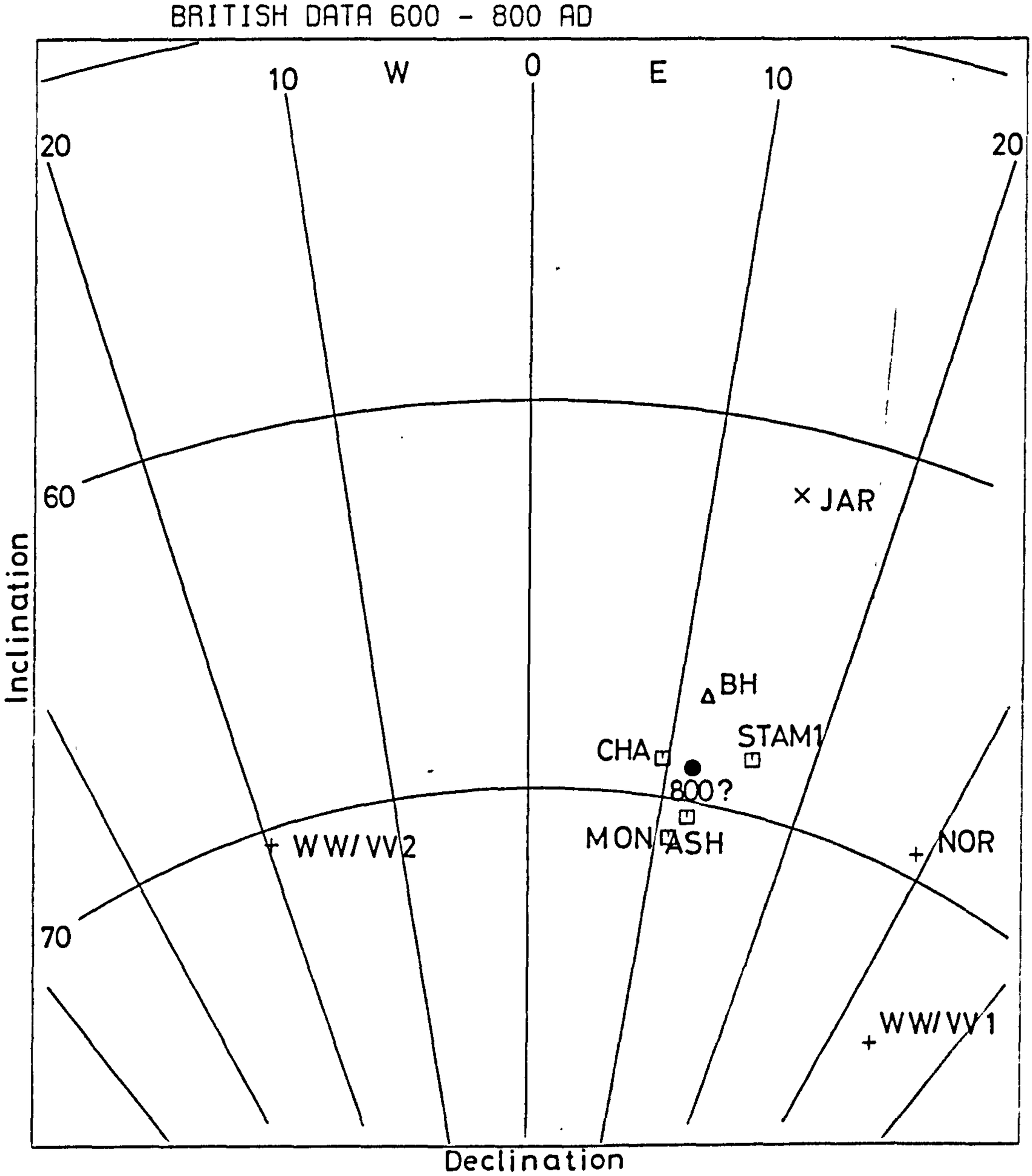
BRITISH DATA 600 - 800 AD
W
E
0
10
10
20
20
60
70
Inclination
Declination
× JAR
BH
STAM1
CHA
800?
MON
ASH
+ WW/VV2
+ NOR
+ WW/VV1

Fig. 4.6

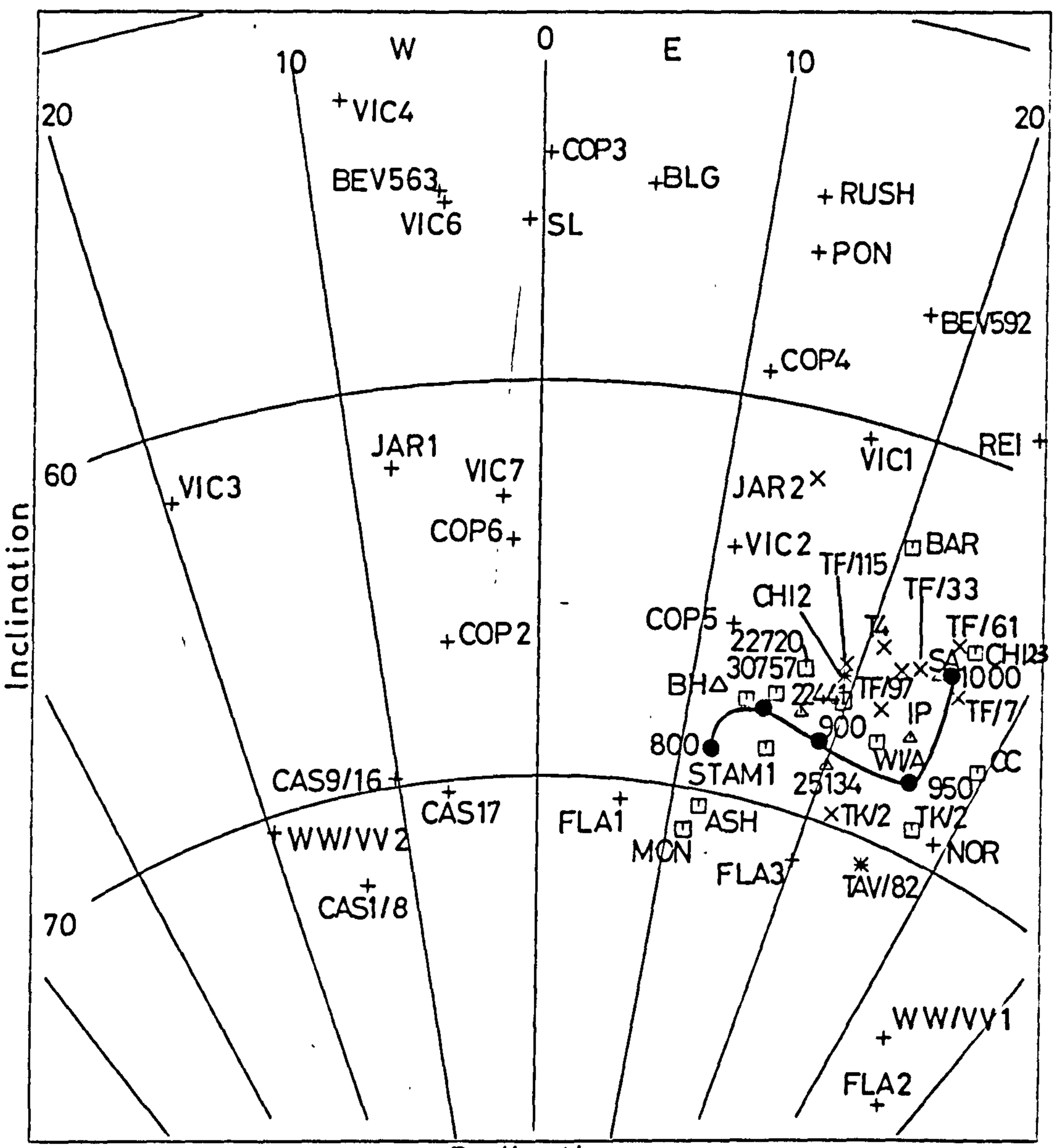
BRITISH DATA 800 - 1000 AD
W
0
E
10
10
20
20
+VIC4
+COP3
+BLG
BEV563
VIC6
+SL
+RUSH
+PON
+BEV592
+COP4
+VIC1
REI +
JAR1
VIC7
60
+VIC3
JAR2
+VIC2
COP6+
BAR
TF/115
TF/33
CH12
COP5
T4
TF/61
22720
CH123
30757
SA
1000
BH
TF/97
IP
TF/7
900
800
STAM1
WVA
CC
25134
950
CAS9/16
CAS17
FLA1
ASH
TK/2
TK/2
MCN
NOR
WW/VV2
FLA3
TAV/82
CAS1/8
70
WW/VV1
FLA2
Inclination
Declination

Fig. 4·7a

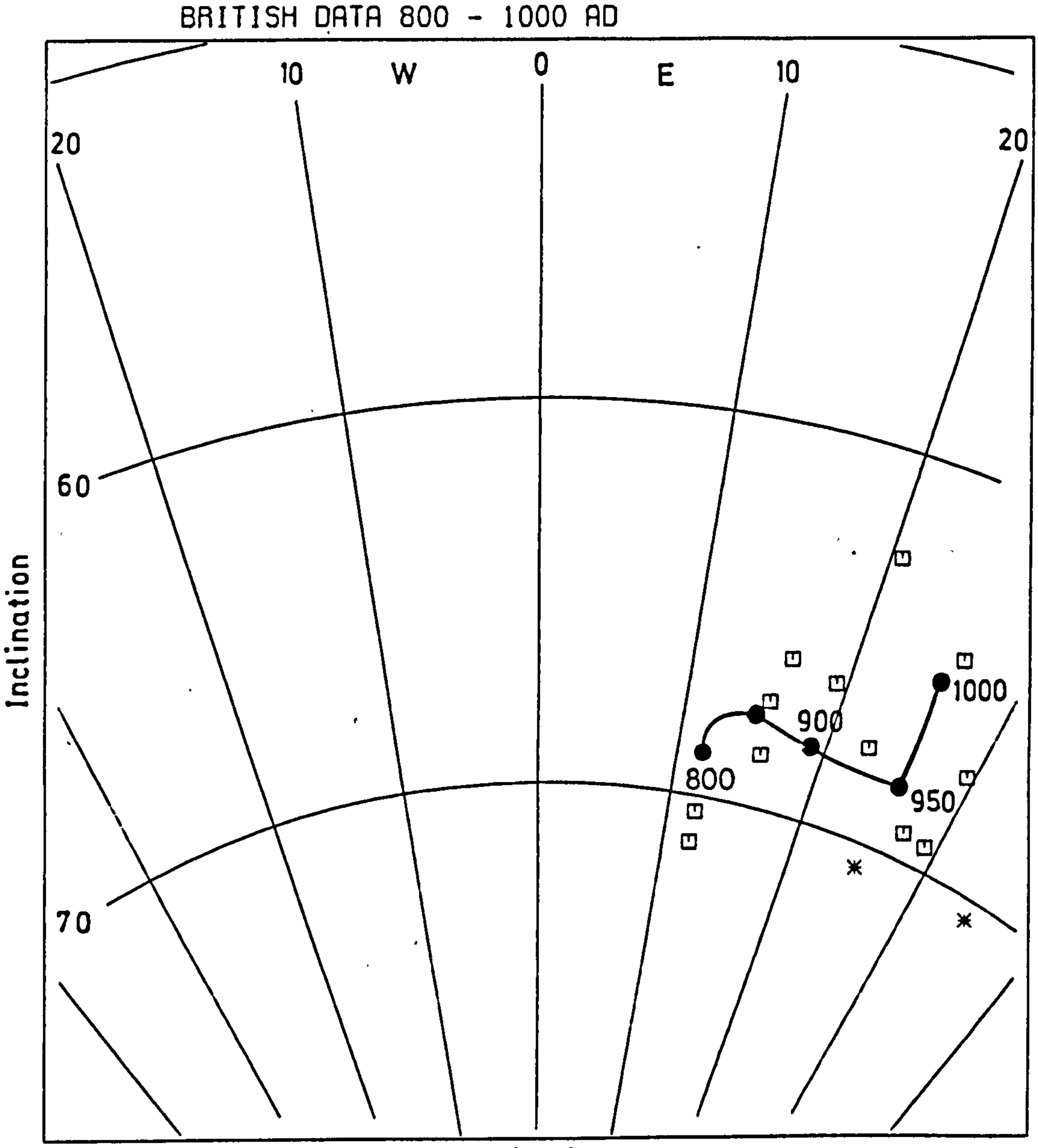

Fig. 4.7 b

Fig. 4.7b The most reliable sites (wt. 4 and 5) for the period 8PP - 1000 AD

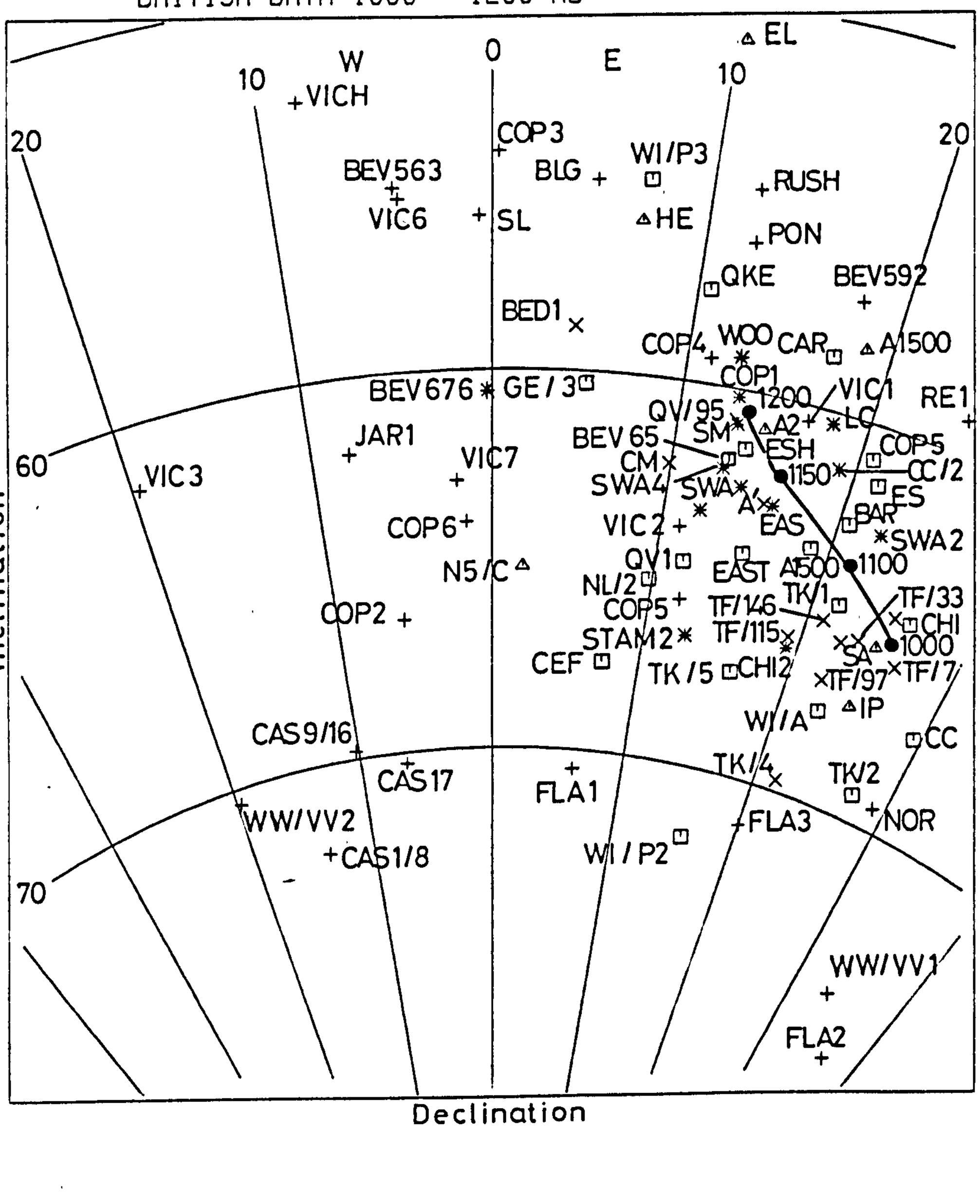
BRITISH DATA 1000 - 1200 AD
W
0
E
10
10
20
20
60
70
Inclination
Declination
EL
VICH
COP3
WI/P3
BLG
BEV563
RUSH
VIC6
SL
HE
PON
QKE
BEV592
BED1
COP4
WOO
CAR
A1500
COP1
BEV676
GE/3
1200
VIC1
RE1
QV/95
LC
JAR1
BEV65
SM
A2
COP5
VIC7
ESH
CM
1150
CC/2
VIC3
SWA4
SWA
A'
ES
BAR
COP6
VIC2
EAS
SWA2
QV1
EAST
A500
1100
N5/C
NL/2
TK/1
TF/33
COP2
COP5
TF/146
CHI
STAM2
TF/115
1000
CEF
TK/5
CHI2
SA
TF/97
TF/7
IP
WI/A
CC
CAS9/16
TK/4
TK/2
CAS17
FLA1
WW/VV2
FLA3
NOR
CAS1/8
WI/P2
WW/VV1
FLA2

Fig. 4.8a

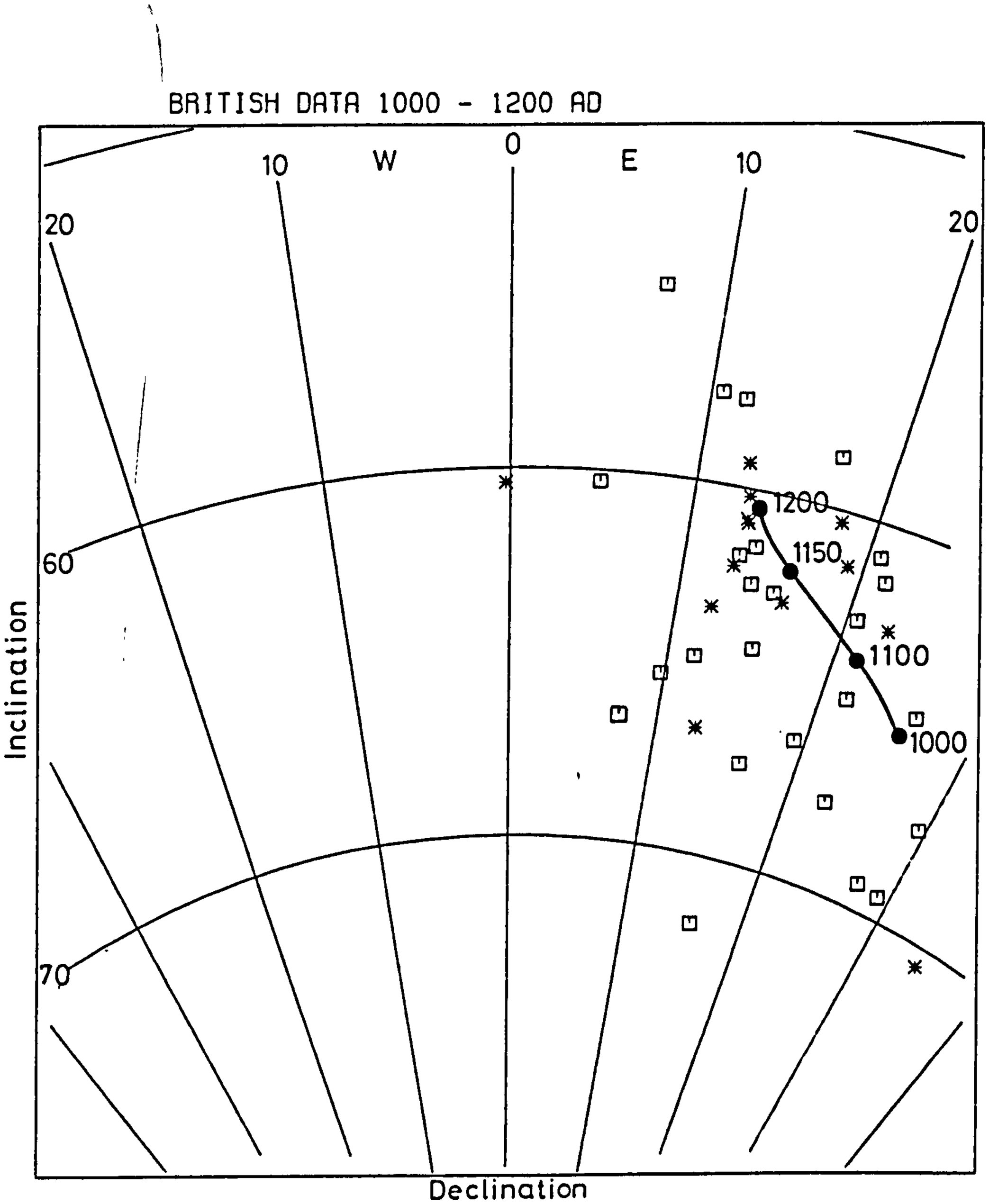

Fig. 4.8b

Fig. 4.8b The most reliable sites (wt. 4 and 5) for the period 1000 - 1200 AD

BRITISH DATA 1200 - 1400 AD

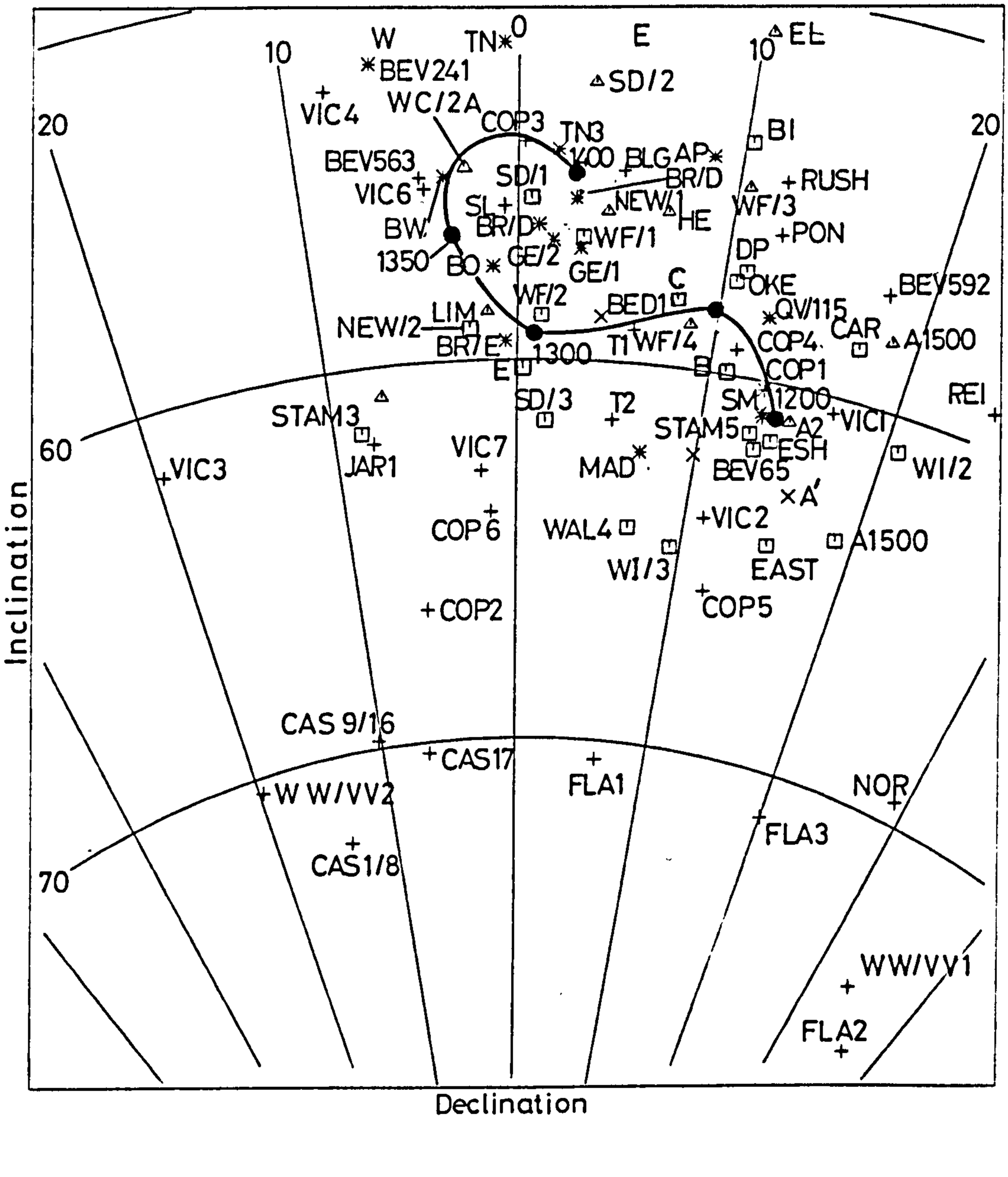

Fig. 4·9a

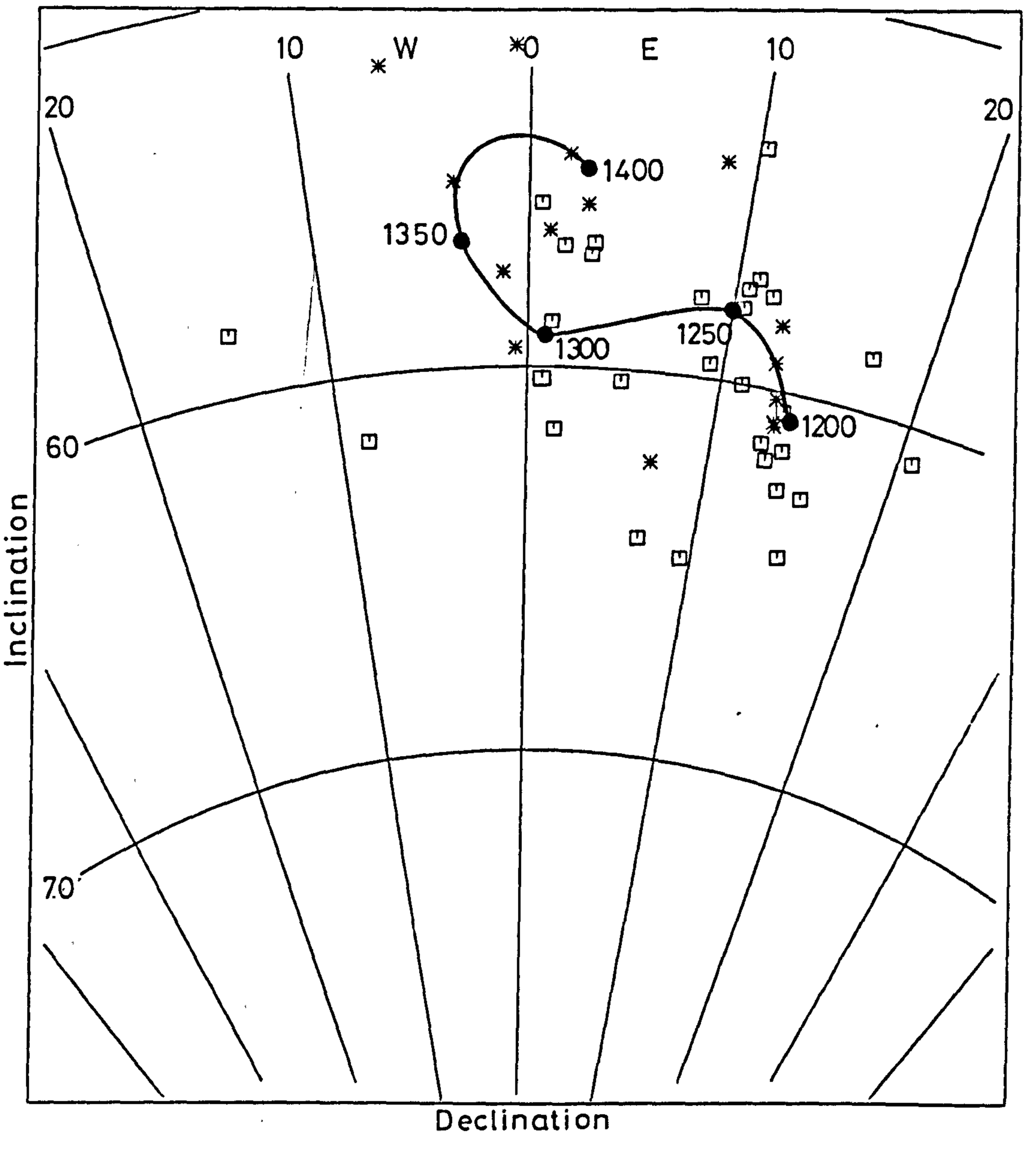

Fig. 4.9 b

The most reliable sites (wt. 4 and 5) for the period 1200 - 1400 AD

(1300-1340 AD), BI (1250-1350 AD), TN (1275-1325 AD), MAD (1325-1350 AD). The 1350 AD is not very well defined but it can be assumed to be between Sites BO (1300-1350 AD), NEW/2 (1230-1360 AD), BW (1300-1350 AD) and LIM (1230-1366 AD). The curve should then change towards the east, where the 1400 AD direction is located between Sites SD/1 (1400-1500 AD), SD/2 (1400-1500 AD) and NEW/1 (1375-1450 AD). This will leave Site WI/3 (1370-1430 AD), SD/3 (1400-1500) and BEV65 (1300-1400 AD), which cover the same age and have high weights, away from the curve.

1400-1600 AD

A total of 69 sites are available within this range (Figure 4.10). These sites show steeper inclinations after 1400 AD and towards 1600 AD. The direction at 1450 AD could be between Sites WC/1D (1450-1530 AD), WC/1B (1450-1530 AD), FF (1470-1530 AD), T1 (1300-1560 AD) and T2 (1300-1560 AD). The 1500 AD direction was located using sites TN/2 (1500 AD), RY (1500-1540 AD) WAL4 (1400-1500 AD), WAK (1535-1540 AD), KIN (1510 AD) and RK/1 (1500-1600 AD). The 1550 AD direction can also be assumed to be near Sties BP/1 (1550-1600 AD) and BP/2 (1550-1600 AD). and the 1600 AD is in between Sites GY (1600 AD), CR (1575-1640 AD) and PP (1600-1700 AD). These directions, between 1400-1600 AD, make some sites with reasonable weights away from the curve, such as Sites RK/2 (1500-1600 AD), NSYK (1538-1547 AD), SL2(3) (1560-1575 AD), LAN (1400-1700 AD) and SD2 (1400-1500 AD).

BRITISH DATA 1400 - 1600 AD

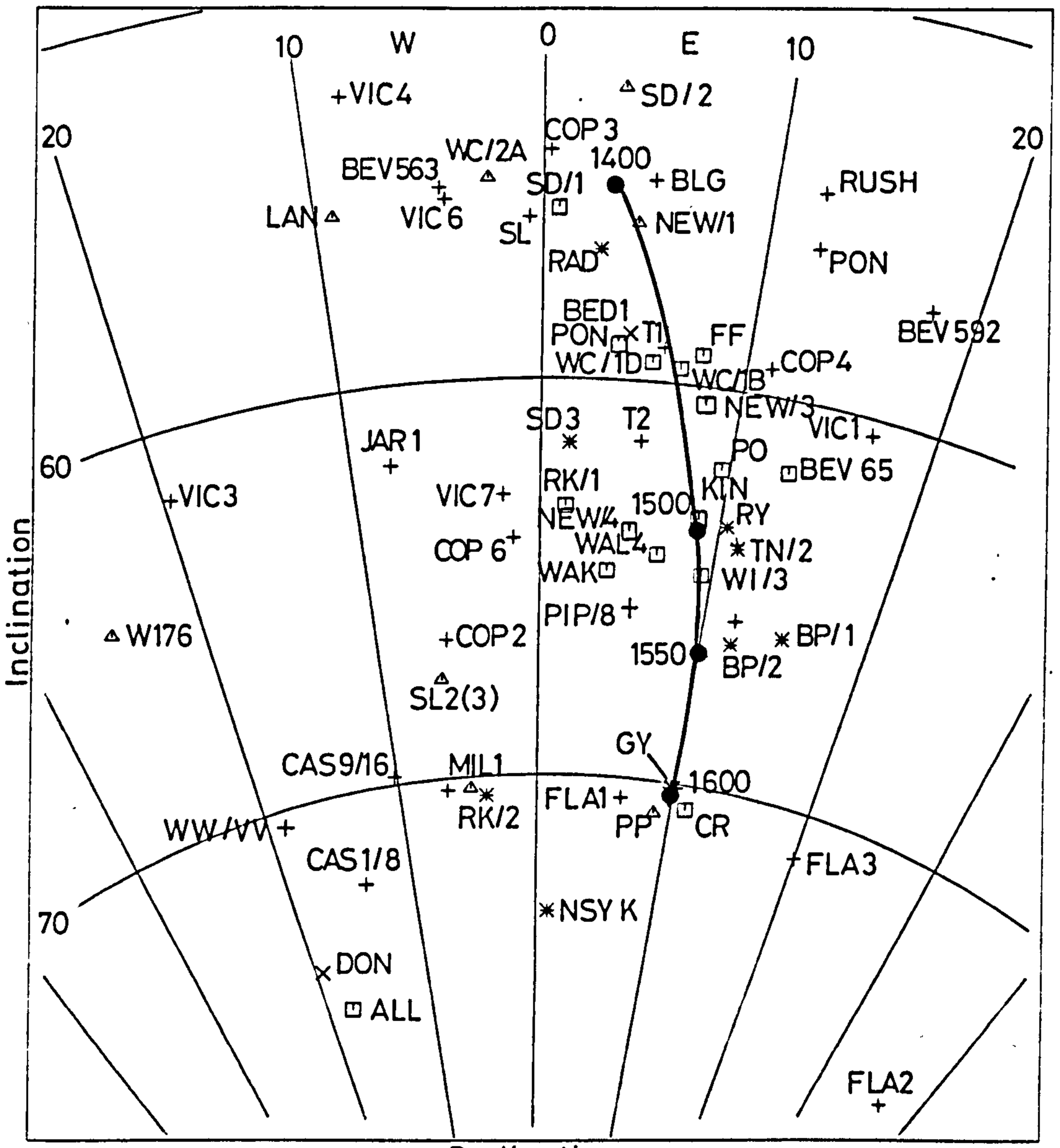

Fig. 4 · 10

1600 - Present

A total of 20 sites are available (Figure 4.11). Some of these sites were not plotted because of their scattered directions. The remaining sites are not very well grouped and they could not be used to plot the curve, if observatory data were not available. However, using the available sites the 1650 AD direction was located near Site WR (1649-1679 AD) and 1950 AD was located near Sites BO/EK1 (1961 AD) and BO/EK2 (1962 AD), and the curve between these two points was dotted. A comparison between the recorded observatories and the available archaeomagnetic data after 1600 AD is somewhat difficult because of the limited number of sites. However, the well defined directions between 1600-1650 AD and at 1950 AD . deviate from the available records. This deviation is within about $\pm$ 2^{o} in declination and inclination.

Summary

The revised archaeomagnetic curve is similar in shape to the previous British archaeomagnetic curve (Aitken 1970), but with some changes in the Roman period and between 1200-1400 AD. The difference between the two curves can be summarized as follows:

(1) The shallow inclination value for the Roman period was obtained at 250 AD, rather than 200 AD and the direction at 300 AD was to the east of 100-200 part of the curve, and not to the west of it.

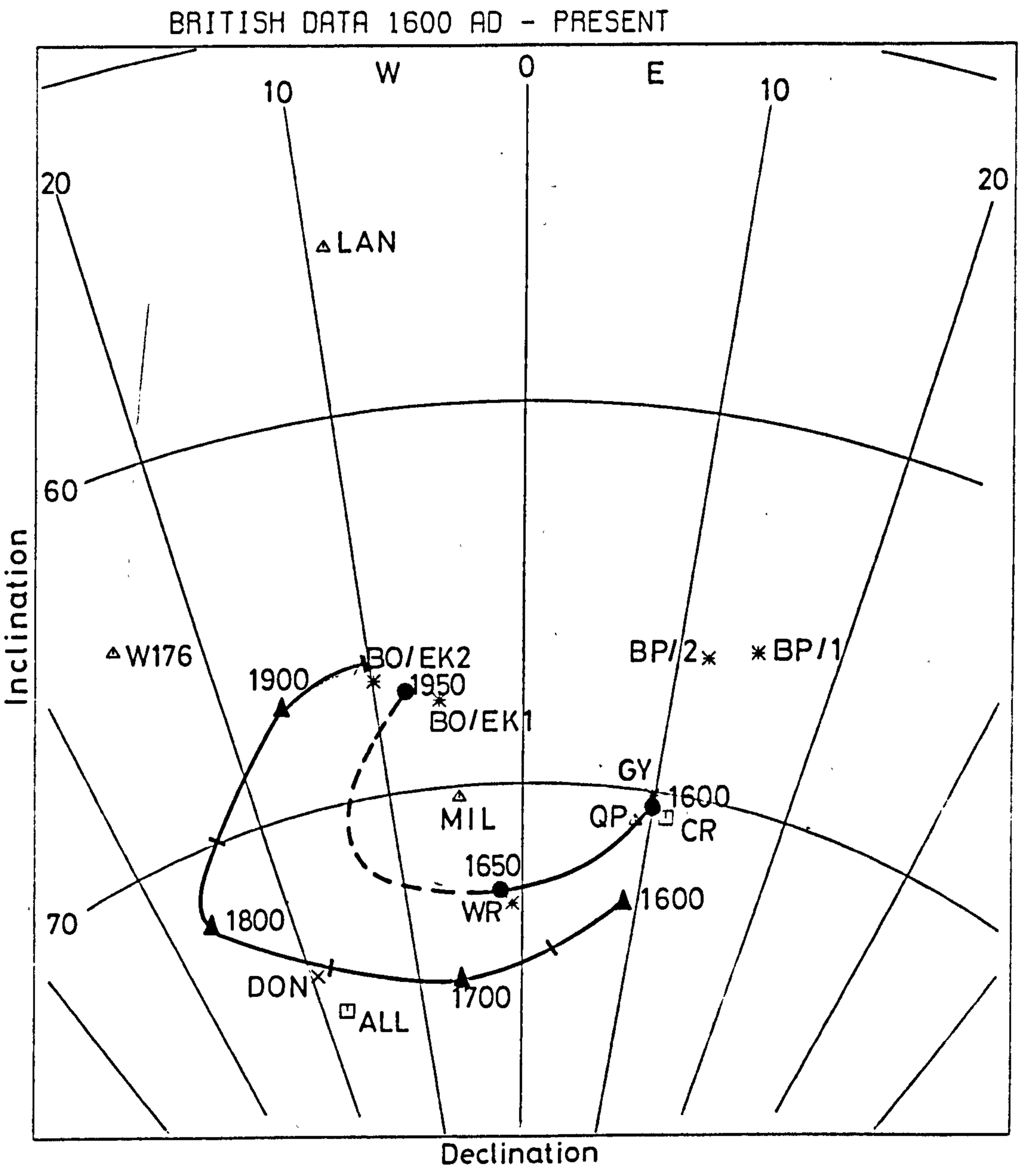
BRITISH DATA 1600 AD - PRESENT
W
0
E
10
10
20
20
60
70
Inclination
Declination
LAN
W176
BO/EK2
1900
1950
BO/EK1
BP/2
BP/1
GY
1600
MIL
QP
CR
1650
WR
1600
1800
1700
DON
ALL

Fig. 4·11

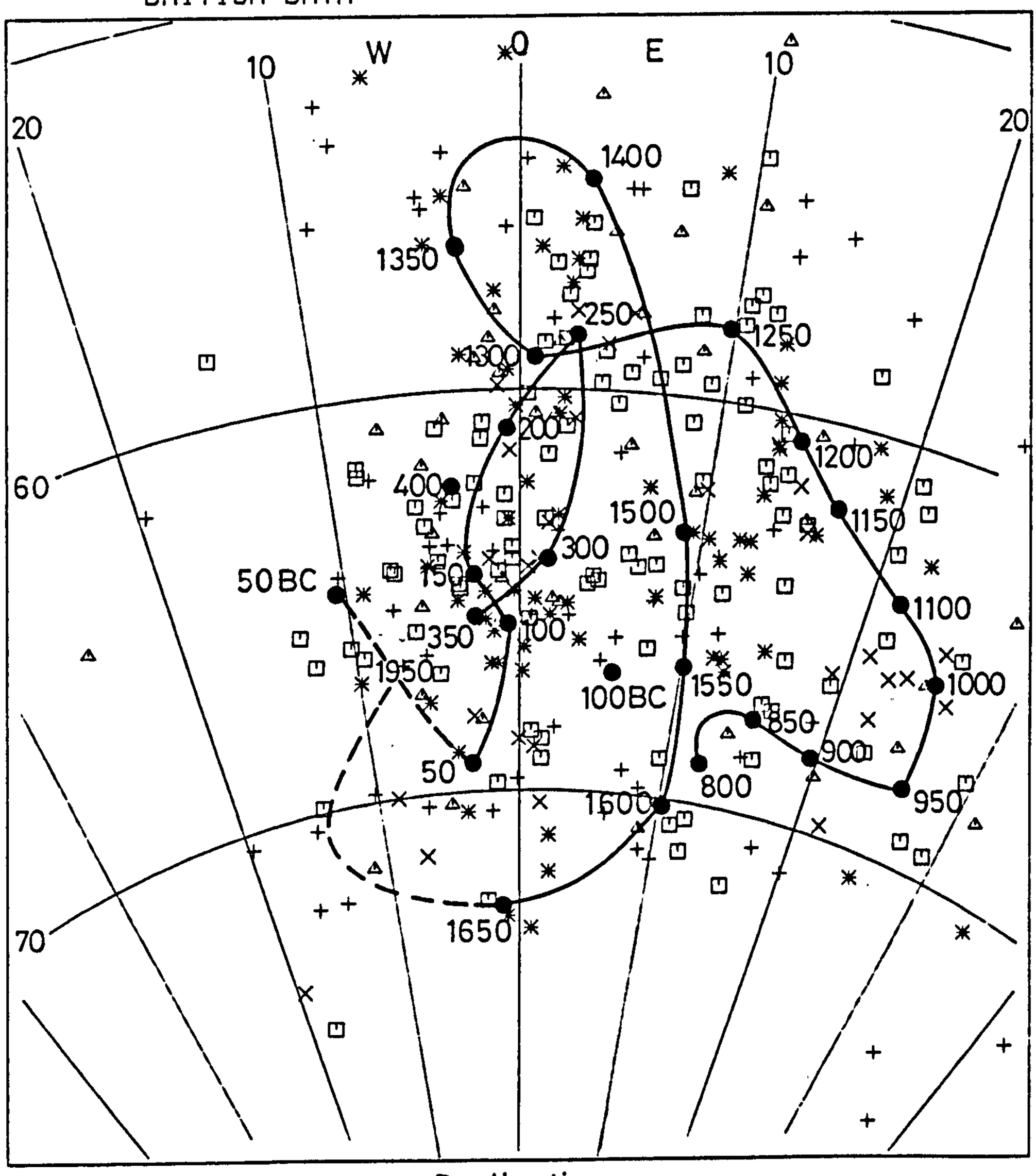

Fig. 4.12a

Revised British archaeomagnetic curve

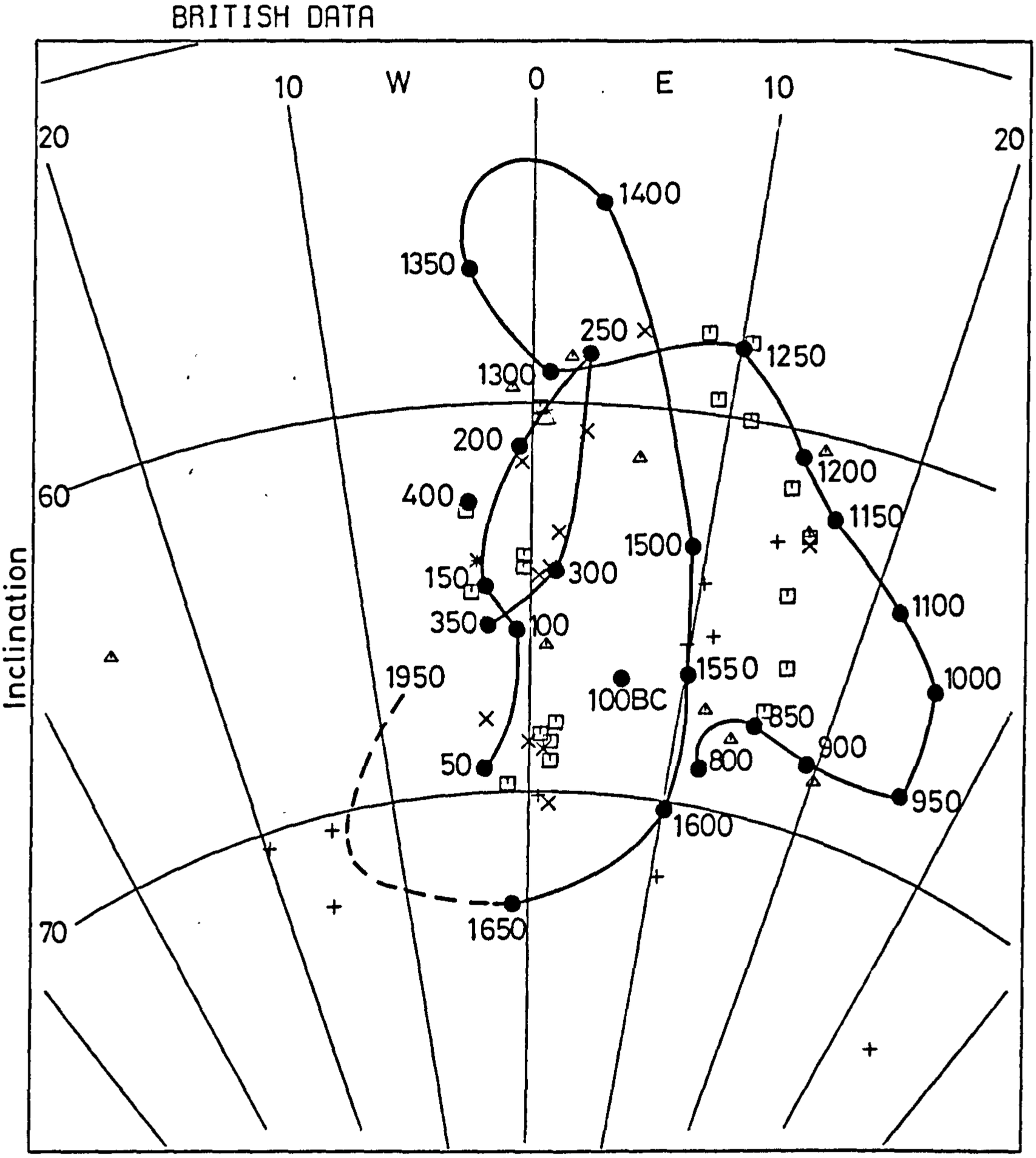

Fig. 4.12 b

Revised British archaeomagnetic curve with the present data

(2) The directions between 1200-1400 showed a loop towards the west with the 1300 AD direction having steeper inclination value than the 1400 AD while the original curve showed a smooth loop with shallow inclination around 1300 AD.

(3) The directions between 800 and 1000 have now been plotted and this part was not established in the original curve.

The main differences between the two curves are related to the additional data which adds more control points in some of the sectors, particularly 1100-1400 AD. The revised weighting system only resulted in some small changes throughout the curve.

Towards the end of the work additional data were accumulated from dating further sites. These have not been discussed in detail within the text, but are included in the Appendices and in the analyses of the curve. The present archaeomagnetic data are plotted with revised curve in Figure 4.12. However, further work is recommended for the sectors which show limited numbers of sites, particularly all ages BC and for 400-800 AD. In order to check the accuracy of the archaeomagnetic dating, further sites are still required for the period between 1600 and the present, in order to allow a better comparison between archaeomagnetic data and observatory records.

4.3 The French Archaeomagnetic Data (Thellier 1981)

The French curve was built using the magnetic directions of 137 sites distributed throughout France. The curve stretches from 40 AD to the present with the magnetic directions after 1600 being based on recorded geomagnetic observations (Figure 4.13) (Appendix 2). The curve starts at 40 AD with an inclination of about 68^{o}. This inclination increases with the declination changing towards the east until 70 AD where there is a significant westerly trend followed by a sharp easterly change in declination. The inclination reaches a value of about 58^{o} around 200 AD and then steepens with almost no changes in declination until 750 AD, where it reaches a value of 73^{o}. After this, the declination changes towards the east and the inclination becomes shallower. At 1000 AD the declination starts changing towards the west with the inclination still tending to shallow until 1300 AD, where it reaches a value of about 55^{o}, then the declination changes about 10^{o} towards the west, with about 2^{o} change in inclination. At 1400 AD the inclination steepens very sharply with just a few degrees change in declination until 1600 AD, where it reaches a value of about 70^{o} and the observatory records then continue until the present time.

The plotted curve by Thellier (1981) clearly shows that the curve was achieved only by severe smoothing of the available data as the sampling points are badly scattered around the curve, even bearing in mind reasonable uncertainty factors for orientation and measurement errors. Furthermore, the Paris data showed a wide age range for many of the sites used and this also causes error in relating these sites to a specific part of the curve.

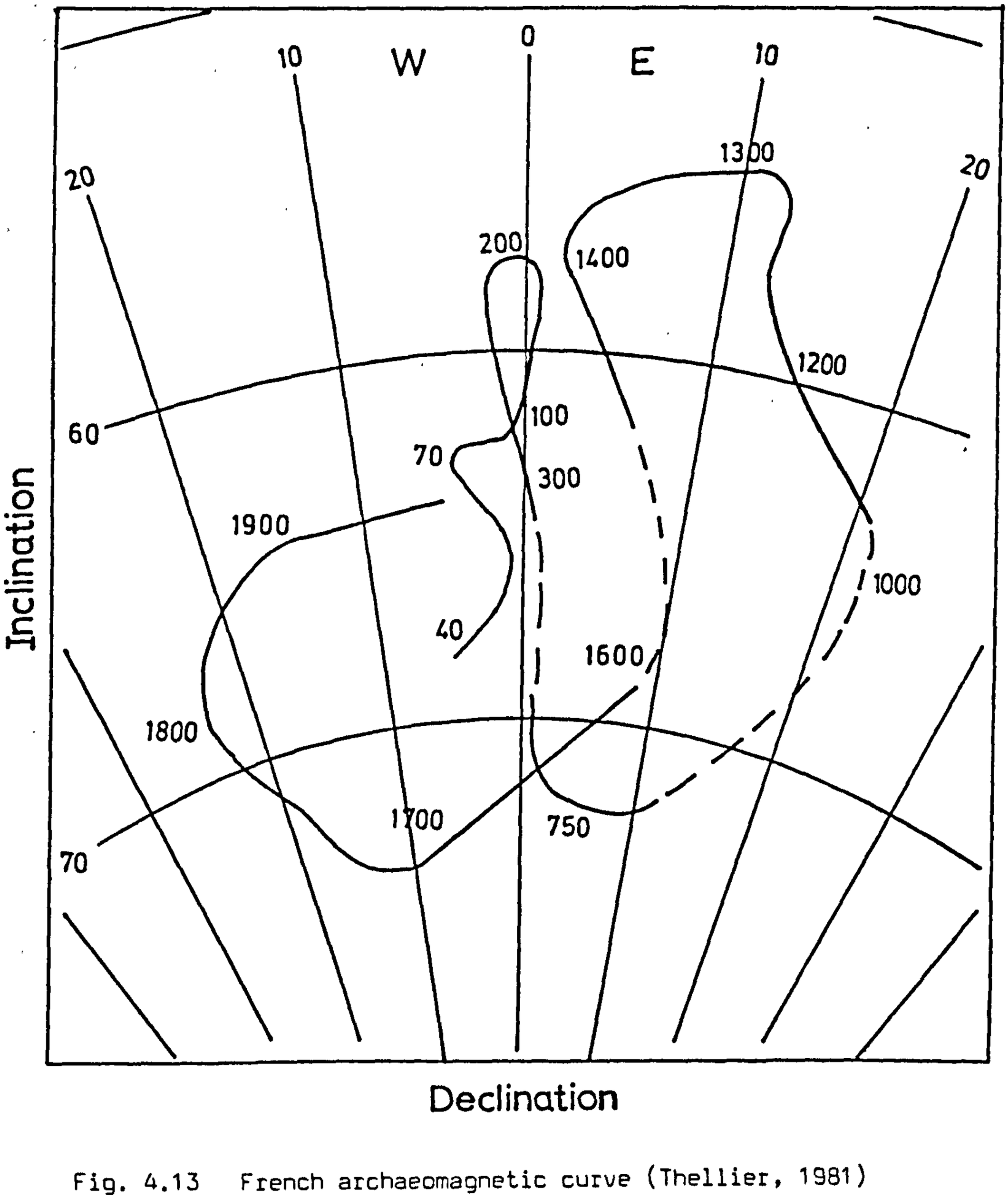

Fig. 4.13 French archaeomagnetic curve (Thellier, 1981)

One of the main limitations in the latest curve (Thellier 1981) was presenting the data without correcting the declination to a reference locality. This could cause some relative differences in the magnetic declinations of different site localities. To overcome the limitation all the original data were corrected to Paris (Lat.48.83, Long. 2.33). After giving weights to all sites the data was re-evaluated as follows:

-200 - 0 AD

Six sites are available within this range which was not included in the original Thellier curve (Figure 4.14). Three of these sites have weights of 5. The directions can be assumed to have been changed from Site 84 to Site 4 and then 183. But because of the limited number of sites such high changes within . . $\pm$ 10 years cannot be considered realistic and hence the direction at 40 BC was only located in between these three sites.

0 - 200 AD

A total of 45 sites are available within this period and so this interval could be subdivided into 50-year intervals (Figure 4.19).

0 - 50 AD

Nineteen sites are available within this range (Figure 4.15). The directions at 0 AD cannot be located due to the lack of sites of this age. The direction at 40 AD was obtained using Sites 6, 24 and 111. The directions can either be drawn passing through these sites or a mean direction can be taken of all three. Since there is about $\pm$ 10

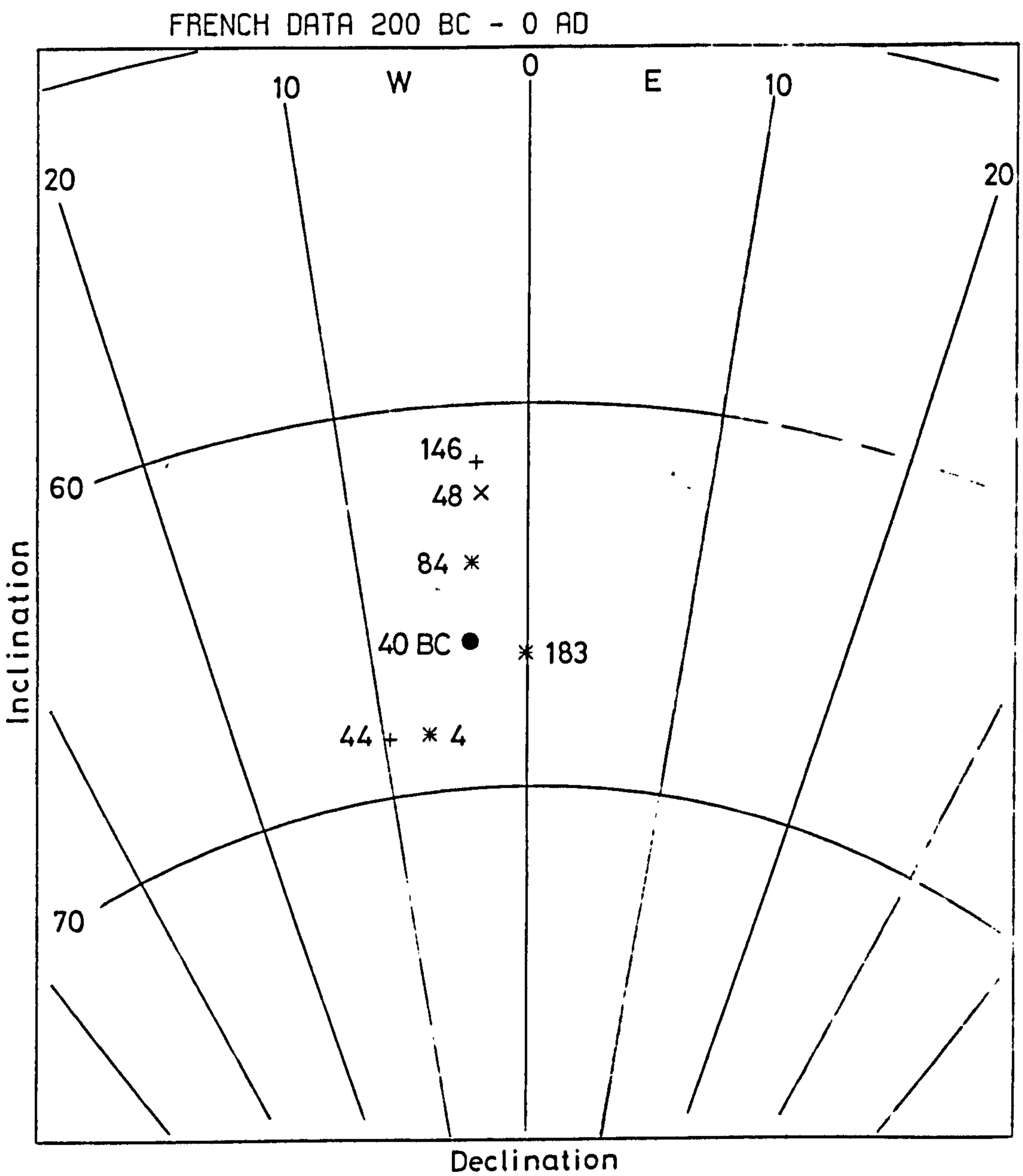
FRENCH DATA 200 BC - 0 AD
W
E
0
10
10
20
20
60
70
146
48
84
40 BC
183
44
4
Inclination
Declination

Fig. 4.14

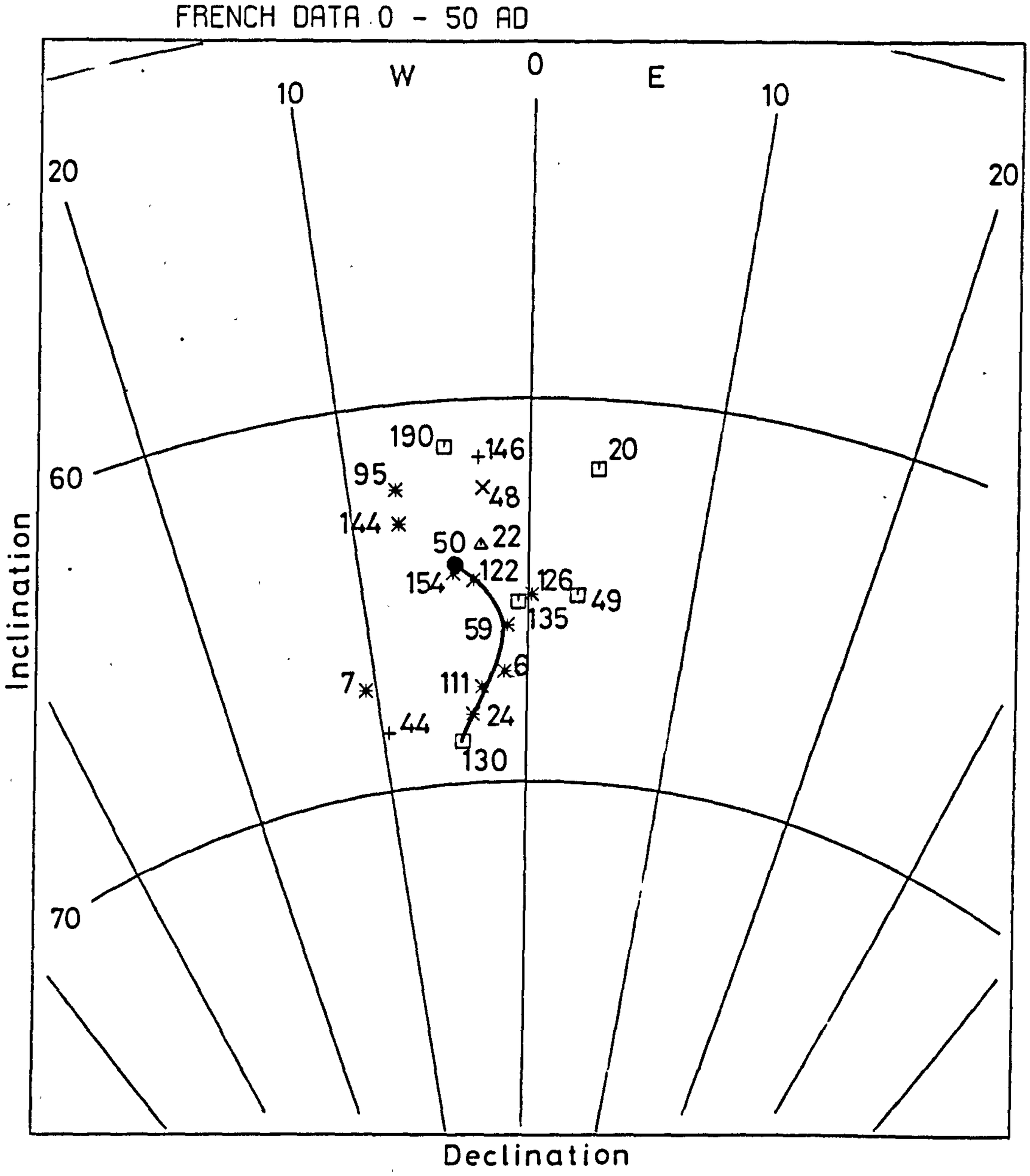
FRENCH DATA 0 - 50 AD
W
0
E
10
10
20
20
60
70
Inclination
Declination
190
+146
20
95
×48
144
50
△22
154
122
126
49
59
135
6
7
111
24
44
130

Fig. 4.15

years between these sites and Sites 130 and 59, hence the curve was drawn to pass through all these sites. This direction will make other reliable sites with high weights and of the same age away from this main grouping (7, 126 and 135). The curve has shallow inclinations after 40 AD and the directions at 50 AD should be in between Sites 22, 122 and 144. These directions seem to be well defined but some of the sites with high weights were still away from the curve as parts of the curve do not correspond with their ages. According to these directions the 0 AD can be located somewhere between -40 and Site 130.

50 - 100 AD

Sixteen sites are available within this range (Figure 4.16). The directions after 50 AD show a slight westerly change in declination. The direction at 100 AD was located between Sites 1, 28, 68 and 123. This will leave Sites 20, 95, and 49, which are of high weights and cover the same age range, away from the area.

100 - 150 AD

Fifteen sites are available within this range (Figure 4.17). The directions after 100 AD are expected to have shallower inclination towards the 150 point which is located near Site 100 (50-250 AD). This will make Site 49 (50-150 AD) and 67 (120 AD) away from this direction.

150 - 200 AD

A total of 23 sites are available within this range (Figure 4.18). According to sites 62, 65, 192, 142, 185, 12 and 117 (good weights),

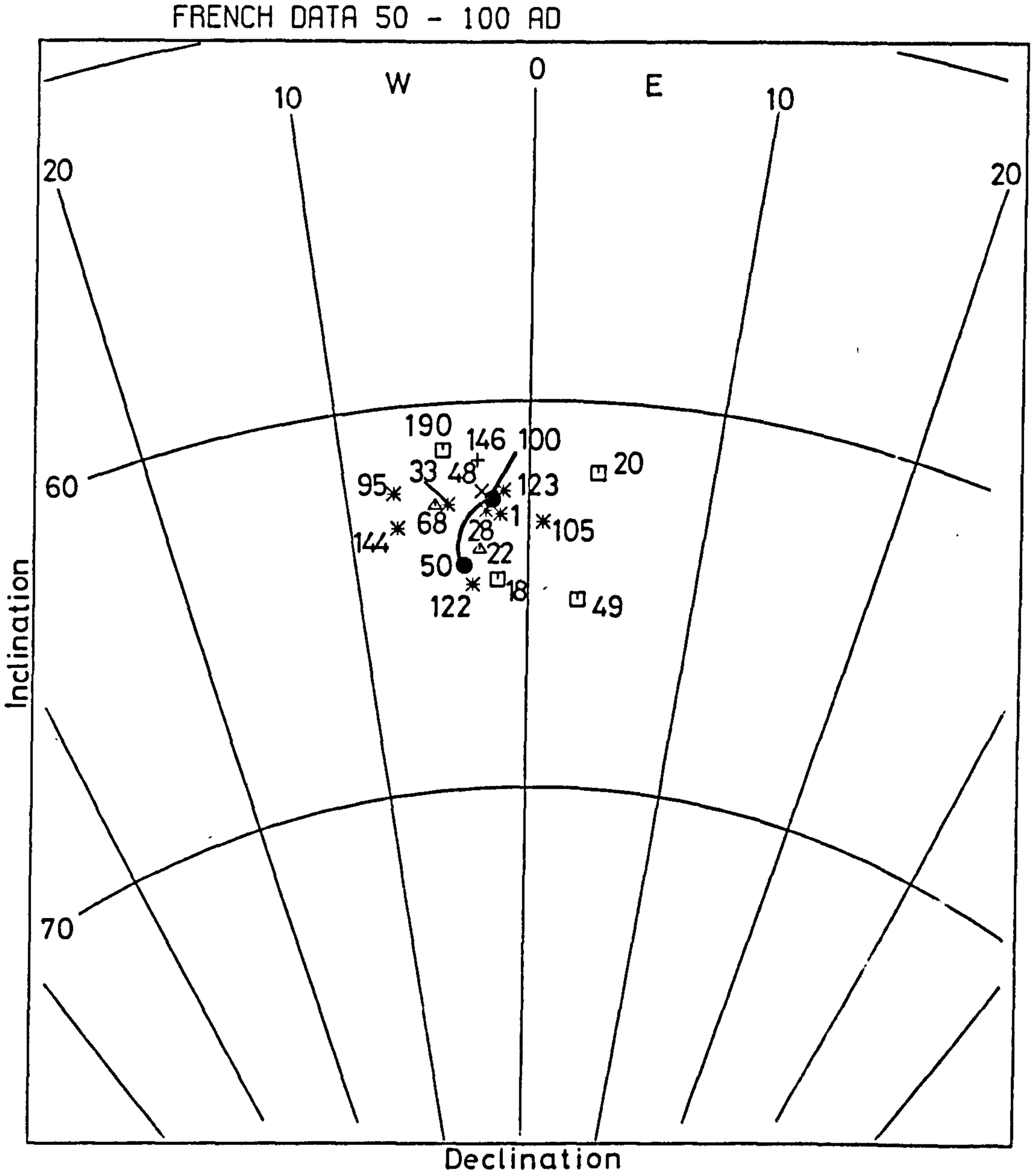
FRENCH DATA 50 - 100 AD
W
0
E
10
10
20
20
60
70
Inclination
Declination
190
146
100
33
48
95
123
20
68
28
1
144
105
22
50
18
122
49

Fig. 4.16

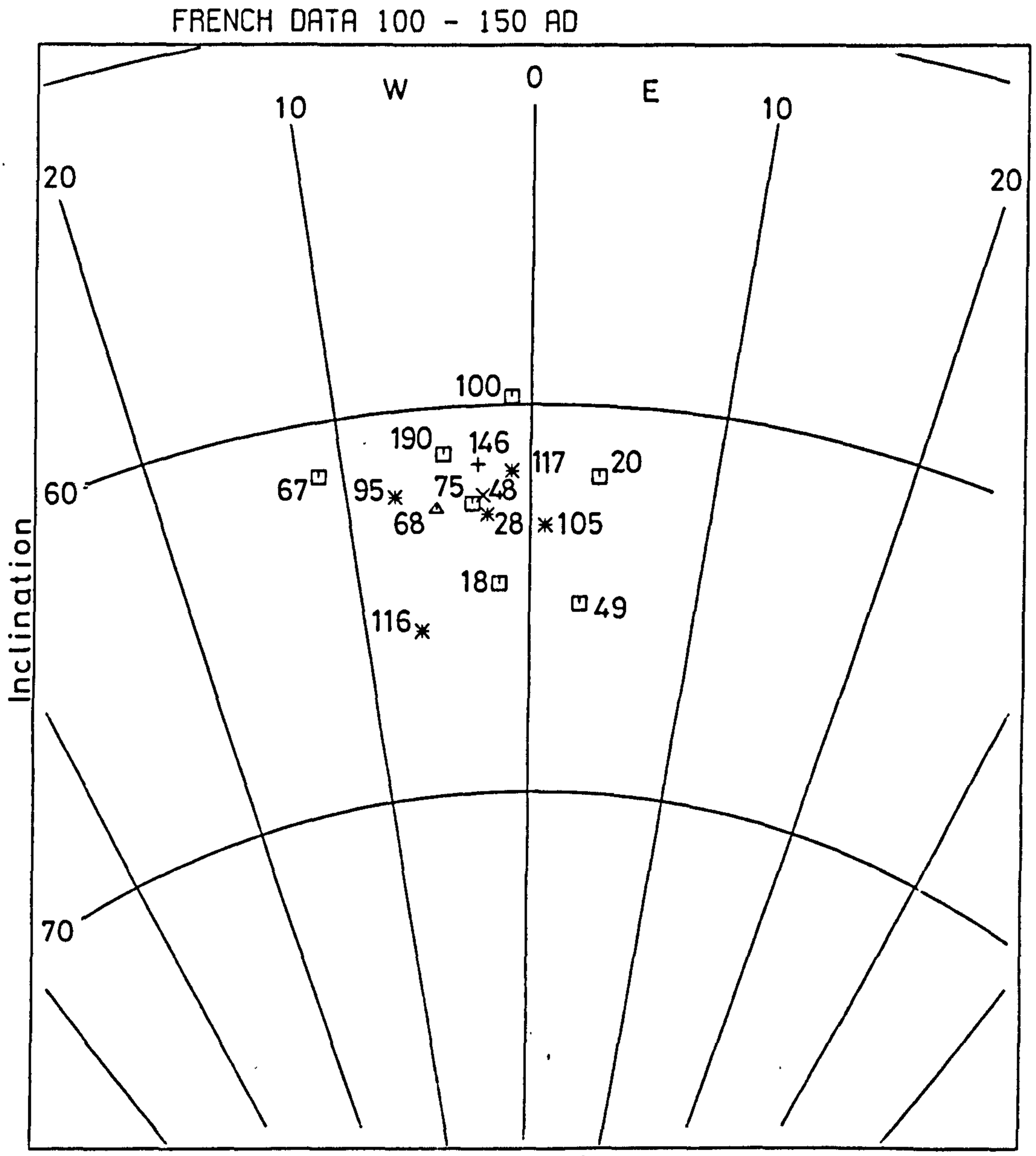
FRENCH DATA 100 - 150 AD
W
0
E
10
10
20
20
100
60
70
190
146
117
20
67
95
75
48
68
28
105
18
49
116
Inclination
Declination

Fig. 4·17

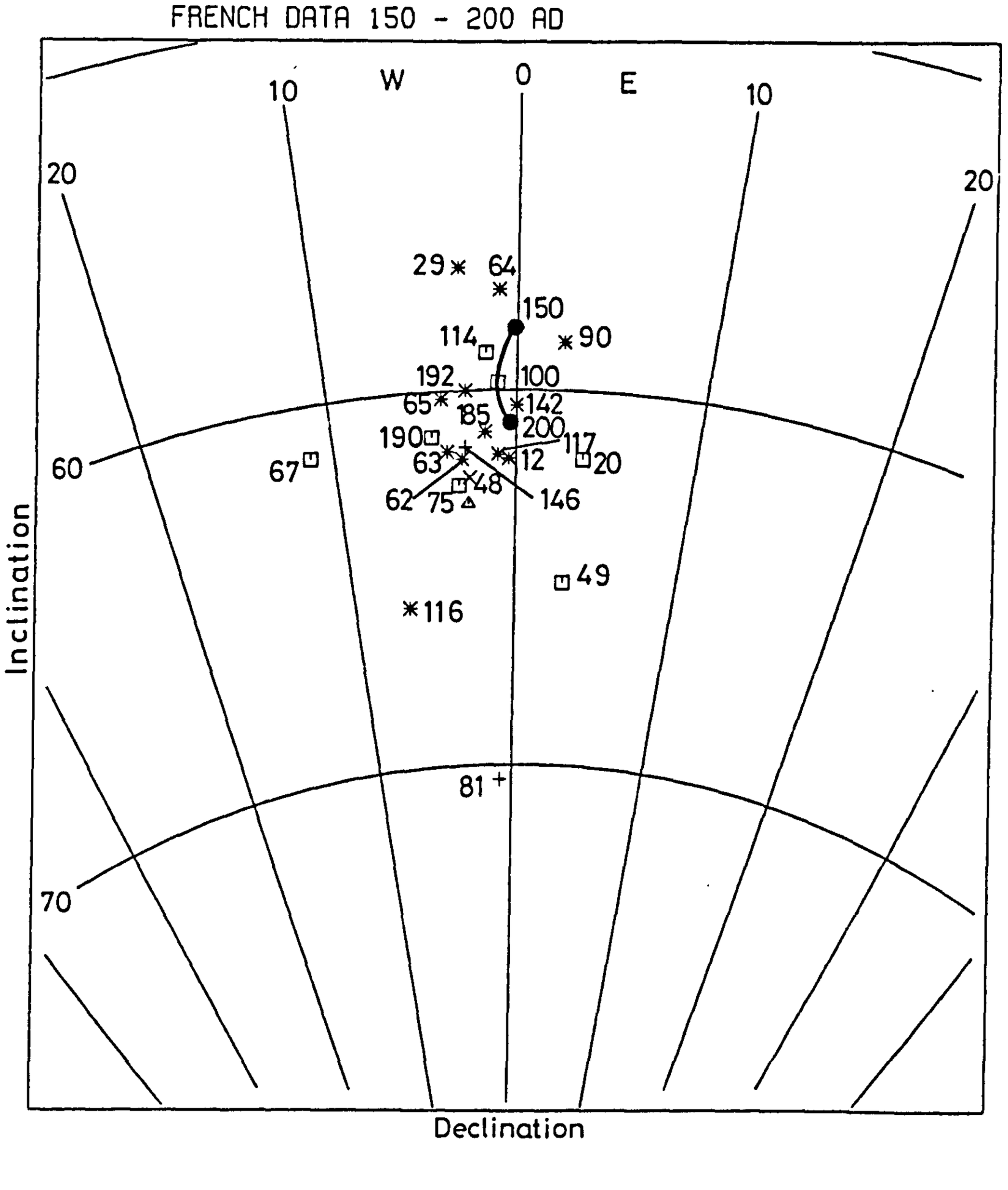
FRENCH DATA 150 - 200 AD
W
E
10
0
10
20
20
29
64
150
114
90
192
100
65
142
185
200
190
117
63
12
20
67
48
62
75
146
49
116
81 +
70
60
Inclination
Declination

Fig. 4·18

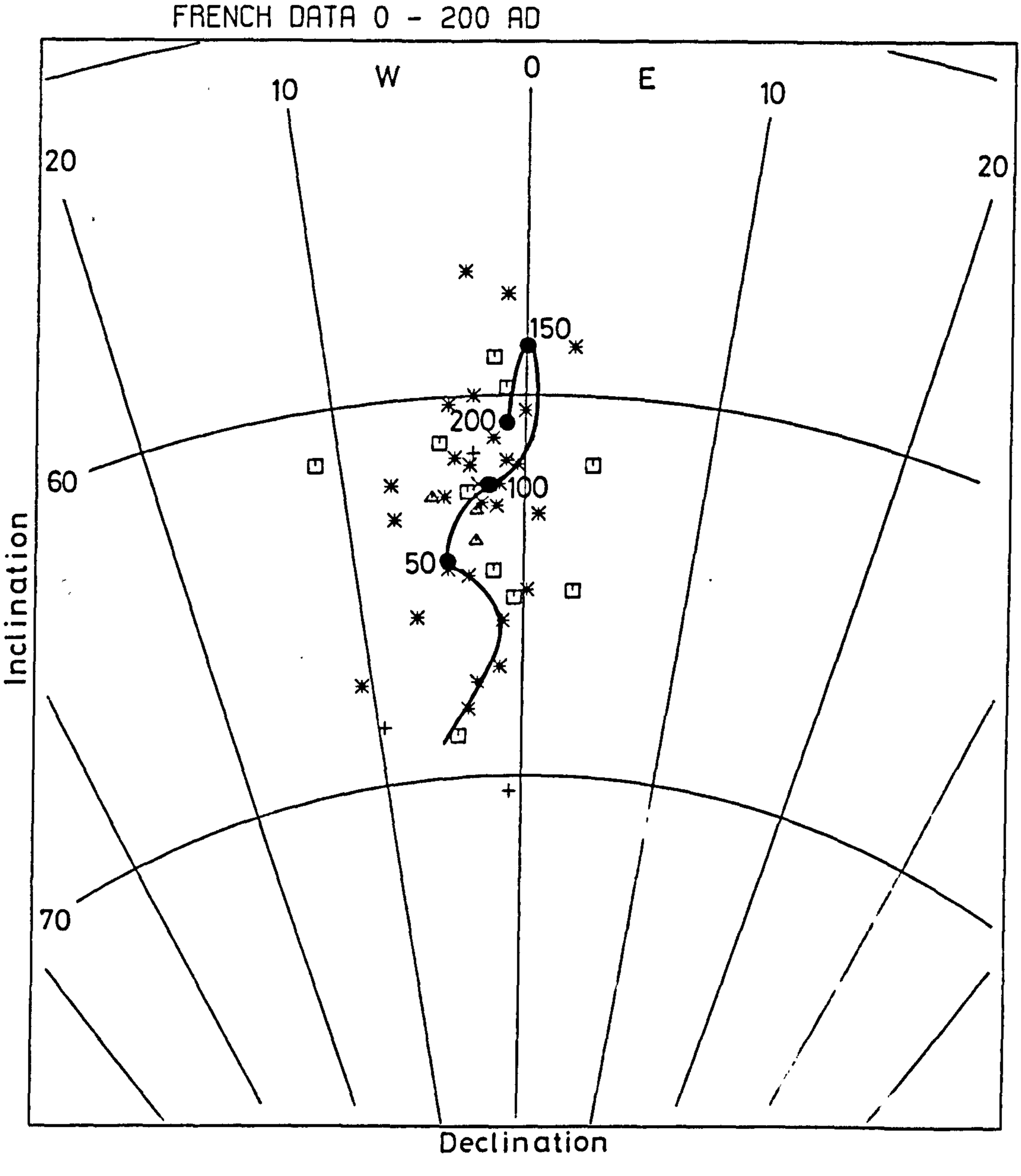
FRENCH DATA 0 - 200 AD
W
0
E
10
10
20
20
150
200
100
50
60
70
Inclination
Declination

Fig. 4.19

the directions after 150 AD should have steeper inclination and the 200 AD should be in between these sites. This will make many of the other reliable sites of the same ages away from this grouping (116, 29, and 90).

200 - 400 AD

A total of 31 sites are available within this period (Figure 4.20). The directions of these sites showed steeper inclination after 200 AD. The directions at 300 AD are well defined by the good grouping of about seven sites with high weights, although some of the other high weight sites are still away from this main grouping (104, 155', 155", 127, 133' and 133"). The direction at 400 AD was located using Sites 47, 76, 125 and 178, which are the only sites covering this range. Although Sites 47 and 178 have similar age ranges (400-500), there is a difference of about 6^{o} in inclination and 10^{o} in declination. Accordingly, the direction at 400 AD was chosen to be in between Sites 76, 47 and 125.

400 - 600 AD

Seven sites are available within this range (Figure 4.21). The age range of most of these sites are distributed around 400 AD. According to the available sites, the 400 AD can be located between Sites 47, 57, 76 and 125, but nearer to Sites 47, 76 and 125. This will make the direction at 400 AD close to the direction at 300 AD. After 400 AD, the sites show little information about the geomagnetic directions, as only two sites (27 and 81) with low weights cover an

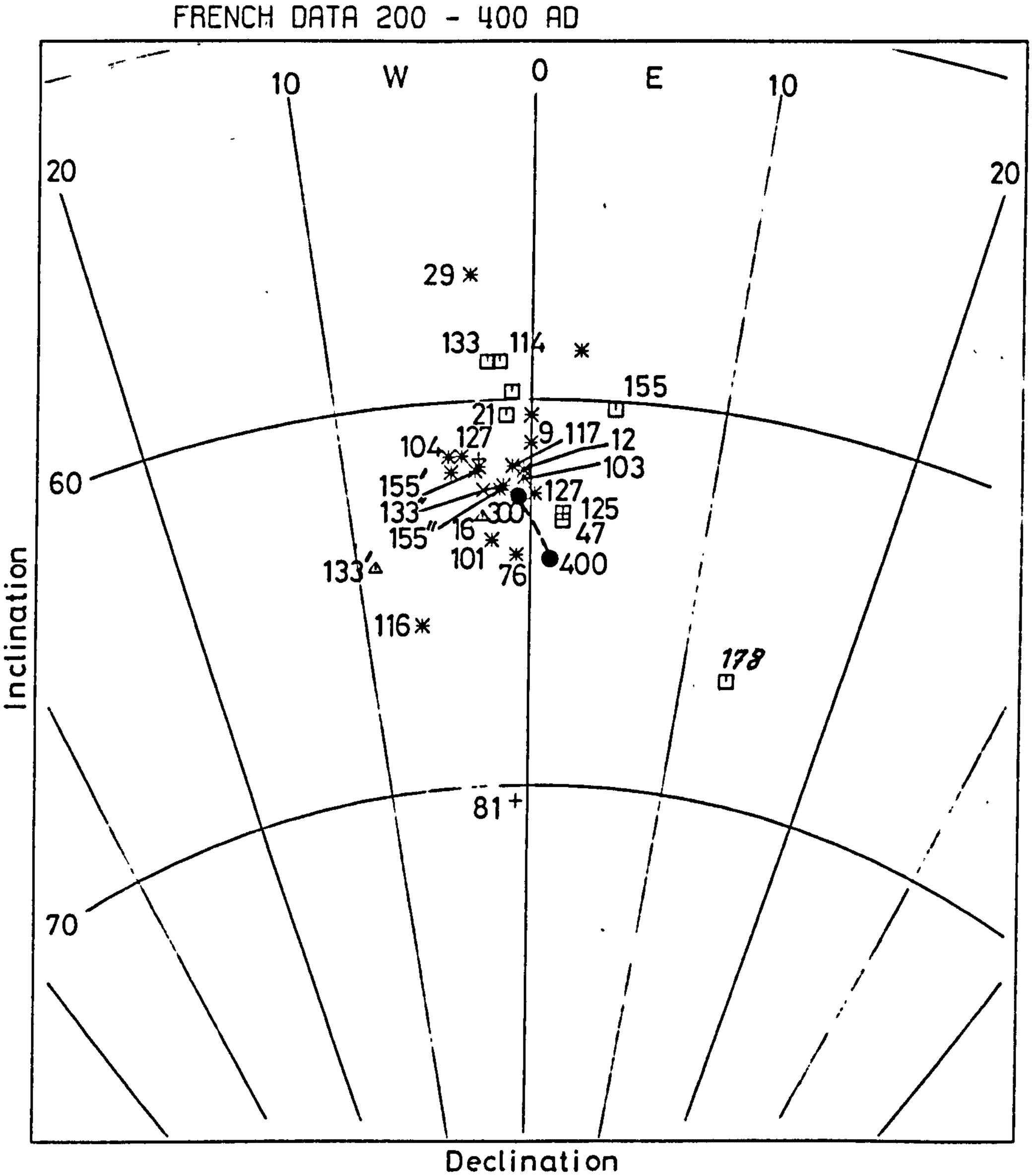
FRENCH DATA 200 - 400 AD
10 W
0
E
10
20
20
29
133
114
155
21
9
117
12
104
127
103
155'
127
133"
300
125
16
47
155"
101
76
400
133'
116
178
81+
60
70
Inclination
Declination

Fig. 4·20

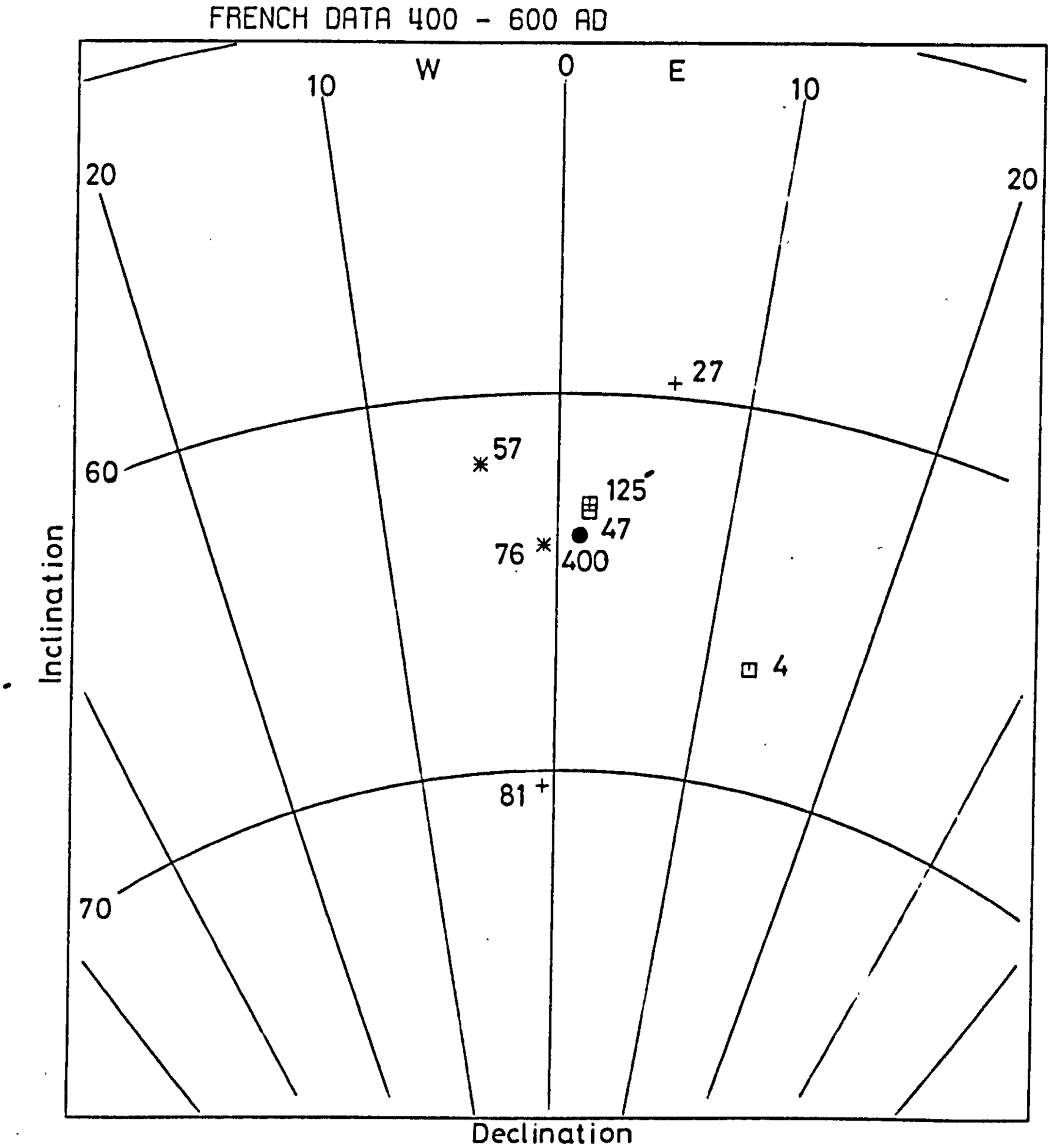
FRENCH DATA 400 - 600 AD
W
0
E
10
10
20
20
27
60
57
125
47
76
400
4
81
70
Inclination
Declination

Fig. 4.21

age range of 550-750 AD and 200-700 AD. Accordingly, the directions at 500 and 600 can hardly be located.

600 - 800 AD

Nine sites are available within this range (Figure 4.22). These sites show that the magnetic inclination steepens sharply towards 700 AD, which is near Sites 87 and 125 (chosen because of their high weights). After 700 AD the sites only poorly indicate the magnetic directions at 800 AD where only three sites are available, two of them with somewhat low weights (23 and 131).

800 - 1000 AD

A total of 14 sites are available within this range (Figure 4.23). Some of these sites could show the directions at 850 AD, particularly sites 110 and 91. This position helped in locating the directions at 800 AD, which showed some difficulties in the previous age range (600-800 AD), but this left Site 113 away from these directions. According to Sites 91, 92, and 131, the directions at 900 AD could be to the east of 800 AD, but this will make Sites 96 and 97 (950 AD) about 10^{o} shallower than this evaluated direction, and statistically, the 950 AD should be somewhere in between Sites 96 and 97. Such directional changes, within a 50-year period, cannot be expected to be real. In addition, another two sites, 26 and 43, cover an age range of 800-900 AD and 900-1200 AD, but show some 15^{o} shallower inclination. Accordingly, the directions between 800 and 900 are not well defined and using the available data it was not possible to locate the position of

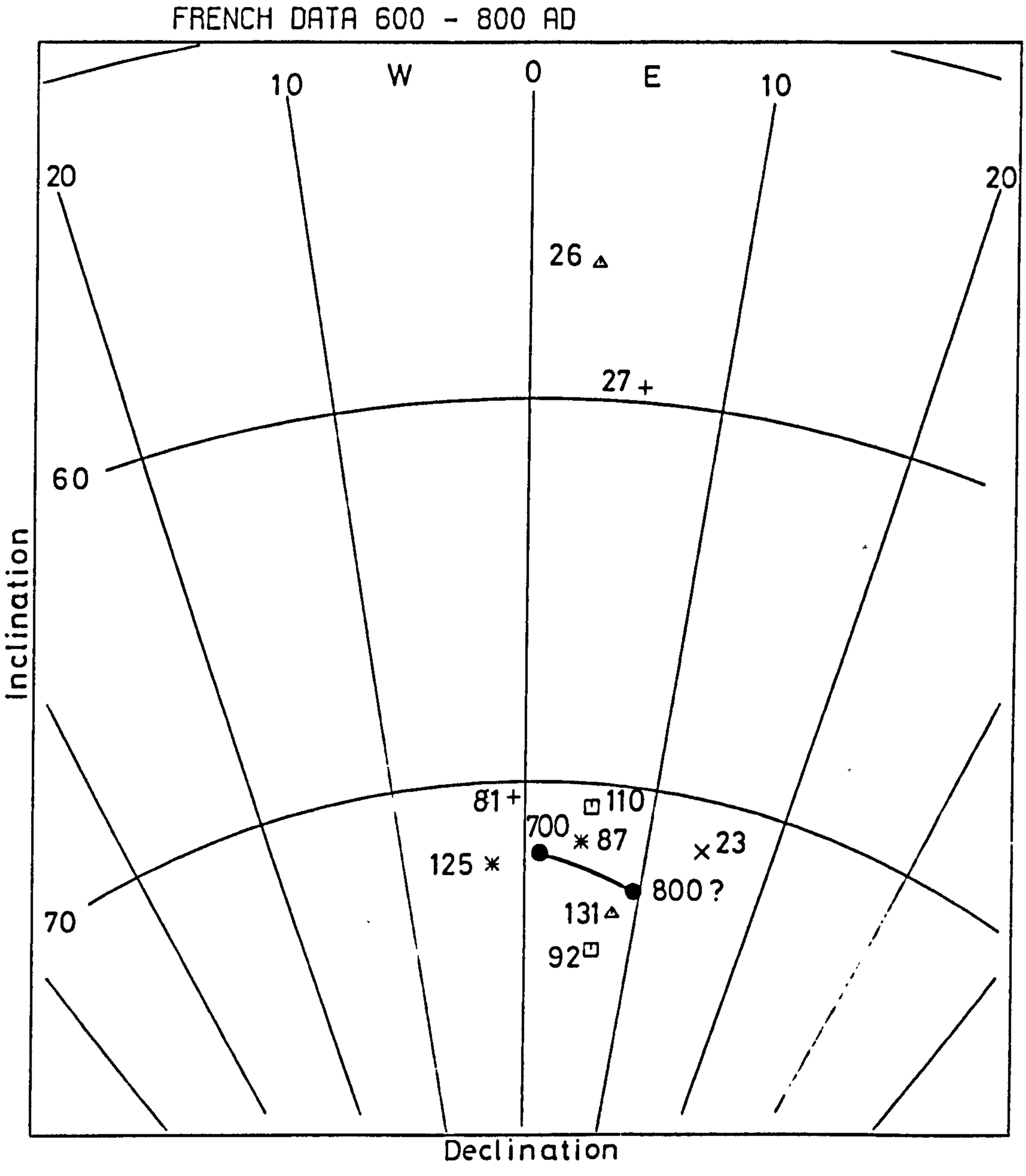
FRENCH DATA 600 - 800 AD
W
E
10
0
10
20
20
26 △
27 +
60
Inclination
81 +
□110
700
✳87
125 ✳
×23
800?
131 △
92 □
70
Declination

Fig. 4·22

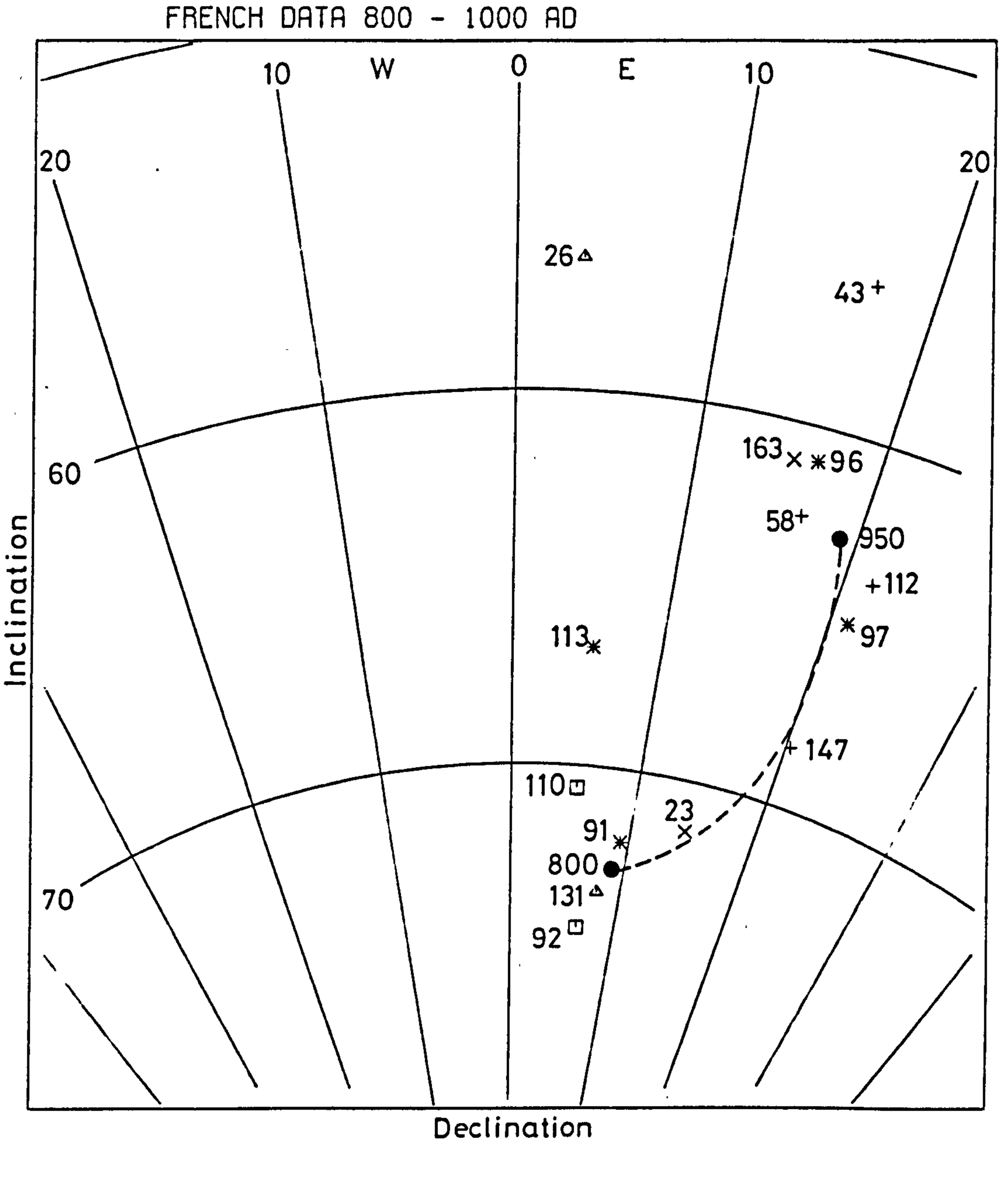
FRENCH DATA 800 - 1000 AD
10 W
0
E
10
20
20
26
43
60
163
96
58
950
112
113
97
147
110
23
91
800
131
70
92
Inclination
Declination

Fig. 4·23

1000 AD part of the curve as the only site available covering this range (43 (900-1200) and 58 (950-1100)) had low weights and about 7^{o} difference in inclination, and was also overlapping with the directions of Sites 96 and 97 (950 AD).

1000 - 1200 AD

Fourteen sites are available within this range (Figure 4.24). The directions at 1000 AD were still not located due to the lack of reliable sites. 1100 AD was located in between Sites 151 (1100, wt. = 4) and 32 (1150-1200, wt = 5) but somewhere near Site 151. The curve is then expected to pass through Sites 166 (1170 AD) and 163 (960-1140 AD). The direction at 1200 AD is defined by Site 78 (1200 AD) and Site 191 (1200 AD). The direction from 1100-1200 AD seems to be well defined, but some of the sites with reasonable weights were still away from the curve (Sites 55 and 148).

1200 - 1400 AD

Nineteen sites are available within this range (Figure 4.25). According to Sites 79 (1250-1275 AD), 80 (1225 AD) and 171 (1225 AD), the directions after 1200 should change towards the east passing between these three sites, and then the 1300 AD is expected to be between Sites 54 (1340), 158 (1300-1400), 159 (1250-1350 AD), 169 (1250-1360) and 176 (1270). The curve is then expected to move westerly towards Site 56 (1350) and 175 (1300-1450), where the 1350 is expected to be near these two sites. The inclinations after 1350 AD are expected to steepen towards Sites 77 (1380 AD) and 137 (1400-1500 AD).

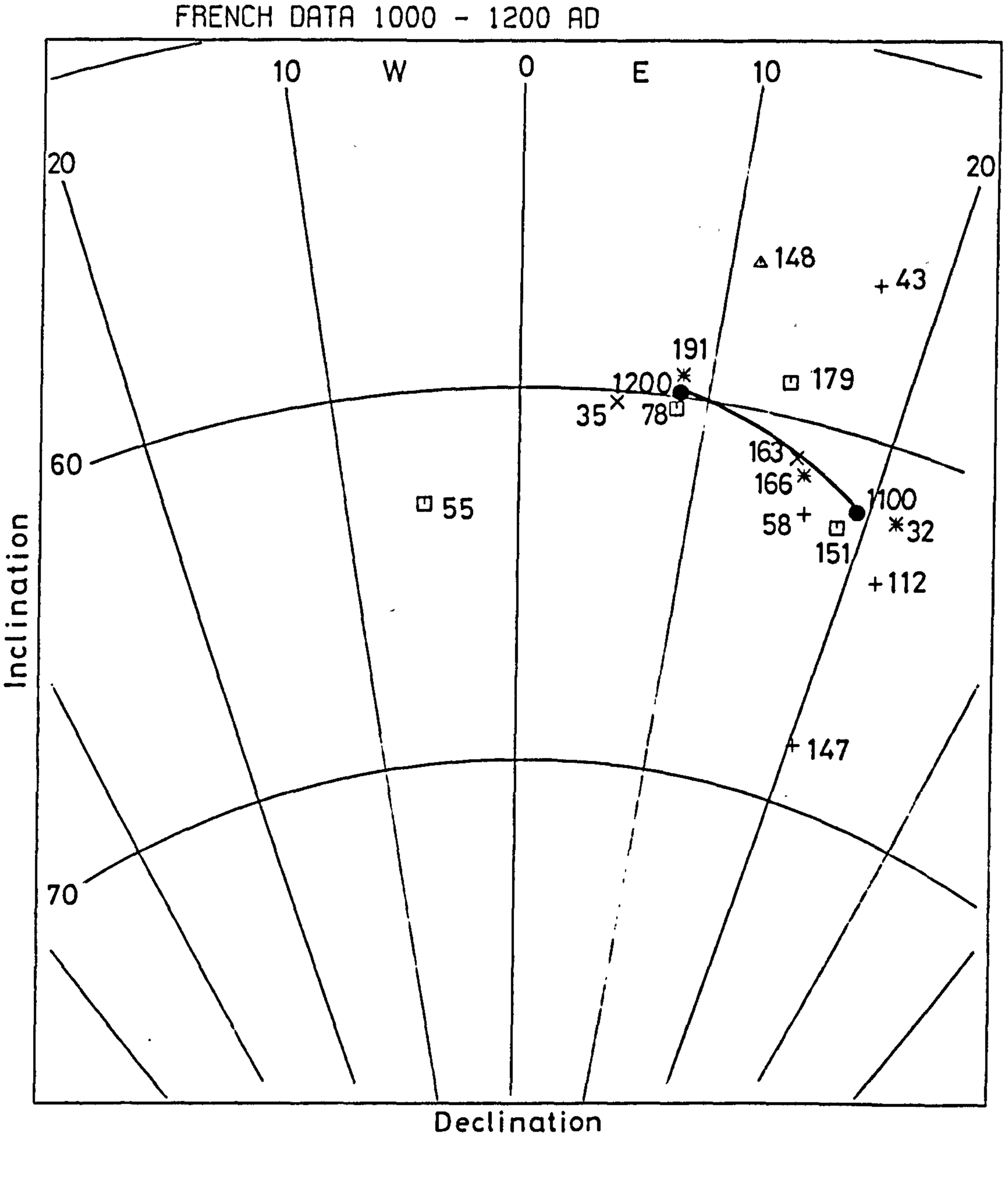
FRENCH DATA 1000 - 1200 AD
10 W
0
E
10
20
20
148
+43
191
1200
179
35
78
60
163
166
1100
58
32
151
+112
55
+147
70
Inclination
Declination

Fig. 4·24

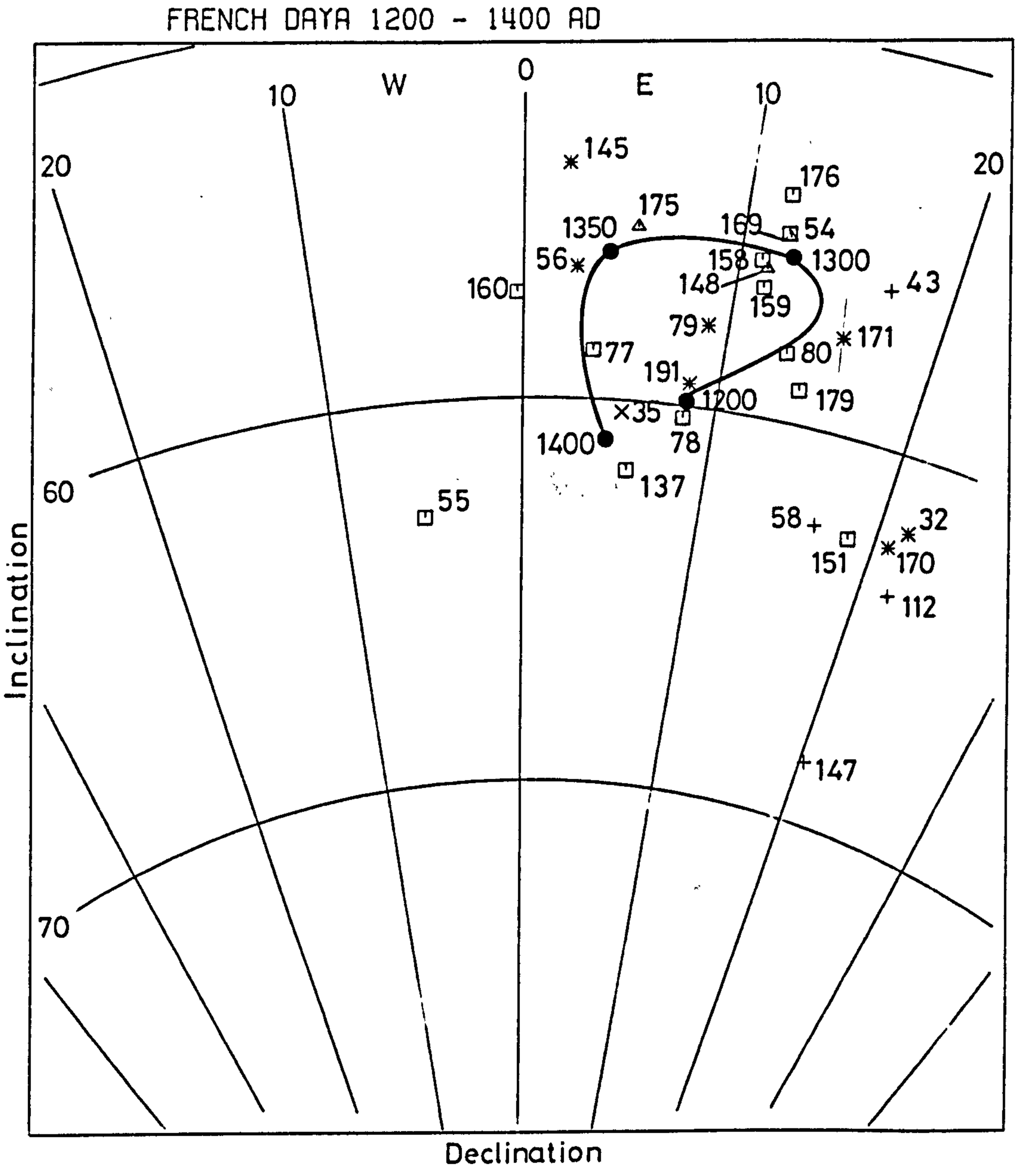
FRENCH DAYA 1200 - 1400 AD
W
E
0
10
10
20
20
60
70
Inclination
Declination
1350
1300
1200
1400
56
160
175
169
54
158
148
159
43
79
171
77
80
191
179
×35
78
137
55
58
151
32
170
112
147
145
176

Fig. 4.25

However, Sites 77 and 137 are the only sites with ages near 1400 AD and they are not very well grouped but, according to these directions, the curve is expected to have steeper inclination around 1400 AD. The directions after 1200 AD until 1350 AD seem to be well defined but there are still some sites with the same age range well away from the curve like Sites 55 (1200-1300 AD), 170 (1225 AD), 179 (1300 AD) and 145 (1370 AD, wt = 5).

1400 - 1600 AD

A total of fifteen sites are available within this range (Figure 4.26). The position at 1400 AD was still only indicated by the direction of Site 137 (discussed within 1200-1400 AD range). According to the available sites it is more reliable to locate the 1550 AD rather than the 1500 AD because the sites covering the 1500 AD age are scattered (39 and 159) and if the 1500 AD is assumed to be near Site 159, then this will make Sites 162, 51 and 121 at a location which is earlier than 1500 AD. Accordingly, the direction at 1550 AD was located using the directions of Sites 162, 51 and 121. This will make the direction at 1500 AD (between 1400 and 1550 AD) very near to the 1400 AD and it will also leave some other reliable sites away from the curve (39, 34 and 160). Using the available sites the inclinations are expected to steepen after 1550 and towards the poorly defined 1600 AD pointer.

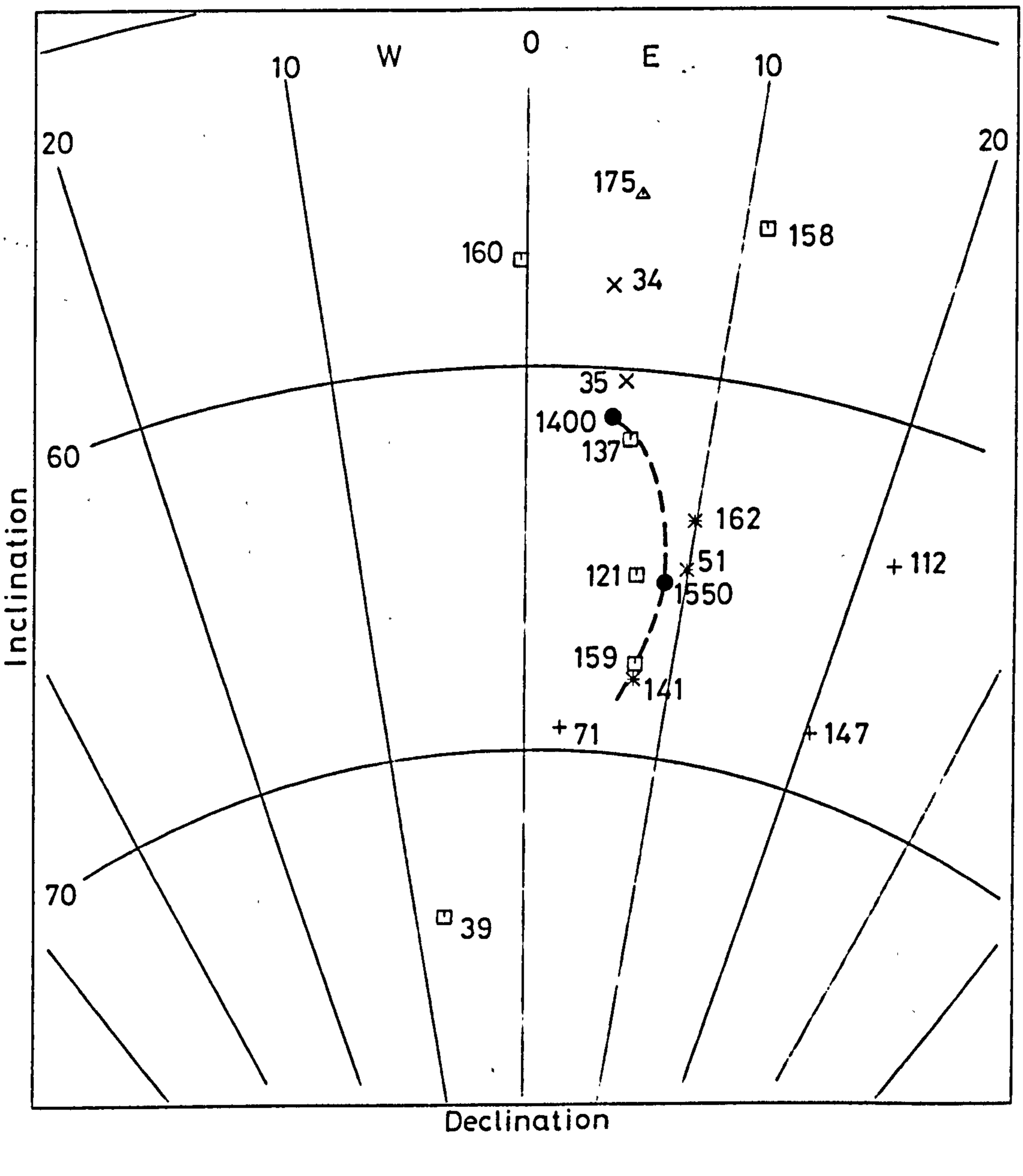
FRENCH DATA 1400 - 1600 AD
W
0
E
10
10
20
20
175
160
158
34
35
1400
137
162
121
51
1550
112
159
141
71
147
60
70
39
Inclination
Declination

Fig. 4·26

1600 - Present

Ten sites were given with their ages ranging between 1600 and 1830 AD (Figure 4.27). Five of these sites had good weights. The directions obtained using these sites were compared with the available Paris observatory records obtained after 1600 AD. The data showed shallow inclinations of about 0.5^{o}-1.5^{o} and also a shift in declination mainly around 1700 AD (about 7^{o}).

This difference in inclination could be due to measurement error, but because the overall curve is smoothly displaced from its actual position it could possibly indicate that some of these directions needed tilting corrections (Aitken and Hawley 1971). This will depend mainly on the nature of individual sites and whether they show any tilting evidence.

Summary

The revised curve has been re-drawn after giving each site a specific weight and hence the sites were not treated equally. The overall shape of the curve was similar to that given by Thellier, but the two curves differ at some periods due to age uncertainties or lack of data. In such periods plotting the curve is highly dependent on the interpreter's judgement and this might affect some parts of the curve by $\pm$ 100 years.

The difference and comments on the two curves can be summarized as follows:

(1) The Thellier curve (1981) shows a declination change at 70 AD of about 5^{o} towards the west. This westerly change appears to be less and smoother in the revised curve.

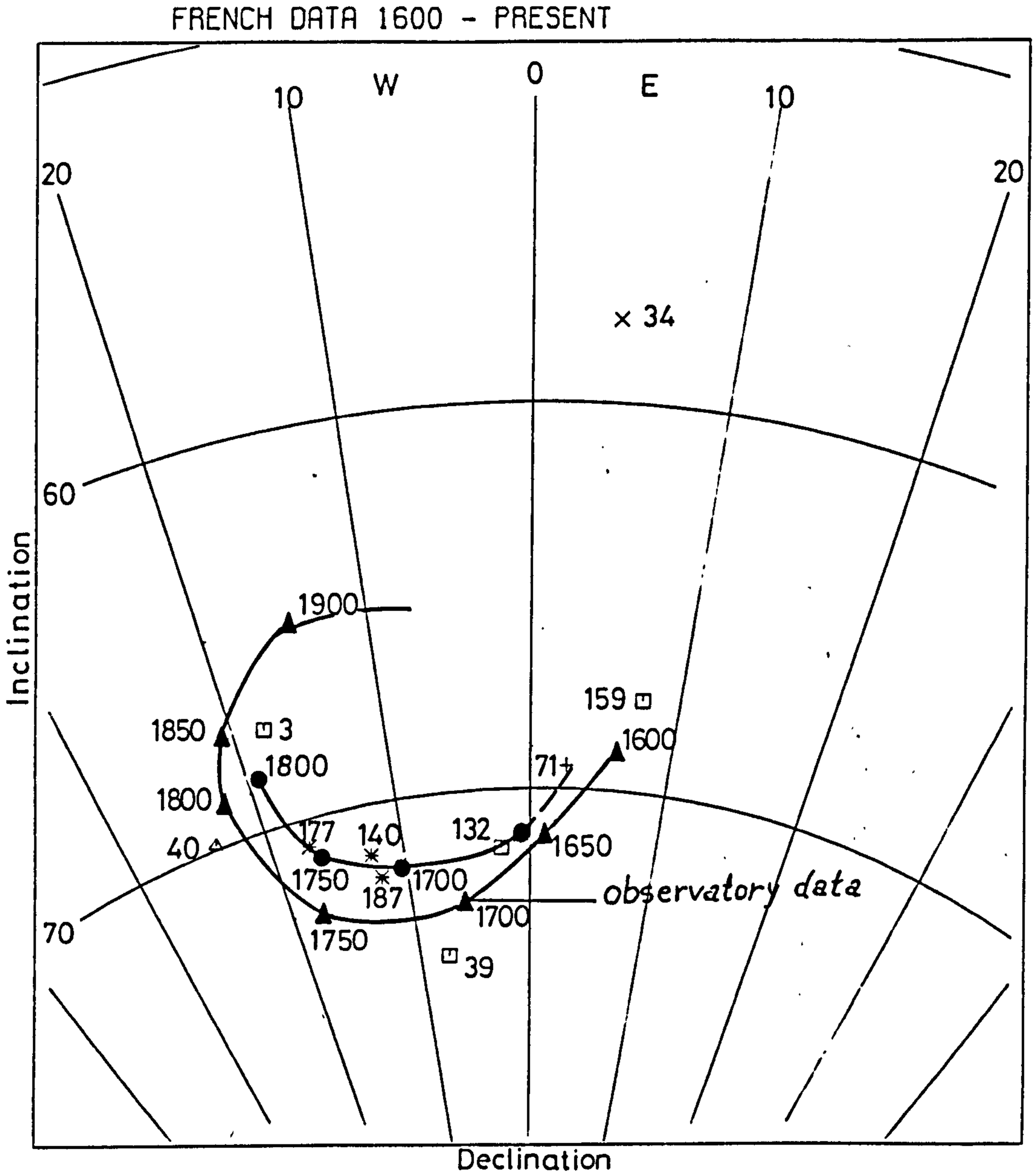
FRENCH DATA 1600 - PRESENT
W
E
0
10
10
20
20
60
70
× 34
Inclination
Declination
1900
1850
3
1800
1800
40
177
140
132
1750
187
1700
1750
1700
1650
1600
159
71
39
observatory data

Fig. 4·27

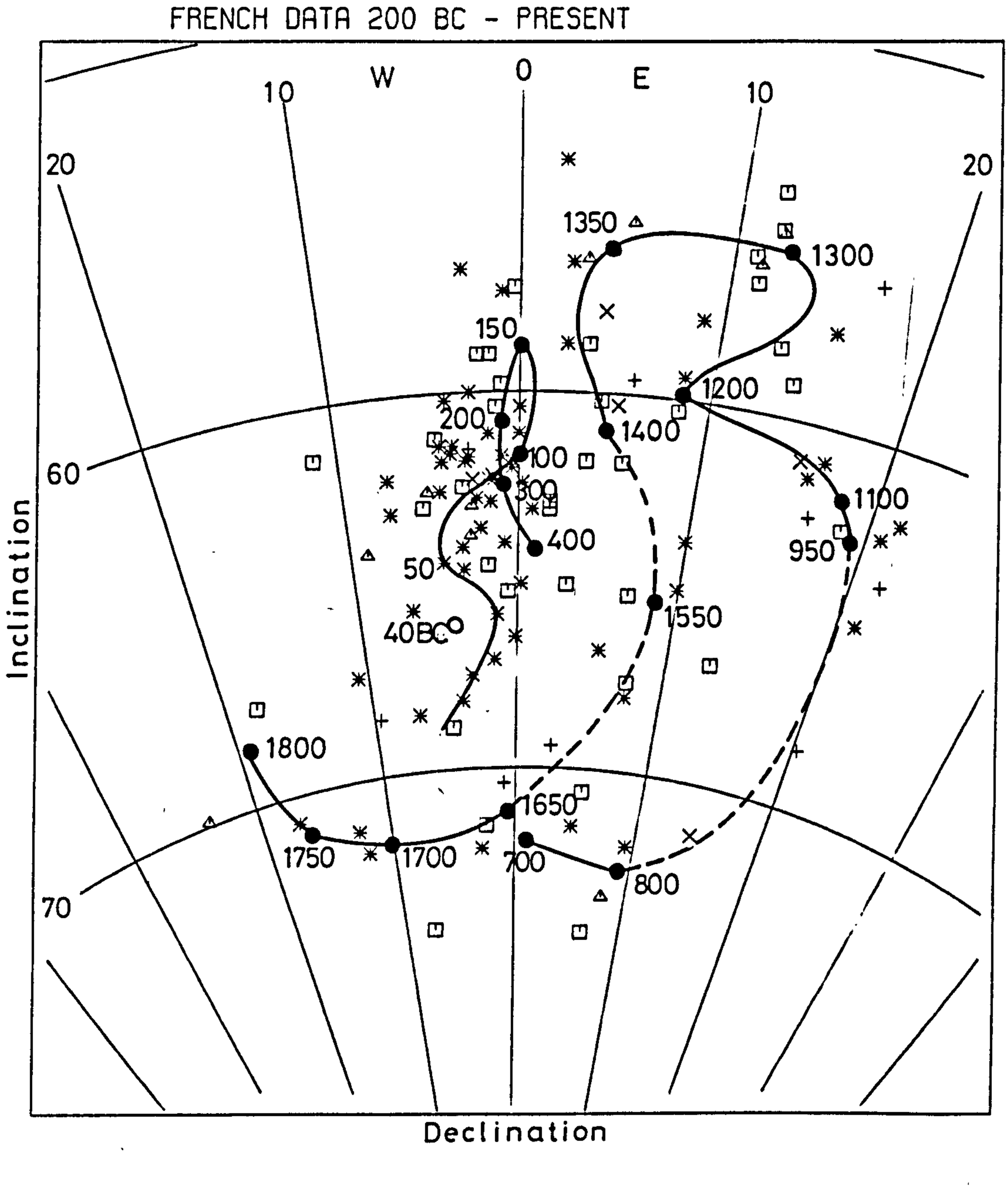

Fig. 4·28

Revised French Archaeomagnetic Curve

(2) Shallower inclination values were obtained at 200 AD in the Thellier curve, while in the revised curve shallower inclinations were obtained at 150 AD and the 200 AD showed steeper inclination.

(3) The directions between 400 and 700 AD are poorly defined and cannot be traced and hence they were left for further dating.

(4) The directions between 800 and 1000 AD were also found to be poorly defined and according to the available sites the directions at 950 AD differ from the directions at 1100 AD by only about 3^{o}. This indicates that this part of the curve is not well defined and accordingly the period between 800 and 950 AD was also left as a gap.

(5) The declination at 1200 AD in Thellier curve reaches a value of about 14^{o}, while the revised curve shows a declination value of only about 9^{o} at 1200 AD, and then the direction tends to move towards the east until 1300 AD, where the two curves are again similar.

(6) The 1400 AD period in the revised curve was found to be steeper than the original position of 1400 AD, and it was also possible to locate the 1550 AD part of the curve (dotted originally) but that made the 1500 AD point (expected between 1400 and 1550 AD) very near to the

1400 AD point. On the other hand, the 1550 AD point was then found to be away from the 1600 AD point (available from recorded observations) implying a change within 50 years greater than would be expected.

4.4 Conclusions

The revised archaeomagnetic curves for both Britain and Paris show similar ranges of declinations and inclinations. Magnetic directions for the Roman period in both curves show sharp inclination changes with only a few degrees change in declination. Both show shallowing inclinations after 50 AD but with a significant westward declination change around 70 AD in the Paris curve. The inclination values steepen to their maximum values at different dates (250 AD in the British curve and 150 AD in the Paris curve). The two curves continue to have steeper inclination towards 400 AD with the French curve showing much slower rate changes afterwards.

The British curve for the period 850-950 AD shows an eastward change in declination with almost no changes in inclinations, while the French curve is not very well defined during this period but, according to the available data, the 950 AD inclination shallows and increases between 700-800 AD and then a decrease in inclination after 800 AD and towards 950 AD.

The most dramatic differences between the two curves are observed during the period 1200-1400 AD. The French curve shows a

westward change in declination around 1200 AD, followed by an eastward change after 1200 AD and until 1300 AD, after which the declination changes westerly with almost no changes in inclination until 1350 AD, then the inclination steepens towards 1400 AD with almost no change in declination. The British curve shows a different path, as the declination changes towards the west after 1200 AD with the inclination getting slightly steeper until 1350 AD, after which the declination changes towards the east with slight changes in inclination. At 1400 AD, the inclination starts to steepen with nearly no change in declination. As the British curve is better substantiated, this 1200-1400 AD discrepancy may disappear if further French data become available.

The British and French observatory data were compared with each other and they were found similar, within a few degrees difference which is attributable to their different locations. A comparison of the archaeomagnetic data with the recorded observatory data showed a deviation of about $\pm 3^{o}$. This value is comparable with the range of declination values over the Roman period and hence the present discrepancies are within the present limits of the technique.

The archaeomagnetic curves of Britain and France both have many sites with directions away from the curve, yet most of these directions were magnetically stable and apparently well dated. One of the main reasons for this deviation may be that many of the samples were collected from rescue archaeological sites that are not as well dated as sometimes reported. Such a scatter in magnetic directions could also occur as a

result of errors in measurements during sampling, particularly when using magnetic compasses which may sometimes be affected by the structure itself. The sampled structure may also have tilted either uniformly or irregularly. Comparison between recorded observations and archaeomagnetic data could indicate that a correction for some of the sites is needed, although such a correction would be of only a few degrees.

The magnetic stability was also found different for different archaeological structures; as an example, kilns and furnaces were found to be generally more stable than walls and hearths. Sediments were found to have the lowest magnetic stability.

Archaeomagnetic curves will always be subject to modifications and alterations with the accumulation of new data. Hence, for optimum archaeomagnetic master curves, intensive sampling is still required to increase the reliability of the available curves, particularly in the missing age ranges. Such observations must be of well dated archaeological samples from stable structures like kilns and furnaces.

CHAPTER FIVE

ARCHAEOMAGNETIC WORK IN IRAQ

5.1 Introduction

The chronology of the principal rulers and dynasty of Mesopotamia were all recorded corresponding with the findings of most historians and with the king lists compiled by Sumerian and Babylonian scribes about 2000 BC, which were found at Nippur, Larsa and other ancient cities. These agree with other recent translations with the Assyrian king lists discovered at Khorsabad, and with other texts inscribed on clay tablets with the names and deeds of the kings. The lengths of the reigns have been based by historians and archaeologists on estimates using such criteria as the occurrence of the kings' names in neighbouring countries and on wars and other events which are recorded on clay tablets. However, calculations based on such a basis are often misleading and show differences, gaps, and errors. Nevertheless, the durations of reigns after the middle of the second Millennium B.C. are generally considered to be fairly accurate, although reigns from 1500 B.C. to 900 B.C. are still only approximate, being liable to be raised or lowered by some 65 years (Basmachi, 1976).

Chronological checks on these ancient records have also been obtained using eclipses which are frequently mentioned in ancient records, usually as bad omens. Their occurrence can be calculated and correlated with known eclipses. The brighter comets also attracted considerable attention and so were likely to be mentioned in ancient records, and their occurrences can also be dated (Bray and Tramp, 1970).

Archaeological dating in Iraq mainly depends on the

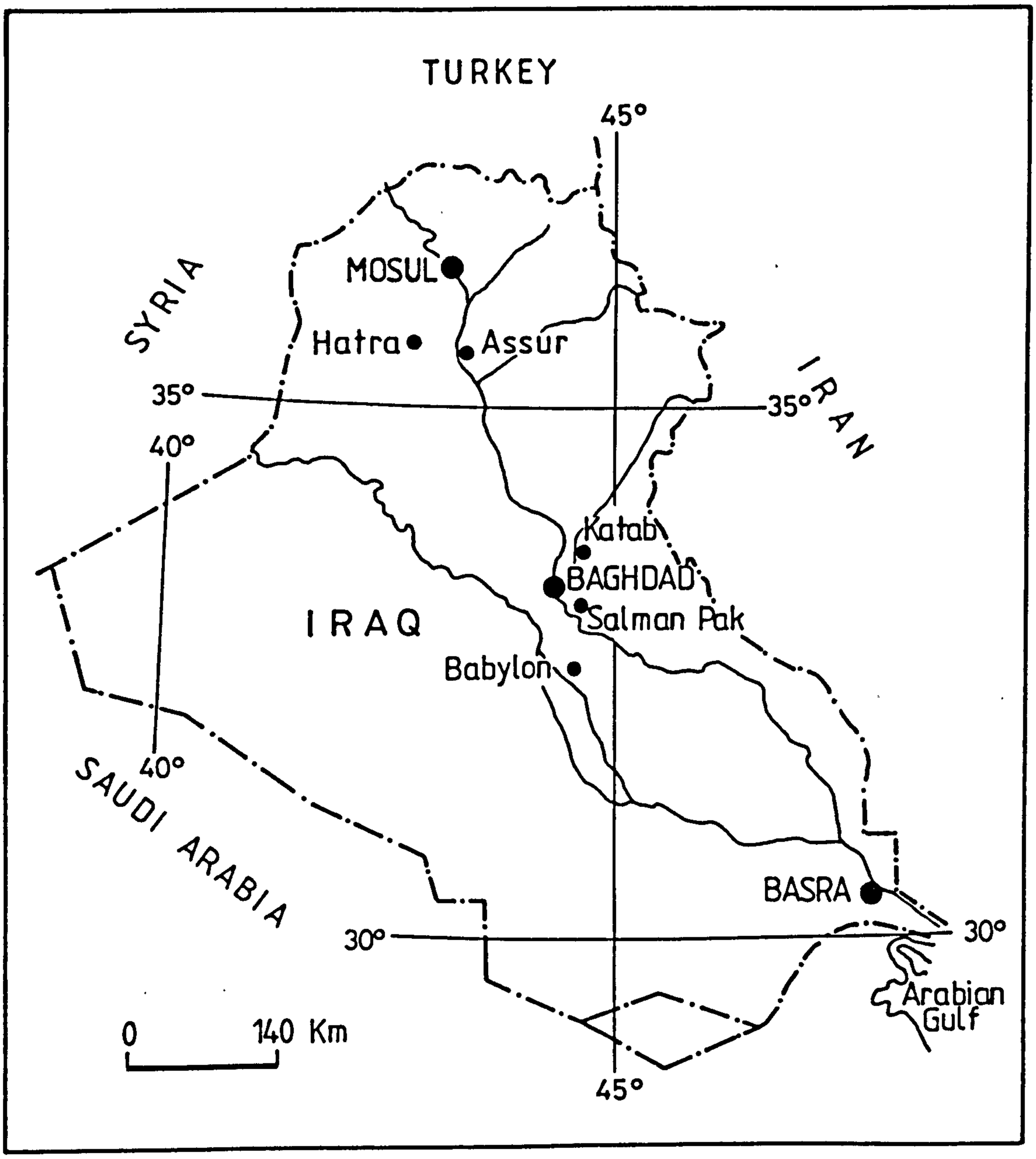

Fig. 5.1 Locality map of the studied Iraq sites

historical records. Radiocarbon dating has only recently been used in a few sites. Most of the Iraqi samples described here were dated by the local archaeologists, based on their archaeological context, i.e. on historical records.

5.2 Sampling Locations

Iraq is a country with well over 1,000 archaeological sites. Many of these sites are still awaiting excavation, although work is going on by both Iraqi and foreign expeditions. Despite this, no archaeomagnetic work has been done and so this draft is the first attempt to construct an archaeomagnetic curve for Iraq. Five well-known archaeological locations were visited and samples were collected from kilns, furnaces and hearths. A total of 96 samples were collected from 19 sites, with 4 - 6 samples taken from each site (the limitation on the number of samples was due to archaeologists wishing to keep all sites intact). All samples were collected using the usual archaeomagnetic method of sampling (Chapter 1). The five archaeological localities were:- Assur, Babylon, Hatra, Katab and Salman Pak (fig. 5.1). The initial, most stable directions, stability indices and the mean values of each site are all given in table 5.1. Examples of changes during AC-demagnetization of both intensity and directions are given in fig. 5.2 and the NRM and most stable direction of all samples are presented in fig. 5.3.

5.3 Assur:-

The locality is in the northern part of Iraq, about 100 km. south of Mosul, at Lat. 35.5E, Long. 43.2N. Assur was the city of the Assyrian dynasty and was founded after the downfall of the third dynasty of Ur.

Samples were collected from four sites. The first group were from remains of a rectangular fireplace of about 1m. length and 30 cm. wide (226 B.C.-226.A.D.). The second group were from two rounded kilns near each other and of the same age (226 B.C. - 226 A.D.); these kilns had diameters between 40-60 cm. The other samples were from a burnt wall (700-614 B.C.). The last group were from a kiln about 60cm. diameter (700-614 B.C.). These sites were named respectively as A_1, A_2, A_3 and A_4.

5.4 Babylon:-

This locality is about 60 km. south of Baghdad (Lat. 32.5E, Long. 44.5N). It was built by the king Hammurabi, who succeded in building the old Babylonian empire. During that time the ancient civilization of Iraq reached its peak.

Five sites were sampled in Babylon. The first was a rounded kiln about 50 cm. diameter (604-539 B.C.), the second was from the remains of a small hearth (669-604 B.C.), the third site was a pottery kiln (141-247 B.C.) and the last two sites were rounded kilns about 50 cm. diameter (539-450 B.C., 323-270 B.C.). These sites have been named as B_1, B_2, B_3, B_4 and B_5 respectively.

5.5 Hatra:-

This is located in the northern part of Iraq (Lat. 35.6E, Long. 42.7N) about 120 km. south-west of Mosul and is well known as the "City of the Sun". Only one kiln was sampled in this locality and this had a rounded shape of about 60 cm diameter (50 B.C.-241 A.D.).

5.6 Katab:-

This locality (Lat. 33.6E, Long. 44.6N) is about 35 km. north-east of Baghdad. Excavation started in this site a few years ago, and it contains furnaces from the Esin Larsa period (2000-3000 B.C.)

and also from the Babylonian period (1800-2000 B.C.).

Five sites were sampled. The first site was a square furnace about 1m length (2300-2000 B.C.), the second was a rounded furnace about 60 cm. diameter (2000-1800 B.C.), the third was a furnace outlet (1800-1500 B.C.), the fourth was a rounded kiln about 40 cm. diameter (2000-1800 B.C.) and the last was from the remains of a square furnace (2300-2000 B.C.). These sites were named as K_1, K_2, K_3, K_4 and K_5 respectively.

5.7 Salman Pak:-

This locality (Lat. 33.1E, Long. 44.6N) is about 57 km. south-east of Baghdad. Four sites were sampled (all 800-900 A.D., except S_3 which is 622 A.D.). The first site was a rounded pottery kiln. about 60 cm. diameter, the second site was a kiln with irregular shape, and the last two sites were square pottery furnaces with sides about 1m. length. These sites were named as S_1, S_2, S_3 and S_4 , respectively.

5.8 Archaeomagnetic Results

The NRM of all samples was measured and the directions at each site were mutually consistent except four sites (B_1, K_1, K_5 and S_3), in which the NRM directions were somewhat scattered. The intensity of NRM ranged between 3 and 1683 mAm^{-1} for Assur samples, 2-1598 mAm^{-1} for Babylon samples, 5-64 mAm^{-1} for Hatra samples, 0.6-833 mAm^{-1} for Katab samples and 1-995 mAm^{-1} for Salman Pak samples.

Most of the samples showed similar behaviour during AC-demagnetization which was carried out up to a peak field of 40mT. Most of the samples were very stable during demagnetization having stability indices greater than 10. Only three samples had stability indices less than 3 and even these were considered to be fairly stable. The components remaining after AC-demagnetization were well-grouped in all samples and

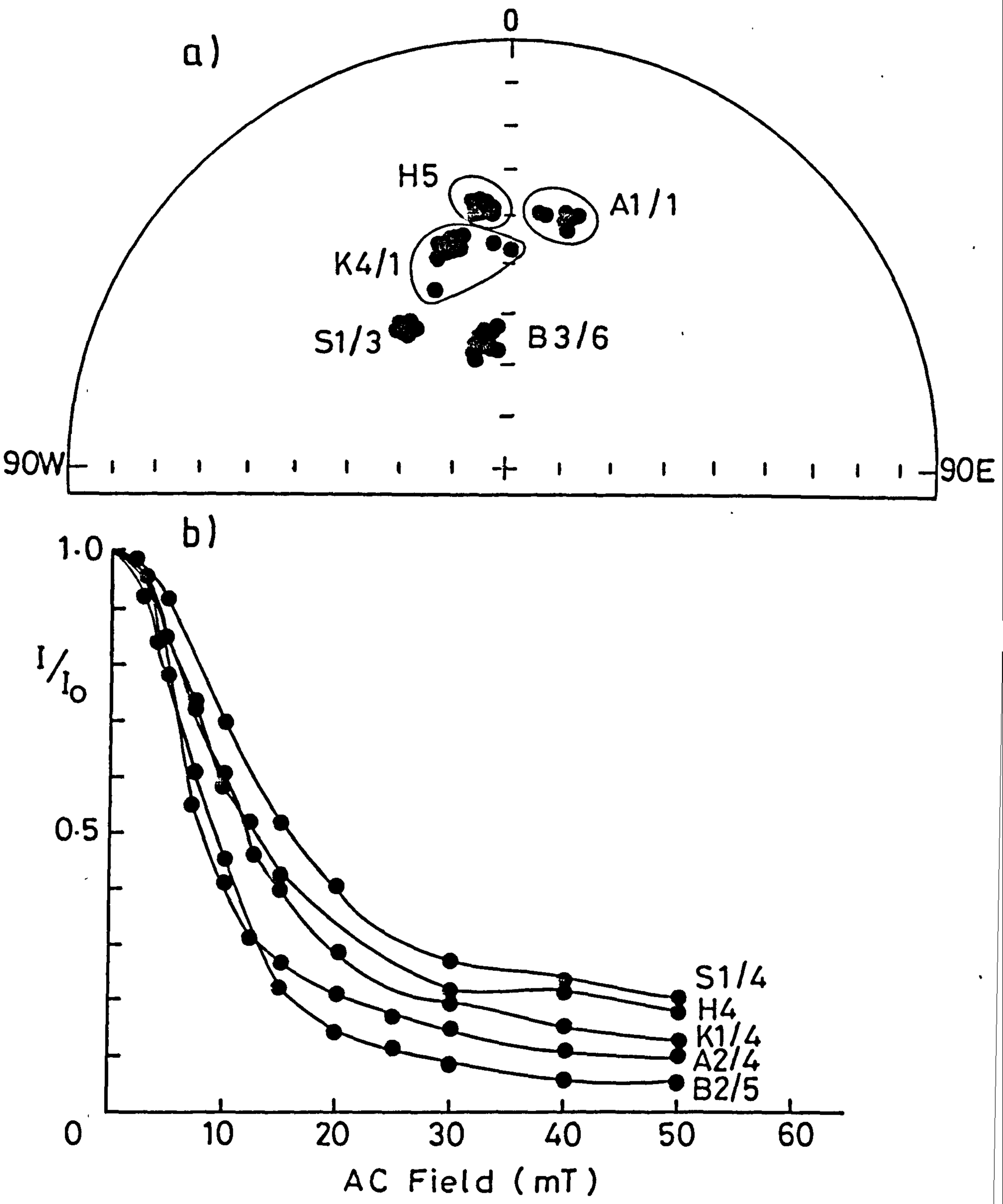

Fig. 5.2 Examples of changes during AC demagnetization of the Iraqi samples

a) Directions
b) Intensity

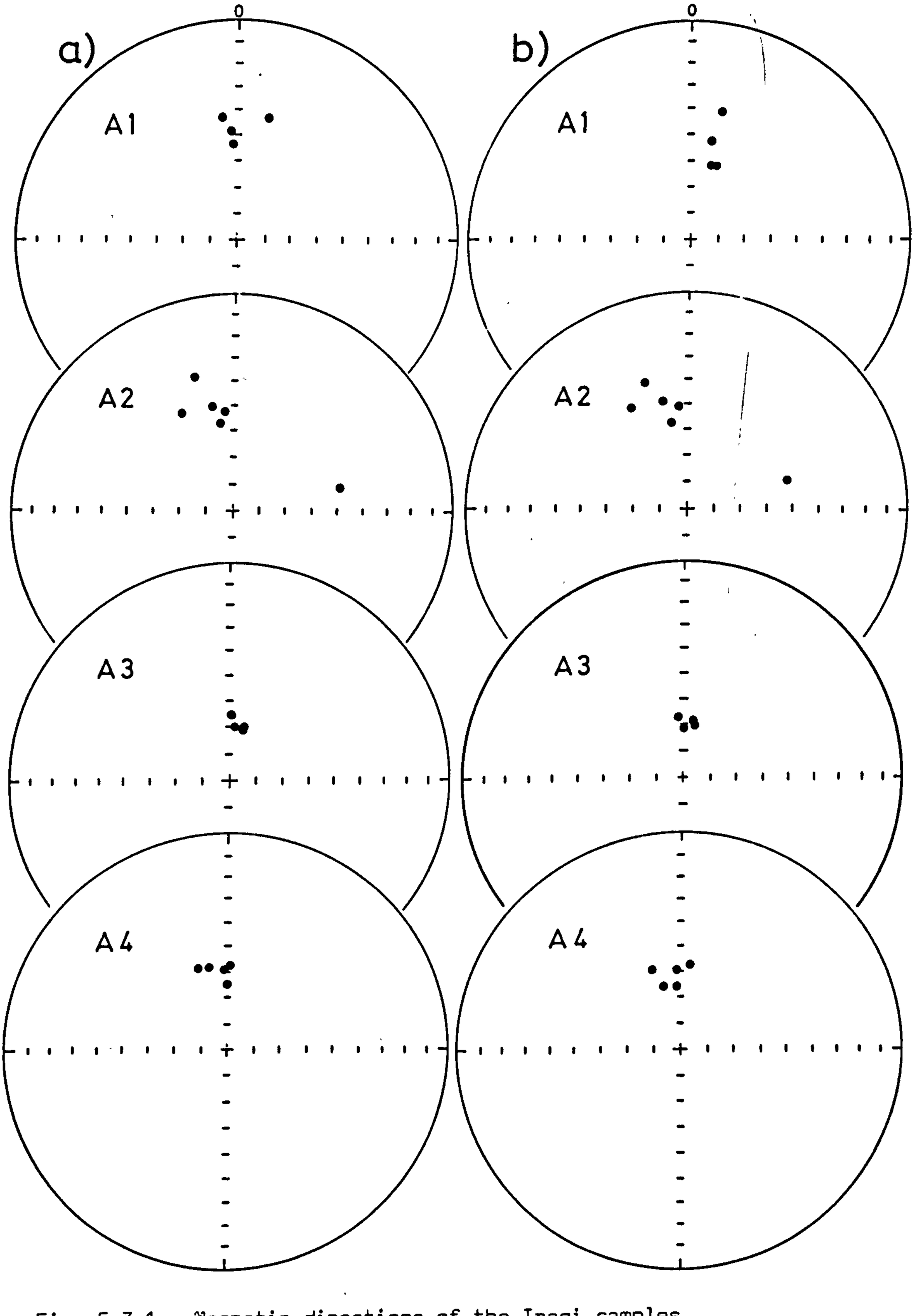

Fig. 5.3.1 Magnetic directions of the Iraqi samples
a) NRM b) Most stable
Assur

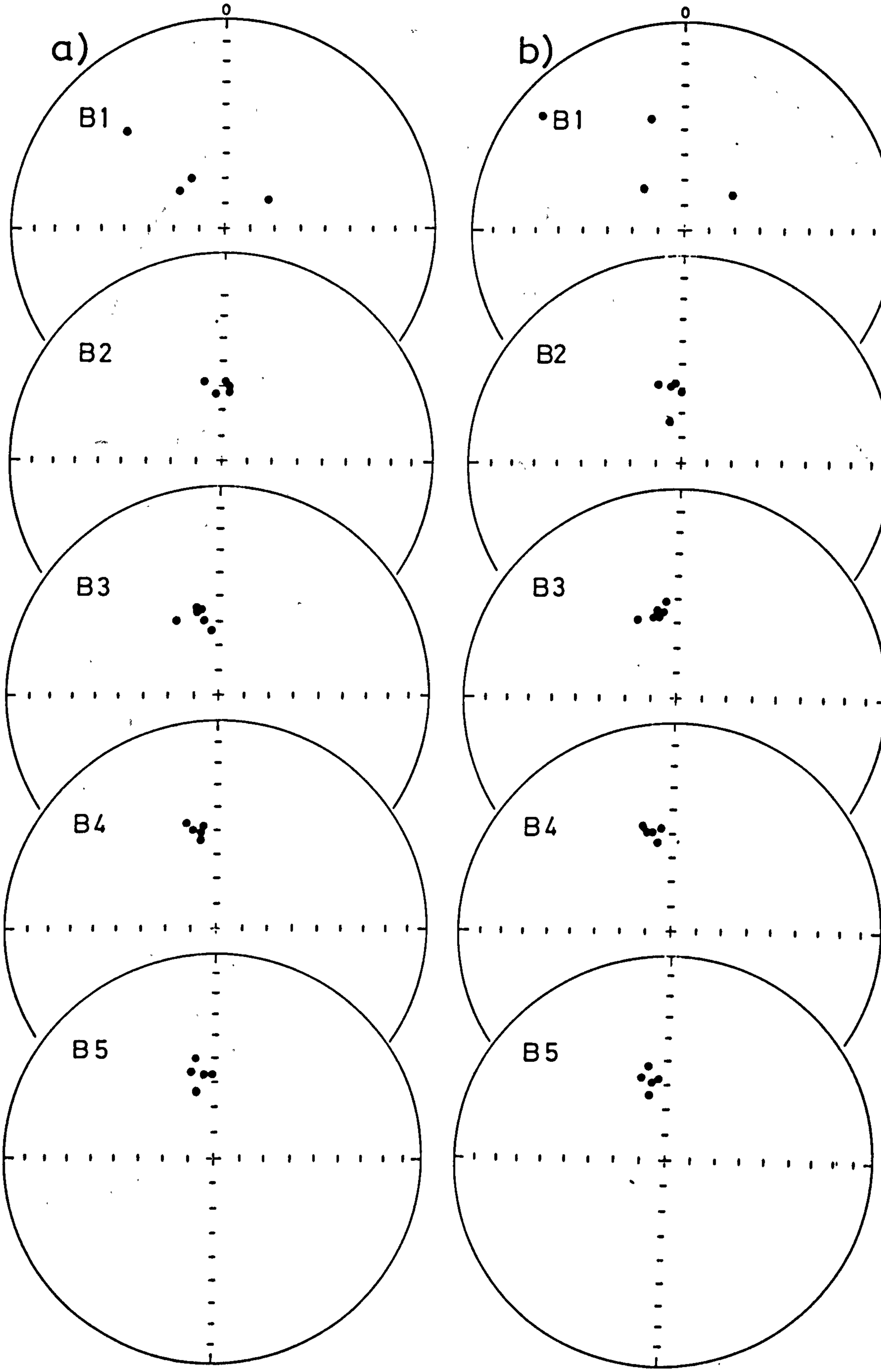

Fig. 5.3.2 Babylon

a) NRM
b) Most stable

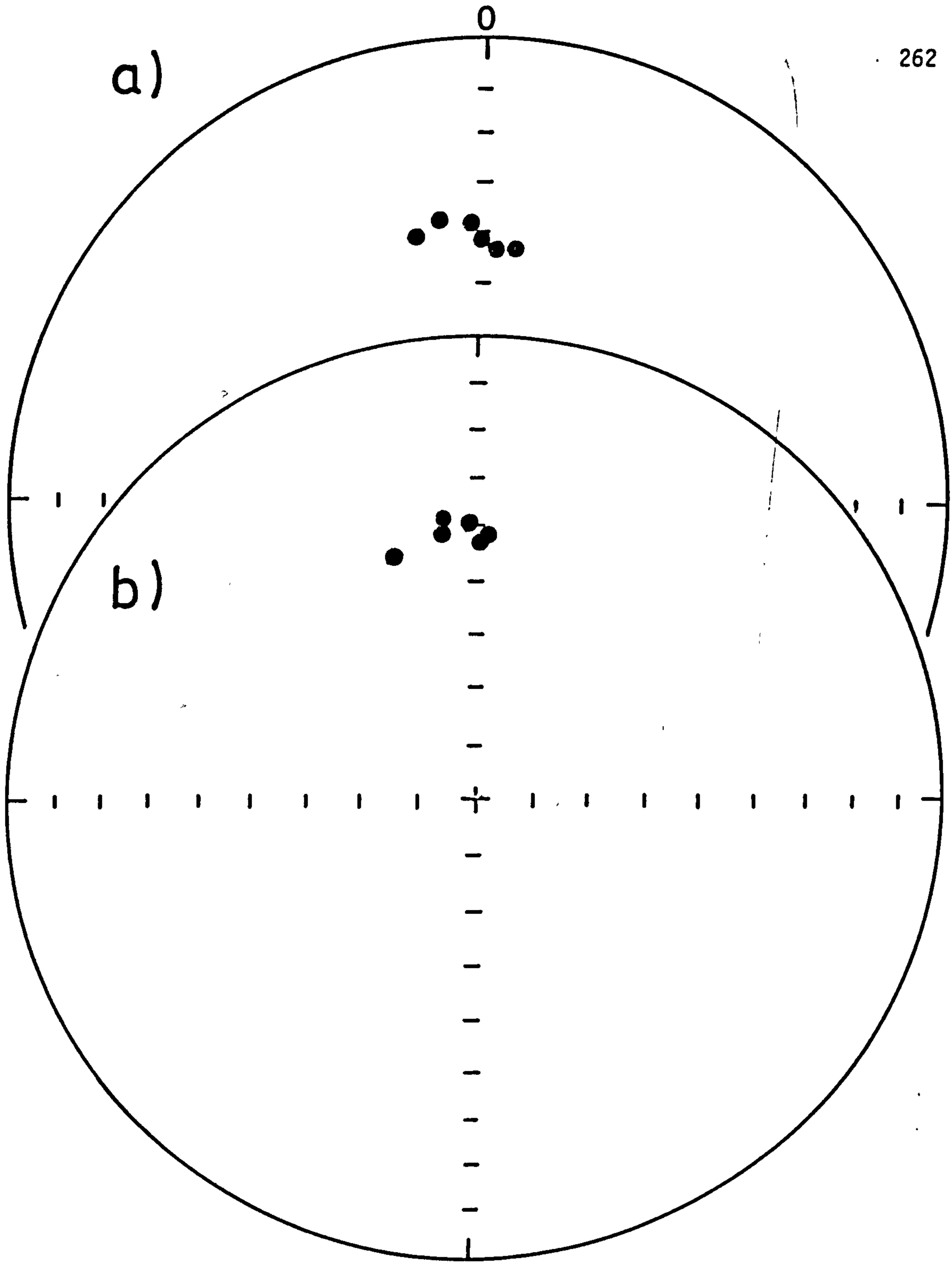

Fig.5.3.3 Magnetic directions of Hatra archaeological site samples
a) NRM
b) Most stable

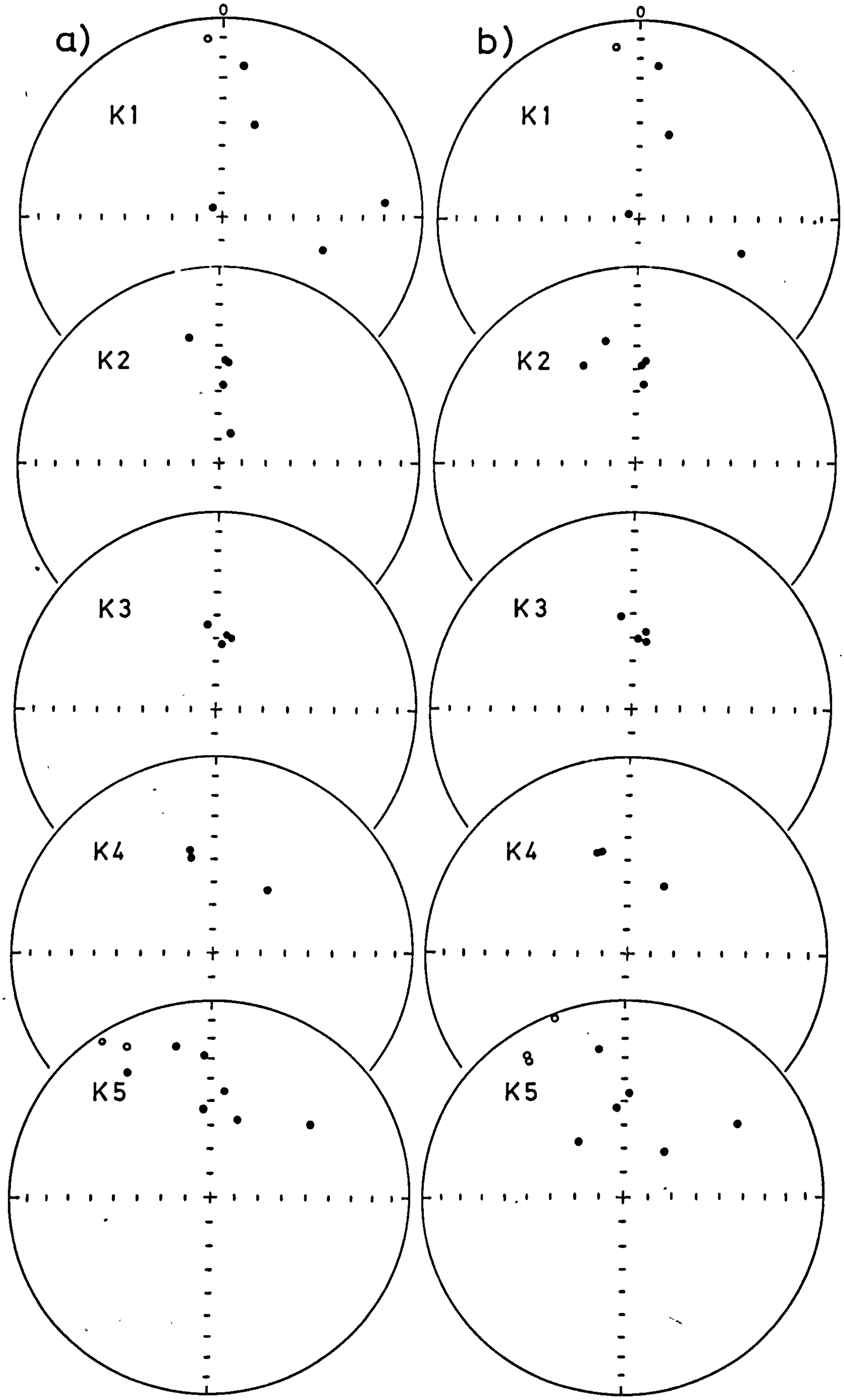

Fig. 5.3.4 Katab

a) NRM
b) Most stable

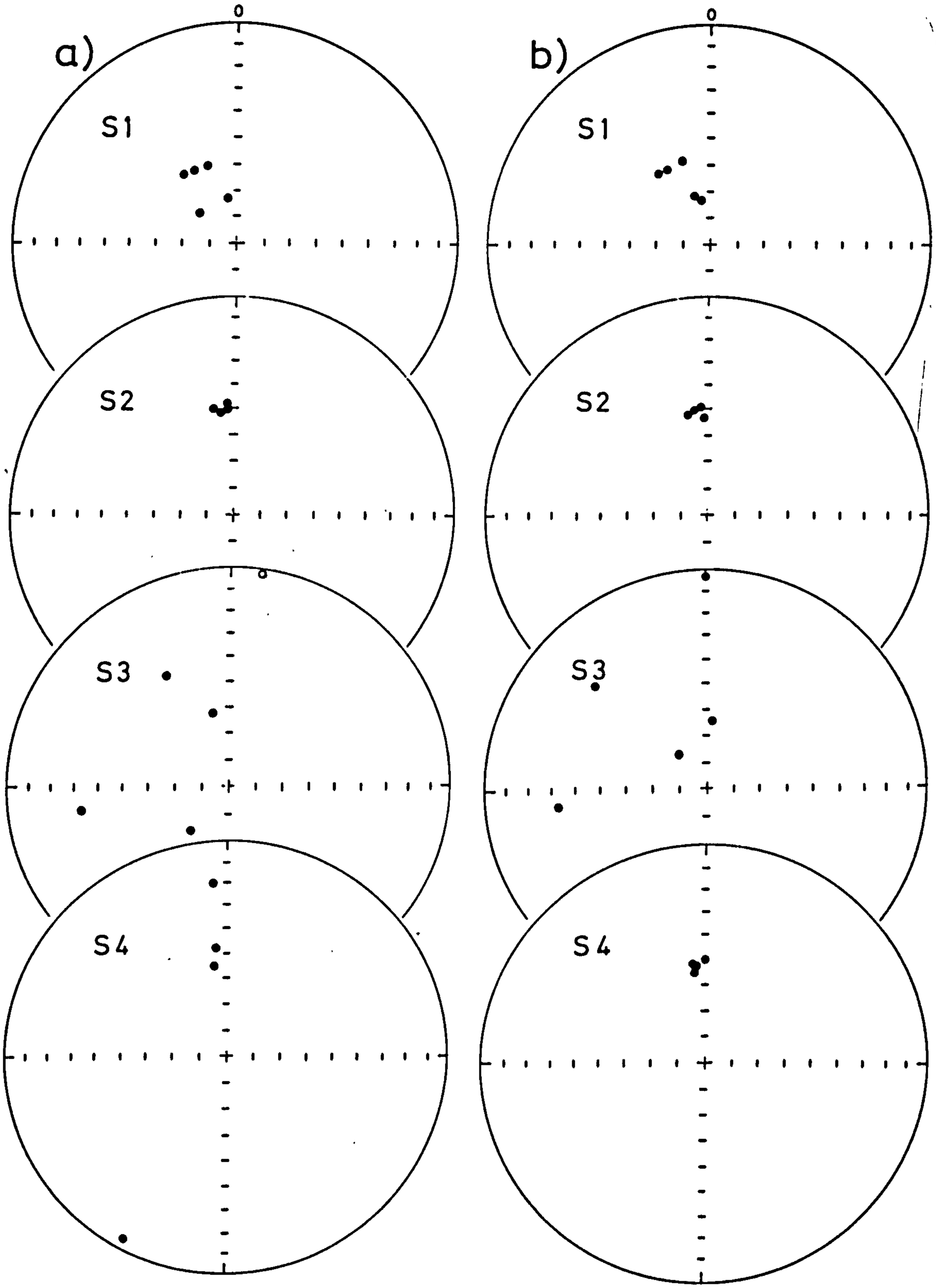

Fig. 5.3.5 Salman Pak

a) NRM
b) Most stable

the removed components showed similar grouping as the remaining components, indicating the existence of only one component of magnetization.

Four sites had scattered directions (B_1, K_1, K_5 and S_3). These scattered directions are not due to:-

1. Instability : all samples were stable during demagnetization.
2. Orientation:- directions in the field were taken using a sun compass.
3. Magnetic refraction:- no systematic scatter in directions was observed in all four sites.

Hence the reasons for the scattered directions could be due to:-

1. The effect of sediments loading and compaction, causing dislocation within the structure. Site S_3, K_1 and K_5 were filled with piles of sediment, but the actual structure itself appeared unaffected.
2. Inhomogeneity in the heat distribution, i.e. some parts may not have been completely fired above 700°C. This is only possible for site B_1 because samples from the other sites were from inside the furnace, while site B_1 was a small kiln. Also, no evidence for more than one component of remanence (other than VRM) was shown during demagnetization.
3. Brick movement during excavation by the archaeologists. This was not suspected at the time of collection, but, particularly when dealing with bricks, it is very easy for one to have been removed and then replaced, but possibly inverted (this is possible for sites S_3, K_1 and K_5).
4. Local disturbance in the earth's magnetic field, as a result of iron lumps near the structure. Hence the magnetic field which the structure acquires will not correspond to the earth's magnetic field at the time of cooling.

5.9 Archaeomagnetic Curve of Iraq

The mean values of the most stable directions of samples from each site were calculated and then plotted to form the preliminary archaeomagnetic curve for Iraq. The middle of the age ranges given by the archaeologists was used to represent the age of each site (fig. 5.4, table 5.2).

The mean directions for the oldest available sites K_1 and K_5 (2300-2000 B.C.) had a very high α_{95} value with the declination of site K_1 not consistent with the overall declination values. Accordingly, the direction of site K_5 was plotted, but has not been joined with the curve because of its high α_{95} value. The direction at 1900 B.C. was obtained using sites K_2 and K_4, and is considered to be the oldest reliable point on the curve. It shows somewhat similar inclination to the present earth's magnetic field of the central part of Iraq, but with the declinations shifted towards the west. Moving to the second point, 1650 B.C. (K_3), the inclination starts to steepen and the declination moves easterly. The directions at 660 B.C. are defined by sites A_3 and A_4, with site A_3 10^{o} east of site A_4 and about 10^{o} steeper. These differences in directions could be due to age differences between the two sites. Logically, site A_4 could probably correspond to directions of an earlier age as it was more consistent with the directions at 630 B.C. However, at this stage the directions at 660 B.C. should be taken in between the two sites until further studies. The inclination after 660 B.C. starts to shallow as shown by the directions at 630 B.C. (site B_2) and also site B_1 (604-539 B.C.) which had high α_{95} value, but directions agreeing with the other two sites (B_2 and A_3). The inclination values shallow after 630 B.C. until 500 B.C. (B_4) after which

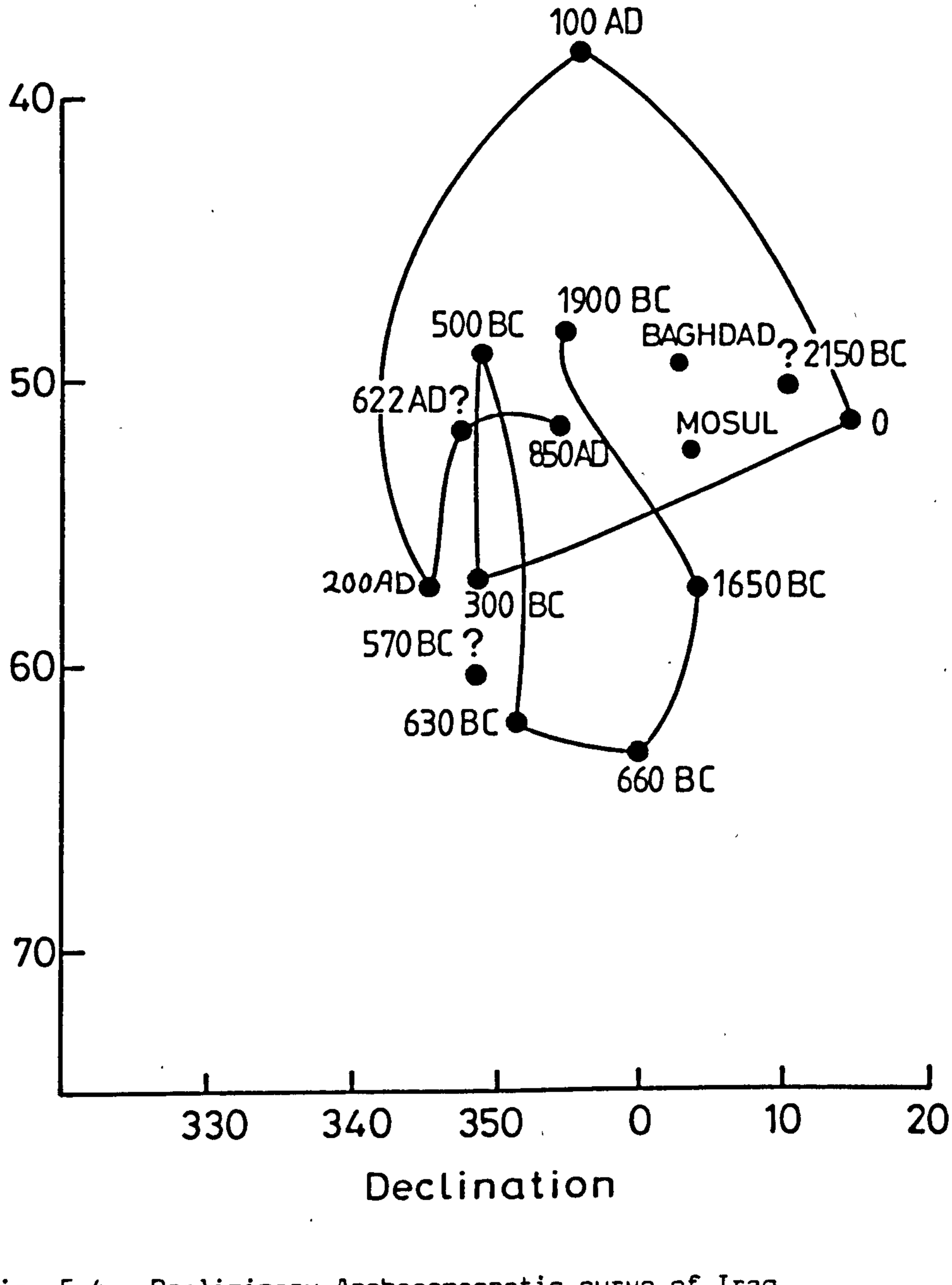

Fig. 5.4 Preliminary Archaeomagnetic curve of Iraq (1900 BC - 850 AD) (corrected to Baghdad)

it steepens with virtually no change in declination until 300 B.C. (B_5). 0 A.D. is defined by two sites (A_1 and A_2) with their ages between 226 B.C.-226 A.D. The direction of these sites are away from each other with about 30^o difference in declination and 5^o in inclination. Since the archaeological dating of these two sites lies within about 450 years, the direction differences probably correspond to differences in ages between the two sites. Accordingly, the direction at 0 A.D. was considered to be near site A_1 on the basis that site A_2 is more likely to be A.D., because its direction agrees with the 100-200 A.D. direction. The period between B.C. - A.D. is accompanied with changes in declination only as it moves easterly until at least 0 A.D. (A_1), after which the declination starts to move westerly with about 15^o change in inclination until 100 A.D. (Hatra site), the inclination then starts to steepen with declinations still moving westerly until 200 A.D. (site B_3) after which the declination moves easterly and the inclination shallows, until 850 A.D. (sites S_1 and S_2) with the poorly defined directions of site S_3 (622 A.D.) near to the 850 A.D. directions.

At the moment the curve stops at 850 A.D., at which the direction is somewhat similar to the 1900 B.C. directions. From the overall curve, it seems that changes during this period of time in declination are between 20E and 20W and the inclinations are between 40^o-65^o. This magnitude of secular variation is essentially comparable to those observed in western and southern Europe, although those are only for the last 2000 years, while some of the new Iraqi curve is mostly B.C.

This curve is clearly only a preliminary curve and the ages are not too well established, often having a possible range between 50 and 450 years. The intervals between the observed points are also large and significant changes in the geomagnetic field could have occurred

Archaological Age	Directions Age Used	Corrected D	I	to Baghdad δ_D	δ_I
ASSUR					
A1. 226 BC - 226 AD	0	14.3	51.5	18.9	11.3
A2. 226 BC - 226 AD	0	344.3	46.1	13.1	8.6
A3 700 BC - 614 BC	660 BC	3.2	67.4	10.5	3.8
A4. 700 BC - 614 BC	660 BC	353.7	59.3	12.3	5.9
BABYLON					
B1. 604 BC - 537 BC	570 BC	348.9	60.4	27.8	25.2
B2 669 BC - 604 BC	630 BC	351.7	62.1	14.6	7.0
B3. 141 BC - 247 AD	200 AD	345.4	57.4	8.9	4.9
B4. 539 BC - 450 BC	500 AD	348.8	49.2	5.2	3.5
B5. 323 BC - 270 BC	300 BC	348.3	57.2	8.3	4.6
HATRA					
50 BC - 241 AD	100 AD	355.6	38.5	6.7	5.0
KATAB					
K1. 2300 BC - 2000 BC	2150 BC	55.7	54.2	69.7	47.3
K2. 2000 BC - 1800 BC	1900 BC	352.9	46.8	17.9	12.1
K3. 1800 BC - 1500 BC	1650 BC	4.0	57.3	13.9	7.5
K4. 2000 BC - 1800 BC	1900 BC	356.3	50.2	40.9	26.0
K5. 2300 BC - 2000 BC	2150 BC	10.6	50.1	25.6	23.5
SALMAN PAK					
S1. 800 BC - 900 AD	850 AD	336.6	63.7	19.0	8.5
S2. 800 BC - 900 AD	850 AD	353.7	51.3	4.8	3.0
S3. 622 AD	622 AD	347.9	51.9	34.3	29.8
S4. 800 BC - 900 AD	850 AD	355.1	52.5	4.7	2.9

Table 5.2 The archaeological ages, directions and the errors in D and I in the mean value of each site.

between successive points.

The value of α_{95} has been converted so that the error in declination δD and incliation δI can be plotted against the age (fig. 5.5). The errors in declination and inclination were found to be the highest around the 1900 BC, for which there is a narrow age range given by the archaeologists, and the directions are more reliably established on the other part of the curve and even for the less well dated material. More samples are needed to fill the gaps in the curve, particularly in the periods between 1800 - 600 BC and between 200 - 800 AD. Also further samples

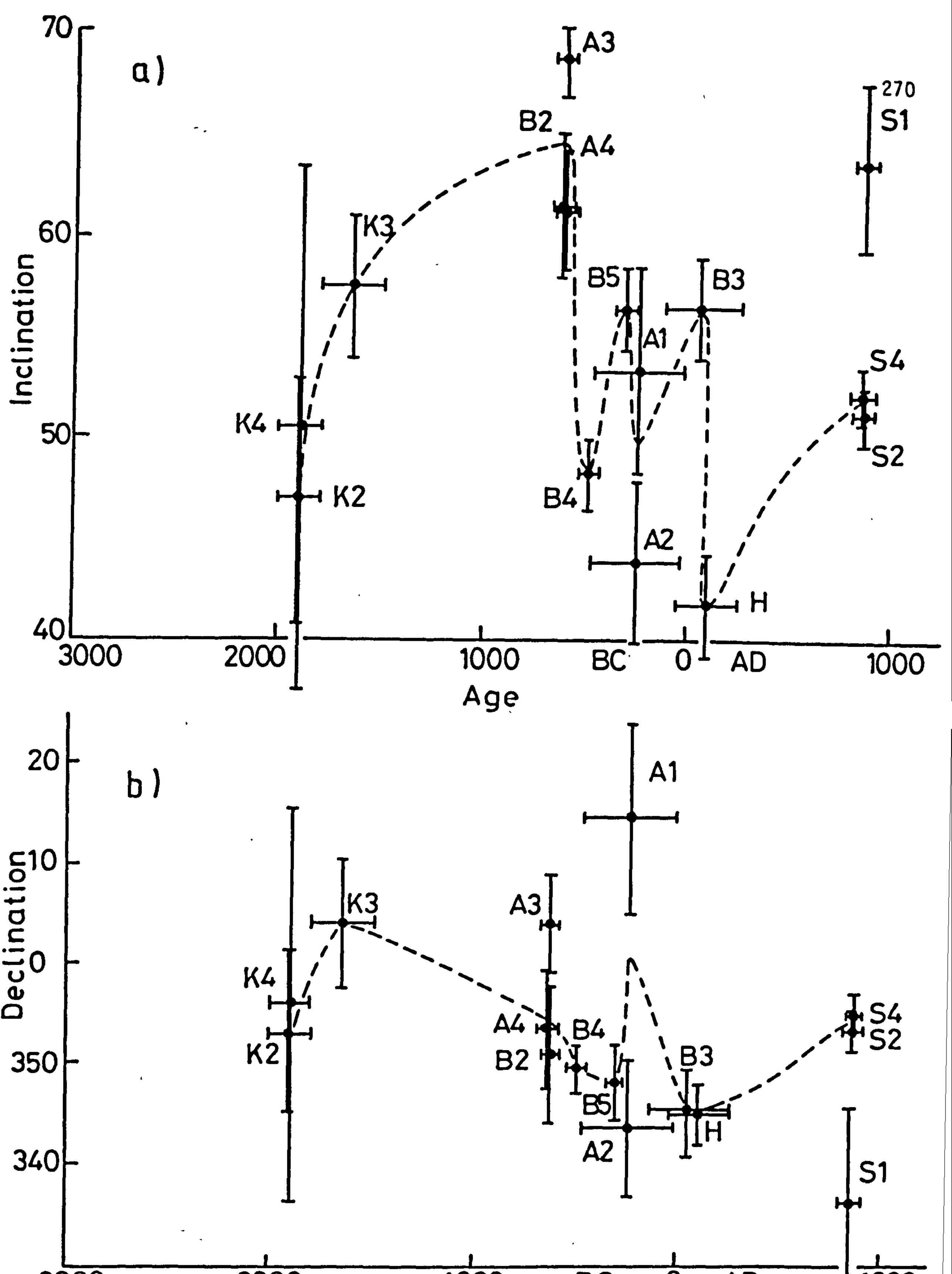

Fig. 5.5 Magnetic secular variation in Iraq (1900 BC - 850 AD)
a) Inclination
b) Declination

are needed to extend the curve to the present time.

In order to get additional information on the magnetic secular variations of Iraq and the surrounding areas, and to check the reliability of the present results, the Iraqi directions were compared with the Ukraine-Moldavia (Rusakov and Zagniy, 1973) and Iranian (Kawen et al., 1972) archaeomagnetic results which are the nearest available archaeomagnetic data to Iraq.

Archaeomagnetic results from Ukraine and Moldavia (Ukraine Lat. 47°N, Long. 30°E) (Rusakov and Zagniy, 1973) had all their inclination values reduced to Kiev (50°5). These values were all corrected back to their original site latitude and were then corrected to Baghdad (Lat. 33.2°N, Long. 44.26°E), using the Meriden program (Appendix 3). Only the directions of the sites which are close to the Iraqi age range were plotted on the Iraqi secular variation curve. In both curves the number of sites showing the magnetic secular variation for about 2000 years are not yet sufficient to define the declination and inclination changes. Accordingly, comparison should be done using the directions of individual sites rather than the shape of the curve, particularly for sections with a limited number of sites. In addition, the Ukraine and Moldavia results had only four sites from B.C. to A.D. and so comparison of the two results for this period of time is difficult (Fig. 5.6).

The inclination for one of the Ukraine sites for age 700 - 800 BC. is shallower than the Iraqi inclination values, while they are similar at 500 B.C. and 300 B.C. as the inclination of sites from the two areas nearly coincides. The Iraqi inclination between 0 A.D. and 900 A.D. shows shallow inclination during the first century and this is followed by steeper inclination at about 900 A.D. The Ukraine and Moldavia data show

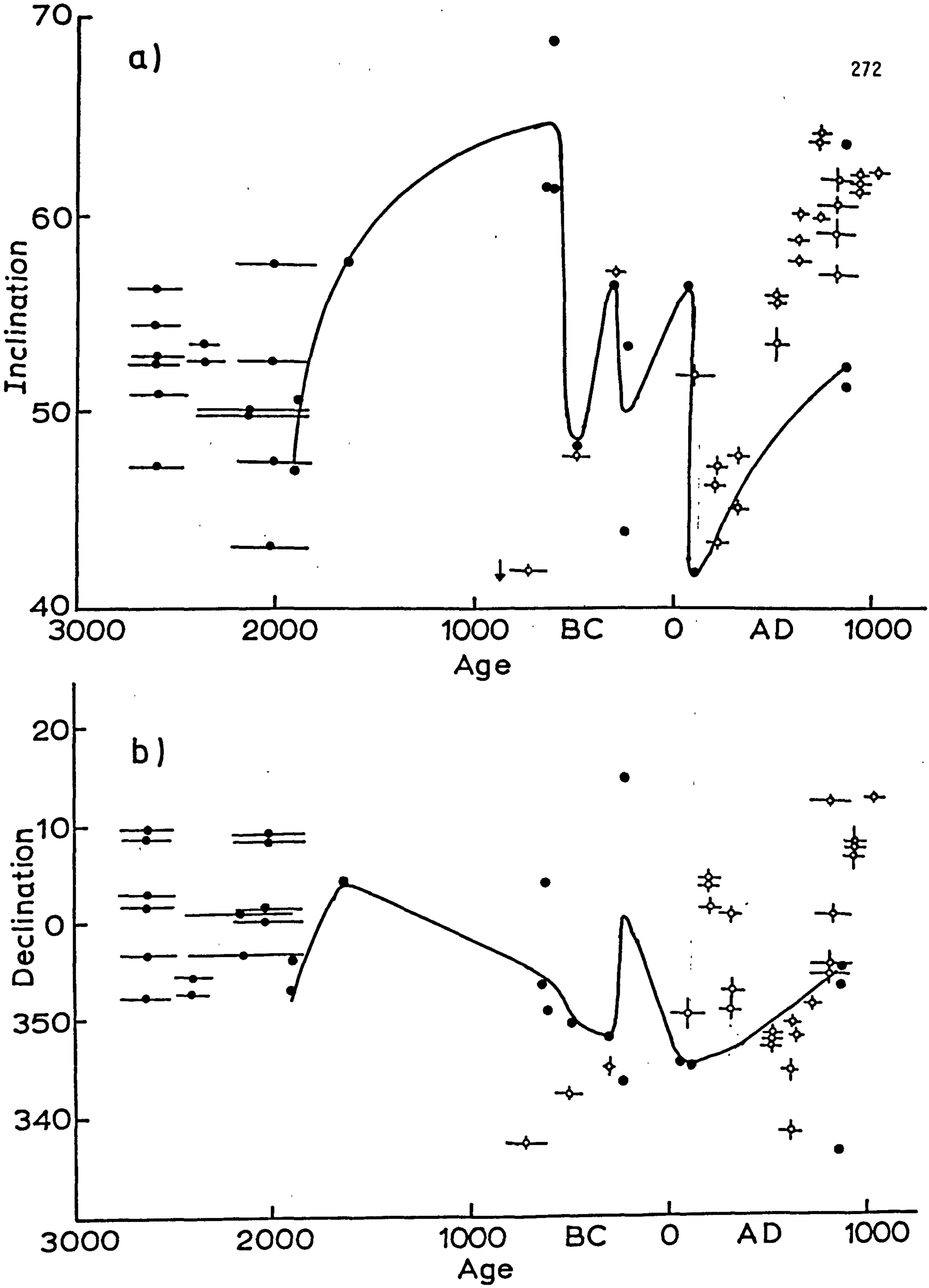

Fig. 5.6 Comparisons between Iraq, and Iran and Ukraine and Moldávia archaeological data

the same sequence as the data also show shallow inclinations at the beginning of AD which is followed by steeper inclination towards 900 A.D. However, two of the Iraqi sites (S_2 and S_4) show a shallower inclination of about 7^o when compared with Ukraine and Moldavia data while the inclination of the other site of a similar age (S_1) is nearly similar to the Ukraine and Moldavia inclination at 800 - 900 A.D.

The declination value for the three B.C. sites from Ukraine and Moldavia show differences ranging between 3 -17^o, from the Iraqi data. The declination of the Ukraine and Moldavia at 100 A.D. is defined by one site only. This declination shows a difference of about 5^o from the Iraqi declination which is defined by two sites. The Iraqi declinations at 800 - 900 A.D. are very similar to those of the Ukraine and Moldavia for 700 - 800 A.D., but they differ by about 10^o from the 900 A.D. declinations.

A total of 14 archaeomagnetic directions has been obtained by Kawen et al (1972) for Iran. These directions cover a period between 2000 - 2500 B.C. with their error in age ranging between ±100 - ±200 years. The inclination and declination were corrected to Baghdad and then plotted on the Iraqi magnetic secular variation. The age of only site K_5 (high α_{95} value) overlaps with the Iranian sites, and despite the scattered direction of site K_5, its inclination was equal to the inclination of two of the Iranian sites with about 2^o difference in declination. The other sites do not overlap with the Iraqi dates, but some of the age errors overlap near 2000 B.C. The Iranian inclination values near 2000 B.C. (4 sites) vary between 43 and 57^o, with high α_{95} value of error ranges. However, the mean inclination values for these sites will give a value which is close to the expected Iraqi inclination around 2000 B.C. On the other hand, the mean declination of these sites is about 10^o different from the Iraqi

declination at 2000 B.C. The comparison between the Iraqi and Iranian data is not very practicable as the Iranian data around 2000 B.C. show low reliability, indicated by their high α_{95} values and error ranges.

Theoretically these archaeomagnetic data should be reasonably similar to each other after the corrections to the same reference locality. Some differences were found; these are statistically expected due to the small number of sites. However, the sources of the differences could be due to different techniques used in sampling (differences between sun and magnetic compasses), instruments, processing and the reliability of the archaeological dating of each site. On the other hand errors in direction could be due to the distance between localities (about 2000 km. between Iraq and Ukraine), accordingly about 5^{o} (solid angle) difference is expected between the two sites after correction (see Chapter 1).

Despite the limited number of samples, the Iraqi material gave interesting results and proved to be very easy to work on, as they were very stable, and strongly magnetized.

Palaeointensity work was also carried out on nine Iraqi samples, using the Thellier method. These results are given in Chapter 6.

Table 5.1 Initial, Most Stable, S.I., Mean Values and α_{95} of the Iraqi Samples

5.1.1 ASSUR

No.	Initials Dec.	Inc.	Int. (mAm^{-1})	Most stable Dec.	Inc.	S.I.
A1/1	14.4	42.4	19.89	13.6	40.0	14.1
A1/2	356.6	49.0	350.8	15.0	60.9	6.8
A1/3	357.4	54.2	173.5	19.1	60.5	9.2
A1/4	352.7	42.9	139.7	12.1	52.1	7.1
Mean	14.6	53.4	α_{95}=11.3			
A2/1	354.5	52.3	3.4	354.4	51.4	4.3
A2/2	343.6	36.8	121.5	341.3	38.9	8.4
A2/3	332.0	48.0	23.5	330.6	46.8	10.3
A2/4	348.4	50.1	20.8	347.2	48.6	17.1
A2/6	77.8	48.7	209.8	75.3	51.7	27.4
A2/7	351.6	56.7	29.5	348.7	57.7	13.2
Mean	343.9	48.9	α_{95}=8.6			
A3/1	14.7	70.4	171.7	11.5	69.3	23.9
A3/2	15.4	69.5	78.2	9.0	68.3	32.6
A3/3	1.7	65.3	1232.6	354.9	66.5	28.3
A3/4	7.0	70.1	1683.9	1.0	71.1	20.1
Mean	3.9	68.9	α_{95}=3.8			
A4/1	358.3	59.6	38.2	357.4	59.9	22.5
A4/2	1.9	57.9	16.8	6.2	57.5	28.8
A4/3	347.6	57.9	58.9	346.4	64.8	34.8
A4/4	341.0	56.9	20.6	341.2	57.4	13.6
A4/5	0.1	65.1	136.3	356.8	65.4	29.9
Mean	353.7	61.3	α_{95}=5.9			

5.1.2 BABYLON

Initials				Most Stable		
No	Dec.	Inc.	Int. (mAm^{-1})	Dec.	Inc.	S.I.
B1/1	311.5	67.0	208.2	326.2	66.9	18.9
B1/2	57.6	69.9	388.6	3.5	66.8	67.6
B1/3	315.2	34.0	262.7	309.5	12.8	8.5
B1/4	327.1	66.1	381.2	353.3	43.1	8.1
Mean	349.3	59.7	α_{95} = 25.2			
B2/1	346.5	57.7	24.3	343.9	56.4	6.1
B2/2	5.4	62.7	33.2	360.2	61.1	7.2
B2/3	3.5	60.1	2.2	344.0	72.9	4.9
B2/4	354.8	59.0	28.5	355.3	57.9	6.2
B2/5	354.0	63.2	27.2	353.5	58.5	11.3
Mean	351.8	61.4	α_{95}=7.0			
B3/1	345.5	53.7	97.2	352.8	51.6	9.8
B3/2	331.2	55.7	1598.7	333.4	54.9	15.7
B3/3	349.5	59.1	813.2	344.3	56.7	18.2
B3/4	346.0	55.2	1007.9	346.5	56.0	14.9
B3/5	346.3	54.6	306.2	347.8	54.4	13.9
B3/6	353.3	63.8	150.5	349.5	65.1	13.8
Mean	345.6	56.6	α_{95}=4.9			
B4/1	350.1	53.3	113.9	350.6	53.0	20.1
B4/2	350.8	48.3	71.3	346.5	47.4	8.4
B4/3	346.9	48.0	223.2	349.3	48.0	12.1
B4/4	344.5	44.9	66.2	344.8	45.1	10.7
B4/5	353.0	47.9	38.4	353.8	47.9	10.6
Mean	348.9	48.3	α_{95}=3.5			
B5/1	348.9	56.6	42.0	349.8	57.6	10.1
B5/2	353.8	56.8	147.0	354.2	56.4	13.6
B5/3	346.2	63.0	125.8	345.9	62.8	11.8
B5/4	345.4	54.2	82.5	343.7	54.4	7.4
B5/5	350.1	49.5	16.7	348.5	50.9	3.8
Mean	348.4	56.4	α_{95}=4.6			

5.1.3 HATRA

Initials				Most Stable		
No	Dec.	Inc.	Int (mAm^{-1})	Dec.	Inc.	S.I.
H1						
H2	3.2	43.1	64.2	3.1	42.0	13.1
H3	6.9	43.3	44.5	1.5	43.0	19.4
H4	351.3	37.6	5.4	352.5	41.5	7.2
H5	357.1	38.7	25.3	353.2	39.0	17.4
H6	346.1	40.3	27.9	341.5	43.9	19.9
Mean	355.2	41.8	α_{95}=5.0			

5.1.4 KATAB

K1/1	354.8	-10.6	7.1	352.0	-13.6	21.1
K1/2	208.6	45.8	8.7	109.0	45.7	11.0
K1/3	7.8	24.4	4.9	7.0	23.6	5.7
K1/4	314.6	84.6	5.7	295.9	85.6	8.5
K1/5	18.8	49.8	1.0	19.1	52.8	1.9
K1/6	85.4	20.1	21.4	90.7	13.9	15.0
overall mean	37.8	45.8	α_{95}=52.4			
Mean(rejects)	55.7	54.2	α_{95}=47.3			
K2/1	22.8	77.0	0.67	332.0	43.0	1.5
K2/2	347.0	35.2	39.3	345.6	36.2	8.6
K2/3	5.8	47.7	93.8	2.9	48.5	11.2
K2/4	4.9	46.7	21.2	4.5	46.9	21.4
K2/5	2.8	57.4	10.1	5.1	57.2	13.1
Mean	352.9	47.1	α_{95}=12.1			
K3/1	10.9	59.9	122.5	11.4	61.3	39.9
K3/2	352.8	54.2	221.2	352.7	50.7	19.8
K3/3	7.9	59.0	29.1	9.5	57.6	25.4
K3/4	4.4	62.5	66.5	5.4	60.0	25.8
Mean	4.0	57.6	α_{95}=7.5			

5.1.4 (continued) KATAB

	Initials			Most Stable		
No	Dec.	Inc.	Int. (mAm^{-1})	Dec.	Inc.	S.I.
K4/1	347.1	45.5	4.1	345.9	44.7	7.3
K4/2	347.0	48.3	5.2	344.2	44.7	7.9
K4/3	41.1	55.4	33.1	27.7	57.7	12.8
Mean	356.3	50.5	α_{95}=26.0			
K5/1	53.9	39.1	28.6	57.8	33.2	14.4
K5/2	7.3	45.6	12.3	3.3	46.6	6.5
K5/3	354.7	53.3	16.9	355.9	52.6	6.4
K5/4	325.6	-4.1	638.1	325.3	-17.3	8.4
K5/5	331.0	-13.2	833.5	325.9	-16.4	11.3
K5/6	357.0	29.1	4.1	339.1	-0.2	7.7
K5/7	326.6	24.7	11.3	321.4	61.1	15.9
K5/8	18.5	56.7	12.1	43.2	54.9	5.5
K5/9	347.2	22.6	2.6	350.4	24.8	3.2
overall mean	352.3	30.9	α_{95}=29.5			
Mean rejects (4,5,6)	10.6	50.1	α_{95}=23.5			

5.1.5 SALMAN PAK

S1/1	340.1	58.8	995.4	344.5	57.4	34.1
S1/2	330.3	58.2	56.9	331.0	57.8	14.1
S1/3	323.5	57.7	105.5	325.0	57.5	14.2
S1/4	349.0	73.1	34.6	342.4	71.0	27.5
S1/5	309.5	72.6	14.9	348.0	72.9	12.1
Mean	336.7	63.5	α_{95} = 8.5			
S2/1	349.0	50.0	601.0	350.1	51.0	30.1
S2/3	352.7	51.4	894.5	352.5	50.0	47.3
S2/2	356.3	48.0	557.2	355.5	49.6	39.9
S2/4	356.5	50.5	619.6	357.2	53.6	33.4
Mean	353.7	51.0	α_{95} = 3.0			

5.1.5 (cont'd) SALMAN PAK

	Initials			Most stable		
No.	Dec	Inc	Int (mAm^{-1})	Dec	Inc	S.I.
S3/1	8.5	-0.2	365.8	0.1	3.0	26.5
S3/2	218.5	69.7	694.4	320.3	73.6	9.7
S3/3	349.7	62.1	489.3	4.5	64.9	16.1
S3/4	331.3	42.0	252.9	333.8	31.3	14.3
S3/5	261.5	34.1	34.29	263.3	32.4	18.6
Mean	348.0	51.7	α_{95}=29.8			
S4/1	355.1	48.4	12.3	359.7	50.3	3.6
S4/2	355.6	20.7	52.7	354.7	52.7	12.5
S4/3	351.9	55.7	10.7	352.9	54.3	8.8
S4/4	209.3	4.8	1.2	353.0	52.0	2.6
Mean	355.1	52.3	α_{95} = 2.9			

CHAPTER 6 PALAEOINTENSITY

6.1 Introduction

A rock sample that has been cooled from a temperature above the Curie point of its magnetic constituents has an intensity of Natural Remanent Magnetization (NRM) of Thermal origin (TRM) that is proportional to the strength of the geomagnetic field in which it cooled (Thellier, 1938). In order to determine the strength of the palaeofield (H_a), the sample can be heated to a temperature above its Curie point, and then cooled in a known field (H_ℓ) so that it acquires a laboratory thermal remanence.

The NRM and the laboratory TRM are both linearly proportional to the external field, a palaeointensity determination can be obtained from the equation:-

$$\frac{J_n}{J_t} = \frac{H_a}{H}\left(\frac{\chi}{\chi}\right) = \frac{H_a}{H}$$

where J_n is the measured intensity of NRM, J_t is the intensity of TRM produced in the laboratory in a field equal H_ℓ, H_a is the unknown ancient field and $J_t = \chi$. H_a, where χ is the constant of proportionality, susceptibility, which is linear in weak field (<1mT).

On this basis, Thellier and Thellier (1959) proposed that the value J_n/J_t can be obtained by a single heating but an evaluation of the error and detection of other effects requires a sequence of paired heatings ($T_1 < T_c$) which can then be used to determine the partial NRM (ΔJ_n) that would be lost in heating from room temperature, T_r to T_1 in zero field, and a partial TRM (ΔJ_t) obtained by cooling the sample in a known field, H_ℓ, from T_1 to T_r (Thellier and Thellier, 1959). This is

known as the Thellier method in which temperature of the paired heatings is progressively increased from T_r until all blocking temperatures are exceeded, giving a data set of $(\Delta J_n(T), \Delta J_t(T))$ for the different temperature steps. Each step gives an independent determination of $\frac{H_a}{H_\ell}$. A plot of ΔJ_n vs. ΔJ_t for different temperatures should thus result in a straight line with slope H_a/H_ℓ for ideal behaviour of an NRM which is entirely of TRM origin. Non-linearity can occur due to viscous and other non-TRM magnetization present in the NRM and to chemical changes causing changes in susceptibility or remanence during heating and cooling of either the NRM, the TRM or both. Most of all of any viscous magnetizations can be removed by either low temperature thermal demagnetization or low field AC-demagnetization. The higher temperature components of NRM and TRM can then be compared over different temperature ranges. On this basis, it is possible to reject the non-linear parts of the curve that have been affected by such viscous magnetizations or chemical changes.

Chemical changes can also be detected by changes in the low field susceptibility which is measured after each heating step in the results reported here. Susceptibility changes can sometimes be misleading as slight changes in either the susceptibility or the TRM may not affect the other. For example, formation of a small percent of hematite could drastically affect the TRM at high temperatures but could still be within the error of the susceptibility reading.

The deviation of $J_n - J_t$ values from the ideal behaviour is also affected by other factors. Studies on the grain size of magnetic particle showed that these deviations increase with a) an increasing proportion of multi-domain grain particles (due to the lack of symmetry of the domain .

wall movement during two successive heatings); b) increasing mean size of the magnetic particles and c) decreasing median demagnetizing field in the case of alternating field demagnetizing methods.

For the relation NRM:TRM against $H_a:H_\ell$ to hold, the laboratory conditions also need to be as similar to the probable field conditions as possible. In particular the cooling rates and heating durations should ideally be identical. These factors are difficult to estimate and it is generally impractical to control their effects. However, the most drastic effects usually arise from physical-chemical changes resulting from laboratory heating, so most recent palaeointensity determination methods have concentrated on decreasing the number of heatings steps. An extreme example of this is the use of Anhysteretic Remanent Magnetization (ARM) instead of the TRM, as this involves no heating but assumes a knowledge of the ratio between intensities of TRM and ARM.

The ARM is generally considered to be the analog of TRM (Dunlop and West, 1969; Gillingham and Stacey, 1971) and has similar additive properties to thermoremanent magnetization, i.e.

$$PARM_{H_1}^{H_3} = PARM_{H_1}^{H_2} + PARM_{H_2}^{H_3}$$

where $PARM_{H_x}^{H_{x+1}}$ .... etc., is the ARM required when the peak value of the alternating field is reduced from H_{x+1} to H_x. However the degree of similarity between the TRM and ARM depends particularly on grain size. For small grain size (<5μm) the ARM and TRM have similar coercivity spectra but for larger grains they are dissimilar. For inhomogeneous materials, with large and fine grains, the relation between the TRM and ARM is even more complicated (Dunlop et al. 1973). The similarity in the coercivity spectra of TRM and

ARM increases with decreasing grain size, and for MD grains, the TRM is more stable than ARM for both AF and thermal treatment. However, the median destructive field for ARM is less than TRM for all grain size in the PSD and MD range (Hartstra, 1983). Additionally, the packing density of the magnetic grains directly affects the TRM/ARM ratio, (Sugiura, 1979).

In this work, four palaeointensity determination methods were carried out on specimens taken from a single Roman Brick from the Black Gate site in Newcastle upon Tyne (BG_1- BG_8) (Lat. 54.6N, Long, 1.3W). This was done in an attempt to compare different palaeointensity methods, particularly between the TRM and ARM method. The heating and cooling rates were essentially constant, throughout all the experiments, and the anisotropy of low field susceptibility of the brick was low (<1%). Accordingly, no corrections should be required for these factors. Any disparity in the results should thus reflect differences due to the actual techniques themselves. (The Thellier method was subsequently used to obtain the ancient intensity preserved in nine Iraqi samples. A modified Thellier method (Kono and Ueno, 1977), was also used to compare the palaeointensity values of three Roman bricks from Chignal St. James, Essex (Lat. 51.4N, Long. 0.05E)).

The methods used are those proposed by:-

1. Thellier and Thellier (1959)
2. Van Zijl (1962)
3. Shaw (1974)
4. Bagina nd Petrova (1977)
5. Konn and Ueno (1976).

The samples were cut into identical cubes, with sides of 2.1cm., in order to fit inside the magnetometer holder and the furnace.

As the samples were unoriented, an arbitrary fiducial line was drawn on top of each sample. For the Kono and Ueno method (1977), smaller samples were used and these were placed in pyrex cylinders and, after identifying the direction of NRM, the cylinders were filled with non-magnetic gypsum (Downey, 1983). All measurements were carried out using a Digico magnetometer, and susceptibility measurements were made after each heating step, using a susceptibility bridge.

The slope of the best fit line (regression line) was plotted using the least square method. In order to test for differences between the best-fit slopes of two samples, the student (t) test was applied. The procedure and equations of the analysis were derived from Edwards (1972, 1973) and the computer program is listed in Appendix (5).

6.2 Theory and Results

6.2.1 Thellier Method (1959)

This method, outlined earlier, consists of a sequence of paired heatings to a given temperature; after the first heating the specimens are cooled in a zero field and after the next they are cooled in a known field. Palaeointensity values should be identical for each pair of heatings, i.e.

$$\frac{\Delta J_n\ (T_2,\ T_1,\ H)}{\Delta J_t\ (T_2,\ T_1,\ H_\ell)} = \frac{|H|}{|\overline{H_\ell}|}$$

where $\Delta J_n\ (T_2,\ T_1,\ H)$ is the magnetization acquired during cooling from T_2 to T_1 in unknown magnetic field H. Such identity of the J_t - J_n ratios can only occur when no chemical changes occur during heating and when the NRM is entirely of TRM origin.

The main advantage of this method is that the decay of the NRM and the acquisition of artificial TRM are both determined in a series of heatings, hence if irreversible alteration of the TRM spectrum begins at a particular temperature during heating in the laboratory then the results determined previously at lower temperature can still be used for palaeointensity as long as the viscous magnetization has been removed. The main risk is in the number of heatings increasing the time and the possibility of thermochemical changes. Additionally the need for re-heating to exactly the same temperature is technically difficult.

Samples BG_1 and BG_2 were heated to 100, 200, 300, 400, 500 and 550°C. At each temperature, the samples were cooled once in a zero field and then in a field of 0.48×10^{-4}T. The $J_n - J_t$ values obtained at 100°C were deviated from the other values at high temperatures, indicating that different viscous magnetizations were removed at temperatures between 100 and 200°C. Above 100°C the susceptibility values were constant at all heating steps. However, it seems that the values of $J_n - J_t$ at 500°C for sample BG_1, and at 550°C for sample BG_2 depart from the best fit line (Fig. 6.1, 6.2, Table 6.1), possibly due to measurement errors or slight chemical changes that did not affect the total susceptibility.

The initial NRM intensity of sample BG_1 was higher than BG_2, and the TRM acquired for sample BG_1 between 200 - 450°C was higher than that acquired by sample BG_2. Conversely the TRM acquired between 500 and 550°C for sample BG_1 was lower than that for BG_2. Accordingly there were slight differences in the palaeointensity values obtained for the two samples. The values at 100°C were departed from the other values, and hence the values were rejected during calculating the slopes. The

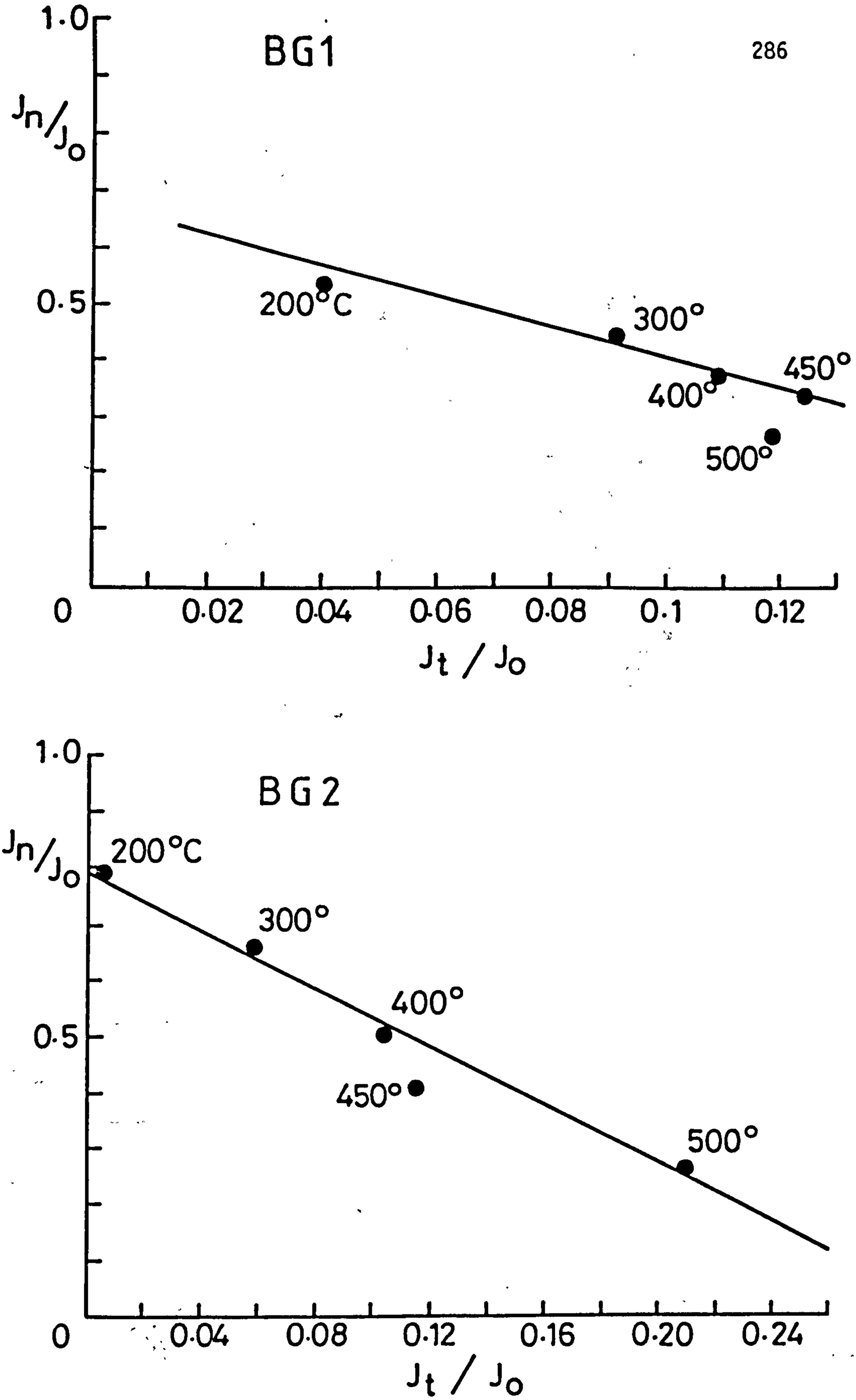

Fig. 6.1 The application of Thellier's method on two samples from Black Gate site (BG_1 and BG_2)

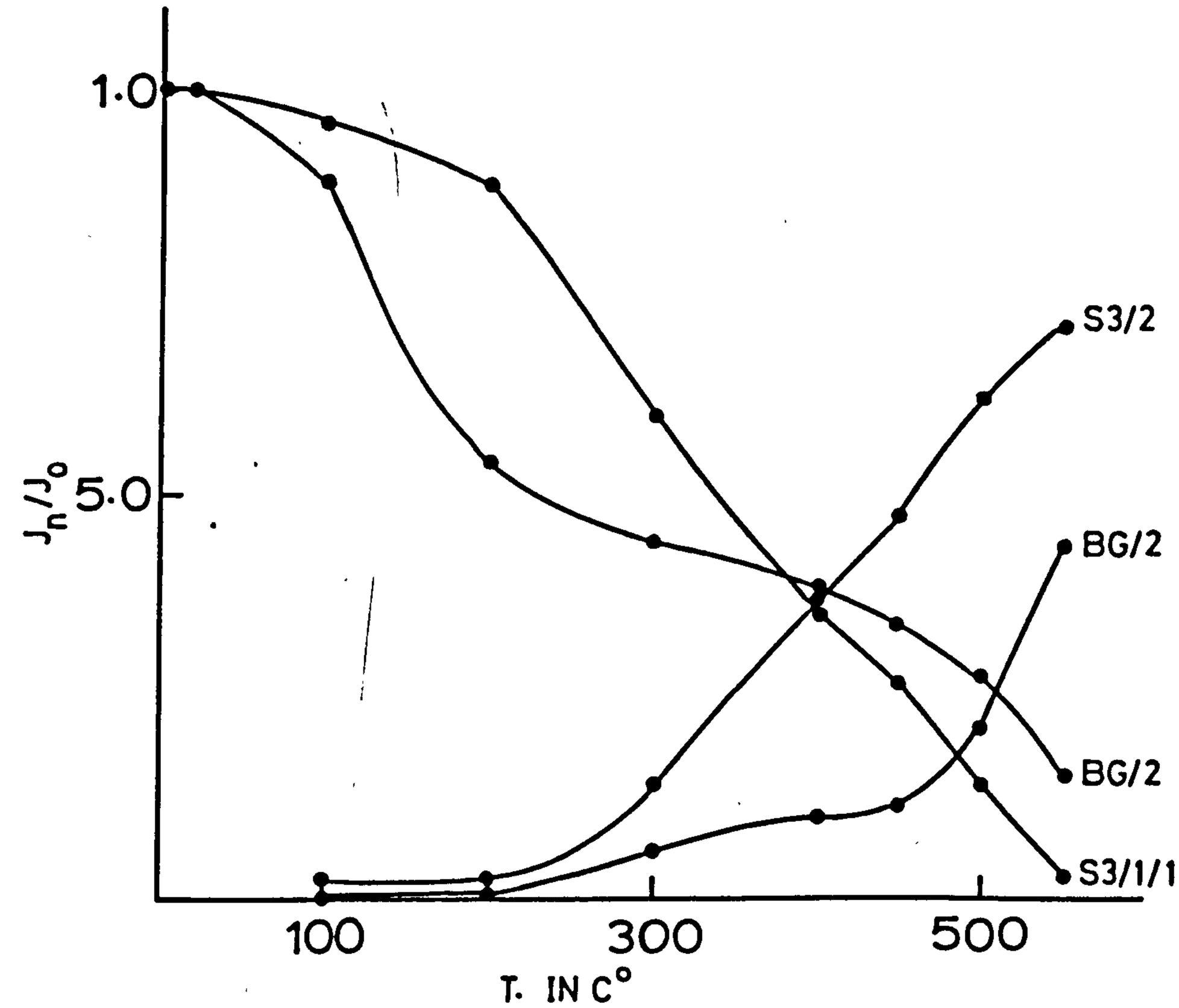

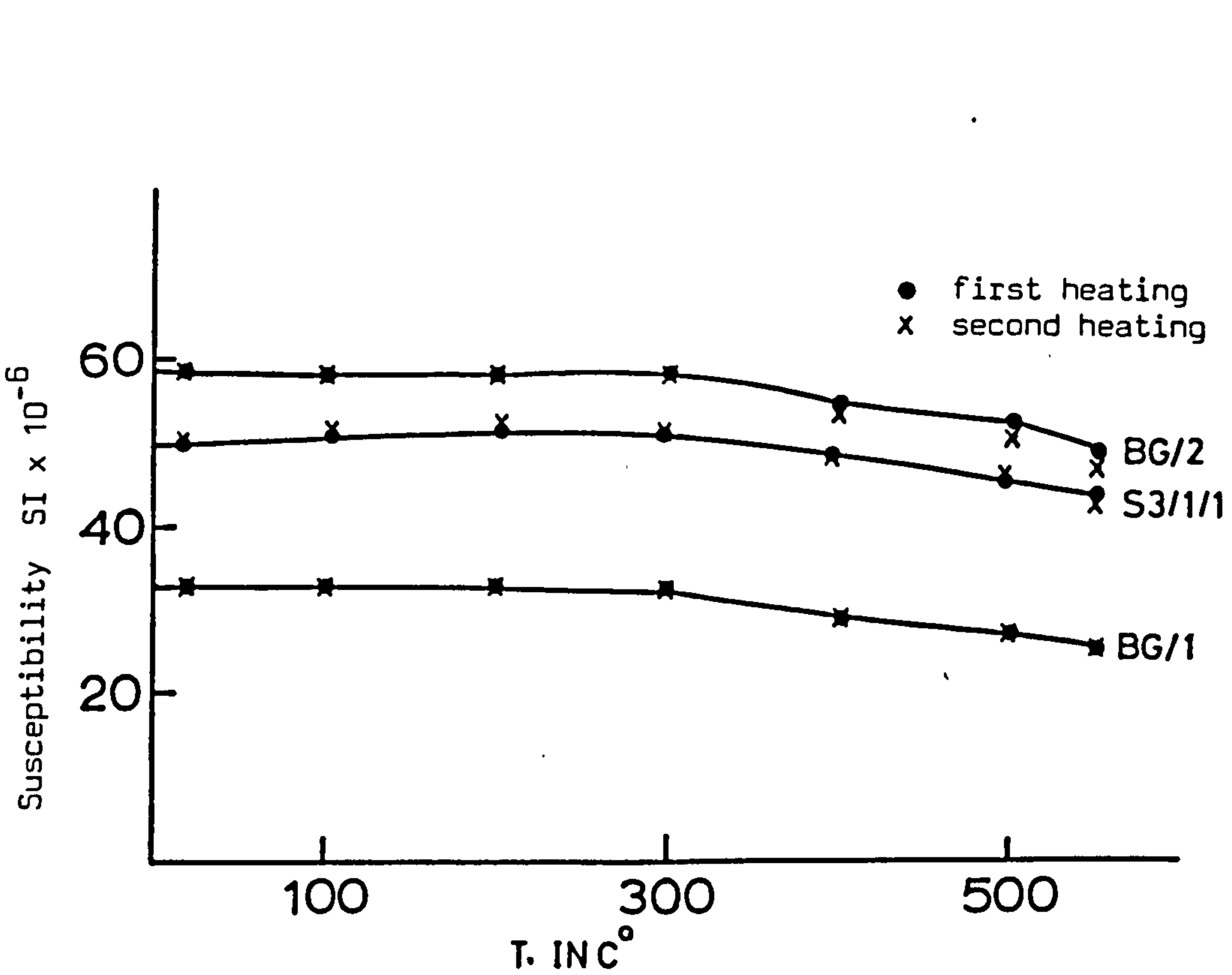

Fig. 6.2 Examples of changes in NRM, TRM and susceptibility during the application of Thellier method on Black Gate and Iraqi samples

Table 6.1 Palaeointensity Results Obtained using Thellier Method

Temp	J_n mAm^{-1}	J_a mAm^{-1}	J_t mAm^{-1}	J_n/J_o	J_t/J_o
	S a m p l e	$BG_{/1}$			
100	639.82	622.70	-17.12	0.89	-0.02
200	383.45	412.09	28.64	0.54	0.04
300	316.80	381.98	65.18	0.44	0.09
400	270.18	348.39	78.21	0.38	0.11
450	243.12	331.61	88.49	0.34	0.12
500	191.44	276.01	84.56	0.27	0.12
550	104.97	312.16	207.18	0.15	0.29

J_o = 714.00

	S a m p l e	$BG_{/2}$			
100	493.89	487.90	-5.99	0.95	-0.01
200	409.73	412.84	3.11	0.79	0.006
300	342.39	373.01	30.62	0.66	0.06
400	267.35	321.21	53.86	0.52	0.10
450	214.10	273.95	59.85	0.41	0.11
500	139.15	247.61	108.45	0.27	0.21
550	42.68	263.86	221.18	0.08	0.43

J_o = 517.11

J_a = Intensity after cooling in known field ($J_a = J_t + J_n$)

J_t = T.R.M. acquired ($J_t = J_a - J_n$)

J_n = N.R.M remaining after cooling in a zero field

value of 500°C for BG_1 and 450°C for BG_2 were also excluded because they deviated from the other values, possibly due to chemical changes (figs. 6.1, 6.2, Table 6.1).

The student t value for the two slopes was 0.472, with 4 d.f. , (degree of freedom), i.e. the slopes show no significant difference at the 0.05 probability, and both values are within the central 95% of distribution and can therefore be considered statistically equal.

Although the two values are statistically equal, slight difference could be due to:-

a) chemical changes

b) errors in reheating to the same temperature

c) inhomogeneity in the brick.

6.2.2 Van Zijl Method (1962)

This method involves a comparison between the coercivity of the NRM and TRM, by demagnetizing in progressively higher alternating magnetic fields, then measuring the remanence at room temperature. The procedure followed in this method can be summarized as follows:-

1. A.F. demagnetization of the NRM in progresively higher fields until no NRM is left. Complete destruction of NRM is often impossible by A.F. method and so in this study, demagnetization was carried out up to 80 mT peak field.

2. The specimen is then given a TRM by cooling from above T_c to room temperature in a field of about 0.46 mT.

3. This TRM is then A.F. demagnetized in the same fields as in step (1).

Ideal behaviour in this method would result in a straight line for the relationship:-

$$\frac{\Delta J_n}{\Delta J_t} = \frac{H_a}{H_\ell}$$

The advantage of this method is the speed and that only one heating is required. However the main disadvantage is that the rock must be heated above its Curie temperature before the demagnetization of the laboratory induced TRM can be measured, so that if any magnetic minerals are altered at any stage of heating, all comparisons between the NRM and TRM will be invalid. In addition, fired archaeological materials may contain a high percentage of hematite, with possible coercivities of more than 2T which cannot be removed by available A.F. demagnetizing instruments.

The TRM and NRM of samples BG_3 and BG_4 were partially demagnetized at steps of 10, 20, 30, 40, 50, 60, 70 and 80 mT. Neither the NRM nor the TRM were completely demagnetized. Hence two intensity values were calculated for each sample, one using a best fit line that did not pass through the origin and a second passing through the origin. The results, excluding the origin, were considered more reliable because demagnetization had not been achieved (fig. 6.3, table 6.2). The value of $J_n - J_t$ at 80 mT for sample BG_3 was away from the best fit line and hence it was excluded during calibrating the slope. Deviation from the best fit was not very high and is likely to be due to a small measurement error or errors during demagnetization at high fields.

The calculated student t for the two slopes is 0.18 with 11 d.F., i.e. the slopes show no significant differences at a 0.05 probability and the two slopes are within the central 95% of the distribution and therefore statistically they are considered equal. The minor differences between the two values could be attributed to:-

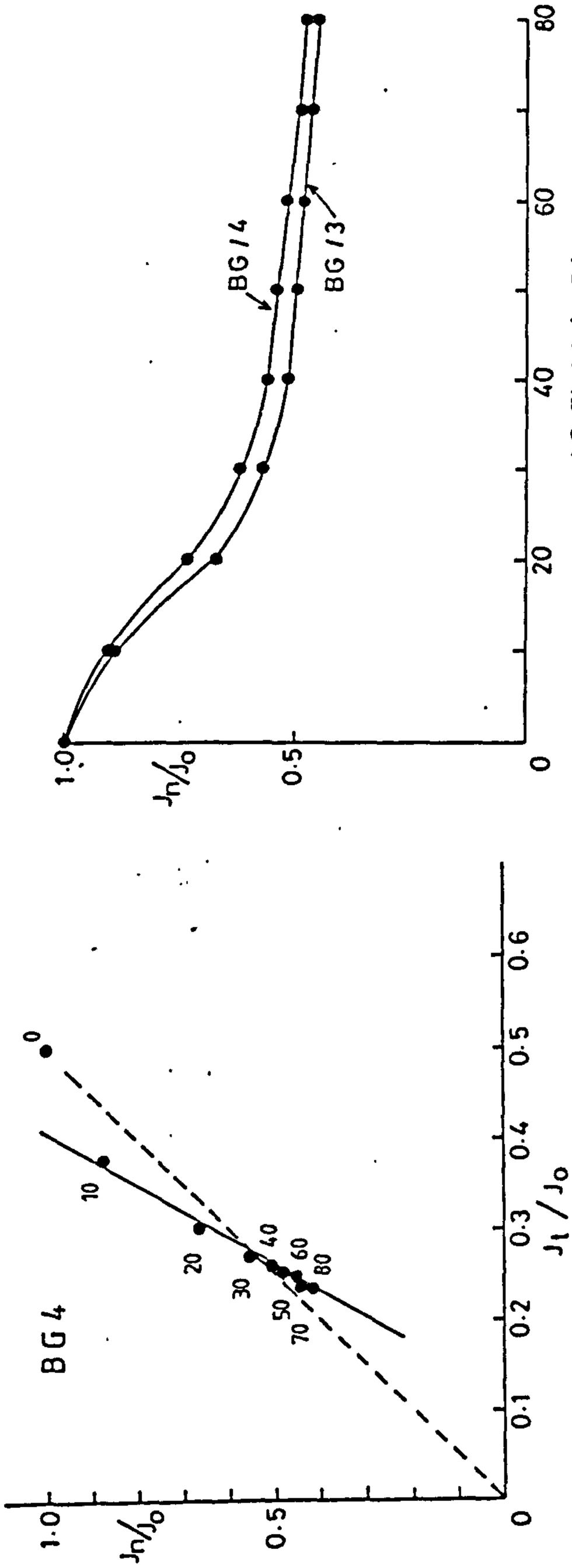

Fig. 6.3 The application of Van Zijl palaeointensity method on samples BG_3 and BG_4

Table 6.2 Palaeointensity Results obtained using Van Zijls method

A.C. field mT	J_n mAm^{-1}	J_t mAm^{-1}	J_n/J_o	J_t/J_o
Sample BG/3				
			1	0.50
10	1092.61	478.57	0.89	0.39
20	831.78	372.67	0.67	0.30
30	698.13	339.13	0.57	0.27
40	635.64	323.56	0.52	0.26
50	605.74	314.61	0.49	0.25
60	586.97	309.27	0.48	0.25
70	567.37	300.22	0.46	0.24
80	551.89	313.67	0.45	0.25

J_o = 1228.73 mAm^{-1}

J_{TRM}= 820.82 mAm^{-1}

Sample BG/4				
			1	0.48
10	1254.22	537.30	0.90	0.38
20	1017.24	434.13	0.73	0.31
30	861.7	397.40	0.62	0.28
40	786.72	374.25	0.56	0.27
50	757.04	368.11	0.54	0.26
60	716.67	354.59	0.52	0.25
70	690.41	342.35	0.49	0.24
80	662.06	331.32	0.47	0.24

J_o = 1390.94 mAm^{-1}

J_{TRM}= 664.49 mAm^{-1}

a) incomplete demagnetization of the NRM and TRM.

b) inhomogeneity in the brick.

6.2.3 Shaw Method

This method (Shaw, 1974) involves comparison between ARMs, one created before and one after heating. The comparison permits selection of a coercive force region within which the heating has not changed the magnetic properties. The NRM and TRM are compared to deduce the palaeo-field only within that selected coercive force region. The region can be determined by comparing ARM demagnetization curves before and after heating. Equality of the two ARM coercive force spectra can then be defined by a straight line relationship of 45^{o} slope. The procedure is as follows:-

1. A.F. demagnetization of NRM, with incremented values of the peak alternating magnetic field. The remaining NRM is measured after each sucessive demagnetization up to the maximum demagnetizing field, which was 120 mT in this work (the same demagnetization intervals are used in later demagnetizations).
2. An ARM (ARM_1) is then given to the sample by putting the sample inside a holder with a coil around the sample and magnets on both sides (in the holder). An alternating field of 120 mT was applied and then decreased slowly. ARM is then progressively demagnetized and measured as in (1).
3. The sample is then given a TRM by heating to $700^{o}C$ and allowing it to cool to room temperature in a constant magnetic field. In this experiment the field was 0.48 mT. This TRM is then demagnetized and measured as in (1).
4. ARM_2 is given to the sample, as in (2), and demagnetized as in (1). A

plot of ARM_2 against ARM_1, using the AF demagnetizing field as a parameter, should give a straight line with a gradient of 1.0 if the rock was unaltered by heating. The appropriate range of TRM is then plotted against the NRM over the same range of demagnetizing field. The best line is fitted within this and constrained to pass through the origin which corresponds to an infinite demagnetizing field and the best average value of the ratio TRM/NRM is then used to determine the ancient field.

Although this method is slow, it is considered to be reliable because it involves the use of only that part of the coercive force spectrum which has not been altered by heating. However this method will still have the same limitations as the Van Zijl method, that is reaching the infinite destructive demagnetizing field, and hence the best line is not constrained to pass through the origin. On the other hand, with the ARM method, there is the possibility of the acquisition of a spurious but possibly systematic ARMs like GRMs and RRMs.

A large number of steps were used in order to obtain a better idea of the ARM behaviour during demagnetization and also to more closely define the coercive force spectrum (Table 3.3). The ARM plots showed that the lower and some of the high coercive force spectrum deviated from the straight line fit and therefore they were rejected (fig. 6.4). This is probably due to viscous magnetization effect at low fields and chemical changes as a result of heating affecting the high coercive spectrum. This was also noticed in the TRM-NRM plots as the values at low fields and high fields showed linear behaviour (nearly similar in the two samples).

The student t for the two slopes was 2.05 with 18 d.f. The value is higher than the previous value and it indicates significant

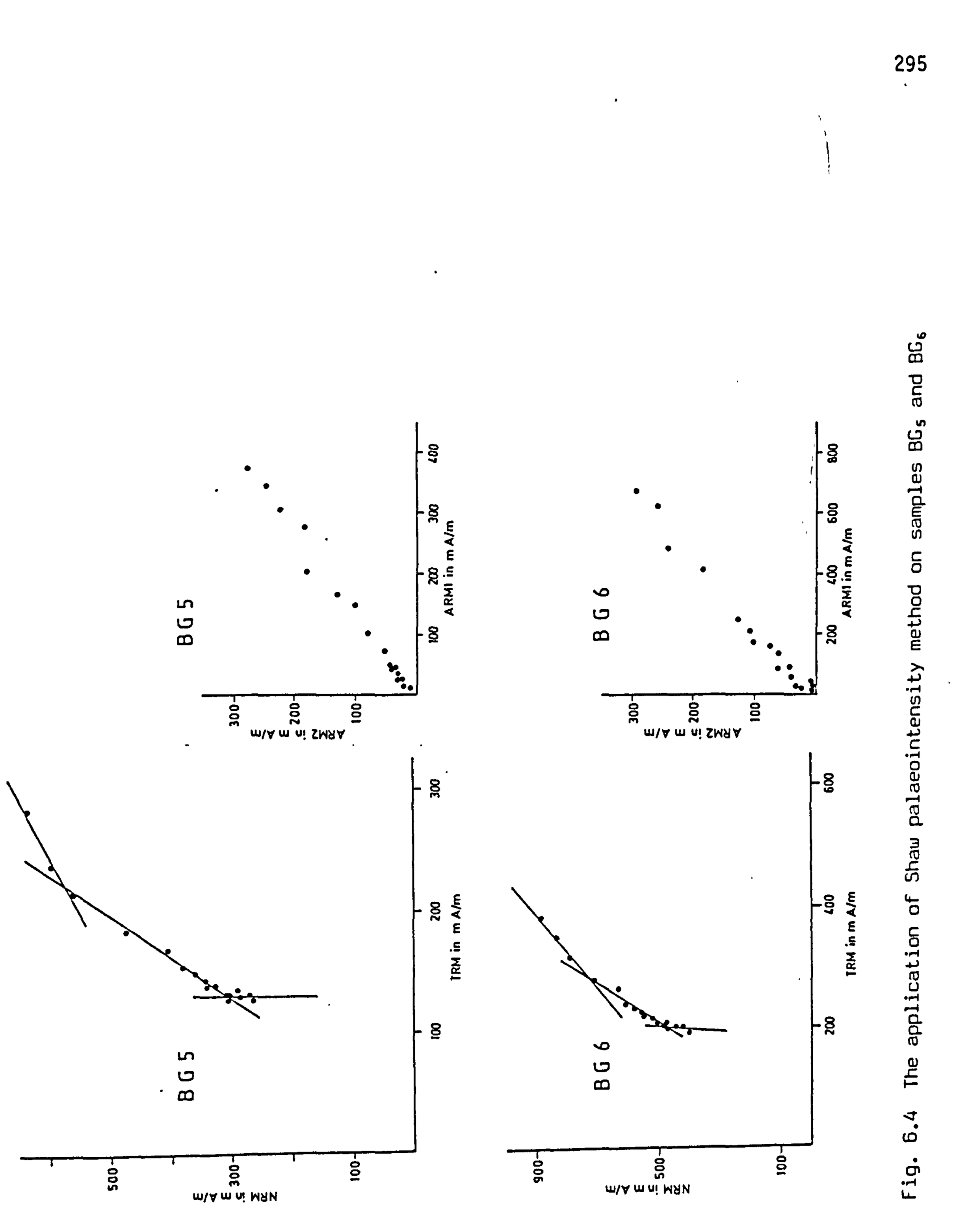

Fig. 6.4 The application of Shaw palaeointensity method on samples BG_5 and BG_6

	BG/5				BG/6			
A.C. Field	NRM	ARM_1 mAm^{-1}	TRM	ARM_2	NRM	ARM_2 mAm^{-1}	TRM	ARM_2
0	635.5	385.2	284.4	283.0	885.5	674.8	385.7	295.4
5	597.3	345.1	249.3	250.1	838.9	623.4	351.2	260.1
10	563.0	304.4	219.6	225.6	798.3	481.2	318.6	244.3
15	477.5	278.6	184.7	184.9	707.1	417.9	283.6	186.4
20	405.6	263.9	171.5	180.4	638.0	243.7	266.3	127.9
25	383.3	165.8	155.3	130.2	612.6	202.4	239.2	109.4
30	361.1	150.0	150.6	100.1	583.7	171.5	232.4	102.4
35	344.8	102.7	144.3	73.8	565.9	160.1	225.3	75.0
40	341.8	73.6	140.9	55.7	556.2	132.0	220.6	62.5
50	327.2	75.9	139.2	46.9	526.7	83.4	215.5	63.9
60	308.0	45.0	132.8	47.8	504.5	91.7	210.6	45.3
70	303.4	46.1	133.0	36.9	482.4	51.9	202.7	42.4
80	307.4	35.1	133.7	33.4	483.6	27.9	200.8	36.0
90	293.7	25.2	135.5	32.6	470.7	23.6	209.7	27.1
100	285.0	25.0	132.2	25.0	444.2	44.3	200.8	7.9
110	265.6	16.9	133.1	19.3	422.9	33.5	201.1	4.8
120	263.2	12.2	129.0	11.4	400.0	20.0	193.0	4.9

Table 6.3 Palaeointensity Results Obtained Using the Shaw Method

difference at about 5% probability. Statistically neither of these two values are within the 95% central distribution, i.e. the slopes are not equal, and there is a high probability that the difference between the two slopes are due to some factors apart from chance. These differences could be due to:-

1) dissimilarity between ARM and TRM behaviour as a result of inhomogeneity in mineral composition and grain size.
2) incomplete demagnetization of the NRM and TRM
3) acquisition of spurious ARM.

6.2.4 Bagina and Petrova Method (1977)

This method is based on a comparison of alternating field demagnetization curves of ARM and NRM. The amplitude changes of the ARM and NRM are compared over the interval of alternating field where the coercive force spectra of these two magnetizations coincide, on the basis that the intersection of the coercive spectra of the ARM and NRM occurs when the fields generating the NRM and ARM are equal.

An ARM was given to the samples using the same procedure of section 6.2.3 and the NRM and ARM of samples BG_7 and BG_8 were demagnetized at 10, 15, 20, 25, 30, 35, 40 and 50 mT. The coercive force spectra were then plotted for both NRM and ARM (using 2.5mT range).

The intensity of ARM of sample BG_8 started to increase slightly after demagnetizing in a field equal to 30 mT. (fig. 6.5, table 6.4), while that of the NRM continued to decrease. This means that the coercive force spectra of the ARM and NRM cannot intersect and so no palaeo-intensity value could be calculated for this sample, while for sample BG_7 there was no increase in the intensities of NRM and ARM and hence the intersection of the coercive force spectra of the ARM and NRM was used to deduce

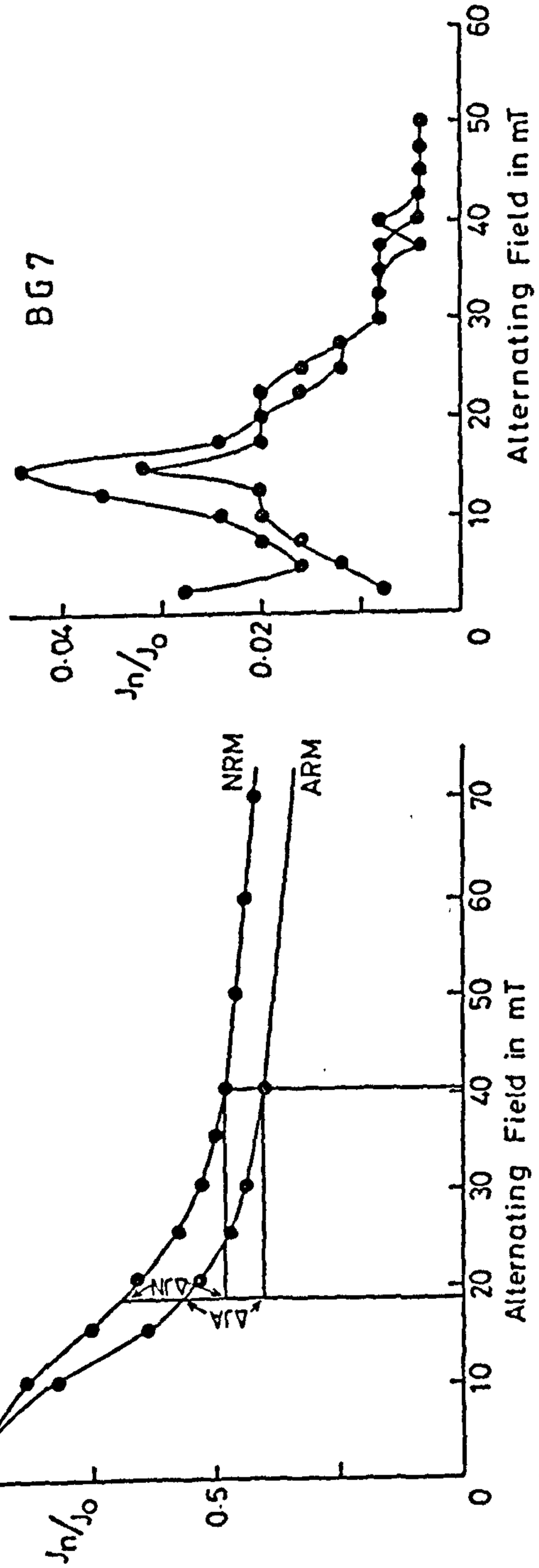

The application of Bagina and Petrova paleointensity method on samples BG7 and BG8

Fig. 6.5

the ancient intensity.

This method depends only on the behaviour of NRM and ARM during demagnetization, but if either the earth's magnetic field has not been completely cancelled during demagnetization or the AF is not harmonically pure, then there is a chance for the acquisition of a spurious ARM which will change the curves of both the coercive force spectra and the demagnetization curve. Hence the two curves may not necessarily intersect (table 6.4).

Table 6.4 A.F. demagnetization of samples BG_7 and BG_8 (Bagina and Petrova method)

A.F. field mT	Sample BG_7 NRM mAm^{-1}	Sample BG_7 ARM mAm^{-1}	Sample BG_8 NRM mAm^{-1}	Sample BG_8 ARM mAm^{-1}
10	903.1	833.8	962.7	614.7
15	758.9	639.6	829.8	483.1
20	663.3	539.4	746.2	432.5
25	582.1	475.6	686.9	400.1
30	539.1	444.4	643.8	407.2
35	503.9	422.0	602.9	416.8
40	460.8	381.5	558.3	406.3
	J_o = 1004.1 mAm^{-1}		J_o = 1042.7 mAm^{-1}	
	J_{ARM} = 1059.1 mAm^{-1}		J_{ARM} = 800.0 mAm^{-1}	

Summary for Black Gate Roman Brick:

Results obtained from the application of the four palaeointensity methods on samples from a Roman brick show a general range of values between 0.753 - 1.449 mT, with most of the results suggesting the higher part of the range, i.e. 1.161 - 1.449 mT (table 6.5). Comparison of these results with the available intensity values for the Roman period (Smith, 1967, 1968), show that the obtained intensities for Black Gate brick are higher than the intensities of the available records. Since these high palaeointensity values were consistent with different methods and on 6 samples, hence it is possible that the site of the sample was in a locally high intensity magnetic field. Therefore the ancient intensity of the brick is distorted by local disturbances.

The nature of the disturbance could be explained more easily in terms of magnetic direction but unfortunately the brick was not in situ as it was obtained for intensity studies and therefore further explanation for the high intensity are not possible.

6.2.5 Modified Thellier Method (Kono and Ueno, 1976)

If the direction of NRM does not change much during AF demagnetization, it should not change much during thermal demagnetization, provided that the demagnetization is not close to the Curie point of the sample. Hence, if the direction of the NRM component is constant $J_n(T)$ then the value of $J_n(T)$ and $J_t(T)$ (TRM acquired) can be separated from a single value of $J_n(T) + J_n(T)$ (i.e. a single heating), if the actual direction of the laboratory field is known and not parallel to $J_n(T)$. This forms the basis of the modified Thellier method (Kono and Ueno, 1976). To minimize the possible error due to misalignment of the sample and to detect effects

	All points					Best points				
Sample	Slope	F_A	S.E.	t	d.F.	Slope	F_A	S.E.	t	d.F.
BG1	2.20	1.05	0.52			2.42	1.16	0.24		
				0.58	10				0.47	4
BG2	1.80	0.86	0.34			2.57	1.23	0.14		
BG3	2.23	1.07	0.20			2.98	1.43	0.18		
				0.25	14				0.18	11
BG4	2.30	1.10	0.20			3.02	1.45	0.15		
BG5	2.49	1.19	0.14			2.97	1.42	0.11		
				0.06	30				2.05	18
BG6	2.48	1.19	0.14			2.61	1.25	0.12		
BG7						-	0.75			
Iraqi Samples										
A1/4/1	0.32	0.15	0.06			0.32	I.15	0.06		
A1/4/2	0.25	0.12	0.08	10.55	10	0.53	0.25	0.06	3.64	9
A1/4/3	0.73	0.35	0.09			0.53	0.25	0.07		
S3/1/1	1.19	0.57	0.21			0.83	0.39	0.06		
S3/1/2	1.28	0.61	0.10	0.12	14	1.04	0.83	0.04	5.92	9
S3/1/3	1.20	0.57	0.11			0.93	0.44	0.03		
Roman Brick										
1A	1.40	0.67	0.05			1.48	0.71	0.02		
				0.45	8				2.16	6
1B	1.52	0.72	0.17			1.75	0.84	0.08		
2A	1.11	0.53	0.07			1.17	0.56	0.03		
				0.52	8				1.17	6
2B	1.21	0.58	0.11			1.04	0.49	0.08		
3A	1.74	0.83	0.56			1.69	0.81	0.40		
				0.34	8				0.66	4
3B	2.57	1.23	1.40			2.83	1.36	0.88		

F_A = Ancient intensity in mT t = Student t

S.E.= Standard error d.F= degree of freedom

Table 6.5 Palaeointensity Results

caused by heating, it is thus better to make J_n and J_t orthogonal.

The palaeointensity of three Roman brick samples (Chignell St. James, Essex) was determined using this method. Since this method is based on the stability of the NRM directions during thermal heating, specimens were taken from each brick and demagnetized at 7.5, 15, 30, 40 and 50 mT. These samples were all very stable during demagnetization (S.I. >5) and so two further specimens were taken from each of the three bricks for the palaeointensity experiment. These were partially demagnetized at 2.5 mT in order to remove the viscous magnetization and then placed in the furnace holder in a position so that the NRM vector lies in a plane parallel to the axis of the furnace tube. A direct magnetic field was then applied perpendicular to the NRM direction. The sample was then heated to different temperatures and cooled in a known field of 0.048mT. Arai diagram of $J_n(T)$ vs. $J_t(T)$ (Arai diagram, Nagata et al., 1963) was plotted, and the best fit was determined using least squares fit. The direction of magnetizations should move on a great circle NRM-TRM showing that $J_n(T) + J_t(T)$ is confined in a plane defined by the NRM and TRM directions. The components of remanence vectors in the NRM and TRM direction correspond to $J_n(T)$ and $J_t(T)$ respectively so that the end points of the measured resultant vectors lie on a straight line if the experiment is successful. The end point of the vector, corresponding to higher temperature, may not fall on the straight line indicating that the TRM capacity of the sample was irreversibly altered by heating.

The halving of the number of heating in this method decreases the probability of thermochemical changes caused by double heating and also halves the time required for the original Thellier technique.

Errors during the application of this method might result from misalignment of the sample in the furnace, which induces error in the NRM components.

Two samples were taken from each of three bricks; 1A, 1B, for brick 1; 2A,2B for brick 2 and 3A, 3B for brick 3. After checking the A.F. stability of the samples, they were heated to 200°, 300°, 350°, 400°, 450° and 500°C (table 6.6).

Palaeointensity values obtained from samples 1A and 1B were similar to each other, with a student t value of 2.16 (d.f = 6), i.e. statistically the data show no significant difference at a 0.05 probability. The t value for samples 2A and 2B was 1.17 (d.f = 6) also indicating no signifcant difference at a 0.05 probability.

Samples 3A and 3B showed directional changes during heating and also intensity increases at 400°, 450° and 500°C. It is evident from fig. (6.6a) that the TRM-NRM values of samples 3A and 3B are less consistent with each other than in the other bricks, and it is more difficult to draw a regression line between these points.

The slopes of the best fit statistically show no significant difference at a 0.05 probability (t - 0.661, d.f = 4), but from the values of the two slopes and their standard errors, it is clear that there is a large difference between the two slopes accompanied by high standard errors. The high standard errors will statistically give low t values hence no significant difference, i.e. that both treatments are under the effect of similar factors (samples from similar distribution). Such errors in the results could be due to:-

1) misalignment in the furnace during heating steps

2) instability of the samples during thermal heating.

Table 6.6 Directions and Intensity Changes during Thermal Treating of Roman Bricks from Chignall St. James, Essex (modified Thellier method by Kono and Ueno, 1976)

Temp.	Dec.	Inc.	Int. (mAm^{-1})	Dec.	Inc.	Int. (mAm^{-1})
1A				1B		
Tr.	96.2	1.4	636.2	328.0	0.4	1267.3
200	96.1	1.5	620.0	328.5	0.3	1260.1
300	96.7	7.8	593.9	329.0	7.8	1248.9
350	102.9	23.2	471.6	328.2	12.4	1154.5
400	102.7	33.0	423.7	327.2	18.1	1086.9
450	111.3	56.3	395.8	321.7	45.1	816.7
500	155.5	79.4	431.7	255.7	83.3	833.8
2A				2B		
Tr.	119.1	1.6	239.8	131.3	-1.2	643.6
200	119.2	1.2	239.2	131.2	-1.2	640.5
300	118.5	15.0	197.7	130.6	10.1	552.4
350	119.3	22.8	176.8	131.9	17.0	478.9
400	115.3	32.4	167.9	127.5	25.5	469.7
450	125.8	53.0	176.8	134.3	41.5	438.8
500	116.9	77.9	183.3	122.1	66.0	400.1
3A				3B		
Tr.	147.9	7.5	89.5	126.2	1.1	26.2
200	147.8	7.4	87.1	126.0	1.1	26.0
300	147.9	23.7	82.3	127.6	14.6	23.7
350	155.3	32.1	48.8	130.0	37.0	9.4
400	146.7	48.5	50.2	137.0	44.9	10.4
450	168.2	63.1	57.4	150.8	50.8	10.4
500	171.6	78.5	49.8	121.4	71.2	5.9

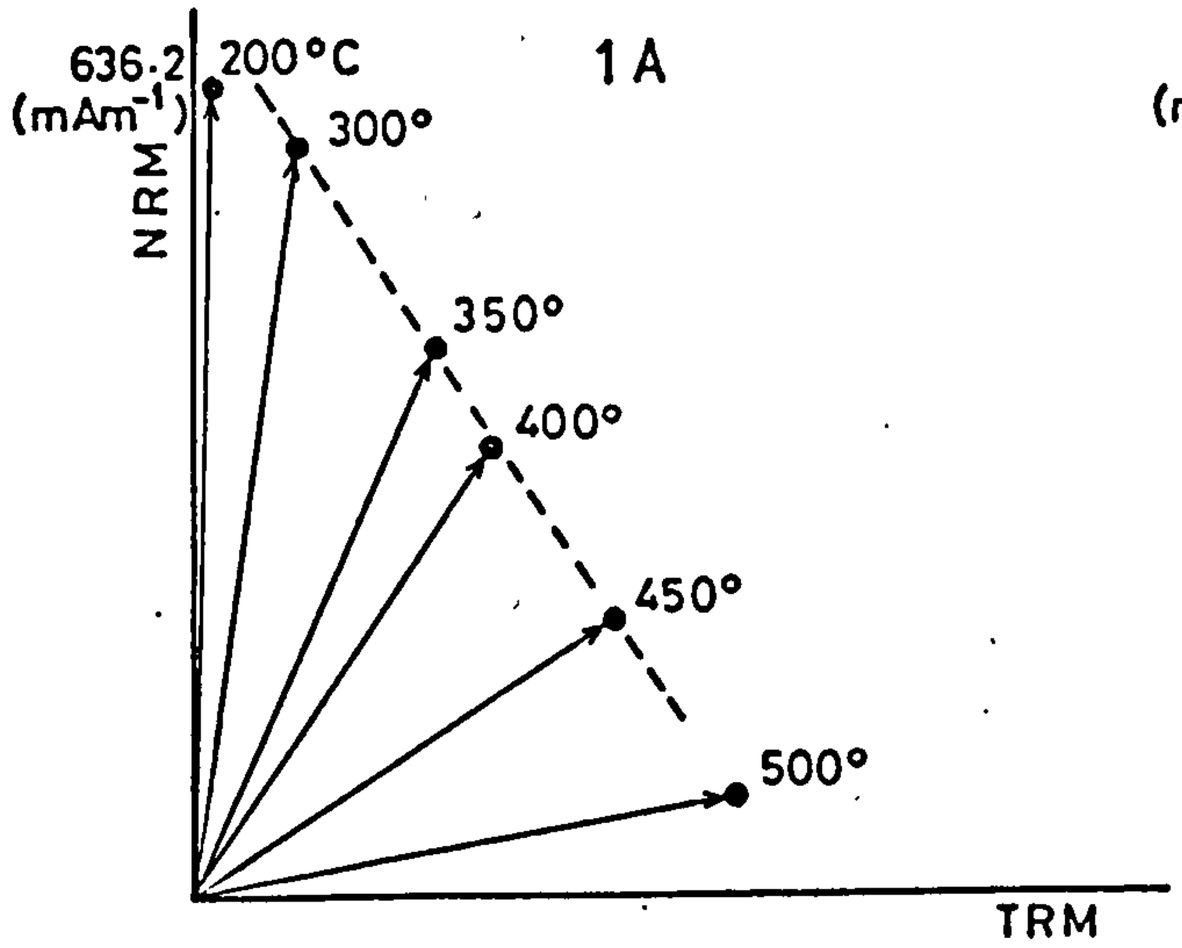

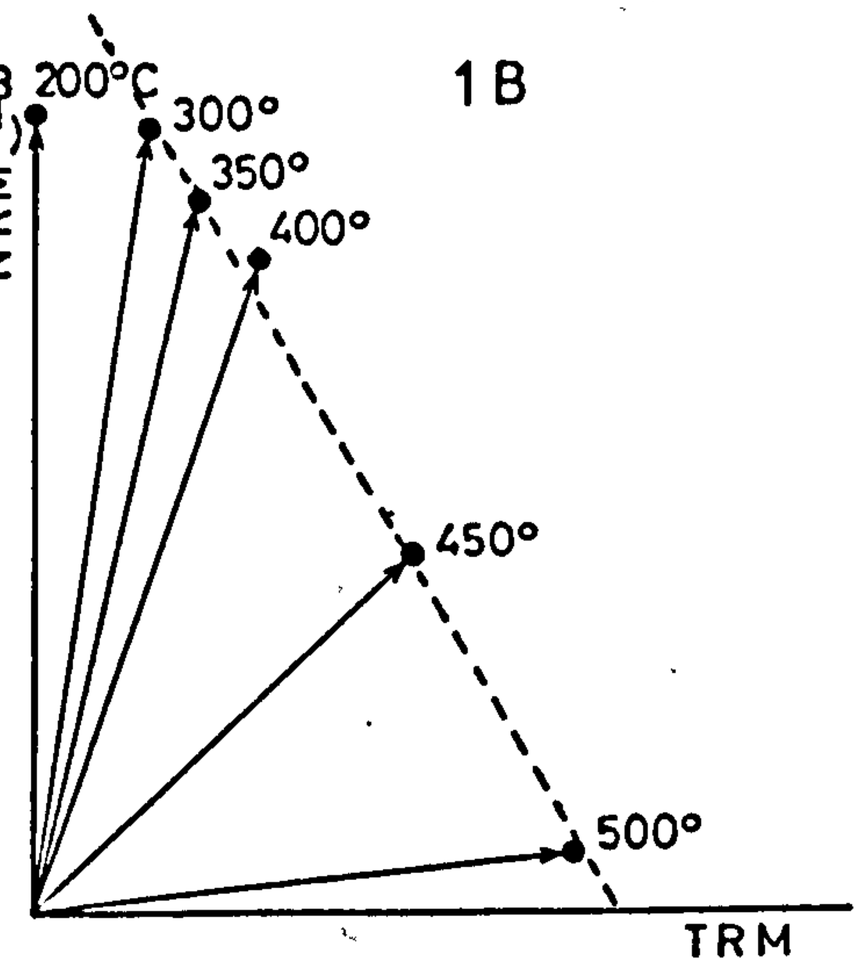

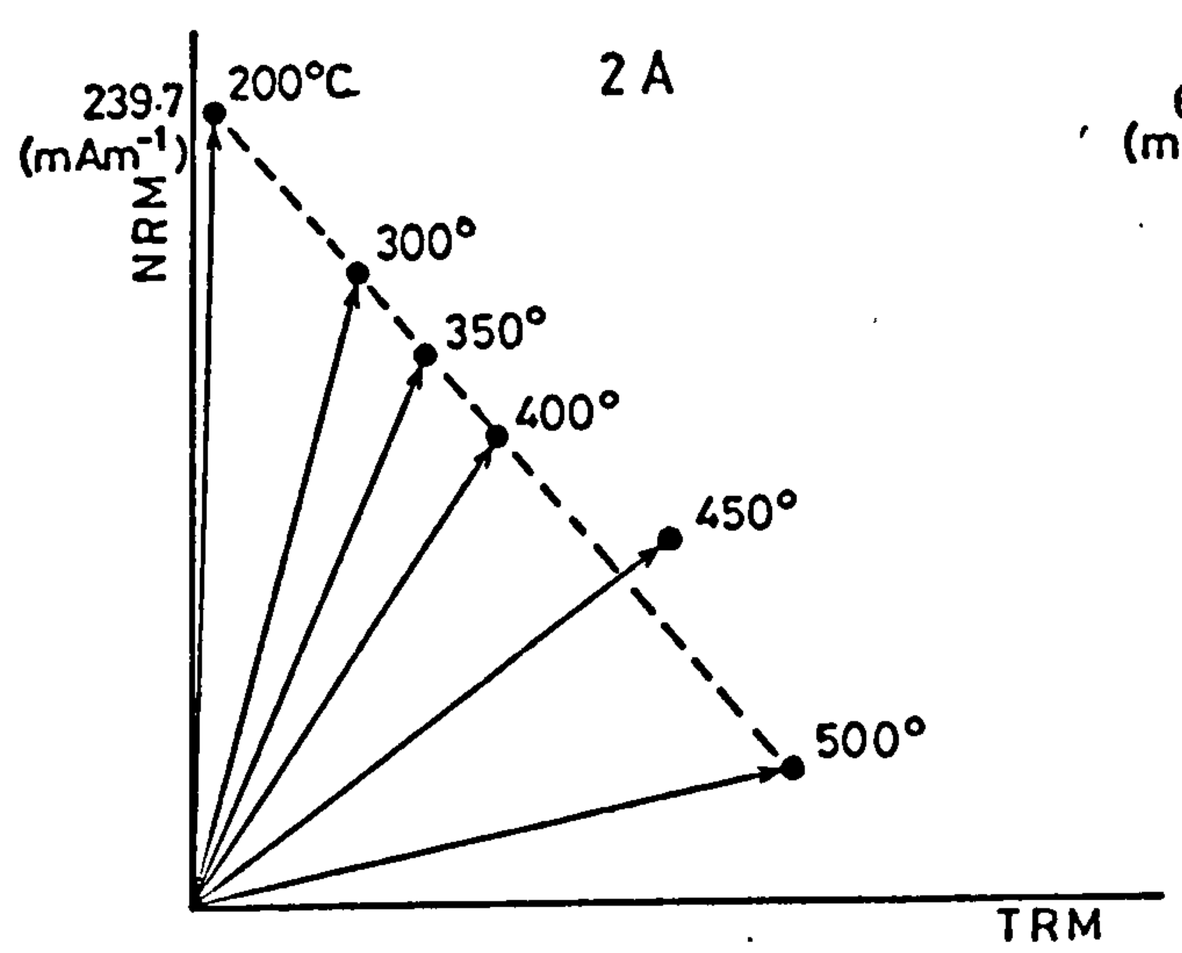

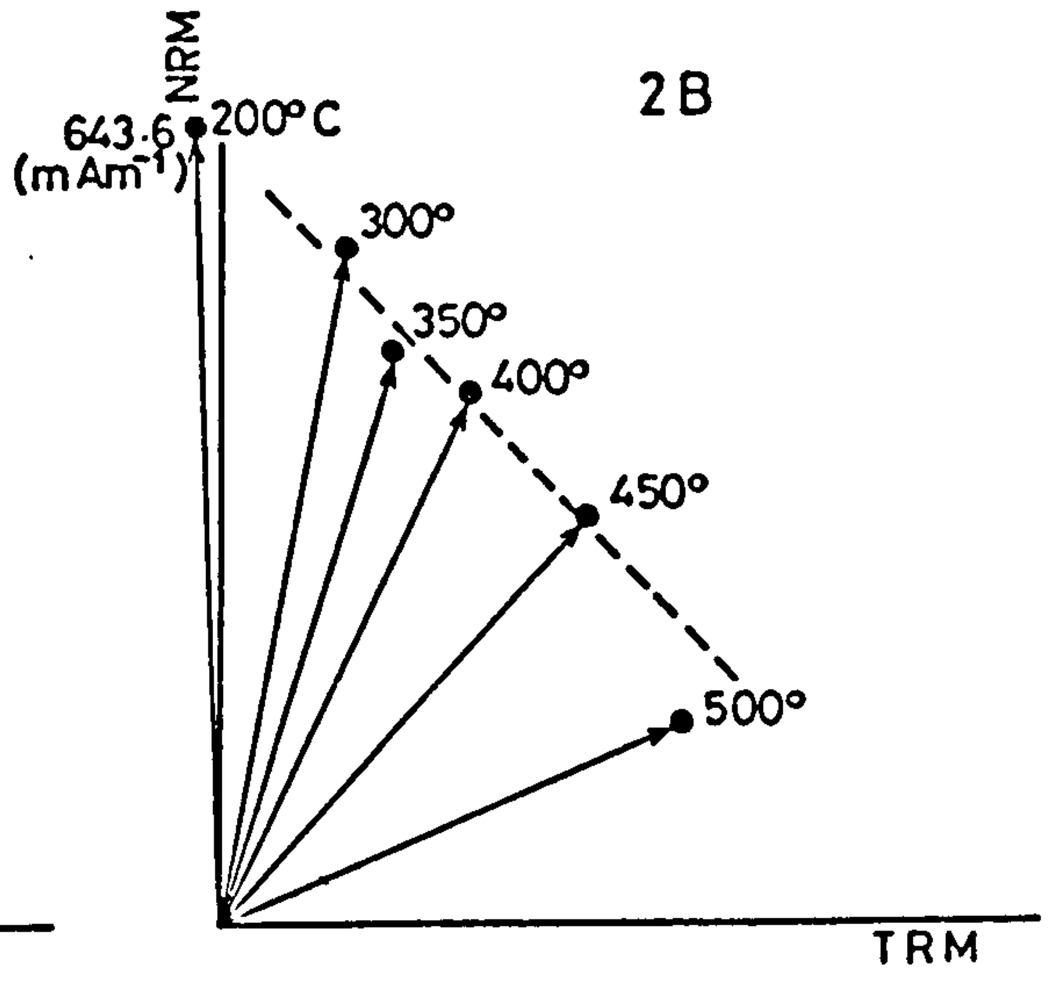

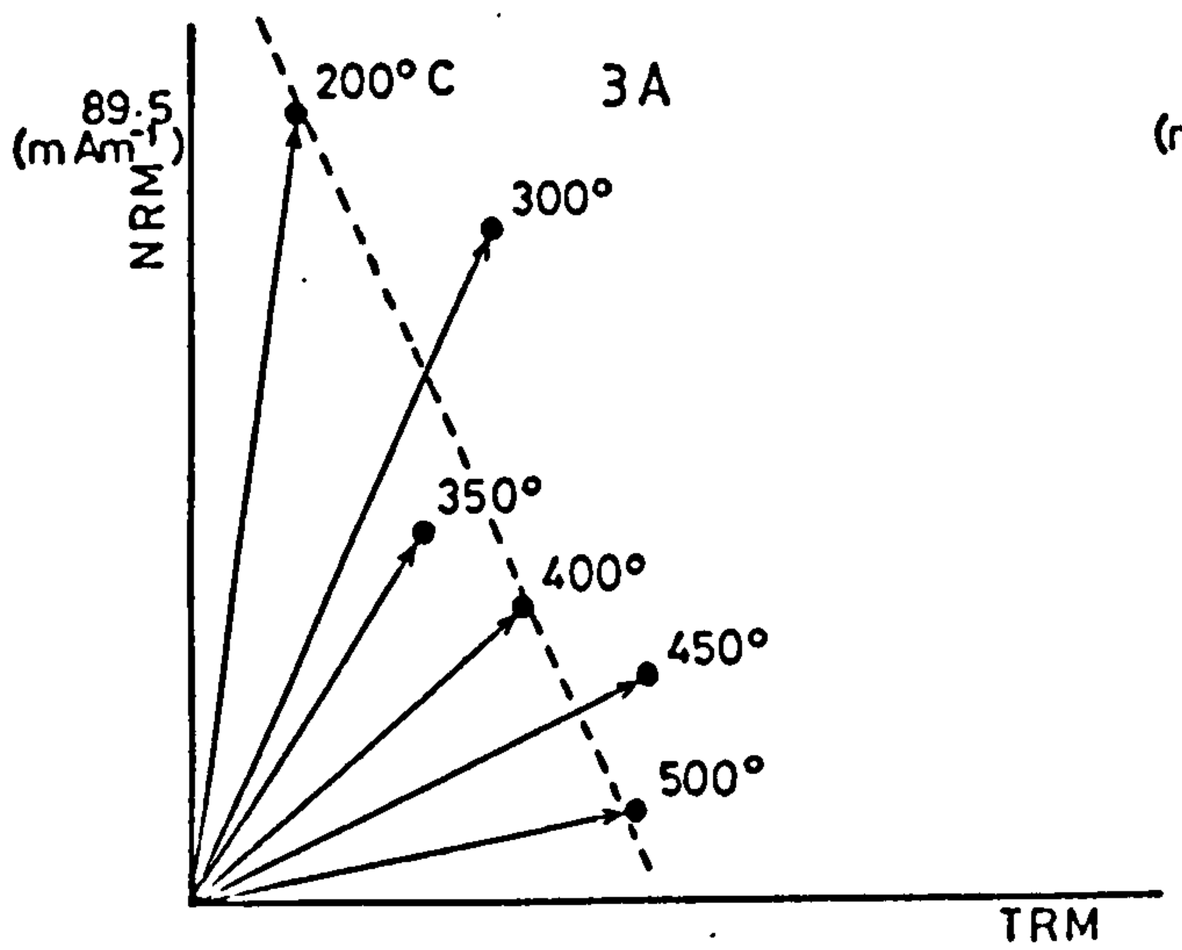

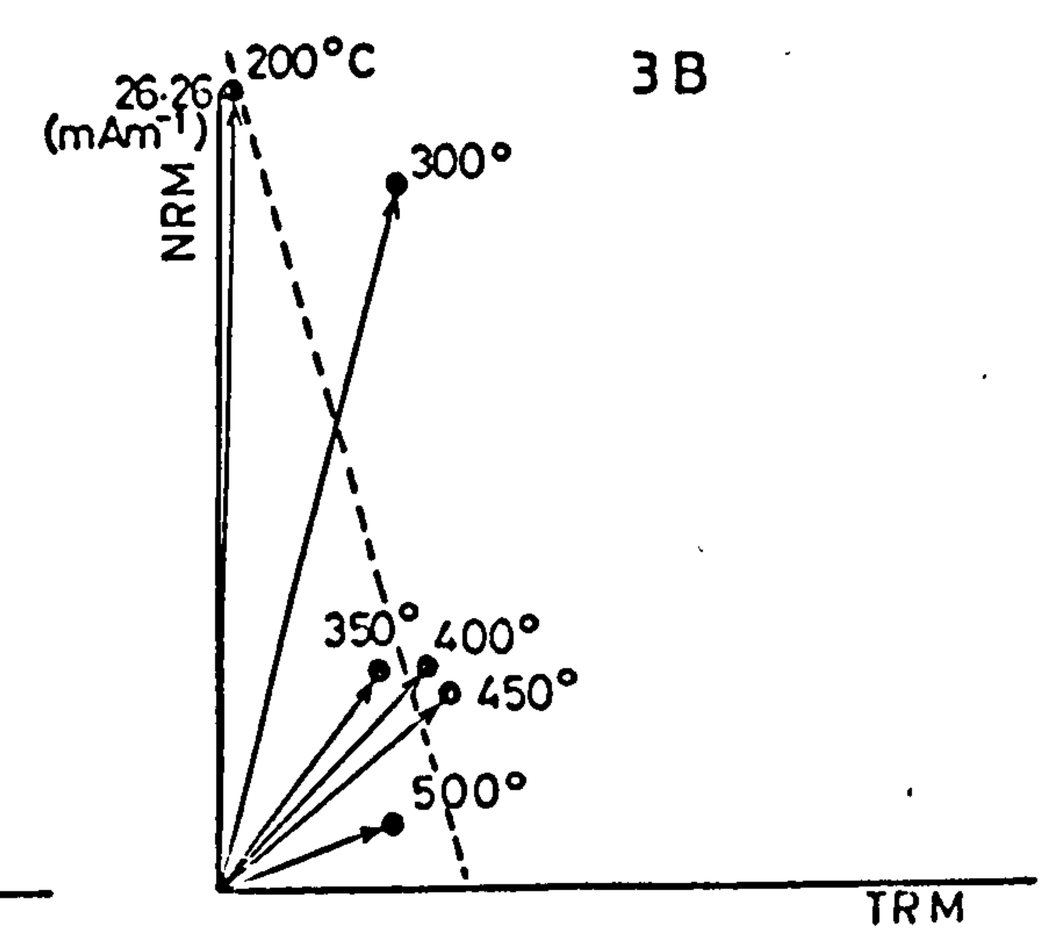

Fig. 6.6(a) The application of the modified Thellier palaeointensity method on Roman bricks from Chignal St. James, Essex

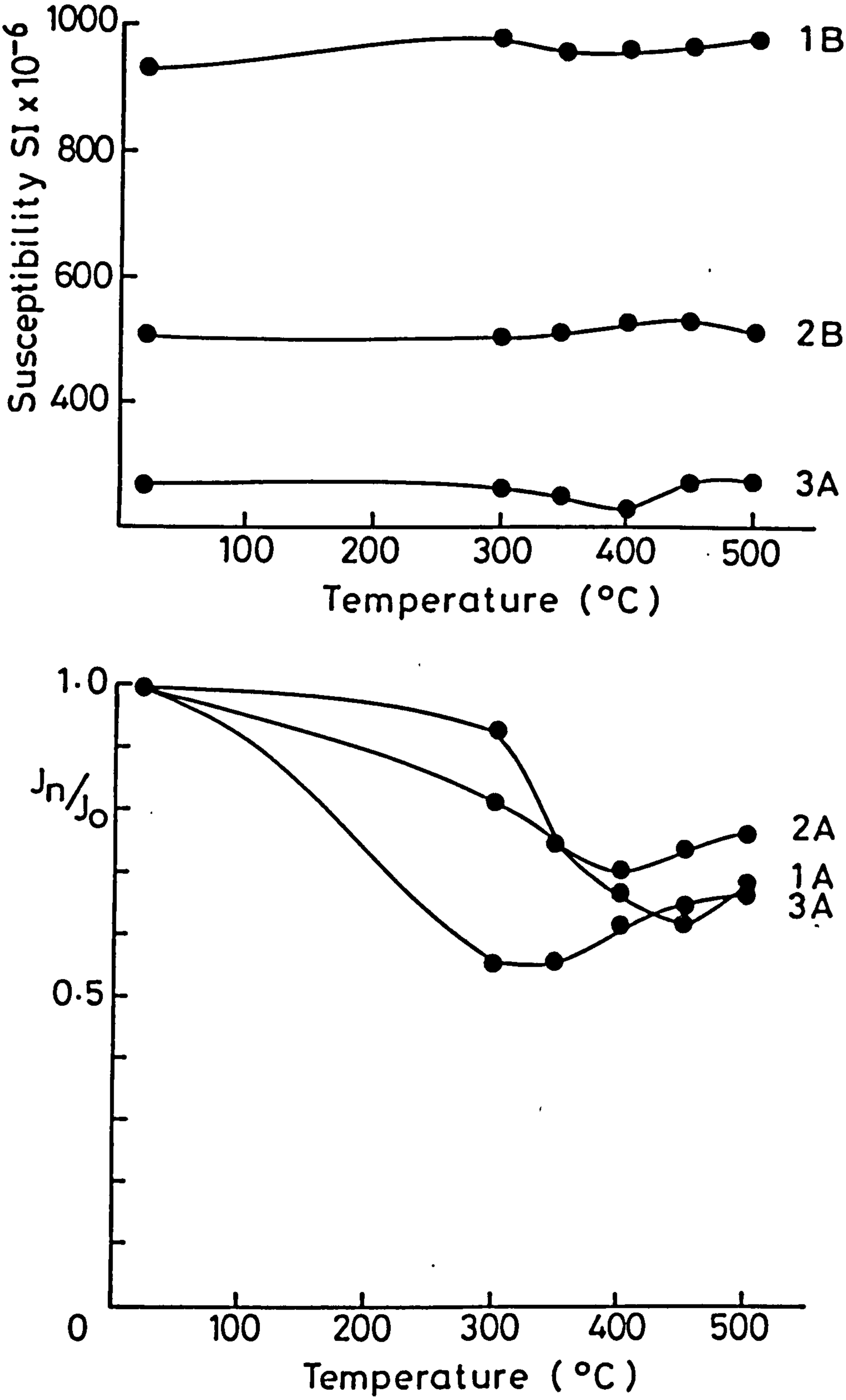

Fig. 6.6 (b) Examples of changes in Susceptibility and Intensity during thermal heating of Roman brick from Chignal St. James, Essex

However the stability of these samples was checked using A.F. demagnetization, but it is possible that they are less stable to thermal heating. This was proved by the directional changes (particularly in sample 3), and also intensity increases which occurred at 500°C in sample 1, 450° and 500°C for sample 2 and 400°, 450° and 500°C for sample 3 (fig. 6.6.).

6.2.6 The Application of Thellier Method on Iraqi Samples

The palaeointensity of nine Iraqi samples taken from three sites, A1 (Islamic), S3 and S4 (Parthian) was determined using the Thellier method (1959).

All samples were heated up to 50°, 100°, 200°, 300°, 400°, 450°, 500° and 550°C. The three samples taken from site A1 showed that they were unstable at lower temperatures. Samples A1/4/1 and A1/4/3 started to have consistent $J_n - J_t$ values at 300°C, while consistent results were obtained for sample A1/4/2 at high temperatures, despite having the $J_n - J_t$ values at 50° nearly on the best fit line. This indicates that chemical changes (within the susceptibility range) occurred at 200°C and 300°C. The palaeointensity values were nearly identical except sample A1/4/1 which had a lower value. The t value was 3.64 for d.f. = 9, i.e. these three values show no significant difference at a 0.05 probability. A similar behaviour was noticed in the three samples from site S3. Consistent $J_n - J_t$ values were obtained above 300°C and values at lower temperatures were rejected. The calculated t was 5.91 (d.f. = 9), i.e. these values are significantly different at a 5% probability.

Samples S4/2/1 and S4/2/2 from site S4 did not acquire sufficient TRM after increasing heating steps, hence the readings were not

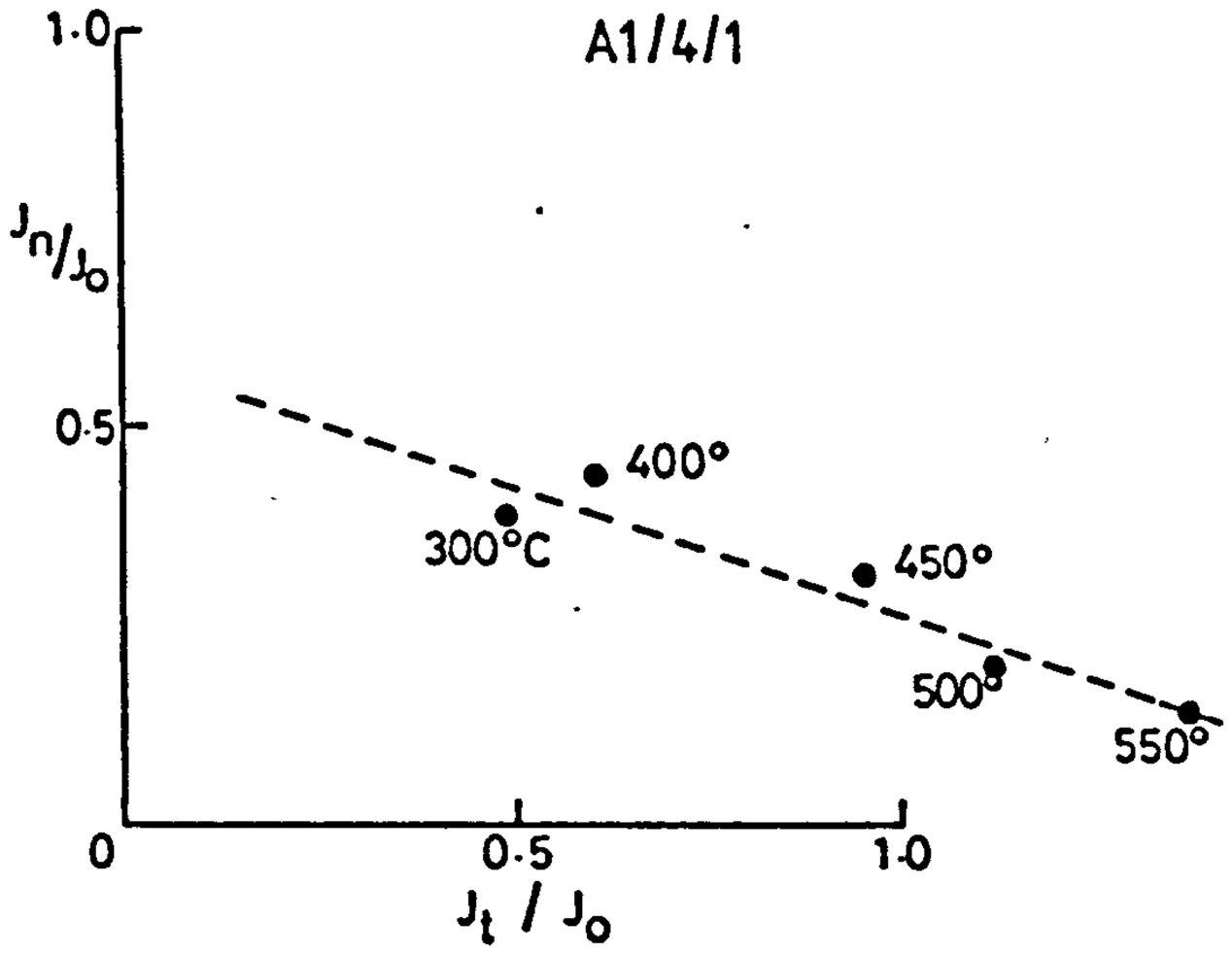

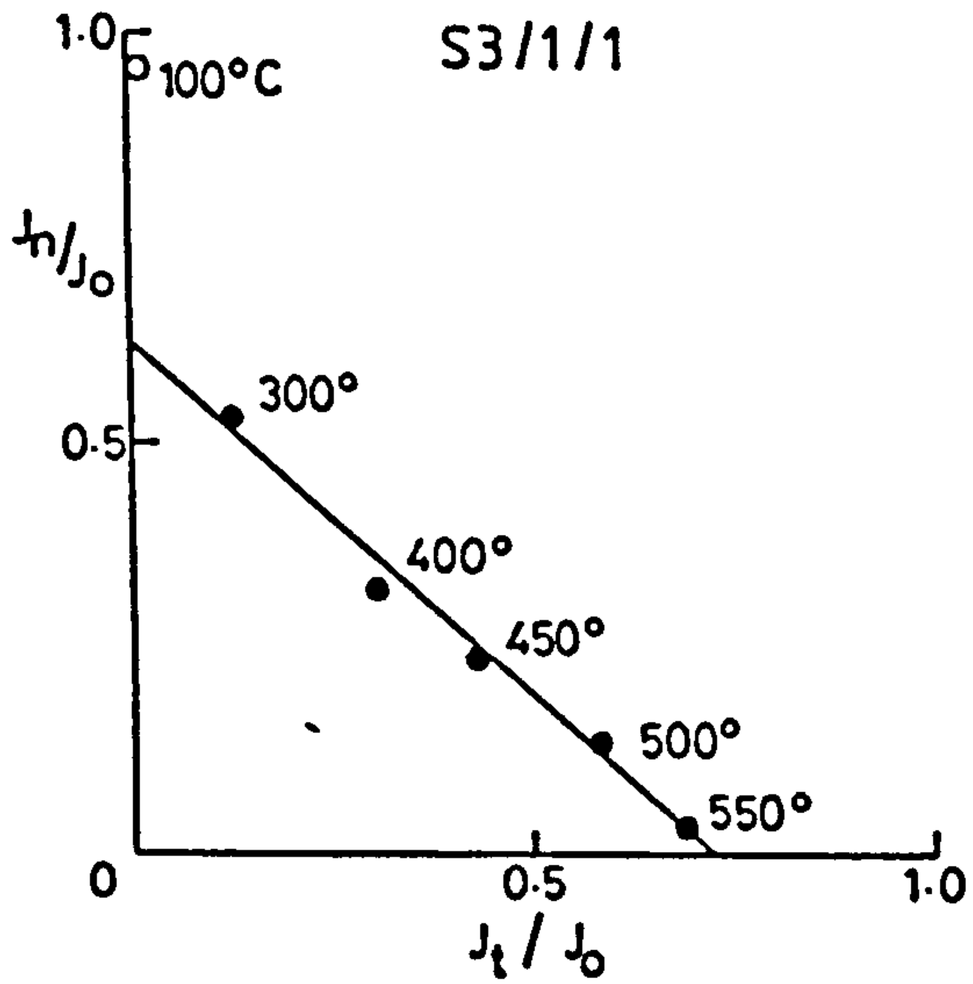

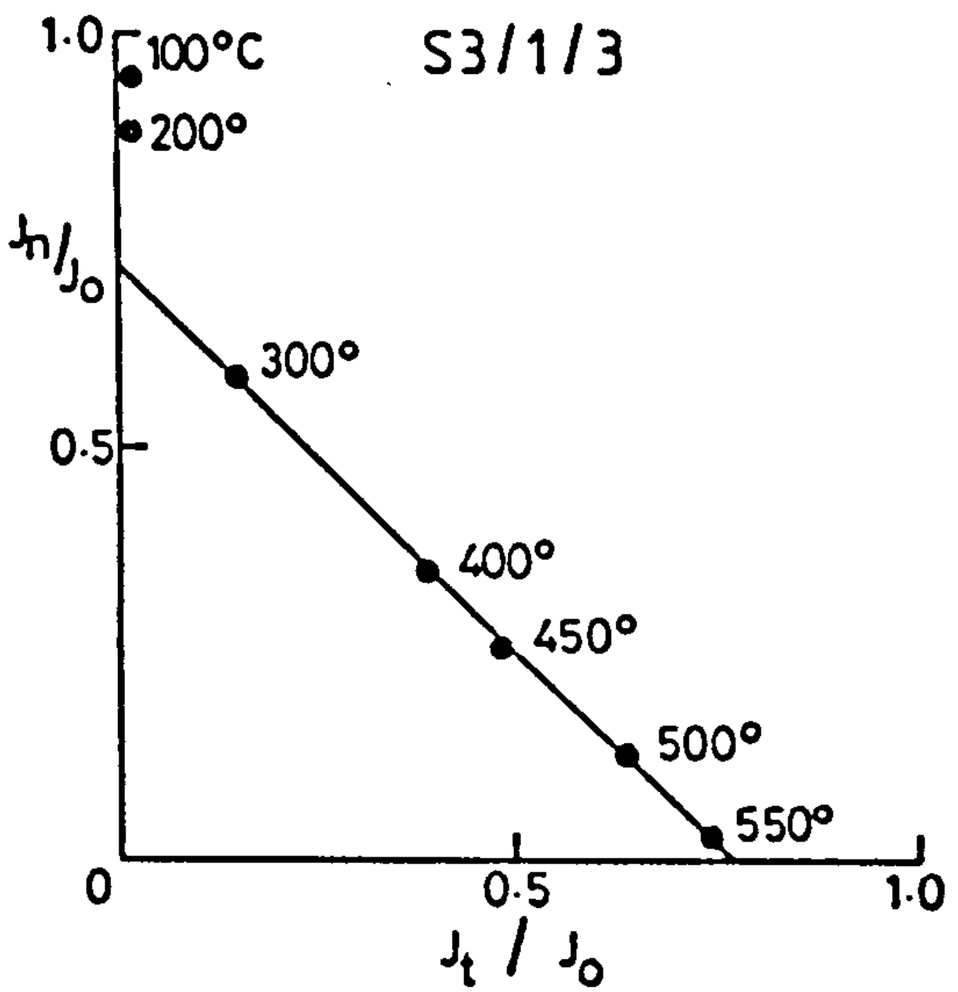

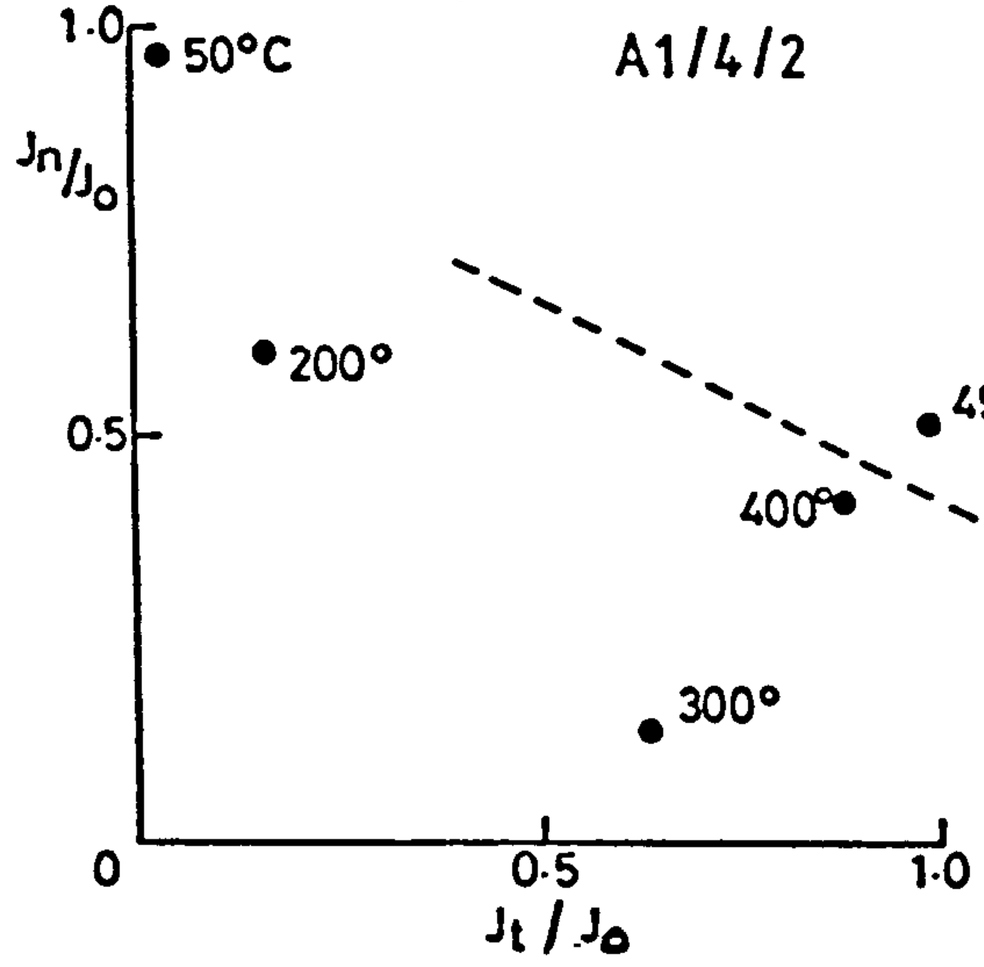

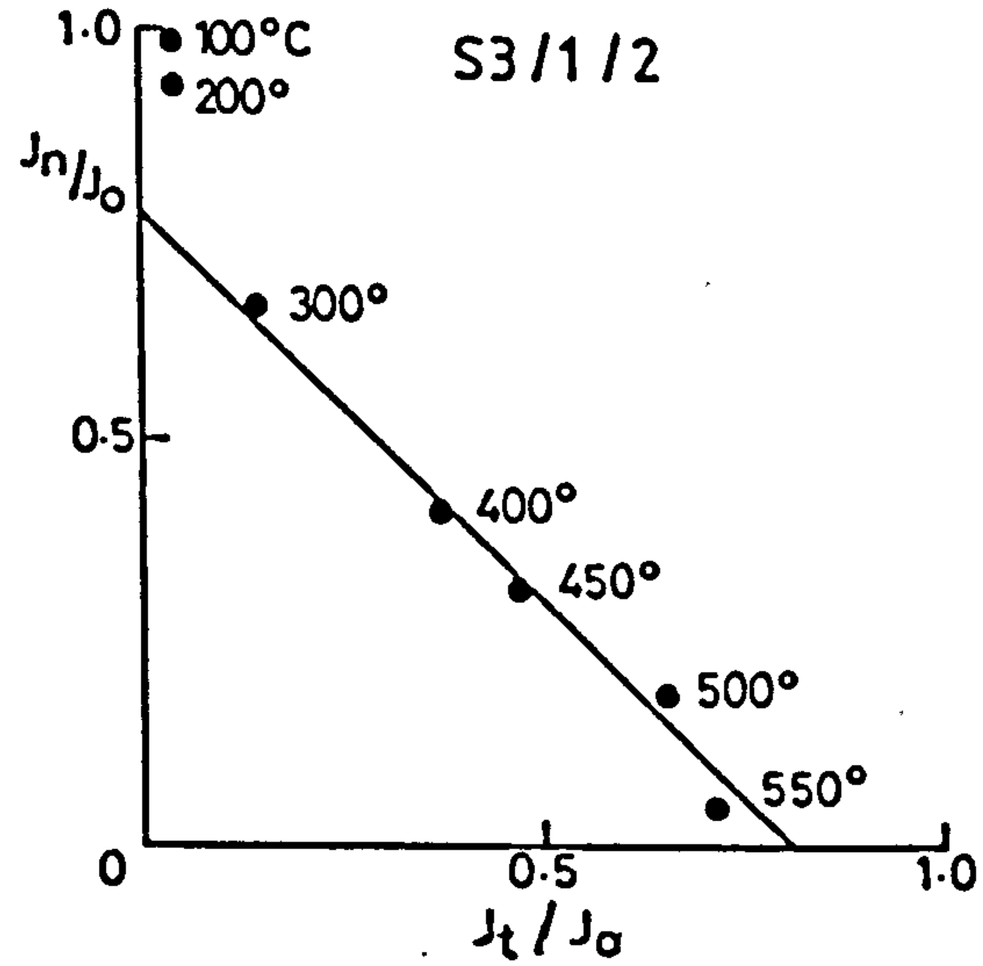

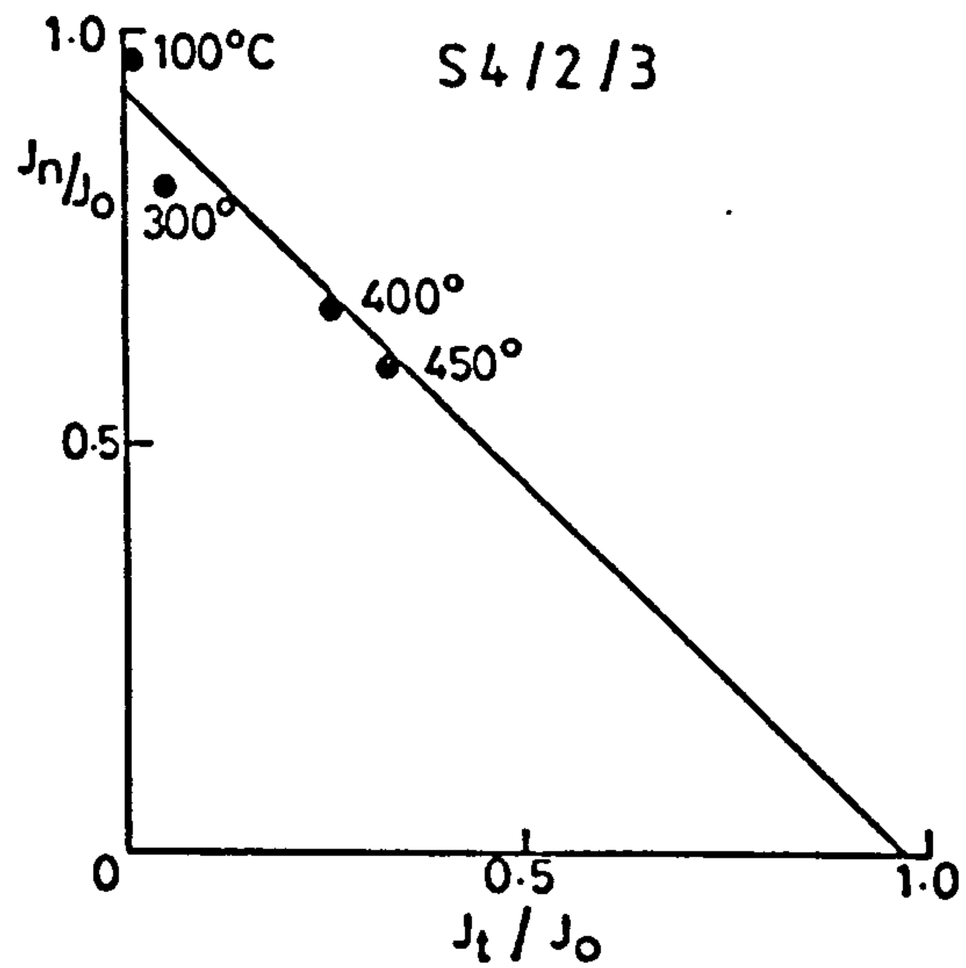

Fig. 6.7 The application of Thellier palaeointensity method on six Iraqi samples

Table 6.7 Palaeointensity Results of the Iraqi samples obtained using the Thellier method

Temp	J_n mAm^{-1}	J_a mAm^{-1}	J_t mAm^{-1}	J_{n/J_o}	J_{t/J_o}
A1/4/1					
50	502.4	476.40			
100	388.7	179.10			
200	218.3	122.20			
300	200.6	456.35	255.74	0.39	0.49
400	227.12	540.55	313.43	0.44	0.61
450	163.73	655.31	489.58	0.32	0.95
500	103.88	706.74	602.85	0.20	1.17
550	76.35	783.42	707.07	0.15	1.37
J_o = 513.93 mAm^{-1}					
A1/4/2					
50	224.4	231.70	7.3	0.95	0.03
100	210.2	122.50	-	-	-
200	141.90	179.44	37.53	0.61	0.16
400	98.53	293.20	194.67	0.42	0.88
450	120.56	350.39	229.84	0.51	0.98
500	93.14	351.07	257.93	0.39	1.10
550	71.22	359.24	288.03	0.30	1.23
J_o = 233.69 mAm^{-1}					
A1/4/3					
50	710.5	709.80			
100	704.3	388.7			
200	687.52	740.76	53.24	0.99	0.07
300	390.97	681.84	290.87	0.56	0.42
400	269.49	698.97	429.47	0.39	0.62
450	112.44	797.69	685.26	0.16	0.99
500	116.09	897.86	781.77	0.17	1.13
550	85.05	925.54	840.48	0.12	1.21
J_o = 692.25 mAm^{-1}					

Table 6.7 (continued)

Temp	J_n	J_a	J_t	J_{n/J_o}	J_{t/J_o}
	mAm^{-1}	mAm^{-1}	mAm^{-1}		
S3/1/1					
100	2585.21	2589.59	4.38	0.96	0.001
200	2390.09	2333.65	-	-	-
300	1443.59	1778.97	335.38	0.53	0.12
400	875.31	1698.41	823.10	0.32	0.30
450	650.76	1804.74	1153.98	0.24	0.43
500	349.33	1921.09	1571.76	0.13	0.58
550	96.89	1978.53	1881.64	0.04	0.69
	J_o = 2691.57 mAm^{-1}				
S3/1/2					
100	2335.15	23^8.00	62.85	0.98	0.03
200	2212.21	2268.62	56.41	0.93	0.02
300	1576.52	1915.37	338.85	0.66	0.14
400	976.08	1863.54	882.46	0.41	0.37
450	739.67	1859.22	1119.55	0.31	0.47
500	431.75	1912.50	1480.75	0.18	0.62
550	121.23	1816.57	1695.34	0.05	0.71
	J_o = 2367.79 mAm^{-1}				
S3/1/3					
100	2804.81	2862.03	57.22	0.96	0.02
200	2585.93	2621.46	35.53	0.88	0.01
300	1739.44	2184.45	445.01	0.59	0.15
400	1043.60	2192.35	1148.75	0.35	0.39
450	765.95	2181.88	1415.93	0.26	0.48
500	406.09	2274.32	1868.23	0.14	0.64
550	104.04	2269.83	2165.79	0.03	0.74
	J_o = 2928.73 mAm^{-1}				

Table 6.7 (continued)

Temp	J_n mAm^{-1}	J_a mAm^{-1}	J_t mAm^{-1}	J_{n/J_o}	J_{t/J_o}
S4/2/3					
100	131.09	131.94	0.85	0.97	0.0006
200	128.10	125.50	-	-	-
300	109.78	117.34	7.55	0.81	0.05
400	90.28	125.99	35.71	0.67	0.26
450	79.88	124.31	44.42	0.59	0.33
500	33.60	98.11	64.50	0.25	0.73

J_o = 134.41 mAm^{-1}

J_t = T.r.m. acquired

J_n = NRM remaining after cooling in a zero field

enough to plot NRM-TRM curves. This could either be due to the composition of the samples which is possibly of minerals with low Curie points as the TRM was only acquired at low temperatures, or it could be due to chemical changes affecting the TRM values only (fig. 6.7, table 6.7). However, the palaeointensity values obtained for sample S4/2/3 from the same site were consistent with the intensity of site S3 which is only a few years older than site S4 (table 6.5).

6.3 Conclusions

The reliability of any palaeointensity methods depends on many factors within each procedure, such as the number of heating steps, and which of the parameters (ARM or TRM) are taken into consideration. During the application of the Bagina and Petrova method one of the samples failed to give any results due to the fact that the behaviour of the ARM and NRM curves did not satisfy the conditions controlling the application of the method, i.e. the intersection of NRM and ARM coercive spectra. In addition the method depends on a similarity between ARM and NRM, which are often dissimilar, and the displacement between their maximum peaks. These are considered to be major limitations in the method. In addition, the Bagina and Petrova method, like other ARM palaeointensity methods, might still suffer from problems with the acquisiton of a spurious ARMs, which can cause non-linearity and dissimilarity between the ARM and NRM. Accordingly some doubts must be raised about the general reliablity of the Bagina and Petrova palaeointensity method.

The Shaw method was used to obtain the palaeointensity of two samples. These results showed significant differences at a 5% level with a difference of 0.36 between the slopes. This was higher than the

differences obtained in the Thellier and Van Zijl methods. Although the Shaw method depends on a comparison of the TRM and NRM using the regions of unaltered coercive force spectra, the method still suffers from problems with spurious ARM, and also incomplete demagnetization of the NRM and TRM. Hence the best fit regression line is not constrained to pass through the origin (method assumes complete demagnetization). . Shaw method was also found to be very slow.

The Van Zijl method gave results which are nearly identical with slope difference of only 0.04 and also with low standard errors. The method was found easy and quick, but since it assumes a complete demagnetization of the NRM, the palaeointensity results obtained from samples with incompletely removed NRM could be misleading. On the other hand, since the sample must be heated above its Curie temperature before the demagnetization of the laboratory induced TRM can be measured, then there is the possibility of chemical changes during heating which will make the comparisons between the NRM and TRM consistent but unreliable.

While the Van Zijl method gave the most consistent results, there is the possibility of consistent error in the technique, therefore in conclusions it was found that the Thellier method is still considered to be the most reliable, despite problems with possible chemical changes. The Kono and Ueno method (1976) could also yield reliable results if oriented properly in the furnace, and also if the anisotropy effect is negligible.

CHAPTER 7 CHARACTERIZATION OF IRAQI OBSIDIAN SAMPLES

7.1 Introduction

Obsidian (volcanic glass) is a form of lava which has been completely fused. It has a conchoidal fracture and a hardness that made it particularly useful for the manufacture of artefacts. The source material can only be derived from particular strata, and worked materials must have been carried by trade if found at any distance from these centres. The presence of obsidian objects in a non-volcanic country is thus proof of trade with some centre of volcanic activity (Wainwright, 1927, 1977). Wainwright demonstrated the use of obsidian as an indicator of contact and communications. If obsidian artefacts associated with archaeological sites can be identified with the particular geological source from which the material was obtained, then the geographical extent of cultural contact and indeed the routes followed by the traders, can be proven.

The procedure of distinguishing the sources from one another is termed 'characterisation' (Cann et al., 1969). A characterisation study involves the detection of properties of the samples under study which ideally are uniquely characteristic of material from a particular obsidian flow. When all the geological obsidian sources in a particular archaeological region have been thus 'fingerprinted' the archaeological material can then be assigned to specific sources. An adequate characterisation of obsidian thus entails demonstrating homogeneity within a geological source and heterogeneity between sources. This necessitates intensive within-source sampling to show the degree of internal consistency and thus assess the bounds within which the material may be considered as homogeneous,

(McDougall, 1978).

Several methods of analysis have been used with varying success to characterize obsidian. These methods were mainly based on refractive index, colour, density, petrology and a variety of geochemical analyses, including quantitative analysis, such as neutron activation and x-ray fluorescence (Taylor, 1976). More recently, McDougall (1978) investigated the possibility of using the magnetic properties as a means of discrimination. The intensity of remanent magnetization, the low field susceptibility and the saturation magnetization may be expected to vary from one obsidian flow to another with difference in composition, form and concentration of ferrimagnetic oxides, and the intensity of natural remanence will also be related to the strength of the geomagnetic field which is also likely to differ for different aged flows. After examination of her results, McDougall suggested that sources could be best distinguished on the basis of two variables; intensity of saturation magnetization and intensity of natural remanent magnetization. A third variable, the low field mass susceptibility, also proved, on occasions, to be a useful discrimination. Effective saturation magnetization was defined as that attained on application of a direct magnetic field of 350 mT, thus avoiding subjective estimation of the intensity value by visual examination of the magnetization curve.

Known obsidian sources in the Mediterranean region are shown in Fig. (7.1). The map should be comprehensive for Europe, but several new sources have recently been reported in West Anatolia, and the extent of those in the south and in Armenia is not yet known. No sources are yet known from Iraq, Syria, Lebanon and Jordan but there are several volcanic districts in this region, such as the Jebel Druz and the possibility of new sources being discovered cannot be ruled out.

In the Iraqi archaeological sites, obsidians are reported from virtually all settlements although the sites are distant from the natural sources (fig. 7.1). However, it has been stated that no obsidian sources are believed to exist between Anatolia and Arabia west of the Zagros mountain range. The nearest known obsidian sources to Iraq can be classified as follows:-

1. Armenia
2. South Anatolia
3. Lake Van
4. Abyssinia and Arabia

The Arpachiyah site in northern Iraq utilised 3 different obsidian sources: Lake Van, Armenia, and South Anatolia (Cann and Renfrew, 1964).

The refractive indices (R.I.) and density of obsidian were considered by Cann and Renfrew (1964), for a number of samples in and around the Mediterranean. Obsidians with refractive indices less than 1.495 are generally alkaline or calc-alkaline; this includes obsidians from Armenia and South Anatolia. Obsidians with refractive indices greater than 1.505 belong to the perkaline type and include obsidians from Lake Van, Abyssinia and Arabia. Chemical analysis of the Lake Van, Abyssinian and Arabian sources showed that these sources have similarities in the content of Barium-Zirconium and Niobium-Yttrium (Cann and Renfrew, 1964). Appearance proved to be another reliable guide. The peralkaline obsidians appeared to be greenish or brown in transmitted light and calc-alkaline and alkaline obsidian appeared grey or colourless (Renfrew et al., 1965).

McDougall (1978) showed that obsidians from South Anatolia and Lake Van are characterized by high saturation magnetization, as reflected

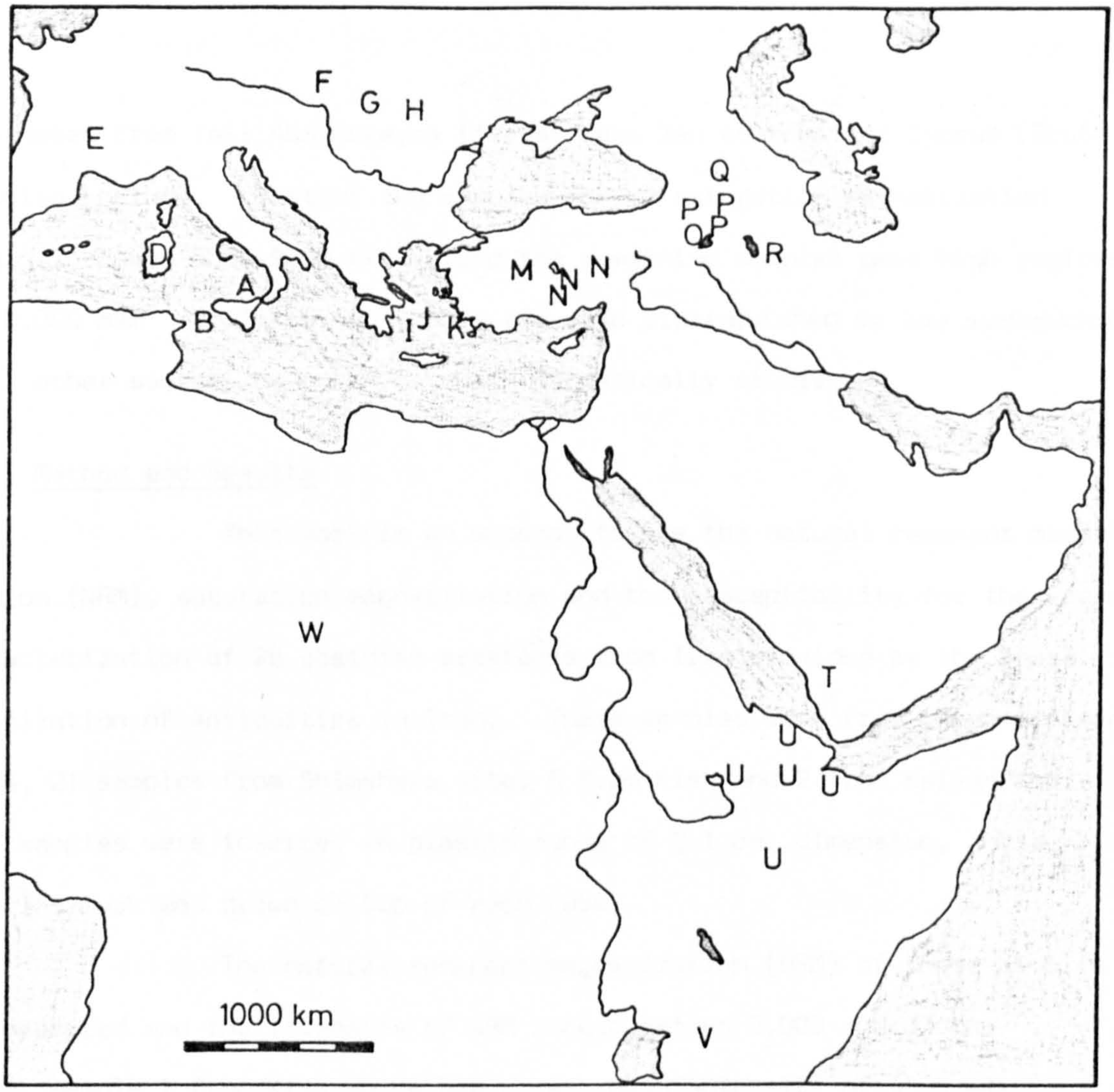

Fig. 7.1 Obsidian sources in and near the Mediterranean region

A: Lipari, B: Pantelleria, C: Palmarola, D: Sardinia, E: Auvergne,
F: Slovakia, G: Tokay region in Hungary, H: Mt. Hargitta in Rumania,
I: Melos, J: Antiparos, K: Giali, M: Afyon, N: South Anatolian sources,
O: Lake Van, P: Armenian sources, Q: Caucasus, R: Lake Urmia, T: Arabia,
U: Abyssinian sources, V: Kenya, W: Tibesti.

by samples from Tell Abu Hureyra (Syria, Lake Van source) and Cyprus (South Anatolia source). Most of the samples showed saturation magnetization ranging between 5000-9000 mAm^{-1}, and the remaining samples gave high regions of 20,000 mAm^{-1}. These two groups are also distinguished by low susceptibility. The other sources have not yet been magnetically studied.

7.2 Method and Results

This work is an attempt to use the natural remanent magnetization (NRM), saturation magnetization and the susceptibility for the source characterization of 28 obsidian artefacts from Iraq provided by the State Organization of Antiquities in Iraq. These samples were from three different sites, 21 samples from Shimshara site, 5 from Kish and 2 from Kaleag Aga. All samples were inserted in plastic cubes of 2.1 cm. dimension, and a fiducial mark was drawn on top of each cube.

The natural remanent magnetization (NRM) of these samples was measured and the intensity of NRM ranged betwen 0.009 - 0.33 mAm^{-1} except sample 1 from Kish which had a very high intensity of 45.5 mAm^{-1} (Table 7.1). During measuring the susceptibility, all samples gave either negative or no deflection on the susceptibility bridge. This was the case even with the largest samples, and hence no values for the susceptibility were obtained, although it is clearly very low. Saturation magnetization was achieved using an iron-cored electromagnet producing a high field in a 3 cm. gap. Samples were inserted into the pole gap and the field was applied in the direction of the fiducial mark. All samples were given fields of 150, 300 and 350 mT. Changes in magnetization were small with increasing applied field, and some of the samples showed similar inten-

sity values in all the three applied fields (Table 7.1). Sample 1 from Kish was again anomalous, showing very much higher saturation values than all other samples.

After determining the magnetic properties, their refractive indices were determined (Table 7.1). Small pieces from each sample were crushed and put on thin section slides. These crystals were then mixed with liquids of known refractive indices. The sections were then studied under the microscope and the refractivity of each sample was obtained depending on the direction towards which the light aureole surrounding the grain moves, as they usually move towards the substance with high refractive index. Accordingly, different liquids were used until the aureole disappears, indicating equality in the refractivity between the crystals and the surrounding liquid.

All but one sample had refractive indices of 1.506, which is greater than 1.505 (peralkaline) and is typical for the Lake Van, Abyssinian and Arabian sources. A single sample from Kish gave a lower value, 1.484.

Conclusion

The NRM and susceptibility of all samples did not show any variability, except for one anomalous sample from Kish which showed a relatively higher initial intensity of magnetization. The saturation magnetization showed a much better grouping than the Syrian and Cyprus groups (previously characterized by McDougall, 1978) (fig. 7.2). The grouping of the Iraqi obsidian is characterized by low saturation magnetizations ranging betwen 0.01 - 0.35 mAm^{-1} with the exception of one anomalous sample from Kish, which gave a higher saturation magnetization value. Using the Refractive Indices and colour (dark greenish) (fig. 7.2) these obsidians

are classified as Peralkaline, which is typical of Lake Van, Abyssinian and Arabian sources. Since Lake Van obsidians show higher magnetization, the most probable obsidian sources for these Iraqi samples is Abyssinian, Arabian or another un-named source. However, the Kish sample, which is anomalous in terms of both refractive index and magnetization, is magnetically close to the Lake Van group. On this basis, this sample is thought to have originated from Lake Van source, although the low refractive index of this sample would then have to be due to local inhomogeneity within that source.

The present work proved that the magnetic characterization method can be used as a tool to distinguish between the obsidian sources of Lake Van, Abyssinia and Arabia, which were very difficult to separate using chemical and other physical analysis.

Table 7.1 NRM Saturation magnetization and Refractive Indices of Iraqi Obsidian Samples

Sample No.	I_{NRM} mA/m	$I_{150\ mT}$ mA/m	$I_{300\ mT}$ mA/m	$I_{350\ mT}$ mA/m	R.I.
Site - Shimshara					
1	0.02	1.75	3.31	3.53	
2	0.15	17.23	20.41	19.62	
3	0.03	1.49	3.86	3.51	
4	0.01	1.15	2.34	1.90	
5	0.04	4.35	6.99	4.47	
6	0.28	6.26	7.19	6.41	
7	0.04	7.91	8.88	7.73	
9	0.04	2.83	4.25	3.87	
10	0.1	7.28	7.91	6.98	
11	0.03	4.22	4.72	4.84	1.506
12	0.13	36.46	43.98	38.55	
13	0.01	5.69	5.37	4.95	
14	0.01	9.68	9.82	8.71	
15	0.05	3.85	4.29	3.34	
16	0.03	3.55	3.44	2.59	
17	0.07	4.58	4.98	4.21	
18	0.13	4.58	4.98	4.21	
19	0.07	4.82	4.92	5.38	
20	0.07	4.16	4.46	3.71	
21	0.33	7.49	6.72	5.58	
Site - Kish					
1	45.50	336.64	551.13	566.96	1.484
2	0.06	4.48	4.86	6.40	
3	0.07	4.53	4.72	5.67	
4	0.02	4.06	4.15	5.15	
5	0.04	3.28	3.39	3.39	
					1.506
Site - Kaleag Aga					
1	0.04	4.11	3.97	3.80	
2	0.14	5.81	7.16	7.63	

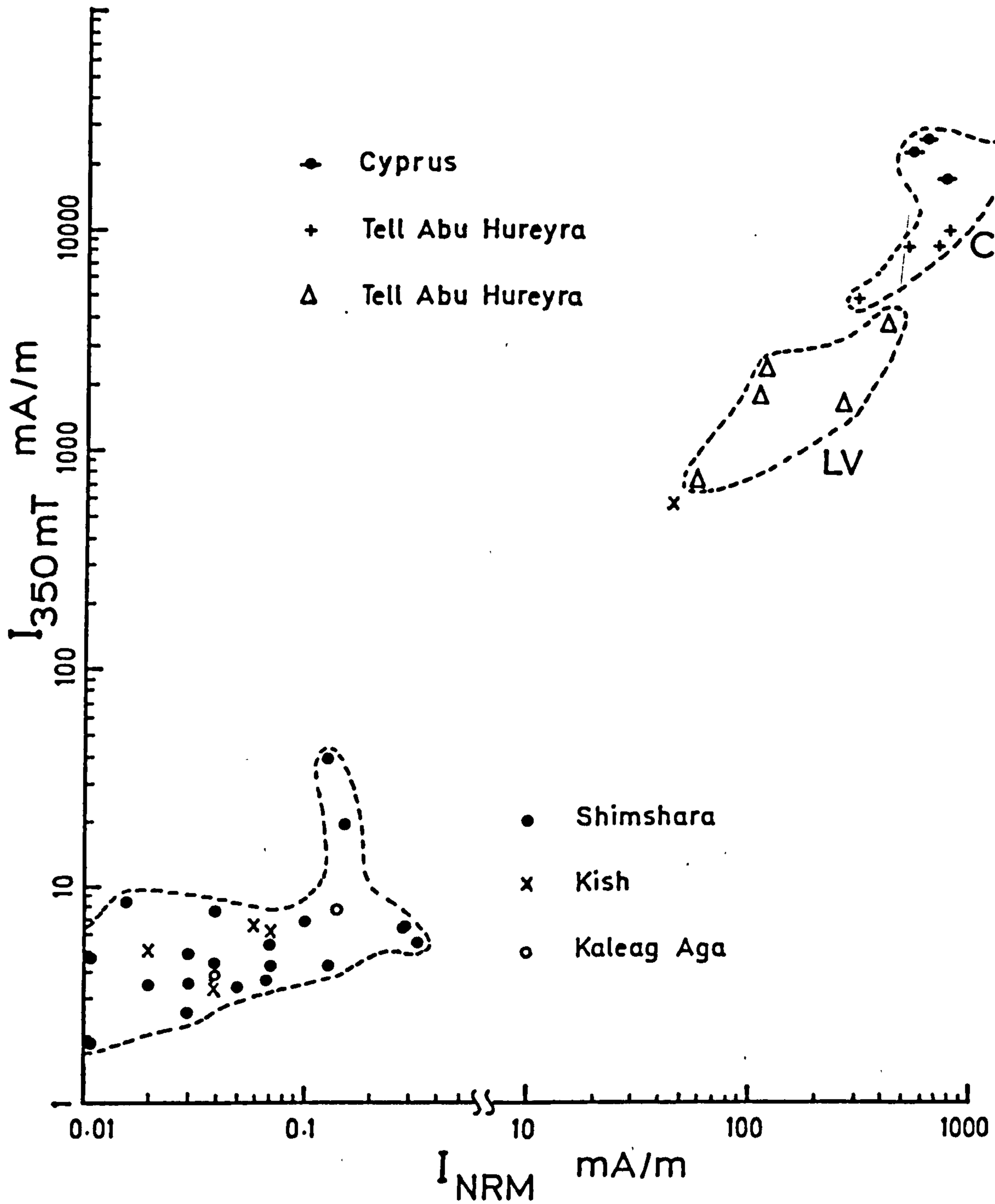

Fig. 7.2 Initial intensity and saturation magnetization of Iraqi, Syrian and Cyprus obsidians

LV : Lake Van Source

CI : Çiftlik

REFERENCES

Addyman P.V. (1980) Excavating Viking Age York. (Salvage archaeologists rescue trade center) Archaeology, V.33, No.3.

Aitken M.T. (1970) Dating by Archaeomagnetism and Thermoluminescent methods. Phil. Trans. R.Soc. Lond. A.269, 77-88.

Aitken M.J., Alcok P.A., Bussell G.D. and Shaw C.J. (1981) Archaeomagnetic determination of the past geomagnetic intensity using ancient ceramics, allowance for anistropy. Archaeometry, 23, 53-64.

Aitken M.J., Hawley H.N. and Weaver G.H. (1963) Magnetic dating: Further archaeomagnetic measurements in Britain. Archaeometry, 6, 76-80.

Aitken M.J. and Hawley H.N. (1966) Magnetic dating III. Further archaeomagnetic measurements in Britain. Archaeometry, 9, 187-97.

Aitken M.J. and Hawley H.N. (1967) Archaeomagnetic measurements in Britain, IV. Archaeometry, 10, 129-35.

Aitken M.J. and Hawley H.N. (1971) Archaeomagnetism: Evidence for magnetic refraction in kiln structures. Archaeometry, 13, 1, 83-5.

Aitken M.J. and Weaver G.H. (1962) Magnetic dating: Some archaeomagnetic measurements in Britain. Archaeometry 5, 4-22.

Aitken M.J. and Weaver G.H. (1964) Recent archaeomagnetic results in England. J. Geomagn. Geoelect. 17, 393-96.

As J.A. and Zijderveld J.O.A. (1958) Magnetic cleaning of rocks in palaeomagnetic research. Geophys.J. Roy.Astr.Soc., 1, 308-19.

Bagina O.L. and Petrova G.N. (1977) Determination of palaeomagnetic field intensity using Anhysteretic Remanent Magnetization. Physics of the Earth and Planetary Interiors. 13, 363-67.

Basmachi F. (1976) Treasures of the Iraqi Museum. Ministry of Information, Al-Jumhuriya Press.

Bathal R.S. (1971) Magnetic anisotropy in rocks. Earth Sci. Res., 7, 227-53.

Baur L.A. (1899) On the Secular Variation of free magnetic needle. Phys. Rev., 3, 34-8.

Bray W. and Tramp D. (1970) The Penguin Dictionary of Archaeology. Hazell Watson and Viney Ltd.

Briden J.C. (1972) A stability index of remanent magnetism. Journal of Geophysical Research 77, 8.

Bucha V. (1970) Influence of the Earth's magnetic field on radiocarbon dating. In RadioCarbon Variations and Absolute Chronology (ed. Olsen). p.501 Wiley-Interscience, New York.

Bullard E.C. and Gellman H. (1950) Homogeneous dynamoes and terrestrial magnetism. Phil. Trans. Roy.Soc. Lond.A. 243, 67-159.

Cann J.R. and Renfrew C. (1964) The characterisation of obsidian and its application to the Mediterranean region. Proc. Prehistoric Society, 30, 111-32.

Cann J.R., Dixon J.E. and Renfrew C. (1969) Obsidian Analysis and Obsidian trade. In Brothwell D. and Higgs E.S. Science and Archaeology, 578-991.

Clark A.J. (1979) Archaeomagnetic dating. In Thompson F.H., Three Surrey hillforts: Excavations at Anstiebury, Holmbury and Hascombe, 1972-77. Ant. J. LIX, 245-318.

Clark A.J. (1980) Magnetic Dating. Sussex Archaeological Collections 118, 7-12.

Clark A.J. (1983) Archaeomagnetic measurements on the Neatham hearth. Ancient Monuments Laboratory (Unpublished Report).

Clark A.J. (1983) Archaeomagnetic dating at Bigberry. Ancient Monuments Laboratory (Unpublished Report).

Clark A.J. (1983) Archaeomagnetic dating of the Medieval pottery kiln at Carrickfergus, Co. Antrim. Ancient Monuments Laboratory (Unpublished Report).

Collinson D.W. (1965a) Origin of remanent magnetization and initial susceptibility of certain red sandstone. Geophys. J. Roy Astr. Soc., 9, 203-17.

Collinson D.W. (1965b) Depositional remanent magnetization in sediments. J. Geophys. Res., 70. p.4663

Collinson D.W. (1966) Magnetic properties of the Taiquati Formation. Geophys. J. Roy Astr.Soc., 11, 337-47.

Collinson D.W. and Molyneux L. (1967) An instrument for the measurement of isotropic initial susceptibility of rock samples. In Methods in Palaeomagnetism (eds. D.W. Collinson, K.M. Creer and S.K. Runcorn) Elsevier, Amsterdam, pp.368-71.

Cook R.M. and Belshe J.C. (1958) Archaeomagnetism: a preliminary report on Britain. Antiquity, 32, 167-78.

Cox A. (1961) Anomalous remanent magnetization of basalt. Geol. Surv. Bull. 1083-6, 131-160.

Creer K.M. and Kopper J.S. (1976) Secular oscillations of the geomagnetic field recorded by sediments deposited in caves in the Mediterranean region. Geophys. J.Roy. Astr. Soc., 45, 35-58.

Crew P. (1981) An Interim Report on the first two seasons of the excavations in Bryn Y. Castell, Plas Tan y Bwlch. Snowdonia National Park Study Centre, Maentwrog, Gwynedd.

Dammon P.E., Long A and Grey D.C. (1966) Fluctuations of atmospheric C^{14} during the last six millennia. J. Geophys. Res., 71, 1055-063.

David A.E. and Clark A.J. (1983) Archaeomagnetic dating: Llawhaden, Dyfed. Ancient Monument Laboratory (Unpublished Report)

Dixon D. (1981) An interim report on the excavation in Eshott, Medieval kiln and settlement. Northumberland NZ 196981.

Dodson M.H. and McCelland-Brown E.A. (1980) Magnetic blocking temperatures of single-domain grains during slow cooling. J. Geophys. Res. 85, 2625-637.

Downey W.S. (1983) Magnetic investigation of Santorini Tephra Mimoan archaeological materials. Ph.D. Thesis (Unpublished) Univ. of Newcastle upon Tyne.

Dunlop D.J. (1975) Theory of the magnetic viscosity of Lunar and terrestrial rocks. Revs. Geophys. Spac Phys., 11., p. 855

Dunlop D.J., Hanes J.A. and Bucha K.L. (1973) Indication of multidomain magnetic behaviour in basic igneous rocks: alternating field demagnetization, hysteresis and oxide petrology.
J. Geophy. Res., 78, 1387-393.

Dunlop D.J. and West G.F. (1969) An experimental evaluation of single domain theories.
Rev. Geophys. 7, 709-57.

Edwards A.L. (1972) Experimental design in psychological research (4th ed.).
New York: Holt, Rinehard and Winston.

Edwards A.L. (1973) Statistical Methods.
New York: Holt, Rinehart and Winston.

Fisher R.A. (1953) Dispersion on a sphere.
Roy. Soc. Lond. A, 217, 295-309.

Fox J.M.W. and Aitken M.J. (1980) Cooling rate dependence of thermoremanent magnetisation.
Nature, 283, No. 5746, 462-63.

Gilingham D.E.W. and Stacey F.D. (1971) Anhysteretic Remanent Magnetization (ARM) in magnetite Grains.
Pure Applied Geophysics, 8, p.160.

Haigh G. (1958) The process of magnetization by chemical change.
Phil. Mag., 3, 267-87.

Harold M.R. (1960) Magnetic dating: kiln wall fall-out.
Archaeometry, 3, 47-9.

Hartstra R.L. (1983) TRM, ARM and Ist of two natural magnetites of MD and PSD grain size.
Geoph.J.Roy.Astr. Soc., 73, 719-37.

Hoye G.S. (1982) A magnetic investigation of kiln wall distortion.
Archaeometry, 24, 80-4.

Irving E. (1964) Paleomagnetism and its application to geological and geophysical problems. pp. 135-143
New York: Wiley.

Ising G. (1943) On the magnetic properties of varved clay.
Arkiv.f. Matematik, Ast. Fysik 29A, 1-37.

Johnson E.A., Murphy T. and Torreson O.W. (1948) The prehistcry of the Earth's magnetic field.
Terr. Magn. Atmós Elect., 53, 349-72.

Kawai N., Hirookak, Nakajime T., Tokieda K. and Tosi M. (1972 Nature 236, N5344.

Kent D.V. and Lowrie W. (1975) On Magnetic Susceptibility Anisotropy of Deep Sea Sediment. Earth and Plant. Sci. Lett. 28, pp.1-12.

King R.F. (1955) The remanent magnetism of artificially deposited sediments. Mon. Not.Roy.Ast.Soc. 7, 115-34.

Klein J., Lerman J.C., Damon P.E. and Ralph E.K. (1982) Calibration of radiocarbon dates. Radiocarbon .24, 2, 103-50.

Kobayashi K. (1959) Chemical remanent magnetization of Ferromagnetic Minerals and its application to rock magnetism. J. Geomag. Geolelec. 10, 99-117.

Kono M. and Meno N. (1977) Paleointensity determination by a modified Thellier method. Phy.Earth. Planet. Inter. ..13, 305-14.

Latham A.G., Schwarcz H.P., Ford D.C. and Pearce G.W. (1979) Palaeomagnetism of stalagmite deposits. Nature 280, 383-85.

McDougall J.M. (1978) An analytical study of Obsidian from Europe and the near east by examination of magnetic parameters. M.A. Dissertation, Bradford University.

McElhinny M.W. (1979) Palaeomagnetism and palte tectonics. Cambridge Earth Science series. p.38 Cambridge University Press.

Molyneux L. (1971) A complete result magnetometer for measuring the remanent magnetization of rocks. Geophys. J. Roy Astr. Soc. 24, 429-33.

Mullins C.E. (1977) Magnetic susceptibility of the soil and its significance in soil science - a review. J. Soil Sci., 28, 223-46.

Munsell Soil Color Charts (1973) Munsell Production, Macbett Color and Photometry Division of Kollmorgen Corporation, Baltimore, Maryland.

Nagata T., Arai Y. and Momose K. (1963) Secular variation of the geomagnetic total force during the last 5000 years. J. Geoph. Res., 68.

Noel M. (1976) Palaemagnetic Studies of Swedish Varved Sediments. Ph.D. Thesis, University of Newcastle upon Tyne.

Noel M. (1980) Surface tension phenomena in the magnetization of Sediments. Geophys. J. Roy. Astr.Soc. 62, 15-25.

O'Reilly W. (1976) Magnetic minerals in the crust of the Earth. Rep. prog. Phys. 39, 857-908.

Porath K. (1968) Magnetic studies on specimens of intergrown Maghemite and Haematite. J. Geophys. Res. 73, 5959-965.

Ralph E.K. (1972) A cyclical solution for the relationship between magnetic and atmospheric C-14 changes. Proc. 8th Internat. Conf. Radiocarbon Dating A76-84.

Renfrew C., Cann J.R. and Dixon J.E. (1965) Obsidian in the Aegean. British School at Athens 60, 225-47.

Roger J., Fox J.M.W. and Aitken M.J. (1979) Magnetic anisotropy in ancient pottery. Nature 277, 644-46.

Rusakov O.M. and Zagniy G.F. (1973) Archaeomagnetic secular variation study in the Ukraine and Moldavia. Archaeometry 15, 1, 153-57.

Shaw J. (1974) A new method of determining the magnitude of the Paleomagnetic field. Application to fine historic lavas and fine archaeological samples. Geophys. J. Roy. Astr. Soc. V39, 133-41.

Smith P.J. (1967a) Ancient geomagnetic field intensities I Historic and archaeological data. Geophys. J. Roy. Astr. Soc. 13, 417-19.

Smith P.J. (1967b) Ancient geomagnetic field intensities II Geophys. J. Roy. Astr. Soc. 13, 483-86.

Smith P.J. (1968) Ancient geomagnetic field intensities III Historic and archaeological data. Geophys. J. Roy. Astr. Soc. 16, 457-60.

Smith C. (1979) The hut circles at Holyhead Mountain; an interim report on excavations carried out in 1978 and 1979.

Sommerfeld A. (1952) Electrodynamics, lectures on Theoretical Physics, V.111. New York: Academic Press.

Stacey F.D. (1977) Physics of the Earth. p.245 John Wiley and Sons New York.

Stacey F.D. and Banerjee S.K. (1974) The physical principle of rock magnetism. pp.195 Elsevier, Amsterdam.

Stephenson A. (1980a) Gyromagnetism and the remanence acquired by a rotating rock in an alternating field. Nature 284. p.48

Stephenson A. (1980b) A gyroremanent magnetisation in anisotropic magnetic material. p.49 Nature 284.

Stephenson A. (1980c) Rotational remanent magnetization and the torque exerted on a rotating rock in an alternating magnetic field. Geophys. J. Roy. Astr. Soc., 62. p.113

Stinger C.B., Andrews P. and Currant A. (1979) The search for early man at Westbury Sub-Mendip, Somerset. Dept. of Palaeontology, British Museum (Natural History) London.

Strangway D.W. (1970) History of the earth's magnetic field. McGraw-Hill, New York. p.168

Stuiver M. (1982) A high-precision calibration of the AD radiocarbon time scale. Radiocarbon 24, 1, 1-26.

Suess H.E. (1970) The three causes of the secular C14 fluctuations, their amplitudes and time constants. In Radiocarbon variations and absolute chronology (ed. I.V. Olsson). Wiley-Interscience.

Sugiura N. (1979) ARM, TRM and magnetic interactions concentration dependence. Earth Plant Sci. Lett. 42, 451-55.

Tarling D.H. (1983) Palaeomagnetism, principles and applications in geology, geophysics and archaeology. Chapman and Hall. p.145 , p.181

Tarling D.H. and Symons D.T.A. (1967) A stability index of remanence in paleomagnetism. Geophys. J. Roy. Astr. Soc. 12, 443-48.

Taylor R.E. (1976) Advance in Obsidian glass studies: archaeological and geochemical perspectives. p.360 Park Ridge, Noyen Press.

Thellier (1937) Sur la disparition de l'aimantation permanet des terres Cuites, par rechauffment en champ magnetique. p.334 Aul. C.R. Acad. Sci. Paris 205.

Thellier E. (1938) Sur l'aimantation des terres cuites et ses applications geophysiques. Ph.D. Thesis, Paris.

Thellier E. (1981) Sur La Direction du Champ Magnetique Terrestre, En France Durant Les Deux Derniers Millenaires. Phys. of the Earth and Plant. Int., 24, 89-132.

Thellier E. and Thellier O. (1959) Sur l'intensité due champ magnetique terrestre dans le passé historique et geologique. Ann. Geophys. 15, 285-376.

Tite M.S. and Mullins C. (1971) Enhancement of the magnetic susceptibility of soils on archaeological sites. Archaeometry 13, 208-19.

Turner P. and Tarling D.H. (1975) Implication of new palaeomagnetic results from the Carboniferous system of Britain. J. Geol.Soc., London 131, 2469-488.

Turner G.M. and Thompson R. (1979) Behaviour of the earth's magnetic field as recorded in sediment of Loch Lomond. Geophys. J. Roy. Astr. Soc. 70, 789-92.

Van Zijl J.S.V., Graham K.W.T. and Hales A.L. (1962) The Paleomagnetism of the Stormberg Lavas of South Africa. Parts 1 and 2. Geophys. J. Roy Astr. Soc. 7, 23-39, 169-82.

Wainwright G.A. (1927) Obsidian Ancient Egypt, 88, 77-93.

Walton D. (1982) Errors and resolution of thermal techniques for obtaining the geomagnetic intensity. Nature 295, 512-15.

Watson G.S. (1956) Analysis of dispersion on a sphere. Roy Astron. Soc. Mon. Not, 7, 153-59.

Weaver G.H. (1961) The firing of a pottery kiln of a Romano-British type at Boston, Lincs. Appendix III, Archaeometry 4, 23-7.

Weaver G.H. (1962) Archaeomagnetic measurements on the second Boston experimental kiln. Archaeometry 5, 93-107.

Weaver G.H. (1964) B.Sc. Thesis, Oxford.

Wilson R.L. and Lomax R. (1972) Magnetic remanence related to slow rotation of ferromagnetic material in alternating magnetic fields. p.295 Geophysics J. Roy. Astr. Soc. 30

Xu T.C. (1984) Palaeomagnetic investigation of upper palaeozoic rocks of Scotland. Ph.D. Thesis, University of Newcastle upon Tyne.

* * *

NOTES ON APPENDICES I and II

1. Code
2. Number of samples
3. TRM, DRM and CRM (T,D,C)
4. Site Name
5. Latitude
6. Longitude
7. Declination
8. Inclination
9. α_{95}
10. K
11. Age Range (9999 = unknown age)
12. Weight (0 = undefined)

APPENDIX I

BRITISH ARCHAEOMAGNETIC DATA

	1	2 3	4	5	6	7	8	9	10	11	12
1	1GW/3	15T	GWITHIAN XV	50.24	-5.30	7.1	64.41	0.0		0-1700-1700	4
2	2		PRE-ROMAN HEARTH								
3	3 BRITAIN . AITKEN & WEAVER, ARCH. 5(1962)										
4	1GW/1	8T	GWITHIAN X	50.24	-5.30	11.5	64.31	2.57		0-1000 -950	5
5	2		PRE-ROMAN HEARTH								
6	3 BRITAIN . AITKEN & WEAVER, ARCH. 5(1962)										
7	1GW/2	13T	GWITHIAN X	50.24	-5.30	11.5	61.11	3.03		0 -950 -900	5
8	2		PRE-ROMAN HEARTH								
9	3 BRITAIN . AITKEN & WEAVER, ARCH. 5(1962)										
10	1HR	7T	HIGH ROCKS	50.10	0.20	14.7	53.41	3.85		0 -700 100	1
11	2		PRE-ROMAN HEARTH. IRON AGE.								
12	3 BRITAIN . AITKEN & WEAVER, ARCH. 5(1962)										
13	1SH	6T	STANTON HARCOURT	50.80	-1.40	-7.0	65.51	4.20		0 -700 100	1
14	2		PRE-ROMAN,HEARTH. IRON AGE.								
15	3 BRITAIN . AITKEN & WEAVER, ARCH. 5(1962)										
16	1CA/35	18T	CANTLEY	53.50	-1.05	4.3	60.01	3.15		0 200 300	4
17	2		ROMAN,POTTERY KILN								
18	3 BRITAIN . AITKEN & WEAVER, ARCH. 5(1962)										
19	1CA/33	6T	CANTLEY	53.50	-1.05	6.0	59.01	0.0		0 280 400	3
20	2		ROMAN,POTTERY KILN								
21	3 BRITAIN . AITKEN & WEAVER, ARCH. 5(1962)										
22	1CA/34	10T	CANTLEY	53.50	-1.05	-1.0	59.01	0.0		0 280 400	3
23	2		ROMAN,POTTERY KILN								
24	3 BRITAIN . AITKEN & WEAVER, ARCH. 5(1962)										
25	1CA/37	14T	CANTERY	53.50	-1.05	2.0	61.51	0.0		0 280 400	3
26	2		ROMAN,POTTERY KILN								
27	3 BRITAIN . AITKEN & WEAVER, ARCH. 5(1962)										
28	1CA/38	17T	CANTERY	53.50	-1.05	1.0	61.51	0.0		0 280 400	3
29	2		ROMAN,POTTERY KILN								
30	3 BRITAIN . AITKEN & WEAVER, ARCH. 5(1962)										
31	1CA/39	8T	CANTERY	53.50	-1.05	-3.8	61.61	1.98		0 280 400	3
32	2		ROMAN,POTTERY KILN								
33	3 BRITAIN . AITKEN & WEAVER, ARCH. 5(1962)										
34	1CT	13T	CASTOR	52.50	-0.40	4.7	64.81	1.98		0 270 350	4
35	2		ROMAN,POTTERY KILN								
36	3 BRITAIN . AITKEN & WEAVER, ARCH. 5(1962)										
37	1CG/8	6T	COX GREEN	51.50	-1.70	-5.5	62.01	1.52		0 315 400	4
38	2		ROMAN,HYPOCAUST								

```
 39      3 BRITAIN  . AITKEN & WEAVER, ARCH. 5(1962)
 40      1CG/3    7T COX GREEN              51.50  -1.70  -7.0 63.71 2.92    0  300  385 4
 41      2    ROMAN, HYPOCAUST
 42      3 BRITAIN  . AITKEN & WEAVER, ARCH. 5(1962)
 43      1HM/1    9T HAMSTEAD MARSHALL      51.40  -1.40  -2.3 61.41 2.45    0  300  400 4
 44      2    ROMAN, POTTERY KILN. AGE 4TH C.(?).
 45      3 BRITAIN  . AITKEN & WEAVER, ARCH. 5(1962)
 46      1HM/2    8T HAMSTEAD MARSHALL      51.40  -1.40  -0.7 62.41 2.45    0  300  400 4
 47      2    ROMAN, POTTERY KILN. AGE 4TH C.(?).
 48      3 BRITAIN  . AITKEN & WEAVER, ARCH. 5(1962)
 49      1HM/3    9T HAMSTEAD MARSHALL      51.40  -1.40  -5.0 60.91 8.75    0  300  400 3
 50      2    ROMAN, POTTERY KILN. AGE 4TH C.(?).
 51      3 BRITAIN  . AITKEN & WEAVER, ARCH. 5(1962)
 52      1HL/1   16T HARTSHILL              52.50  -1.55  -9.0 64.81 1.75    0  300  350 5
 53      2    ROMAN, POTTERY KILN.
 54      3 BRITAIN  . AITKEN & WEAVER, ARCH. 5(1962)
 55      1HL/4    9T HARTSHILL              52.50  -1.55  -4.2 62.81 1.40    0  340  370 5
 56      2    ROMAN, POTTERY KILN.
 57      3 BRITAIN  . AITKEN & WEAVER, ARCH. 5(1962)
 58      1HL/6   25T HARTSHILL              52.50  -1.55  -6.2 65.91 2.33    0  300  400 4
 59      2    ROMAN, POTTERY KILN.
 60      3 BRITAIN  . AITKEN & WEAVER, ARCH. 5(1962)
 61      1HL/7    8T HARTSHILL              52.50  -1.55  -2.0 61.31 2.80    0  300  370 4
 62      2    ROMAN, POTTERY KILN.
 63      3 BRITAIN  . AITKEN & WEAVER, ARCH. 5(1962)
 64      1HL/8    9T HARTSHILL              52.50  -1.55   2.7 58.11 2.33    0  180  350 2
 65      2    ROMAN, POTTERY KILN.
 66      3 BRITAIN  . AITKEN & WEAVER, ARCH. 5(1962)
 67      1HL/9   11T HARTSHILL              52.50  -1.55  -1.2 64.61 1.75    0  240  300 4
 68      2    ROMAN, POTTERY KILN.
 69      3 BRITAIN  . AITKEN & WEAVER, ARCH. 5(1962)
 70      1HL/11   7T HARTSHILL              52.50  -1.55  -2.0 65.81 2.33    0  100  150 5
 71      2    ROMAN, POTTERY KILN.
 72      3 BRITAIN  . AITKEN & WEAVER, ARCH. 5(1962)
 73      1HL/12  12T HARTSHILL              52.50  -1.55   4.0 59.91 3.50    0  100  200 4
 74      2    ROMAN, POTTERY KILN.
 75      3 BRITAIN  . AITKEN & WEAVER, ARCH. 5(1962)
 76      1HL/14A  7T HARTSHILL              52.50  -1.55   3.6 66.31 2.22    0  100  130 5
 77      2    ROMAN, POTTERY KILN.
```

```
 78      3 BRITAIN  . AITKEN & WEAVER, ARCH. 5(1962)
 79      1HL/15  11T HARTSHILL          52.50  -1.55   2.2 60.31 3.03    0  260  300 5
 80      2    ROMAN,POTTERY KILN.
 81      3 BRITAIN  . AITKEN & WEAVER, ARCH. 5(1962)
 82      1HL/18  10T HARTSHILL          52.50  -1.55   2.4 57.41 2.10    0  240  290 5
 83      2    ROMAN,POTTERY KILN.
 84      3 BRITAIN  . AITKEN & WEAVER, ARCH. 5(1962)
 85      1HL/19  11T HARTSHILL          52.50  -1.55  -5.2 64.41 1.87    0  135  160 5
 86      2    ROMAN,POTTERY KILN.
 87      3 BRITAIN  . AITKEN & WEAVER, ARCH. 5(1962)
 88      1HL/22  22T HARTSHILL          52.50  -1.55  -1.7 66.91 1.52    0  120  145 5
 89      2    ROMAN,POTTERY KILN.
 90      3 BRITAIN  . AITKEN & WEAVER, ARCH. 5(1962)
 91      1HL/24  12T HARTSHILL          52.50  -1.55  -9.5 66.41 3.15    0  100  140 4
 92      2    ROMAN,POTTERY KILN.
 93      3 BRITAIN  . AITKEN & WEAVER, ARCH. 5(1962)
 94      1HL/28  16T HARTSHILL          52.50  -1.55  -0.3 65.11 1.75    0  270  320 5
 95      2    ROMAN,POTTERY KILN.
 96      3 BRITAIN  . AITKEN & WEAVER, ARCH. 5(1962)
 97      1HL/31   8T HARTSHILL          52.50  -1.55  -4.3 56.41 2.68    0  180  230 5
 98      2    ROMAN,POTTERY KILN.
 99      3 BRITAIN  . AITKEN & WEAVER, ARCH. 5(1962)
100      1HL/32  11T HARTSHILL          52.50  -1.55 -12.5 66.41 4.08    0  100  150 4
101      2    ROMAN,POTTERY KILN.
102      3 BRITAIN  . AITKEN & WEAVER, ARCH. 5(1962)
103      1LH      6T LONG HANBORO       51.80  -1.40 -11.0 71.21 0.0     0   25   75 3
104      2    ROMAN,POTTERY KILN.
105      3 BRITAIN  . AITKEN & WEAVER, ARCH. 5(1962)
106      1PW     13T PICKWORTH          52.70  -0.60  -5.6 65.51 0.0     0  100  200 3
107      2    ROMAN,IRON SMELTING FURNACE. AGE 2ND C.(?).
108      3 BRITAIN  . AITKEN & WEAVER, ARCH. 5(1962)
109      1RB/1    7T ROSSINGTON BRIDGE  53.50  -1.05  -2.8 60.01 3.03    0  150  180 5
110      2    ROMAN,POTTERY KILN.
111      3 BRITAIN  . AITKEN & WEAVER, ARCH. 5(1962)
112      1RB/2    6T ROSSINGTON BRIDGE  53.50  -1.05   2.4 59.71 1.63    0  150  180 4
113      2    ROMAN,POTTERY KILN.
114      3 BRITAIN  . AITKEN & WEAVER, ARCH. 5(1962)
115      1RB/4   14T ROSSINGTON BRIDGE  53.50  -1.05   2.2 61.51 1.17    0  160  175 5
116      2    ROMAN,POTTERY KILN.
```

```
)  117      3 BRITAIN  . AITKEN & WEAVER, ARCH. 5(1962)
)  118      1SV     11T SAVERNAKE            51.40  -1.70   9.3 62.51 2.92    0   70  110 5
)  119      2    ROMAN,POTTERY KILN.
)  120      3 BRITAIN  . AITKEN & WEAVER, ARCH. 5(1962)
)  121      1SB/B    5T SIBSON              52.50  -0.35  -4.0 60.91 4.43    0  230  270 4
)  122      2    ROMAN,POTTERY KILN.
)  123      3 BRITAIN  . AITKEN & WEAVER, ARCH. 5(1962)
)  124      1SB/C   10T SIBSON              52.50  -0.35  -3.2 64.91 2.57    0  300  400 4
)  125      2    ROMAN,POTTERY KILN.
)  126      3 BRITAIN  . AITKEN & WEAVER, ARCH. 5(1962)
)  127      1SB/E    5T SIBSON              52.50  -0.35  -5.0 63.31 1.28    0  300  400 4
)  128      2    ROMAN,POTTERY KILN.
)  129      3 BRITAIN  . AITKEN & WEAVER, ARCH. 5(1962)
)  130      1ST     15T STOKE-ON-TRENT      53.00  -2.20  -1.4 67.21 1.40    0   50   70 5
)  131      2    ROMAN,POTTERY KILN.
)  132      3 BRITAIN  . AITKEN & WEAVER, ARCH. 5(1962)
)  133      1WP/1    4T WAPPENBURY          52.30  -1.45  -1.1 65.61 1.17    0  300  350 3
)  134      2    ROMAN,POTTERY KILN.
)  135      3 BRITAIN  . AITKEN & WEAVER, ARCH. 5(1962)
)  136      1DT      9T DORCHESTER,THAMES   51.65  -1.05  -0.7 62.01 4.08    0  525  575 4
)  137      2    SAXON,HEARTH.
)  138      3 BRITAIN  . AITKEN & WEAVER, ARCH. 5(1962)
)  139      1CC     10T CH.  . OXFORD       51.75  -1.25  29.2 67.01 2.39    0  950 1050 4
)  140      2    SAXON-NORMAN,HEARTH.
)  141      3 BRITAIN  . AITKEN & WEAVER, ARCH. 5(1962)
)  142      1NS/C    4T CUDDINGTON          51.35  -0.25   2.0 64.41 2.92    0 1050 1100 3
)  143      2    SAXON-NORMAN,BURNT BEAM SLOT.
)  144      3 BRITAIN  . AITKEN & WEAVER, ARCH. 5(1962)
)  145      1ES     10T EASTON SOCON        52.20  -0.30  21.7 61.61 2.10    0 1050 1150 4
)  146      2    SAXON-NORMAN,HEARTH.
)  147      3 BRITAIN  . AITKEN & WEAVER, ARCH. 5(1962)
)  148      1IP     18T IPSWICH             52.00   1.15  24.7 67.41 1.17    0  850 1150 1
)  149      2    SAXON-NORMAN,POTTERY KILN.
)  150      3 BRITAIN  . AITKEN & WEAVER, ARCH. 5(1962)
)  151      1TK/I   11T TORKSEY 1           53.30  -0.75  22.1 65.61 1.17    0 1050 1150 4
)  152      2    SAXON-NORMAN,POTTERY KILN.
)  153      3 BRITAIN  . AITKEN & WEAVER, ARCH. 5(1962)
)  154      1TK/2    7T TORKSEY 2           53.30  -0.75  27.9 70.01 1.87    0  900 1000 4
)  155      2    SAXON-NORMAN,POTTERY KILN.
```

```
156     3 BRITAIN  . AITKEN & WEAVER, ARCH. 5(1962)
157     1BW     15T BLUNDENS WOOD       51.10  -0.60  -3.0 53.71 1.28    0 1300 1350 5
158     2    GLASS FURNACE
159     3 BRITAIN  . AITKEN & WEAVER, ARCH. 5(1962)
160     1BO     18T BOSTON              53.00   0.0   -0.7 58.01 0.64    0 1300 1350 5
161     2    TILE KILN
162     3 BRITAIN  . AITKEN & WEAVER, ARCH. 5(1962)
163     1BR/D   17T BRILL D             51.80  -1.05   1.2 55.81 2.57    0 1300 1350 5
164     2    POTTERY KILN
165     3 BRITAIN  . AITKEN & WEAVER, ARCH. 5(1962)
166     1BR/E   14T BRILL E             51.80  -1.05  -0.4 58.91 2.45    0 1300 1350 5
167     2    POTTERY KILN
168     3 BRITAIN  . AITKEN & WEAVER, ARCH. 5(1962)
169     1AP      7T CLAR'DON PALACE     51.10  -1.75   8.5 52.91 2.80    0 1237 1251 5
170     2    TILE KILN
171     3 BRITAIN  . AITKEN & WEAVER, ARCH. 5(1962)
172     1DP      9T DOWNPATRICK         54.30  -5.75   9.9 58.51 0.93    0 1250 1325 4
173     2    POTTERY KILN
174     3 BRITAIN  . AITKEN & WEAVER, ARCH. 5(1962)
175     1SE      6T SEACOURT            51.75  -1.30  -7.0 60.21 0.0     0 1325 1350 3
176     2    HEARTH
177     3 BRITAIN  . AITKEN & WEAVER, ARCH. 5(1962)
178     1TN     21T TOYNTON ALL STS.    53.15   0.10   0.1 52.41 1.75    0 1275 1325 5
179     2    POTTERY KILN
180     3 BRITAIN  . AITKEN & WEAVER, ARCH. 5(1962)
181     1GY      8T ST.LEONARDS         51.90  -2.75   9.7 69.71 2.33    0 1600 1600 5
182     2    POST MEDIAEVAL,GLASS FURNACE.
183     3 BRITAIN  . AITKEN & WEAVER, ARCH. 5(1962)
184     1NS/K    7T NONSUCH             51.35  -0.25   0.7 72.71 1.28    0 1538 1547 5
185     2    POST MEDIAEVAL,BRICK OR LIME KILN. AGE OR 1665
186     3 BRITAIN  . AITKEN & WEAVER, ARCH. 5(1962)
187     1BO/EK1 16T BOSTON              53.00   0.0   -5.7 68.01 1.40    0 1961 1961 5
188     2    EXPERIMENTAL POTTERY KILN
189     3 BRITAIN  . AITKEN & WEAVER, ARCH. 5(1962)
190     1BO/EK2 40T BOSTON              53.00   0.0   -9.9 67.31 0.93    0 1962 1962 5
191     2    EXPERIMENTAL POTTERY KILN
192     3 BRITAIN  . AITKEN & WEAVER, ARCH. 5(1962)
193     1AW      7T ASCOTT              51.90  -1.60   9.9 71.21 2.76    0-4000-2500 1
194     2    PRE-ROMAN,HEARTH
195     3 BRITAIN  . AITKEN & HAWLEY, ARCH. 10(1967)
```

```
196     1CF     15T CITY FARM          51.80  -1.40  -2.5 72.31 3.10    0 -100  -50 4
197     2    PRE-ROMAN,FIRE PIT
198     3 BRITAIN  . AITKEN & HAWLEY, ARCH. 10(1967)
199     1FN     24T FINAVON            56.70  -2.80  -9.6 72.81 2.24    0 -500 -300 2
200     2    PRE-ROMAN,VITRIFIED STONE
201     3 BRITAIN  . AITKEN & HAWLEY, ARCH. 10(1967)
202     1DG     17T DRAGONBY           53.60  -0.60  -0.9 65.61 5.17    0   50  100 3
203     2    ROMAN,POT KILN(F,W.)
204     3 BRITAIN  . AITKEN & HAWLEY, ARCH. 10(1967)
205     1DG     12T DRAGONBY           53.60  -0.60   2.7 61.91 3.62    0   50  100 4
206     2    ROMAN,POT KILN(F.)
207     3 BRITAIN  . AITKEN & HAWLEY, ARCH. 10(1967)
208     1GL     35TGLOUCESTER          51.90  -2.20   2.7 64.91 2.58    0   60   80 5
209     2    ROMAN,POT KILN(F,W,P.)
210     3 BRITAIN  . AITKEN & HAWLEY, ARCH. 10(1967)
211     1GL     14TGLOUCESTER          51.90  -2.20  -0.7 62.81 0.69    0   60   80 5
212     2    ROMAN,POT KILN(F.)
213     3 BRITAIN  . AITKEN & HAWLEY, ARCH. 10(1967)
214     1HW     10T HAY ON WYE         52.10  -3.10  -5.0 63.31 6.20    0   40   70 3
215     2    ROMAN,OVEN,(W,F.) , MAG. DEC. ABOUT 5 W.
216     3 BRITAIN  . AITKEN & HAWLEY, ARCH. 10(1967)
217     1FB      8T HOLBROOK          53.00  -1.50   9.4 62.81 4.30    0  100  300 3
218     2    ROMAN,POT KILN(W)
219     3 BRITAIN  . AITKEN & HAWLEY, ARCH. 10(1967)
220     1MC/1   25T MANCETTER          52.60  -1.50  -2.0 65.11 1.38    0  155  180 5
221     2    ROMAN,POT KILN(F,W,P.)
222     3 BRITAIN  . AITKEN & HAWLEY, ARCH. 10(1967)
223     1MC/2   31T MANCETTER          52.60  -1.50  -7.3 64.41 3.79    0  200  260 4
224     2    ROMAN,POT KILN(F,W.)
225     3 BRITAIN  . AITKEN & HAWLEY, ARCH. 10(1967)
226     1MC/2   10T MANCETTER          52.60  -1.50  -1.9 60.91 3.44    0  200  260 4
227     2    ROMAN,POT KILN(F.)
228     3 BRITAIN  . AITKEN & HAWLEY, ARCH. 10(1967)
229     1MC/3A  14T MANCETTER          52.60  -1.50  13.0 64.21 2.07    0  150  180 5
230     2    ROMAN,POT KILN(F,W,P.)
231     3 BRITAIN  . AITKEN & HAWLEY, ARCH. 10(1967)
232     1MC/4   11T MANCETTER          52.60  -1.50   4.2 64.71 3.96    0  155  190 4
233     2    ROMAN,POT KILN(W,P.)
234     3 BRITAIN  . AITKEN & HAWLEY, ARCH. 10(1967)
```

```
)  235      1MC/9   16T MANCETTER          52.60  -1.50   0.9 65.31 2.41    0  260  310 5
)  236      2    ROMAN,POT KILN(F,W,P.)
)  237      3 BRITAIN  : AITKEN & HAWLEY, ARCH. 10(1967)
)  238      1MC/9    7T MANCETTER          52.60  -1.50   2.1 63.21 2.07    0  260  310 5
)  239      2    ROMAN,POT KILN(F.)
)  240      3 BRITAIN  . AITKEN & HAWLEY, ARCH. 10(1967)
)  241      10B      7T OLD BURROW         51.20  -3.70  -4.8 63.31 4.82    0   50   70 4
)  242      2    ROMAN,OVEN(F)
)  243      3 BRITAIN  . AITKEN & HAWLEY, ARCH. 10(1967)
)  244      1PI     15T PITT'S WOOD        50.90  -1.70  -1.5 64.81 1.21    0  330  370 5
)  245      2    ROMAN,POT KILN(W.)
)  246      3 BRITAIN  . AITKEN & HAWLEY, ARCH. 10(1967)
)  247      1SO/1   20T SOLDEN             50.90  -1.70  -4.8 65.91 3.10    0  300  330 4
)  248      2    ROMAN,POT KILN(F,W.)
)  249      3 BRITAIN  . AITKEN & HAWLEY, ARCH. 10(1967)
)  250      1SO/1    4T SOLDEN             50.90  -1.70   2.2 64.11 5.17    0  300  330 3
)  251      2    ROMAN,POT KILN(F.)
)  252      3 BRITAIN  . AITKEN & HAWLEY, ARCH. 10(1967)
)  253      1SO/2   21T SOLDEN             50.90  -1.70   0.2 65.91 1.21    0  300  330 5
)  254      2    ROMAN,POT KILN(W.)
)  255      3 BRITAIN  . AITKEN & HAWLEY, ARCH. 10(1967)
)  256      1SG     23T STANGROUND         52.50  -0.20   0.7 62.41 2.76    0  200  230 5
)  257      2    ROMAN,POT KILN(W,P.)
)  258      3 BRITAIN  . AITKEN & HAWLEY, ARCH. 10(1967)
)  259      1CC/2   18T CHRIST CHURCH      51.70  -1.20  19.0 60.91 2.76    0 1100 1130 5
)  260      2    SAXON-NORMAN,HEARTH
)  261      3 BRITAIN  . AITKEN & HAWLEY, ARCH. 10(1967)
)  262      1NC/2    9T NORTHAMPTON        52.20  -0.90   9.9 65.21 3.79    0 1050 1100 4
)  263      2    SAXON-NORMAN,HEARTH
)  264      3 BRITAIN  . AITKEN & HAWLEY, ARCH. 10(1967)
)  265      1LC      8T LUDGERSHALL        51.30  -1.60  17.8 59.41 2.41    0 1125 1175 5
)  266      2    SAXON-NORMAN,HEARTH
)  267      3 BRITAIN  . AITKEN & HAWLEY, ARCH. 10(1967)
)  268      1GE/1   14T GREAT EASTON       51.90   0.30   3.6 56.61 0.86    0 1300 1400 4
)  269      2    MEDIEVAL,OVEN(F) .  AGE 1400 C. OR EARLIER
)  270      3 BRITAIN  . AITKEN & HAWLEY, ARCH. 10(1967)
)  271      1GE/2   17T GREAT EASTON       51.90   0.30   2.3 56.31 1.03    0 1300 1400 4
)  272      2    MEDIEVAL,HEARTH .  AGE 1400 C. OR EARLIER
)  273      3 BRITAIN  . AITKEN & HAWLEY, ARCH. 10(1967)
```

```
)   274      1GE/3   15T GREAT EASTON          51.90   0.30   5.4 59.91 0.69    0 1100 1200 4
)   275      2    MEDIEVAL,HEARTH .  AGE 1200 C. OR EARLIER
)   276      3 BRITAIN  . AITKEN & HAWLEY, ARCH. 10(1967)
)   277      1SD/1   15T SANDAL                53.60  -1.50   0.7 56.81 2.41    0 1400 1500 4
)   278      2    MEDIEVAL,HEARTH .  AGE 1500 C.
)   279      3 BRITAIN  . AITKEN & HAWLEY, ARCH. 10(1967)
)   280      1SD/2    8T SANDEL                53.60  -1.50   3.4 53.81 6.89    0 1400 1500 3
)   281      2    MEDIEVAL,SMELTING PIT . AGE 1500 C.
)   282      3 BRITAIN  . AITKEN & HAWLEY, ARCH. 10(1967)
)   283      1SD/3    8T SANDEL                53.60  -1.50   1.6 62.61 2.93    0 1400 1500 4
)   284      2    MEDIEVAL,HEARTH .  AGE 1500 C.
)   285      3 BRITAIN  . AITKEN & HAWLEY, ARCH. 10(1967)
)   286      1TN/3   55T TOYNTON               53.10   0.10   2.5 55.11 0.86    0 1275 1325 5
)   287      2    MEDIEVAL,POT KILN(2F)
)   288      3 BRITAIN  . AITKEN & HAWLEY, ARCH. 10(1967)
)   289      1WF/3   15T WOODHOUSE             54.10  -1.60  10.7 56.61 1.21    0 1250 1375 3
)   290      2    MEDIEVAL,POT KILN(F)
)   291      3 BRITAIN  . AITKEN & HAWLEY, ARCH. 10(1967)
)   292      1WF/4   16T WOODHOUSE             54.10  -1.60   8.9 60.31 2.07    0 1250 1375 3
)   293      2    MEDIEVAL,POT KILN(F)
)   294      3 BRITAIN  . AITKEN & HAWLEY, ARCH. 10(1967)
)   295      1CR     42T CROCKERTON            51.20  -2.20  10.8 69.71 1.03    0 1575 1640 4
)   296      2    POST MEDIEVAL,POT KILN(W,P.)
)   297      3 BRITAIN  . AITKEN & HAWLEY, ARCH. 10(1967)
)   298      1RY     27T RAMSEY                52.40  -0.10  10.7 63.51 0.69    0 1500 1540 5
)   299      2    POST MEDIEVAL,BRICK KILN(F)
)   300      3 BRITAIN  . AITKEN & HAWLEY, ARCH. 10(1967)
)   301      1RK/1    6T ROCKLEY               53.50  -1.50   1.4 64.11 3.96    0 1500 1600 4
)   302      2    POST MEDIEVAL,IRON FURNACE . AGE 1600 C.
)   303      3 BRITAIN  . AITKEN & HAWLEY, ARCH. 10(1967)
)   304      1RK/2    9T ROCKLEY               53.50  -1.50  -3.8 71.21 2.07    0 1500 1600 4
)   305      2    POST MEDIEVAL,IRON FURNACE . AGE 1600 C.
)   306      3 BRITAIN  . AITKEN & HAWLEY, ARCH. 10(1967)
)   307      1TN/2   26T TOYNTON               53.10   0.10  11.6 64.61 0.69    0 1475 1525 5
)   308      2    POST MEDIEVAL,POT KILN(F)
)   309      3 BRITAIN  . AITKEN & HAWLEY, ARCH. 10(1967)
)   310      1BC      7T BURY CAMP             51.40  -2.30 -10.1 65.41 4.30    0 -200 -100 4
)   311      2     PRE ROMAN, HEARTH(STONE)
)   312      3 BRITAIN  . AITKEN & HAWLEY, ARCH. 9(1966)
```

```
313     1EA      8T EASINGTON          53.60   0.10  -7.4 72.21 2.41    0-1600-1300 1
314     2     PRE ROMAN, HEARTH
315     3 BRITAIN  . AITKEN & HAWLEY, ARCH. 9(1966)
316     1RA      7T RAINSBOROUGH        52.00  -1.20  -2.4 67.91 2.76    0 -450 -300 3
317     2     PRE ROMAN, HEARTH
318     3 BRITAIN  . AITKEN & HAWLEY, ARCH. 9(1966)
319     1WE      9T WEEPING CROSS       52.80  -2.70  -5.2 64.11 2.41    0 -700  100 1
320     2     PRE ROMAN, HEARTH . AGE MBE
321     3 BRITAIN  . AITKEN & HAWLEY, ARCH. 9(1966)
322     1WW      7T WESTON WOOD         51.20  -0.50  33.5 65.31 5.51    0 -620 -400 1
323     2     PRE ROMAN, HEARTH . AGE LBA/EIA, 510 +- 110 .
324     3 BRITAIN  . AITKEN & HAWLEY, ARCH. 9(1966)
325     1TF/7   30T THETFORD          52.40   0.70  26.7 66.31 3.62    0  900 1100 2
326     2     SAXON-NORMAN,POT KILN(F,W.)
327     3 BRITAIN  . AITKEN & HAWLEY, ARCH. 9(1966)
328     1TF/33  20T THETFORD          52.40   0.70  23.9 65.91 2.24    0  900 1100 2
329     2     SAXON-NORMAN,POT KILN(W)
330     3 BRITAIN  . AITKEN & HAWLEY, ARCH. 9(1966)
331     1TF/46  33T THETFORD          52.40   0.70  21.4 65.71 1.89    0  900 1100 2
332     2     SAXON-NORMAN,POT KILN(F,W.)
333     3 BRITAIN  . AITKEN & HAWLEY, ARCH. 9(1966)
334     1TF/61  22T THETFORD          52.40   0.70  25.6 65.01 3.27    0  900 1100 2
335     2     SAXON-NORMAN,POT KILN(W)
336     3 BRITAIN  . AITKEN & HAWLEY, ARCH. 9(1966)
337     1TF/97  21T THETFORD          52.40   0.70  22.5 67.21 3.44    0  900 1100 2
338     2     SAXON-NORMAN,POT KILN(W)
339     3 BRITAIN  . AITKEN & HAWLEY, ARCH. 9(1966)
340     1TF/115 42T THETFORD          52.40   0.70  19.5 66.31 1.55    0  900 1100 2
341     2     SAXON-NORMAN,POT KILN(F,W.)
342     3 BRITAIN  . AITKEN & HAWLEY, ARCH. 9(1966)
343     1TF(AV)168T THETFORD          52.40   0.70  22.9 66.11 0.17    0  900 1100 2
344     2     SAXON-NORMAN,6 KILNS . THETFORD AVERAGE.
345     3 BRITAIN  . AITKEN & HAWLEY, ARCH. 9(1966)
346     1TK/4   16T TORKSEY           53.30  -0.70  22.1 70.41 1.89    0  900 1100 2
347     2     SAXON-NORMAN,POT KILN(F,W.)
348     3 BRITAIN  . AITKEN & HAWLEY, ARCH. 9(1966)
349     1TK/5   32T TORKSEY           53.30  -0.70  16.6 68.01 2.07    0 1050 1150 4
350     2     SAXON-NORMAN,POT KILN(F,W,P.)
351     3 BRITAIN  . AITKEN & HAWLEY, ARCH. 9(1966)
```

```
352     1WI/A   11T WINCHESTER          51.10  -1.30  22.1 66.81 2.07    0  900 1000 4
353     2     SAXON-NORMAN,HEARTH .
354     3 BRITAIN  . AITKEN & HAWLEY, ARCH. 9(1966)
355     1BI     16T BINSTEAD            50.80  -0.60  10.5 52.31 1.89    0 1250 1350 4
356     2     MEDIEVAL,POT KILN (F)
357     3 BRITAIN  . AITKEN & HAWLEY, ARCH. 9(1966)
358     1CM     19T CAMLEY              51.50  -0.70  10.0 61.51 1.03    0 1100 1300 2
359     2     MEDIEVAL,POT KILN (F,W,P)
360     3 BRITAIN  . AITKEN & HAWLEY, ARCH. 9(1966)
361     1EL      4T ELLINGTON           52.30  -0.30  10.9 50.91 8.09    0 1170 1230 3
362     2     MEDIEVAL,TILTED HEARTH
363     3 BRITAIN  . AITKEN & HAWLEY, ARCH. 9(1966)
364     1FF      7T FOLLIFOOT           54.00  -1.50   8.0 60.61 2.07    0 1470 1530 4
365     2     MEDIEVAL,POT KILN
366     3 BRITAIN  . AITKEN & HAWLEY, ARCH. 9(1966)
367     1HE      6T HEN DOMEN           52.60  -3.20   6.5 56.01 6.20    0 1200 1300 3
368     2     MEDIEVAL,BURNT AREA
369     3 BRITAIN  . AITKEN & HAWLEY, ARCH. 9(1966)
370     1WI/2    7T WINCHESTER          51.10  -1.30  20.4 59.91 2.93    0 1200 1330 3
371     2     MEDIEVAL,HEARTH
372     3 BRITAIN  . AITKEN & HAWLEY, ARCH. 9(1966)
373     1WI/3   12T WINCHESTER          51.10  -1.30   9.2 63.71 1.72    0 1370 1430 4
374     2     MEDIEVAL,HEARTH
375     3 BRITAIN  . AITKEN & HAWLEY, ARCH. 9(1966)
376     1WI/P2  14T WINCHESTER          51.10  -1.30  15.2 71.01 3.79    0 1100 1130 4
377     2     MEDIEVAL,BELL FURNACE(W)
378     3 BRITAIN  . AITKEN & HAWLEY, ARCH. 9(1966)
379     1WI/P3  15T WINCHESTER          51.10  -1.30   7.2 53.51 4.65    0 1100 1130 4
380     2     MEDIEVAL,BELL FURNACE(W)
381     3 BRITAIN  . AITKEN & HAWLEY, ARCH. 9(1966)
382     1WF/1   16T WOODHOUSE           54.10  -1.60   3.2 58.31 1.21    0 1250 1350 4
383     2     MEDIEVAL,POT KILN(F)
384     3 BRITAIN  . AITKEN & HAWLEY, ARCH. 9(1966)
385     1WF/2   21T WOODHOUSE           54.10  -1.60   1.2 60.31 1.03    0 1250 1350 4
386     2     MEDIEVAL,POT KILN(F)
387     3 BRITAIN  . AITKEN & HAWLEY, ARCH. 9(1966)
388     1BP/1    7T BAGOTS PARK         52.80  -1.90  15.0 66.11 2.07    0 1550 1600 5
389     2     POST MEDIEVAL,ANNEALING HEARTH
390     3 BRITAIN  . AITKEN & HAWLEY, ARCH. 9(1966)
```

```
391     1BP/2   33T BAGOTS PARK          52.80  -1.90  12.0 66.51 0.52    0 1550 1600 5
392     2    POST MEDIEVAL,GLASS FURNACE(F)
393     3 BRITAIN . AITKEN & HAWLEY, ARCH. 9(1966)
394     1PP      4T POTTERSBURY          52.10  -0.90   8.7 70.61 1.72    0 1600 1700 3
395     2    POST MEDIEVAL,POT KILN
396     3 BRITAIN . AITKEN & HAWLEY, ARCH. 9(1966)
397     1WR     16T WRENTHORPE           53.70  -1.50  -1.0 73.91 0.69    0 1649 1679 5
398     2    POST MEDIEVAL,POT KILN(F)
399     3 BRITAIN . AITKEN & HAWLEY, ARCH. 9(1966)
400     1IV     21T IRTHING VALLEY       54.9  357.25   0.2 68.21 0.34        90  120 5
401     2   TILE KILN ,WALL
402     3 BRITAIN . AITKEN, HAWLEY, AND WEAVER, ARCH. 6(1963)
403     1SA     16T STAMFORD CO-OP       52.7  359.5   25.0 65.9              900 1100 3
404     2   HEARTHS
405     3 BRITAIN . AITKEN, HAWLEY, AND WEAVER, ARCH. 6(1963)
406     1GR     22T GRIMSTON             52.75   0.53  12.6 63.81 2.1        1100 1150 5
407     2   POTTERY KILN,WALL
408     3 BRITAIN . AITKEN, HAWLEY, AND WEAVER, ARCH. 6(1963)
409     1SM     26T STAMFORD SCHOOL      52.7  359.5   13.5 61.31 0.8        1200 1230 5
410     2   POTTERY KILN,WALL
411     3 BRITAIN . AITKEN, HAWLEY, AND WEAVER, ARCH. 6(1963)
412     1WC-3B  32T WEST COWICK          53.70 358.99   3.0 56.91 0.7        1300 1350 5
413     2   POTTERY KILN ,FLOOR
414     3 BRITAIN . AITKEN, HAWLEY, AND WEAVER, ARCH. 6(1963)
415     1WC-2A   9T WEST COWICK          53.7  358.99 357.8 56.11 1.6        1370 1500 3
416     2   POTTERY KILN FLOOR
417     3 BRITAIN . AITKEN, HAWLEY, AND WEAVER, ARCH. 6(1963)
418     1WC-1D  26T WEST COWICK          53.7  358.99   5.7 60.61 0.4        1450 1530 4
419     2   POTTERY KILN FLOOR
420     3 BRITAIN . AITKEN, HAWLEY, AND WEAVER, ARCH. 6(1963)
421     1WC-1B  33T WEST COWICK          53.7  358.99   7.1 60.71 0.8        1450 1530 4
422     2   POTTERY KILN FLOOR
423     3 BRITAIN . AITKEN, HAWLEY, AND WEAVER, ARCH. 6(1963)
424     1PO     16T POTTERN              53.5  358.77   9.9 62.91 1.0        1450 1550 4
425     2   POTTERY KILN FLOOR
426     3 BRITAIN . AITKEN, HAWLEY, AND WEAVER, ARCH. 6(1963)
427     1ALL    12T ALLENSFORD           54.85 358.22 340.8 76.71 1.20    0 1600 1700 4
428     2   BLAST FURNACE, MAG. RESULT INDICATES 1750
429     3 BRITAIN. NOEL, M., DEP. OF ENV.(UNPUBLISHED)
```

```
430   1BAR     20T BARTON UPON HUMBER 53.68 359.57  21.3 63.81 1.20    0 1000 1100 4
431   2    HEARTH.
432   3 BRITAIN. CLARK, A.J., DEP. OF ENV.(UNPUBLISHED)
433   1BIG/1  12T BIGBURY HILLFORT.   51.28   1.04   8.0 64.41 8.50    0  -70 -100 3
434   2   LATE 1A HEARTH RESULTS.
435   3 BRITAIN. CLARK, A.J., DEP. OF ENV.(UNPUBLISHED)
436   1BIG/2   9D BIGBURY HILLFORT    51.28   1.04   8.1 69.21 2.70    0  -70 -100 5
437   2   SILT IN LATE 1A 'WATER HOLE'
438   3 BRITAIN. CLARK, A.J., DEP. OF ENV.(UNPUBLISHED)
439   1BED1    9T BEDEARN ,YORK       53.97 358.92   4.5 60.21 3.80    0 1200 1400 2
440   2   KILN
441   3 BRITAIN. NOEL, M., DEP. OF ENV.(UNPUBLISHED)
442   1BED2    8T BEDEARN ,YORK       53.97 358.92 358.3 52.01 6.50    0 1355 1405 3
443   2   HEARTH .
444   3 BRITAIN. NOEL, M., DEP. OF ENV.(UNPUBLISHED)
445   1BIN1    8T BINCHESTER          54.66 358.34   2.4 69.91 5.40    0   43  410 1
446   2   HEARTH , ROMAN
447   3 BRITAIN. NOEL, M., DEP. OF ENV.(UNPUBLISHED)
448   1BIN2   16T BINCHESTER          54.70 358.30   0.7 67.31 4.00    0   43  410 1
449   2   KILN , ROMAN
450   3 BRITAIN. NOEL, M., DEP. OF ENV.(UNPUBLISHED)
451   1BIN3   10T BINCHESTER          54.70 358.30 351.8 55.91 4.90    0   43  410 1
452   2   HEARTH , ROMAN
453   3 BRITAIN. NOEL, M., DEP. OF ENV.(UNPUBLISHED)
454   1BLG    13T BLACKGATE NCL       54.97   1.60   6.2 57.51 4.00    0 1000 1500 1
455   2   MEDIEVAL HEARTH
456   3 BRITAIN. NOEL, M., DEP. OF ENV.(UNPUBLISHED)
457   1BYC     4T BRYN Y CASTELL      52.96 356.12 344.2 71.01 9.60    0 9999 9999 0
458   2    ARC. AGE UNKNOWN
459   3 BRITAIN. NOEL, M., DEP. OF ENV.(UNPUBLISHED)
460   1CAR    10T CARRICKFERGUS       54.72 354.18  16.4 59.91 3.90    0 1200 1250 4
461   2   MEDIEVAL POTTERY KILN .
462   3 BRITAIN. NOEL, M., DEP. OF ENV.(UNPUBLISHED)
463   1CAS1/8  8T CASTLE ACRE CASTLE  52.70   0.68 345.8 72.31 0.0     0 1000 1500 1
464   2
465   3 BRITAIN. NOEL, M., DEP. OF ENV.(UNPUBLISHED)
466   1CAS916  8D CASTLE ACRE CASTLE  52.70   0.68 349.7 69.81 5.10    0 1000 1500 1
467   2   SILTING OF DIVERTED CHANNEL, MIDDLE LAYER
468   3 BRITAIN. NOEL, M., DEP. OF ENV.(UNPUBLISHED)
```

```
1CAS17   8D CASTLE ACRE CASTLE  52.70   0.68 353.3 70.41 0.0     0 1000 1500 1
2   SILTING OF DIVERTED CHANNEL, BOTTOM LAYER
3 BRITAIN. NOEL, M., DEP. OF ENV.(UNPUBLISHED)
1CAR1    7T CARLISLE 1          54.90 357.10  19.8 68.81 6.40    0   43  410 1
2   ROMAN , KILN
3 BRITAIN. NOEL, M., DEP. OF ENV.(UNPUBLISHED)
1CEF    13T CEFN GRIEANOG        0.0    0.0    6.0 67.01 0.0     0 1200 1300 4
2
3 BRITAIN. NOEL, M., DEP. OF ENV.(UNPUBLISHED)
1CHA    13T CHALTON HANTS       50.92 359.03   9.3 68.01 3.70    0  600  700 4
2   SMALL CLAY CHALK HEARTH
3 BRITAIN. CLARK, A.J., DEP. OF ENV.(UNPUBLISHED)
1COP1   15T COPPERGATE 1        53.97 358.92  13.5 61.51 2.10    0 1175 1225 5
2   MEDIEVAL HEARTH
3 BRITAIN. NOEL, M., DEP. OF ENV.(UNPUBLISHED)
1COP2   13T COPPERGATE 2        53.97 358.92 354.2 67.6110.10    0 1000 1500 1
2   MEDIEVAL HEARTH
3 BRITAIN. NOEL, M., DEP. OF ENV.(UNPUBLISHED)
1COP3    9T COPPERGATE 3        53.97 358.92 359.6 57.41 4.20    0 1000 1500 1
2   MEDIEVAL HEARTH
3 BRITAIN. NOEL, M., DEP. OF ENV.(UNPUBLISHED)
1COP4    9T COPPERGATE 4        53.97 358.92  11.6 60.71 3.30    0 1000 1500 1
2   MEDIEVAL HEARTH
3 BRITAIN. NOEL, M., DEP. OF ENV.(UNPUBLISHED)
1COP5   10T COPPERGATE 5        53.97 358.92  12.3 66.91 5.00    0 1000 1500 1
2   MEDIEVAL HEARTH
3 BRITAIN. NOEL, M., DEP. OF ENV.(UNPUBLISHED)
1COP6    6T COPPERGATE 6        53.97 358.92 358.6 65.2111.20    0 1000 1500 1
2   MEDIEVAL HEARTH
3 BRITAIN. NOEL, M., DEP. OF ENV.(UNPUBLISHED)
1DON1   19T DONYATT SOMERSET    50.93 357.05 341.7 73.51 4.50    0 1600 1800 2
2   17TH. OR 18TH. C. POTTERY KILN , YOUNGER OF TWO
3 BRITAIN. NOEL, M., DEP. OF ENV.(UNPUBLISHED)
1DON2   17T DONYATT SOMERSET    50.93 357.05  21.2 79.21 2.50    0 1600 1700 4
2   17TH. C. POTTERY KILN , OLDER OF TWO.
3 BRITAIN. NOEL, M., DEP. OF ENV.(UNPUBLISHED)
1EAS    12T EASTBOURNE          50.77   0.27  16.1 61.81 1.80    0 1160 1190 5
2   MEDIEVAL LIMEKILN.
3 BRITAIN. CLARK, A.J., DEP. OF ENV.(UNPUBLISHED)
```

```
 508      1SL     16T FARNBOROUGH HANTS   51.30 359.25   0.6 53.01 1.40    0 1000 1500 1
 509      2   MEDIEVAL KILN
 510      3 BRITAIN. CLARK, A.J., DEP. OF ENV.(UNPUBLISHED)
 511      1SL2(3) 11T FARNBOROUGH HANTS   51.30 359.25 354.0 66.61 6.00    0 1560 1575 3
 512      2            FLOOR OF POTTERY KILN, POST MEDIEVAL
 513      3 BRITAIN. CLARK, A.J., DEP. OF ENV.(UNPUBLISHED)
 514      1FLA1   10D FLAXENGATE YORK     53.23 359.45   6.3 71.11 7.50    0 1000 1500 1
 515      2   STRATIFIED BROWN SOIL. MEDIEVAL?.
 516      3 BRITAIN. NOEL, M., DEP. OF ENV.(UNPUBLISHED)
 517      1FLA2    4D FLAXENGATE YORK     53.23 359.45  37.3 76.3136.90    0 1000 1500 1
 518      2   STRATIFIED YELLOW SOIL. MEDIEVAL?.
 519      3 BRITAIN. NOEL, M., DEP. OF ENV.(UNPUBLISHED)
 520      1FLA3   16D FLAXENGATE YORK     53.23 359.45  20.4 71.71 4.30    0 1000 1500 1
 521      2   STRATIFIED BROWN SOIL. PROB. MEDIEVAL.
 522      3 BRITAIN. NOEL, M., DEP. OF ENV.(UNPUBLISHED)
 523      1GHS1   25T GREAT HOLMES ST.    52.63 358.92   5.1 66.91 2.50    0   43  410 1
 524      2   ROMAN KILN
 525      3 BRITAIN. NOEL, M., DEP. OF ENV.(UNPUBLISHED)
 526      1GHS2   15T GREAT HOLMES ST.    52.63 358.92  15.1 68.81 2.40    0   43  410 1
 527      2
 528      3 BRITAIN. NOEL, M., DEP. OF ENV.(UNPUBLISHED)
 529      1HAM1   12T HAMWIH 1            50.92 358.58  40.5 71.51 0.70    0  500 1066 1
 530      2   DOMED HEARTH, SAXON
 531      3 BRITAIN. CLARK, A.J., DEP. OF ENV.(UNPUBLISHED)
 532      1JAR    12T JARROW ABBEY        55.00 358.50  15.4 63.71 1.20    0  600  800 2
 533      2   FURNACE, AGE 7TH. TO 8TH C.
 534      3 BRITAIN. NOEL, M., DEP. OF ENV.(UNPUBLISHED)
 535      1JAR    13T JARVIS BROOK        51.03   0.20 352.7 60.71 7.20    0   43  410 1
 536      2   WALLS OF HEARTH, PROB. ROMAN
 537      3 BRITAIN. CLARK, A.J., DEP. OF ENV.(UNPUBLISHED)
 538      1KIN    10D KINGSTON BRIDGE     51.37 359.60   7.8 63.41 4.90    0 1510 1510 4
 539      2   SILT
 540      3 BRITAIN. CLARK, A.J., DEP. OF ENV.(UNPUBLISHED)
 541      1LAN    14T LANGLEY BURRELL     51.48 359.90 351.4 54.51 5.10    0 1400 1700 1
 542      2   POTTERY KILN FLOOR
 543      3 BRITAIN. CLARK, A.J., DEP. OF ENV.(UNPUBLISHED)
 544      1LIM    13T LIMPSFIELD          51.24   0.03 359.0 57.61 3.40    0 1230 1366 3
 545      2   POTTERY KILN
 546      3 BRITAIN. CLARK, A.J., DEP. OF ENV.(UNPUBLISHED)
```

```
547     1TAV82  12T LONDON                51.45 359.90  24.4 70.31 0.90    0  900  950 5
548     2   HEARTH
549     3 BRITAIN. CLARK, A.J., DEP. OF ENV.(UNPUBLISHED)
550     1MON    12T LONDON PENINSULAR     51.52 359.90  11.7 70.71 4.00    0  800  900 4
551     2   HEARTH
552     3 BRITAIN. CLARK, A.J., DEP. OF ENV.(UNPUBLISHED)
553     1SWA    60T LONDON SWAN LANE      51.52 359.90  14.2 62.01 1.10    0 1100 1200 4
554     2   HEARTHS
555     3 BRITAIN. CLARK, A.J., DEP. OF ENV.(UNPUBLISHED)
556     1BOW    12T LONDON WELL COURT     51.52 359.90  33.7 70.31 2.00    0  950 1000 5
557     2   HEARTH
558     3 BRITAIN. CLARK, A.J., DEP. OF ENV.(UNPUBLISHED)
559     1WOO    15T LITTLE WOOLSTONE      52.00 359.30  12.0 57.31 3.90    0 1180 1250 4
560     2   HEARTH
561     3 BRITAIN. CLARK, A.J., DEP. OF ENV.(UNPUBLISHED)
562     1M3R4/3  5T HANTS                 51.13 358.75   8.7 70.51 7.30    0-2000 -700 1
563     2   BA BARROW . BURNT GROUND BENEATH
564     3 BRITAIN. CLARK, A.J., DEP. OF ENV.(UNPUBLISHED)
565     1MUC/2  16D MUCKING,ESSEX         51.50   0.43   2.0 64.91 2.00    0  -75 -125 5
566     2   DITCH SILT PRE ROMAN
567     3 BRITAIN. CLARK, A.J., DEP. OF ENV.(UNPUBLISHED)
568     1MUC1   16D MUCKING               51.50   0.43  31.0 68.01 5.10    0 -600 -600 3
569     2   SALT DRYING HEARTH
570     3 BRITAIN. CLARK, A.J., DEP. OF ENV.(UNPUBLISHED)
571     1MIL1    8D MILLMEAD              51.23 359.42 355.3 69.51 8.50    0 1700 1700 3
572     2   POST MEDIEVAL RIVER SILT
573     3 BRITAIN. CLARK, A.J., DEP. OF ENV.(UNPUBLISHED)
574     1ASH    15T MILLBROOK ASHDOWN F   51.06   0.03  11.6 69.61 5.00    0  800  835 4
575     2   HEARTH
576     3 BRITAIN. CLARK, A.J., DEP. OF ENV.(UNPUBLISHED)
577     1NEA    11T NEATHAM HANTS         51.17   0.11 356.7 64.21 1.90    0  325  375 5
578     2   HEARTH LATE RB
579     3 BRITAIN. CLARK, A.J., DEP. OF ENV.(UNPUBLISHED)
580     1MAD    13T MADDISON STREET       50.90 358.60   6.8 61.01 2.20    0 1325 1350 5
581     2   LIME KILN
582     3 BRITAIN. CLARK, A.J., DEP. OF ENV.(UNPUBLISHED)
583     1NEW/1  10T NEWBURY               51.40 358.67   4.2 55.01 6.80    0 1375 1450 3
584     2   PITCHED TILE HEARTH
585     3 BRITAIN. CLARK, A.J., DEP. OF ENV.(UNPUBLISHED)
```

```
586     1NEW/2  10T NEWBURY              51.40 358.67 357.9 58.31 2.30    0 1375 1450 3
587     2   PITCHED TILE HEARTH
588     3 BRITAIN. CLARK, A.J., DEP. OF ENV.(UNPUBLISHED)
589     1NEW/3   7T NEWBURY              51.40 358.67   8.6 59.71 4.60    0 1475 1575 4
590     2   CLAY HEARTH
591     3 BRITAIN. CLARK, A.J., DEP. OF ENV.(UNPUBLISHED)
592     1NEW/4   8T NEWBURY              51.40 358.67   6.0 63.21 2.80    0 1475 1575 4
593     2   PITCHED TILE HEARTH
594     3 BRITAIN. CLARK, A.J., DEP. OF ENV.(UNPUBLISHED)
595     1NEW/5  10T NEWBURY              51.40 358.67 345.6 57.41 3.20    0 1325 1375 4
596     2   BURNT TILE HEARTH
597     3 BRITAIN. CLARK, A.J., DEP. OF ENV.(UNPUBLISHED)
598     1NOR    15T NORWICH              52.63   1.28  29.4 70.11 2.30    0 1000 1100 4
599     2   POTTERY KILN
600     3 BRITAIN. CLARK, A.J., DEP. OF ENV.(UNPUBLISHED)
601     1OKE    18T OKEHAMPTON           50.73   4.00  12.1 56.61 4.30    0 1150 1250 4
602     2   HEARTH PRECEDING 13TH. C. BUILDING
603     3 BRITAIN. CLARK, A.J., DEP. OF ENV.(UNPUBLISHED)
604     1PIP/B  14T PIPPINGFORD          51.06   0.07   5.8 65.21 4.00    0 1000 1500 1
605     2   BLOOMERY FURNACE
606     3 BRITAIN. CLARK, A.J., DEP. OF ENV.(UNPUBLISHED)
607     1PIP/1  10T PIPPINGFORD          51.06   0.07   7.5 62.51 5.30    0   43  100 3
608     2   HEARTH FLOOR
609     3 BRITAIN. CLARK, A.J., DEP. OF ENV.(UNPUBLISHED)
610     1PIP/2  11T PIPPINGFORD          51.06   0.07   0.8 64.71 4.10    0   43  100 4
611     2   HEARTH FLOOR
612     3 BRITAIN. CLARK, A.J., DEP. OF ENV.(UNPUBLISHED)
613     1ORS    11T ORSETT               51.50   0.40   2.4 62.81 3.10    0   43  410 1
614     2   ROMAN KILN
615     3 BRITAIN. CLARK, A.J., DEP. OF ENV.(UNPUBLISHED)
616     1QV1    13T QUILTERS VAULT       50.92 358.58  11.4 63.61 3.40    0 1160 1160 4
617     2   LIMEKILN
618     3 BRITAIN. CLARK, A.J., DEP. OF ENV.(UNPUBLISHED)
619     1QV195   8T QUILTERS VAULT       50.92 358.58  12.9 59.51 2.90    0 1190 1200 5
620     2   LIMEKILN
621     3 BRITAIN. CLARK, A.J., DEP. OF ENV.(UNPUBLISHED)
622     1QV1115  8T QUILTERS VAULT       50.92 358.58  12.3 57.01 1.70    0 1250 1260 5
623     2   LIMEKILN
624     3 BRITAIN. CLARK, A.J., DEP. OF ENV.(UNPUBLISHED)
```

```
)  625      1PON    10T PONTEFRACT PRIORY   53.70 358.70  12.6 57.31 9.00    0 1000 1500 1
)  626      2   MEDIEVAL HEARTH
)  627      3 BRITAIN. CLARK, A.J., DEP. OF ENV.(UNPUBLISHED)
)  628      1RAD     10T RADWINTER          52.00   0.35   3.2 56.31 1.00    0 1420 1420 5
)  629      2   TILE KILN
)  630      3 BRITAIN. CLARK, A.J., DEP. OF ENV.(UNPUBLISHED)
)  631      1LAU     7T RAINHAM             51.51   0.23 356.4 63.01 4.20    0  200  410 1
)  632      2   LATE R-B HEARTH
)  633      3 BRITAIN. CLARK, A.J., DEP. OF ENV.(UNPUBLISHED)
)  634      1RAI/M   9T RAINHAM             51.51   0.23   3.1 64.9111.30    0 -200   43 1
)  635      2   LATE IA DITCH SILT
)  636      3 BRITAIN. CLARK, A.J., DEP. OF ENV.(UNPUBLISHED)
)  637      1RE1    12T REIGATE             51.23 359.83  24.8 58.5112.10    0  900 1200 1
)  638      2   HEARTH
)  639      3 BRITAIN. CLARK, A.J., DEP. OF ENV.(UNPUBLISHED)
)  640      1SAN    18T SANDFORD MANOR      51.48 359.82   2.0 70.51 0.90    0 1636 1652 5
)  641      2   BRICK CLAMP
)  642      3 BRITAIN. CLARK, A.J., DEP. OF ENV.(UNPUBLISHED)
)  643      1SAP1   23T SAPCOTE             52.60 358.75 358.1 70.61 3.80    0   43  410 1
)  644      2   ROMAN KILN OR FURNACE
)  645      3 BRITAIN. NOEL, M., DEP. OF ENV.(UNPUBLISHED)
)  646      1SAP2   15T SAPCOTE             52.60 358.75 359.9 69.81 4.60    0   43  410 1
)  647      2   ROMAN KILN OR FURNACE
)  648      3 BRITAIN. NOEL, M., DEP. OF ENV.(UNPUBLISHED)
)  649      1       20T SPONG  HILL         52.73   0.90 358.7 64.41 3.40    0   43  200 2
)  650      2   EARLY R-B KILN
)  651      3 BRITAIN. CLARK, A.J., DEP. OF ENV.(UNPUBLISHED)
)  652      1STAM1  19T STAMFORD CASTLE     52.65 359.52  15.9 68.91 1.60    0  800  900 4
)  653      2   POTTERY KILN
)  654      3 BRITAIN. CLARK, A.J., DEP. OF ENV.(UNPUBLISHED)
)  655      1STAM2  20T STAMFORD CASTLE     52.65 359.52  12.9 66.91 1.40    0 1150 1170 5
)  656      2   BREAD OVEN
)  657      3 BRITAIN. CLARK, A.J., DEP. OF ENV.(UNPUBLISHED)
)  658      1STAM3  21T STAMFORD CASTLE     52.65 359.52 351.7 61.81 4.50    0 1300 1340 4
)  659      2   FIREPLACE MORTAR
)  660      3 BRITAIN. CLARK, A.J., DEP. OF ENV.(UNPUBLISHED)
)  661      1STAM5  20T STAMFORD CASTLE     52.65 359.52  13.0 61.71 3.30    0 1220 1220 4
)  662      2   HEARTH
)  663      3 BRITAIN. CLARK, A.J., DEP. OF ENV.(UNPUBLISHED)
```

```
664     1THAID   8D THANET INNER DITCH  51.33   1.38  37.3 78.1120.80    0-2000 -600 1
665     2   BA DITCH
666     3 BRITAIN. CLARK, A.J., DEP. OF ENV.(UNPUBLISHED)
667     1THAMD   8D THANET MID DITCH    51.33   1.38   6.9 68.8113.70    0-2000 -600 1
668     2   BA DITCH
669     3 BRITAIN. CLARK, A.J., DEP. OF ENV.(UNPUBLISHED)
670     1THAOD   8D THANET OUT DITCH    51.33   1.38  16.8 70.41 9.60    0-2000 -600 1
671     2   BA DITCH
672     3 BRITAIN. CLARK, A.J., DEP. OF ENV.(UNPUBLISHED)
673     1T1     23T TINTEM  ABBEY       51.70 357.32   5.5 58.41 4.60    0 1300 1540 1
674     2   FURNACE LATE 14TH C OR 1560
675     3 BRITAIN. CLARK, A.J., DEP. OF ENV.(UNPUBLISHED)
676     1T2     13T TINTEM ABBEY        51.70 357.32   4.9 60.81 3.50    0 1300 1540 1
677     2   SMALL CLAY LINED KILN/FURNACE
678     3 BRITAIN. CLARK, A.J., DEP. OF ENV.(UNPUBLISHED)
679     1TRE    10T TRELYSTAN           52.63 356.90 358.5 60.11 2.60    0-2000-1800 2
680     2   HEARTH
681     3 BRITAIN. NOEL, M., DEP. OF ENV.(UNPUBLISHED)
682     1VIC1   10T VICARS CHORAL       53.97 359.92  17.6 61.9120.50    0 1000 1500 1
683     2   MEDIEVAL HEARTH
684     3 BRITAIN. NOEL, M., DEP. OF ENV.(UNPUBLISHED)
685     1VIC2   10T VICARS CHORAL       53.97 359.92  11.7 65.1115.40    0 1000 1500 1
686     2   MEDIEVAL HEARTH
687     3 BRITAIN. NOEL, M., DEP. OF ENV.(UNPUBLISHED)
688     1VIC3   12T VICARS CHORAL       53.97 359.92 340.3 62.61 4.60    0 1000 1500 1
689     2   MEDIEVAL HEARTH
690     3 BRITAIN. NOEL, M., DEP. OF ENV.(UNPUBLISHED)
691     1VIC4   10T VICARS CHORAL       53.97 359.92 352.2 54.0110.30    0 1000 1500 1
692     2   MEDIEVAL HEARTH
693     3 BRITAIN. NOEL, M., DEP. OF ENV.(UNPUBLISHED)
694     1VIC5   13T VICARS CHORAL       53.97 359.92 350.6 43.41 9.70    0 1000 1500 1
695     2   MEDIEVAL HEARTH
696     3 BRITAIN. NOEL, M., DEP. OF ENV.(UNPUBLISHED)
697     1VIC6   13T VICARS CHORAL       53.97 359.92 356.2 56.81 4.10    0 1000 1500 1
698     2   MEDIEVAL HEARTH
699     3 BRITAIN. NOEL, M., DEP. OF ENV.(UNPUBLISHED)
700     1VIC7    7T VICARS CHORAL       53.97 359.92 358.3 64.11 4.70    0 1000 1500 1
701     2   MEDIEVAL HEARTH
702     3 BRITAIN. NOEL, M., DEP. OF ENV.(UNPUBLISHED)
```

```
 703      1SS     20T WAKEFIELD            53.66 358.50   4.0 65.71 3.20    0 1535 1540 4
 704      2   BURNT CLAY FLOOR
 705      3 BRITAIN. CLARK, A.J., DEP. OF ENV.(UNPUBLISHED)
 706      1WAL4    9T WALMGATE             53.97 359.92   7.1 65.61 4.80    0 1400 1500 4
 707      2   HEARTH ASH
 708      3 BRITAIN. NOEL, M., DEP. OF ENV.(UNPUBLISHED)
 709      1WAL    12T WALINGTON            51.37 359.85   1.5 65.2112.80    0 9999 9999 0
 710      2   HEARTH UNCERTAIN AGE
 711      3 BRITAIN. CLARK, A.J., DEP. OF ENV.(UNPUBLISHED)
 712      1WLD3   10D WALTON LE DALE       53.67 357.33 347.4 78.5115.00    0 9999 9999 0
 713      2    SILT . ARC. AGE UNKNOWN
 714      3 BRITAIN. CLARK, A.J., DEP. OF ENV.(UNPUBLISHED)
 715      1WIT    12T WITHAM               51.80   0.65 352.1 61.21 3.80    0  300  300 4
 716      2   R-B POTTERY KILN DATED BY POT TO 300AD APPROX.
 717      3 BRITAIN. CLARK, A.J., DEP. OF ENV.(UNPUBLISHED)
 718      1BEV65  15T BEVERLEY LURK LANE  53.84 359.50  13.7 63.11 3.70    0 1200 1300 4
 719      2   POST 13TH C. PITCHED TILE HEARTH
 720      3 BRITAIN. CLARK, A.J., DEP. OF ENV.(UNPUBLISHED)
 721      1BEV241 15T BEVERLEY LURK LANE  53.84 359.50 354.1 53.41 2.40    0 1350 1350 5
 722      2   MEDIEVAL PITCHED TILE HEARTH ABOUT 1360
 723      3 BRITAIN. CLARK, A.J., DEP. OF ENV.(UNPUBLISHED)
 724      1BEV563 14T BEVERLEY LURK LANE  53.84 359.50 355.8 56.41 4.60    0 1000 1500 1
 725      2   MEDIEVAL PITCHED TILE HEARTH
 726      3 BRITAIN. CLARK, A.J., DEP. OF ENV.(UNPUBLISHED)
 727      1BEV585 13T BEVERLEY LURK LANE  53.84 359.50   2.0 59.51 1.90    0 1000 1500 1
 728      2   MEDIEVAL PITCHED TILE HEARTH
 729      3 BRITAIN. CLARK, A.J., DEP. OF ENV.(UNPUBLISHED)
 730      1BEV592 12T BEVERLEY LURK LANE  53.84 359.50  18.6 58.41 3.10    0 1000 1500 1
 731      2   MEDIEVAL PITCHED TILE HEARTH
 732      3 BRITAIN. CLARK, A.J., DEP. OF ENV.(UNPUBLISHED)
 733      1BEV676 14T BEVERLEY LURK LANE  53.84 359.50   0.1 61.61 1.70    0 1180 1180 5
 734      2   LOWEST OF THE SIX MEDIEVAL PITCHED TILE HEARTHS
 735      3 BRITAIN. CLARK, A.J., DEP. OF ENV.(UNPUBLISHED)
 736      1BDW    24T BEVERLEY DYERS WALK 53.84 359.50  13.2 60.61 2.60    0 1180 1220 5
 737      2   HEARTH
 738      3 BRITAIN. CLARK, A.J., DEP. OF ENV.(UNPUBLISHED)
 739      1CHI 2  11T CHICHESTER SUSSEX   53.84 359.20  20.0 67.41 2.80    0 1000 1066 4
 740      2   SAXON POTTERY FIRING CLAMP
 741      3 BRITAIN. CLARK, A.J., DEP. OF ENV.(UNPUBLISHED)
```

```
1CHI 1  16T CHICHESTER SUSSEX   53.84 359.20  34.2 65.21 1.00    0 1000 1066 4
2   SAXON POTTERY FIRING CLAMP
3 BRITAIN. CLARK, A.J., DEP. OF ENV.(UNPUBLISHED)
1CHI 3   9T CHICHESTER, SUSSES  53.84 359.20  28.9 64.4  6.6       1000 1066 3
2   SAXON POTTERY FIRING CLAMP
3 BRITAIN. CLARK, A.J., DEP. OF ENV.(UNPUBLISHED)
1CH1123 36T CHICHESTER SUSSEX   53.84 359.20  27.0 65.71 2.00    0 1000 1066 4
2   ALL COMBINED
3 BRITAIN. CLARK, A.J., DEP. OF ENV.(UNPUBLISHED)
1GAR82  12T GARDEN HILL SUSSEX  51.00   0.16   2.7 69.31 4.00    0 9999 9999 0
2   BURNT GROUND . ARC. AGE UNKNOWN
3 BRITAIN. CLARK, A.J., DEP. OF ENV.(UNPUBLISHED)
1GAR490 16T GARDEN HILL SUSSEX  51.00   0.16   8.9 57.21 1.80    0 9999 9999 0
2   HEARTH . ARC. AGE UNKNOWN
3 BRITAIN. CLARK, A.J., DEP. OF ENV.(UNPUBLISHED)
1SWA1    8T LONDON SWAN LANE    51.52 359.92  19.0 44.21 2.30    0 1150 1150 5
2   PITCHED TILE HEARTH
3 BRITAIN. CLARK, A.J., DEP. OF ENV.(UNPUBLISHED)
1SWA2   12T LONDON SWAN LANE    51.52 359.92  22.5 62.31 2.40    0 1150 1150 5
2   PITCHED TILE HEARTH
3 BRITAIN. CLARK, A.J., DEP. OF ENV.(UNPUBLISHED)
1SWA3   11T LONDON SWAN LANE    51.52 359.92   0.0 57.4110.00    0 9999 9999 0
2   PITCHED TILE HEARTH . ARC. AGE UNKNOWN
3 BRITAIN. CLARK, A.J., DEP. OF ENV.(UNPUBLISHED)
1SWA4   12T LONDON SWAN LANE    51.52 359.92  13.1 61.51 1.70    0 1150 1150 5
2   PITCHED TILE HEARTH
3 BRITAIN. CLARK, A.J., DEP. OF ENV.(UNPUBLISHED)
1SWA5   11T LONDON SWAN LANE    51.52 359.92  10.3 63.61 1.90    0 9999 9999 0
2   PITCHED TILE HEARTH : ARC. AGE UNKNOWN
3 BRITAIN. CLARK, A.J., DEP. OF ENV.(UNPUBLISHED)
1SWA6    6T LONDON SWAN LANE    51.52 359.92   7.1 57.41 2.20    0 9999 9999 0
2   EARLIEST OF THE SIX SUPERIMPOSED PITCHED TILE HEARTH, ARC. AGE UNKNOWN
3 BRITAIN. CLARK, A.J., DEP. OF ENV.(UNPUBLISHED)
1PEL    20T PELDON ESSEX        51.80   0.92 356.0 68.51 1.30    0    0   43 5
2    HEARTH
3 BRITAIN. CLARK, A.J., DEP. OF ENV.(UNPUBLISHED)
1RED    13T REDCLIFF FARM       50.68 359.10   7.8 63.71 2.60    0  100  150 5
2   POTTERY FIRING CLAMP
3 BRITAIN. CLARK, A.J., DEP. OF ENV.(UNPUBLISHED)
```

```
781     1RAN    17T RAND CHURCH          53.30   0.33  14.0 60.81 4.20    0 9999 9999 0
782     2    METAL WORKING HEARTH, ARC. AGE UNKNOWN
783     3 BRITAIN. CLARK, A.J., DEP. OF ENV.(UNPUBLISHED)
784     1RUSH   19T RUSH GREEN BUCKS    51.57 359.47  12.4 54.01 2.70    0 1000 1500 1
785     2   MEDIEVAL KILN
786     3 BRITAIN. CLARK, A.J., DEP. OF ENV.(UNPUBLISHED)
787     1BIG/S   9D BIGBERRY             51.28   1.04   1.9 71.31 2.1      -100  -70 5
788     2   SILT
789     3 BRITAIN. CLARK, A.J., DEP. OF ENV.(UNPUBLISHED)
790     1BIG/H  10T BIGBERRY             51.28   1.04   5.7 66.41 9.1      9999 9999 0
791     2   HEARTH, ARC. AGE UNKNOWN
792     3 BRITAIN. CLARK, A.J., DEP. OF ENV.(UNPUBLISHED)
793     1ALI/2A 17T ALICE HOLT FOREST   51.15  -0.85   2.5 56.41 1.1       200  300 4
794     2    R-B POTTERY KILN
795     3 BRITAIN. CLARK, A.J., DEP. OF ENV.(UNPUBLISHED)
796     1AL1/2B 16T ALICE HOLT FOREST   51.15  -0.85 357.0 52.61 2.4        43  410 1
797     2    R-B POTTERY KILN
798     3 BRITAIN. CLARK, A.J., DEP. OF ENV.(UNPUBLISHED)
799     1ALC2    9T ALICE HOLT FOREST   51.15  -0.85   5.4 53.71 3.8        43  410 1
800     2    ROMAN POTTERY KILN
801     3 BRITAIN. CLARK, A.J., DEP. OF ENV.(UNPUBLISHED)
802     1GAR436  9T GARDEN HILL SUSSEX  51.06   0.07 350.2 63.11 5.5      -700  100 1
803     2    HEARTH ON RAMPORT OF IRON AGE (AM. 50 BC)
804     3 BRITAIN. CLARK, A.J., DEP. OF ENV.(UNPUBLISHED)
805     1GAR433  9T GARDEN HILL SUSSEX  51.06   0.07 353.0 64.11 9.1        43  410 1
806     2    ROMAN IRON SMELTING FURNACE
807     3 BRITAIN. CLARK, A.J., DEP. OF ENV.(UNPUBLISHED)
808     1GAR315 18T GARDEN HILL SUSSEX  51.06   0.07 347.5 64.41 3.4      -100    0 4
809     2    HEARTH OF IRON AGE (AM. 50 BC)
810     3 BRITAIN. CLARK, A.J., DEP. OF ENV.(UNPUBLISHED)
811     1GAR346·11T GARDEN HILL SUSSEX  51.06   0.07 346.4 68.81 3.3      -100    0 4
812     2    ROMAN IRON FORCING HEARTH (AM. 50 BC)
813     3 BRITAIN. CLARK, A.J., DEP. OF ENV.(UNPUBLISHED)
814     1GAR227 15T GARDEN HILL SUSSEX  51.06   0.07   3.7 54.51 4.1      -100    0 4
815     2    ROMAN IRON FORCING HEARTH (AM. 50 BC)
816     3 BRITAIN. CLARK, A.J., DEP. OF ENV.(UNPUBLISHED)
817     1GAR067  7T GARDEN HILL SUSSEX  51.06   0.07 356.1 61.81 7.0        43  410 1
818     2    ROMAN IRON SMELTING
819     3 BRITAIN. CLARK, A.J., DEP. OF ENV.(UNPUBLISHED)
```

```
820     1DAN    17T DAN-Y-COED          00.00   0.00   9.8 62.81 5.2      9999 9999 0
821     2    BAKED CLAY FLOOR ON HEARTH (AM. 1510-1560 OR 4TH C.)
822     3 BRITAIN. CLARK, A.J., DEP. OF ENV.(UNPUBLISHED)
823     1DAN/2  14T DAN-Y-COED          00.00   0.00 353.5 63.91 4.6      9999 9999 0
824     2    BOWL  SHAPED PIT (AM. 70 +-15)
825     3 BRITAIN. CLARK, A.J., DEP. OF ENV.(UNPUBLISHED)
826     1DAN/3  14T DAN-Y-COED          00.00   0.00 353.7 62.41 5.1      9999 9999 0
827     2    WOODSIDE (AM. 70 +-15)
828     3 BRITAIN. CLARK, A.J., DEP. OF ENV.(UNPUBLISHED)
829     1CARR    8T CARRICKFERGUS       54.43 354.50  12.8 61.71 3.6      1220 1290 4
830     2    MEDIEVAL POTTERY KILN
831     3 BRITAIN. CLARK, A.J., DEP. OF ENV.(UNPUBLISHED)
832     1NEA    11T NEATHAM             00.00   0.00 356.7 64.21 1.9      9999 9999 0
833     2    (AM. 110 - 150 OR 320 - 350)
834     3 BRITAIN. CLARK, A.J., DEP. OF ENV.(UNPUBLISHED)
835     1PARR   10T PARROCK HARTFIELD   51.06   0.06  14.0 63.81          9999 9999 0
836     2
837     3 BRITAIN. CLARK, A.J., DEP. OF ENV.(UNPUBLISHED)
838     1PARR/2 10T PARROCK HARTFIELD   51.06   0.06  25.4 58.61          9999 9999 0
839     2    ARC. AGE UNKNOWN
840     3 BRITAIN. CLARK, A.J., DEP. OF ENV.(UNPUBLISHED)
841     1HOLM    5D HOLMBURY, SURREY    51.20 359.75 350.4 64.81 1.40       -70    0 4
842     2    SILT
843     3 BRITAIN. CLARK, A.J., IN THOMPSON. ANT. J. 1979
844     1HASC1  21T HASCOMBE, SURREY    51.20 359.75 351.4 65.31 1.90       -70    0 5
845     2    GREENSAND ROCK, BURNT
846     3 BRITAIN. CLARK, A.J., IN THOMPSON. ANT. J. 1979
847     1HASC2  22D HASCOMBE, SURREY    51.20 359.75 352.1 66.11 3.20       -70    0 4
848     2    SILT
849     3 BRITAIN. CLARK, A.J., IN THOMPSON. ANT. J. 1979
850     1ALC     5T ALICE HOLT          51.20 358.60   1,9 57.71 5.60   0  200  250 3
851     2    KILN
852     3 BRITAIN. HAMMO YASSI, N. . NCL. UN.
853     125134   9T COPPERGATE YORK     53.80 359.92  20.8 69.71 5.10   0  900  940 3
854     2    HEARTH
855     3 BRITAIN. HAMMO YASSI, N. . NCL. UN.
856     122441   7T COPPERGATE YORK     53.80 359.92  14.3 69.21 5.90   0  900  920 3
857     2    HEARTH
858     3 BRITAIN. HAMMO YASSI, N. . NCL. UN.
```

```
 859      130757   9T COPPERGATE YORK     53.80 359.92  16.1 68.31 3.90    0  850  900 4
 860      2   HEARTH
 861      3 BRITAIN. HAMMO YASSI, N. . NCL. UN.
 862      122720   6T COPPERGATE YORK     53.80 359.92  16.9 67.21 1.90    0  900  900 4
 863      2   HEARTH
 864      3 BRITAIN. HAMMO YASSI, N. . NCL. UN.
 865      1        3T COPPERGATE YORK     53.80 359.92   6.6 66.41 9.20    0 9999 9999 0
 866      2   BRICKS VIKING
 867      3 BRITAIN. HAMMO YASSI, N. . NCL. UN.
 868      1ESH    11T ESHOTT ALNWICK      55.10 358.40  14.5 63.61 3.60    0 1200 1300 4
 869      2   HEARTH
 870      3 BRITAIN. HAMMO YASSI, N. . NCL. UN.
 871      1S004   11T HARLECH             52.80 355.90 350.5 79.51 2.70    0   43  410 1
 872      2   KILN
 873      3 BRITAIN. HAMMO YASSI, N. . NCL. UN.
 874      1S036   11T HARLECH             52.80 355.90 344.1 72.81 2.50    0   43  410 1
 875      2   ROMAN KILN
 876      3 BRITAIN. HAMMO YASSI, N. . NCL. UN.
 877      1HH/1    3T HOLYHEAD            53.30 355.40  13.3 63.2117.80    0  100  400 1
 878      2   KILN
 879      3 BRITAIN. HAMMO YASSI, N. . NCL. UN.
 880      1HH/2    5T HOLYHEAD            53.30 355.40  23.6 47.2120.10    0  100  400 1
 881      2   KILN
 882      3 BRITAIN. HAMMO YASSI, N. . NCL. UN.
 883      1HH/3    8T HOLYHEAD            53.30 355.40 345.0 71.3130.10    0  100  400 1
 884      2   KILN
 885      3 BRITAIN. HAMMO YASSI, N. . NCL. UN.
 886      1PIEG    8T PIERCEBRIDGE        54.40 358.40 356.4 66.31 4.40    0  150  150 4
 887      2   KILN
 888      3 BRITAIN, HAMMO YASSI, N. . NCL. UN.
 889      1A1500   9T PRUDHOE             54.90 358.20  16.0 64.41 6.90    0 1100 1200 3
 890      2   HEARTH A USING 9 SAMPLES
 891      3 BRITAIN. HAMMO YASSI, N. . NCL. UN.
 892      1A'      4T PRUDHOE             54.90 358.20  16.2 64.7111.10    0 1100 1200 2
 893      2   MORE SAMPLES FROM A
 894      3 BRITAIN. HAMMO YASSI, N. . NCL. UN.
 895      1A1500  12T PRUDHOE             54.90 358.20  16.1 64.51 5.00    0 1100 1200 4
 896      2   OVERALL SAMPLES
 897      3 BRITAIN. HAMMO YASSI, N. . NCL. UN.
```

```
)  898      1A''      5T PRUDHOE              54.90 358.20  15.8 62.41 5.10     0 1200 1250 3
)  899      2   HEARTH ON TOP OF A
)  900      3 BRITAIN. HAMMO YASSI, N. . NCL. UN.
)  901      1B1523  13T  PRUDHOE              54.90 358.20  11.5 62.01 4.10     0 1225 1275 4
)  902      2   HEARTH ABOUT 1250AD
)  903      3 BRITAIN. HAMMO YASSI, N. . NCL. UN.
)  904      1B1523  19T  PRUDHOE              54.90 358.20   9.6 61.71 3.40     0 1225 1275 4
)  905      2   OVERALL SAMPLES OF B
)  906      3 BRITAIN. HAMMO YASSI, N. . NCL. UN.
)  907      1B1523   6T  PRUDHOE              54.90 358.20   5.9 63.31 8.30     0 1225 1275 3
)  908      2   EXTRA SAMPLES FOR B
)  909      3 BRITAIN. HAMMO YASSI, N. . NCL. UN.
)  910      1C       9T  PRUDHOE              54.90 358.20   8.6 60.11 4.40     0 1250 1300 4
)  911      2   FURNACE
)  912      3 BRITAIN. HAMMO YASSI, N. . NCL. UN.
)  913      1D       6T  PRUDHOE              54.90 358.20  10.8 60.21 5.00     0 1250 1300 4
)  914      2   KILN
)  915      3 BRITAIN. HAMMO YASSI, N. . NCL. UN.
)  916      1E       8T  PRUDHOE              54.90 358.20   0.3762.71 4.60     0 1300 1300 4
)  917      2   KILN
)  918      3 BRITAIN. HAMMO YASSI, N. . NCL. UN.
)  919      1F      12T  PRUDHOE              54.90 358.20 347.8 46.7110.20     0 1200 1200 2
)  920      2   BURNT WALL
)  921      3 BRITAIN. HAMMO YASSI, N. . NCL. UN.
)  922      1AF37    6T  BRYN CASTELL         52.57 356.40   2.3 60.81 3.60     0    0  200 2
)  923      2   KILN
)  924      3 BRITAIN. HAMMO YASSI, N. . NCL. UN.
)  925      1BF49    6T  BRYN CASTELL         52.57 356.40 359.0 61.61 5.20     0    0  200 2
)  926      2   KILN
)  927      3 BRITAIN. HAMMO YASSI, N. . NCL. UN.
)  928      1CF28    4T  BRYN CASTELL         52.57 356.40   4.7 58.01 6.70     0    0  200 2
)  929      2   KILN
)  930      3 BRITAIN. HAMMO YASSI, N. . NCL. UN.
)  931      1DF41    4T  BRYN CASTELL         52.57 356.40   0.2 64.51 1.70     0    0  200 2
)  932      2
)  933      3 BRITAIN. HAMMO YASSI, N. . NCL. UN.
)  934      1WW/VV  11D WHARRAM PERCY DAM     51.20 357.40 326.9 64.91 8.20     0  600 1300 1
)  935      2   DAM SITE GREY LAYER 170/171
)  936      3 BRITAIN. HAMMO YASSI, N. . NCL. UN.
```

```
 937      1WW/VV   5D WHARRAM PERCY       51.20 357.40  32.4 73.4111.00    0  600 1300 1
 938      2   DAM SITE BLACK LAYER
 939      3 BRITAIN. HAMMO YASSI, N. . NCL. UN.
 940      1WW/VV  17D WHARRAM PERCY       51.20 357.40 340.9 69.81 7.90    0  600 1300 1
 941      2   DAM SITE OVERALL
 942      3 BRITAIN. HAMMO YASSI, N. . NCL. UN.
 943      1W176    7D WHARRAM SILT       51.20 357.40 335.2 63.71 6.30    0 1500 1600 3
 944      2   WHARRAM SILT
 945      3 BRITAIN. HAMMO YASSI, N. . NCL. UN.
 946      1        3D WHARRAM SILT       51.20 357.40 313.1 69.91 4.70    0 1500 1600 3
 947      2   SILT
 948      3 BRITAIN. HAMMO YASSI, N. . NCL. UN.
 949      1KK172   6D WHARRAM PERCY       51.20 357.40  13.9 29.7112.40    0 1000 1300 2
 950      2   POND SILT
 951      3 BRITAIN. HAMMO YASSI, N. . NCL. UN.
 952      1EAST    7D WHARRAM PERCY       51.20 357.40  14.6 63.11 3.90    0 1200 1300 4
 953      2   EASTERN FACE OF PP/QQ/171
 954      3 BRITAIN. HAMMO YASSI, N. . NCL. UN.
 955      1WEST    4D WHARRAM PERCY       51.20 357.40  81.8 67.5110.30    0 1200 1300 2
 956      2   WESTERNFACE OFPP/QQ/171
 957      3 BRITAIN. HAMMO YASSI, N. . NCL. UN.
 958      1DITCH   3D WHARRAM PERCY       51.20 357.40  11.6 37.7114.20    0 9999 9999 0
 959      2   DITCH SAMPLES . ARC. AGE UNKNOWN
 960      3 BRITAIN. HAMMO YASSI, N. . NCL. UN.
 961      100/55  10D WHARRAM PERCY       51.20 357.40 295.3 78.6117.70    0  600 1300 1
 962      2   SUMP SILT
 963      3 BRITAIN. HAMMO YASSI, N. . NCL. UN.
 964      1CAR    15D CARLISLE           54.90 357.50 358.7 61.71 7.40    0 -200 -200 3
 965      2   CLAY DEPOSITS
 966      3 BRITAIN. HAMMO YASSI, N. . NCL. UN.
 967      1LIN     6D LINCOLN            53.20 359.64  10.6 72.51 7.10    0   43  410 1
 968      2   CLAY
 969      3 BRITAIN. HAMMO YASSI, N. . NCL. UN.
 970      1LIN     3D LINCOLN            53.20 359.64  11.6 66.31 4.80    0   43  410 1
 971      2    SILT
 972      3 BRITAIN. HAMMO YASSI, N. . NCL. UN.
 973      1LIN     9D LINCOLN            53.20 359.64   0.6 70.61 5.30    0   43  410 1
 974      2   ALL SAMPLES
 975      3 BRITAIN. HAMMO YASSI, N. . NCL. UN.
```

```
)  976      1RBA     9T BRIDGE ABUTMENT     54.90  -2.50   0.2 62.21 1.2  1777  150  250 4
)  977      2    HEARTH
)  978      3    BRITAIN. HAMMO YASSI, N. . NCL. UN.
)  979      1WALL   11T WALLSEND            54.90  -1.60   1.2 66.11 1.2  1276  200  400 2
)  980      2    HEARTH
)  981      3    BRITAIN. HAMMO YASSI, N. . NCL. UN.
)  982      1BRY/H   2T BRYNCASTELL         52.90  -3.60 357.0 68.51 2.0  1559    0  200 2
)  983      2     KILN
)  984      3    BRITAIN. HAMMO YASSI, N. . NCL. UN.
)  985      1BRY/F  14T BRYNCASTELL         52.90  -3.60   0.0 69.01 1.4   773    0  200 2
)  986      2     KILN
)  987      3    BRITAIN. HAMMO YASSI, N. . NCL. UN.
)  988      1BRY/G   6T BRYNCASTELL         52.90  -3.60 358.6 70.11 1.2          0  100 4
)  989      2     KILN
)  990      3    BRITAIN. HAMMO YASSI, N. . NCL. UN.
)  991      1BRY/G2  7T BRYNCASTELL         52.90  -3.60   0.8 68.81 1.5          0  100 4
)  992      2     KILN
)  993      3    BRITAIN. HAMMO YASSI, N. . NCL. UN.
)  994      1BRY/A   8T BRYNCASTELL         52.90  -3.60   1.5 69.51 1.5          0  100 4
)  995      2     KILN
)  996      3    BRITAIN. HAMMO YASSI, N. . NCL. UN.
)  997      1BRY/E   2T BRYNCASTELL         52.90  -3.60   1.6 70.61 2.7          0  150 2
)  998      2     KILN
)  999      3    BRITAIN. HAMMO YASSI, N. . NCL. UN.
) 1000      1BRY/E2  2T BRYNCASTELL         52.90  -3.60   1.0 69.21 5.4          0  200 2
) 1001      2     KILN
) 1002      3    BRITAIN. HAMMO YASSI, N. . NCL. UN.
) 1003      1BRY/E3  6T BRYNCASTELL         52.90  -3.60   1.5 69.01 2.2          0  100 4
) 1004      2     KILN
) 1005      3    BRITAIN. HAMMO YASSI, N. . NCL. UN.
) 1006      1RM1     8T ROMAN WALL NCLE     54.90 357.50 356.6 65.91 1.80  912  125  150 5
) 1007      2    HEARTH (AM. 160)
) 1008      3    BRITAIN. HAMMO YASSI, N. . NCL. UN.
) 1009      1RM2     6T ROMAN WALL NCLE     54.90 357.50 356.1 64.71 3.60  335  125  150 4
) 1010      2    HEARTH (AM. 150 - 200)
) 1011      3    BRITAIN. HAMMO YASSI, N. . NCL. UN.
) 1012      1ST/A    6T STEEL RIG           54.90 357.50  10.5 66.11 2.20  894 1000 1500 1
) 1013      2    MEDIEVAL HEARTH (AM. 1500)
) 1014      3    BRITAIN. HAMMO YASSI, N. . NCL. UN.
```

```
)  1015      1ST/B    3T STEEL RIG          54.90 357.50  10.2 67.61 1.60 5876 1000 1500 1
)  1016      2    MEDIEVAL FIRED BRICKS (AM. 1530)
)  1017      3    BRITAIN. HAMMO YASSI, N. . NCL. UN.
)  1018      1ST/C    5T STEEL RIG          54.90 357.50 359.4 65.81 1.40 2663  120  160 4
)  1019      2    BURNT CLAY (AM. 160)
)  1020      3    BRITAIN. HAMMO YASSI, N. . NCL. UN.
)  1021      1ST/D    6T STEEL RIG          54.90 357.50 359.4 66.11 1.40 2268  120  160 4
)  1022      2    WALL (AM. 155 OR 300)
)  1023      3    BRITAIN. HAMMO YASSI, N. . NCL. UN.
)  1024      1WAL/2  10T WALLSEND           54.90 358.40   1.7 65.21 1.30 1268  200  400 2
)  1025      2    HEARTH (AM. ABOUT 280)
)  1026      3    BRITAIN. HAMMO YASSI, N. . NCL. UN.
)  1027      1LEA     40T LEA KILN LINCOLN  53.20 359.60   1.9 68.81 2.10       250  350 4
)  1028      2    KILN (WALL SAMPLES)
)  1029      3    BRITAIN. HAMMO YASSI, N. . NCL. UN.
)  1030      1BH      12T BURROW HILL       52.10   1.50  11.8 67.51 2.50       700  840 3
)  1031      2    KILN
)  1032      3    BRITAIN. HAMMO YASSI, N. . NCL. UN.
)  1033      1SPO     16T SPONG HILL KILN   52.44   0.54   1.2 66.21 2.30        40  150 3
)  1034      2    KILN PILLAR
)  1035      3    BRITAIN. HAMMO YASSI, N. . NCL. UN.
#End of file
```

APPENDIX II

FRENCH ARCHAEOMAGNETIC DATA
THELLIER, E. (1981)

)	1	1	2 3	4	5	6	7	8	9	10	11	12
)	2											
)	3											
)	4	1 1	17T	YZEURE(LE PAVILLON)	46.57	3.35	-1.4	61.01	0.70	2265	80	80 5
)	5	1 3	6T	THORONET	43.45	6.25	-16.2	62.91	1.40	1626	1830	1830 4
)	6	1 3	8T	FREJUS PIECE	43.47	6.75	-6.4	64.31	1.20	1629	-40	-40 5
)	7	1 6	10T	NZUSE	51.18	6.72	-1.7	68.71	2.40	333	30	30 5
)	8	17,8	22T	NEUSZ III	51.18	6.72	-11.3	68.51	2.70	122	40	40 5
)	9	1 9	11T	MITTELBRON	48.75	7.20	0.8	61.01	1.00	1743	300	300 5
)	10	1 10	8T	ROUTE DE LESPIGNAN	43.28	3.13	3.7	70.51	1.90	688	9999	999910
)	11	1 11	5T	ROUTE DE SALLES	43.28	3.13	1.5	43.21	1.90	1061	9999	999910
)	12	1 12	16T	ABRENS	43.30	2.53	-0.3	56.81	1.10	1031	200	200 5
)	13	1 16	10T	GRIMESTONE END	52.28	0.83	-3.0	65.71	1.70	698	200	320 3
)	14	1 18	6T	WEST STOW HEATH	52.30	0.63	-2.0	67.21	3.20	316	100	100 4
)	15	1 20	6T	EVREUX	48.95	1.08	3.5	61.81	1.00	3187	50	150 4
)	16	2	AGE END OF 1ST C. TO BEGINING OF 2N									
)	17	1 21	14T	SPEICHER	49.93	6.70	-0.5	61.31	1.20	944	280	330 4
)	18	1 22	4T	ASBERG	51.43	6.60	-2.5	65.71	1.40	2500	25	75 3
)	19	2	AGE MID 1ST C.									
)	20	1 23	13T	WALBERBERG	50.78	6.90	14.2	73.01	3.20	143	700	875 2
)	21	1 24	11T	NEUSZ I	51.18	6.70	-4.2	69.71	2.10	418	40	40 5
)	22	1 26	5T	CAVANAC	43.17	2.30	3.0	50.51	2.10	890	800	950 3
)	23	1 27	6T	PALAJA	43.17	2.40	5.5	54.21	1.30	1965	550	750 1
)	24	1 28	8T	LA VILLENEUVE-	48.55	3.60	-2.2	62.51	1.00	2497	70	110 5
)	25	2	AGE 90 +- 20									
)	26	1 29	11T	LEZOUX	45.83	3.40	-2.5	53.71	1.70	548	160	200 5
)	27	1 32	17T	GOULT	43.87	5.30	20.5	58.51	2.40	203	1150	1200 5
)	28	1 33	8T	DORMAGEN	51.08	6.80	-0.5	68.01	1.40	1270	50	70 5
)	29	1 34	12T	SIEGBOURG	50.81	7.20	5.5	59.81	1.00	1571	1500	1700 2
)	30	2	AGE 16TH. C. TO 17TH. C.									
)	31	1 35	9T	SIEGBOURG	50.81	7.20	6.3	62.21	1.00	2370	1200	1400 2
)	32	2	AGE 13TH. C. TO 14TH. C.									
)	33	1 36	6T	SIEGBOURG	50.81	7.20	2.9	60.91	1.80	1039	9999	999910
)	34	1 37	8T	MUNSTER PLATZ	50.77	7.00	19.9	63.71	3.90	189	9999	999910
)	35	1 38	6T	PETIT ROUQUETTE	43.15	3.10	-1.3	58.41	1.10	2503	9999	999910
)	36	1 39	6T	LE PIGEONNIER	43.13	2.90	-6.5	70.51	1.30	1957	1500	1600 4
)	37	2	AGE 16TH. C.									
)	38	1 40	3T	LE PIGEONNIER	43.13	2.90	-21.0	66.01	2.10	1465	1790	1790 3

)	39	2	AGE ABOUT 1790 (?)										
)	40	1 41	4T GASPARETS W	43.02	2.93	-18.0	61.21	1.50	2139	9999	999910		
)	41	1 43	7T LA FONTIVELLE	43.03	2.33	16.0	50.21	3.00	308	900	1300	1	
)	42	2	AGE 10TH.C. TO 13TH C.										
)	43	1 44	4T AMPURIAS	42.12	3.13	-8.5	63.51	1.50	2592	-300	0	1	
)	44	2	AGE 3RD. C. BC TO AD										
)	45	1 45	4T AMPURIAS	42.12	3.13	-5.0	55.71	2.00	1138	9999	999910		
)	46	1 47	7T LE THORONET	43.45	6.25	2.0	58.51	1.50	1333	400	500	4	
)	47	2	AGE 5TH C.										
)	48	1 48	9T MUSCAPEU	43.47	5.93	-2.0	57.51	1.50	887	0	200	2	
)	49	2	AGE 1ST. TO 2ND C.										
)	50	1 49	5T SERAME E	43.25	2.75	2.7	60.51	2.50	607	50	150	4	
)	51	2	AGE END OF 1ST. C. TO BEGINING OF 2										
)	52	1 51	7T TINTAINE	43.13	3.12	9.0	60.51	1.80	985	1570	1570	5	
)	53	2	AGE ABOUT 1570										
)	54	1 54	6T CAEN	49.18	-0.37	11.2	55.01	1.00	3448	1340	1340	4	
)	55	1 55	5T PORTEL	43.05	2.90	-5.0	58.01	1.10	3354	1200	1300	4	
)	56	2	AGE 13 C.										
)	57	1 56	7T AMAY	50.55	5.33	3.3	58.21	2.10	658	1350	1350	5	
)	58	1 57	20T LECTOURE	43.93	0.60	-4.2	57.51	1.70	311	400	450	5	
)	59	2	AGE BRGINING OF 5TH C.										
)	60	1 58	10T CABASSE	43.43	6.20	15.7	58.51	1.10	1608	950	1350	1	
)	61	2	AGE 950 TO 1150 OR 1300 TO 1350										
)	62	1 59	22T LEZOUX LAS65	45.83	3.37	-1.2	63.51	1.30	684	15	20	5	
)	63	1 62	7T LEZOUX LAS4	45.83	3.37	-2.7	59.21	2.00	673	180	200	5	
)	64	2	AGE 180 TO 200										
)	65	1 63	7T COULANGES(I)	46.48	3.90	-3.4	59.51	2.40	505	160	170	5	
)	66	1 64	7T BOUCHEPORN(FOUR 9)	49.15	6.63	0.1	57.51	1.50	1229	160	180	5	
)	67	2	AGE 160 TO 180										
)	68	1 65	9T BOUCHEPORN(FOUR7)	49.15	6.63	-3.2	60.31	2.70	293	160	180	5	
)	69	2	AGE 160 TO 180										
)	70	1 67	9T BOUCLEPORN(FOUR10)	49.15	6.63	-10.6	61.21	3.30	197	120	150	4	
)	71	2	AGE 120 TO 150 (?)										
)	72	1 68	5T BOUCLEPORN(FOUR15)	49.15	6.63	-4.7	62.61	5.10	152	70	100	3	
)	73	1 71	7T CABANE GIRY II	43.28	3.11	2.2	65.41	1.70	1010	1450	1690	2	
)	74	2	AGE 1570 +- 120										
)	75	1 75	5T LA VILLENEUVE	48.55	3.61	-3.0	62.21	1.20	2781	150	180	4	
)	76	1 76	8T BARAT DE VIN	43.53	-1.03	-1.0	59.61	1.50	1079	400	400	5	
)	77	1 77	6T ARGENTAN	48.75	-0.01	3.0	58.51	2.70	457	1380	1380	4	

78	1	78	10T	FORCHTENBERG I(31)	49.30	9.50	9.7	61.31	3.20	187	1200	1200	4	
79	2	AGE ABOUT 1200												
80	1	79	8T	FORCHTENBERG I(43)	49.30	9.50	10.7	58.91	2.00	584	1250	1275	5	
81	1	80	5T	FORCHTENBERG I(49)	49.30	9.50	14.7	59.61	1.80	1294	1225	1225	4	
82	2	AGE ABOUT 1225												
83	1	81	6T	FORCHTENBERG I(549)	49.30	9.50	-2.1	70.61	2.60	467	200	700	1	
84	1	82	9T	JOHLINGEN	49.03	8.57	6.3	69.71	2.30	405	9999	999910		
85	1	84	7T	LIMOUX II(2)	43.11	2.27	-0.1	62.01	2.10	625	-20	-5	5	
86	1	87	11T	FORCHTENBERG(1722)	49.30	9.50	2.9	72.01	1.60	721	700	700	5	
87	1	88	9T	BOUTONVILLE	50.05	4.40	27.2	66.51	2.10	510	9999	999910		
88	2	AGE UNKNOWN												
89	1	90	7T	XANTEN	51.67	6.45	3.4	61.31	1.10	2155	175	200	5	
90	1	91	11T	BRUHL-ECKDORF	50.80	6.91	8.6	73.41	1.30	1057	850	900	5	
91	1	92	14T	BRUHIL-ECKDORF(3)	50.80	6.91	4.8	75.61	1.90	404	800	900	4	
92	1	93	12T	MARILLES II(I)	50.70	4.95	-4.3	64.01	1.70	2942	71	78	5	
93	1	94	11T	MARILLED II(II)	50.70	4.95	1.7	67.51	2.10	404	9999	999910		
94	1	95	11T	AMAY II(I)	50.55	5.33	-7.2	63.41	3.00	196	50	100	5	
95	1	96	13T	DOUE LA FONTAINE	47.20	-0.27	15.7	59.11	2.60	214	950	950	5	
96	2	AGE ABOUT 950												
97	1	97	10T	DOE LA FONTAINE	47.20	-0.27	20.2	63.11	1.80	607	950	950	5	
98	2	AGE ABOUT 950												
99	1	98	12T	GUEUGNON(9)	46.60	4.05	-4.1	59.41	0.90	2095	9999	999910		
100	1	99	10T	GUEUGNON(10)	46.60	4.05	1.2	61.61	1.70	665	9999	999910		
101	1	100	5T	GUEUGNON(6)	46.60	4.05	-0.7	57.71	1.30	2291	150	250	4	
102	2	AGE LATE 2ND. C. TO POST 2ND. C.												
103	1	101	7T	LEZOUX III JARDIN	45.83	3.37	-2.0	61.11	1.30	1622	385	385	5	
104	2	AGE AFTER 385												
105	1	103	8T	IVERSHEIM(4)	50.60	6.77	0.2	63.41	2.20	487	280	280	5	
106	1	104	8T	IVERSHEIM(2)	50.60	6.77	-3.8	62.71	1.30	1351	280	280	5	
107	1	105	7T	VERVOZ HAMEAU	50.40	5.37	1.2	64.31	1.60	1071	100	125	5	
108	1	110	24T	SARAN(B)	47.95	1.88	5.2	70.01	1.00	864	750	850	4	
109	2	AGE 820 TO 850 OR 750												
110	1	111	12T	GIEVRES	47.27	1.67	-2.9	66.31	1.50	760	40	40	5	
111	1	112	7T	CLOITRE	49.18	-0.38	21.4	63.31	0.90	3251	1000	1500	1	
112	2	AGE 11TH. C. OR 12TH. C. TO 15TH.												
113	1	113	12T	SARAN(C)	47.95	1.88	5.3	66.11	1.70	591	820	820	5	
114	2	AGE AFTER 820												
115	1	114	7T	BEAUVAIS	49.43	2.07	-1.7	59.51	1.60	1830	200	300	4	
116	2	AGE 3RD. C.												

→ +220

) 117	1116	8T	POUILLE LES BORDES	47.31	1.30	-6.4	64.61	1.80	771	150	200 5
) 118	2 AGE END OF 2ND. C.										
) 119	1116''	7T	POUILLE LES BORDES	47.31	1.30	-1.1	60.41	1.50	1248	150	200 5
) 120	2 AGE END OF 2ND. C.										
) 121	1118	6T	MARILLES III	50.70	4.95	-1.9	64.51	1.90	875	9999	999910
) 122	1121	9T	PIERRELITTE	49.48	1.98	7.0	65.71	4.70	100	1550	1550 4
) 123	1122	12T	ABBAYE DE VAUCLAIR	49.45	3.75	-3.3	65.11	2.00	420	40	70 5
) 124	1123	5T	COUTELAN I	47.78	2.43	-1.4	61.41	1.60	1452	75	75 5
) 125	1124	7T	TAVAUX	49.73	3.90	6.0	74.31	2.30	504	9999	999910
) 126	1125	9T	HUY (2)	50.53	5.25	-3.6	73.11	2.00	508	700	700 5
) 127	1125'	6T	HUY(23)	50.53	5.25	2.2	64.31	1.80	1029	400	500 4
) 128	1126	7T	PIERREFONDS (10)	49.37	3.00	0.2	65.51	1.50	1154	40	40 5
) 129	1127	10T	VRIGNY I,II,II(2)	48.07	2.25	-3.7	60.71	2.00	512	290	290 5
) 130	1127'	10T	VRIGNY I,II,III(3)	48.07	2.25	0.2	61.71	1.20	1393	290	290 5
) 131	1130	7T	NERIS LES BAINS	46.25	2.67	-4.3	67.01	3.50	226	15	25 4
) 132	1131	4T	SARAN IV(G)	47.95	1.88	7.8	72.71	3.60	375	750	900 3
) 133	1132	6T	TAVAUX II(2)	49.73	3.90	-2.7	72.01	2.10	756	1666	1666 4
) 134	2 AGE ABOUT 1666										
) 135	1133	6T	VRIGNY III(1)	48.07	2.25	-2.2	58.31	3.40	279	275	300 4
) 136	1133'	4T	VRIGNY III(4)	48.07	2.25	-8.9	63.51	1.60	1859	275	300 3
) 137	1133''	9T	VRIGNY III(5)	48.07	2.25	-1.7	61.61	1,40	1098	290	290 5
) 138	1135	6T	GIEVRES II	47.27	1.67	-0.6	64.11	0.80	5047	40	40 4
) 139	1137	9T	CHAMBON LA FORET	48.03	2.30	5.6	61.11	2.30	402	1400	1500 4
) 140	2 AGE 15TH. C.										
) 141	1140	7T	LA MADRAGUE	43.17	5.60	-11.6	67.11	1.20	1796	1700	1700 5
) 142	2 AGE ABOUT 1700										
) 143	1141	17T	MONT ST. JEAN	49.78	4.20	7.5	68.71	0.90	1342	1580	1580 5
) 144	1142	16T	THONON LES BAINS	46.37	6.48	0.7	58.21	2.50	189	190	200 5
) 145	1144	20T	STRASBOURG	48.53	7.70	-6.7	62.51	2.00	254	40	70 5
) 146	1145	7T	ST. URSIN	49.31	-0.45	1.2	54.21	2.70	354	1370	1370 5
) 147	2 AGE ABOUT 1370										
) 148	1146	11T	MOUGON(1)	47.11	0.48	-3.0	60.01	0.90	2285	0	300 2
) 149	2 AGE 1ST. TO 3RD. C.										
) 150	1147	12T	PALAMINY(3)	43.18	1.07	18.2	64.21	1.20	969	1000	1450 1
) 151	2 AGE 11TH. C. TO THE BEGINING OF 15T										
) 152	1148	18T	ST. GILLES DU GARD	43.68	4.43	11.2	51.21	1.00	1040	1100	1200 3
) 153	2 AGE 12TH. C. OR AFTER										
) 154	1151	20T	ST.VICTOR	44.05	4.47	17.5	59.01	0.80	1564	1100	1200 4
) 155	2 AGE 12TH. C.										

```
)   156      1154    17T COULANGES II          46.48   3.90  -4.2 62.51 1.50  455   20   20 5
)   157      1155     5T VRIGNY IV(7)          48.07   2.25   4.2 59.51 1.70 1045  275  300 4
)   158      1155'   11T VRIGNY IV(6)          48.07   2.25  -2.8 61.01 1.30 1125  275  300 5
)   159      1155''  30T VRIGNY (3,5,6)        48.07   2.25  -1.5 61.51 1.50 1159  275  300 5
)   160      1158     6T LA SALVETAT           43.23   1.17  10.0 50.01 3.50  282 1300 1400 4
)   161      2   AGE 14TH. C.
)   162      1159     5T ST. DENIS I(1)        49.00   2.42   7.5 67.71 1.70 1281 1500 1600 4
)   163      2   AGE 16TH. C.
)   164      1159'    5T ST. DENIS II(2)       49.00   2.42  11.3 56.71 2.30  744 1250 1350 4
)   165      1160     7T SAVIGNIES             49.47   1.97  -0.4 57.81 1.20 1809 1500 1600 4
)   166      2   AGE 15TH. C.
)   167      1162     8T MONTREUIL             50.45   1.75  10.1 64.91 2.80  305 1537 1537 5
)   168      1163     7T PLOMEUR               47.85  -4.33  13.8 59.21 2.90  326  960 1140 2
)   169      2   AGE 1050 +-90
)   170      1166     7T RUBERCY               49.28  -0.88  15.4 61.31 1.60 1146 1170 1170 5
)   171      2   AGE ABOUT 1170
)   172      1169    10T BOLLENE               44.27   4.77  12.1 50.91 0.70 3504 1250 1360 3
)   173      1170     8T ST. VICTOR (128L)     44.05   4.47  19.6 58.91 1.60  998 1225 1225 5
)   174      2   AGE ABOUT 1225(?)
)   175      1171     8T ST. VICTOR (128E)     44.05   4.47  15.1 53.31 1.50 1158 1225 1225 5
)   176      2   AGE ABOUT 1225
)   177      1172     8T ST. VICTOR (89B)      44.05   4.47  20.2 61.51 0.70 4523 9999 999910
)   178      1175     7T ST. GERMAIN           49.45   1.98   5.1 55.91 1.30 1804 1300 1450 3
)   179      2   AGE 14TH C. TO THE BEGINING OF 15TH
)   180      1176     6T SORRUS                50.45   1.71  11.8 55.61 1.70 1190 1270 1270 4
)   181      1177     7T ABBAYE DE DOMARTIN    50.31   1.91 -17.7 71.71 0.60 7097 1770 1780 5
)   182      1178     7T NORRENT-FONTES        50.60   2.41  13.4 68.01 2.40  466  300  400 4
)   183      2   AGE 4TH. C.
)   184      1179    11T LEZOUX IV             45.83   3.37  13.6 56.51 0.60 4748 1200 1300 4
)   185      2   AGE 13TH. C.
)   186      1183     9T CAZERES               43.23   1.08  -3.1 59.41 2.50  337  -50  -50 5
)   187      2   AGE -50(?)
)   188      1184     8T BEGUES                46.10   3.20   9.8 59.21 2.30  444 9999 999910
)   189      1185     8T VARENNES/ALLIER       46.31   3.40  -1.5 58.81 1.80  749  180  180 5
)   190      1187     8T ST. QUENTIN           44.01   4.41 -11.2 68.51 1.00 2509 1650 1700 5
)   191      2   AGE 1650 TO 1700
)   192      1190     9T LABUISSIERE II        50.50   2.57  -4.7 62.51 0.60 6055   50  150 4
)   193      2   AGE END OF 1ST. C. TO BEGINING OF 2
)   194      1191     9T MIRVILLE              49.57   0.48   8.2 59.91 1.70  770 1180 1200 5
)   195      1192    17T TOULON/ALLIER         46.57   3.33  -2.4 57.91 0.50 4012  180  180 5
#End of file
```

APPENDIX III

FORTRAN Computer program for geographics correction of Archaeomagnetic data

Meriden : Lat = 52.43 Long = 358.38

Paris : Lat = 48.87 Long = 2.33

```
      C     ************************************************************
      C          GEOGRAPHIC CORRECTION FOR ARCHAEOMAGNETIC DATA
      C     BY N. YASSI ON IDEA OF M. NOEL, MODIFIED BY D.H. TARLING
      C     ************************************************************
      C     *** SLAT IS THE SITE LATITUDE IN DEG. +VE N. HEMIS. *****
      C     ***       AND -VE. S. HEMIS.                        *****
      C     *** SLONG IS THE SITE EAST LONGITUDE (0 TO 360)      *****
      C     *** AINC IS THE MAGNETIC INCLINATION IN DEG. +VE. N.*****
      C     ***       HEMIS. AND -VE. S. HEMIS.                 *****
      C     *** ADEC IS THE MAGNETIC DECLINATION IN DEG.         *****
      C     ***       (0 TO 360).                               *****
      C     *** SNLAT IS THE NEW SITE LATITUDE                  *****
      C     *** SNLONG. IS THE NEW SITE LONGITUDE               *****
      C     ************************************************************
            DIMENSION BA5(300),B5(300),BA4(300),B4(300),BA3(300),B3(300),
           1BA2(300),B2(300),BA1(300),B1(300)
             I=0
             J=0
             K=0
             L=0
             M=0
             E=0.0174532
             E1=57.295779
             E2=1.5707963
             E3=3.1415926
             CHECK=0
      C      ****** INPUT DATA ******
       10    WRITE(6,1000)
       1000 FORMAT(' GIVE LAT LONG OF CORRECTION POINT(2F7.2)',
           & /,'   MERIDEN = 52.43 358.38 ; PARIS = 48.87 2.33',
           & /,'  (TERMINATE WITH TWO BLANK LINES)')
             READ(5,1020) SNLAT,SNLONG
             SNLAT=SNLAT*E
             SNLONG=SNLONG*E
             IF(SNLAT.LE.90.0*E) GOTO 200
             CHECK=1
             WRITE(6,1000)
             READ(5,1020)SNLAT,SNLONG
```

```
      SNLAT=SNLAT*E
      SNLONG=SNLONG*E
  200 WRITE(6,1010)
 1010 FORMAT('GIVE LAT LONG SITE (2F7.2)')
      READ(5,1020) SLAT,SLONG
 1020 FORMAT(2F7.2)
      WRITE(6,1030)
 1030 FORMAT('GIVE DEC INC OF DIRECTION (2F7.2)')
 1021 FORMAT(2F7.2,I2)
      READ(5,1021) ADEC,AINC,JRL
      IF((ADEC.EQ.0).AND.(AINC.EQ.0).AND.(SLAT.EQ.0).AND.(SLONG.EQ.0))
     &GO TO 100
      WRITE(6,1)SLAT,SLONG
    1 FORMAT('SITE LAT.LONG=',F7.2,F9.2)
      WRITE(6,3)ADEC,AINC
    3 FORMAT('MAGNETIC DEC.INC=',F7.2,F9.2)
C     ****** POLE CALCULATION ******
      SLAT=SLAT*E
      SLONG=SLONG*E
      AINC=AINC*E
      ADEC=ADEC*E
      X=-ATAN(0.5*TAN(AINC))+E2
      PLAT=ARSIN(SIN(SLAT)*COS(X)+COS(SLAT)*SIN(X)*COS(ADEC))
      Q=ARSIN(SIN(X)*SIN(ADEC)/COS(PLAT))
      IF(COS(X).GT.SIN(PLAT)*SIN(SLAT)) PLONG=SLONG+Q
      IF(COS(X).EQ.SIN(PLAT)*SIN(SLAT)) PLONG=SLONG+Q
      IF(COS(X).LT.SIN(PLAT)*SIN(SLAT)) PLONG=E3+SLONG-Q
      XLAT=PLAT*E1
      XLONG=PLONG*E1
      WRITE(6,5)XLAT,XLONG
    5 FORMAT('          POLE LAT.LONG=',F7.2,F9.2)
C     ****** CALCULATION OF NEW DEC. INC. ******
      SM=0.0000001
      A4=SNLAT
      A6=SNLONG
      A2=PLAT
      A3=PLONG
      A5=SIN(A2)*SIN(A4)
      A7=COS(A2)*COS(A3-A6)
```

```
     78            A1=ARCOS(COS(A4)*A7+A5)
     79            A8=COS(A1)
     80            A9=SIN(A1)
     81            IF(A9.EQ.0.0) A9=SM
     82            BINC=(ATAN(2*A8/A9))*E1
     83            IF(A5.GT.A8) A7=SIN(A6-A3+E3)
     84            IF(A5.LT.A8) A7=SIN(A3-A6)
     85            IF(A5.EQ.A8) A7=SIN(A3-A6)
     86            BDEC=ARCOS((COS(A2)*A7/A9))
     87            BDEC=90-BDEC*E1
     88            IF(BDEC.LT.0) BDEC=360.0+BDEC
     89            IF(BDEC.GT.360) BDEC=BDEC-360
     90            WRITE(6,7)BDEC,BINC
     91          7 FORMAT('              NEW DEC. INC=',F7.2,F9.2)
     92            BBINC=BINC*(-1)
     93            IF(CHECK.EQ.1) GOTO 1090
     94            GOTO 200
     95        C   ****** DATA PREPARATION FOR PLOT PROGRAM ******
     96         1090 IF(JRL.EQ.5) GOTO 2000
     97            IF(JRL.EQ.4) GOTO 2010
     98            IF(JRL.EQ.3) GOTO 2020
     99            IF(JRL.EQ.2) GOTO 2030
    100            IF(JRL.EQ.1) GOTO 2040
    101            GOTO 200
    102         2000 I=I+1
    103            I1=I
    104            BA5(I)=BBINC
    105            B5(I)=BDEC
    106            GOTO 200
    107         2010 J=J+1
    108            J1=J
    109            BA4(J)=BBINC
    110            B4(J)=BDEC
    111            GOTO 200
    112         2020 K=K+1
    113            K1=K
    114            BA3(K)=BBINC
    115            B3(K)=BDEC
    116            GOTO 200
```

```
)   117      2030 L=L+1
)   118           L1=L
)   119           BA2(L)=BBINC
)   120           B2(L)=BDEC
)   121           GOTO 200
)   122      2040 M=M+1
)   123           M1=M
)   124           BA1(M)=BBINC
)   125           B1(M)=BDEC
)   126           GOTO 200
)   127      100  IF(CHECK.EQ.1) GOTO 3000
)   128           STOP
)   129      3000 IF(I.LT.1) GOTO 3010
)   130           WRITE(9,4000)
)   131      4000 FORMAT(' 110.0   1.0')
)   132           DO 3001 I=1,I1
)   133      3001 WRITE(9,1040) BA5(I),B5(I)
)   134      3010 IF(J.LT.1) GOTO 3020
)   135           WRITE(9,4010)
)   136      4010 FORMAT(' 107.0   0.9')
)   137           DO 3002 J=1,J1
)   138      3002 WRITE(9,1040) BA4(J),B4(J)
)   139      3020 IF(K.LT.1) GOTO 3030
)   140           WRITE(9,4020)
)   141      4020 FORMAT(' 109.0   0.8')
)   142           DO 3003 K=1,K1
)   143      3003 WRITE(9,1040) BA3(K),B3(K)
)   144      3030 IF(L.LT.1) GOTO 3040
)   145           WRITE(9,4030)
)   146      4030 FORMAT(' 101.0   0.1')
)   147           DO 3004 L=1,L1
)   148      3004 WRITE(9,1040) BA2(L),B2(L)
)   149      3040 IF(M.LT.1) GOTO 5000
)   150           WRITE(9,4040)
)   151      4040 FORMAT(' 100.0   0.0')
)   152           DO 3005 M=1,M1
)   153      3005 WRITE(9,1040) BA1(M),B1(M)
)   154      1040 FORMAT(2F6.1)
)   155      5000 STOP
)   156           END
End of file
```

APPENDIX IV

FORTRAN Computer program for sorting Archaeomagnetic data

```
      1     C      ************************************************************
      2     C      *****    SORTING PROGRAM OF THE ARCHEOLOGICAL DATA  *******
      3     C      ************************************************************
      4           DIMENSION ND(1500)
      5           REAL ANEM*8
      6           REAL ANEM1*8
      7           REAL ANEM2*4
      8           REAL REM1*8
      9           REAL REM2*8
     10           REAL REM3*8
     11           REAL REM4*8
     12           REAL REM5*8
     13           REAL REM6*8
     14           REAL REM7*8
     15           REAL REM8*8
     16           REAL REM9*8
     17           REAL REM10*8
     18           REAL REM11*8
     19           REAL REM12*8
     20           REAL CODE*8
     21           READ(5,10,ERR=100)(ND(I),I=1,918)
     22        10 FORMAT(I2)
     23       100 CONTINUE
     24     C      ************************************************************
     25     C      ******* INPUT SWICHES (FILE 7)                        ******
     26     C      ******* ====================                         ******
     27     C      ******* 1-IREM FOR PRINTING REMARKS (I1).             ******
     28     C      *******   IREM=0 NO REMARKS PRINT.                    ******
     29     C      *******   IREM=1 PRINT REMARKS ON LINE 2.             ******
     30     C      *******   IREM=2 PRINT REMARKS ON LINE 3.             ******
     31     C      *******   IREM=3 PRINT REMARKS ON LINE 2 AND 3.       ******
     32     C      *******   IREM=4 TAPE OUTPUT + PRINT OF LINE 1        ******
     33     C      ******* 2-IGEMI MINIMUM AGE (I5).                    ******
     34     C      *******   IGEMA MAXIMUM AGE (I5).                    ******
     35     C      ******* 3-ALTMI MINIMUM AREA LATITUDE (F7.2)         ******
     36     C      *******   ALTMA MAXIMUM AREA LATITUDE (F7.2)         ******
     37     C      *******   GLOMI MINIMUM AREA LONGITUDE (F7.2)        ******
     38     C      *******   GLOMA MAXIMNM AREA LONGITUDE (F7.2)        ******
```

```
C       ******* 4-ISAMP MINIMUM NO. OF SAMPLES (I2)                ******
C       ******* 5-MSTAB MINIMUM M. STABILITY (I5)                  ******
C       ***************************************************************
      READ(7,40)IREM,ISAMP,MSTAB
      IF(IREM.EQ.4) WRITE(9,1200)
 1200 FORMAT(' 100.00 100.00',/,'  52.43 358.38')
   40 FORMAT(I1,I2,I5)
      READ(7,42)ALTMI,ALTMA,GLOMI,GLOMA
   42 FORMAT(4F7.2)
      READ(7,44)IGEMI,IGEMA
   44 FORMAT(2I5)
      K=I
      DO 200 I=1,K
      IF(ND(I).EQ.2) GOTO 300
      IF(ND(I).EQ.3) GOTO 400
      READ(6,50)NLN,CODE,ISP,TRM,ANEM,ANEM1,ANEM2,ALT,GLON,DMAG,CMAG,
     1IA,A95,MST,MIG,MAG,JRL
C       ***************************************************************
C       ******  INPUT DATA(FILES 5 AND 6)                          ******
C       ******  ==========                                         ******
C       ****** 1- NLN IS NO. OF LINE 1,FOR DATA. 2,REMARKS         ******
C       ******    AND 3, COUNTRY AND REFERENCE.                    ******
C       ****** 2- CODE IS THE SITE CODE (A6).                      ******
C       ****** 3- ISP IS THE NO. OF SAMPLES (I3).                  ******
C       ****** 4- TRM T,FOR TRM. C,FOR CRM AND D,DRM (A1).         ******
C       ****** 5- ANEM,1,2 NAME OF SITE (2A8,A4).                  ******
C       ****** 6- ALT SITE LATITUDE (F6.2).                        ******
C       ****** 7- GLON SITE LONGITUDE (F7.2).                      ******
C       ****** 8- DMAG MAGNETIC DECLINATION (F6.1).                ******
C       ****** 9- CMAG MAGNETIC INCLINATION (F5.1).                ******
C       ******10- IA 1,FOR ALPHA 95. 2,80. 3,68. (I1).            ******
C       ******11- ALPHA 95 , 80, OR 68 (F5.2).                    ******
C       ******12- MST MAGNETIC STABILITY (I5).                    ******
C       ******13- MIG MINIMUM AGE (I5).                           ******
C       ******14- MAG MAXIMUM AGE (I5).                           ******
C       ******15- JRL MAGNETIC RELIABILITY (I2).                  ******
C       ***************************************************************
      IF(ALT.EQ.ALTMI.OR.ALT.GT.ALTMI) GOTO 600
      GOTO 200
```

```
     78      600  IF(ALT.EQ.ALTMA.OR.ALT.LT.ALTMA) GOTO 610
     79           GOTO 200
     80      610  IF(GLON.EQ.GLOMI.OR.GLON.GT.GLOMI) GOTO 620
     81           GOTO 200
     82      620  IF(GLON.EQ.GLOMA.OR.GLON.LT.GLOMA) GOTO 700
     83           GOTO 200
     84      700  IF(ISP.EQ.ISAMP.OR.ISP.GT.ISAMP) GOTO 800
     85           GOTO 200
     86      800  IF(MST.EQ.MSTAB.OR.MST.GT.MSTAB) GOTO 850
     87           GOTO 200
     88      850  IF(MIG.GT.IGEMI.AND.MAG.LT.IGEMA) GOTO 900
     89           IF(MIG.LT.IGEMI.AND.MAG.GT.IGEMI) GOTO 900
     90           IF(MIG.LT.IGEMA.AND.MAG.GT.IGEMA) GOTO 900
     91           IF(MIG.EQ.IGEMI.OR.MAG.EQ.IGEMA) GOTO 900
     92           IF(MIG.EQ.IGEMA.OR.MAG.EQ.IGEMI) GOTO 900
     93           IF(MIG.LT.IGEMI.AND.MAG.GT.IGEMA) GOTO 900
     94           GOTO 200
     95      900  NFLAG=1
     96           WRITE(8,50)NLN,CODE,ISP,TRM,ANEM,ANEM1,ANEM2,ALT,GLON,DMAG,CMAG,
     97          1IA,A95,MST,MIG,MAG,JRL
     98       50  FORMAT(I2,A6,I3,A1,2A8,A4,F6.2,F7.2,F6.1,F5.1,I1,F5.2,3I5,I2)
     99           IF(IREM.EQ.4) WRITE(9,1000) ALT,GLON,DMAG,CMAG,JRL
    100      1000 FORMAT(2F7.2,/,2F7.2,I2)
    101      C    **************************************************************
    102      C    ****** OUTPUT DATA FILES 8 AND 9                          ******
    103      C    ****** ========================                          ******
    104      C    ****** FILE 8 OUTPUT LIST OF DATA AND REMARKS.            ******
    105      C    ****** FILE 9 TAPE OUTPUT WHEN IREM=4                     ******
    106      C    ******         FOR ALT,GLON,DMAG,CMAG,RL                 ******
    107      C    ******          IN 2F7.2,/,2F7.2,I2  FORMAT.             ******
    108      C    **************************************************************
    109           GOTO 200
    110      300  READ(6,30)REM1,REM2,REM3,REM4,REM5,REM11
    111      C    **************************************************************
    112      C    ****** INPUT REMARKS(FILES 5 AND 6)                       *******
    113      C    ****** ============                                      *******
    114      C    ****** REM1,2,3,4,5 AND 11 ARE SITE REMARKS (6A8).        *******
    115      C    **************************************************************
    116           IF(IREM.EQ.1.OR.IREM.EQ.3.AND.NFLAG.EQ.1)WRITE(8,30)REM1,REM2,
```

```
     117           1REM3,REM4,REM5,REM11
     118            GOTO 200
     119       400  READ(6,30)REM6,REM7,REM8,REM9,REM10,REM12
     120      C      ************************************************************
     121      C      ****** INPUT REMARKS(FILES 5 AND 6)                  *******
     122      C      ****** =============                                 *******
     123      C      ****** REM6,7,8,9,10 AND 12 ARE COUNTRY OF SITE AND  *******
     124      C      ******                      SITE REFERENCE (6A8).    *******
     125      C      ************************************************************
     126            IF(IREM.EQ.2.OR.IREM.EQ.3.AND.NFLAG.EQ.1)WRITE(8,30)REM6,REM7,
     127           1REM8,REM9,REM10,REM12
     128            NFLAG=0
     129       200  CONTINUE
     130        30  FORMAT(6A8)
     131            IF(IREM.EQ.4) WRITE(9,1100)
     132       1100 FORMAT(/,/)
     133            STOP
     134            END
End of file
```

APPENDIX V

Least square and student (t) test computer program

```
C     ***************************************************
C     ***      LEAST SQUARE, T-TEST AND F-TEST PROGRAM      ***
C     ***                  BY N. YASSI 1983                 ***
C     ***************************************************
      DIMENSIONX(100),XS1(100),YM1(100),ZS1(100),Y(100),
     +LDF(100),BT(100),AA3(100)
      WRITE(6,900)
  900 FORMAT('ENTER NO. OF SETS (I3)')
      READ(5,100)M
      DO 50 J=1,M
      WRITE(6,800)
  800 FORMAT('ENTER NO. OF POINTS  (I3)')
      READ(5,100)N
  100 FORMAT(I3)
      WRITE(6,810)
  810 FORMAT('ENTER X         Y     (2F10.3)')
      DO 10 I=1,N
      READ(5,200)X(I),Y(I)
  200 FORMAT(2F10.3)
   10 CONTINUE
      SX=0.0
      SY=0.0
      XX=0.0
      YY=0.0
      XY=0.0
      DO 30 I=1,N
      SX=SX+X(I)
      SY=SY+Y(I)
      CP=X(I)*Y(I)
      XY=XY+CP
      XX=XX+X(I)**2
      YY=YY+Y(I)**2
C     ***************************
C     **** SX = SUM OF X    ****
C     **** SY = SUM OF Y    ****
C     **** XY = SUM OF X*Y  ****
C     **** XX = SUM OF X SQ.****
C     **** YY = SUM OF Y SQ.****
```

```
      C      **************************
   30 CONTINUE
      CX=SX*SX/N
      CY=SY*SY/N
      CC=SX*SY/N
      XS=XX-CX
      YM=YY-CY
      ZS=XY-CC
      AMX=SX/N
      AMY=SY/N
      B=ZS/XS
      A=AMY-(B*AMX)
      R=(XY-CC)/SQRT((XX-CX)*(YY-CY))
      YS=(XY-CC)**2/(XX-CX)
      TS=YY-CY
      RS=TS-YS
      SS=RS/(N-2)
      SE=SQRT(SS)/SQRT(XX-CX)
      WRITE(6,3500)
      WRITE(6,700)B,A,SE
C     ****************************************
C     **** B = SLOP OF BEST REGRESSION LINE ****
C     **** A = INTERCEPT OF BEST LINE       ****
C     **** SE= STANDERD ERROR OF SLOP       ****
C     ****************************************
      WRITE(6,3500)
  700 FORMAT('SLOP =    ',F10.2,/,'INTERCEPT   =',F10.2,
     +/,'S. E. OF SLOP=',F10.2)
      LDF(J)=N
      BT(J)=B
      XS1(J)=XS
      YM1(J)=YM
      ZS1(J)=ZS
   50 CONTINUE
      IF(M.EQ.1) GOTO 2000
      IF(M.GT.2) GOTO 600
      AA1=YM1(1)-(ZS1(1)**2/XS1(1))
      AA2=YM1(2)-(ZS1(2)**2/XS1(2))
      SYX2=(AA1+AA2)/(LDF(1)+LDF(2)-4)
```

```
     78            SBB=SQRT(SYX2*(1/XS1(1)+1/XS1(2)))
     79            T=(BT(1)-BT(2))/SBB
     80            LDF2=LDF(1)+LDF(2)-4
     81            WRITE(6,1000)T,LDF2
     82            GOTO 2000
     83        600 SSP=0.0
     84            XSP=0.0
     85            YMP=0.0
     86            ZSP=0.0
     87            LDF1=0
     88            DO 500 J=1,M
     89            AA3(J)=YM1(J)-(ZS1(J)**2/XS1(J))
     90            LDF1=LDF1+(LDF(J)-2)
     91            SSP=SSP+AA3(J)
     92            XSP=XSP+XS1(J)
     93            YMP=YMP+YM1(J)
     94            ZSP=ZSP+ZS1(J)
     95        500 CONTINUE
     96            SSC=YMP-(ZSP**2/XSP)
     97            F=((SSC-SSP)/(M-1))/(SSP/LDF1)
     98            BC=ZSP/XSP
     99            WRITE(6,3000)BC
    100       3000 FORMAT('SLOP OF ALL POINTS=',F15.3)
    101            WRITE(6,1500)F,LDF1
    102       1500 FORMAT('F FOR F-TEST=',F15.3,/,'D.F. FOR F-TEST=',I10)
    103            GOTO 2000
    104       1000 FORMAT('T FOR T-TEST=',F15.3,/,'D.F. FOR T-TEST=',I10)
    105          C     ************************************************
    106          C     ****   T OR F VALUES WITH (D.F.) THE DEGREE OF FREEDOM ****
    107          C     **** CAN BE USED TO GET THE SIGNEFICANT PROBABILITY    ****
    108          C     **** FROM TABELS IN ANY STATISTICS TEXT BOOK .         ****
    109          C     ************************************************
    110       2000 STOP
    111       3500 FORMAT('*********************************************')
    112            END
#End of file
```